

**Table 1.** Aerosol Refractive Index Data

Species (1)	Database (2)	Refractive Index (3)	Notes (4)	(Min, Max) $\mu\text{m}$ (5)
<b>Super Hot</b>				
$\text{CaAl}_{12}\text{O}_{19}$	WS15	Mutschke et al. (2002) <sup>D</sup>	Hibonite (crystalline, E  c)	(2, 30)
$\text{Al}_2\text{O}_3$	WS15	Koike et al. (1995)	$\gamma$ Corundum (crystalline)	(0.34, 30)
$\text{Al}_2\text{O}_3$	KH18	Koike et al. (1995)	$\gamma$ Corundum (crystalline)	(0.2, 30)
		Begemann et al. (1997) <sup>D</sup>	Corundum (amorphous, porous)	
$\text{CaTiO}_3$	WS15	Posch et al. (2003) <sup>D</sup>	Perovskite (crystalline)	(2, 30)
$\text{CaTiO}_3$	KH18	Posch et al. (2003) <sup>D</sup>	Perovskite (crystalline)	(0.2, 30)
		Ueda et al. (1998)		
<b>M-L Dwarf</b>				
$\text{TiO}_2$	KH18	Zeidler et al. (2011) <sup>D</sup>	Anatase (crystalline)	(0.2, 30)
		Posch et al. (2003) <sup>D</sup>		
		Siefke et al. (2016)		
$\text{TiO}_2$	gCMCRT	Zeidler et al. (2011) <sup>D</sup>	Rutile (crystalline, E  a,b)	(0.47, 30)
		Ribarsky in Palik (1985) <sup>C</sup>		
$\text{TiC}$	KH18	Koide et al. (1990)	Titanium Carbide (crystalline)	(0.2, 30)
		Henning & Mutschke (2001)		
$\text{VO}$	gCMCRT	Wan et al. (2019)	$\text{VO}_2$ as a VO analog (crystalline)	(0.3, 30)
Nano-Diamond	N/A	Mutschke et al. (2004)	Meteoritic C (crystalline)	(0.2, 30)
<b>Iron</b>				
Fe	KH18	Lynch & Hunter in Palik (1991) <sup>C</sup>	$\alpha$ Fe (crystalline)	(0.2, 30)
FeO	WS15	Begemann et al. (1995)	Wüstite (crystalline)	(0.21, 30)
FeS	KH18	Pollack et al. (1994) <sup>C</sup>	Troilite (Crystalline)	(0.2, 30)
		Henning & Mutschke (1997) <sup>D</sup>		
$\text{Fe}_2\text{O}_3$	WS15	Triaud (2005) <sup>D</sup> (unpublished)	Hematite ( $\alpha \text{Fe}_2\text{O}_3$ )	(0.2, 30)
			(crystalline, E  a,b)	(0.2, 30)
$\text{FeSiO}_3$	WS15	Day (1981)	Ferrosilite (Iron-rich Pyroxene)	(8.22, 30)
			(amorphous)	
$\text{Fe}_2\text{SiO}_4$	KH18	Fabian et al. (2001) <sup>D</sup>	Fayalite (Iron-rich Olivine)	(0.40, 30)
			(crystalline)	
<b>Magnesium</b>				
$\text{MgO}$	KH18	Roessler & Huffman in Palik (1991) <sup>C</sup>	Periclase (crystalline)	(0.2, 30)
$\text{Mg}_{0.8}\text{Fe}_{1.2}\text{SiO}_4$	WS15	Henning et al. (2005) <sup>C</sup>	Forsterite (Fe-rich)	(0.21, 30)
		Dorschner et al. (1995) <sup>D</sup>	(amorphous glass)	
$\text{Mg}_{1.72}\text{Fe}_{0.21}\text{SiO}_4$	WS15	Zeidler et al. (2011) <sup>D</sup>	Forsterite (Fe-poor)	(0.2, 30)
			(crystalline, E  c)	
$\text{Mg}_2\text{SiO}_4$	B21	Scott & Duley (1996) <sup>C</sup>	Forsterite (amorphous)	(0.27, 30)
		Draine & Lee (1984)	'Astronomical' Silicate	
		Nitsan & Shankland (1976)	Forsterite (crystalline, E  a, E  c)	
$\text{Mg}_2\text{SiO}_4$	KH18	Jäger et al. (2003) <sup>D</sup>	Forsterite (amorphous sol gel)	(0.2, 30)
$\text{Mg}_2\text{SiO}_4$	gCMCRT	Suto et al. (2006)	Forsterite (crystalline, E  a, E  b)	(0.2, 30)
$\text{MgFeSiO}_4$	KH18	Dorschner et al. (1995) <sup>D</sup>	Olivine (amorphous glass)	(0.2, 30)
$\text{Mg}_{0.8}\text{Fe}_{1.2}\text{SiO}_4$	WS15	Dorschner et al. (1995) <sup>D</sup>	Olivine (amorphous glass)	(0.2, 30)
$\text{MgSiO}_3$	WS15	Egan & Hilgeman (1975)	Enstatite (crystalline)	(0.2, 30)
		Dorschner et al. (1995) <sup>D</sup>	Enstatite (amorphous glass)	
$\text{MgSiO}_3$	B21	Scott & Duley (1996)	Enstatite (amorphous)	(0.27, 30)
		Draine & Lee (1984)	'Astronomical' Silicate	

**Table 1** *continued*

**Table 1** (*continued*)

Species	Database	Refractive Index	Notes	(Min, Max) $\mu\text{m}$
(1)	(2)	(3)	(4)	(5)
MgSiO <sub>3</sub>	KH18	Nitsan & Shankland (1976) Dorschner et al. (1995) <sup>D</sup>	Forsterite (crystalline, E  a, E  c) Enstatite (amorphous glass)	(0.2, 30)
MgSiO <sub>3</sub>	KH18	Jäger et al. (2003) <sup>D</sup>	Enstatite (amorphous sol gel)	(0.2, 30)
MgSiO <sub>3</sub>	B21	Jaeger et al. (1998) <sup>D</sup>	Ortho-Enstatite (crystalline)	(0.27, 30)
Mg <sub>0.4</sub> Fe <sub>0.6</sub> SiO <sub>3</sub>	KH18	Dorschner et al. (1995) <sup>D</sup>	Pyroxene (amorphous glass)	(0.2, 30)
Mg <sub>0.5</sub> Fe <sub>0.5</sub> SiO <sub>3</sub>	KH18	Dorschner et al. (1995) <sup>D</sup>	Pyroxene (amorphous glass)	(0.2, 30)
Mg <sub>0.8</sub> Fe <sub>0.2</sub> SiO <sub>3</sub>	KH18	Dorschner et al. (1995) <sup>D</sup>	Pyroxene (amorphous glass)	(0.2, 30)
MgAl <sub>2</sub> O <sub>4</sub>	WS15	Fabian et al. (2001) <sup>D</sup>	Spinel (annealed, crystalline)	(1.69, 30)
<b>Silica</b>				
SiC	KH18	Laor & Draine (1993) <sup>C</sup> Bohren & Huffman (1983)	$\alpha$ SiC (crystalline)	(0.2, 30)
SiO	KH18	Philipp & Taft in Caras (1965) Philipp in Palik (1985) <sup>C</sup> Wetzel et al. (2013)	Amorphous (glass)	(0.2, 30)
SiO <sub>2</sub>	WS15	Philipp in Palik (1985) <sup>C</sup> Zeidler et al. (2013) <sup>D</sup>	$\alpha$ Quartz (crystalline) $\beta$ Quartz (crystalline, 928K, E  c)	(0.2, 30)
SiO <sub>2</sub>	N/A	Hervé Herbin & Petitprez (2023)	$\alpha$ Quartz (crystalline)	(0.25, 15.37)
SiO <sub>2</sub>	N/A	Philipp in Palik (1985) <sup>C</sup>	$\alpha$ Quartz (crystalline)	(0.2, 30)
SiO <sub>2</sub>	KH18	Henning & Mutschke (1997) <sup>D</sup> Philipp in Palik (1985) <sup>C</sup>	Amorphous Silica (glass) $\alpha$ Quartz (crystalline)	(0.2, 30)
SiO <sub>2</sub>	N/A	Philipp in Palik (1985) <sup>C</sup>	Amorphous Silica (glass)	(0.2, 30)
<b>T-Y Dwarf</b>				
Cr	KH18	Lynch & Hunter in Palik (1991) <sup>C</sup> Rakić et al. (1998)	Crystalline	(0.2, 30)
MnS	WS15	Huffman & Wild (1967)	Lab Data (crystalline)	(0.2, 13)
MnS	KH18	Huffman & Wild (1967) Montaner et al. (1979)	Extrapolated (crystalline) Na <sub>2</sub> S (15K)	(0.2, 30)
MnS	WS15	Huffman & Wild (1967) KH18 Montaner et al. (1979)	Lab Data + Extrapolated Na <sub>2</sub> S (15K)	(0.2, 30)
Na <sub>2</sub> S	WS15	Morley et al. (2012) Montaner et al. (1979) Khachai et al. (2009)	Crystalline 15K	(0.2, 30)
ZnS	WS15	Querry et al. (1987)	Zinc blende (crystalline)	(0.22, 30)
NaCl	WS15	Eldridge & Palik in Palik (1985) <sup>C</sup>	Halite (crystalline)	(0.2, 30)
KCl	WS15	Palik in Palik (1985) <sup>C</sup>	Sylvite (crystalline)	(0.2, 30)
<b>Ices</b>				
ADP (NH <sub>4</sub> H <sub>2</sub> PO <sub>4</sub> )	N/A	Zernike (1965) Querry et al. (1974)	Crystalline Liquid	(0.2, 19.99)
H <sub>2</sub> O	WS15	Hale & Querry (1973) <sup>C</sup>	Liquid	(0.2, 30)
H <sub>2</sub> O	WS15	Warren (1984) <sup>C</sup>	Ice 1h (266.15K)	(0.2, 30)
NH <sub>4</sub> SH	N/A	Howett et al. (2007) (pers. comm.)	Crystalline (~160K)	(0.5, 30)
NH <sub>3</sub>	optool	Martonchik et al. (1984) <sup>C</sup>	Crystalline (77-88K)	(0.2, 30)
CH <sub>4</sub>	WS15	Martonchik & Orton (1994) <sup>C</sup>	Liquid (111K)	(0.2, 30)
CH <sub>4</sub>	WS15	Martonchik & Orton (1994) <sup>C</sup>	Crystalline (90K)	(0.2, 30)
Ice Tholins	N/A	Khare et al. (1993)	C <sub>2</sub> H <sub>6</sub> -H <sub>2</sub> O Photolysis (amorphous, 77K)	(0.2, 30)
<b>Soots and Hazes</b>				
C	KH18	Draine (2003a) Draine (2003b)	Graphite (crystalline)	(0.2, 30)

**Table 1** *continued*

**Table 1** (*continued*)

Species	Database	Refractive Index	Notes	(Min, Max) $\mu\text{m}$	
	(1)	(2)	(3)	(4)	(5)
ExoHaze (300K)	N/A	He et al. (2023)	$\text{H}_2\text{O}-\text{CH}_4-\text{N}_2-\text{CO}_2-\text{He}$ Photolysis (amorphous)	(0.4, 28.6)	
ExoHaze (400K)	N/A	He et al. (2023)	$\text{H}_2\text{O}-\text{CH}_4-\text{N}_2-\text{CO}_2-\text{H}_2-\text{He}$ Photolysis (amorphous)	(0.4, 28.6)	
Flame Soot	gCMCRT	Lavvas & Koskinen (2017) <sup>C</sup>	Amorphous	(0.2, 30)	
Hexene ( $\text{C}_6\text{H}_{12}$ )	WS15	Anderson (2000)	Liquid	(2, 25)	
$\text{H}_2\text{SO}_4$	N/A	Palmer & Williams (1975)	Sulfuric Acid (liquid, 300K)	(0.36, 24.98)	
$\text{S}_8$	gCMCRT	Fuller, Downing, & Querry in Palik (1998) <sup>C</sup>	$\alpha$ -Sulfur (crystalline)	(0.2, 30)	
Saturn Phosphorus Haze	N/A	Noy et al. (1981) Sromovsky et al. (2020) Fletcher et al. (2023)	$\text{P}_2\text{H}_2$ Proxy (amorphous)	(0.25, 20)	
Soot 6mm	N/A	Chang & Charalampopoulos (1990)	Amorphous	(0.2, 28.4)	
Tholin	WS15	Khare et al. (1984) Ramirez et al. (2002)	$\text{N}_2-\text{CH}_4$ Photolysis (amorphous)	(0.2, 30)	
Tholin CO 1	N/A	Corrales et al. (2023)	$\text{N}_2-\text{CH}_4-\text{CO}_2$ Photolysis (amorphous)	(0.2, 9.99)	
Tholin CO 0.625	N/A	Corrales et al. (2023)	$\text{N}_2-\text{CH}_4-\text{CO}_2$ Photolysis (amorphous)	(0.2, 9.99)	

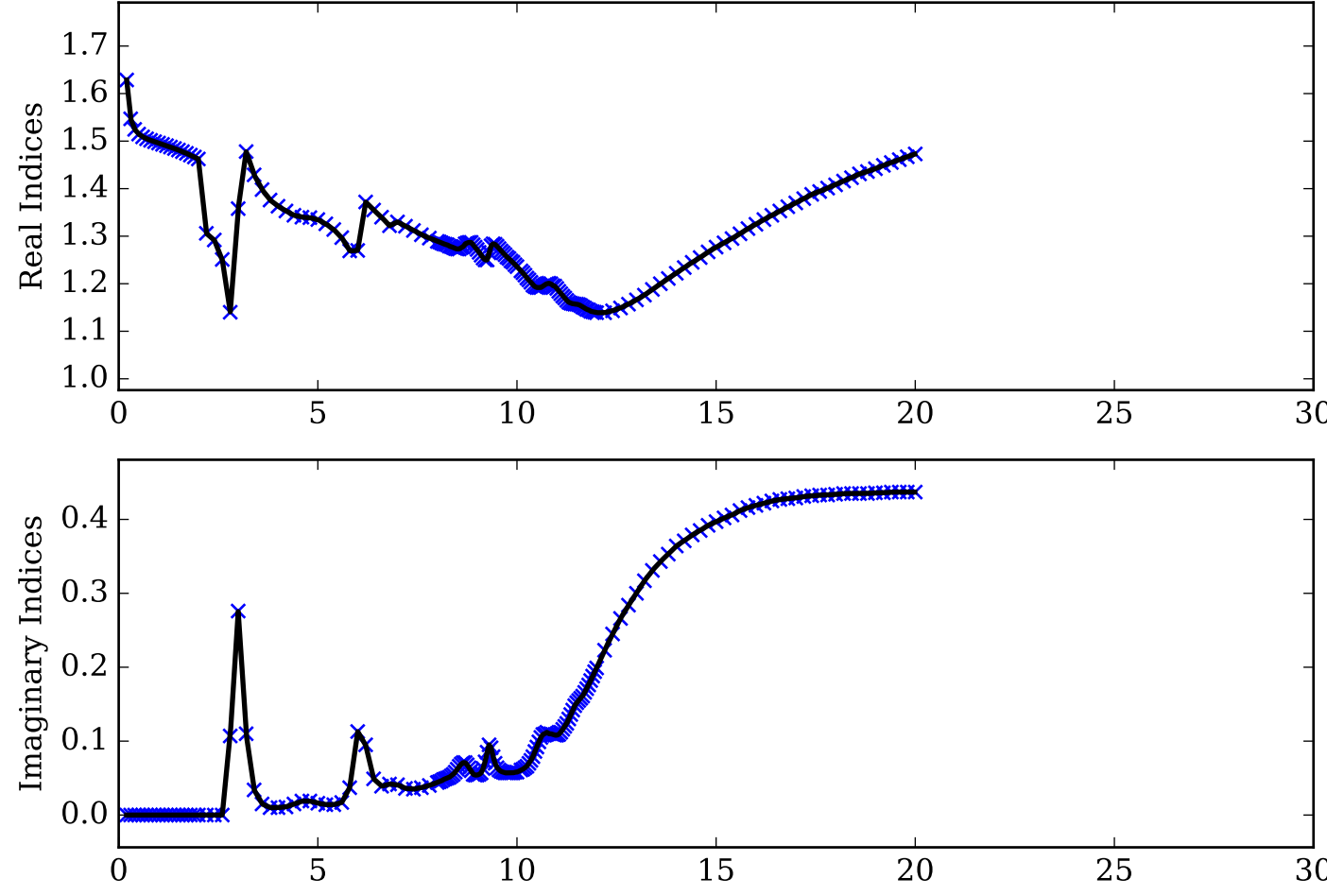
NOTE—Aerosol species included in the precomputed, open-source aerosol database. Categories: Super-Hot (e.g., Wakeford et al. 2017), M-L Dwarf (e.g., Burrows & Sharp 1999; Lodders 2002; Lee et al. 2016), Iron, Magnesium, Silica (e.g., Sudarsky et al. 2003; Visscher et al. 2010; Lee et al. 2016), T-Y Dwarf (e.g., Morley et al. 2012), Ices (e.g., Morley et al. 2014; Fletcher et al. 2023), Soots/Hazes (e.g., Gao et al. 2017; Lavvas & Koskinen 2017; He et al. 2023). Species name (1), refractive index database reference (2) (Wakeford & Sing (2015) (WS15, <https://stellarplanet.org/science/condensates/>), Kitzmann & Heng (2018) (KH18, <https://github.com/NewStrangeWorlds/LX-MIE/tree/master/compilation>), Birmingham et al. (2021) (B21), Dominik et al. (2021) (optool, [https://github.com/cdominik/optool/tree/master/lnk\\_data](https://github.com/cdominik/optool/tree/master/lnk_data)), Lee et al. (2022) (gCMCRT, [https://github.com/ELeeAstro/gCMCRT/tree/main/data/nk\\_tables](https://github.com/ELeeAstro/gCMCRT/tree/main/data/nk_tables)), N/A refers to this work) where refractive index files can be found on the POSEIDON github (<https://github.com/MartianColonist/POSEIDON> under POSEIDON/reference data) or §??, refractive index reference (3), notes (common name, crystalline or amorphous, specific direction/polarization/temperature if one was used) (4). The absolute minimum and maximum wavelength of the database is 0.20 and 30  $\mu\text{m}$ . The minimum and maximum wavelengths of individual species are listed in (5), where we do not extrapolate past the bounds of the refractive index data. Note that refractive indices are interpolated between their minimum and maximum wavelength, and therefore might not be accurate where there are gaps in the refractive index data (see ‘aerosol\_database.pdf’ on Zenodo (§??) or POSEIDON’s Opacity Database to see refractive indices vs interpolated indices). Optical properties are precomputed for particle sizes 1e-3 to 10  $\mu\text{m}$ . <sup>D</sup> refers to refractive indices that can be found on the Database of Optical Constants for Cosmic Dust (DOCCD, <https://www.astro.uni-jena.de/Laboratory/OCDB/index.html>). <sup>C</sup> refers to references that compile refractive index data (sometimes to supplement their own lab data). For more information on aerosols and refractive index citations (such as synthetic vs natural samples, how lab measurements were taken, crystal shape, etc.), see the ‘Aerosol-Database-Readme.txt’ on Zenodo (§??) or POSEIDON’s documentation. We recommend that for colder ices and hydrocarbons, users should refer to the cosmic ice laboratory (<https://science.gsfc.nasa.gov/691/cosmicice/constants.html>) or the optical constants database (<https://ocdb.smce.nasa.gov/>) and add species to the precomputed database following the ‘Making an Aerosol Database’ tutorial in Forward Model Tutorials

## REFERENCES

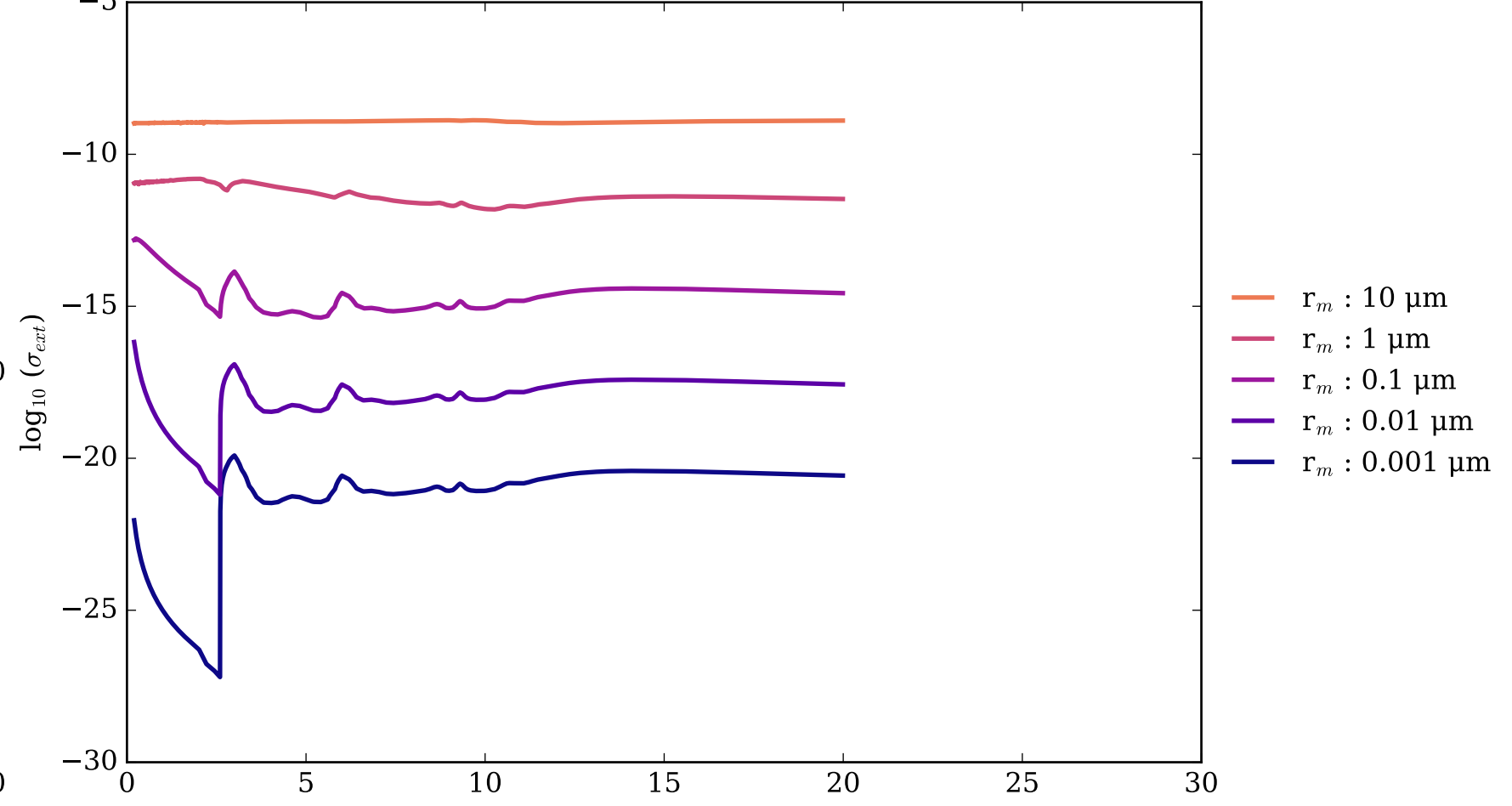
- Anderson, M. R. 2000.  
<https://api.semanticscholar.org/CorpusID:94157827>
- Begemann, B., Dorschner, J., Henning, T., et al. 1997, The Astrophysical Journal, 476, 199, doi: [10.1086/303597](https://doi.org/10.1086/303597)
- Begemann, B., Henning, T., Mutschke, H., & Dorschner, J. 1995, Planet. Space Sci., 43, 1257, doi: [10.1016/0032-0633\(95\)00001-L](https://doi.org/10.1016/0032-0633(95)00001-L)
- Bohren, C. F., & Huffman, D. R. 1983, Absorption and scattering of light by small particles
- Burningham, B., Faherty, J. K., Gonzales, E. C., et al. 2021, MNRAS, 506, 1944, doi: [10.1093/mnras/stab1361](https://doi.org/10.1093/mnras/stab1361)
- Burrows, A., & Sharp, C. M. 1999, ApJ, 512, 843, doi: [10.1086/306811](https://doi.org/10.1086/306811)
- Caras, G. J. 1965, Silicon carbide for semiconductors (Research Branch, Redstone Scientific Information Center)
- Chang, H., & Charalampopoulos, T. T. 1990, Proceedings of the Royal Society of London Series A, 430, 577, doi: [10.1098/rspa.1990.0107](https://doi.org/10.1098/rspa.1990.0107)
- Corrales, L., Gavilan, L., Teal, D. J., & Kempton, E. M. R. 2023, ApJL, 943, L26, doi: [10.3847/2041-8213/acaf86](https://doi.org/10.3847/2041-8213/acaf86)
- Day, K. L. 1981, ApJ, 246, 110, doi: [10.1086/158903](https://doi.org/10.1086/158903)
- Dominik, C., Min, M., & Tazaki, R. 2021, OpTool: Command-line driven tool for creating complex dust opacities, Astrophysics Source Code Library, record ascl:2104.010
- Dorschner, J., Begemann, B., Henning, T., Jaeger, C., & Mutschke, H. 1995, A&A, 300, 503
- Draine, B. T. 2003a, ApJ, 598, 1017, doi: [10.1086/379118](https://doi.org/10.1086/379118)
- . 2003b, ApJ, 598, 1026, doi: [10.1086/379123](https://doi.org/10.1086/379123)
- Draine, B. T., & Lee, H. M. 1984, ApJ, 285, 89, doi: [10.1086/162480](https://doi.org/10.1086/162480)
- Egan, W. G., & Hilgeman, T. 1975, AJ, 80, 587, doi: [10.1086/111782](https://doi.org/10.1086/111782)
- Fabian, D., Henning, T., Jäger, C., et al. 2001, A&A, 378, 228, doi: [10.1051/0004-6361:20011196](https://doi.org/10.1051/0004-6361:20011196)
- Fletcher, L. N., King, O. R. T., Harkett, J., et al. 2023, Journal of Geophysical Research (Planets), 128, e2023JE007924, doi: [10.1029/2023JE007924](https://doi.org/10.1029/2023JE007924)
- Gao, P., Marley, M. S., Zahnle, K., Robinson, T. D., & Lewis, N. K. 2017, AJ, 153, 139, doi: [10.3847/1538-3881/aa5fab](https://doi.org/10.3847/1538-3881/aa5fab)
- Hale, G. M., & Querry, M. R. 1973, ApOpt, 12, 555, doi: [10.1364/AO.12.000555](https://doi.org/10.1364/AO.12.000555)
- He, C., Radke, M., Moran, S. E., et al. 2023, Nature Astronomy, doi: [10.1038/s41550-023-02140-4](https://doi.org/10.1038/s41550-023-02140-4)
- Henning, T., & Mutschke, H. 1997, A&A, 327, 743
- . 2001, Spectrochimica Acta Part A: Molecular Spectroscopy, 57, 815, doi: [10.1016/S1386-1425\(00\)00446-7](https://doi.org/10.1016/S1386-1425(00)00446-7)
- Henning, T., Mutschke, H., & Jäger, C. 2005, Proceedings of the International Astronomical Union, 1, 457–468, doi: [10.1017/S1743921306007472](https://doi.org/10.1017/S1743921306007472)
- Hervé Herbin, Lise Deschutter, A. D., & Petitprez, D. 2023, Aerosol Science and Technology, 57, 255, doi: [10.1080/02786826.2023.2165899](https://doi.org/10.1080/02786826.2023.2165899)
- Howett, C. J. A., Carlson, R. W., Irwin, P. G. J., & Calcutt, S. B. 2007, Journal of the Optical Society of America B Optical Physics, 24, 126, doi: [10.1364/JOSAB.24.000126](https://doi.org/10.1364/JOSAB.24.000126)
- Huffman, D. R., & Wild, R. L. 1967, Phys. Rev., 156, 989, doi: [10.1103/PhysRev.156.989](https://doi.org/10.1103/PhysRev.156.989)
- Jaeger, C., Molster, F. J., Dorschner, J., et al. 1998, A&A, 339, 904
- Jäger, C., Dorschner, J., Mutschke, H., Posch, T., & Henning, T. 2003, A&A, 408, 193, doi: [10.1051/0004-6361:20030916](https://doi.org/10.1051/0004-6361:20030916)
- Khachai, H., Khenata, R., Bouhemadou, A., et al. 2009, Journal of Physics Condensed Matter, 21, 095404, doi: [10.1088/0953-8984/21/9/095404](https://doi.org/10.1088/0953-8984/21/9/095404)
- Khare, B. N., Sagan, C., Arakawa, E. T., et al. 1984, Icarus, 60, 127, doi: [10.1016/0019-1035\(84\)90142-8](https://doi.org/10.1016/0019-1035(84)90142-8)
- Khare, B. N., Thompson, W. R., Cheng, L., et al. 1993, Icarus, 103, 290, doi: [10.1006/icar.1993.1071](https://doi.org/10.1006/icar.1993.1071)
- Kitzmann, D., & Heng, K. 2018, MNRAS, 475, 94, doi: [10.1093/mnras/stx3141](https://doi.org/10.1093/mnras/stx3141)
- Koide, T., Shidara, T., Fukutani, H., et al. 1990, Phys. Rev. B, 42, 4979, doi: [10.1103/PhysRevB.42.4979](https://doi.org/10.1103/PhysRevB.42.4979)
- Koike, C., Kaito, C., Yamamoto, T., et al. 1995, Icarus, 114, 203, doi: <https://doi.org/10.1006/icar.1995.1055>
- Laor, A., & Draine, B. T. 1993, ApJ, 402, 441, doi: [10.1086/172149](https://doi.org/10.1086/172149)
- Lavvas, P., & Koskinen, T. 2017, arXiv e-prints, arXiv:1708.09257, doi: [10.48550/arXiv.1708.09257](https://doi.org/10.48550/arXiv.1708.09257)
- Lee, E., Dobbs-Dixon, I., Helling, C., Bognar, K., & Woitke, P. 2016, A&A, 594, A48, doi: [10.1051/0004-6361/201628606](https://doi.org/10.1051/0004-6361/201628606)
- Lee, E. K. H., Wardenier, J. P., Prinoth, B., et al. 2022, ApJ, 929, 180, doi: [10.3847/1538-4357/ac61d6](https://doi.org/10.3847/1538-4357/ac61d6)
- Lodders, K. 2002, ApJ, 577, 974, doi: [10.1086/342241](https://doi.org/10.1086/342241)
- Martonchik, J. V., & Orton, G. S. 1994, Appl. Opt., 33, 8306, doi: [10.1364/AO.33.008306](https://doi.org/10.1364/AO.33.008306)
- Martonchik, J. V., Orton, G. S., & Appleby, J. F. 1984, ApOpt, 23, 541, doi: [10.1364/AO.23.000541](https://doi.org/10.1364/AO.23.000541)
- Montaner, A., Galtier, M., Benoit, C., & Bill, H. 1979, Physica Status Solidi Applied Research, 52, 597, doi: [10.1002/pssa.2210520228](https://doi.org/10.1002/pssa.2210520228)

- Morley, C. V., Fortney, J. J., Marley, M. S., et al. 2012, ApJ, 756, 172, doi: [10.1088/0004-637X/756/2/172](https://doi.org/10.1088/0004-637X/756/2/172)
- Morley, C. V., Marley, M. S., Fortney, J. J., et al. 2014, ApJ, 787, 78, doi: [10.1088/0004-637X/787/1/78](https://doi.org/10.1088/0004-637X/787/1/78)
- Mutschke, H., Andersen, A. C., Jäger, C., Henning, T., & Braatz, A. 2004, A&A, 423, 983, doi: [10.1051/0004-6361:20034544](https://doi.org/10.1051/0004-6361:20034544)
- Mutschke, H., Posch, T., Fabian, D., & Dorschner, J. 2002, A&A, 392, 1047, doi: [10.1051/0004-6361:20021072](https://doi.org/10.1051/0004-6361:20021072)
- Nitsan, U., & Shankland, T. J. 1976, Geophysical Journal, 45, 59, doi: [10.1111/j.1365-246X.1976.tb00313.x](https://doi.org/10.1111/j.1365-246X.1976.tb00313.x)
- Noy, N., Podolak, M., & Bar-Nun, A. 1981, Journal of Geophysical Research, 86, 11985, doi: [10.1029/JC086iC12p11985](https://doi.org/10.1029/JC086iC12p11985)
- Palik, E. 1998, Handbook of Optical Constants of Solids III, Academic Press handbook series No. v. 3 (Elsevier Science).  
<https://books.google.com/books?id=nxoqxyoHfbIC>
- Palik, E. D. 1985, in Handbook of Optical Constants of Solids Volume 1, ed. E. D. Palik (Academic Press)
- . 1991, Handbook of optical constants of solids II (Academic Press)
- Palmer, K. F., & Williams, D. 1975, ApOpt, 14, 208, doi: [10.1364/AO.14.000208](https://doi.org/10.1364/AO.14.000208)
- Pollack, J. B., Hollenbach, D., Beckwith, S., et al. 1994, ApJ, 421, 615, doi: [10.1086/173677](https://doi.org/10.1086/173677)
- Posch, T., Kerschbaum, F., Fabian, D., et al. 2003, ApJS, 149, 437, doi: [10.1086/379167](https://doi.org/10.1086/379167)
- Querry, M., Chemical Research, D. . E. C. U., United States. Army Armament, M., Command, C., & Service, U. S. N. T. I. 1987, Optical Constants of Minerals and Other Materials from the Millimeter to the Ultraviolet, CRDC-CR (Chemical Research, Development & Engineering Center, US Army Armament, Munitions, Chemical Command).  
<https://books.google.com/books?id=FVeENwAACAAJ>
- Querry, M. R., Waring, R. C., Holland, W. E., et al. 1974, J. Opt. Soc. Am., 64, 39, doi: [10.1364/JOSA.64.000039](https://doi.org/10.1364/JOSA.64.000039)
- Rakić, A. D., Djurišić, A. B., Elazar, J. M., & Majewski, M. L. 1998, Applied optics, 37 22, 5271.  
<https://api.semanticscholar.org/CorpusID:4825387>
- Ramirez, S. I., Coll, P., da Silva, A., et al. 2002, Icarus, 156, 515, doi: [10.1006/icar.2001.6783](https://doi.org/10.1006/icar.2001.6783)
- Scott, A., & Duley, W. W. 1996, ApJS, 105, 401, doi: [10.1086/192321](https://doi.org/10.1086/192321)
- Siefke, T., Kroker, S., Pfeiffer, K., et al. 2016, arXiv e-prints, arXiv:1607.04866, doi: [10.48550/arXiv.1607.04866](https://doi.org/10.48550/arXiv.1607.04866)
- Sromovsky, L. A., Baines, K. H., & Fry, P. M. 2020, Icarus, 344, 113398, doi: [10.1016/j.icarus.2019.113398](https://doi.org/10.1016/j.icarus.2019.113398)
- Sudarsky, D., Burrows, A., & Hubeny, I. 2003, ApJ, 588, 1121, doi: [10.1086/374331](https://doi.org/10.1086/374331)
- Suto, H., Sogawa, H., Tachibana, S., et al. 2006, MNRAS, 370, 1599, doi: [10.1111/j.1365-2966.2006.10594.x](https://doi.org/10.1111/j.1365-2966.2006.10594.x)
- Triaud, A. H. 2005, Database of Optical Constants for Cosmic Dust, unpublished
- Ueda, K., Yanagi, H., Noshiro, R., Hosono, H., & Kawazoe, H. 1998, Journal of Physics Condensed Matter, 10, 3669, doi: [10.1088/0953-8984/10/16/018](https://doi.org/10.1088/0953-8984/10/16/018)
- Visscher, C., Lodders, K., & Fegley, Bruce, J. 2010, ApJ, 716, 1060, doi: [10.1088/0004-637X/716/2/1060](https://doi.org/10.1088/0004-637X/716/2/1060)
- Wakeford, H. R., & Sing, D. K. 2015, A&A, 573, A122, doi: [10.1051/0004-6361/201424207](https://doi.org/10.1051/0004-6361/201424207)
- Wakeford, H. R., Visscher, C., Lewis, N. K., et al. 2017, MNRAS, 464, 4247, doi: [10.1093/mnras/stw2639](https://doi.org/10.1093/mnras/stw2639)
- Wan, C., Zhang, Z., Woolf, D., et al. 2019, Annalen der Physik, 531, 1900188, doi: [10.1002/andp.201900188](https://doi.org/10.1002/andp.201900188)
- Warren, S. G. 1984, ApOpt, 23, 1206, doi: [10.1364/AO.23.001206](https://doi.org/10.1364/AO.23.001206)
- Wetzel, S., Klevenz, M., Gail, H. P., Pucci, A., & Trieloff, M. 2013, A&A, 553, A92, doi: [10.1051/0004-6361/201220803](https://doi.org/10.1051/0004-6361/201220803)
- Zeidler, S., Posch, T., & Mutschke, H. 2013, A&A, 553, A81, doi: [10.1051/0004-6361/201220459](https://doi.org/10.1051/0004-6361/201220459)
- Zeidler, S., Posch, T., Mutschke, H., Richter, H., & Wehrhan, O. 2011, A&A, 526, A68, doi: [10.1051/0004-6361/201015219](https://doi.org/10.1051/0004-6361/201015219)
- Zernike, Frits, J. 1965, Journal of the Optical Society of America (1917-1983), 55, 210.2

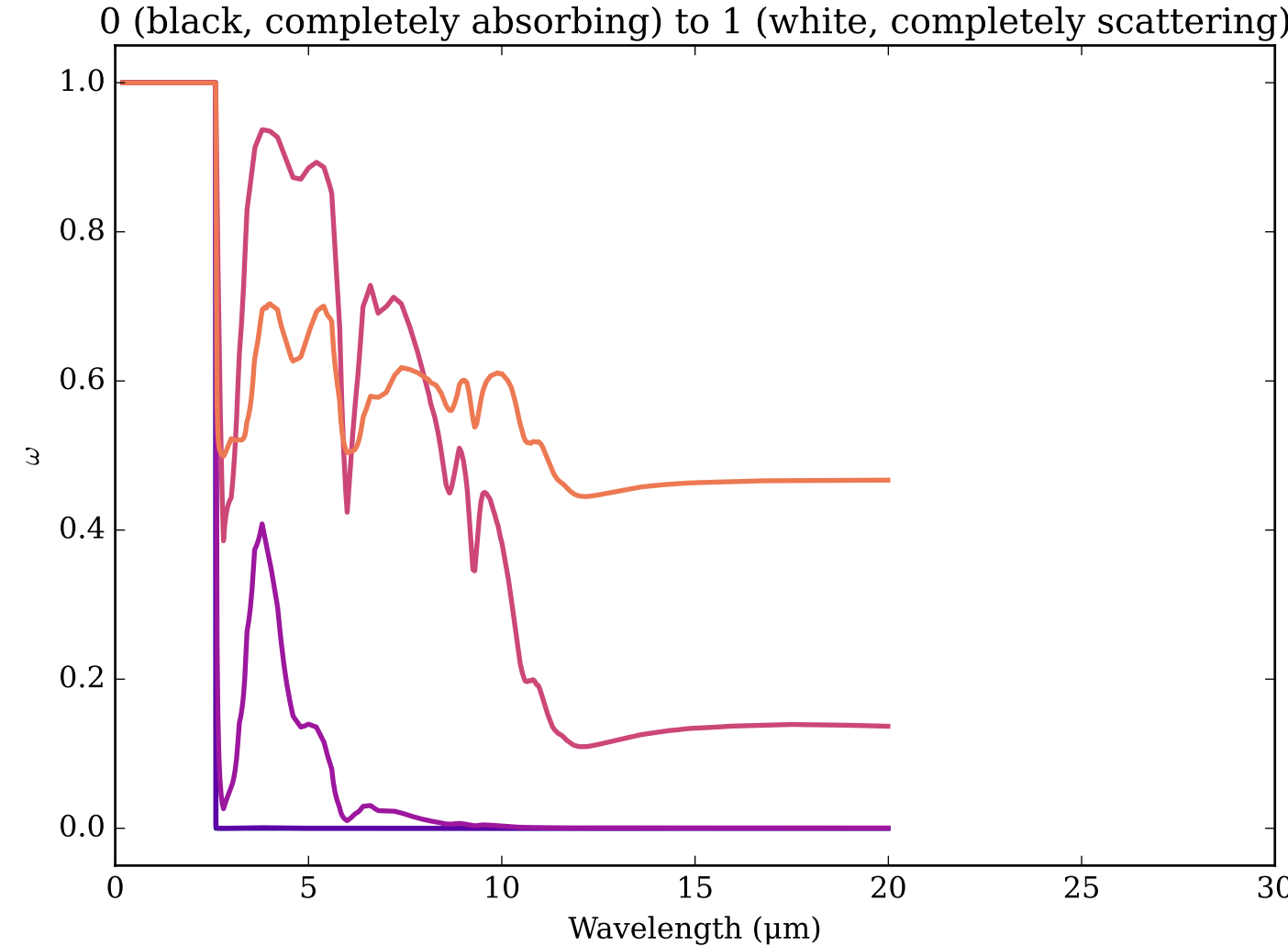
Refractive Indices for ADP  
(0.2, 19.99)  $\mu\text{m}$



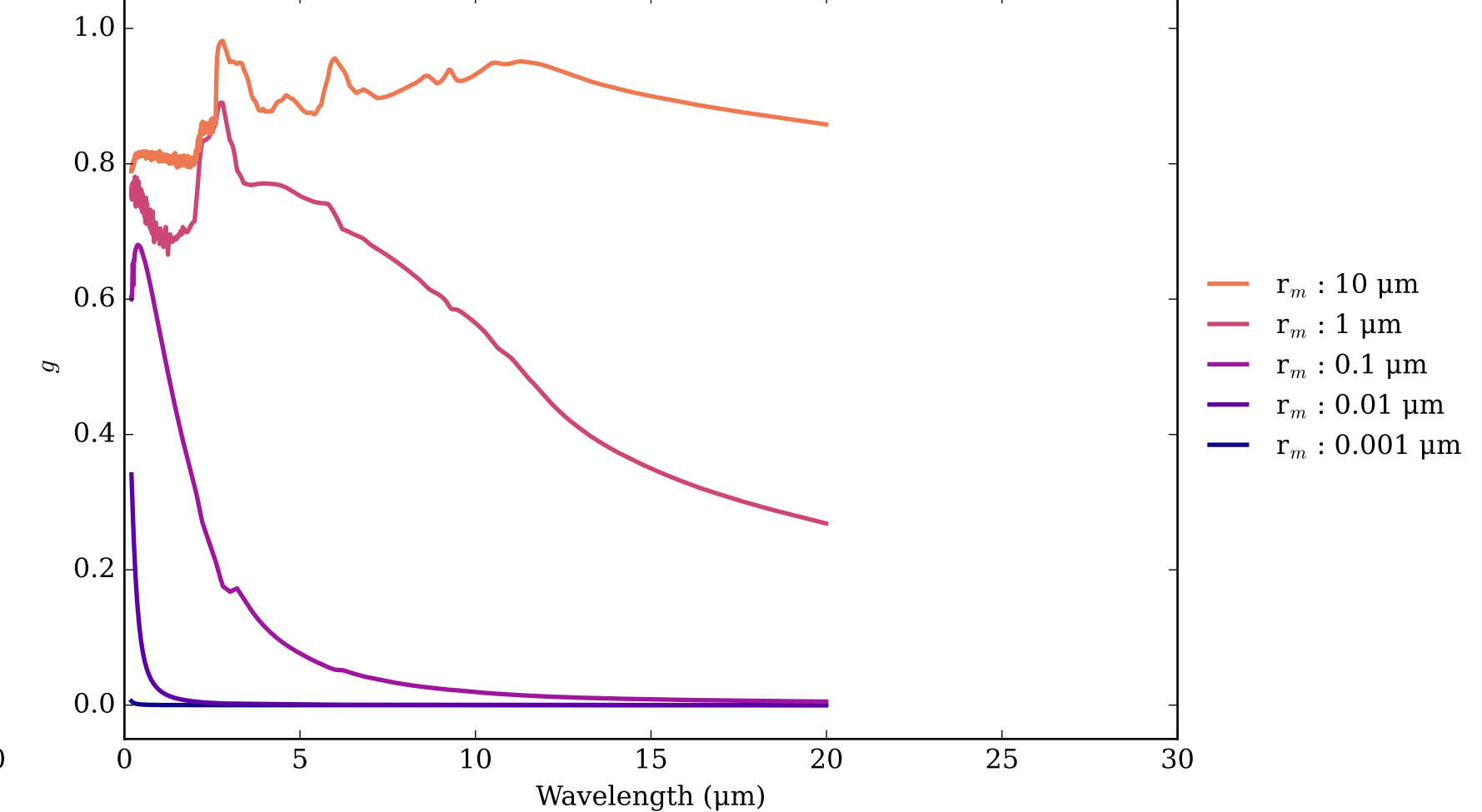
ADP Effective Extinction Cross Section  
 $\sigma_{\text{ext, eff}} = \sigma_{\text{abs, eff}} + \sigma_{\text{scat, eff}}$



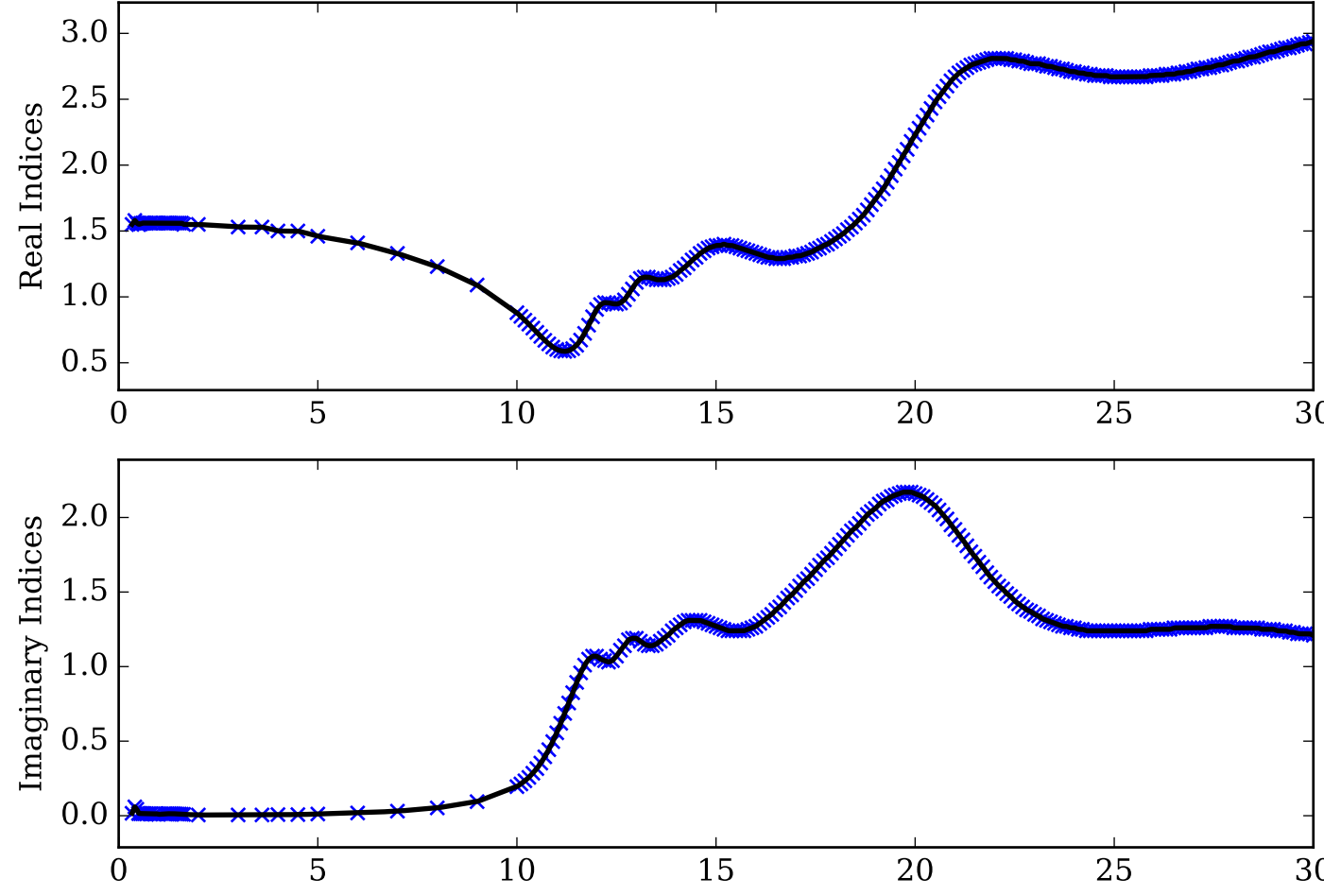
ADP Single Scattering Albedos  $\omega$



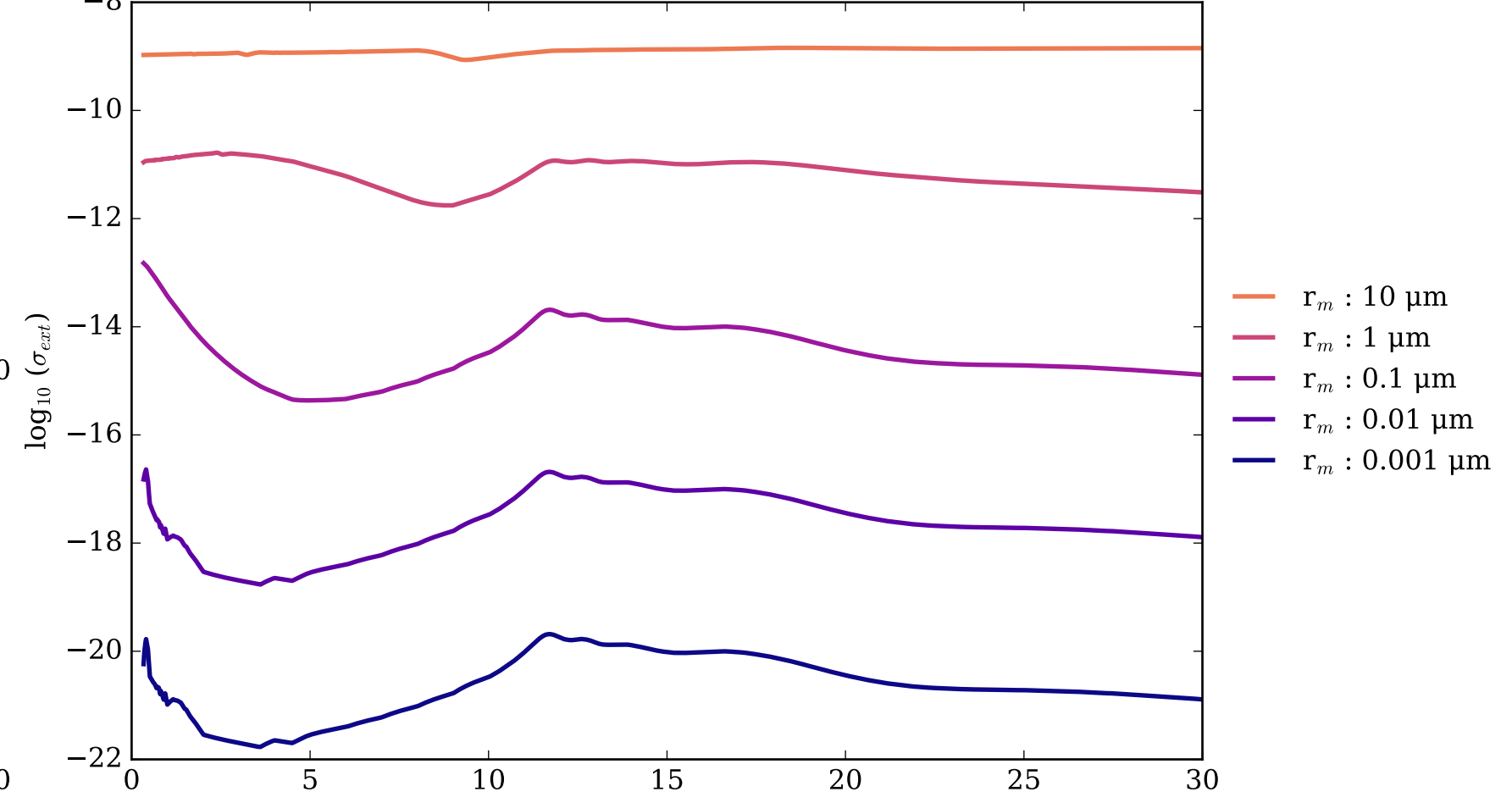
ADP Asymmetry Parameter  $g$   
0 (Rayleigh Limit) to 1 (Total Forward Scattering)



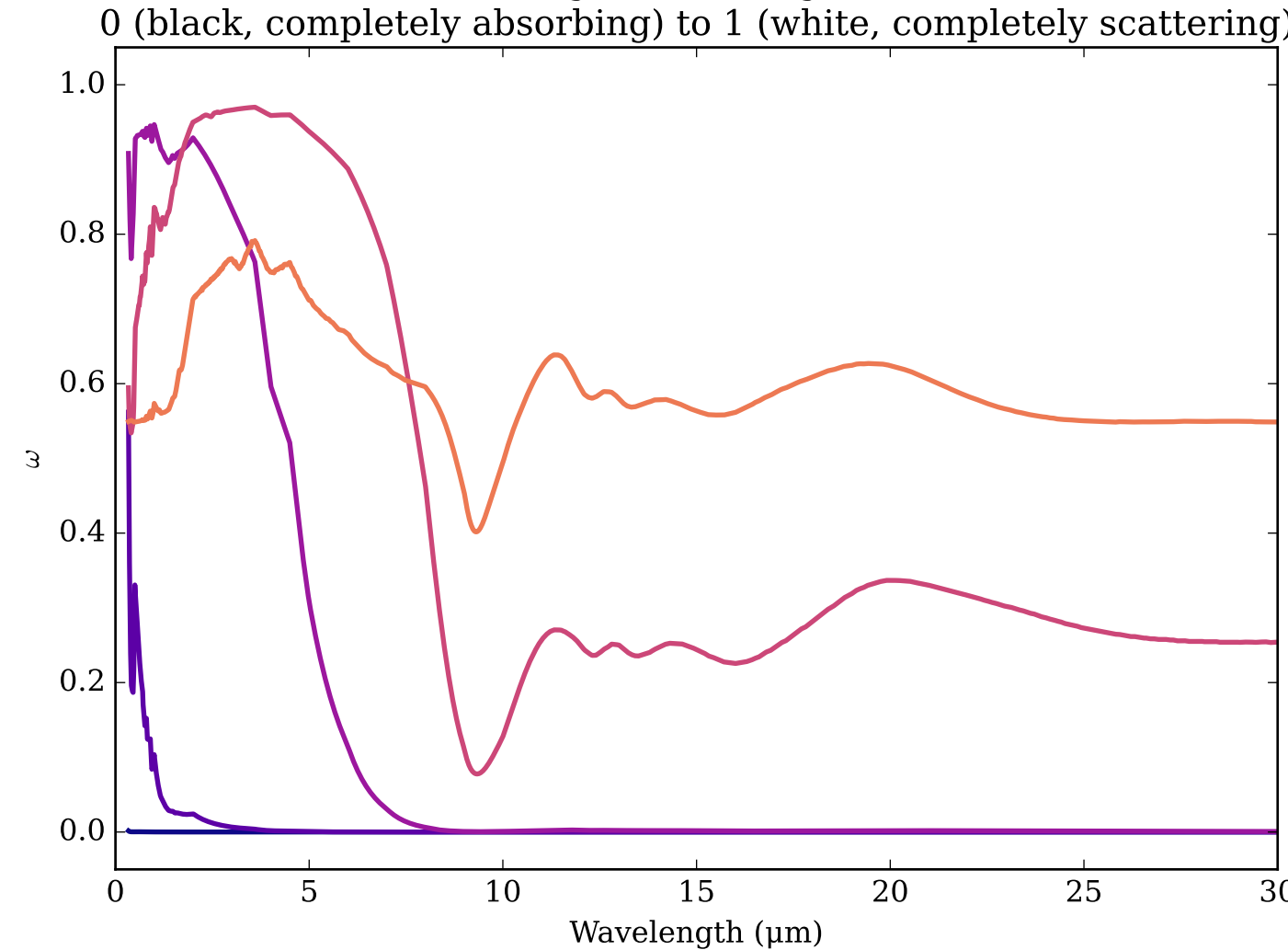
Refractive Indices for Al<sub>2</sub>O<sub>3</sub>  
(0.34, 30.0)  $\mu\text{m}$



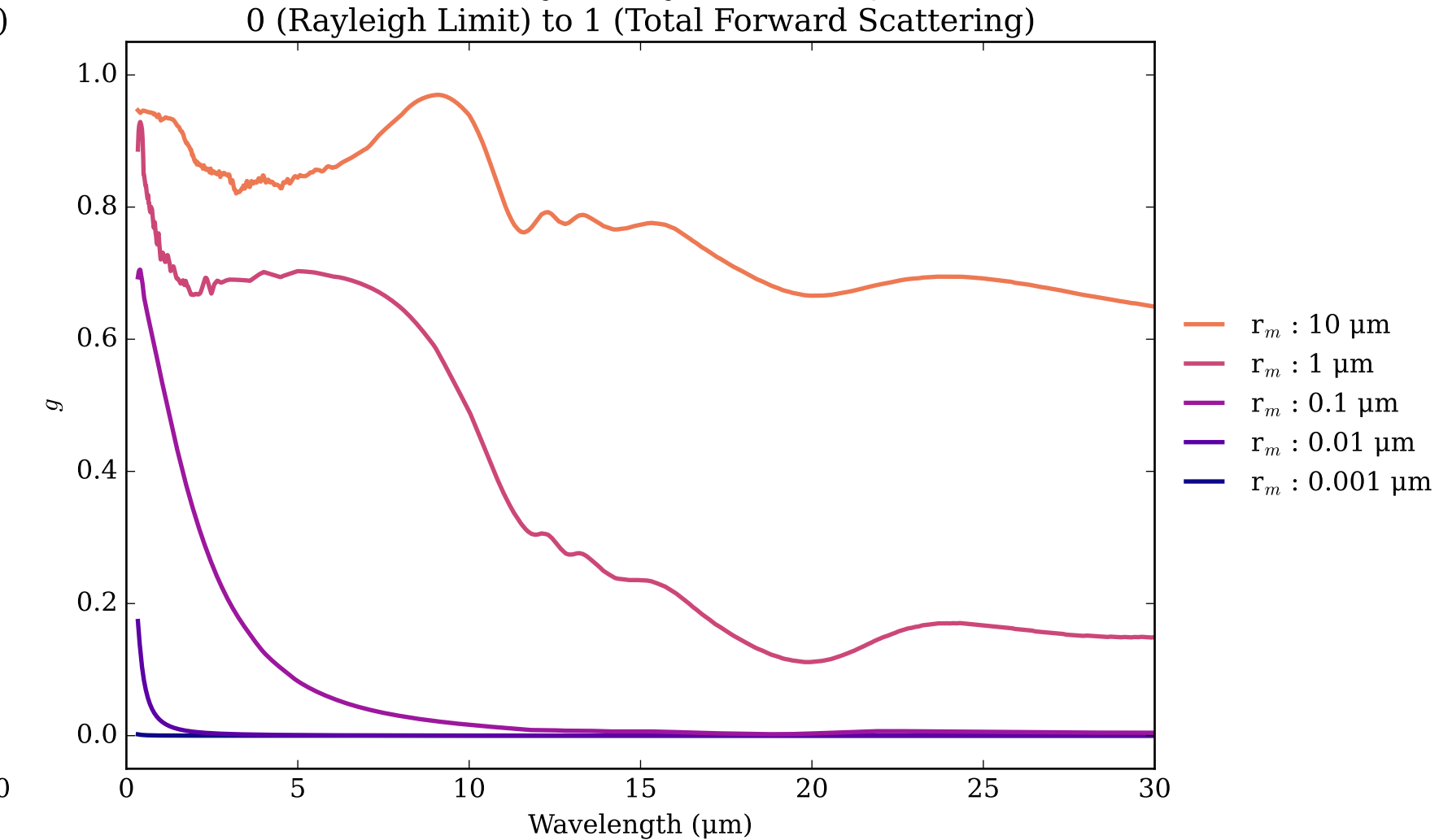
Al<sub>2</sub>O<sub>3</sub> Effective Extinction Cross Section  
 $\sigma_{\text{ext, eff}} = \sigma_{\text{abs, eff}} + \sigma_{\text{scat, eff}}$



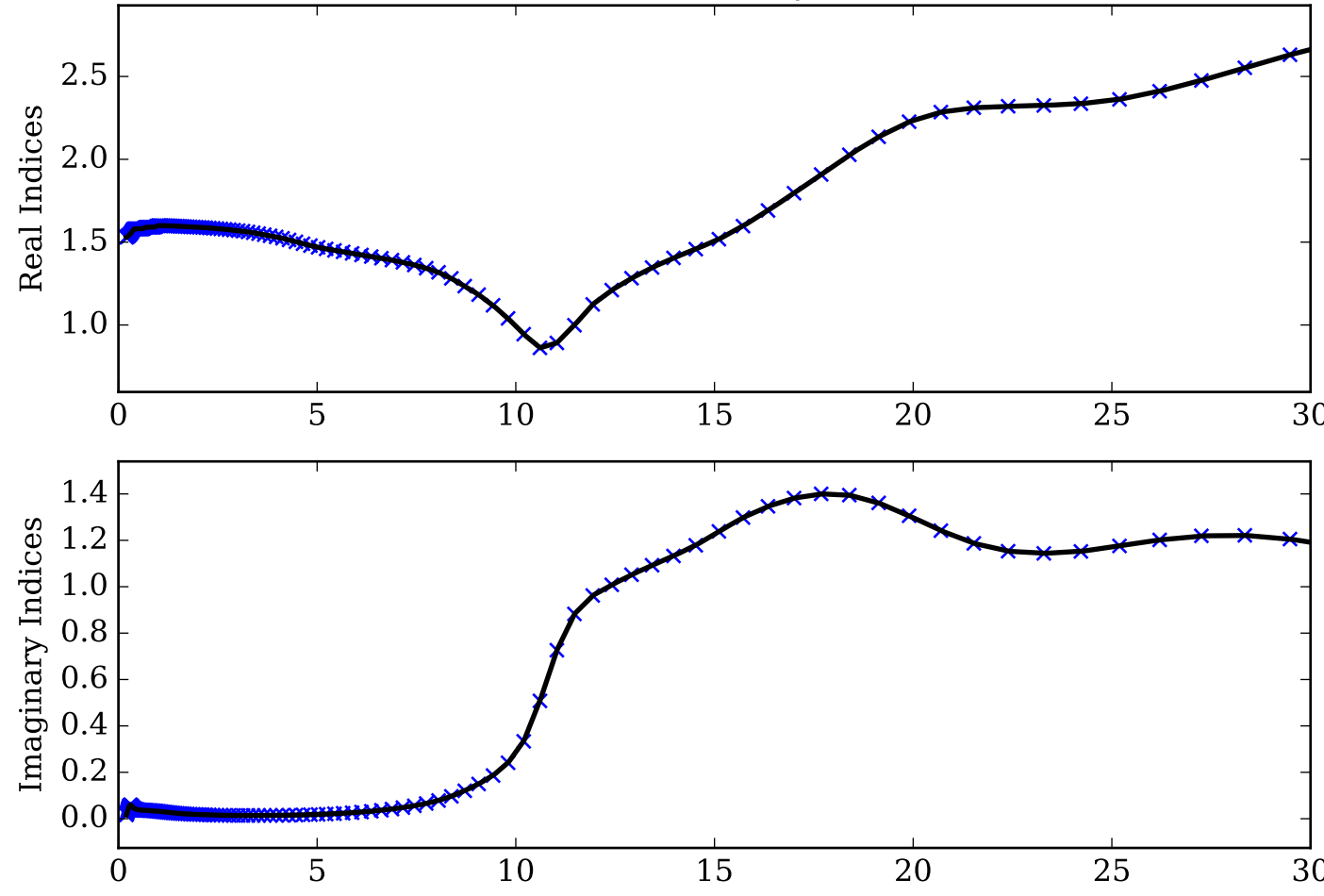
Al<sub>2</sub>O<sub>3</sub> Single Scattering Albedos  $\omega$



Al<sub>2</sub>O<sub>3</sub> Asymmetry Parameter  $g$

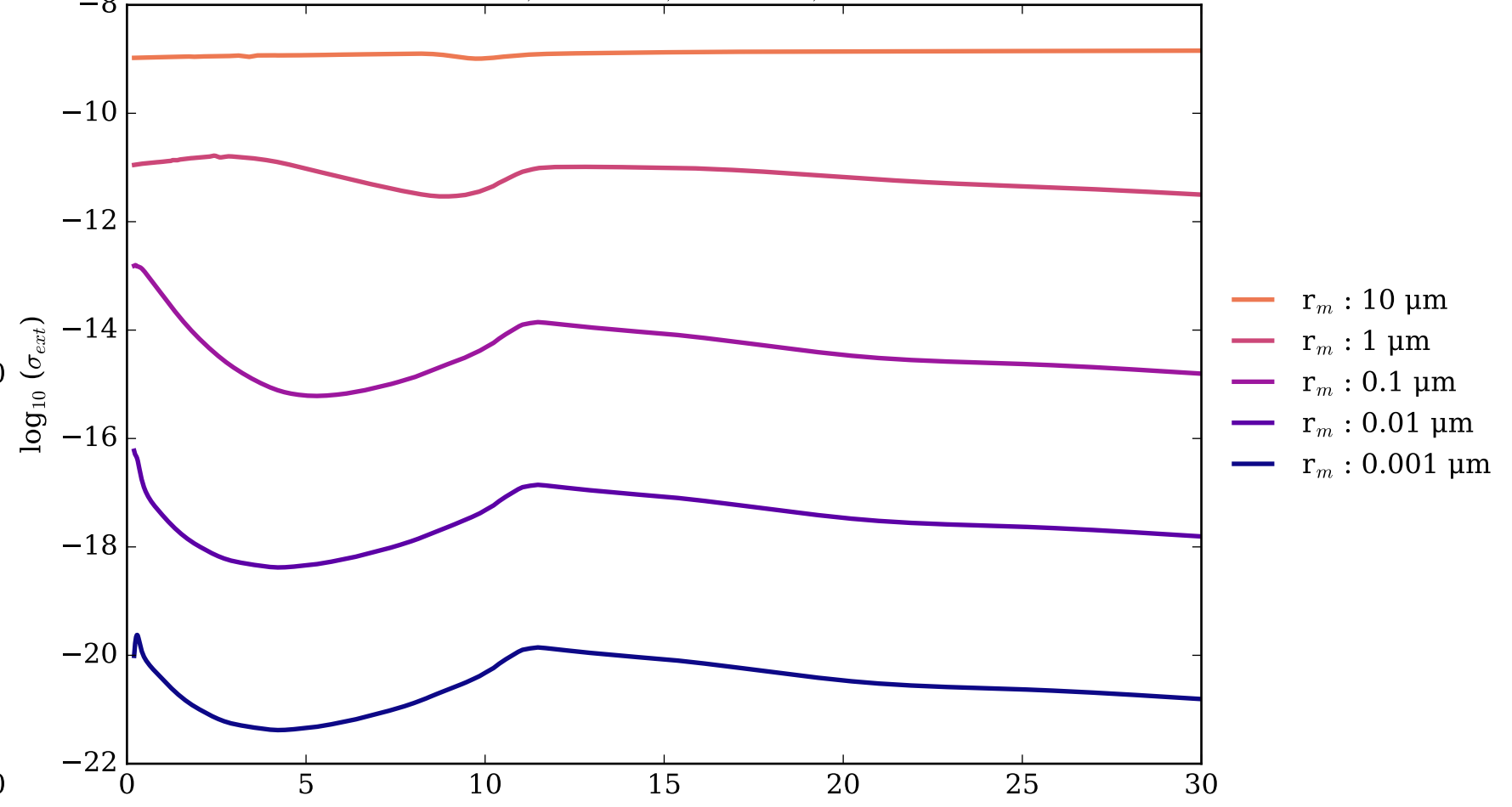


Refractive Indices for Al<sub>2</sub>O<sub>3</sub>  
(0.2, 30.0)  $\mu\text{m}$

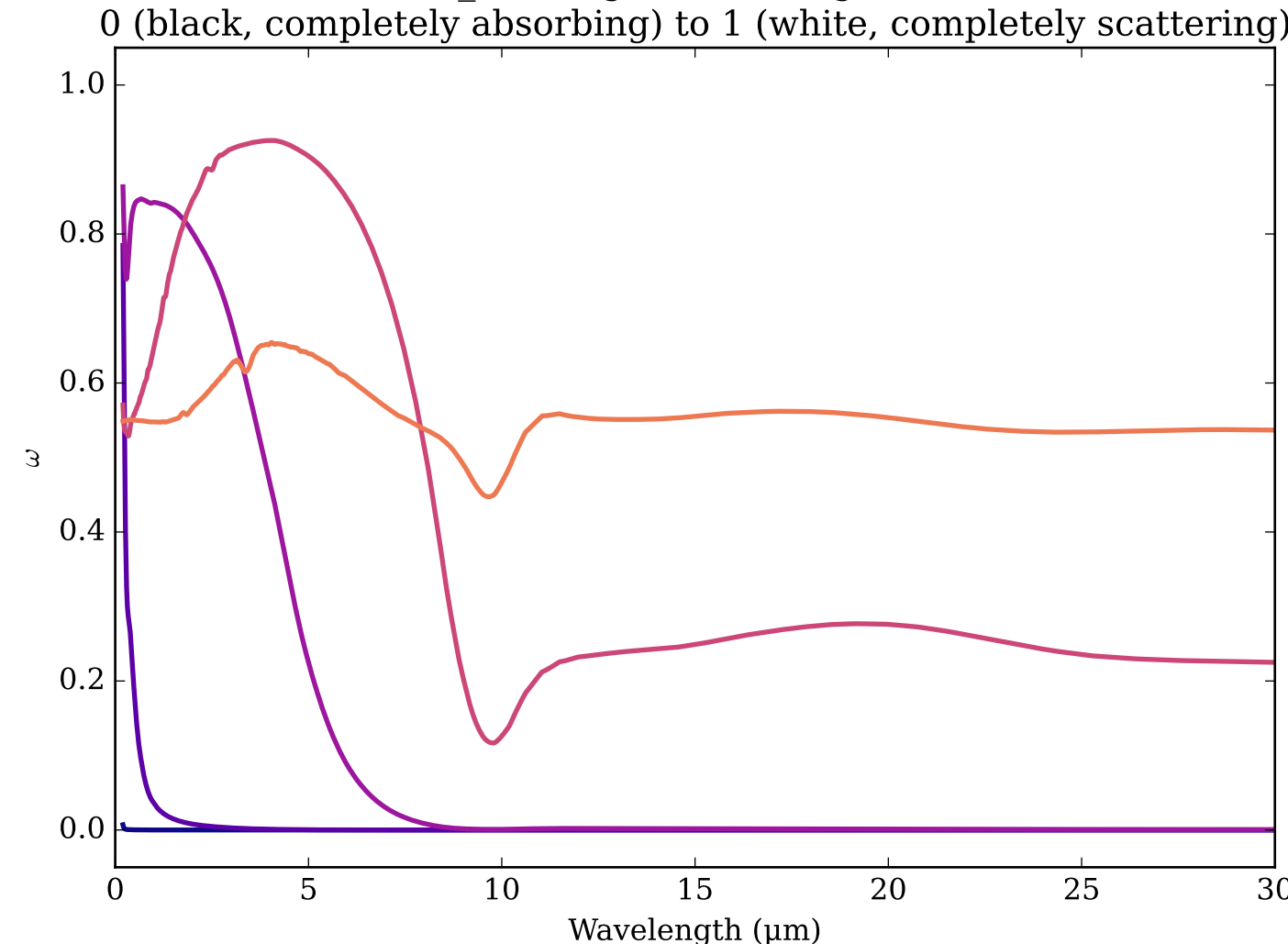


Al<sub>2</sub>O<sub>3</sub>\_KH Effective Extinction Cross Section

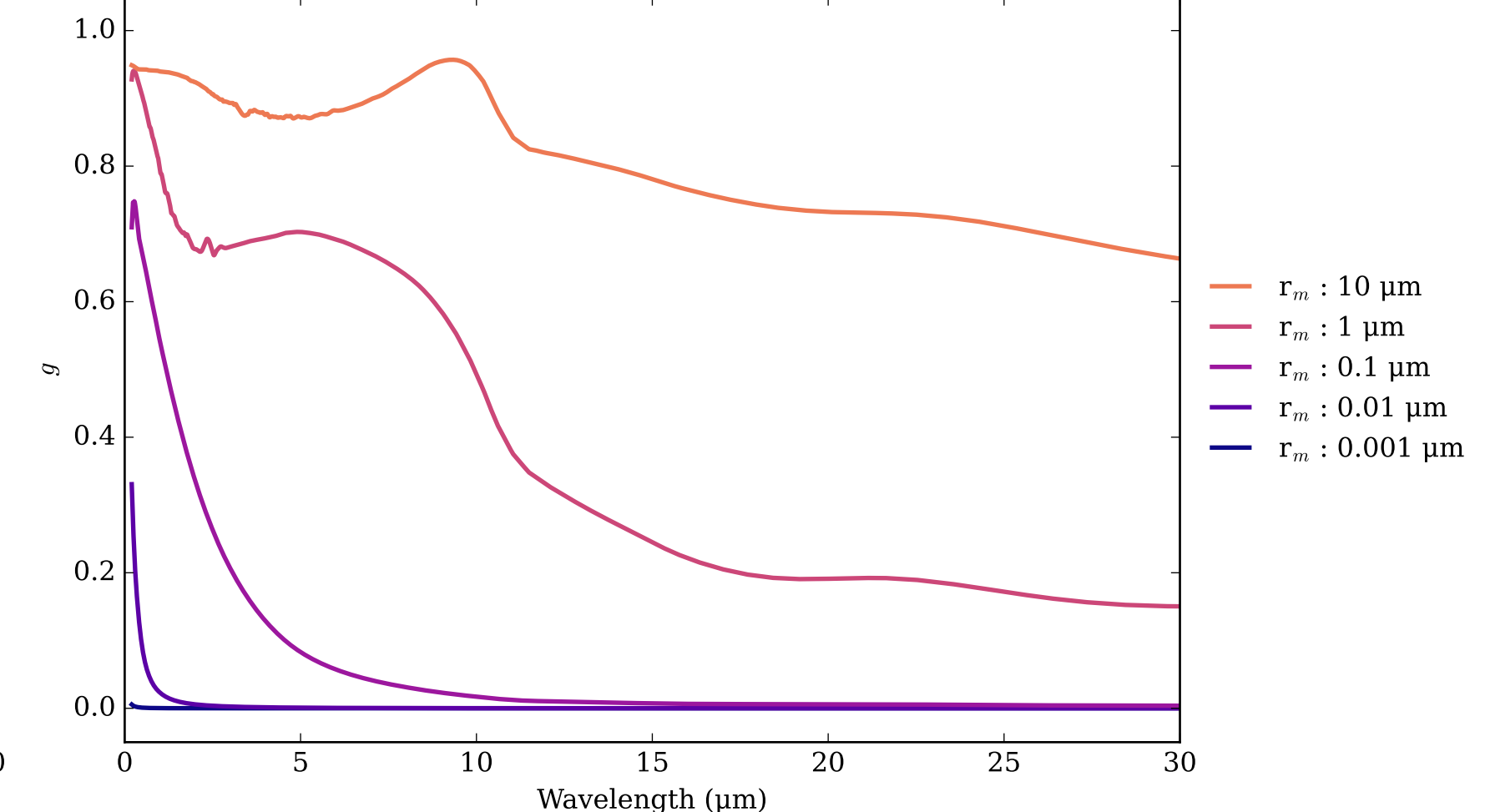
$$\sigma_{\text{ext, eff}} = \sigma_{\text{abs, eff}} + \sigma_{\text{scat, eff}}$$



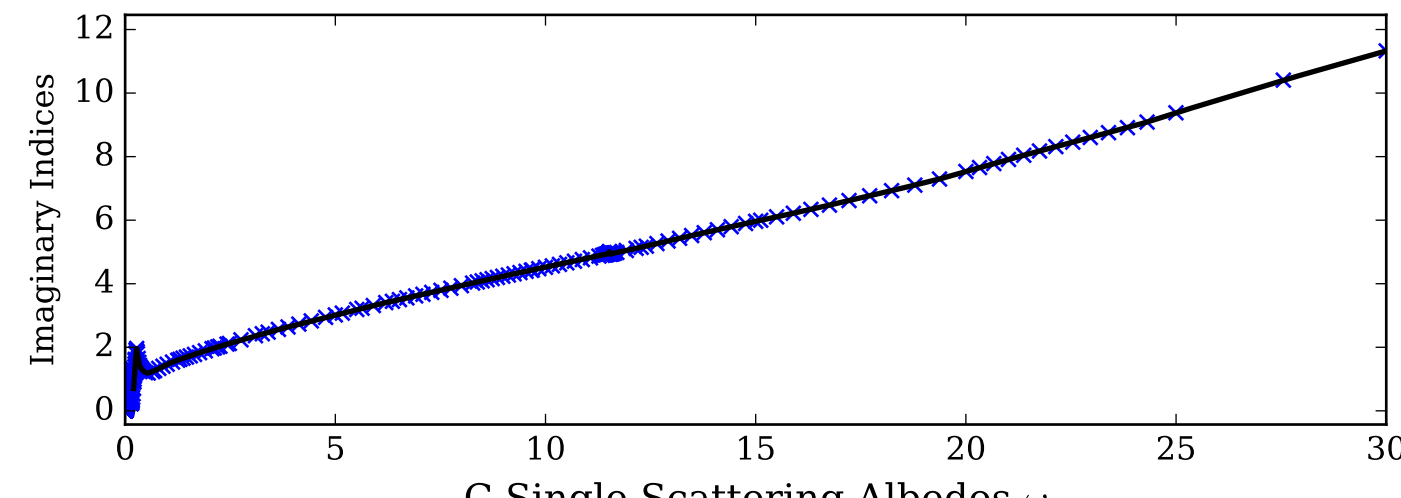
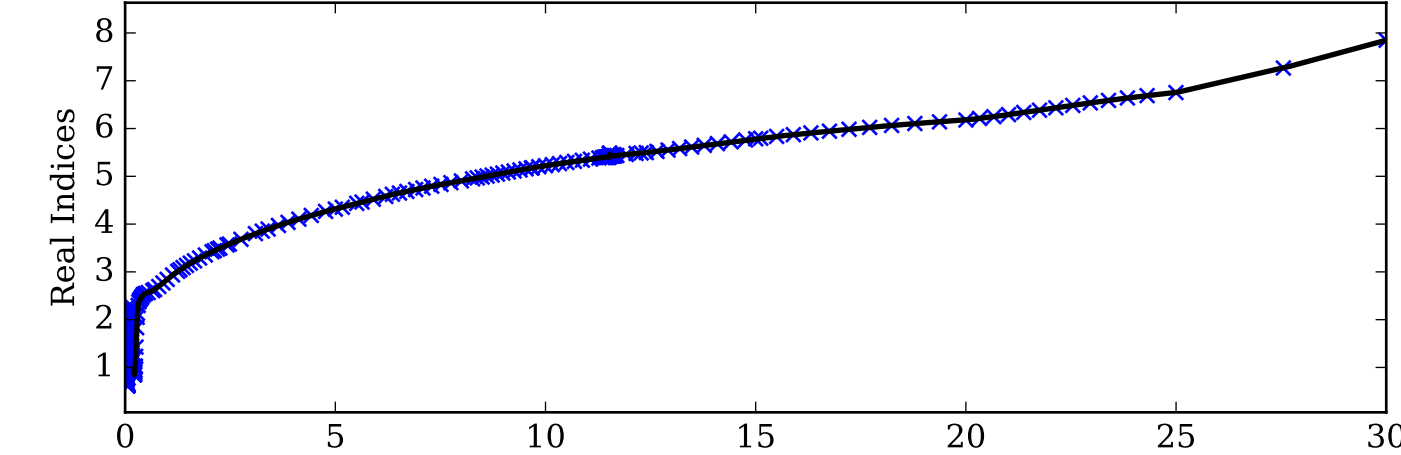
Al<sub>2</sub>O<sub>3</sub>\_KH Single Scattering Albedos  $\omega$



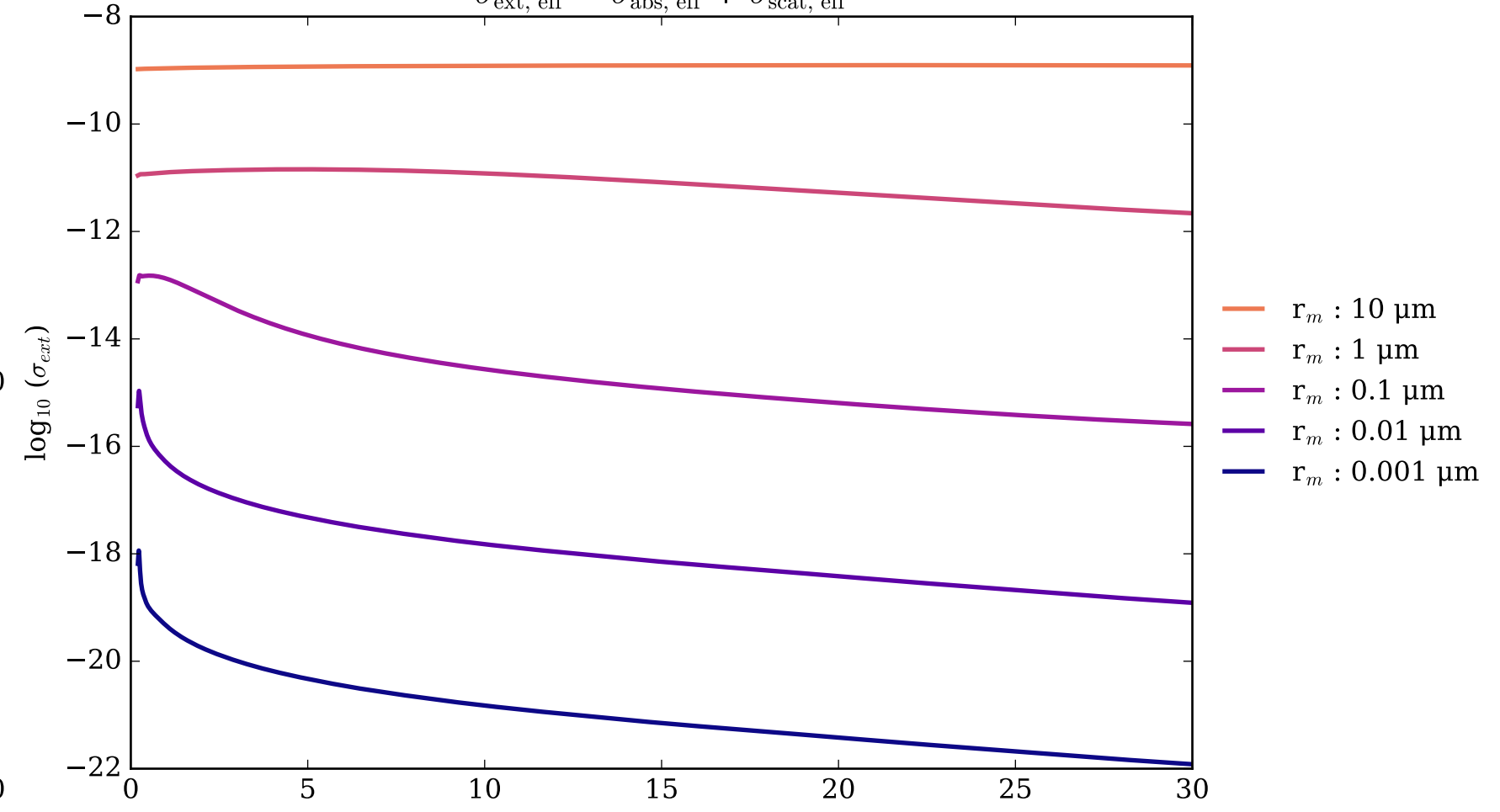
Al<sub>2</sub>O<sub>3</sub>\_KH Asymmetry Parameter  $g$   
0 (Rayleigh Limit) to 1 (Total Forward Scattering)



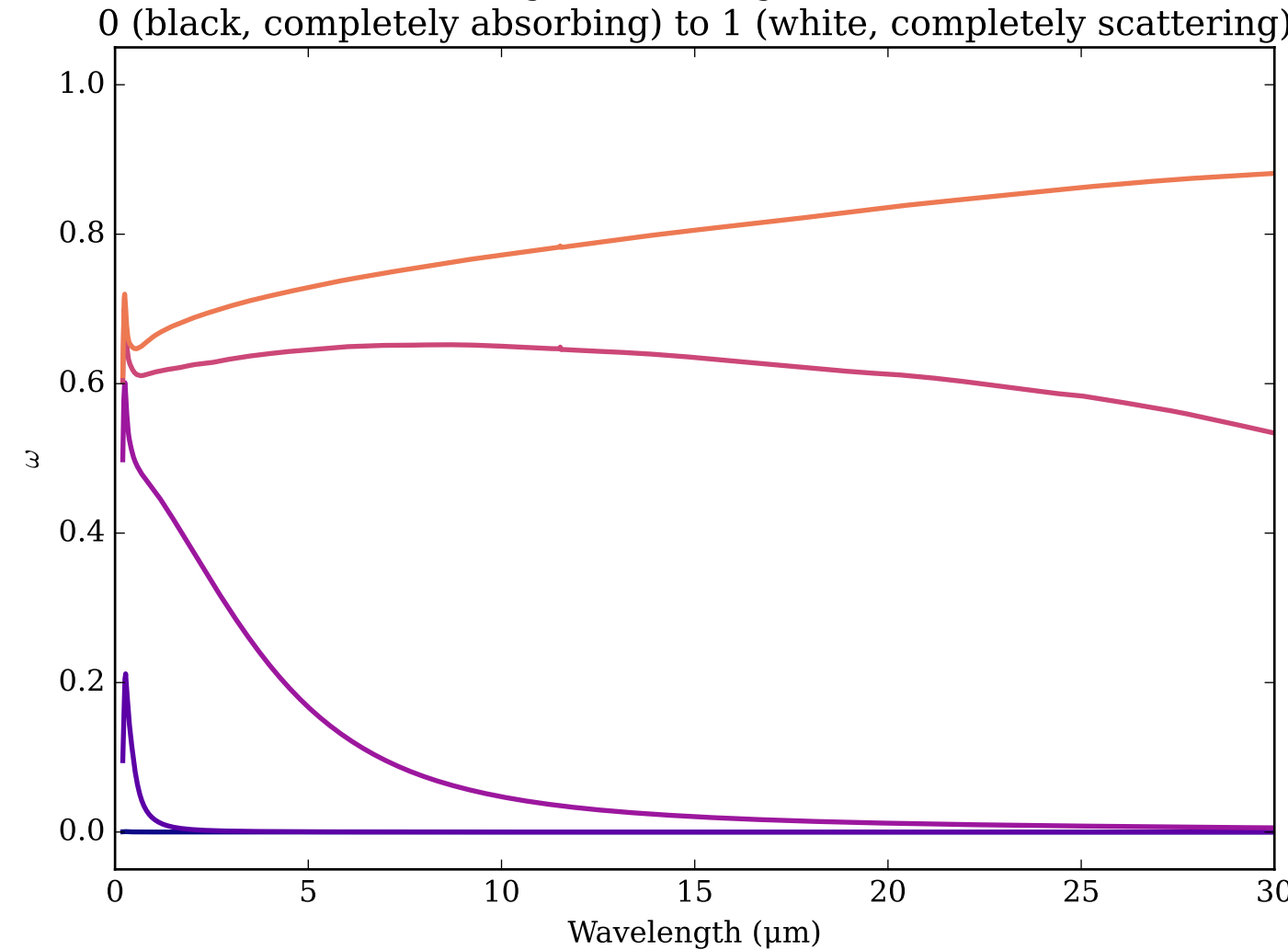
Refractive Indices for C  
(0.2, 30.0)  $\mu\text{m}$



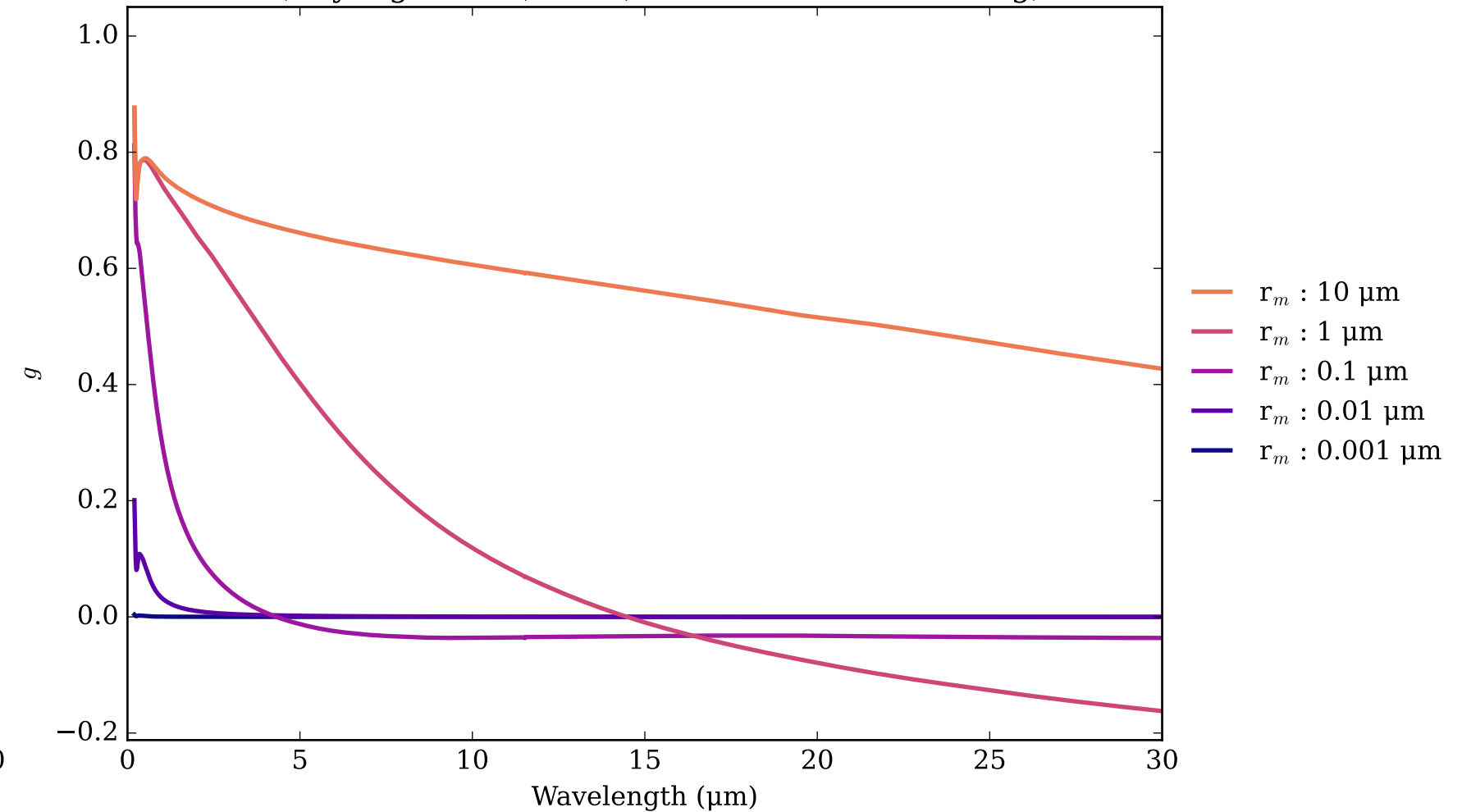
C Effective Extinction Cross Section  
 $\sigma_{\text{ext, eff}} = \sigma_{\text{abs, eff}} + \sigma_{\text{scat, eff}}$



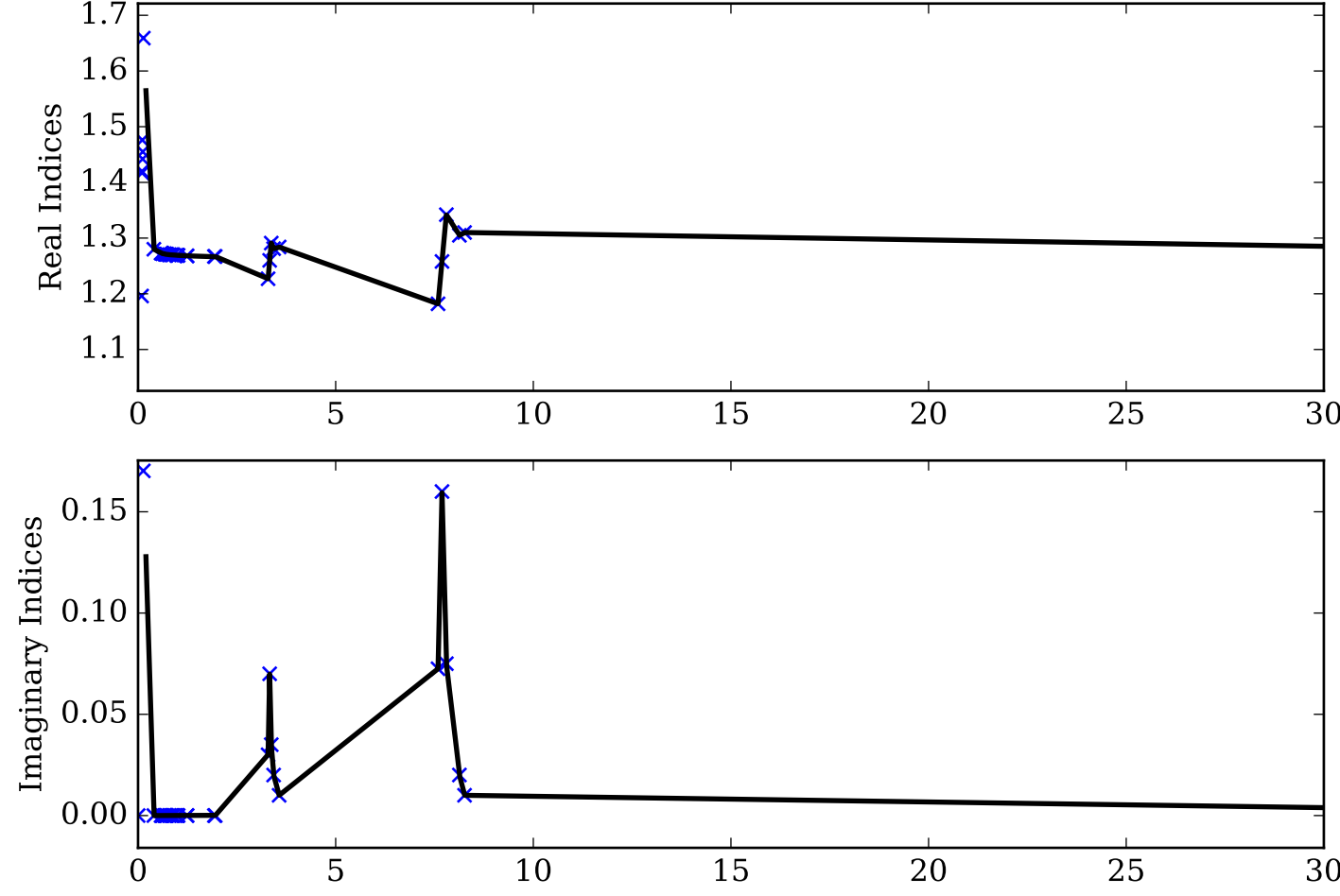
C Single Scattering Albedos  $\omega$



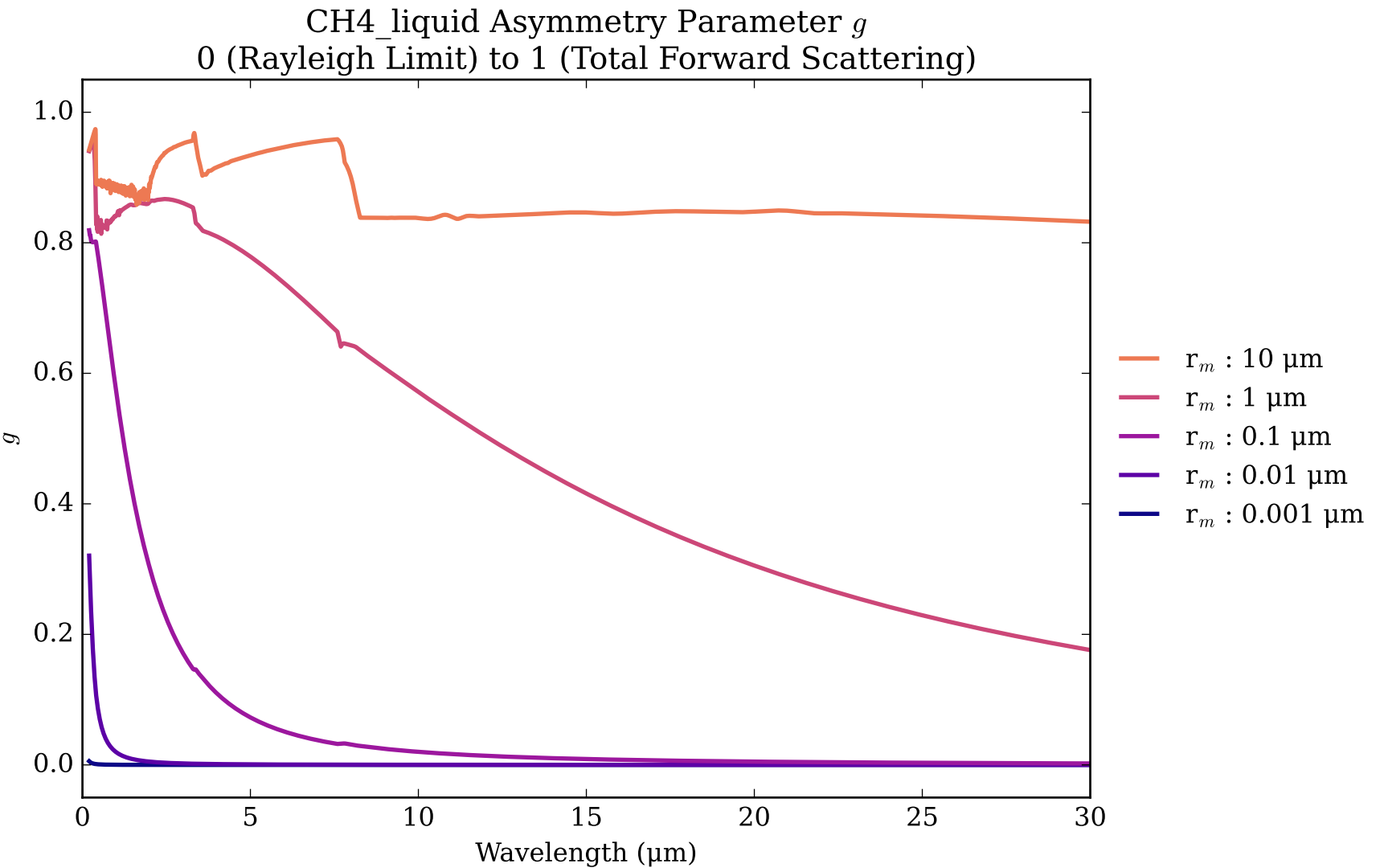
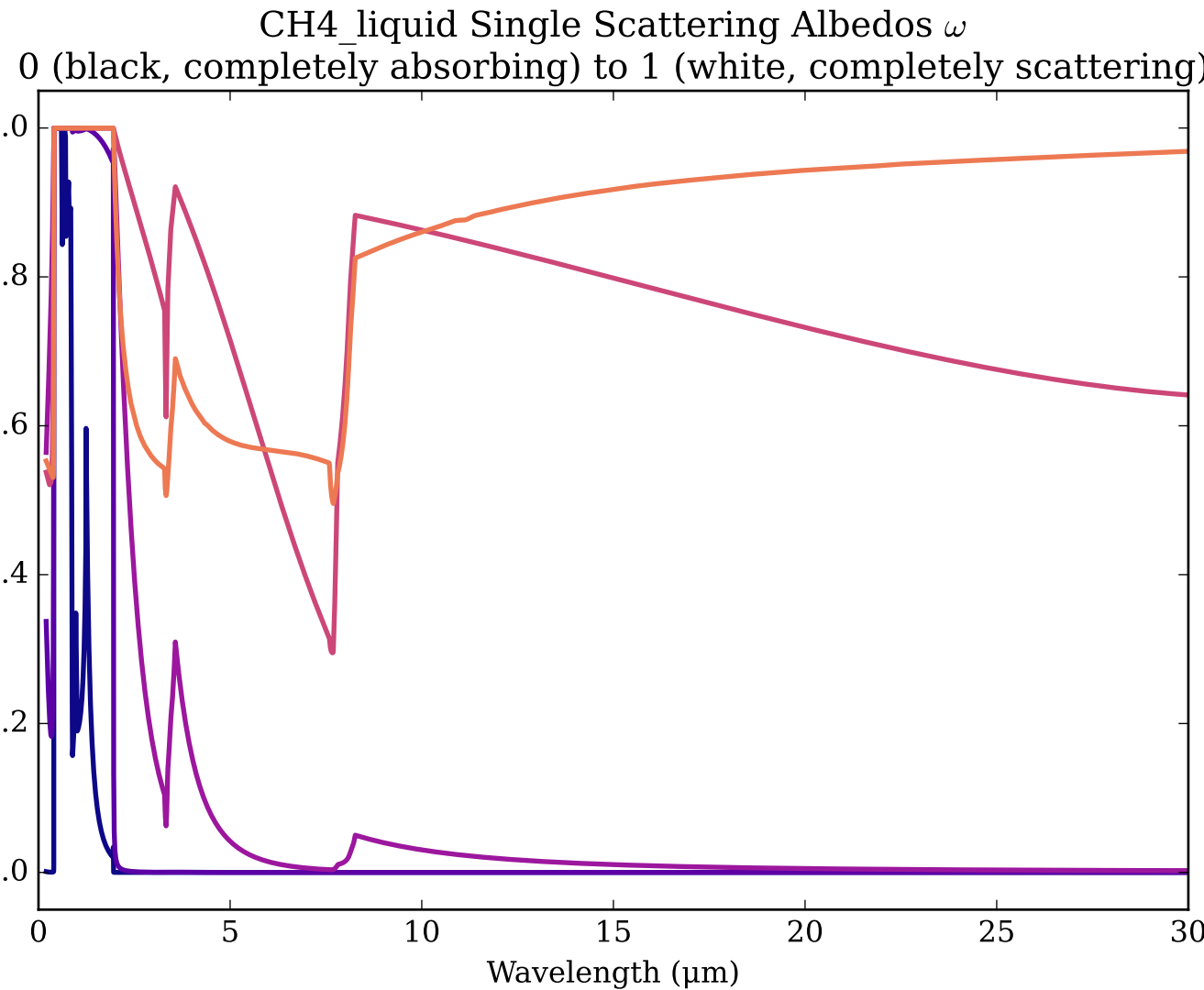
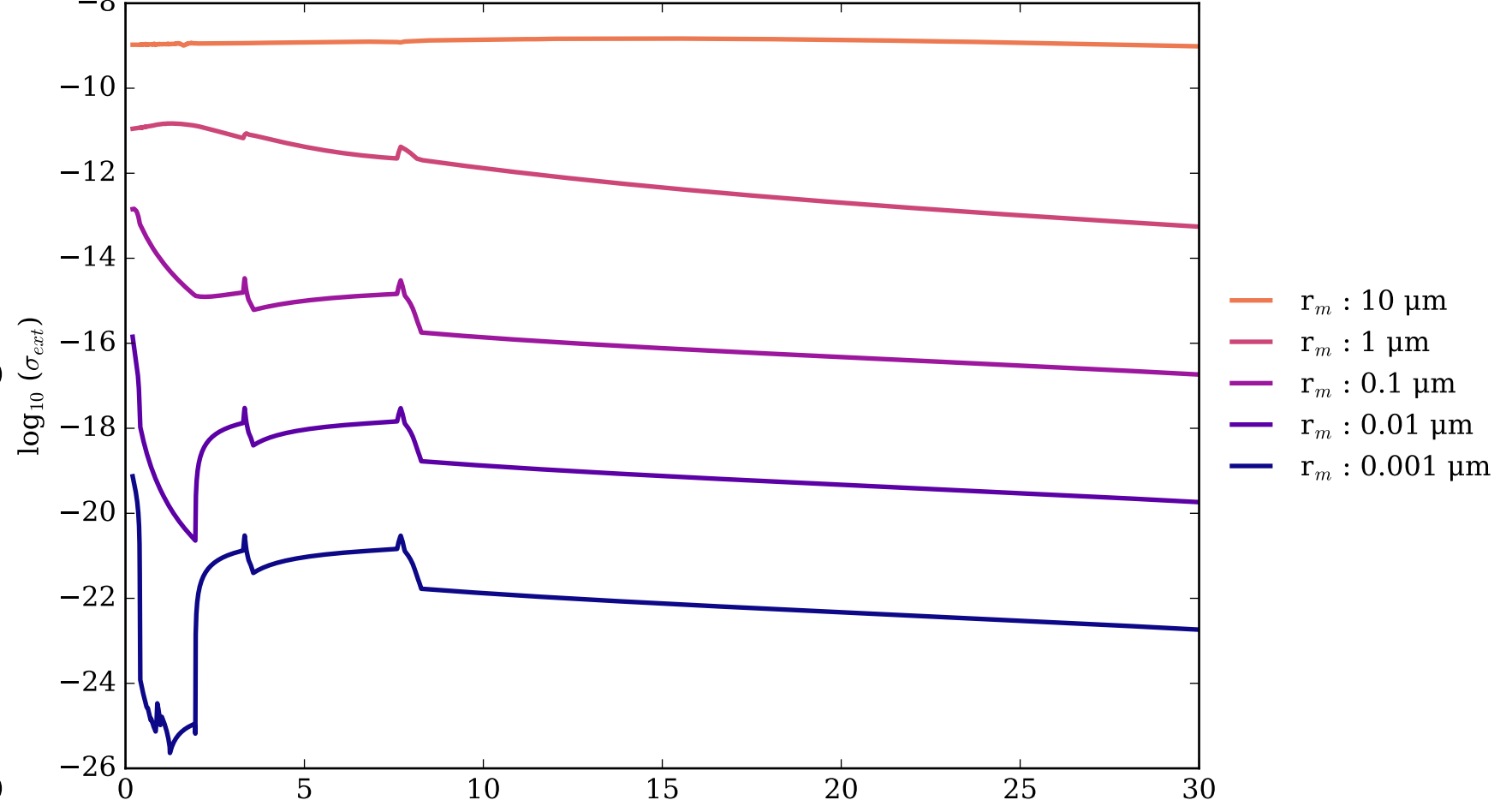
C Asymmetry Parameter  $g$



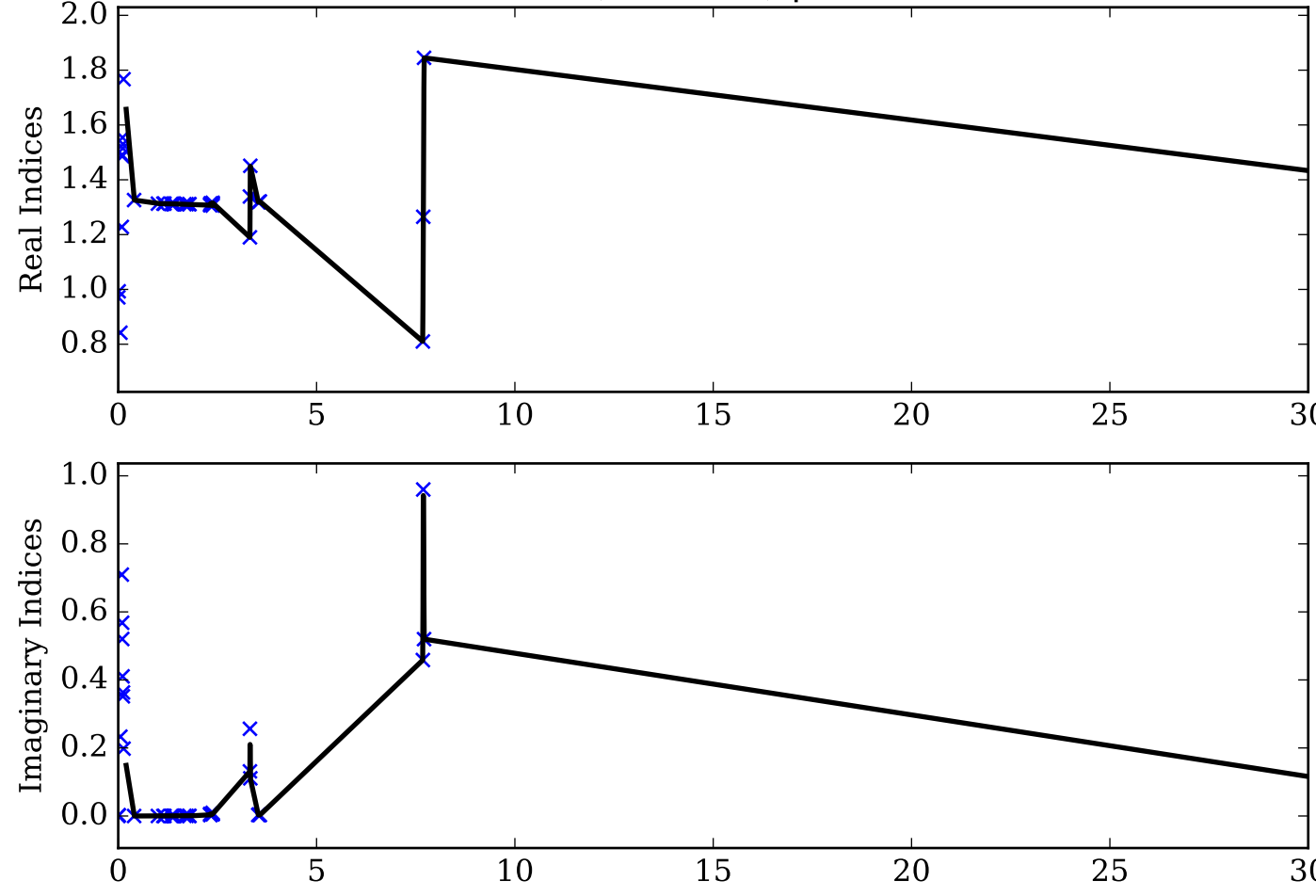
Refractive Indices for CH<sub>4</sub>  
(0.2, 30.0)  $\mu\text{m}$



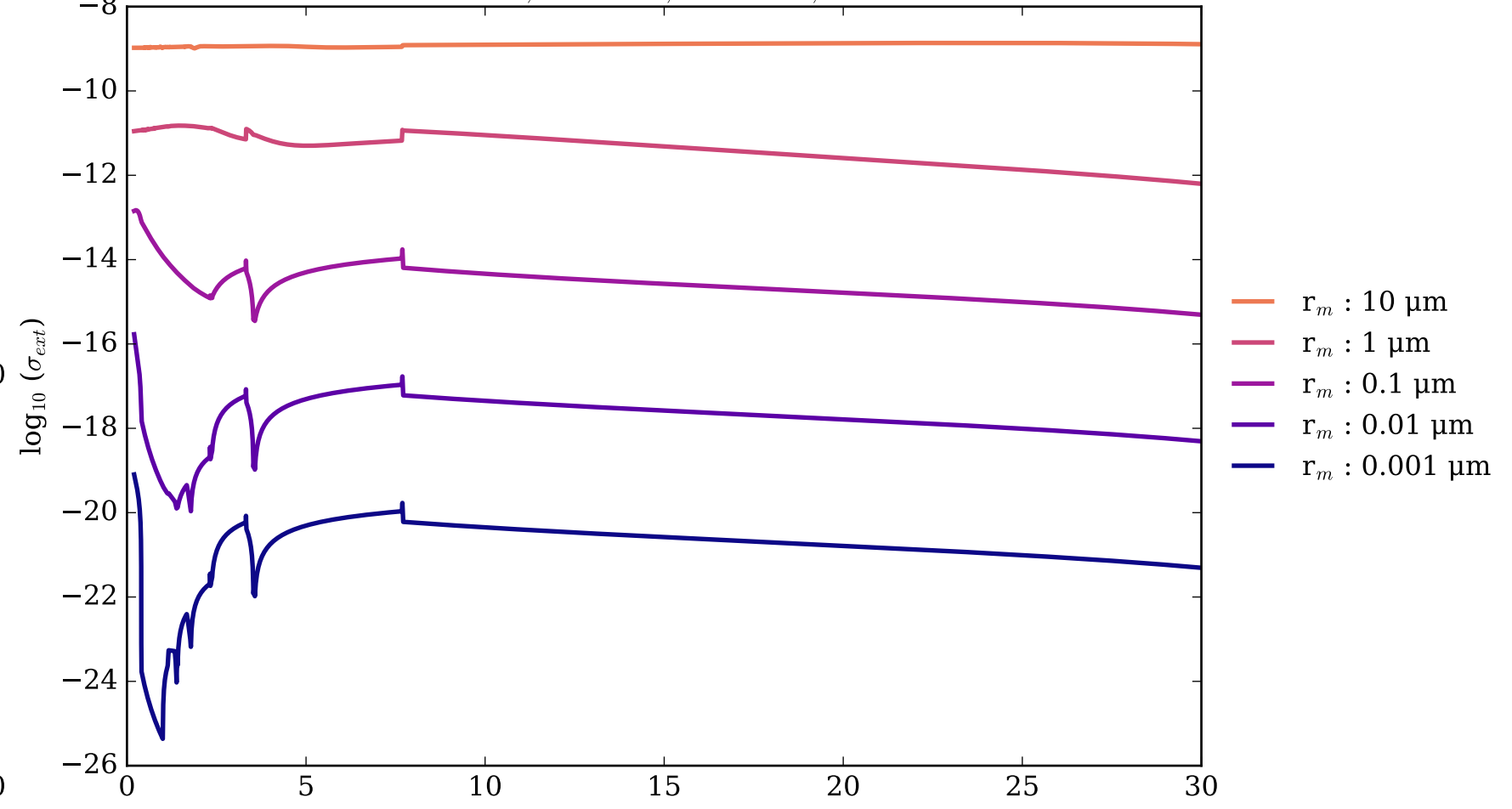
CH<sub>4</sub>\_liquid Effective Extinction Cross Section  
 $\sigma_{\text{ext, eff}} = \sigma_{\text{abs, eff}} + \sigma_{\text{scat, eff}}$



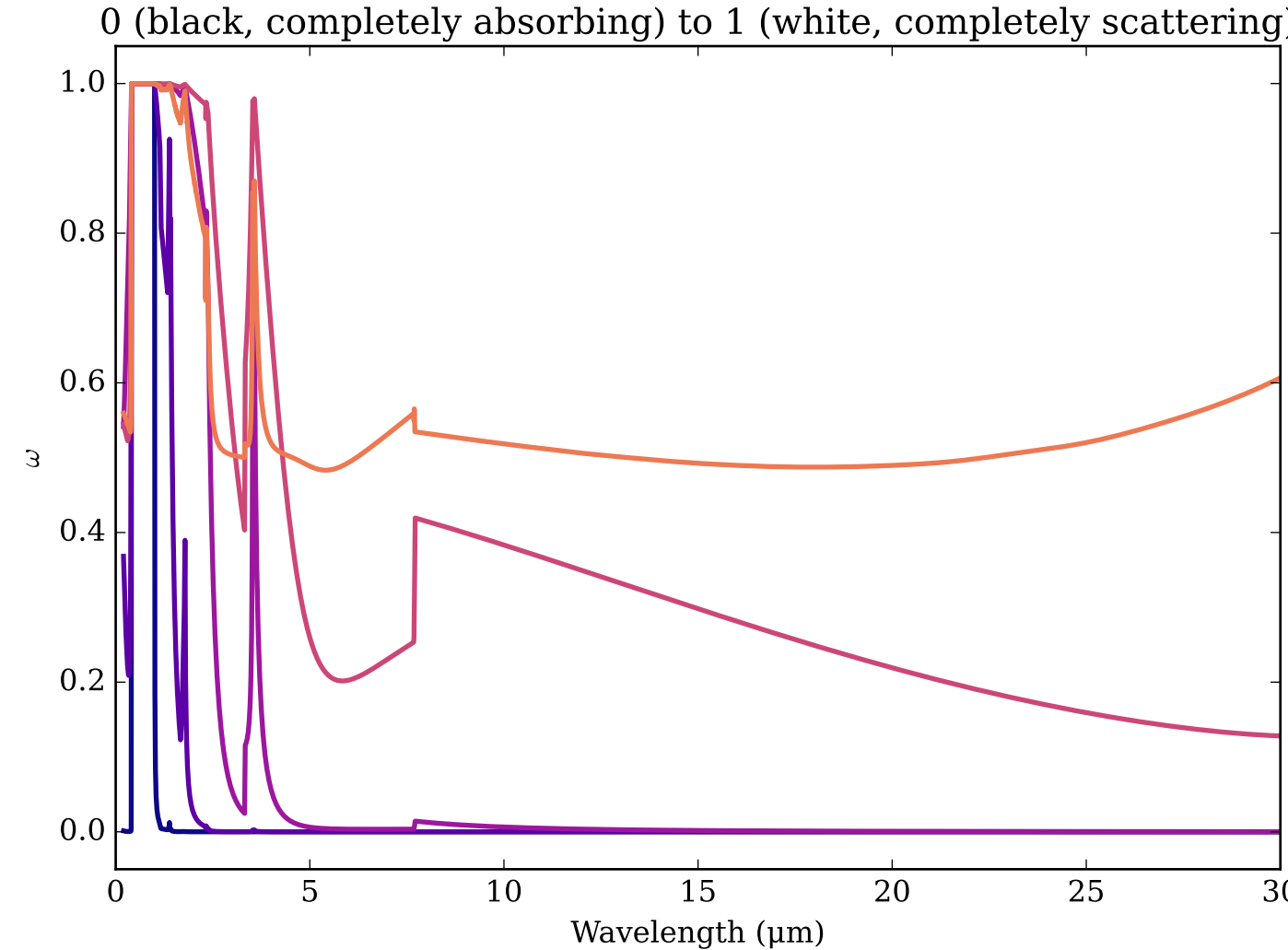
Refractive Indices for CH<sub>4</sub>  
(0.2, 30.0)  $\mu\text{m}$



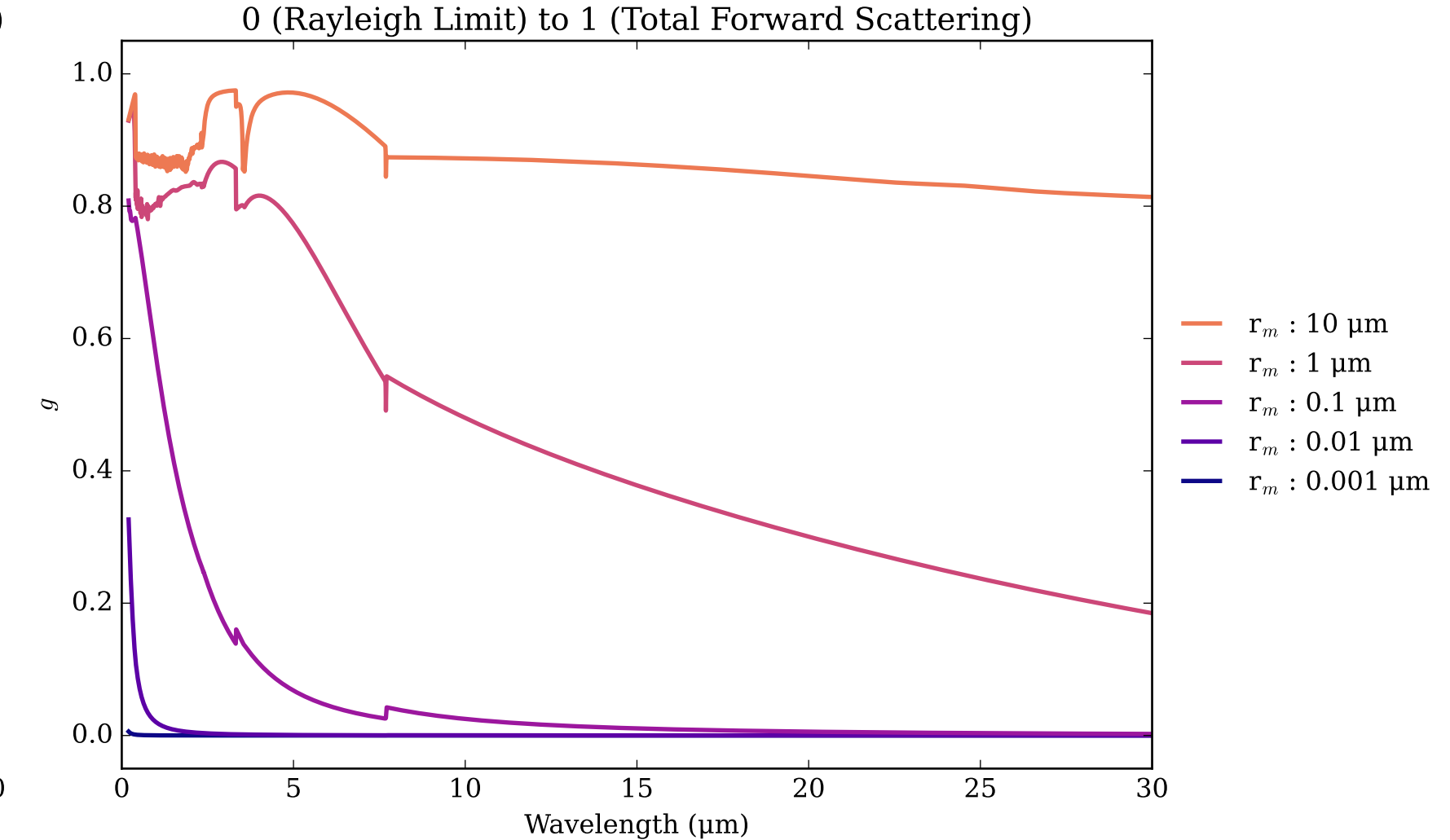
CH<sub>4</sub>\_solid Effective Extinction Cross Section  
 $\sigma_{\text{ext, eff}} = \sigma_{\text{abs, eff}} + \sigma_{\text{scat, eff}}$



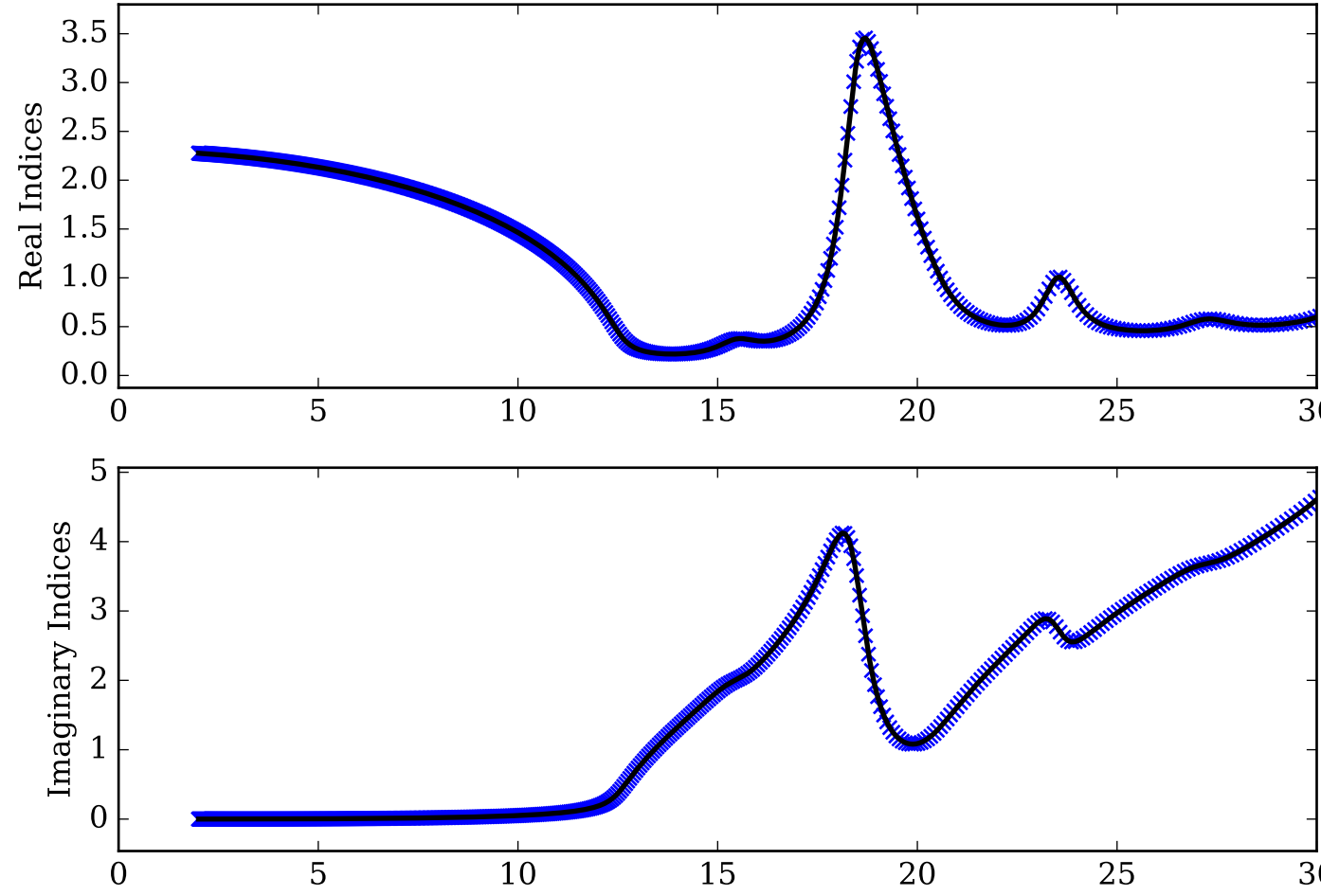
CH<sub>4</sub>\_solid Single Scattering Albedos  $\omega$



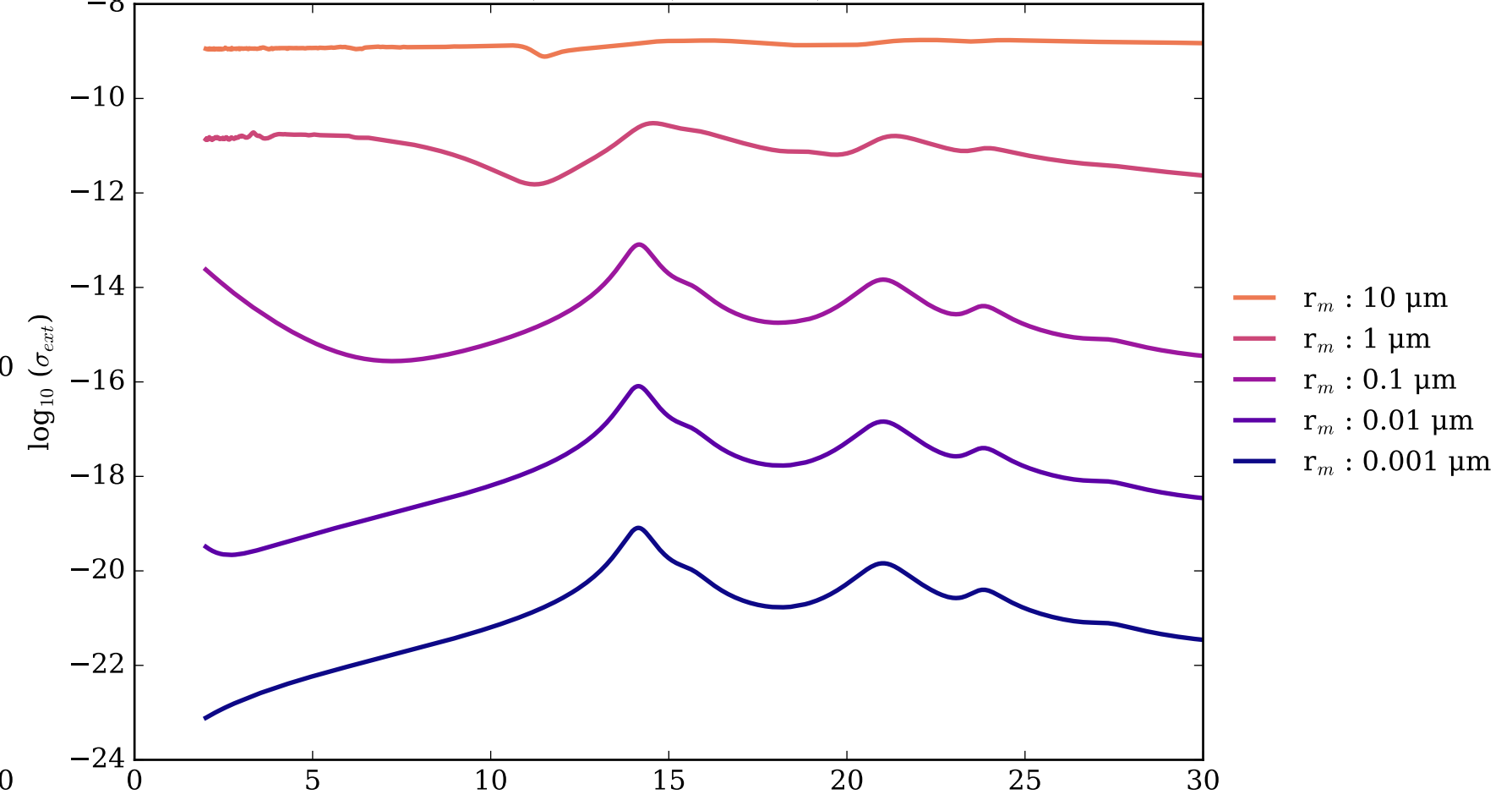
CH<sub>4</sub>\_solid Asymmetry Parameter  $g$



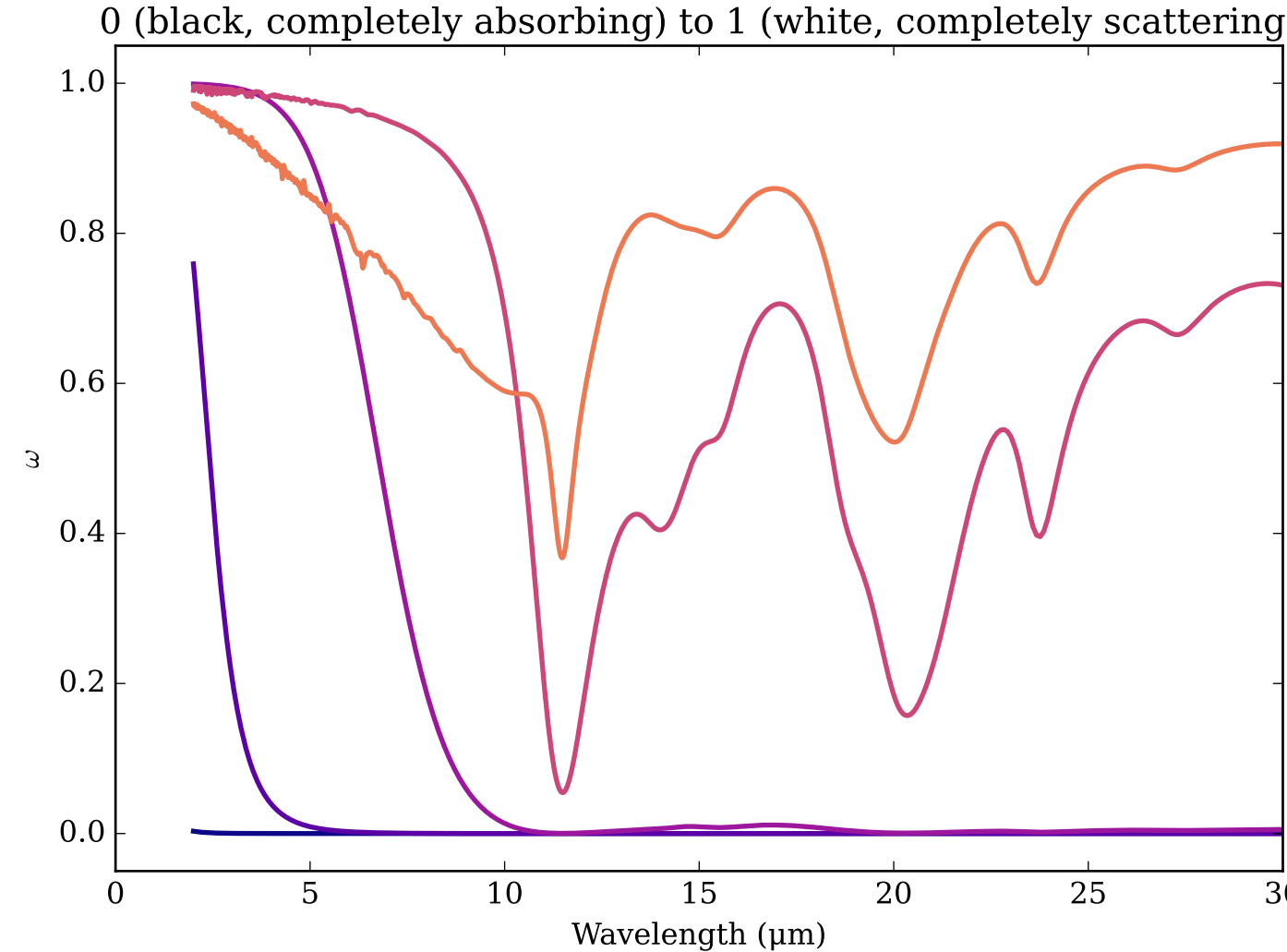
Refractive Indices for CaTiO<sub>3</sub>  
(2.0, 30.0)  $\mu\text{m}$



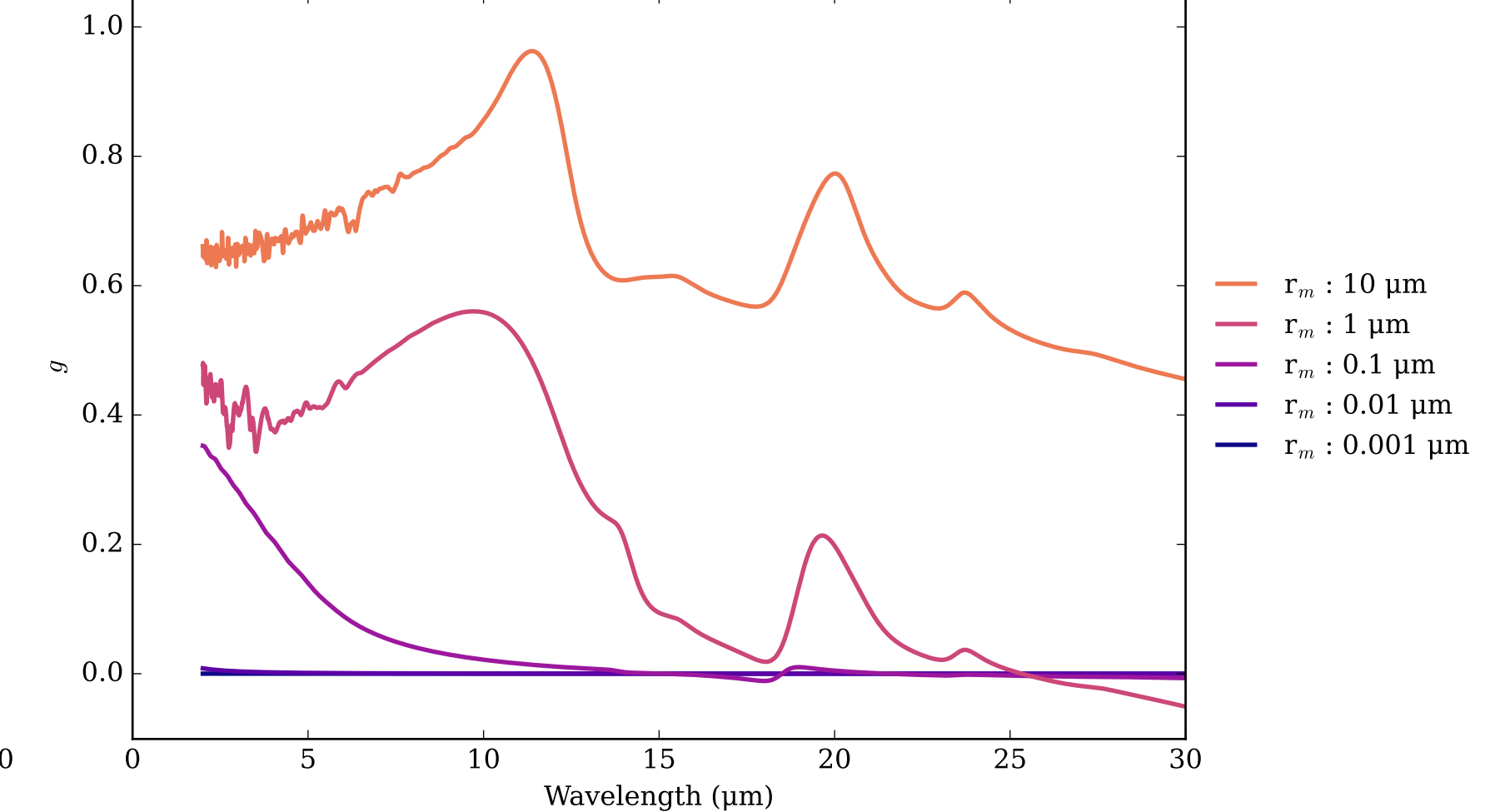
CaTiO<sub>3</sub> Effective Extinction Cross Section  
 $\sigma_{\text{ext, eff}} = \sigma_{\text{abs, eff}} + \sigma_{\text{scat, eff}}$



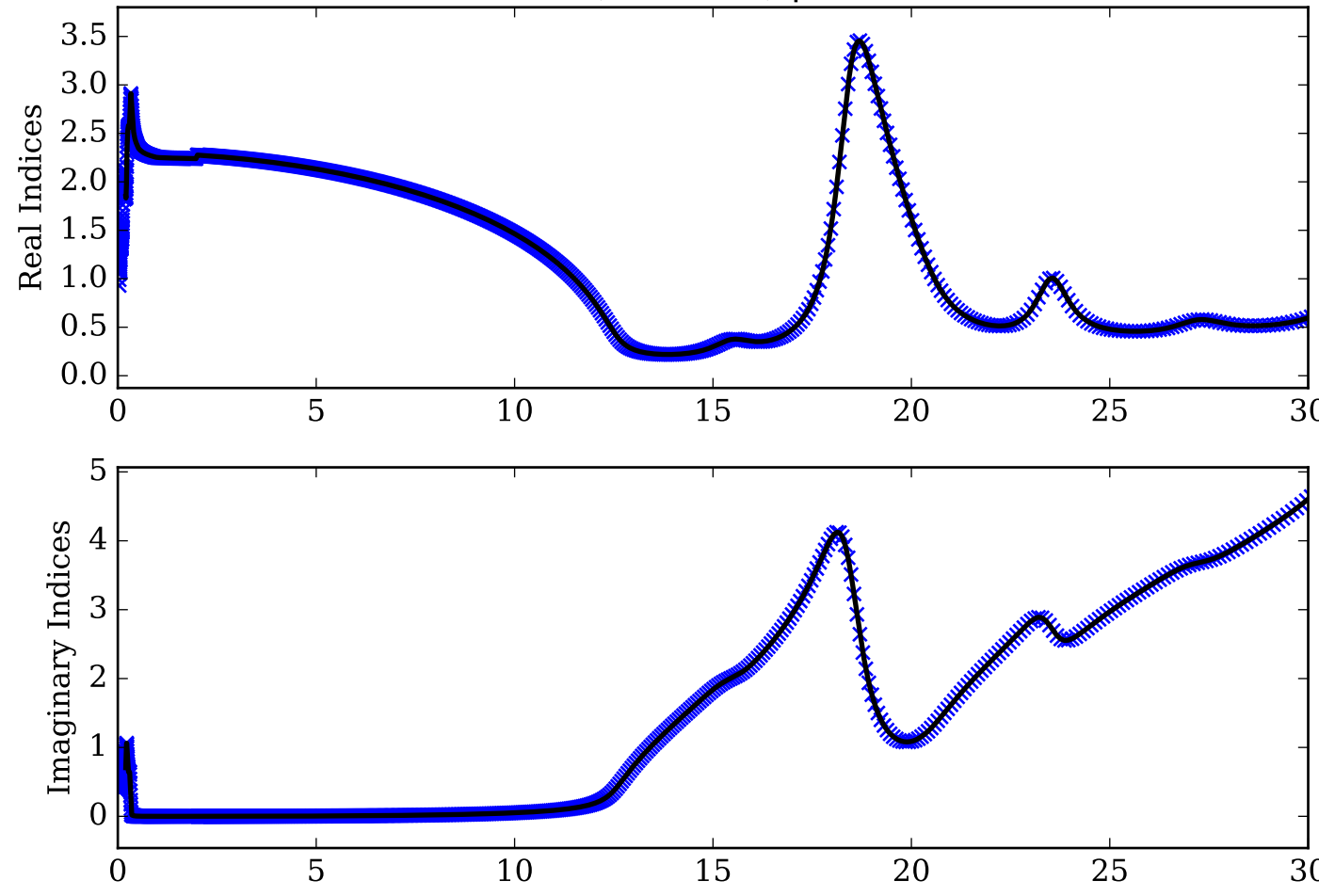
CaTiO<sub>3</sub> Single Scattering Albedos  $\omega$



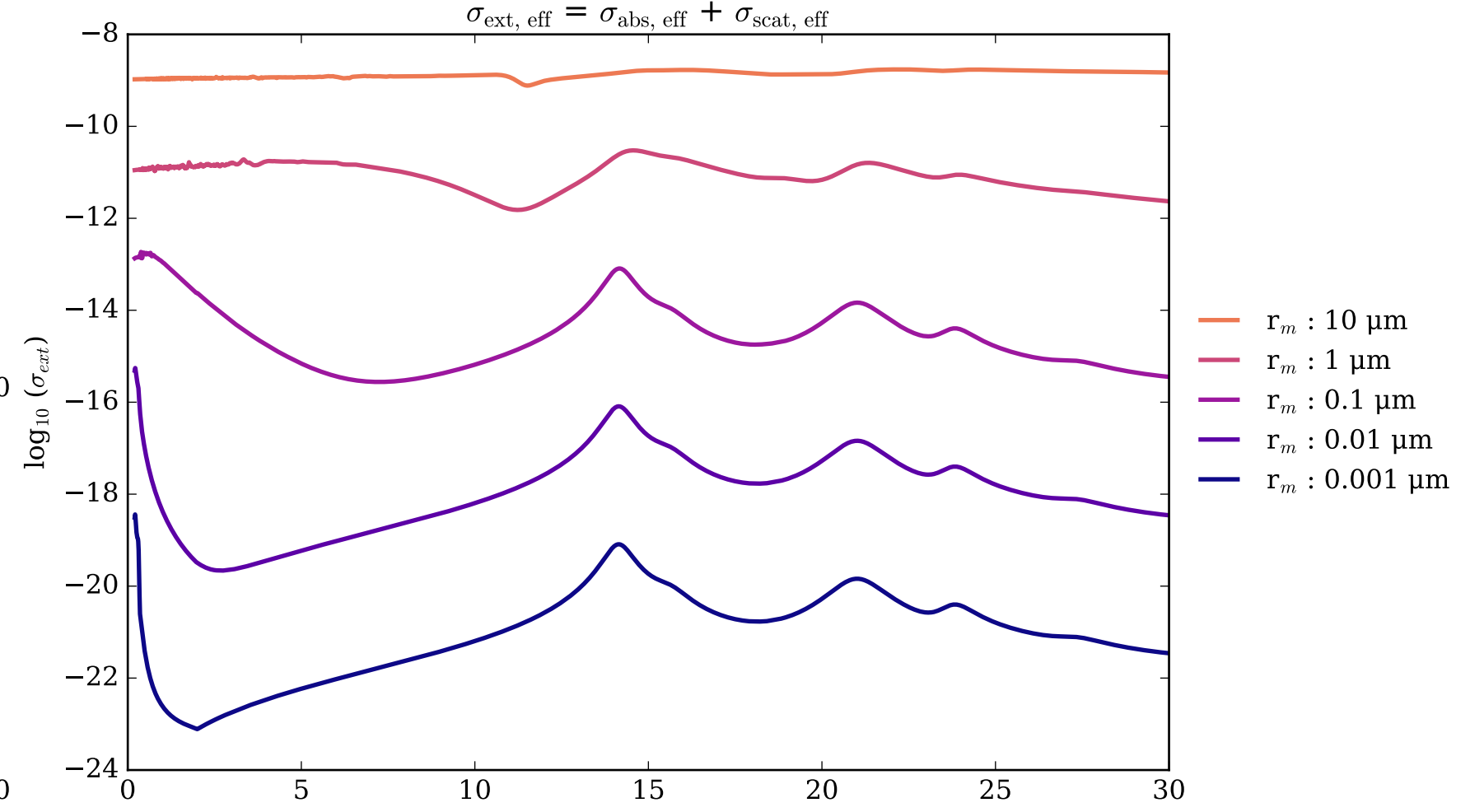
CaTiO<sub>3</sub> Asymmetry Parameter  $g$   
0 (Rayleigh Limit) to 1 (Total Forward Scattering)



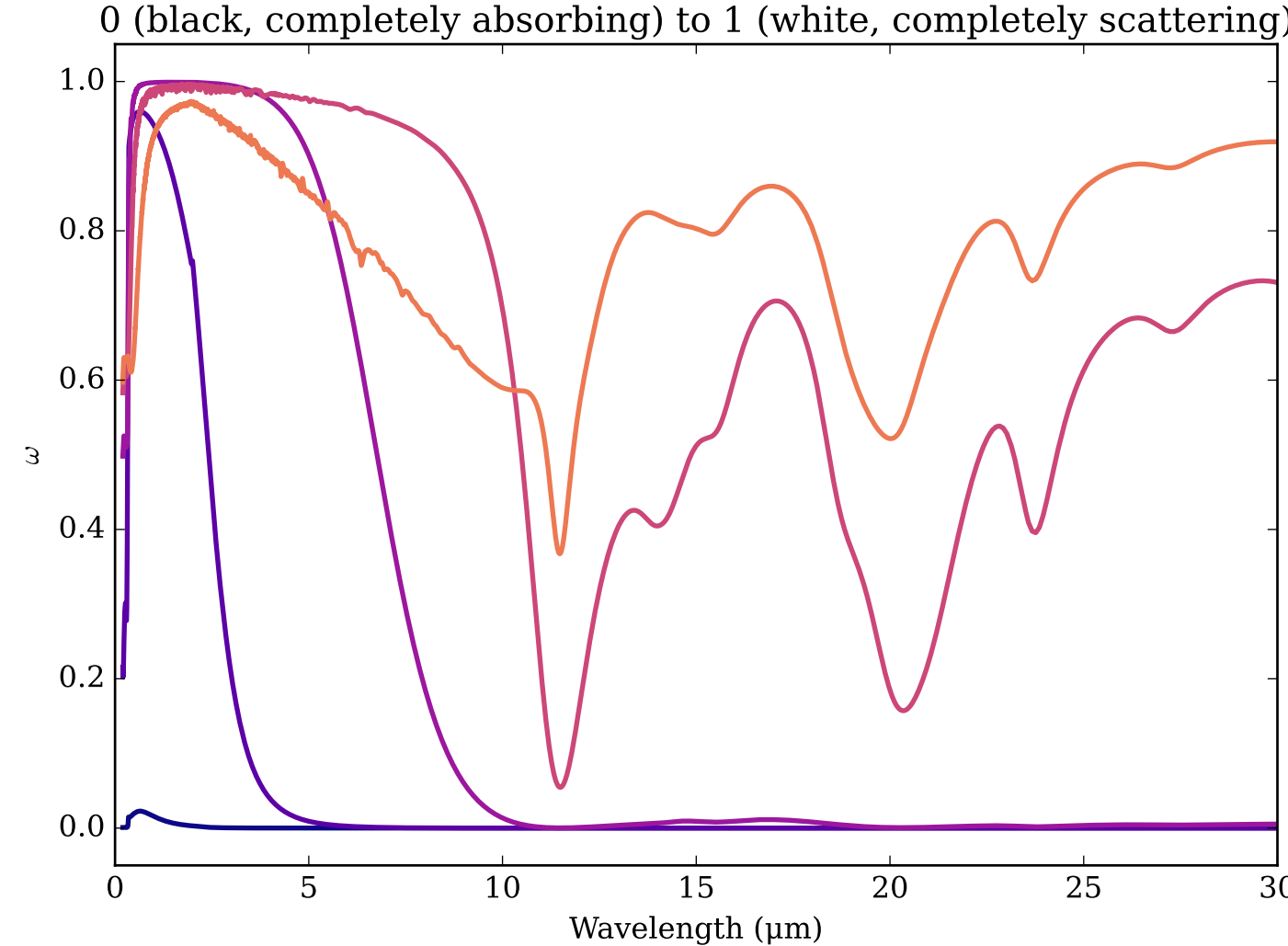
Refractive Indices for CaTiO<sub>3</sub>  
(0.2, 30.0)  $\mu\text{m}$



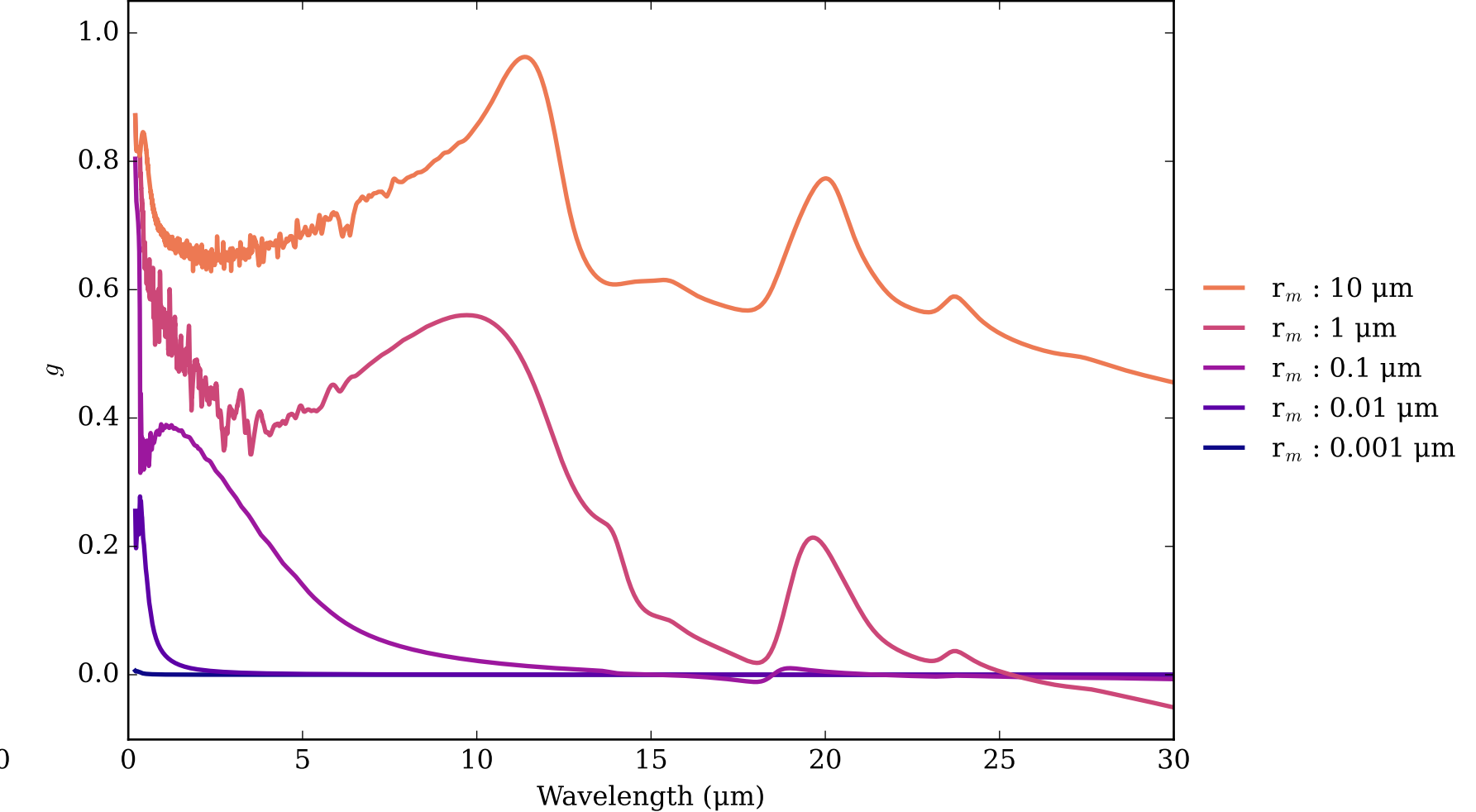
CaTiO<sub>3</sub>\_KH Effective Extinction Cross Section



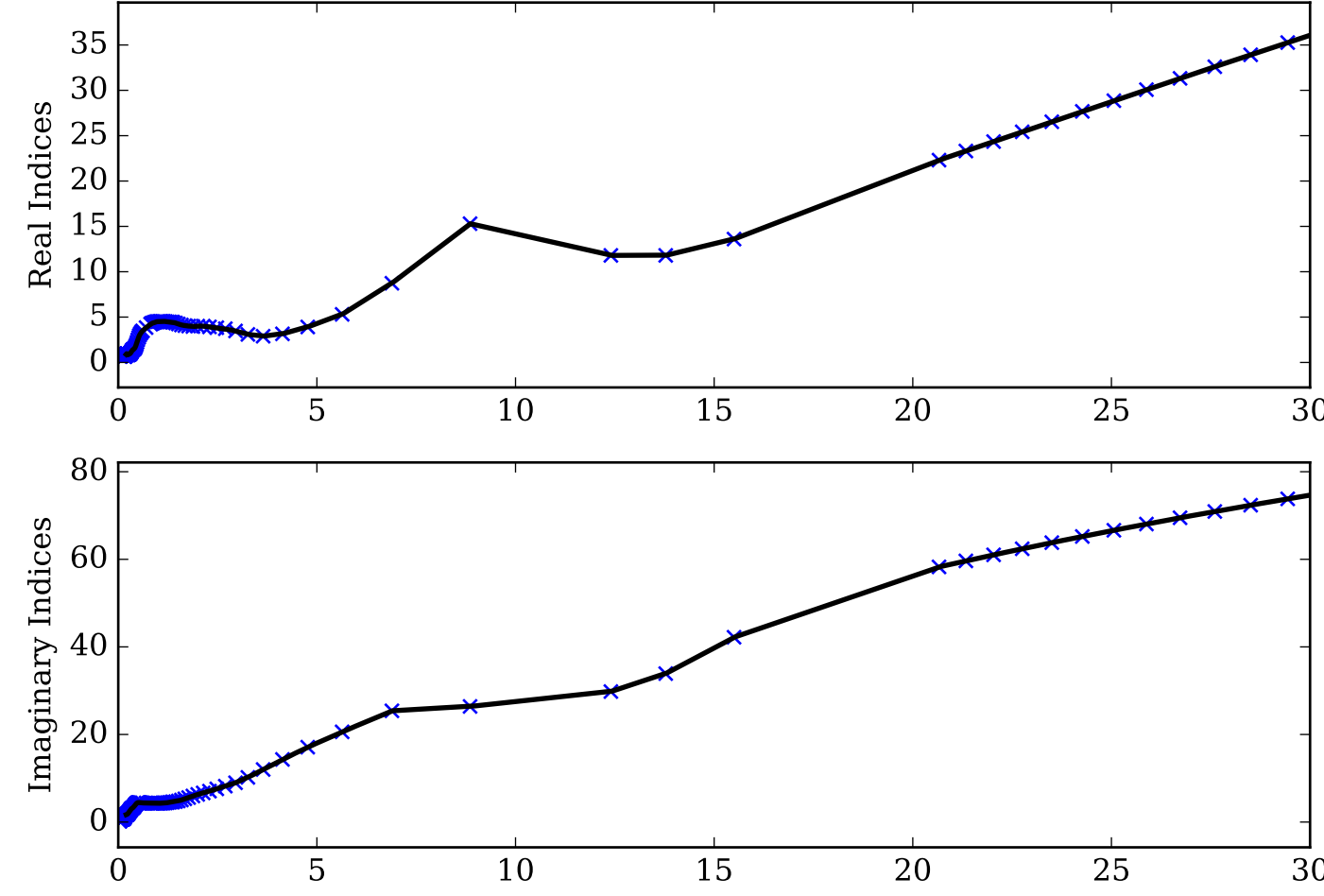
CaTiO<sub>3</sub>\_KH Single Scattering Albedos  $\omega$



CaTiO<sub>3</sub>\_KH Asymmetry Parameter  $g$

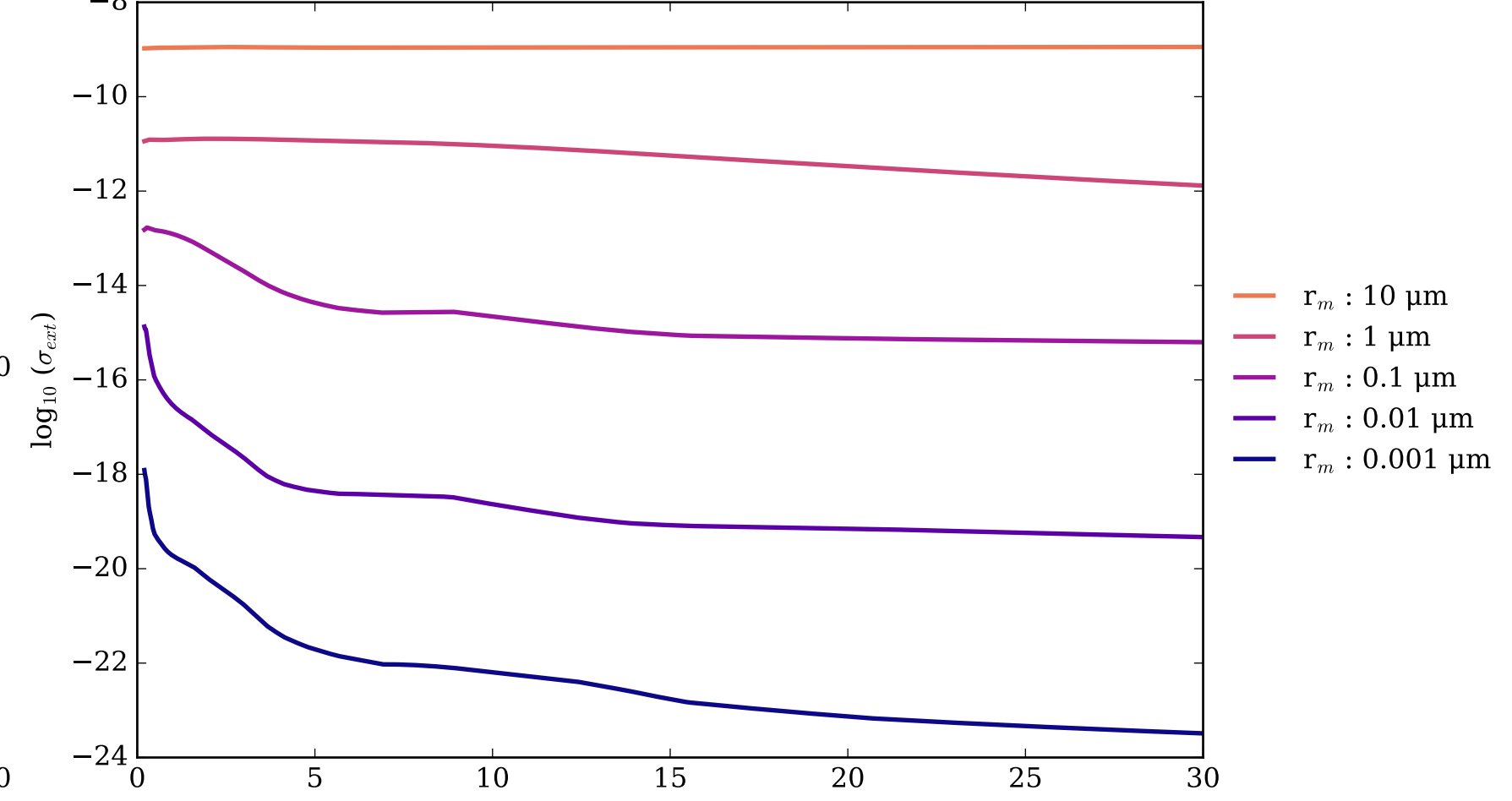


Refractive Indices for Cr  
(0.2, 30.0)  $\mu\text{m}$

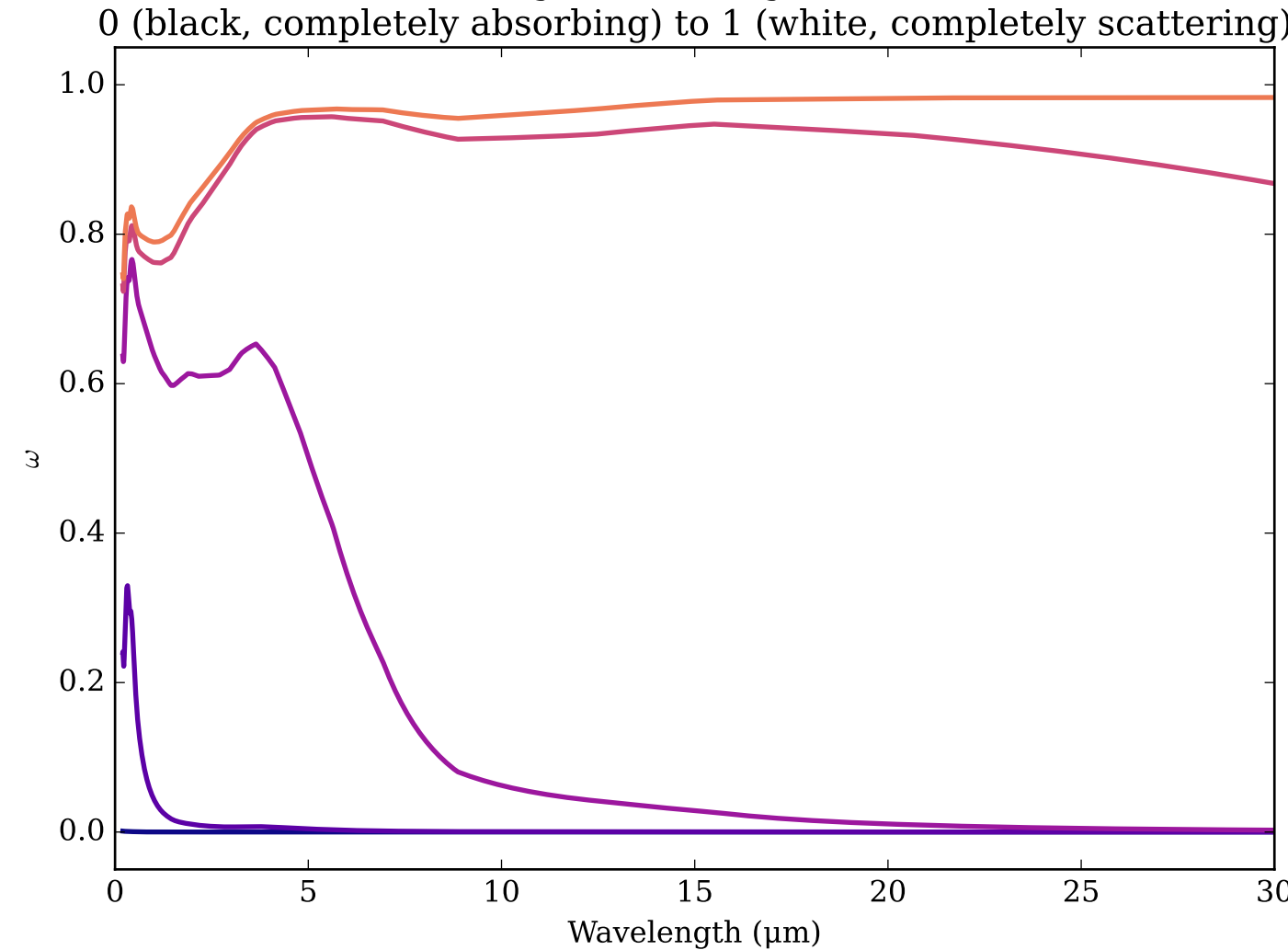


Cr Effective Extinction Cross Section

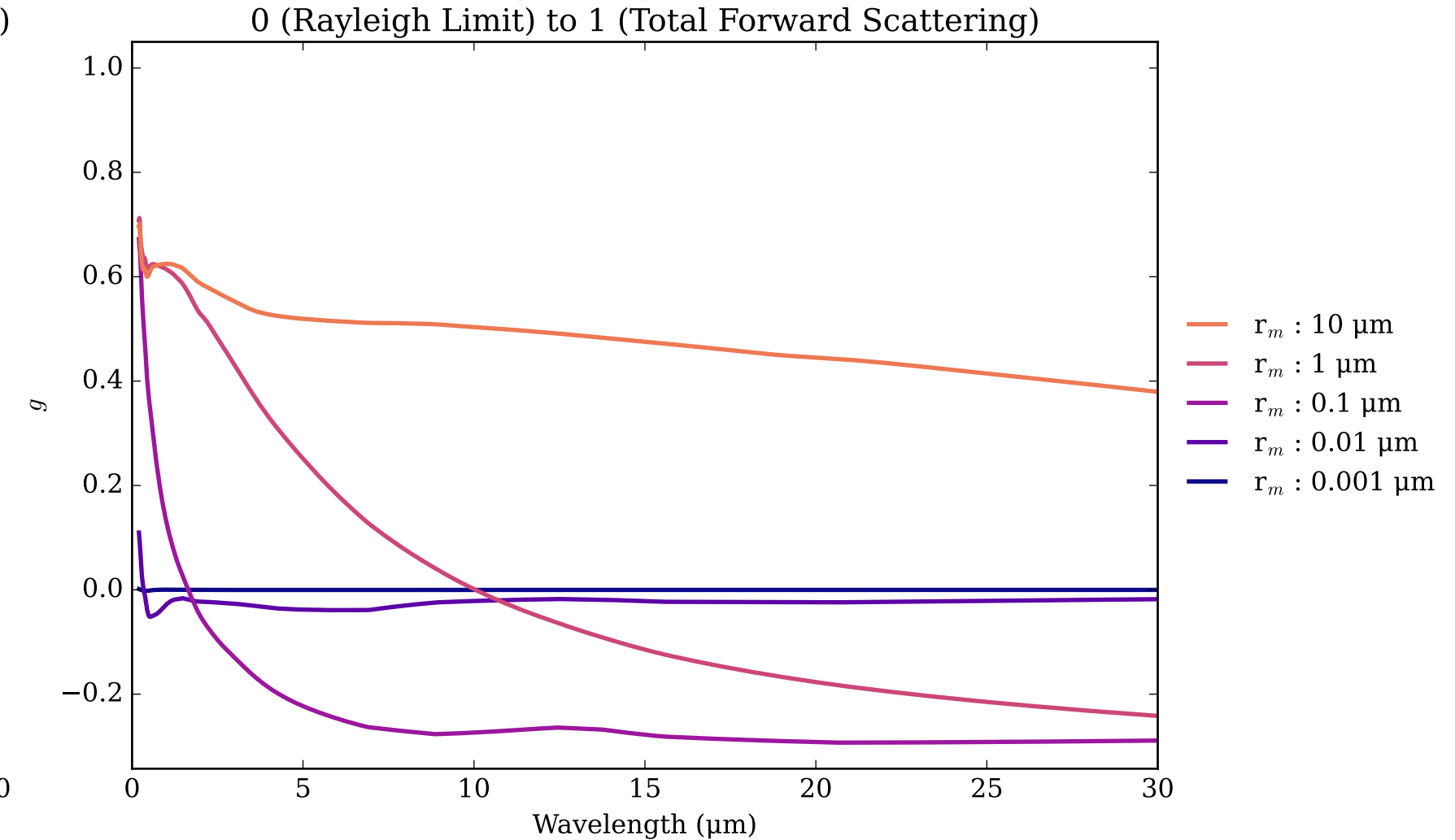
$$\sigma_{\text{ext, eff}} = \sigma_{\text{abs, eff}} + \sigma_{\text{scat, eff}}$$



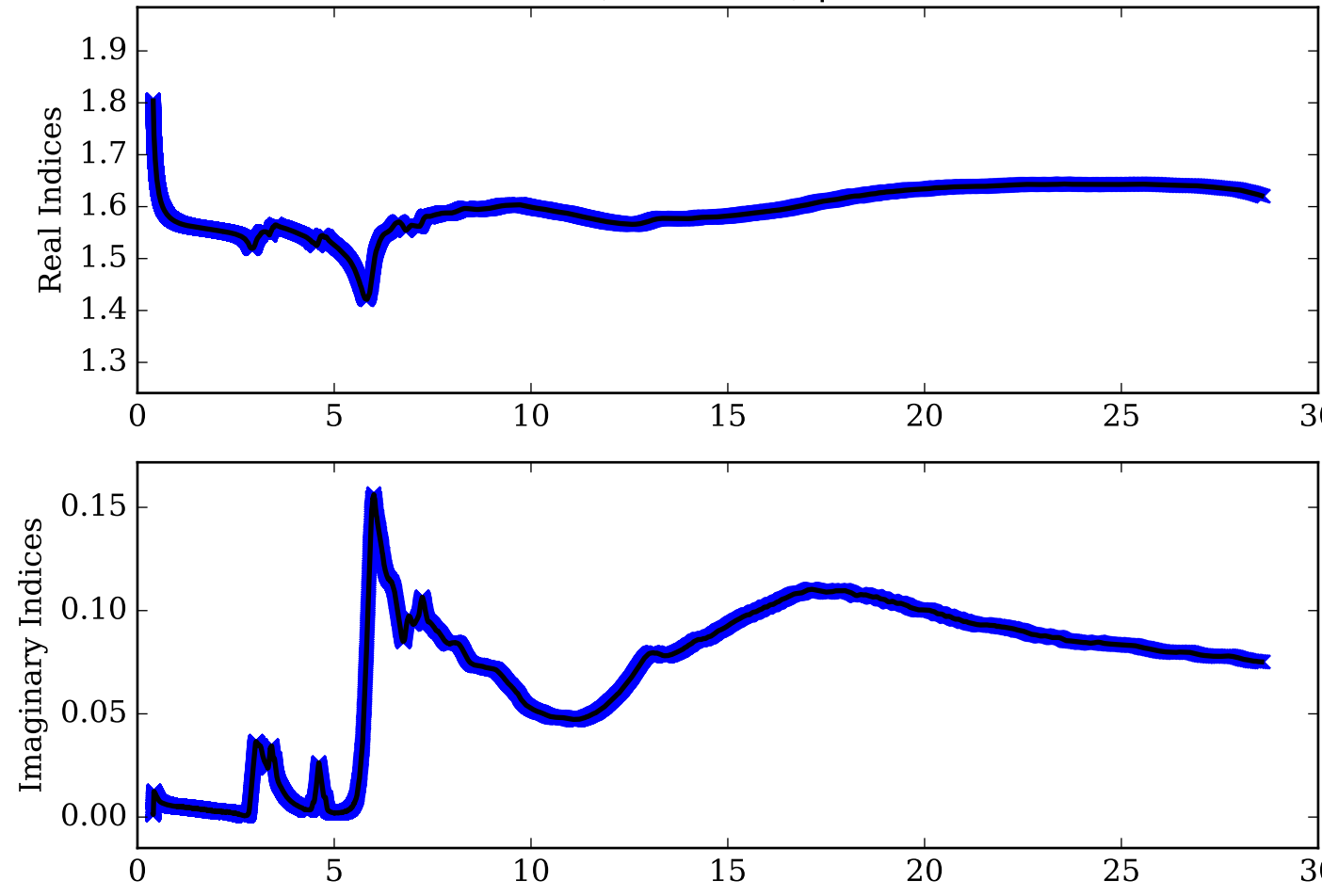
Cr Single Scattering Albedos  $\omega$



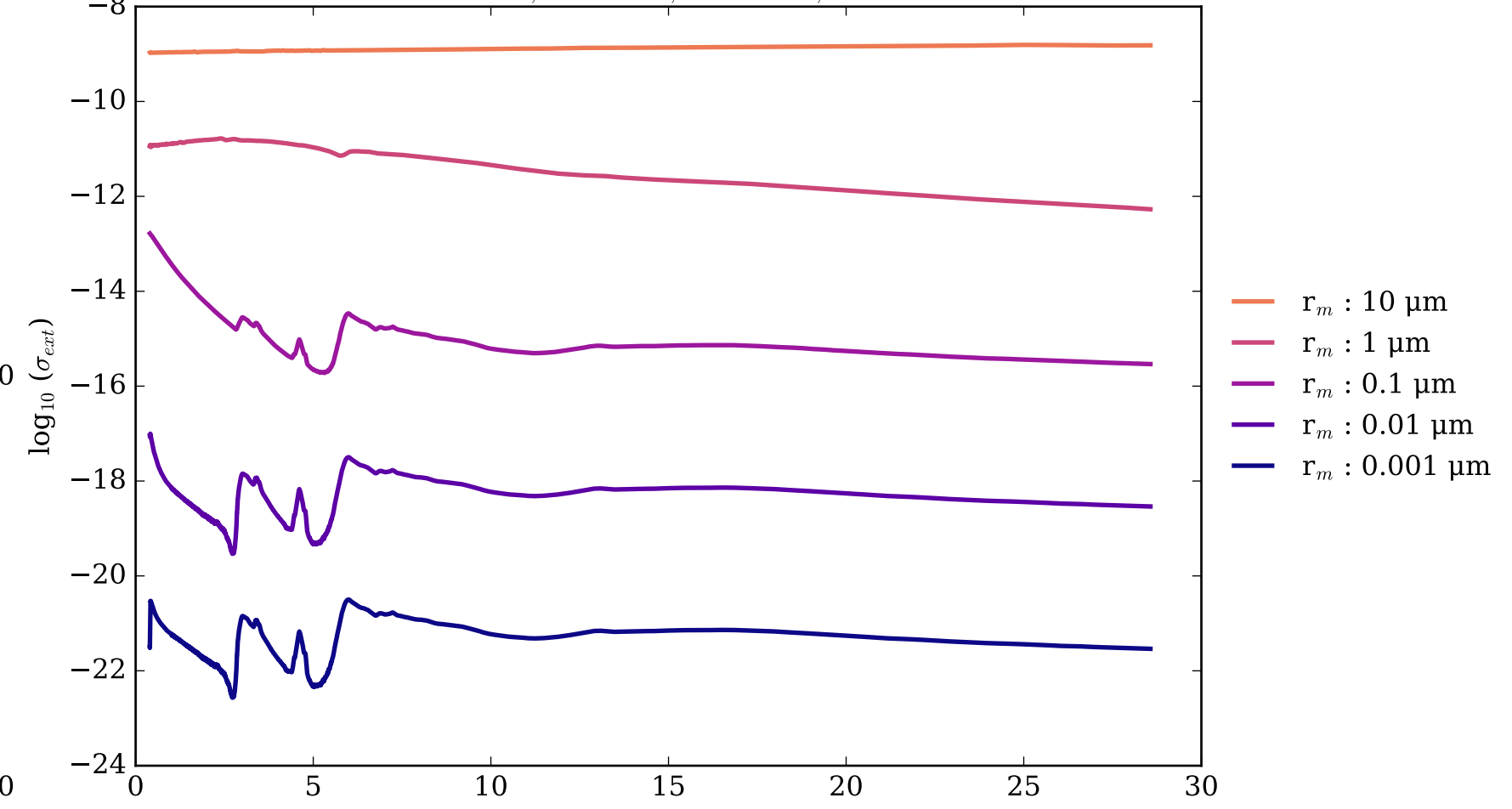
Cr Asymmetry Parameter  $g$



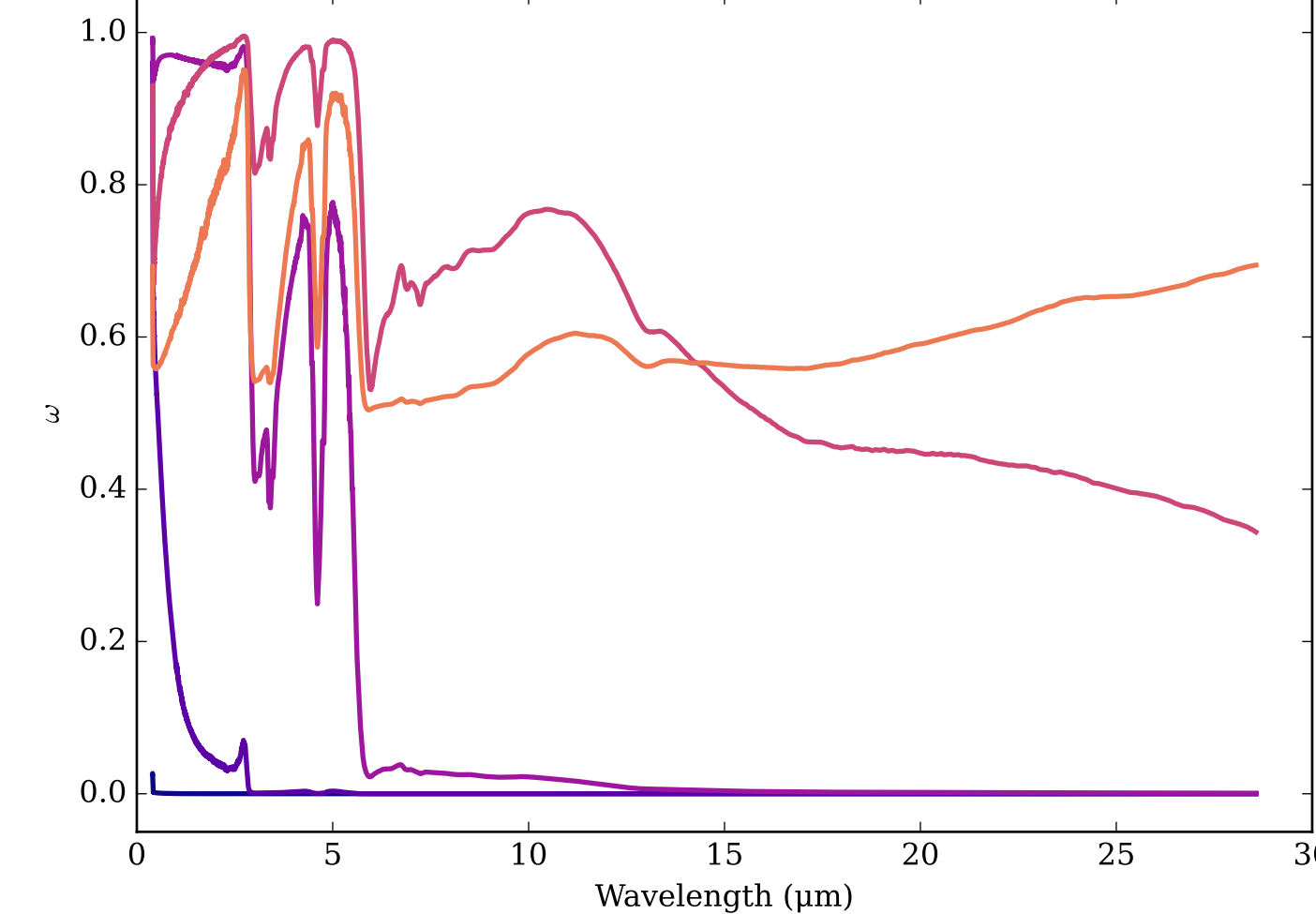
Refractive Indices for ExoHaze  
(0.4, 28.57)  $\mu\text{m}$



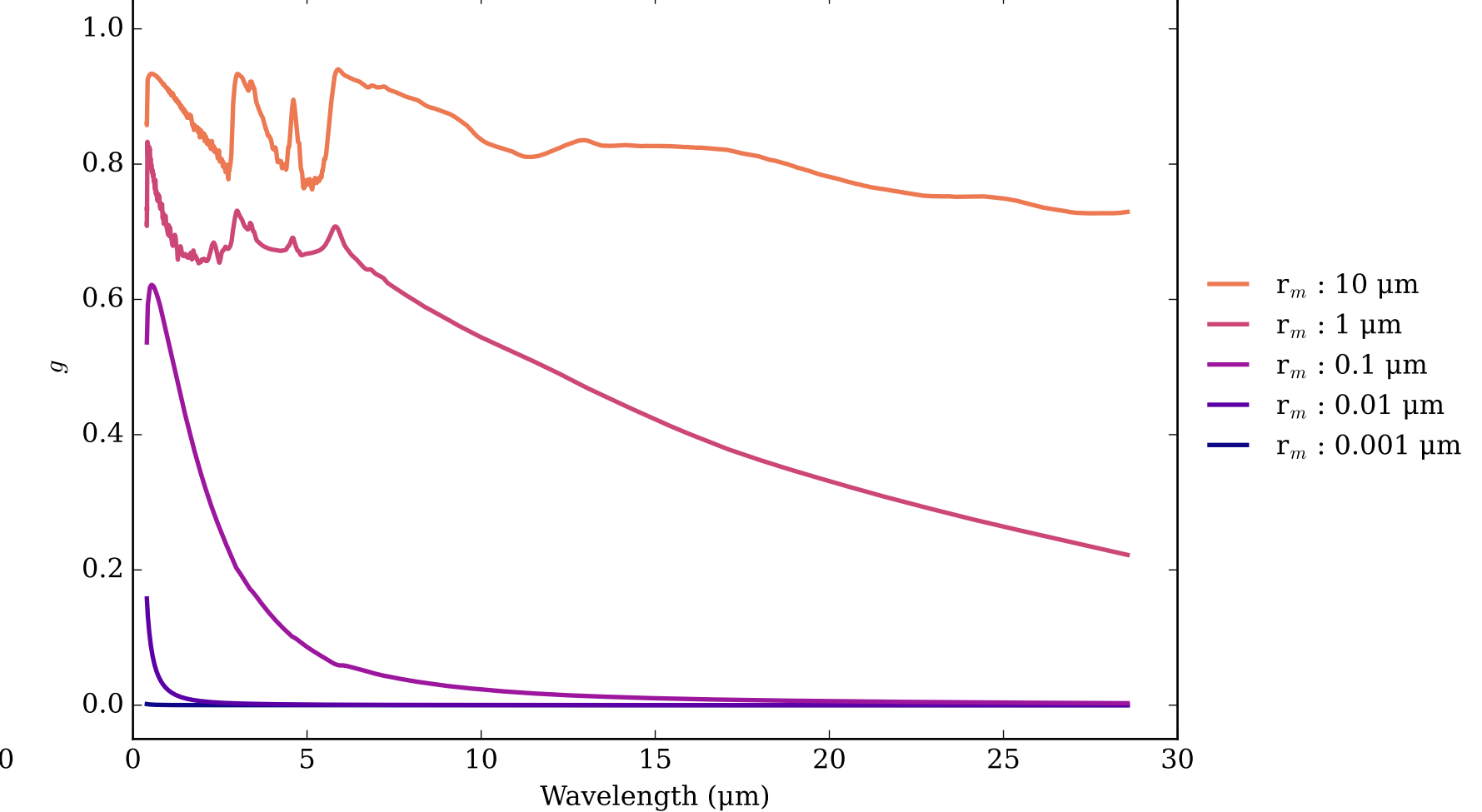
ExoHaze\_1000xSolar\_300K Effective Extinction Cross Section



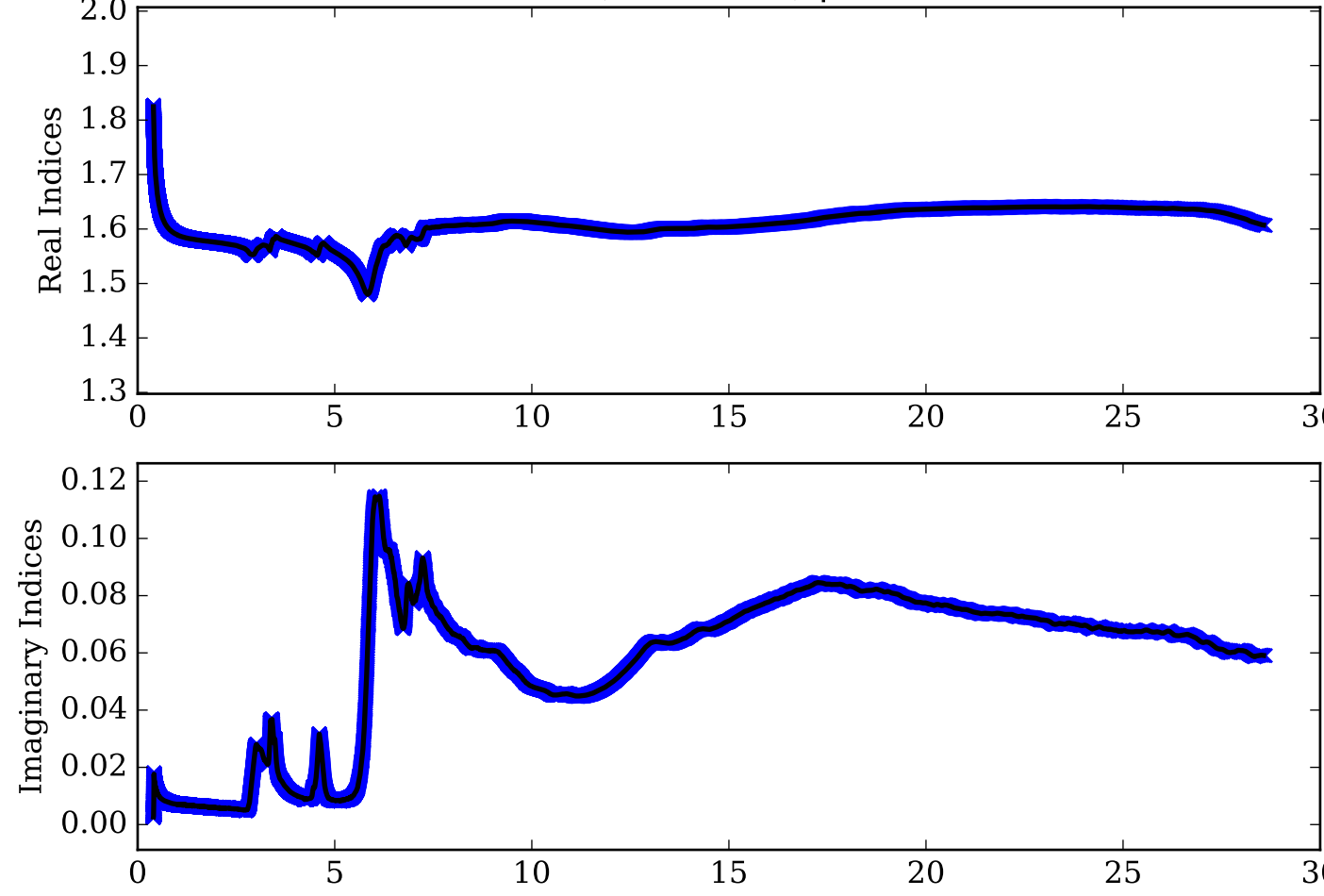
ExoHaze\_1000xSolar\_300K Single Scattering Albedos  $\omega$   
0 (black, completely absorbing) to 1 (white, completely scattering)



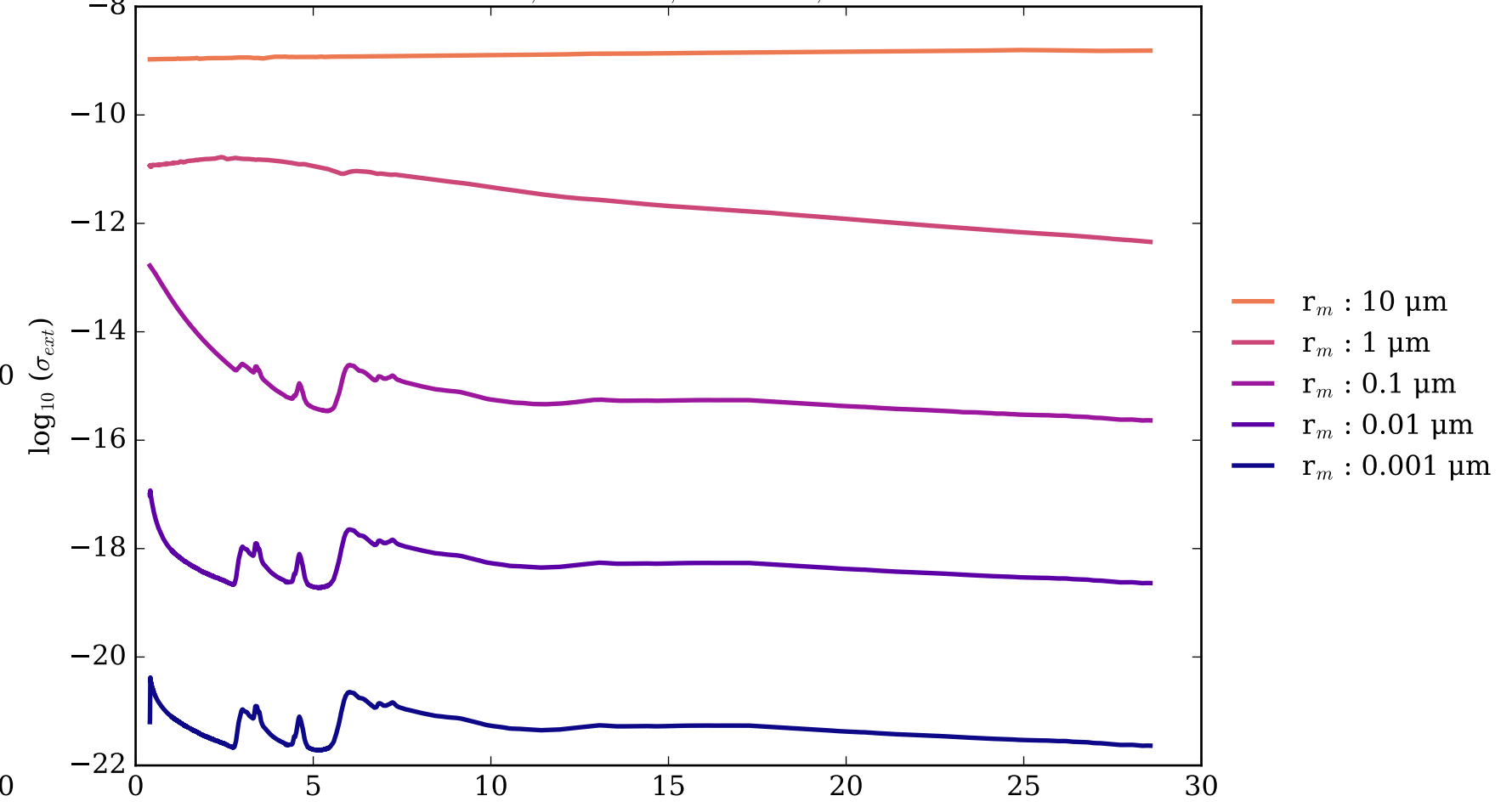
ExoHaze\_1000xSolar\_300K Asymmetry Parameter  $g$   
0 (Rayleigh Limit) to 1 (Total Forward Scattering)



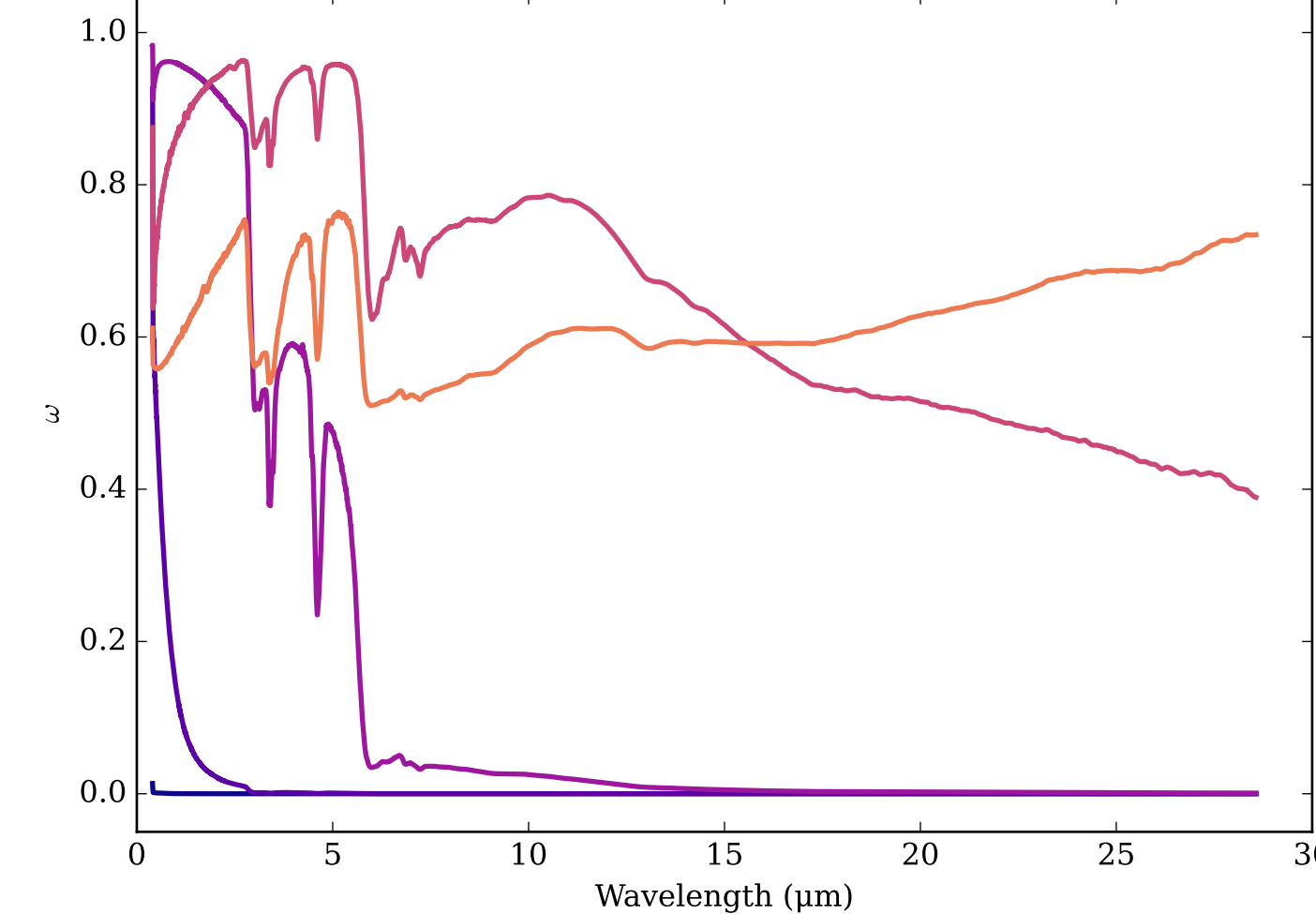
Refractive Indices for ExoHaze  
(0.4, 28.57)  $\mu\text{m}$



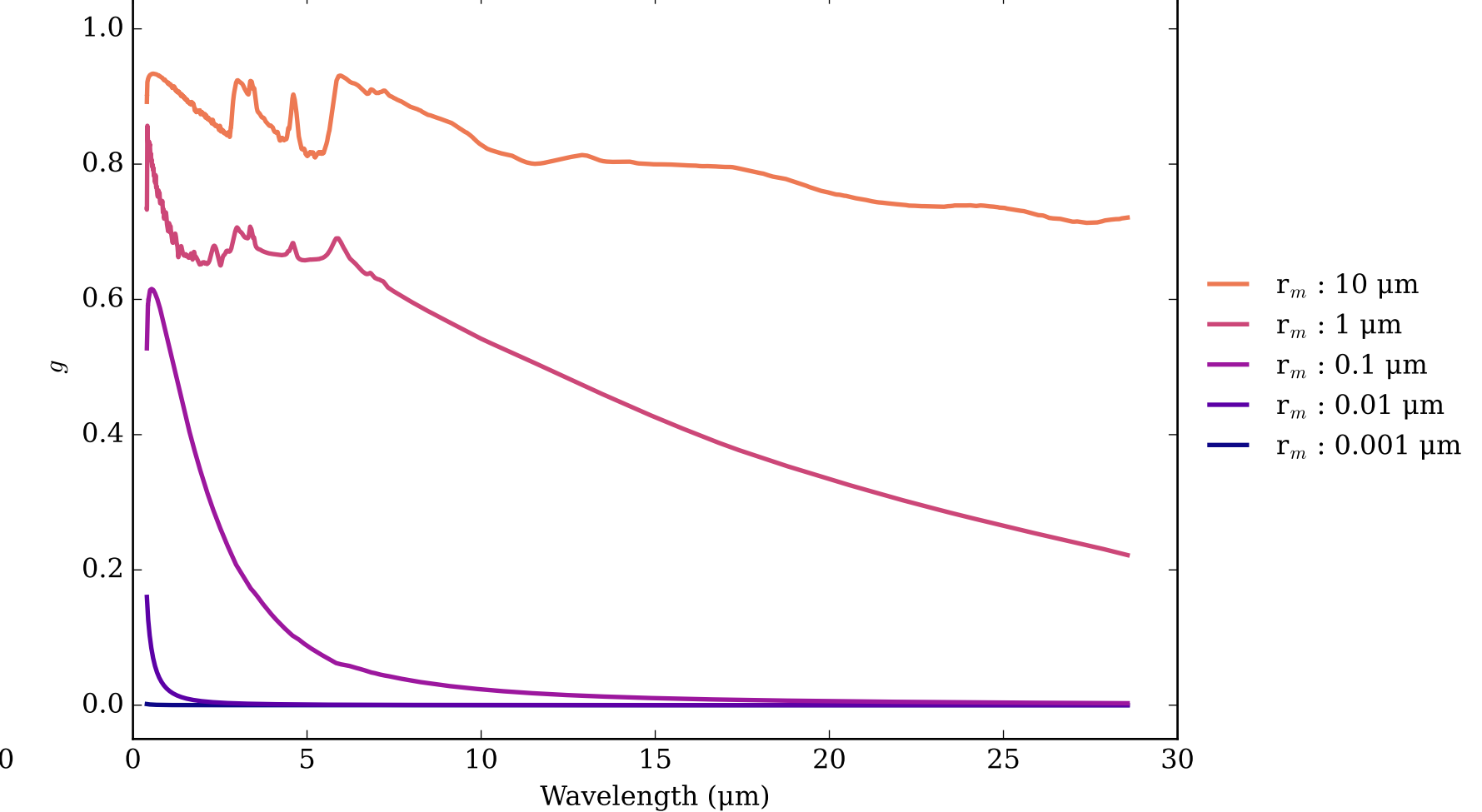
ExoHaze\_1000xSolar\_400K Effective Extinction Cross Section



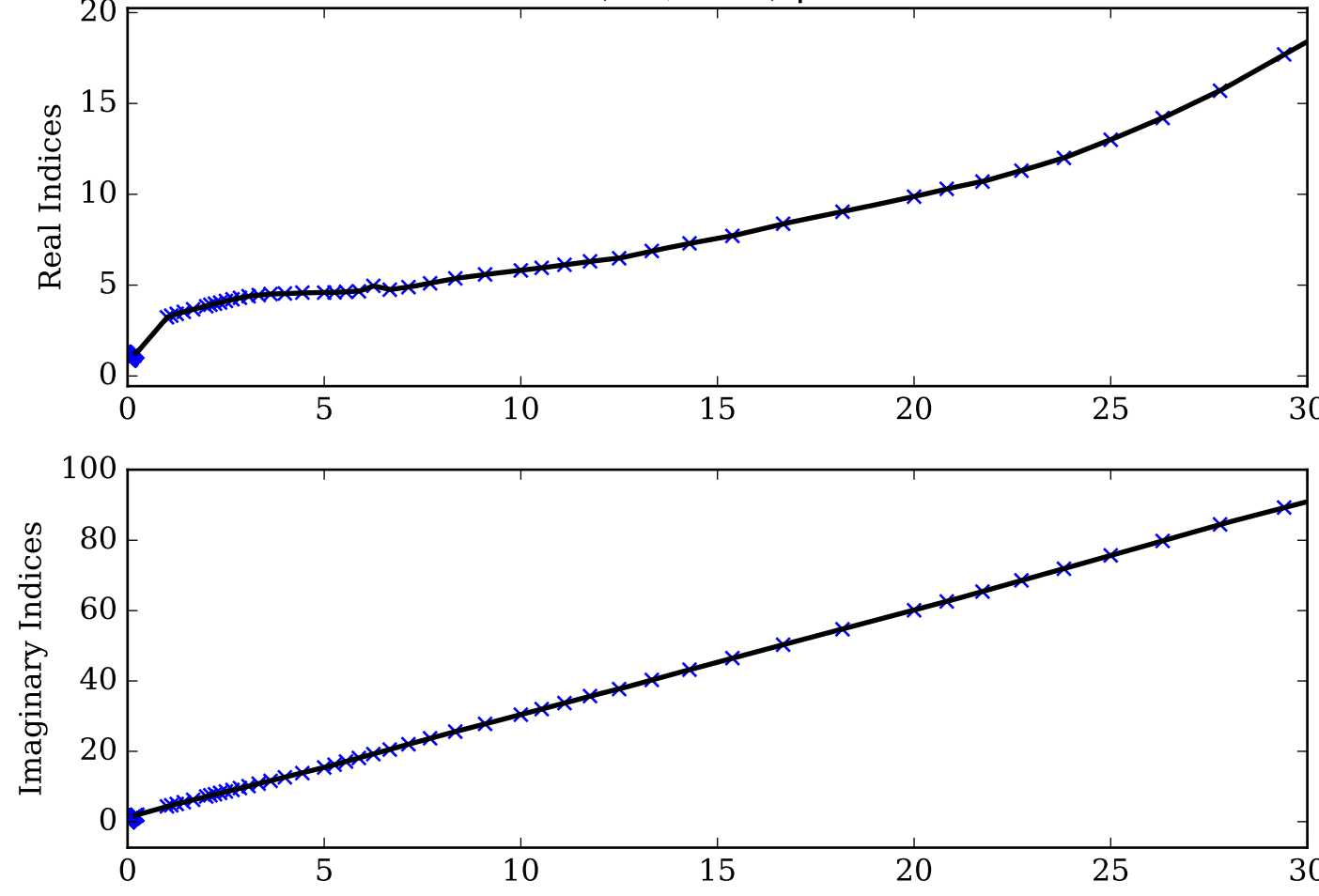
ExoHaze\_1000xSolar\_400K Single Scattering Albedos  $\omega$   
0 (black, completely absorbing) to 1 (white, completely scattering)



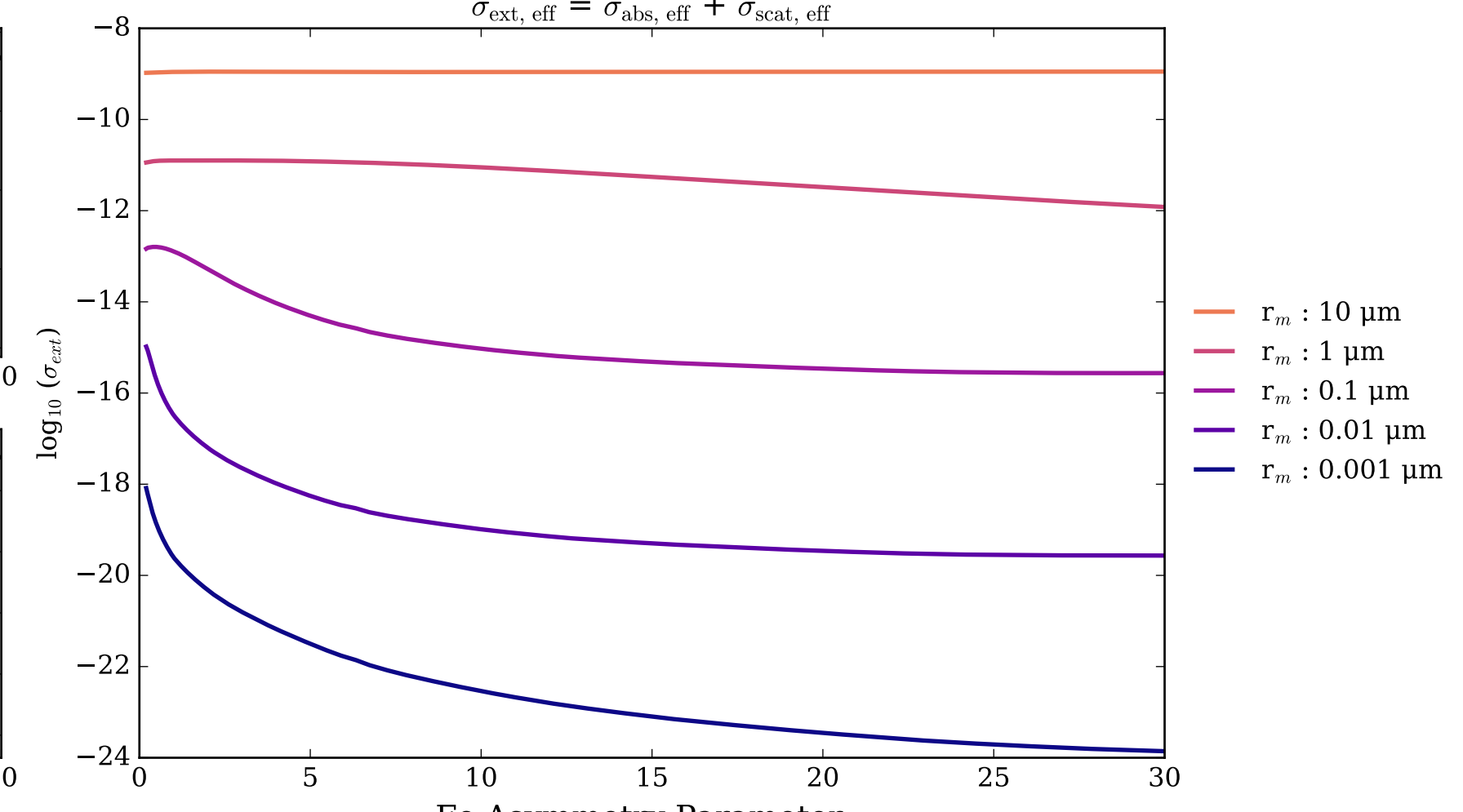
ExoHaze\_1000xSolar\_400K Asymmetry Parameter  $g$   
0 (Rayleigh Limit) to 1 (Total Forward Scattering)



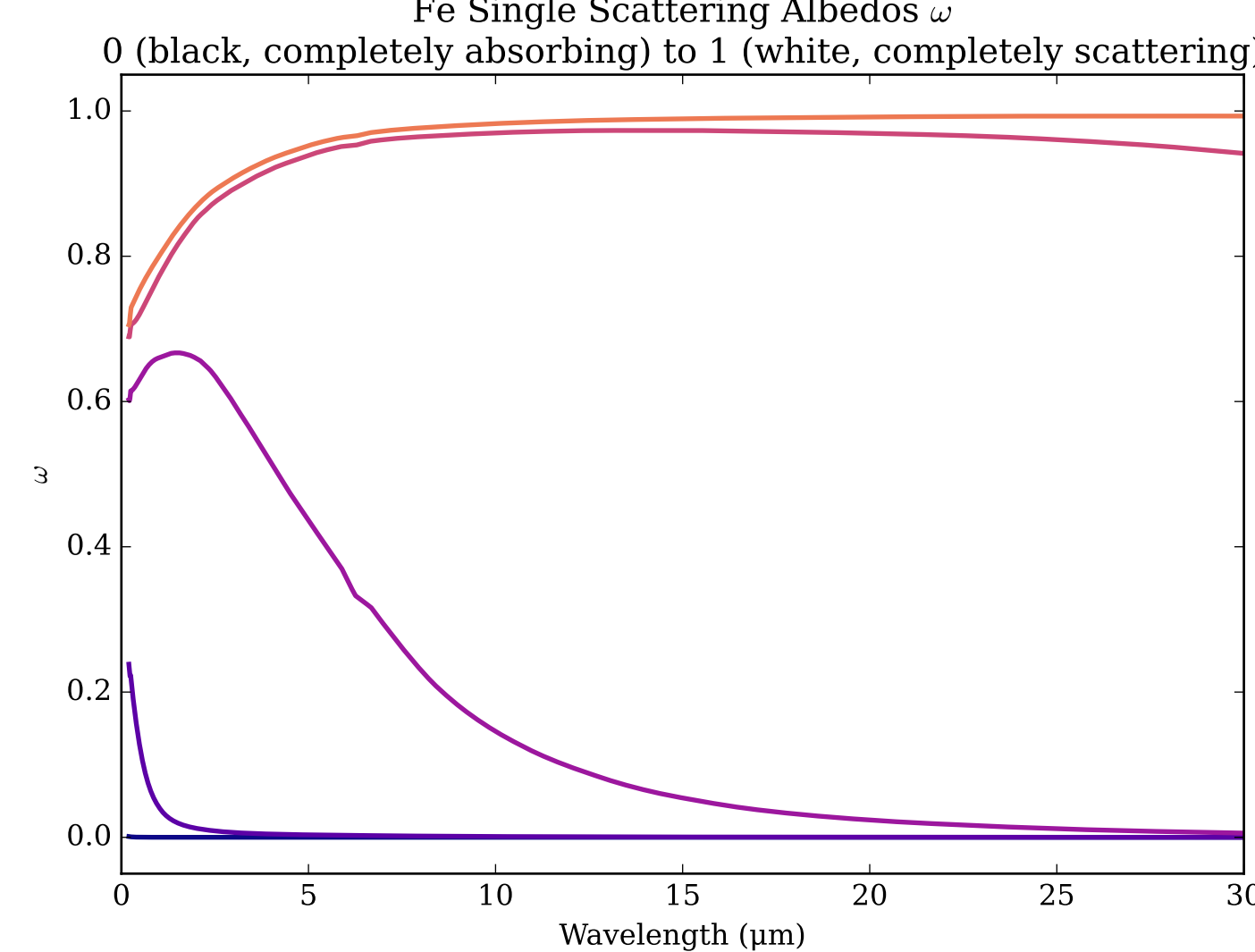
Refractive Indices for Fe  
(0.2, 30.0)  $\mu\text{m}$



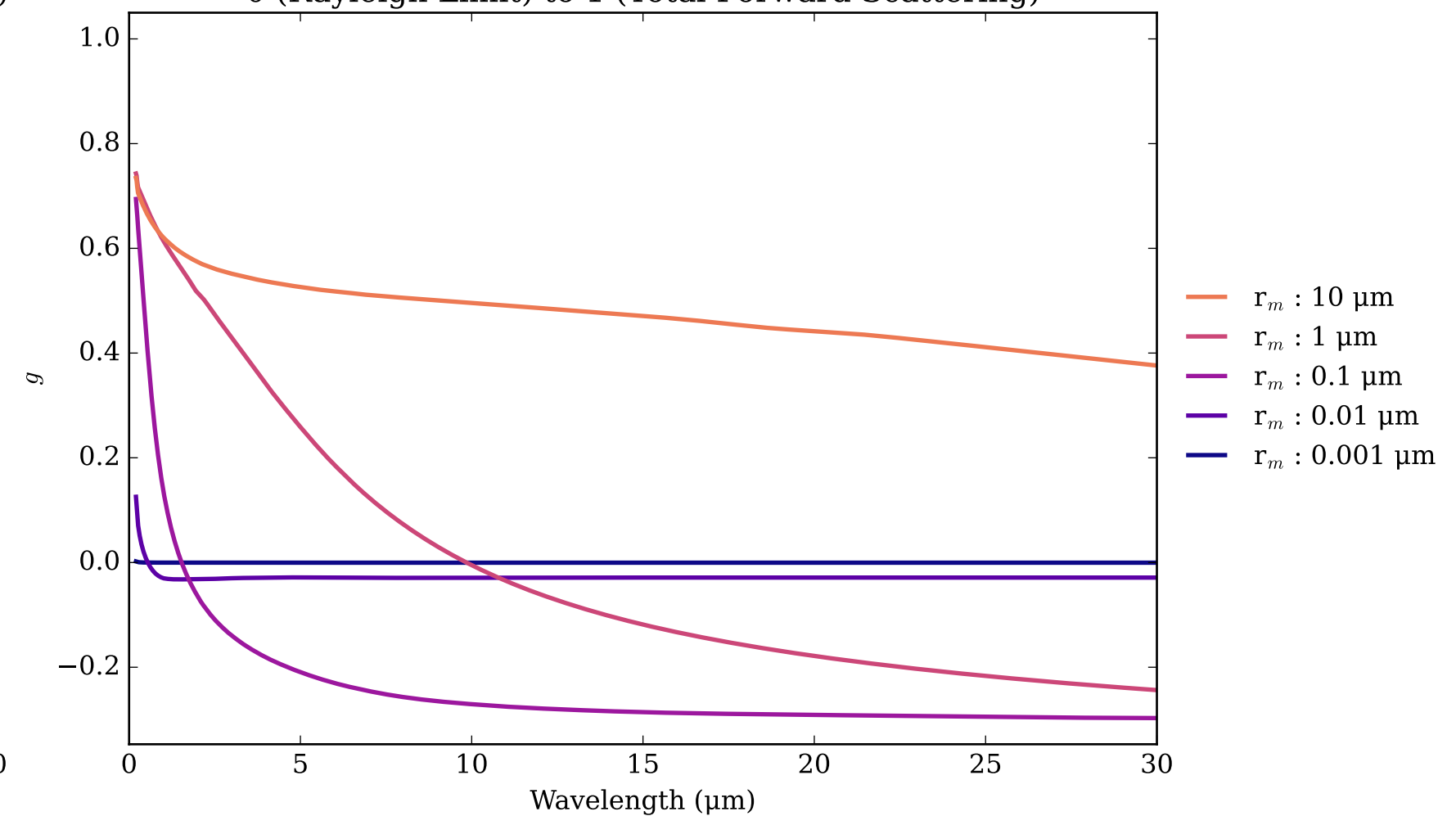
Fe Effective Extinction Cross Section



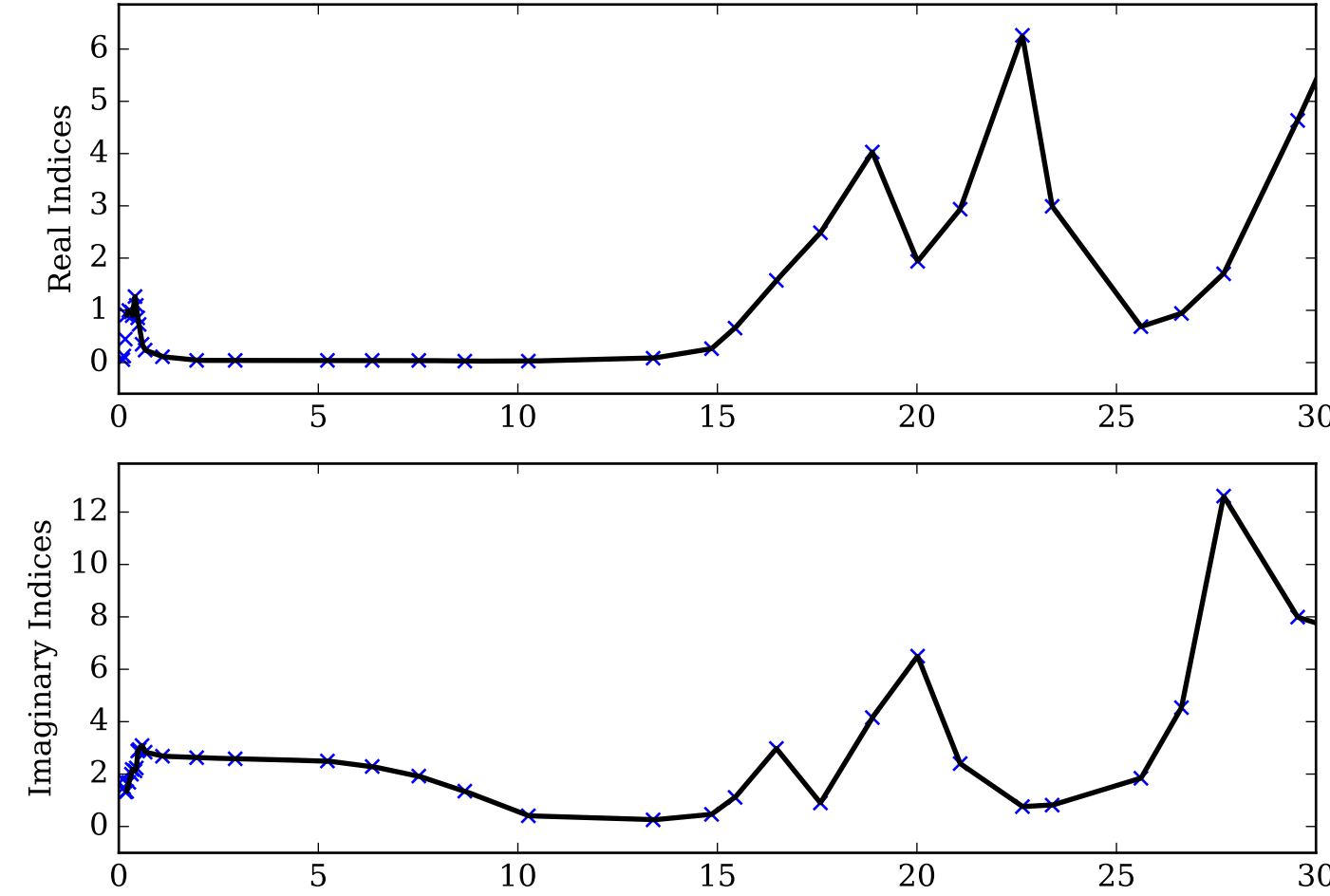
Fe Single Scattering Albedos  $\omega$



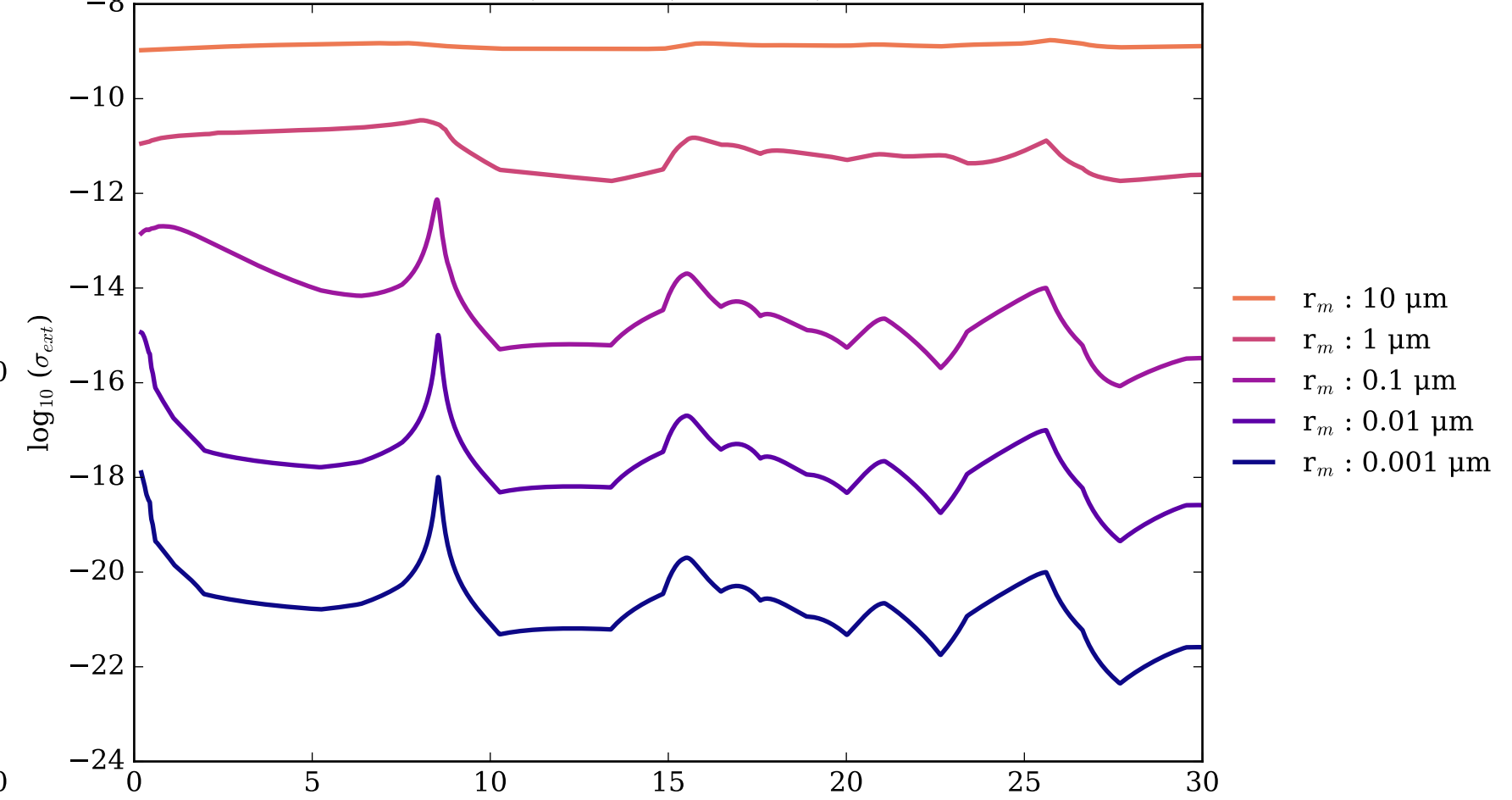
Fe Asymmetry Parameter  $g$



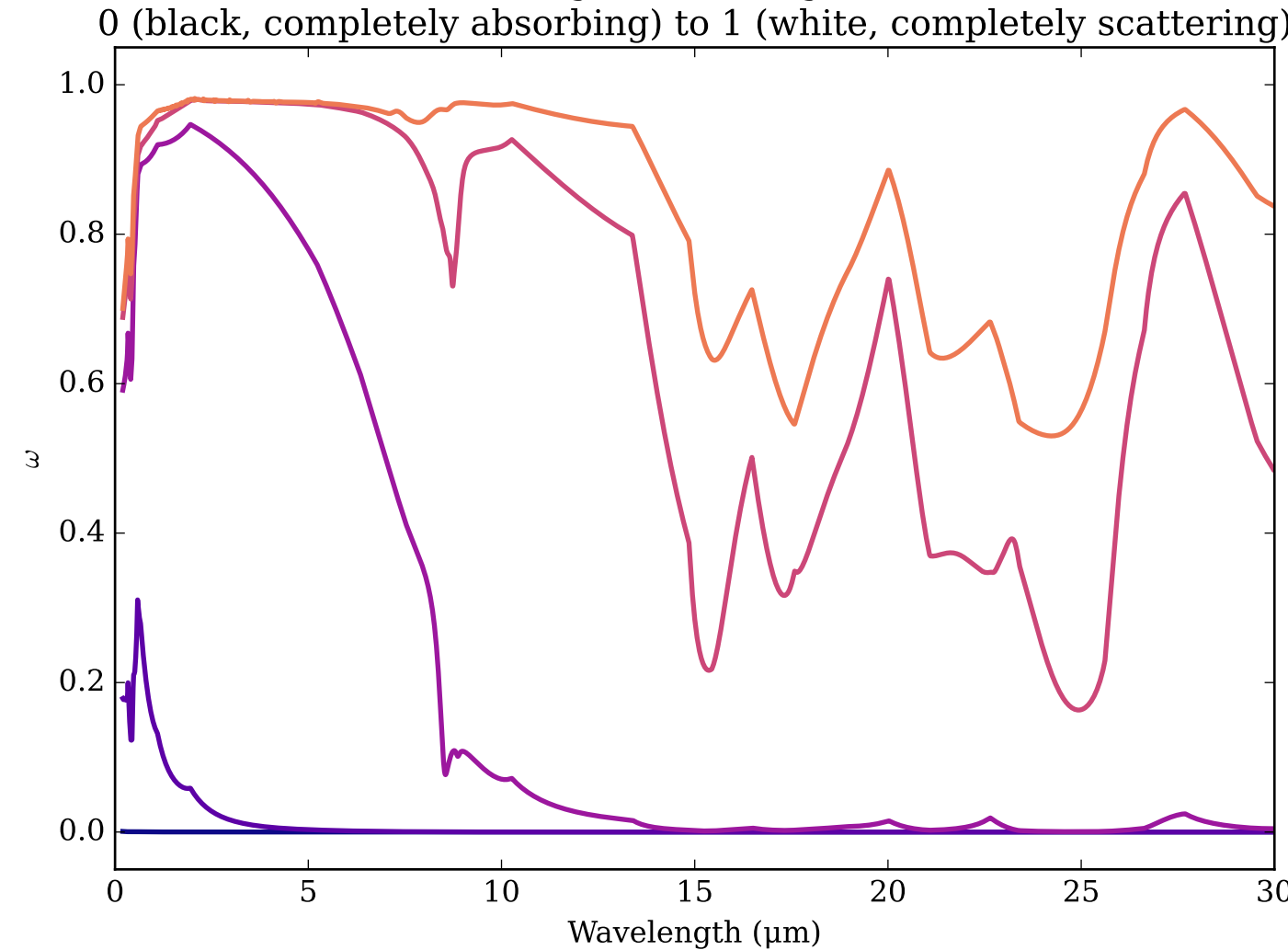
Refractive Indices for Fe<sub>2</sub>O<sub>3</sub>  
(0.2, 30.0)  $\mu\text{m}$



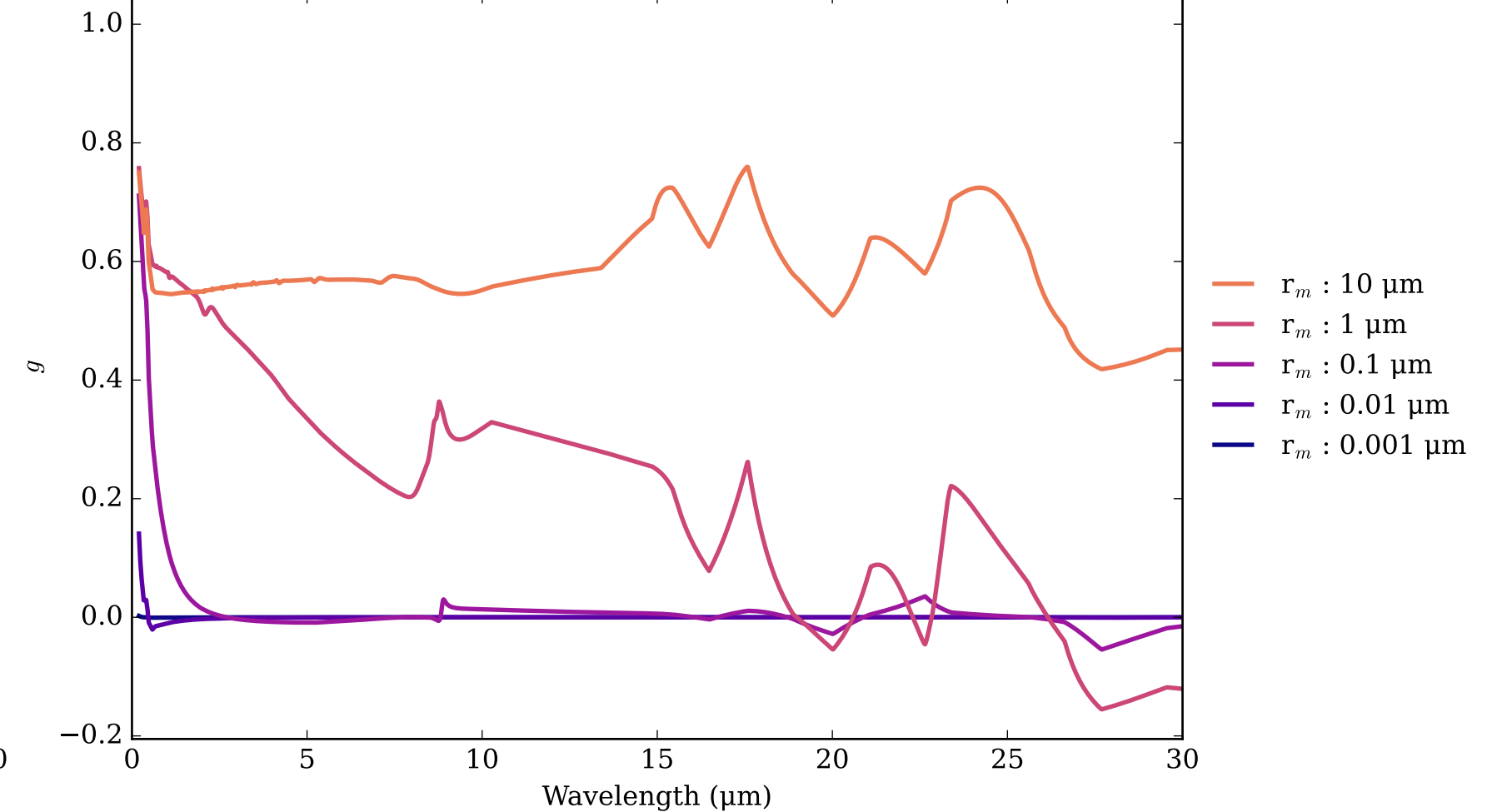
Fe<sub>2</sub>O<sub>3</sub> Effective Extinction Cross Section  
 $\sigma_{\text{ext, eff}} = \sigma_{\text{abs, eff}} + \sigma_{\text{scat, eff}}$



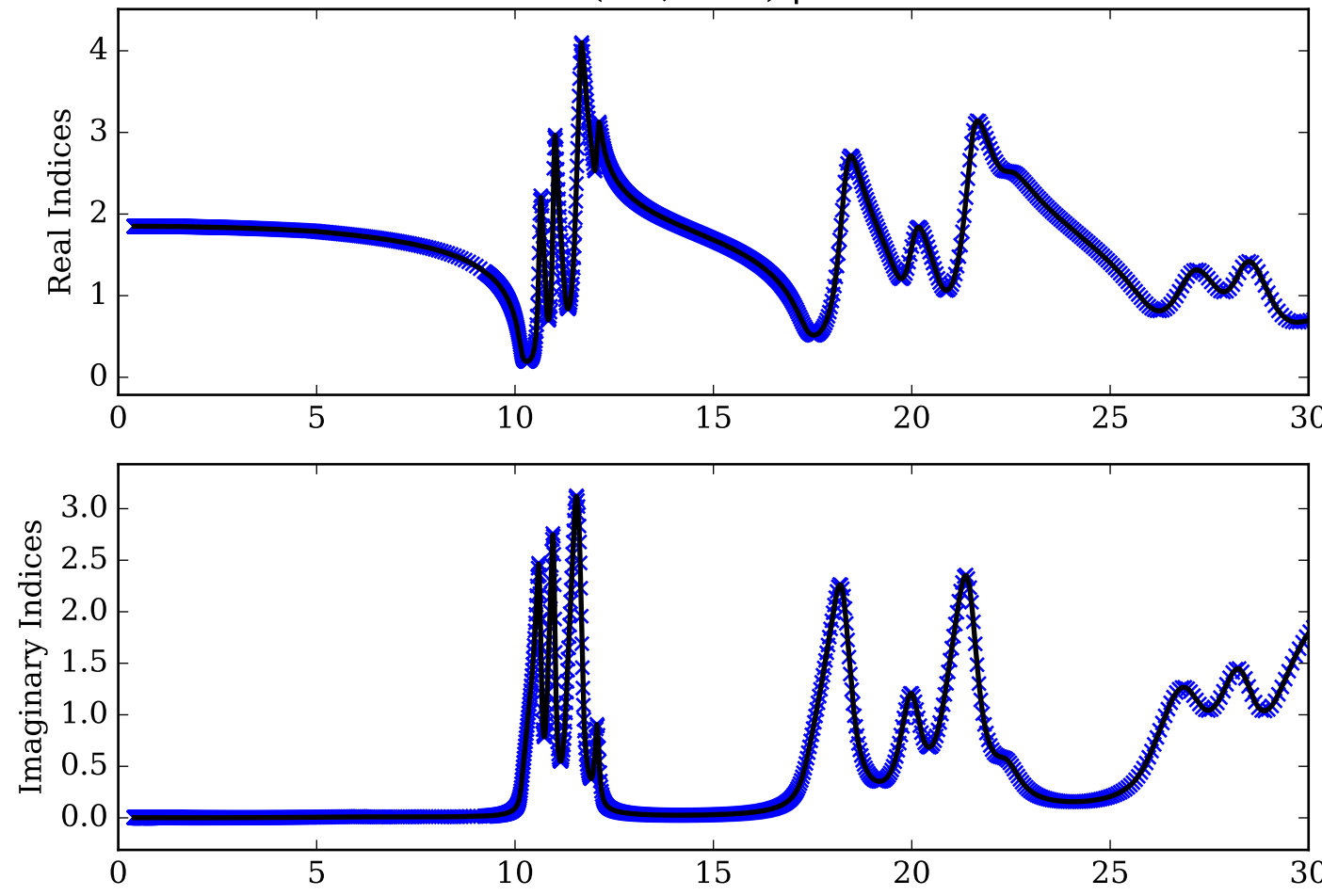
Fe<sub>2</sub>O<sub>3</sub> Single Scattering Albedos  $\omega$



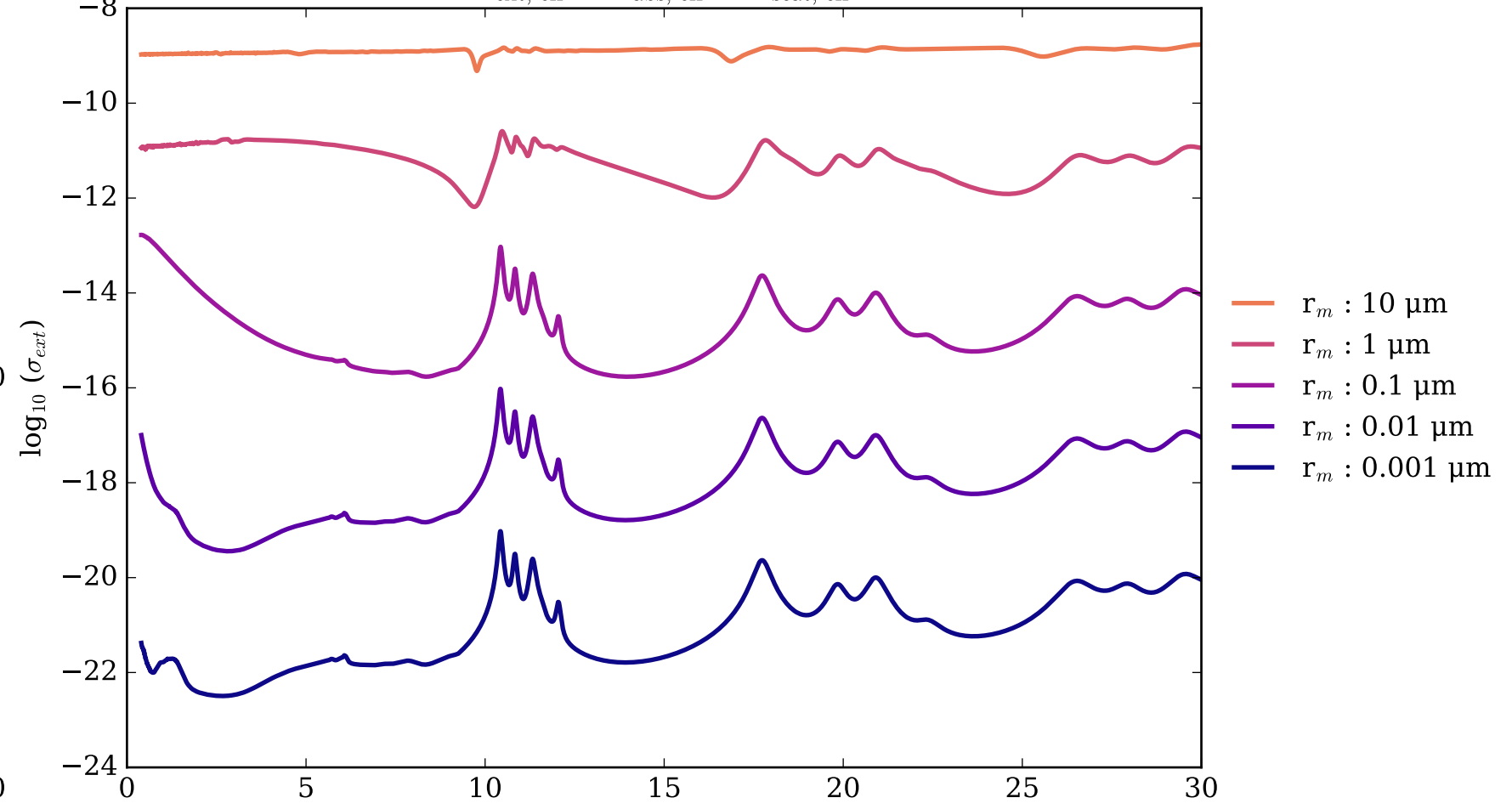
Fe<sub>2</sub>O<sub>3</sub> Asymmetry Parameter  $g$   
0 (Rayleigh Limit) to 1 (Total Forward Scattering)



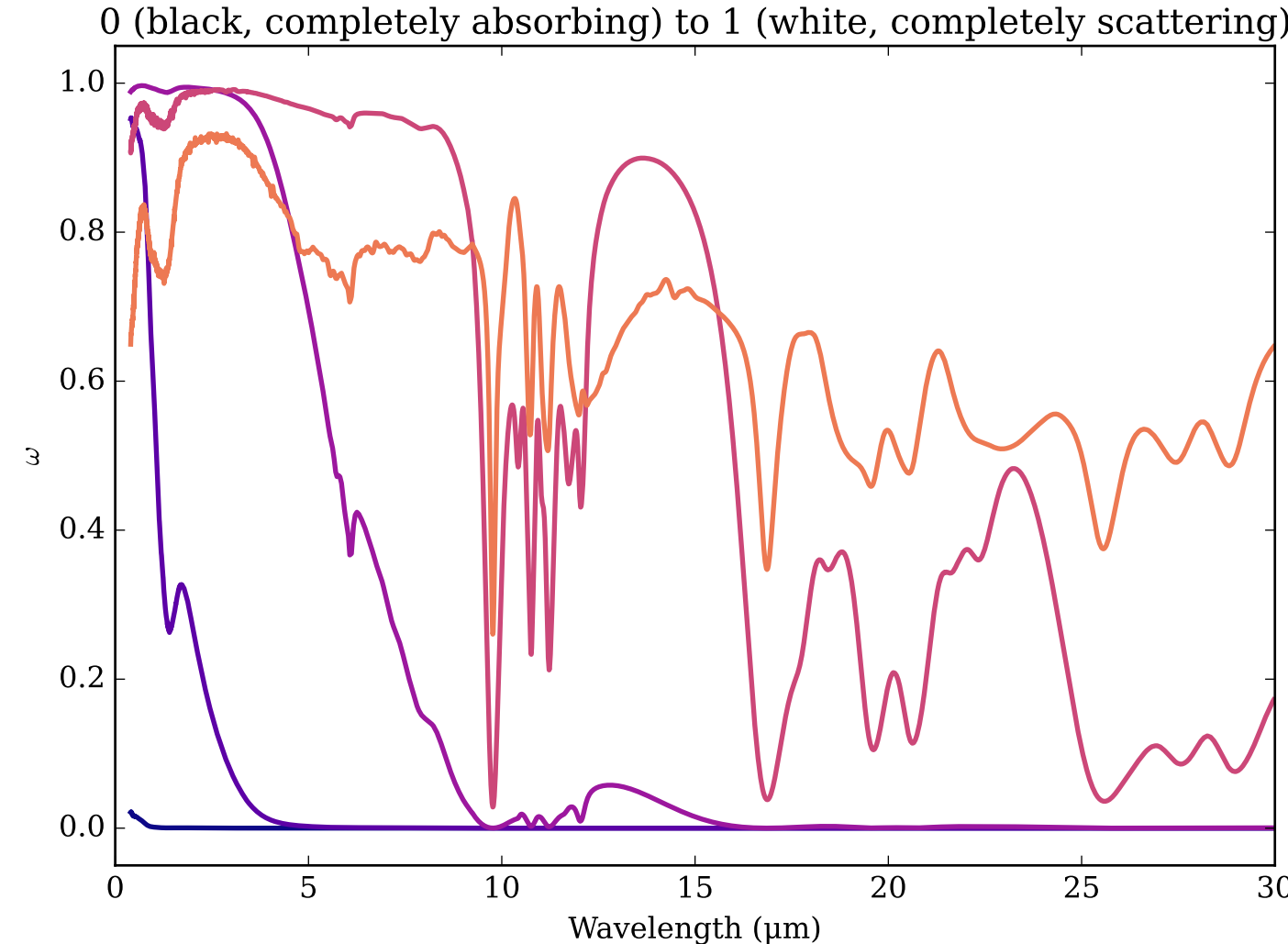
Refractive Indices for Fe<sub>2</sub>SiO<sub>4</sub>  
(0.4, 30.0)  $\mu\text{m}$



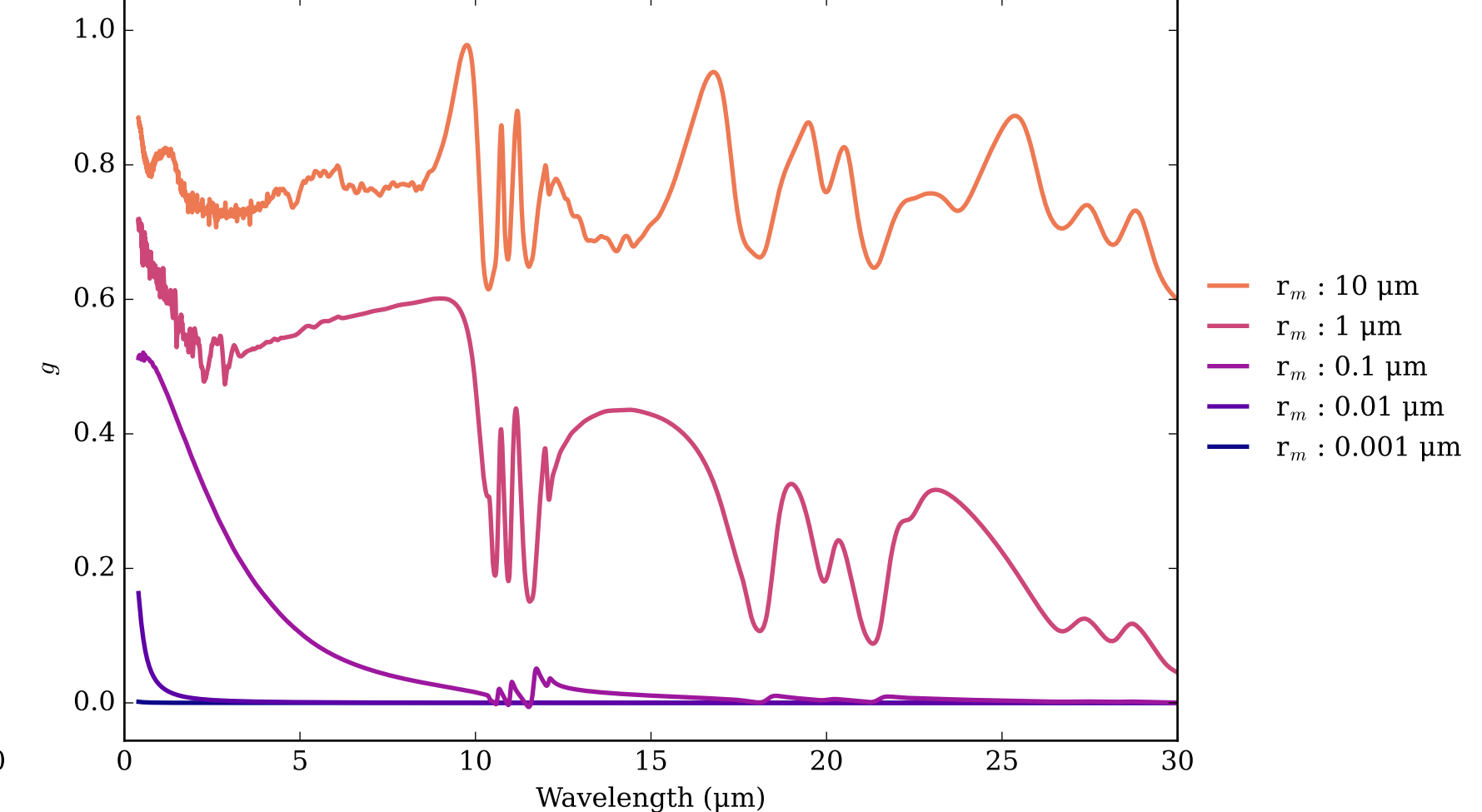
Fe<sub>2</sub>SiO<sub>4</sub>\_KH Effective Extinction Cross Section  
 $\sigma_{\text{ext, eff}} = \sigma_{\text{abs, eff}} + \sigma_{\text{scat, eff}}$



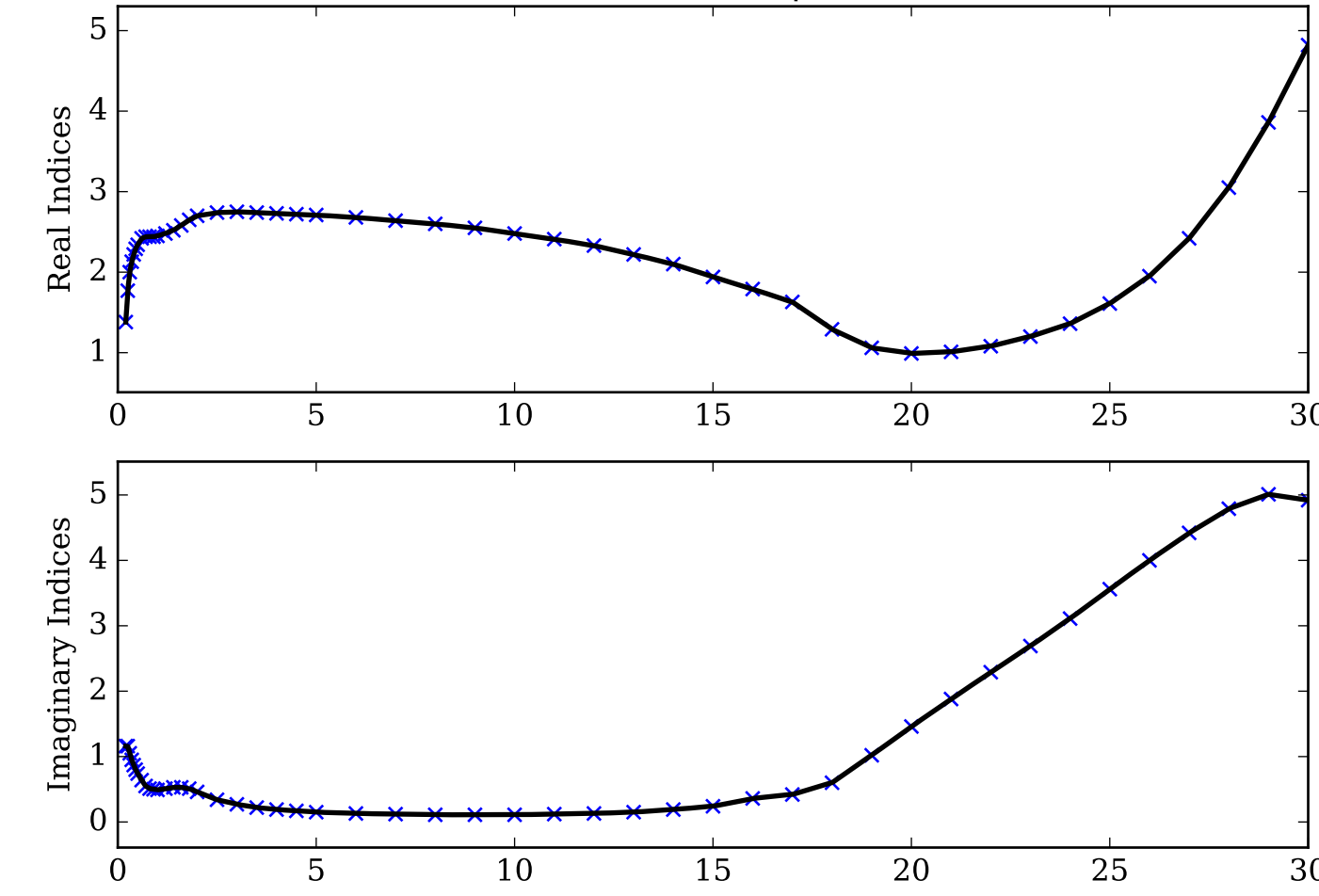
Fe<sub>2</sub>SiO<sub>4</sub>\_KH Single Scattering Albedos  $\omega$



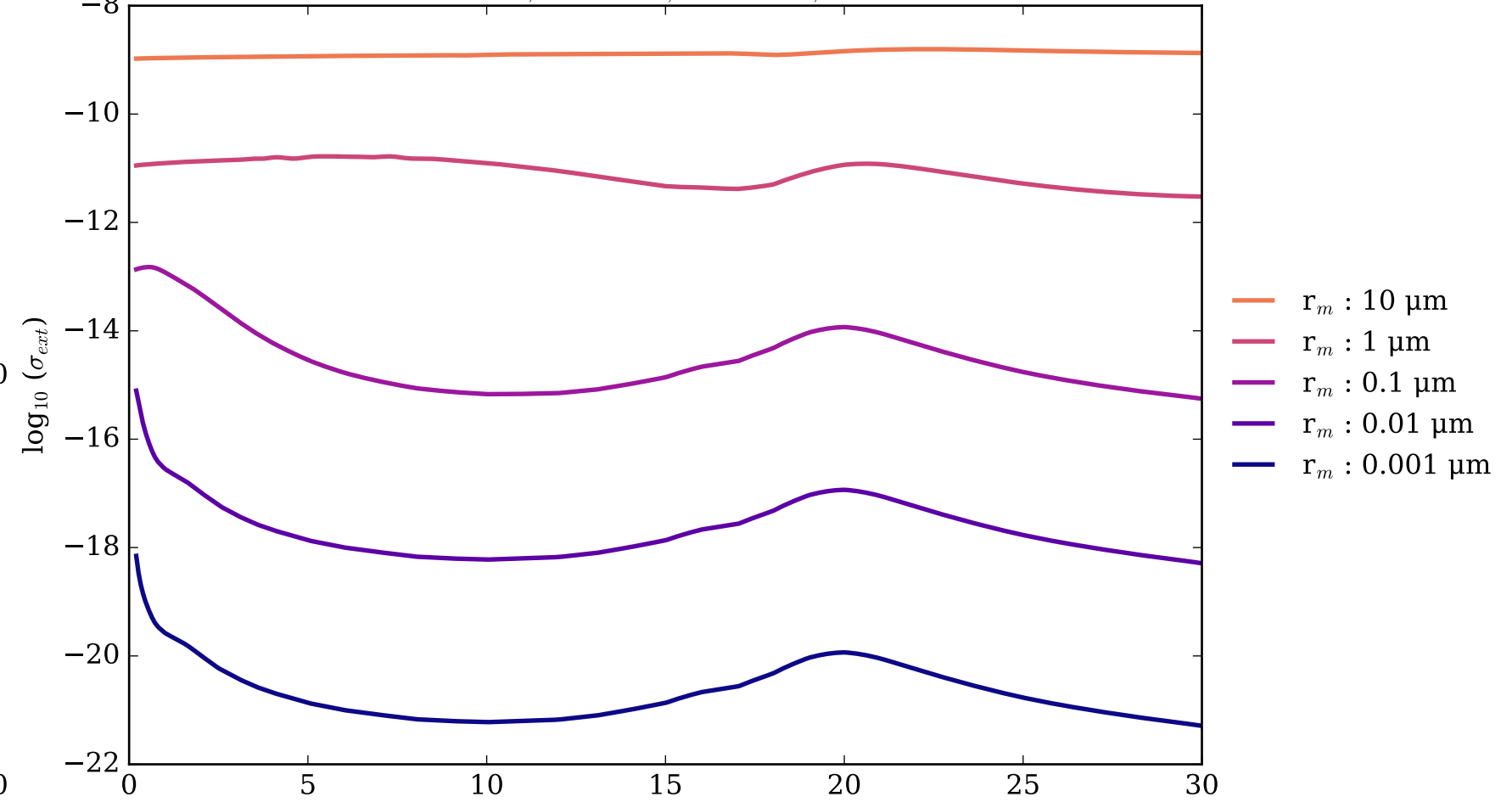
Fe<sub>2</sub>SiO<sub>4</sub>\_KH Asymmetry Parameter  $g$   
0 (Rayleigh Limit) to 1 (Total Forward Scattering)



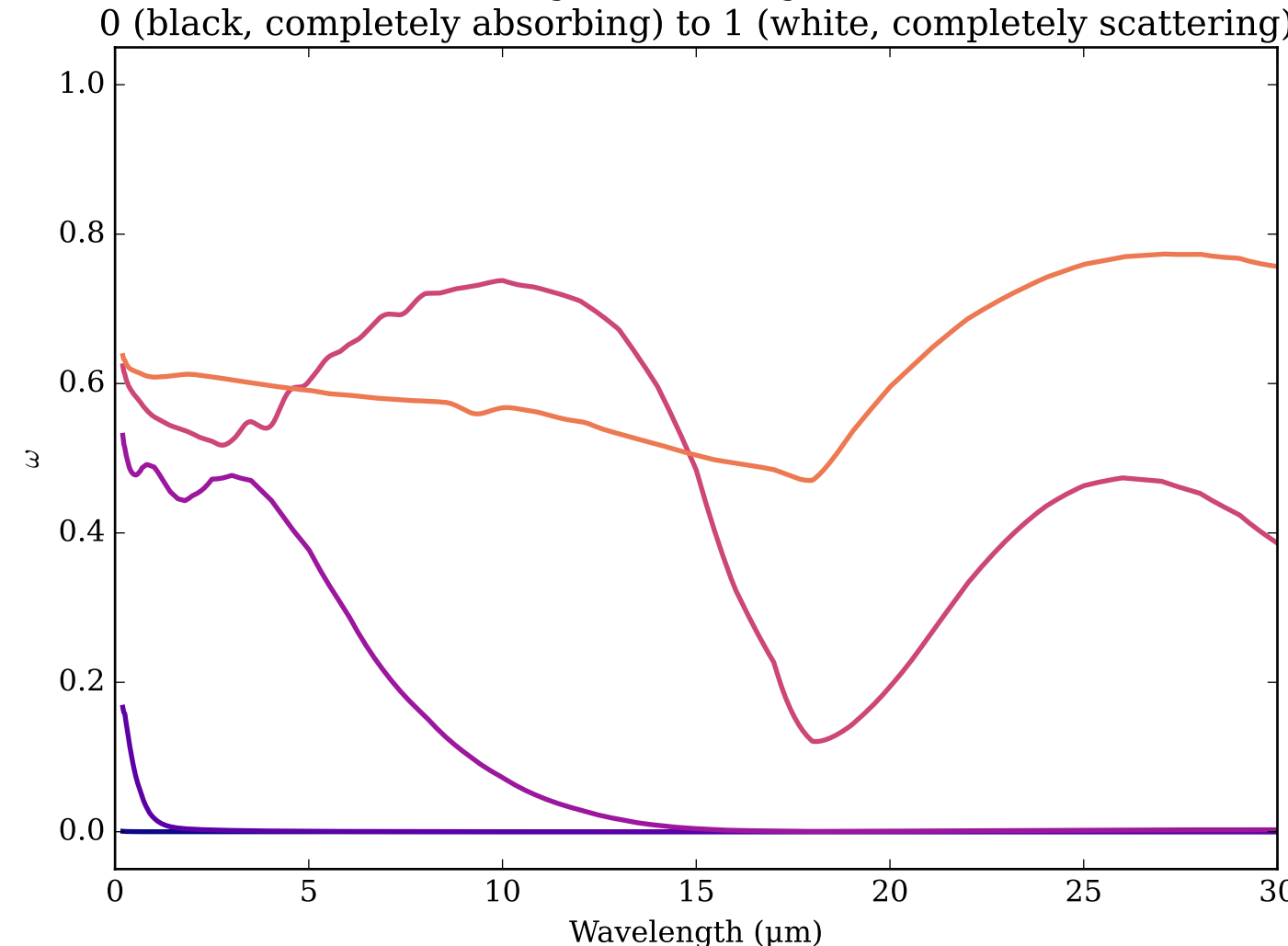
Refractive Indices for FeO  
(0.2, 30.0)  $\mu\text{m}$



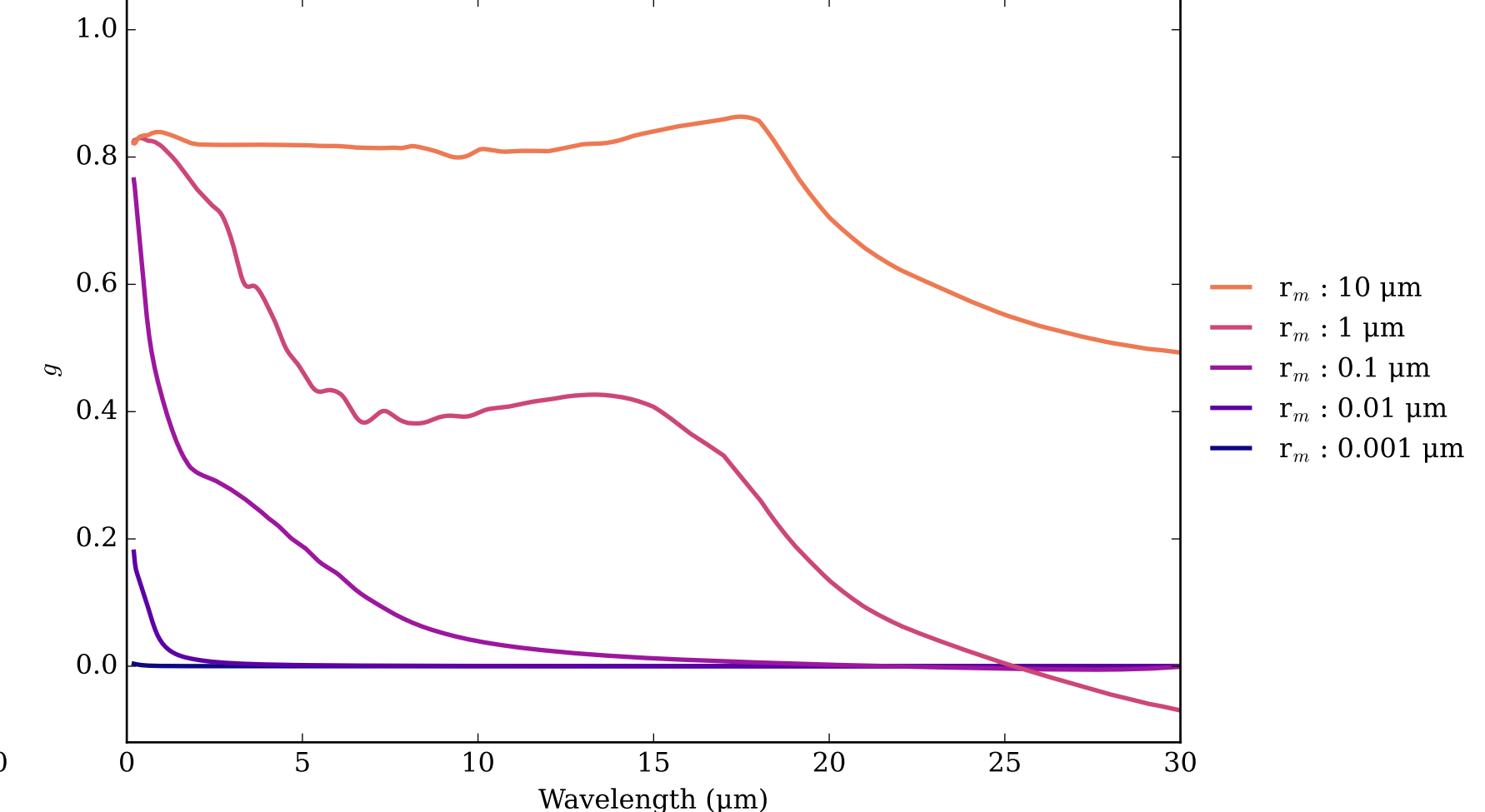
FeO Effective Extinction Cross Section  
 $\sigma_{\text{ext, eff}} = \sigma_{\text{abs, eff}} + \sigma_{\text{scat, eff}}$



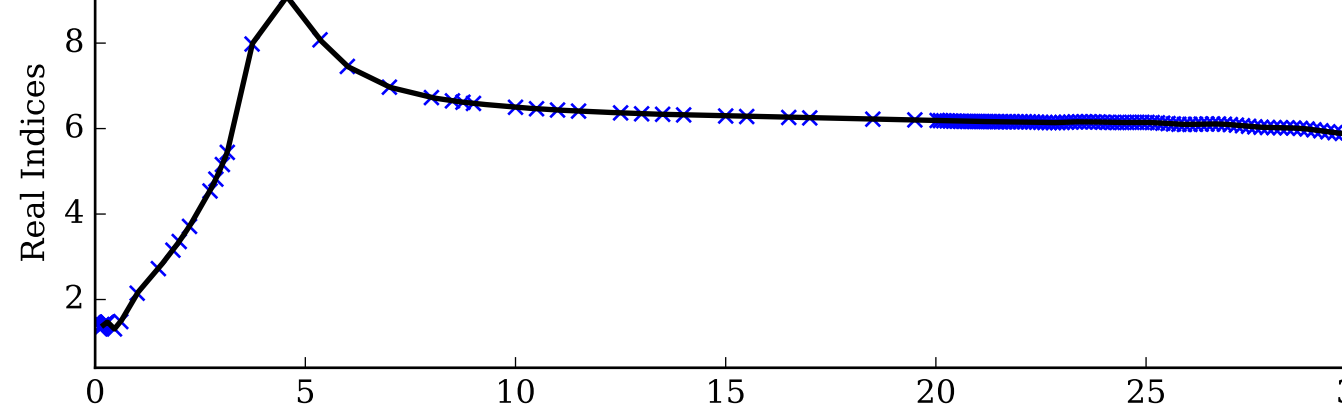
FeO Single Scattering Albedos  $\omega$



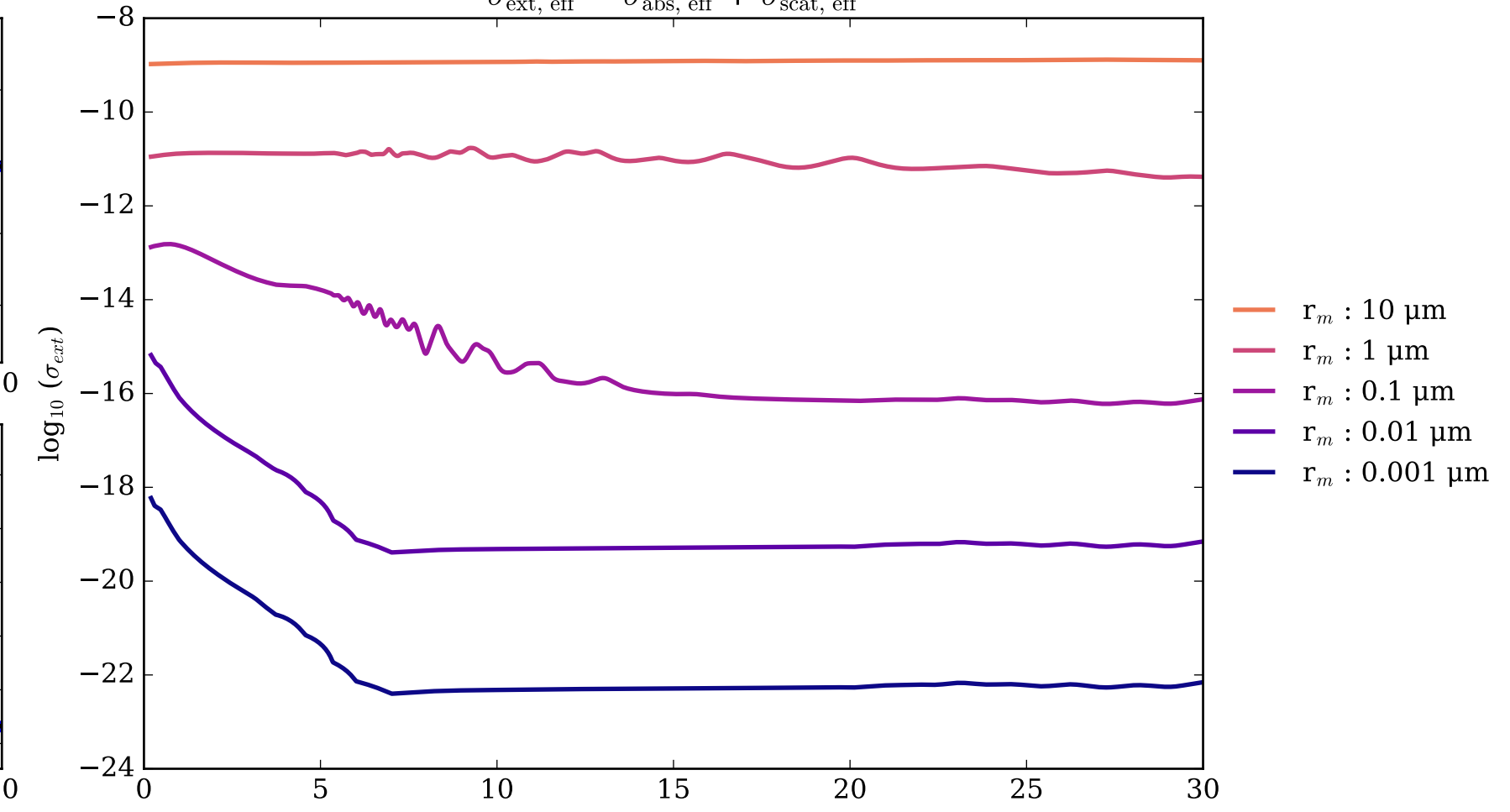
FeO Asymmetry Parameter  $g$   
0 (Rayleigh Limit) to 1 (Total Forward Scattering)



Refractive Indices for FeS  
(0.2, 30.0)  $\mu\text{m}$

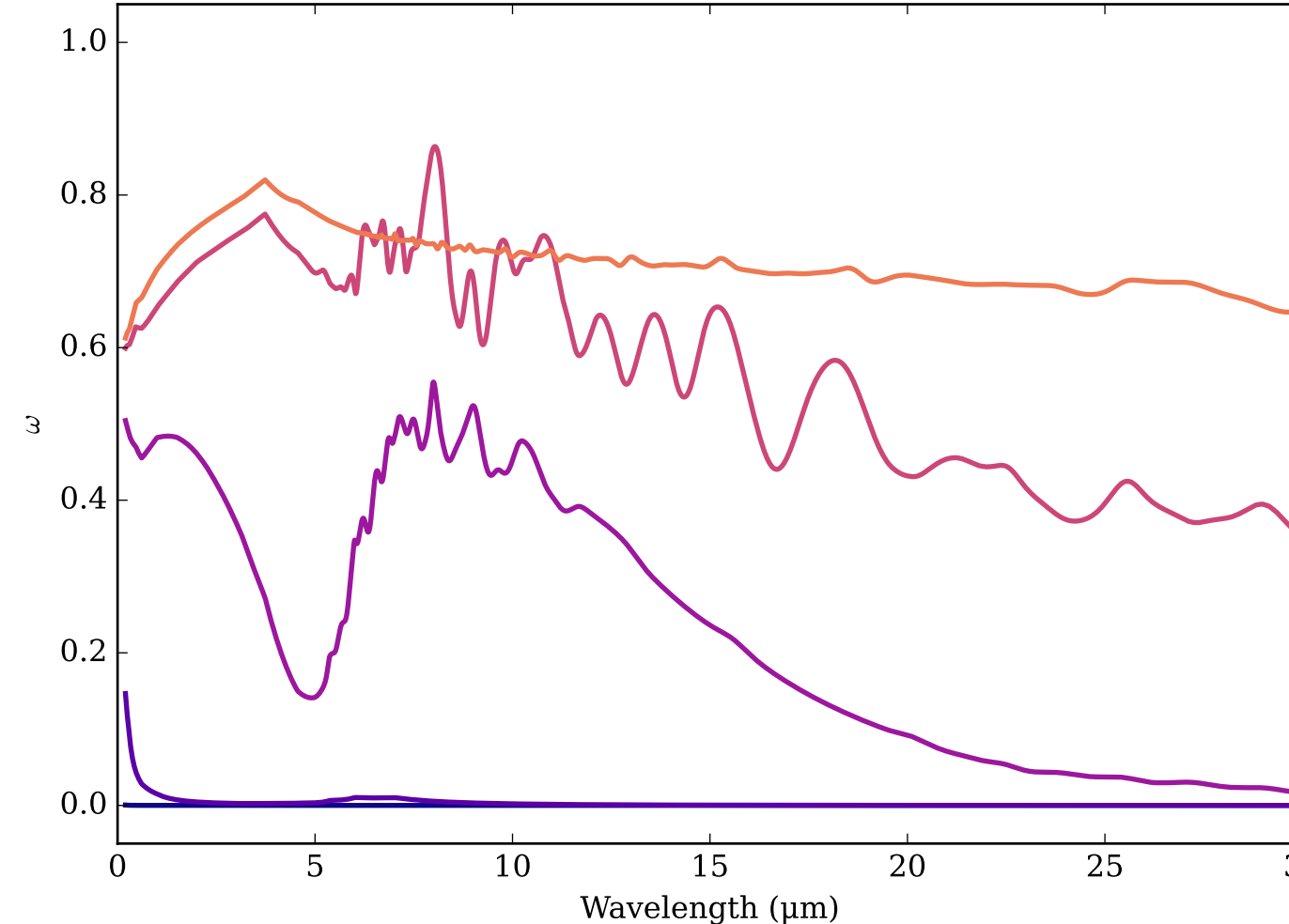


FeS Effective Extinction Cross Section  
 $\sigma_{\text{ext, eff}} = \sigma_{\text{abs, eff}} + \sigma_{\text{scat, eff}}$



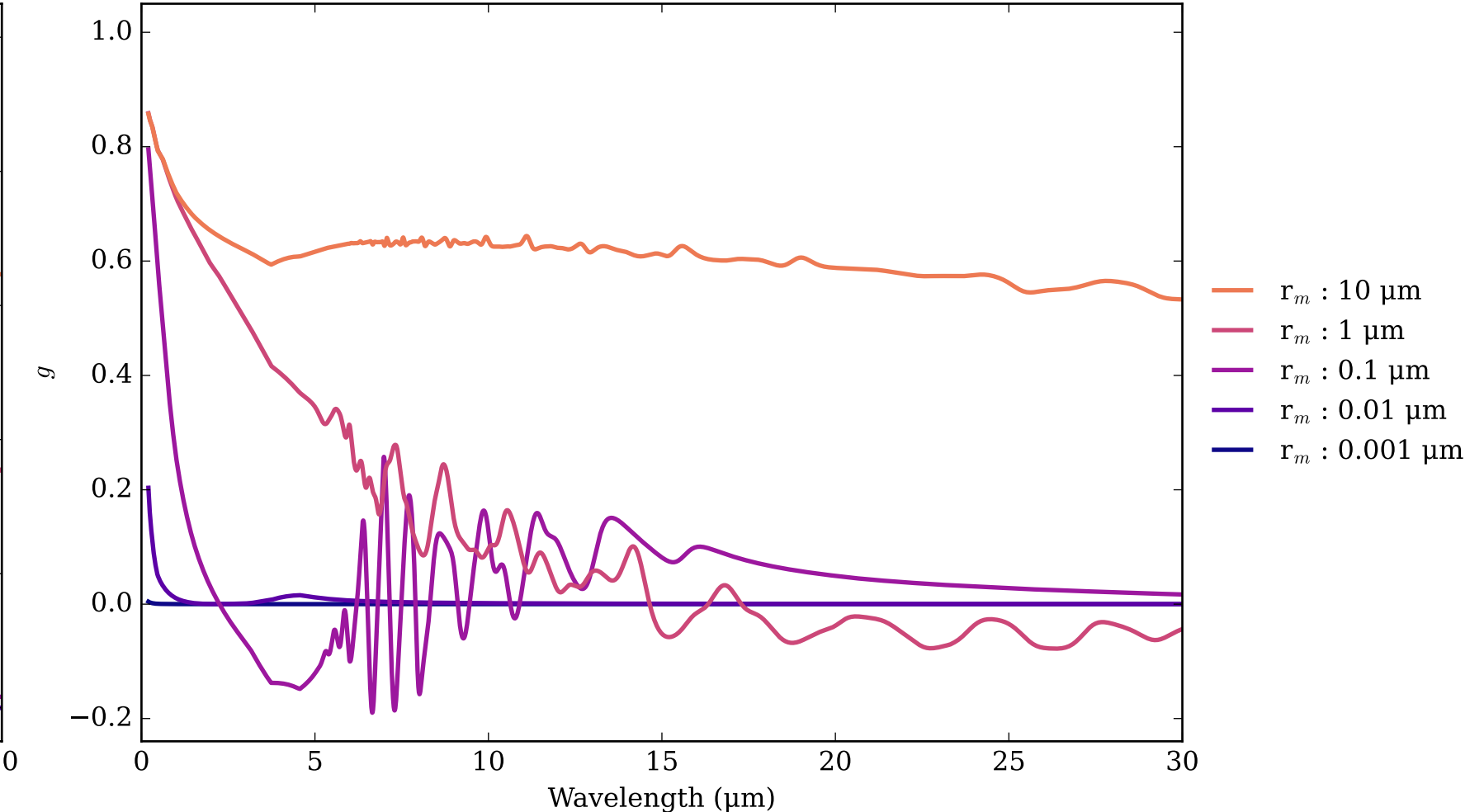
FeS Single Scattering Albedos  $\omega$

0 (black, completely absorbing) to 1 (white, completely scattering)

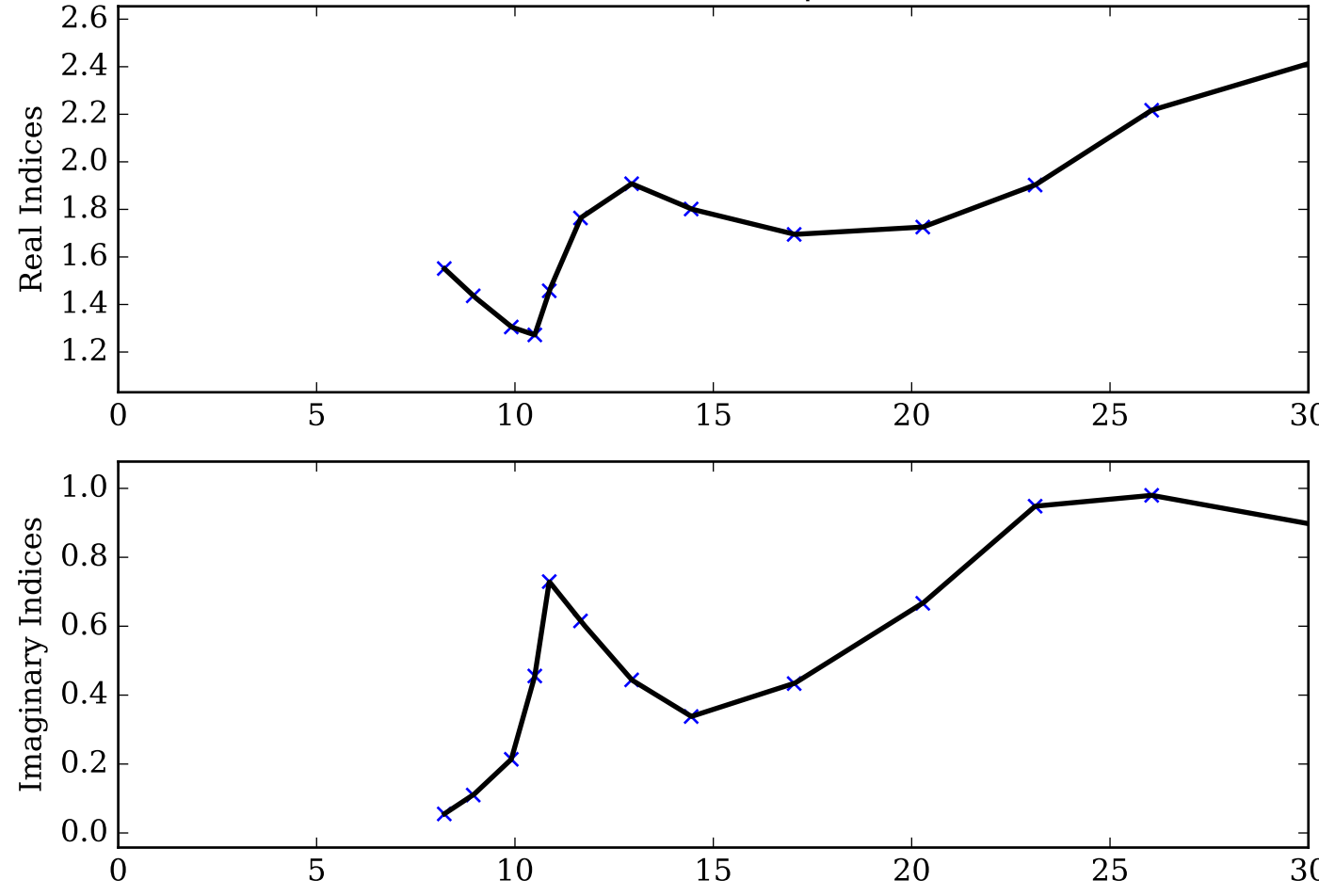


FeS Asymmetry Parameter  $g$

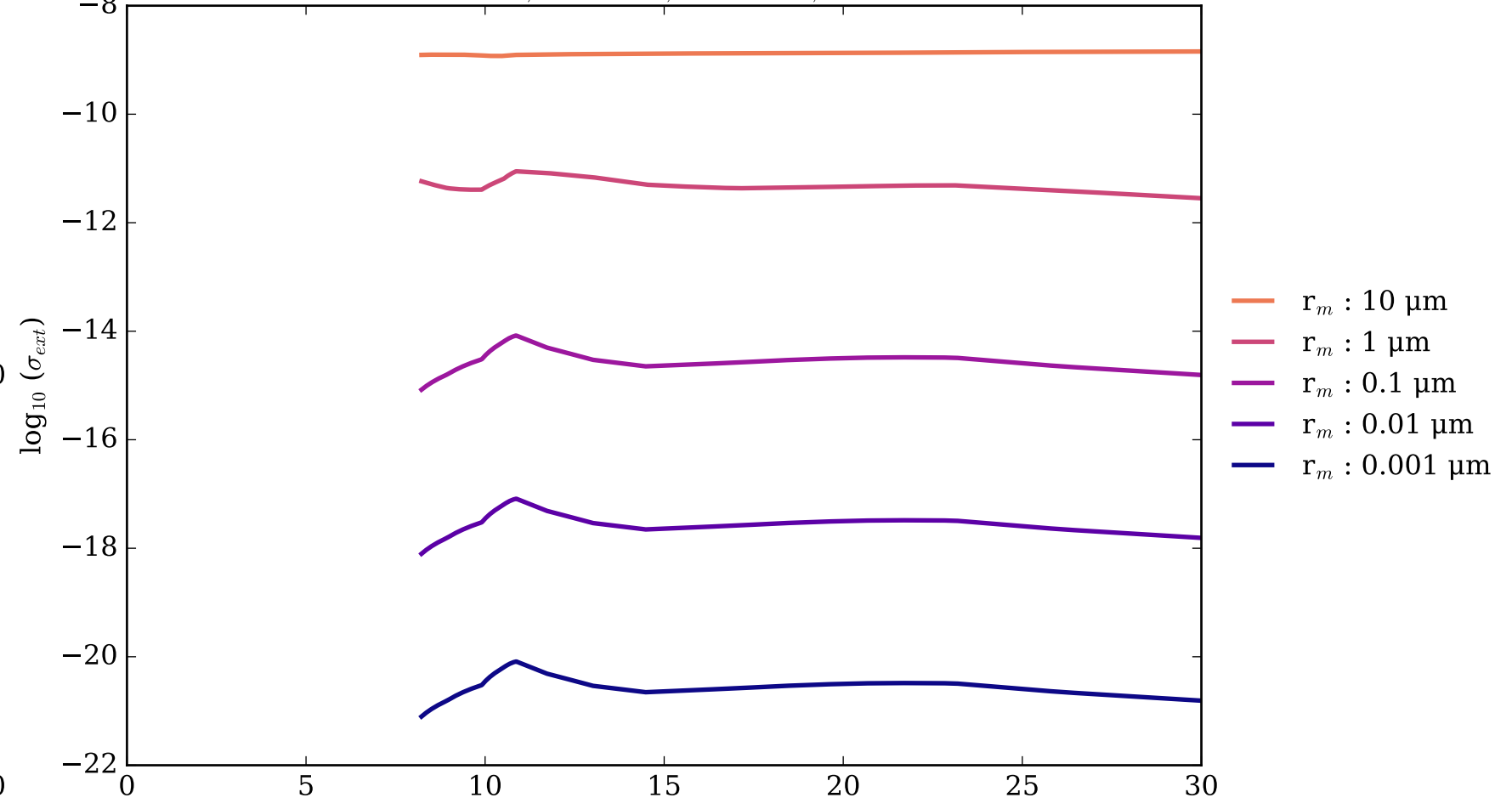
0 (Rayleigh Limit) to 1 (Total Forward Scattering)



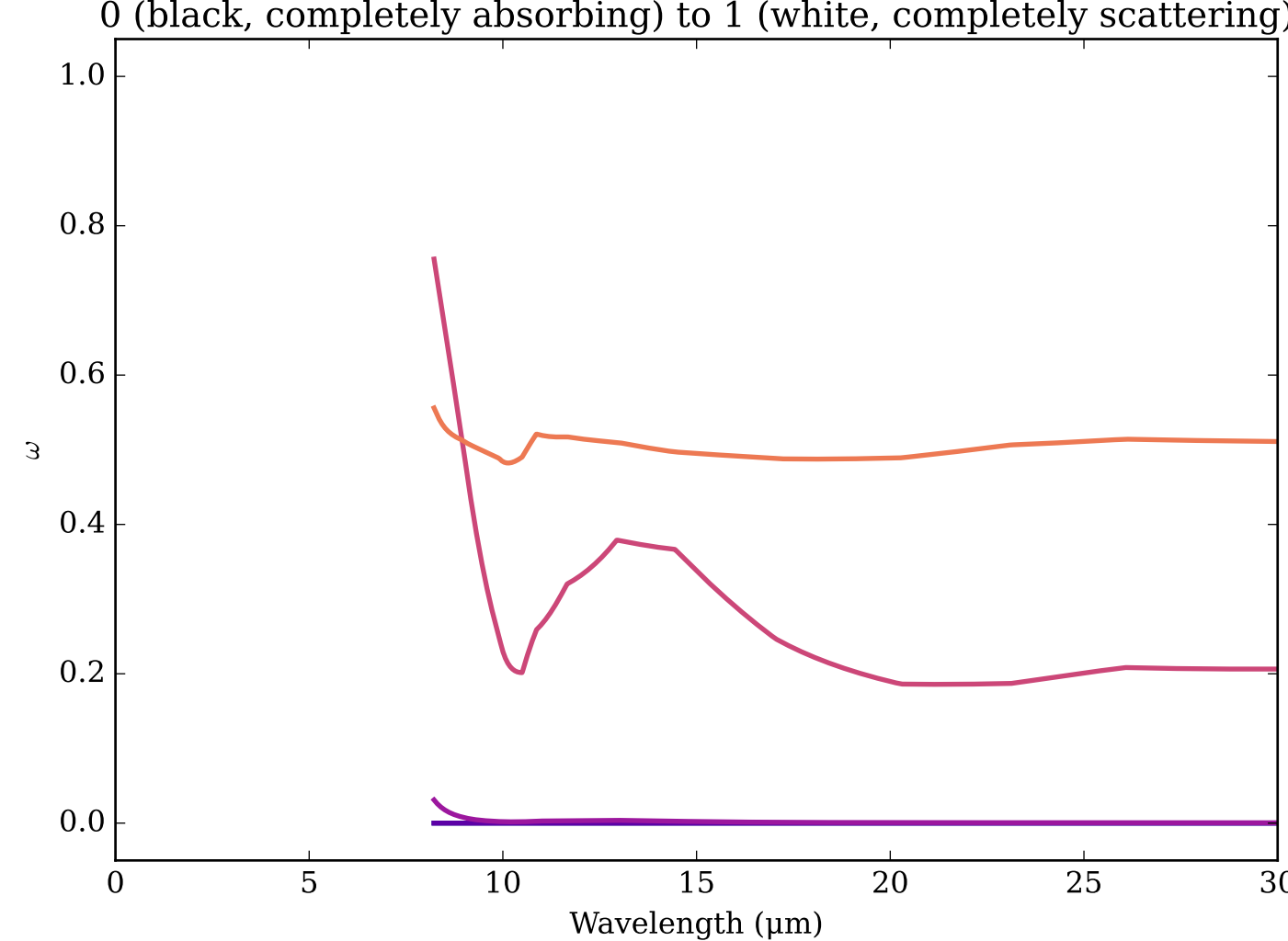
Refractive Indices for FeSiO<sub>3</sub>  
(8.22, 30.0)  $\mu\text{m}$



FeSiO<sub>3</sub> Effective Extinction Cross Section

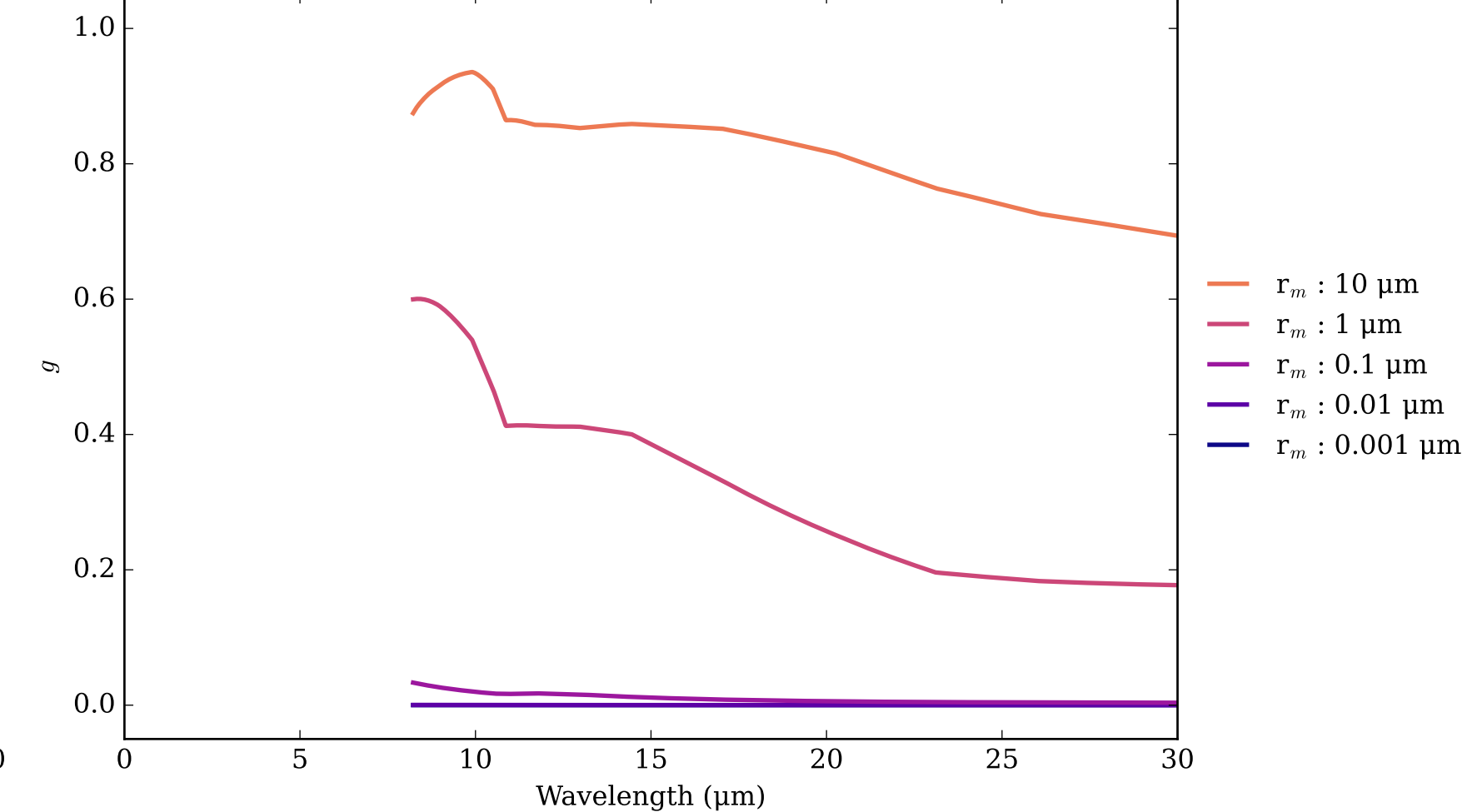


FeSiO<sub>3</sub> Single Scattering Albedos  $\omega$

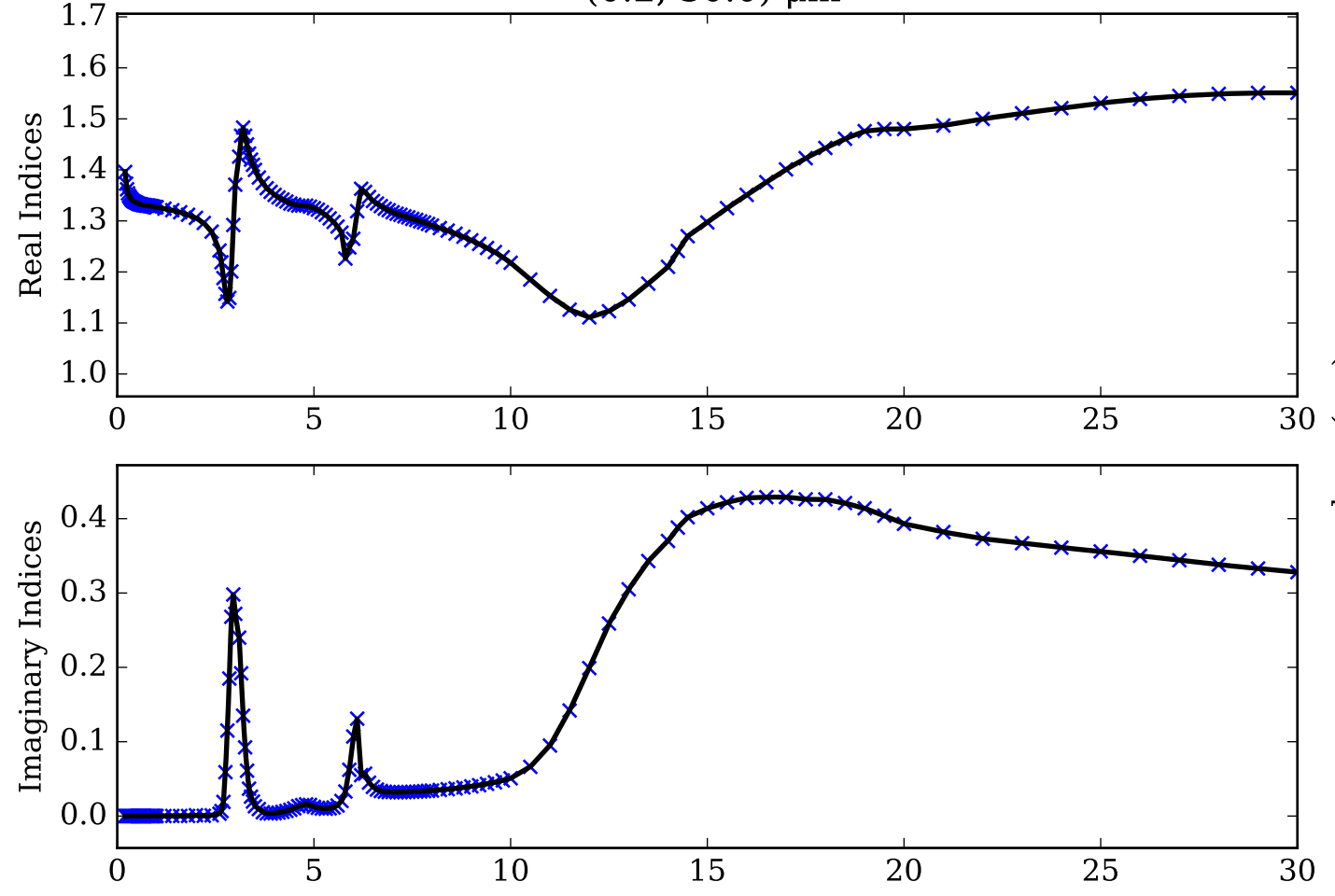


FeSiO<sub>3</sub> Asymmetry Parameter  $g$

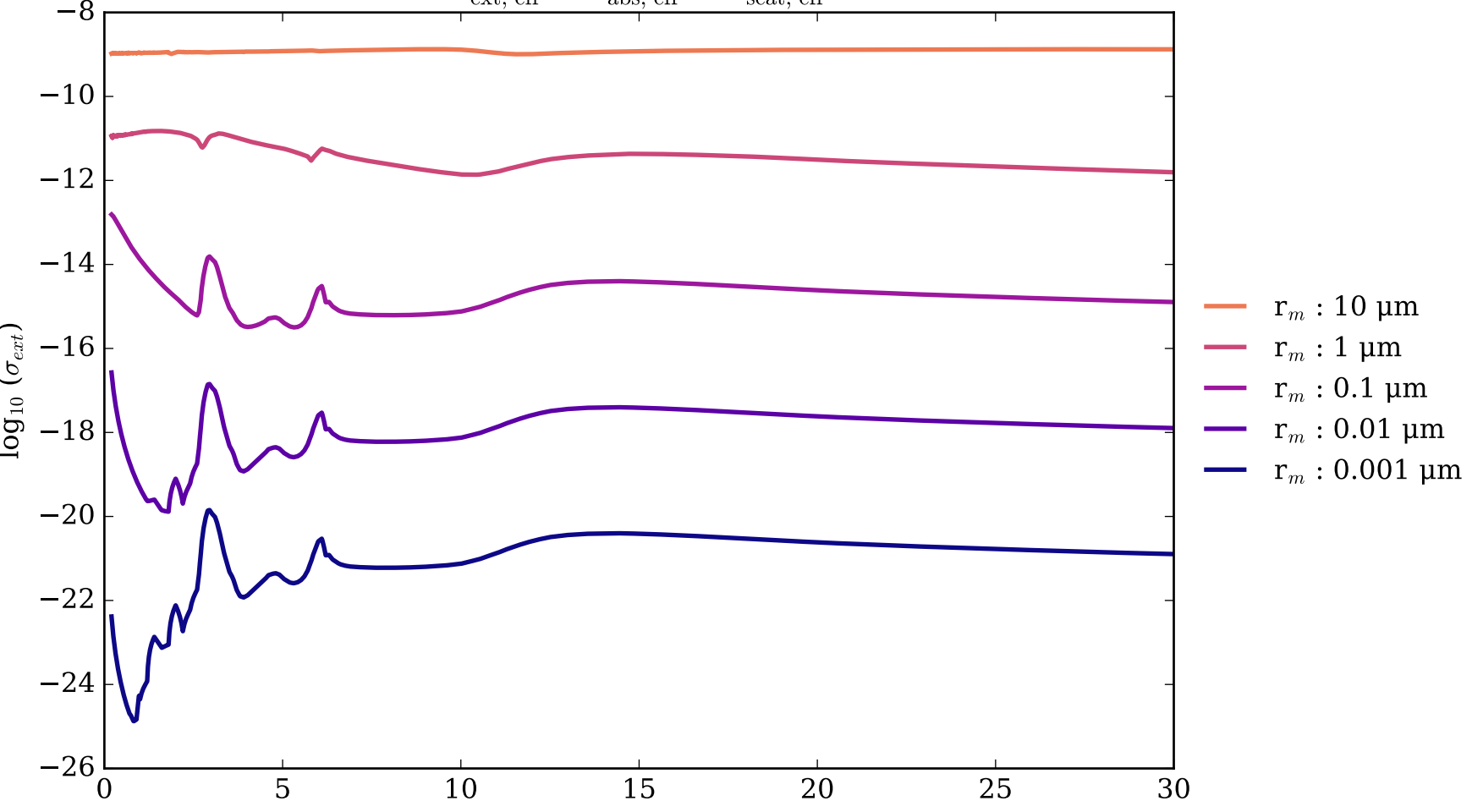
0 (Rayleigh Limit) to 1 (Total Forward Scattering)



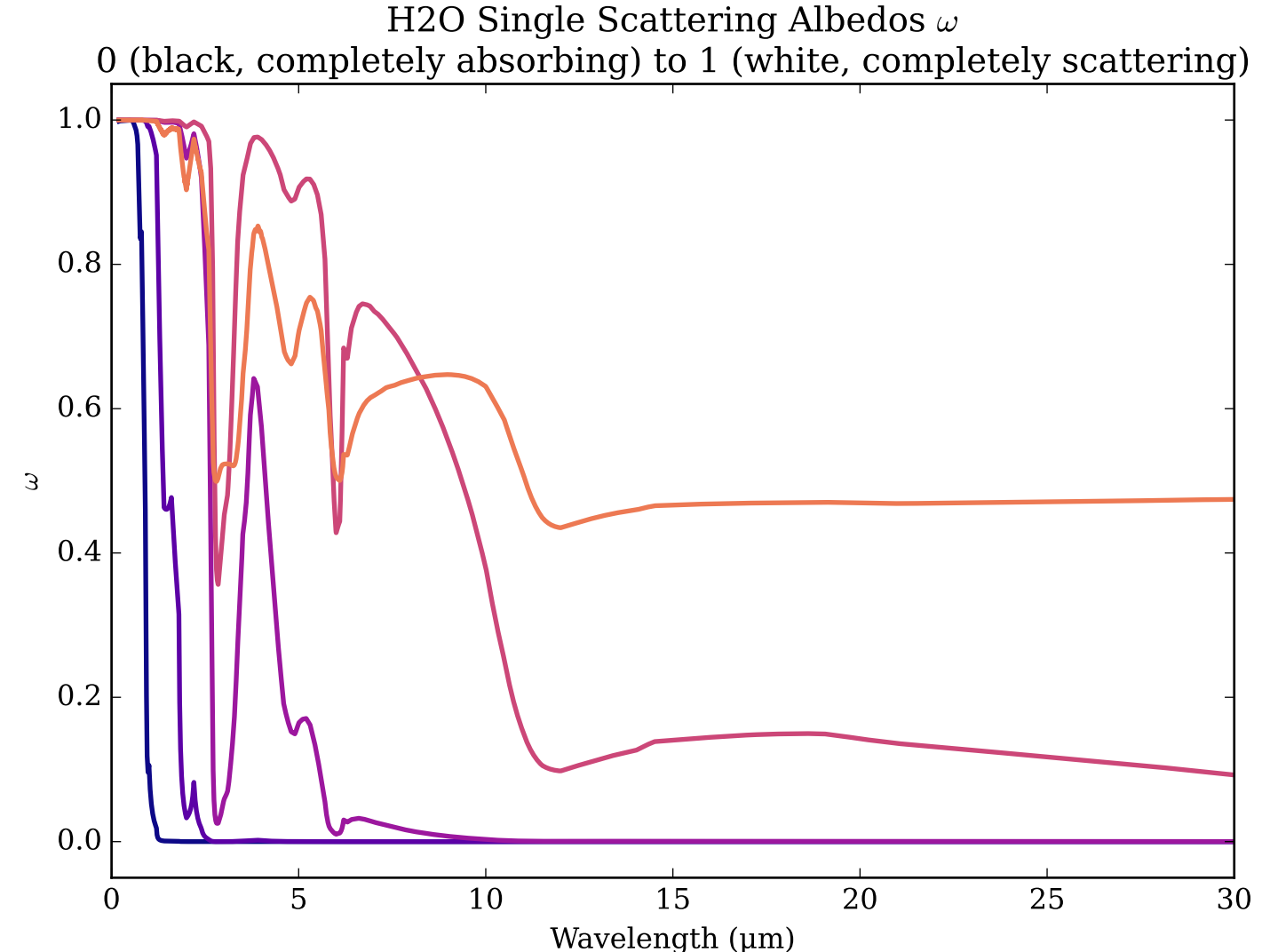
Refractive Indices for H<sub>2</sub>O  
(0.2, 30.0) μm



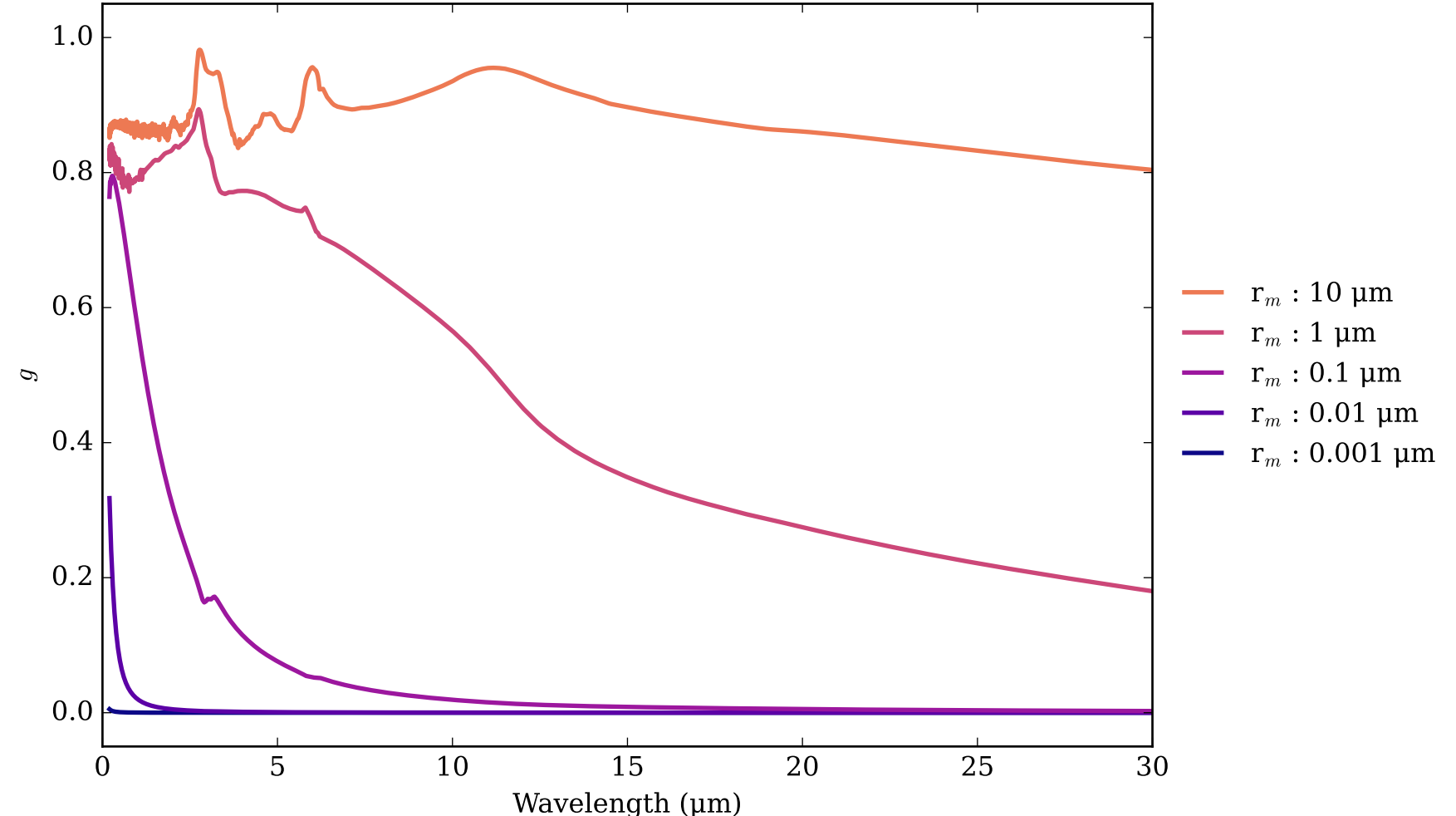
H<sub>2</sub>O Effective Extinction Cross Section



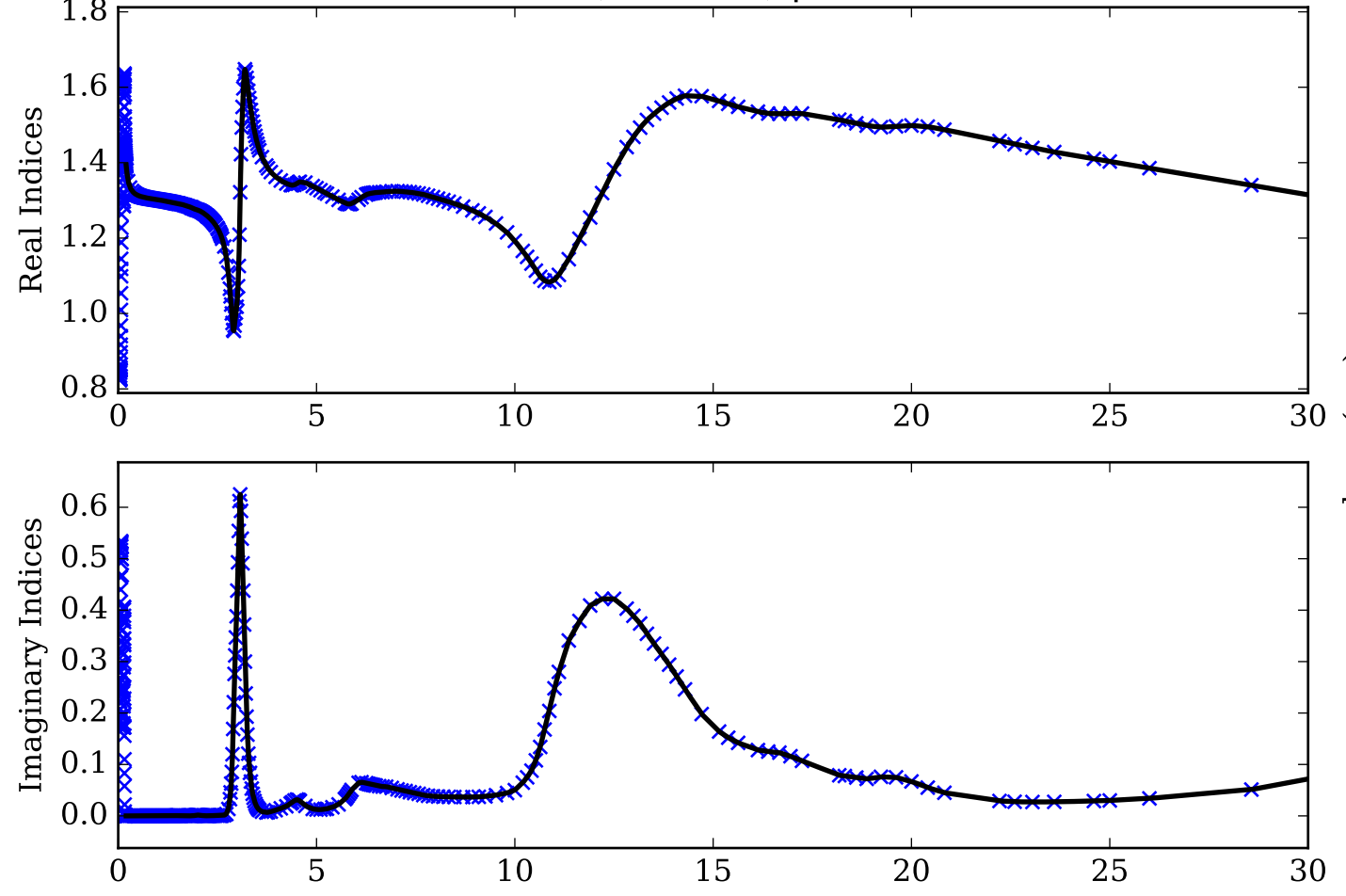
H<sub>2</sub>O Single Scattering Albedos  $\omega$



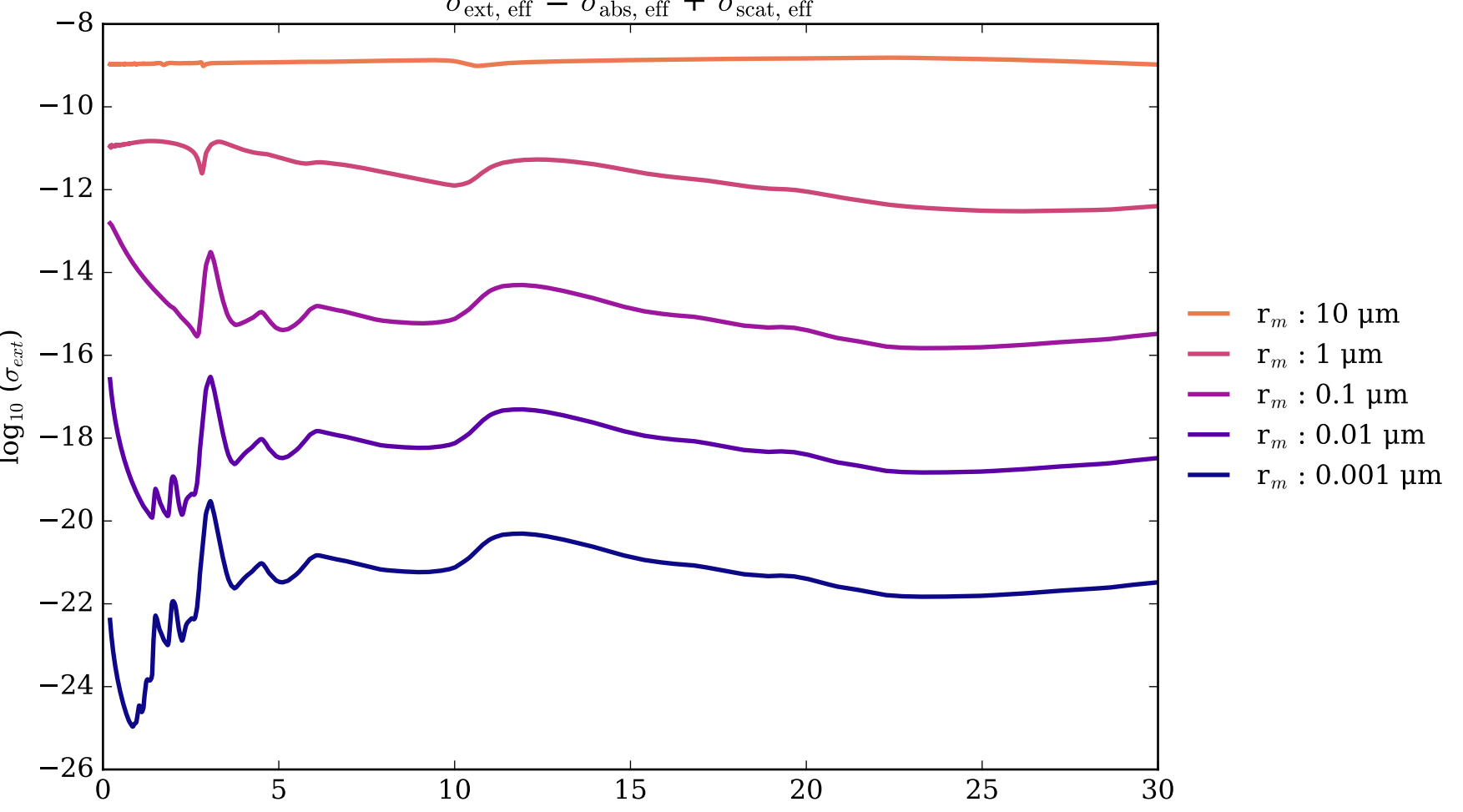
H<sub>2</sub>O Asymmetry Parameter  $g$   
0 (Rayleigh Limit) to 1 (Total Forward Scattering)



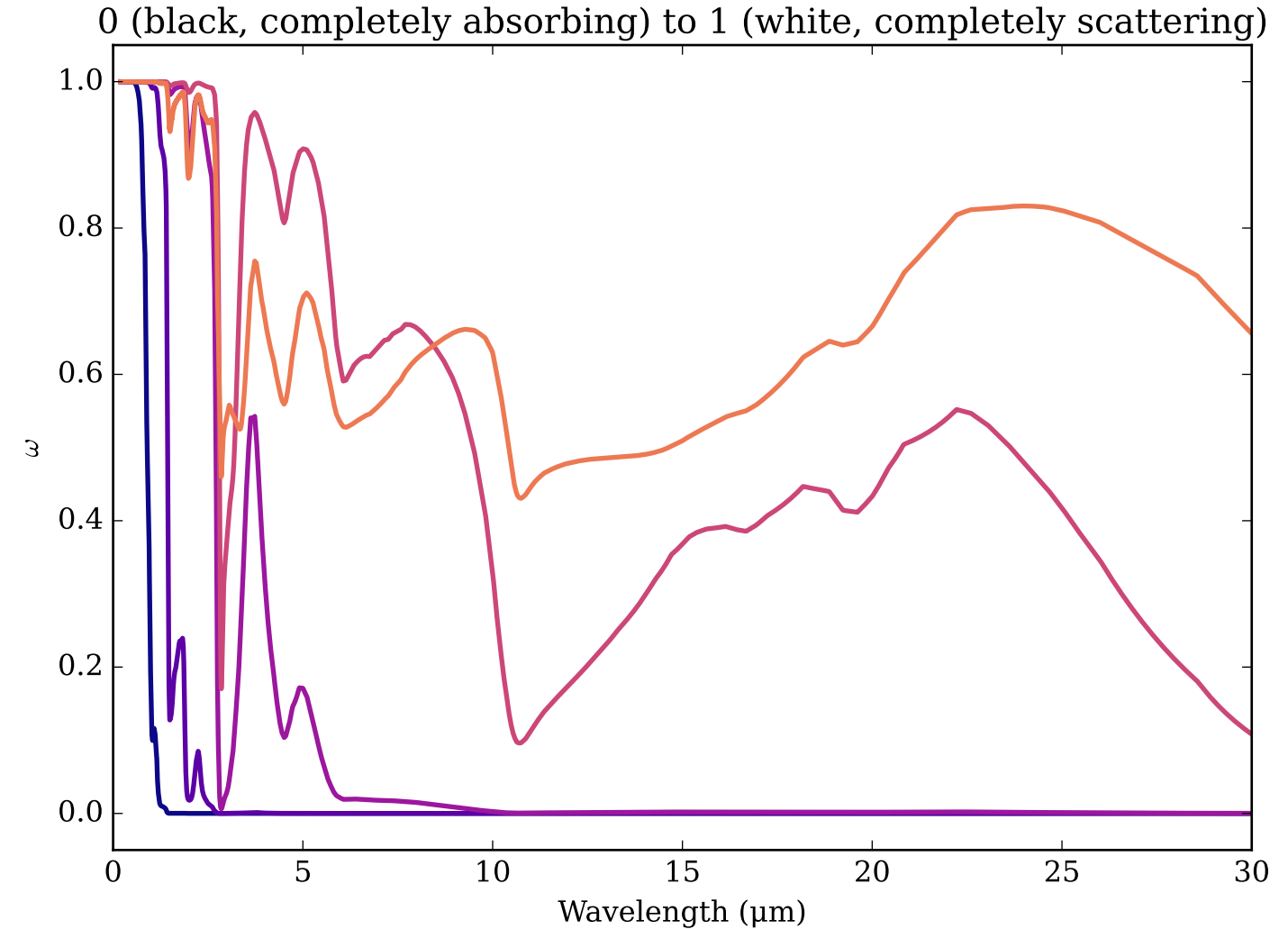
Refractive Indices for H<sub>2</sub>O  
(0.2, 30.0) μm



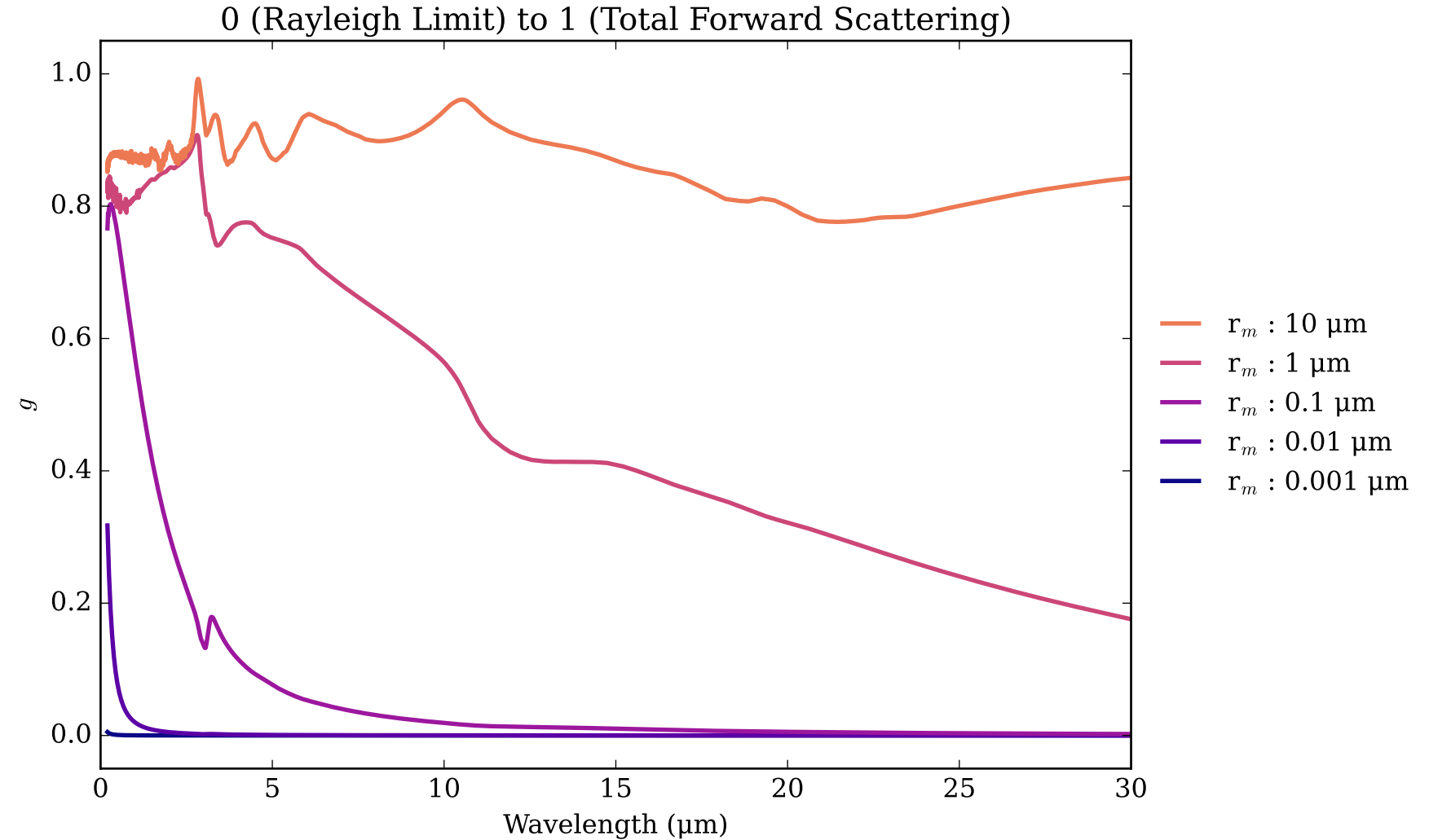
H<sub>2</sub>O\_ice Effective Extinction Cross Section



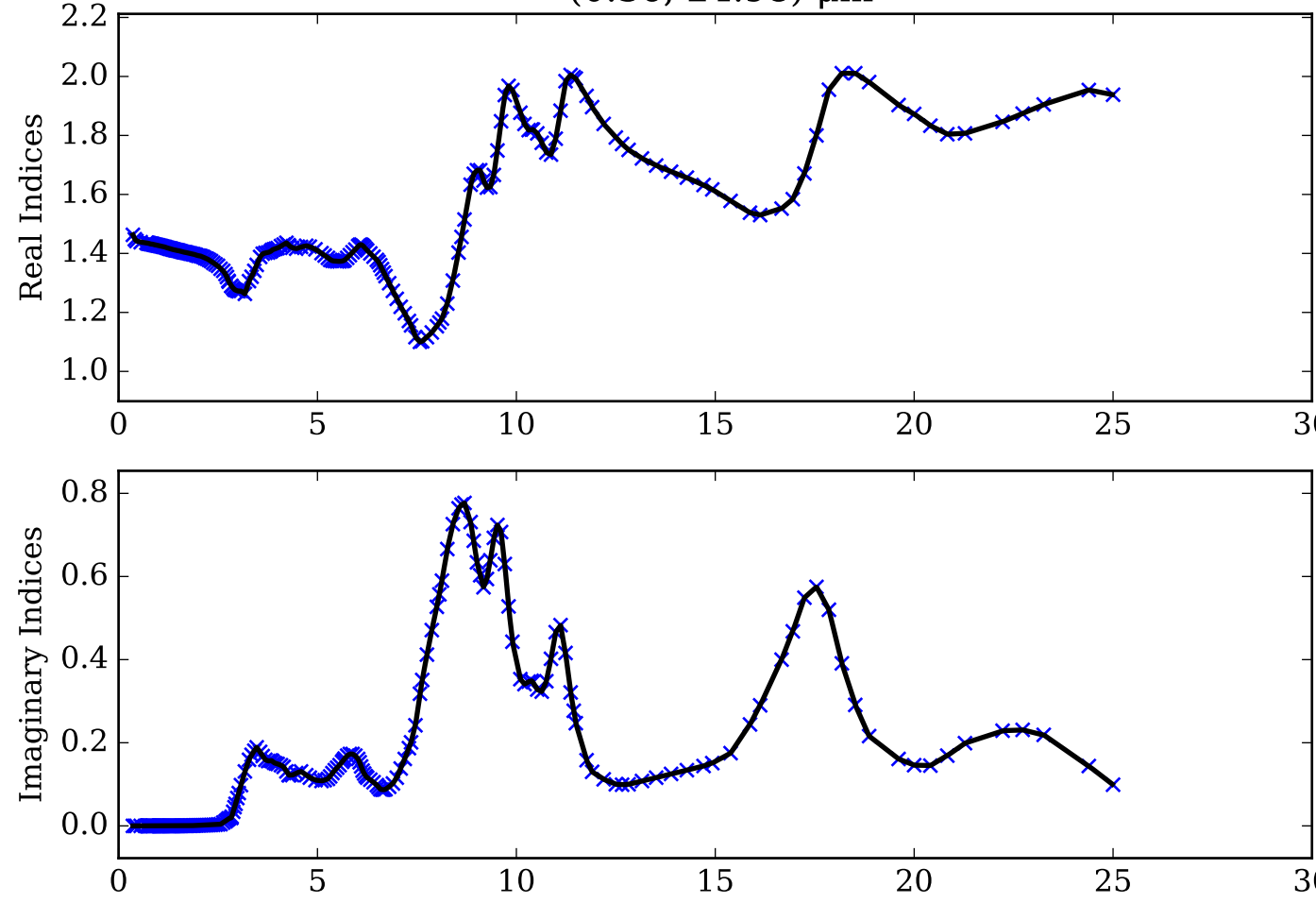
H<sub>2</sub>O\_ice Single Scattering Albedos  $\omega$



H<sub>2</sub>O\_ice Asymmetry Parameter  $g$

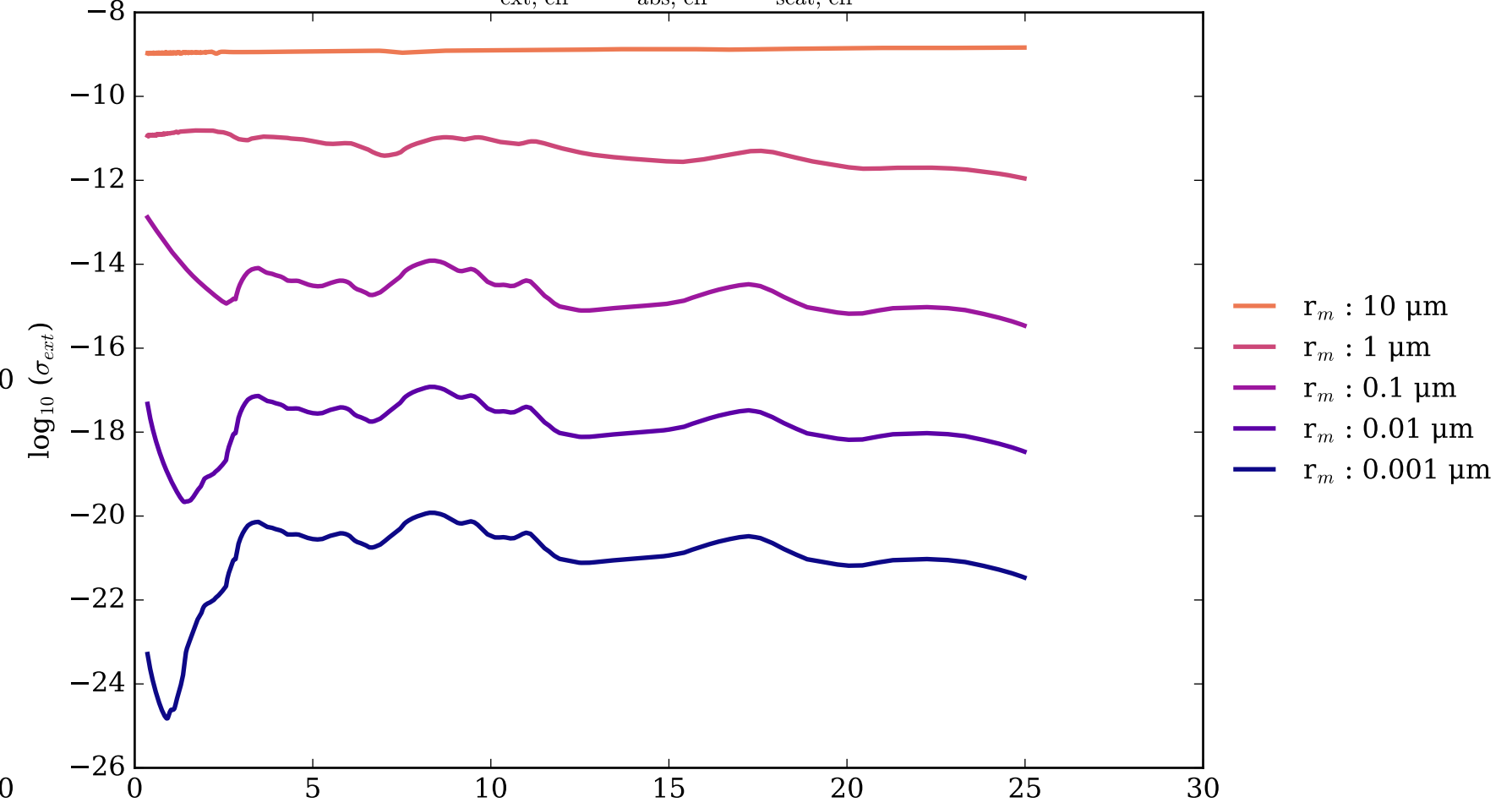


Refractive Indices for H<sub>2</sub>SO<sub>4</sub>  
 (0.36, 24.98)  $\mu\text{m}$

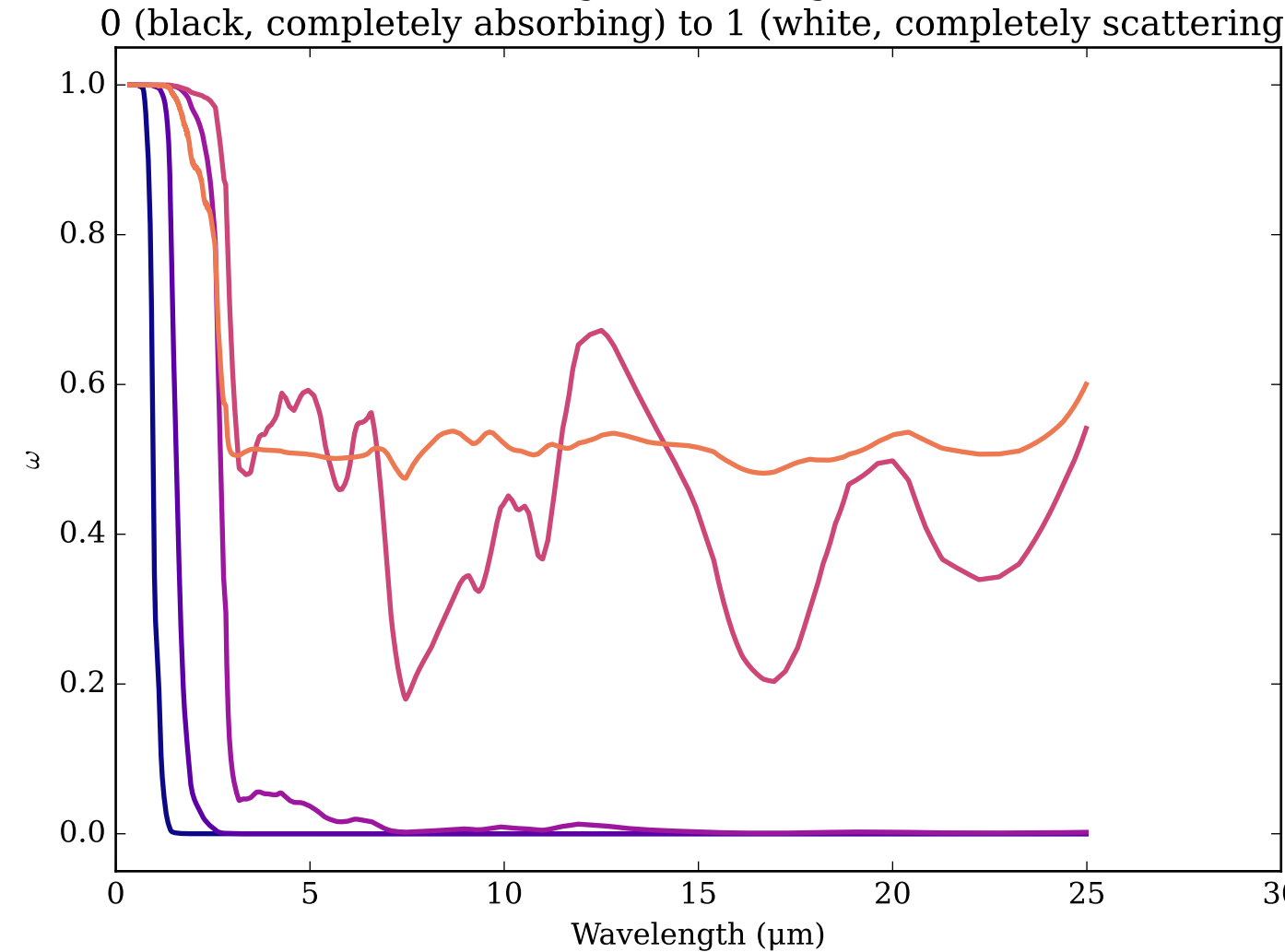


H<sub>2</sub>SO<sub>4</sub> Effective Extinction Cross Section

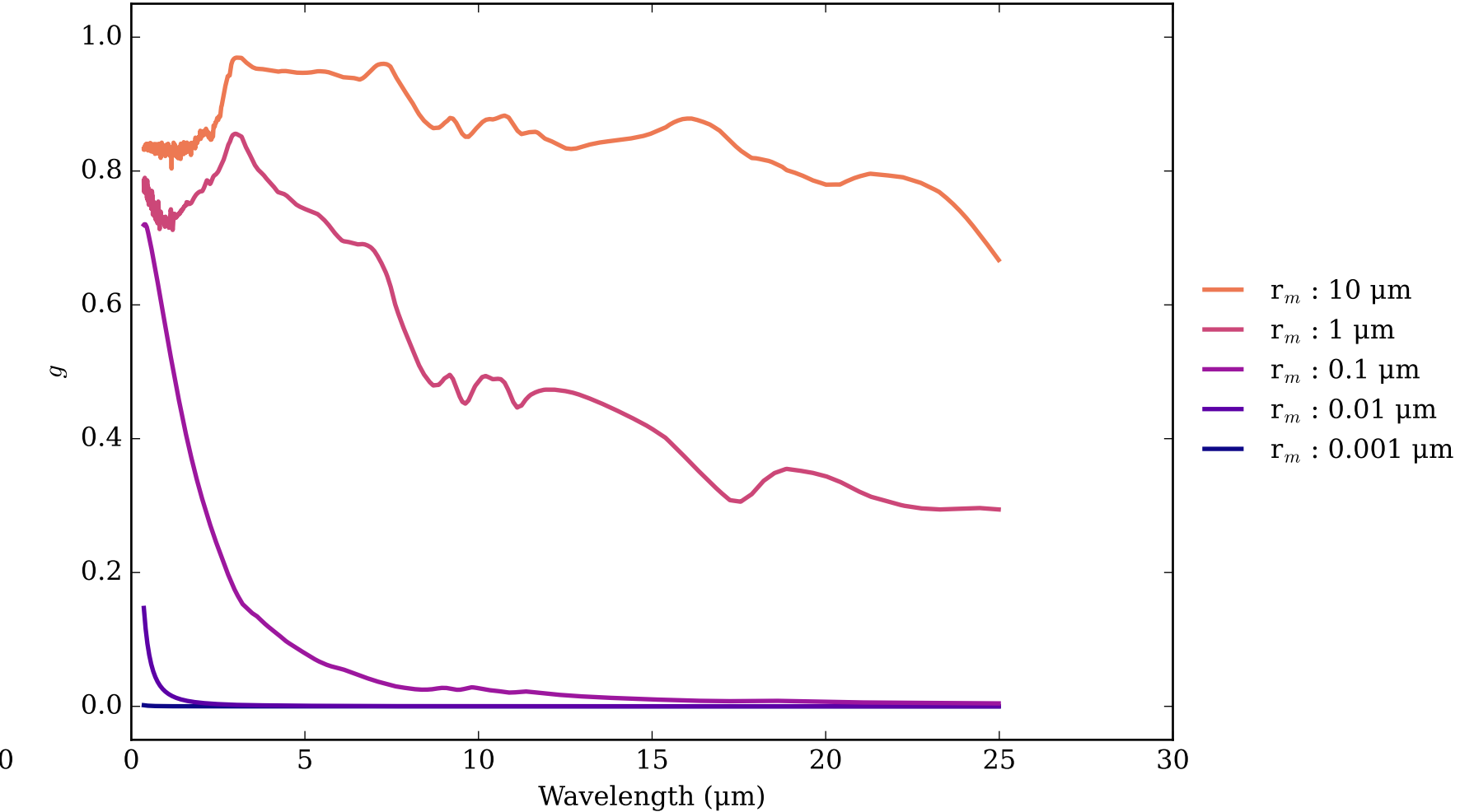
$$\sigma_{\text{ext, eff}} = \sigma_{\text{abs, eff}} + \sigma_{\text{scat, eff}}$$



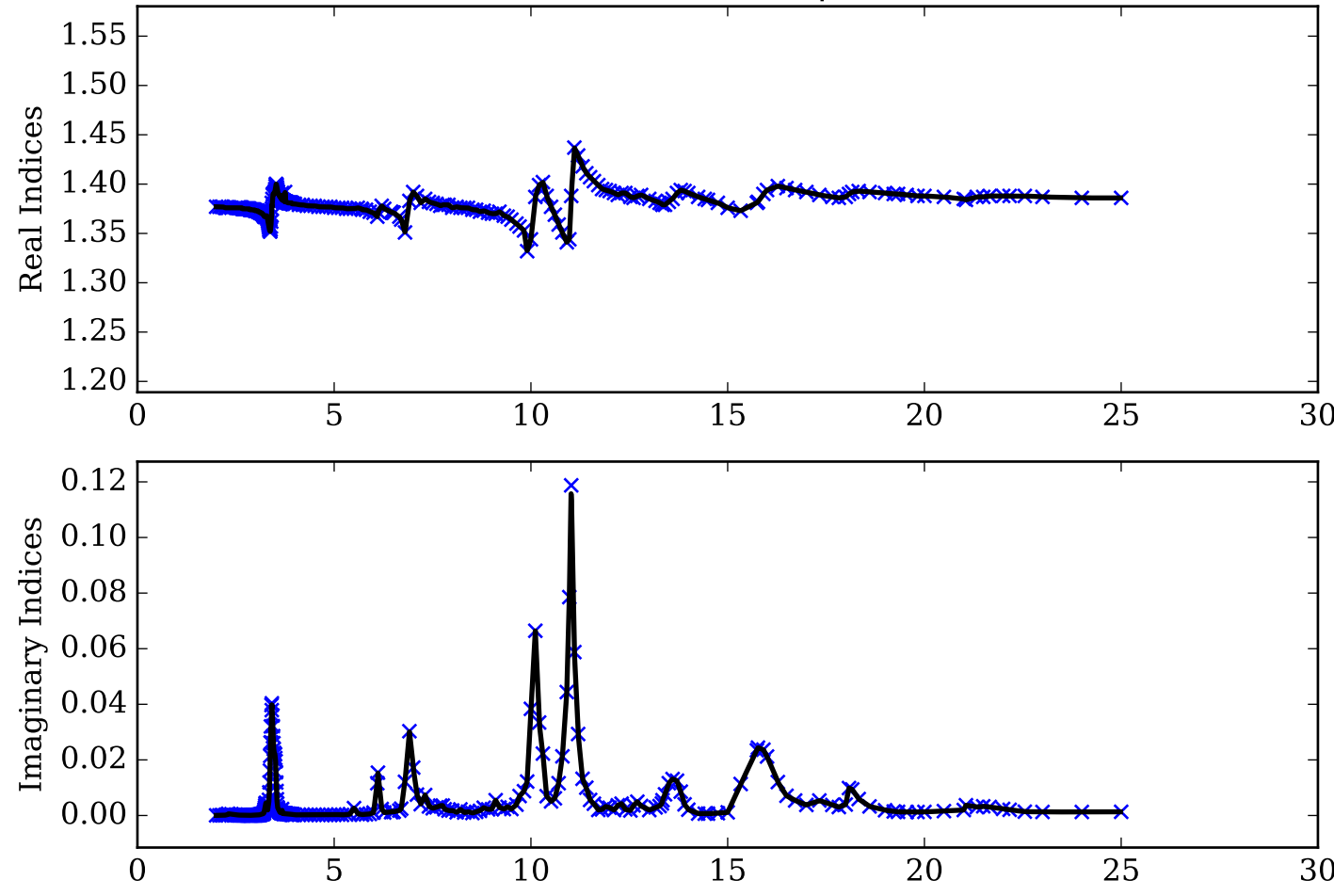
H<sub>2</sub>SO<sub>4</sub> Single Scattering Albedos  $\omega$



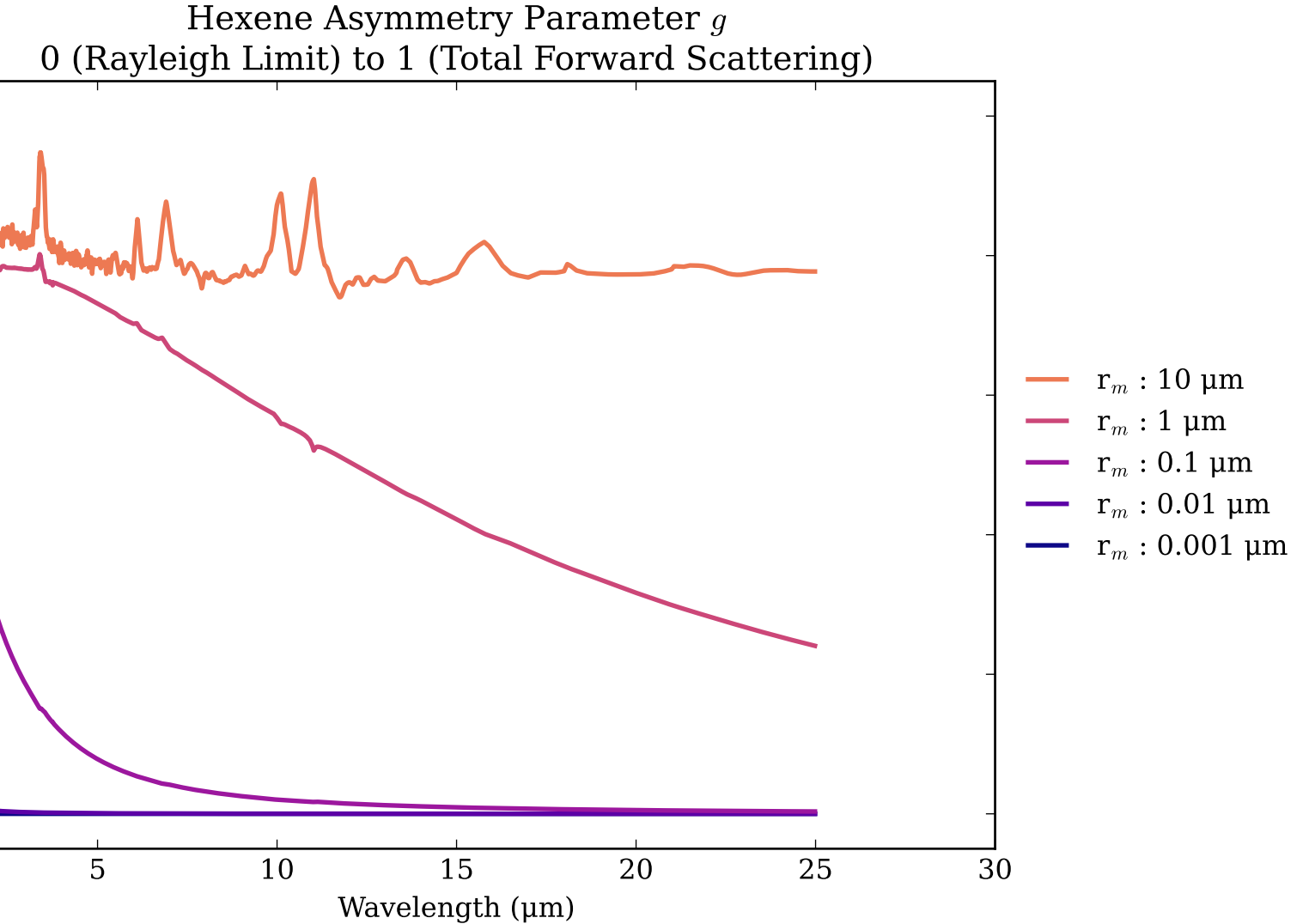
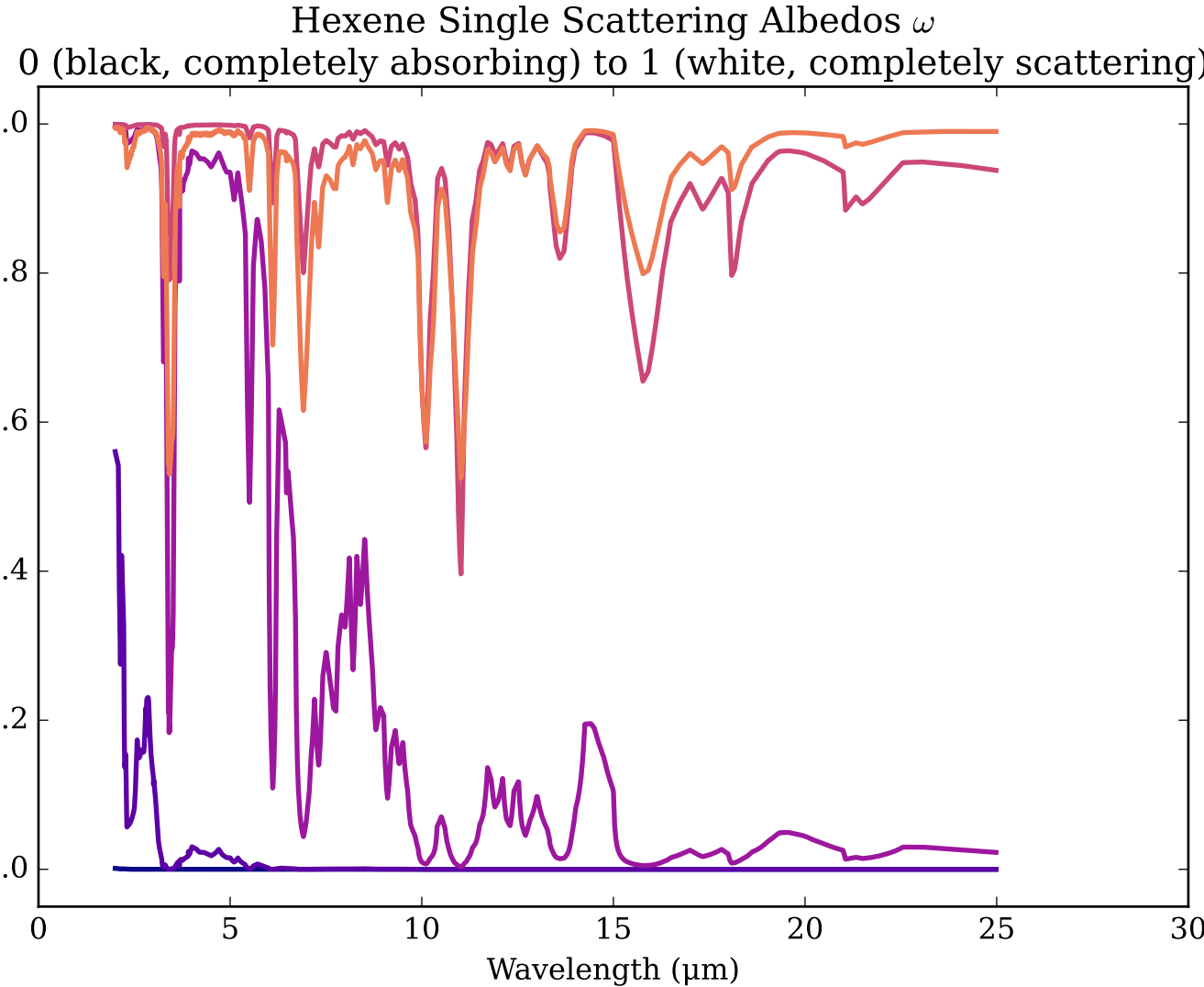
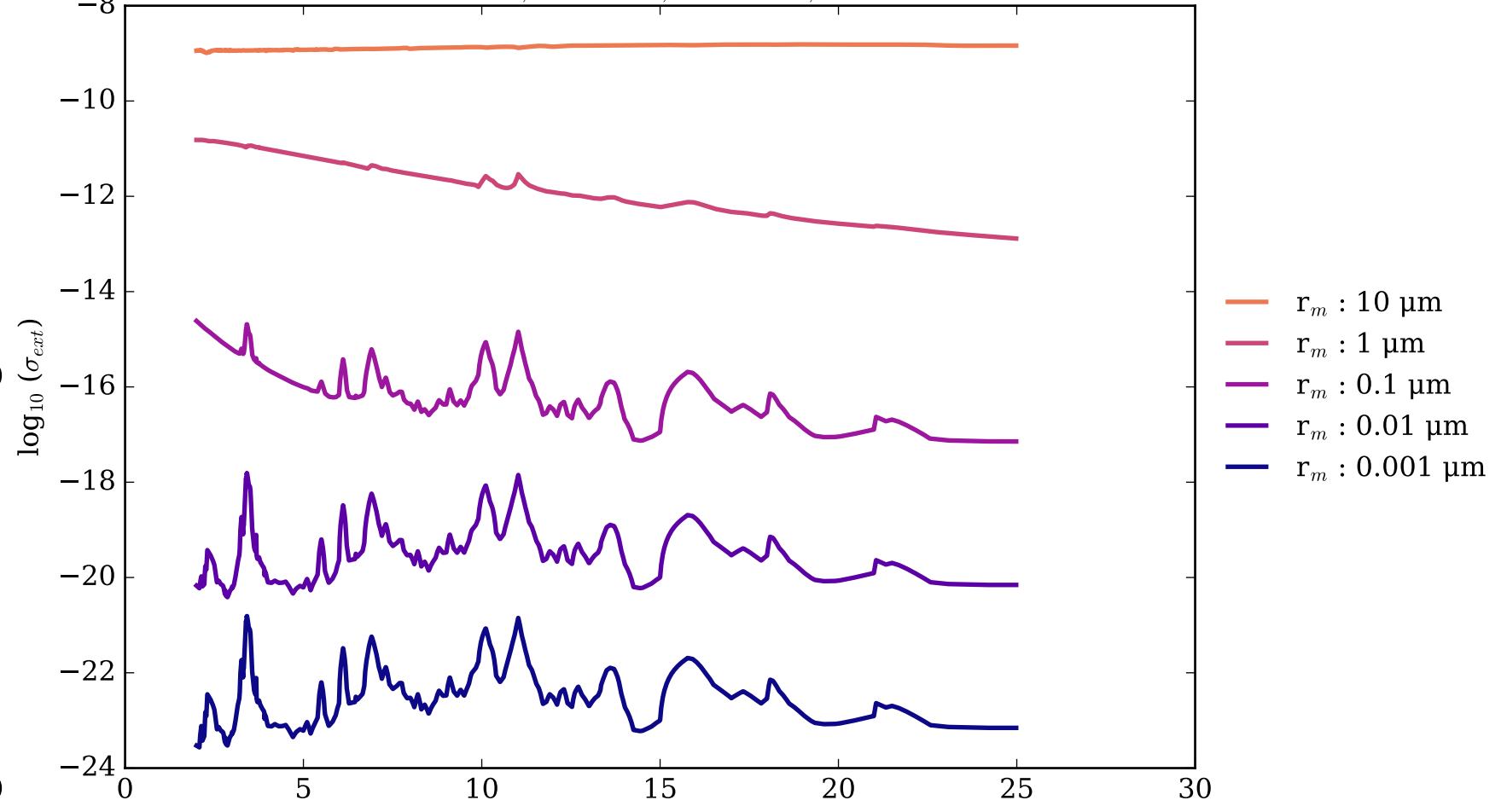
H<sub>2</sub>SO<sub>4</sub> Asymmetry Parameter  $g$



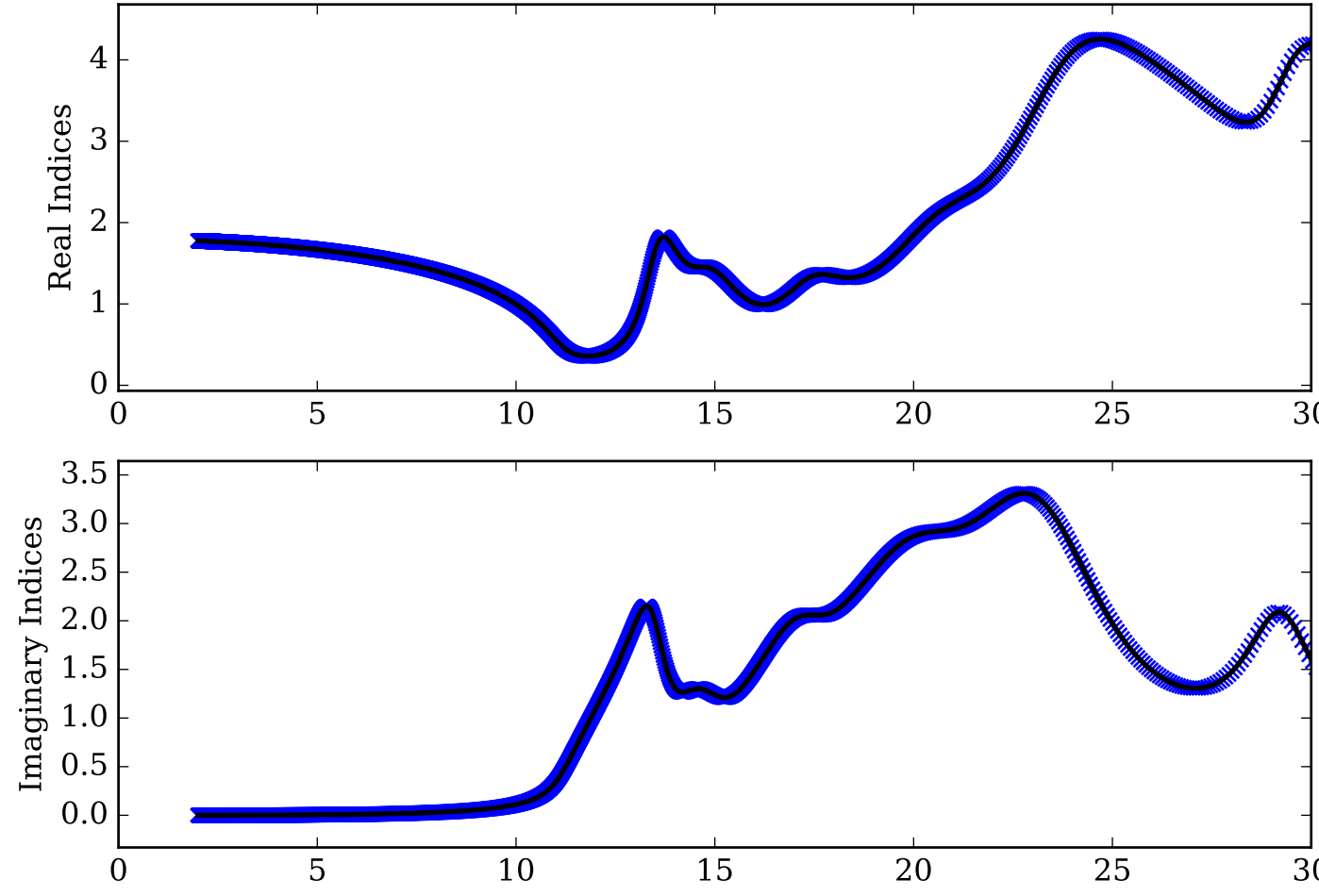
Refractive Indices for Hexene  
(2.0, 24.98)  $\mu\text{m}$



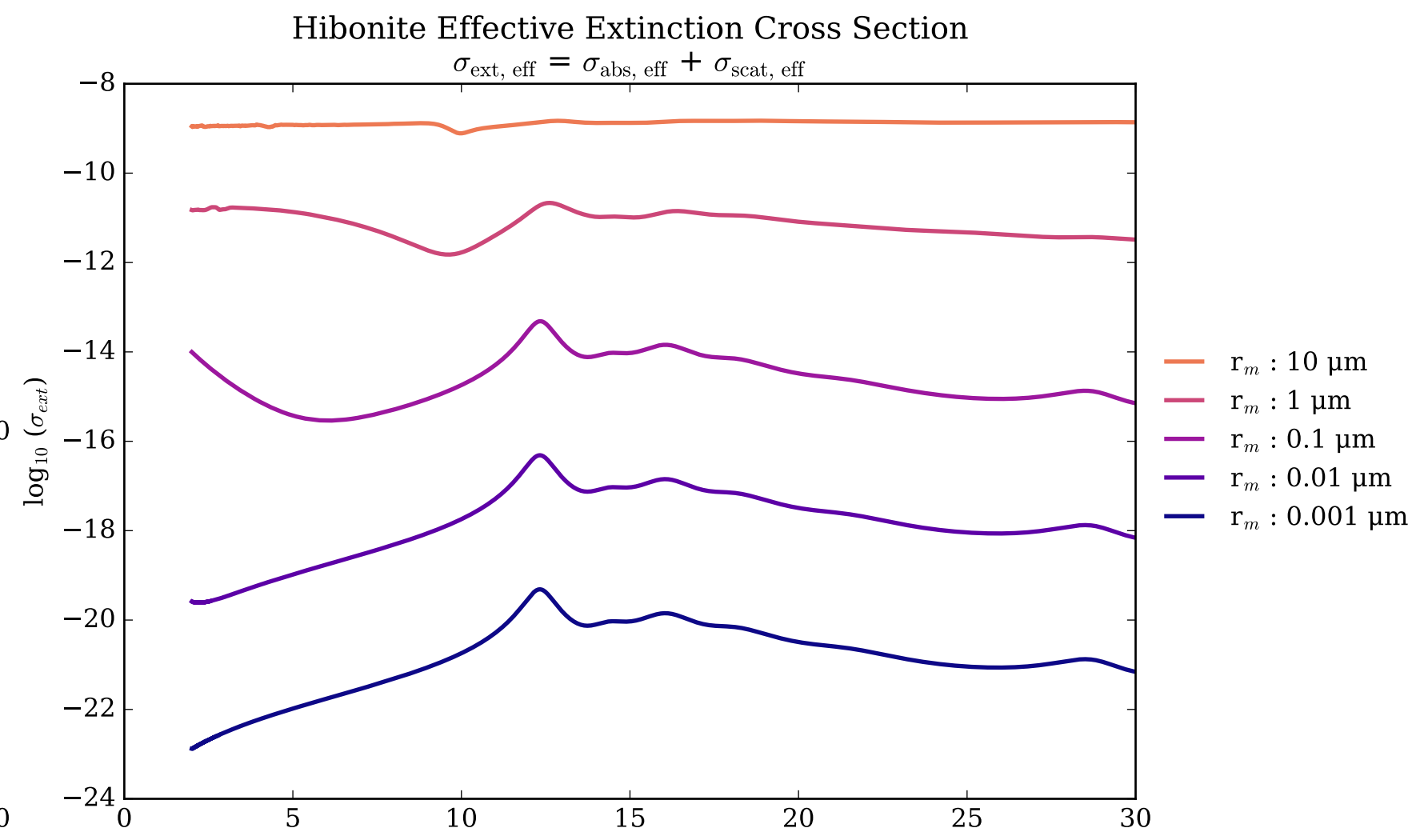
Hexene Effective Extinction Cross Section  
 $\sigma_{\text{ext, eff}} = \sigma_{\text{abs, eff}} + \sigma_{\text{scat, eff}}$



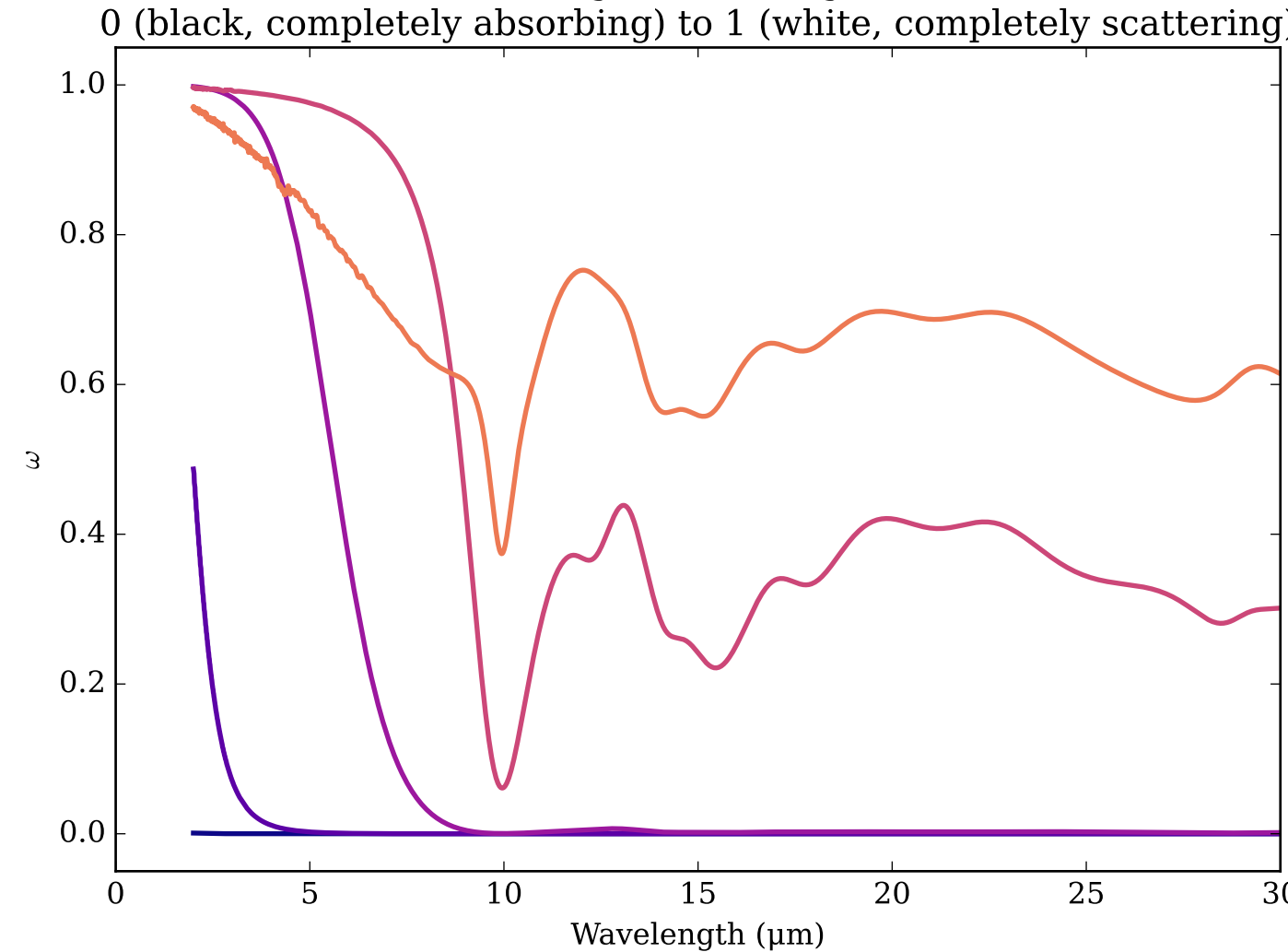
Refractive Indices for Hibonite  
(2.0, 30.0)  $\mu\text{m}$



Hibonite Effective Extinction Cross Section

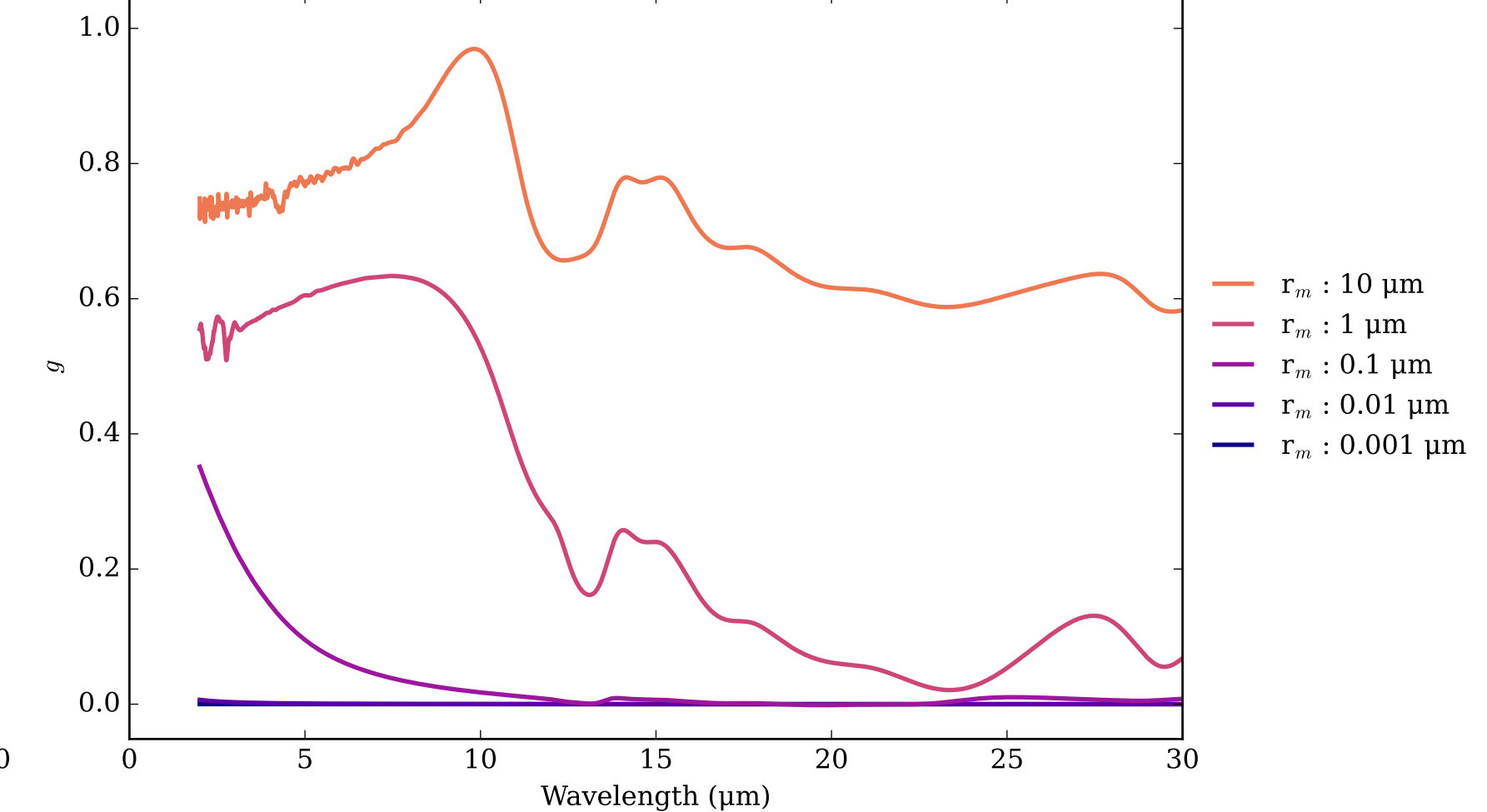


Hibonite Single Scattering Albedos  $\omega$

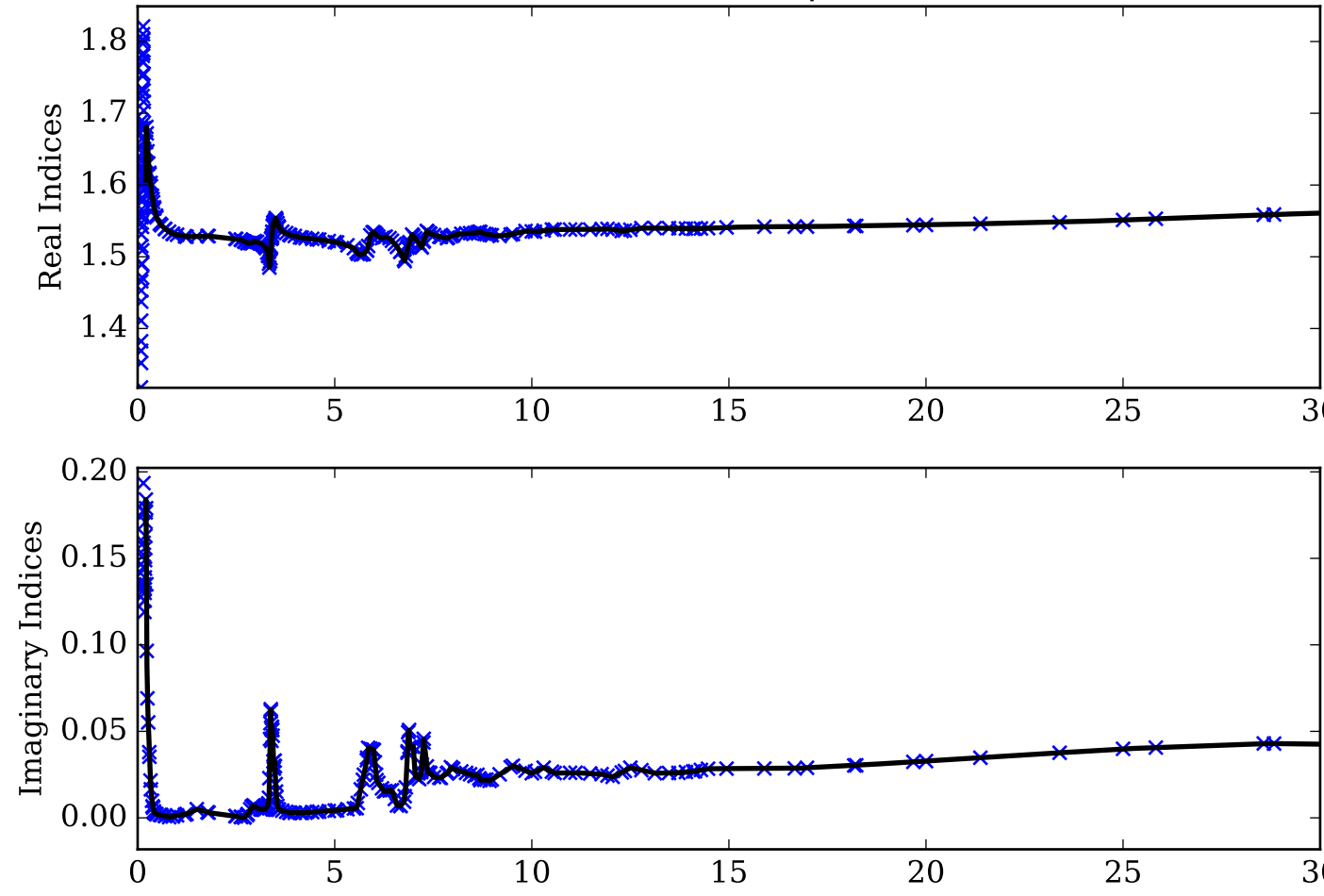


Hibonite Asymmetry Parameter  $g$

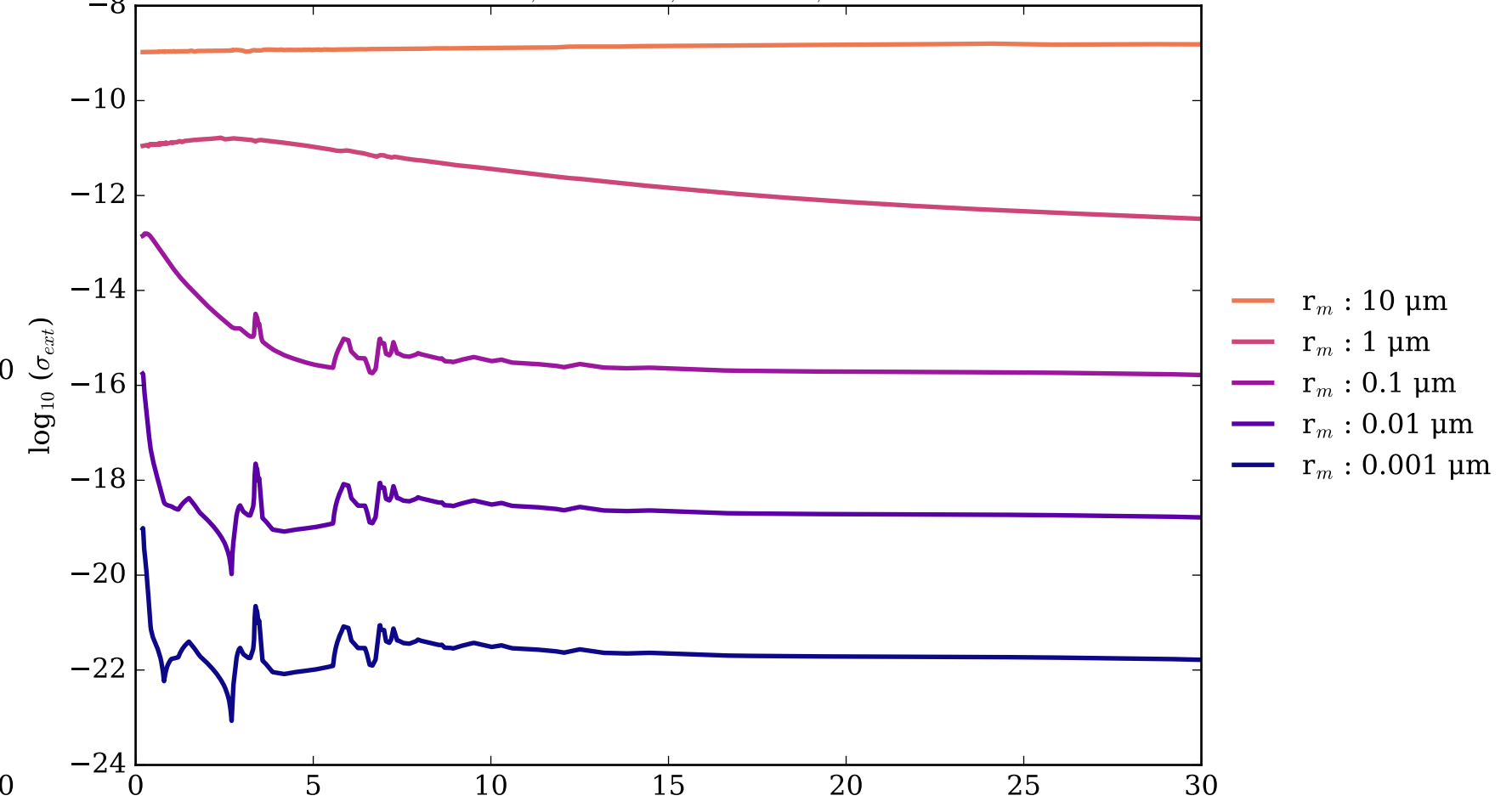
0 (Rayleigh Limit) to 1 (Total Forward Scattering)



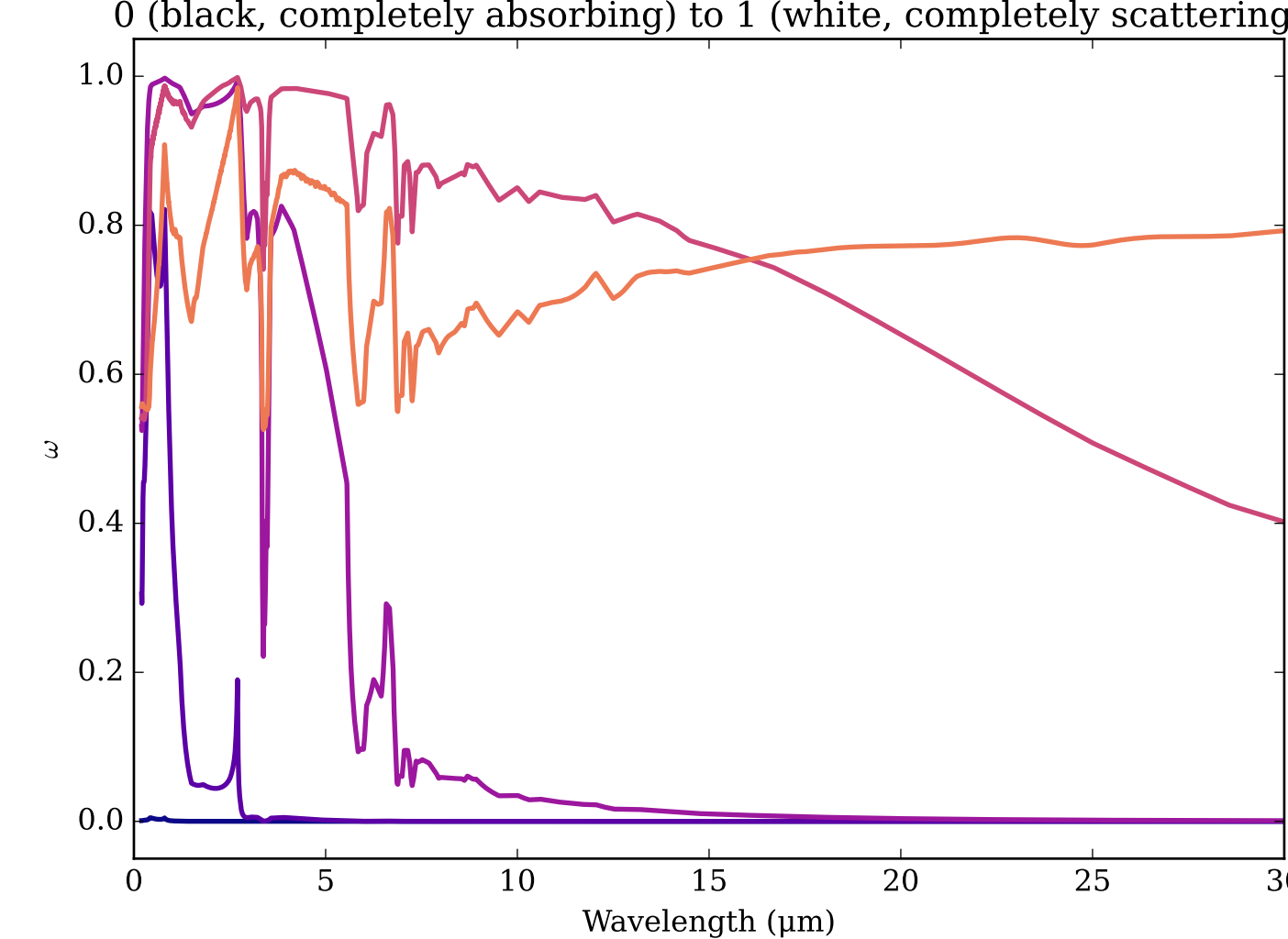
Refractive Indices for IceTholin  
(0.2, 30.0)  $\mu\text{m}$



IceTholin Effective Extinction Cross Section

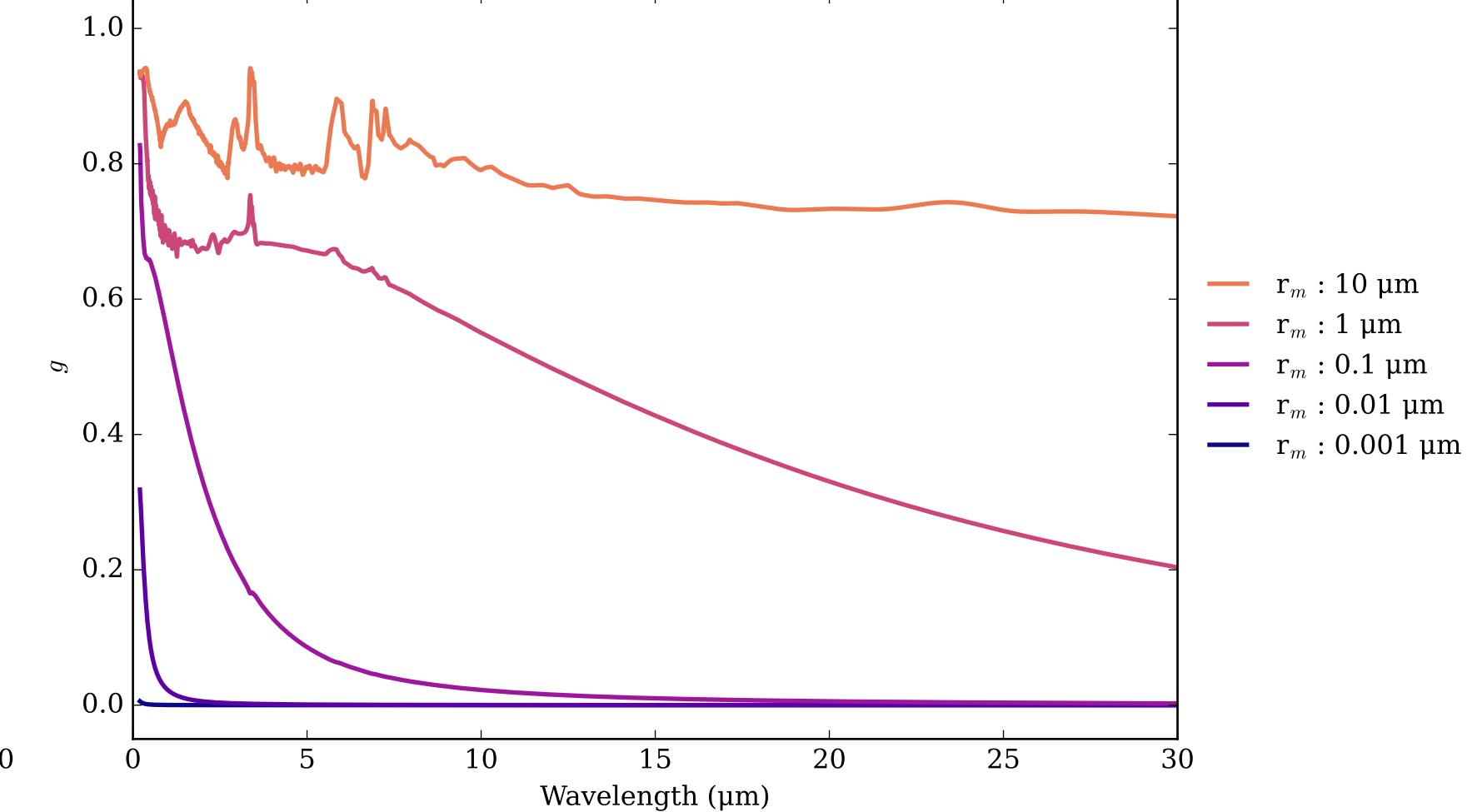


IceTholin Single Scattering Albedos  $\omega$

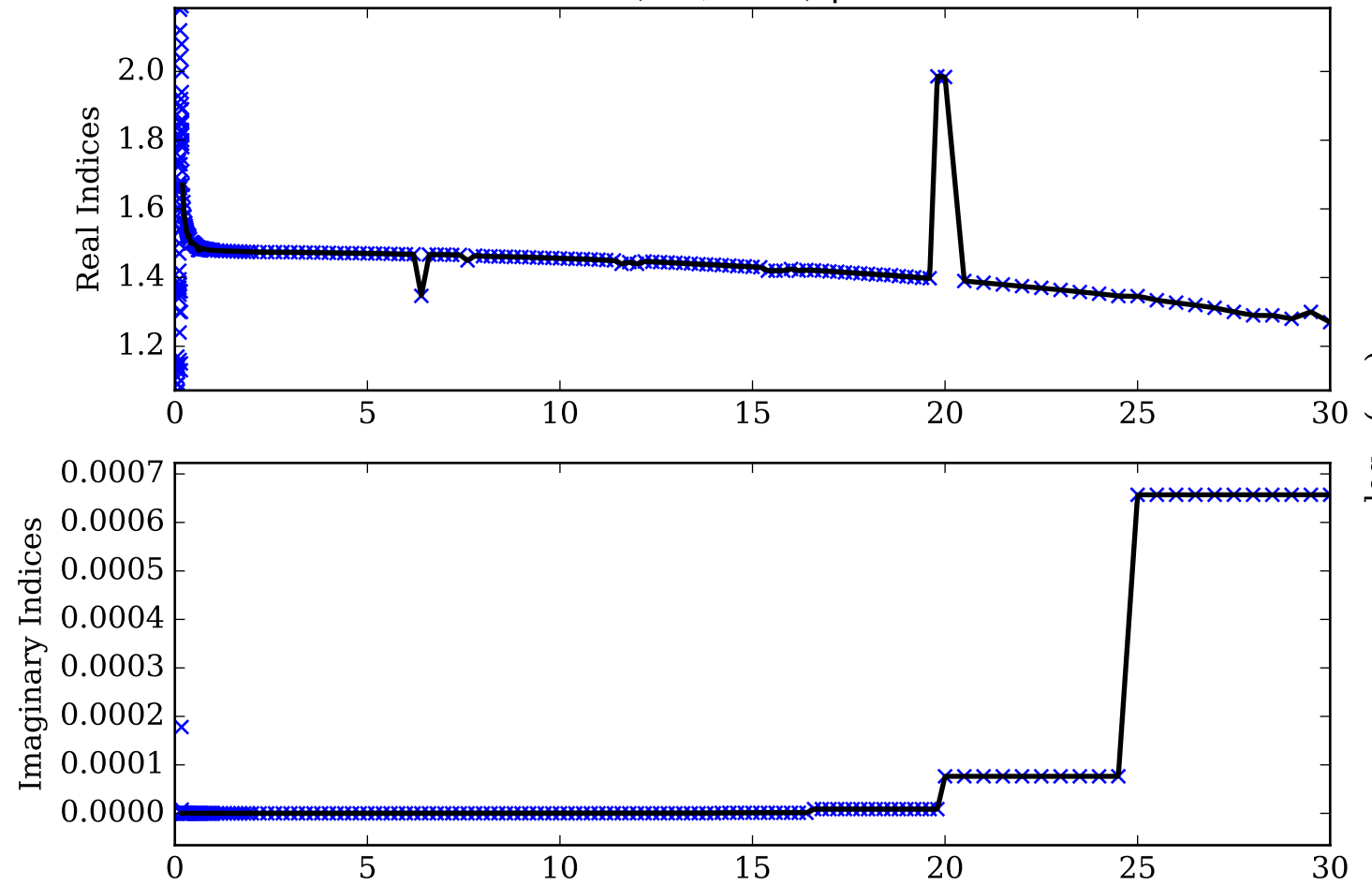


IceTholin Asymmetry Parameter  $g$

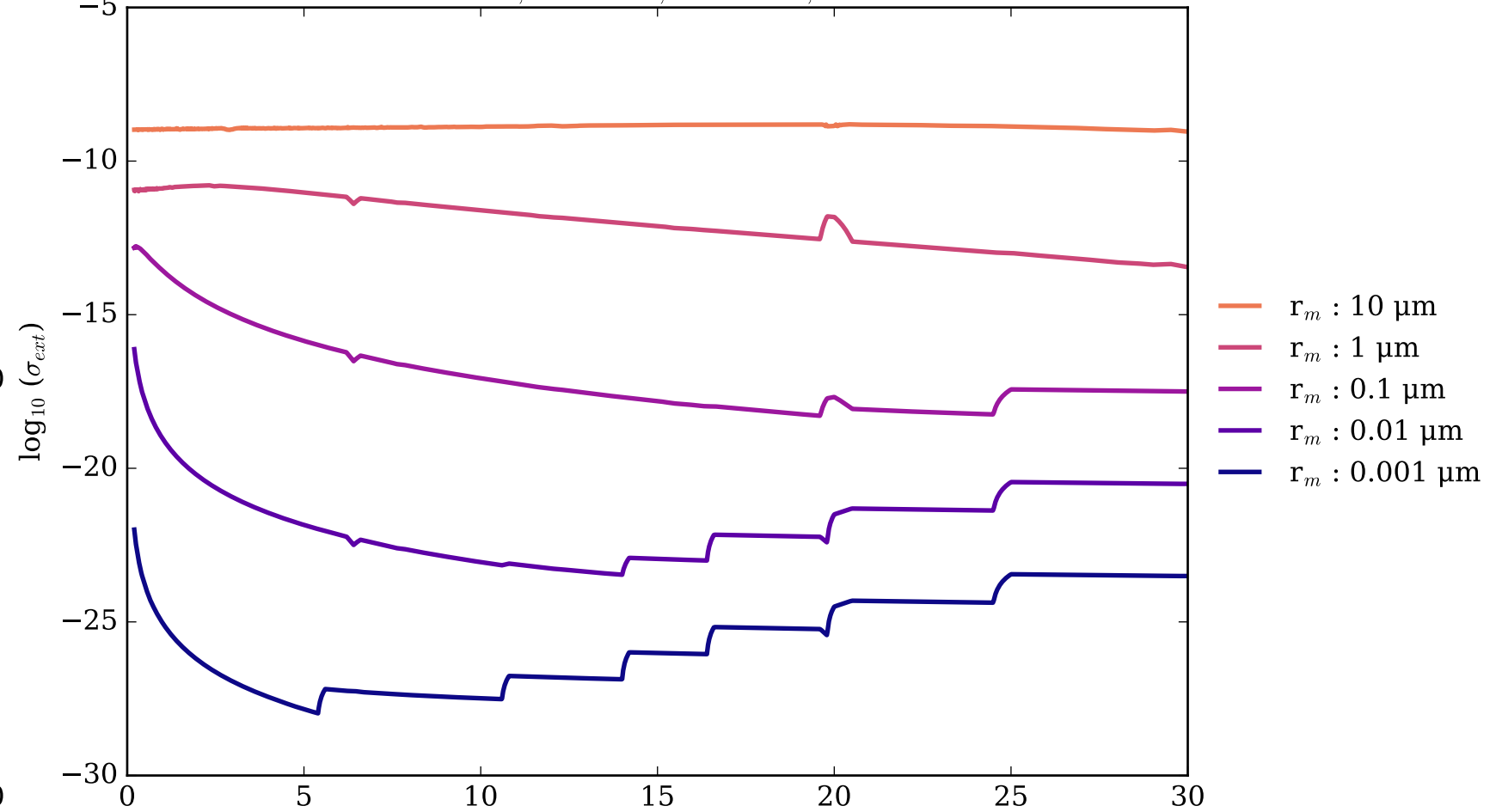
0 (Rayleigh Limit) to 1 (Total Forward Scattering)



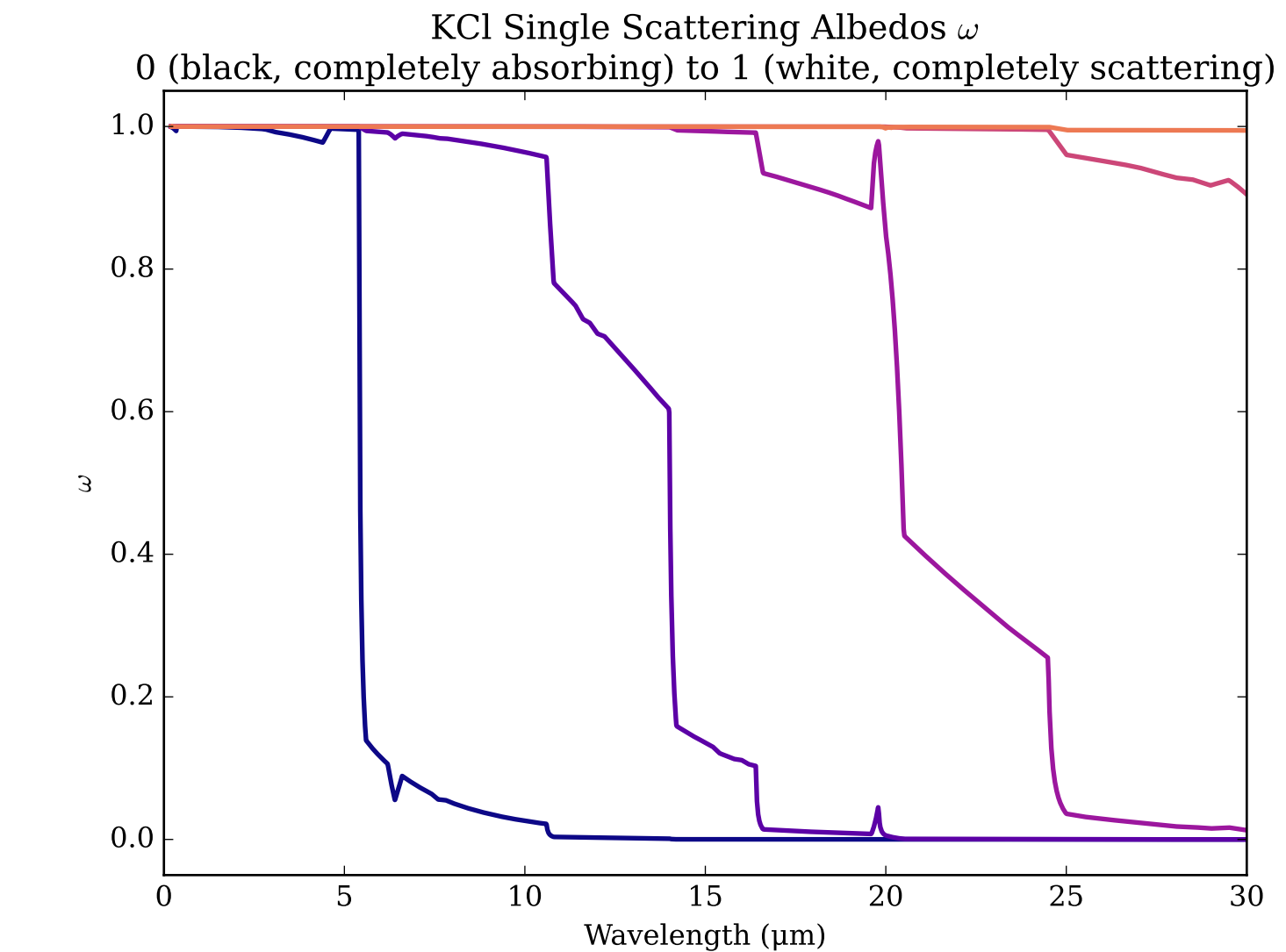
Refractive Indices for KCl  
(0.2, 30.0)  $\mu\text{m}$



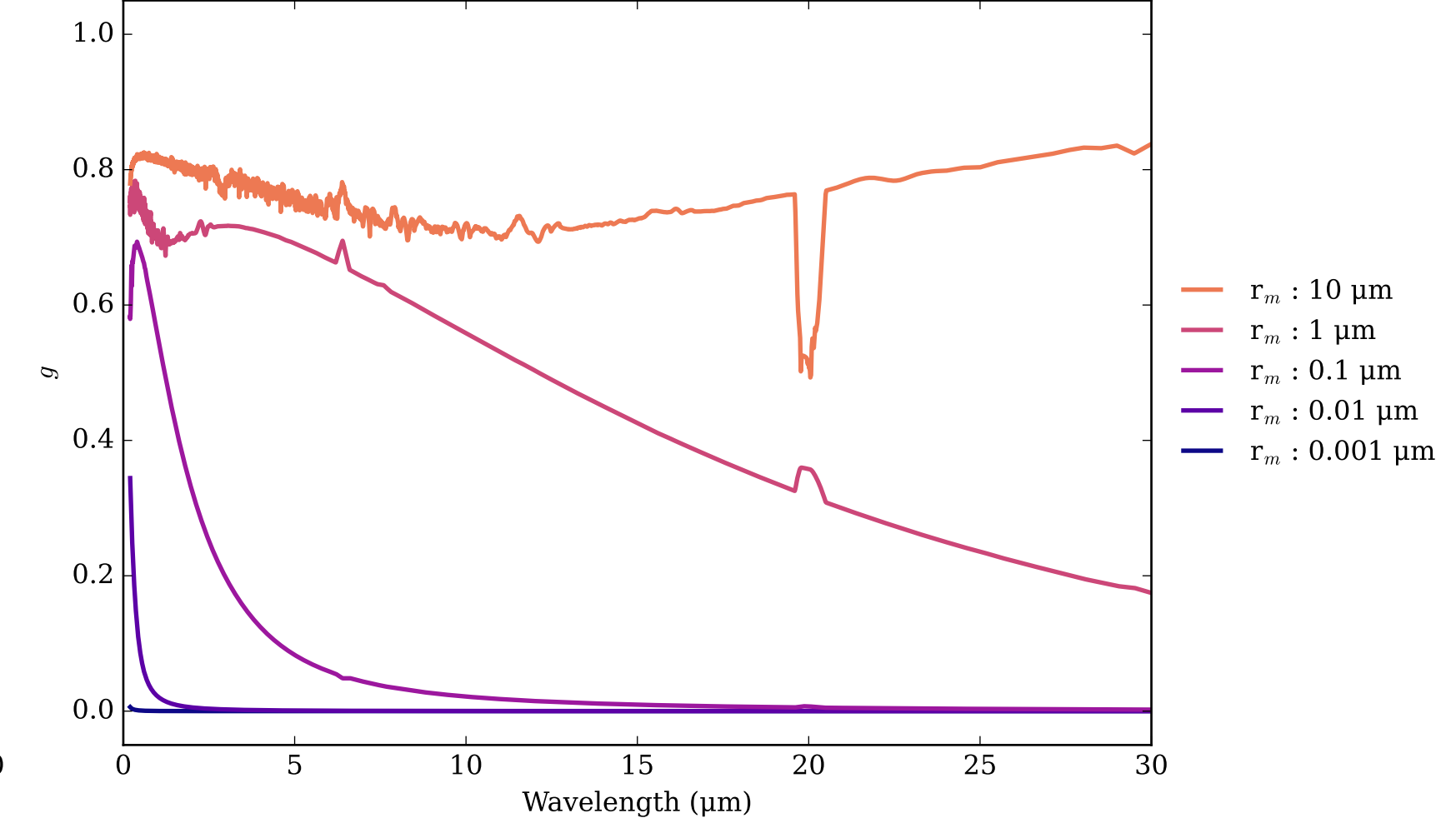
KCl Effective Extinction Cross Section  
 $\sigma_{\text{ext, eff}} = \sigma_{\text{abs, eff}} + \sigma_{\text{scat, eff}}$



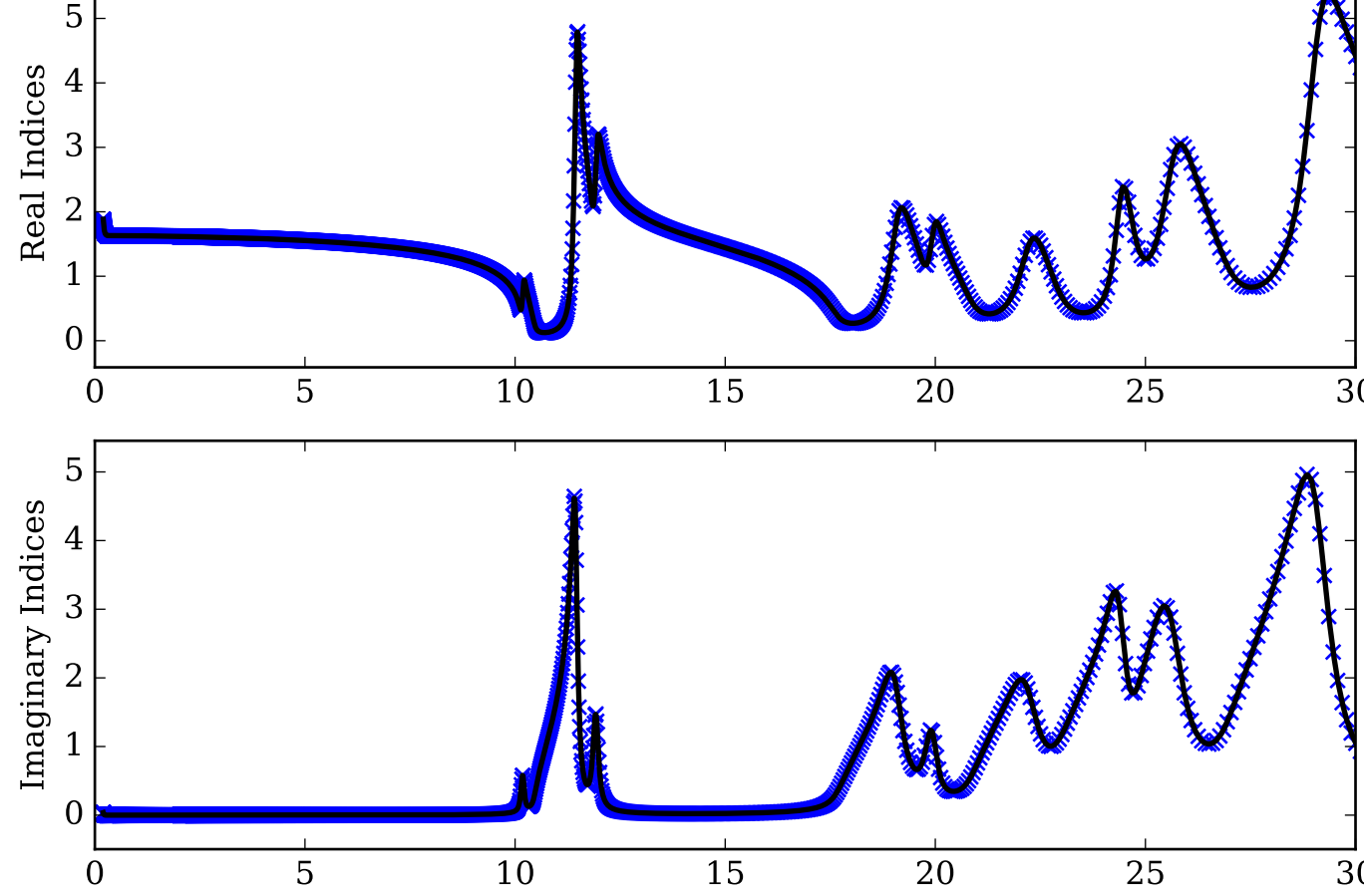
KCl Single Scattering Albedos  $\omega$



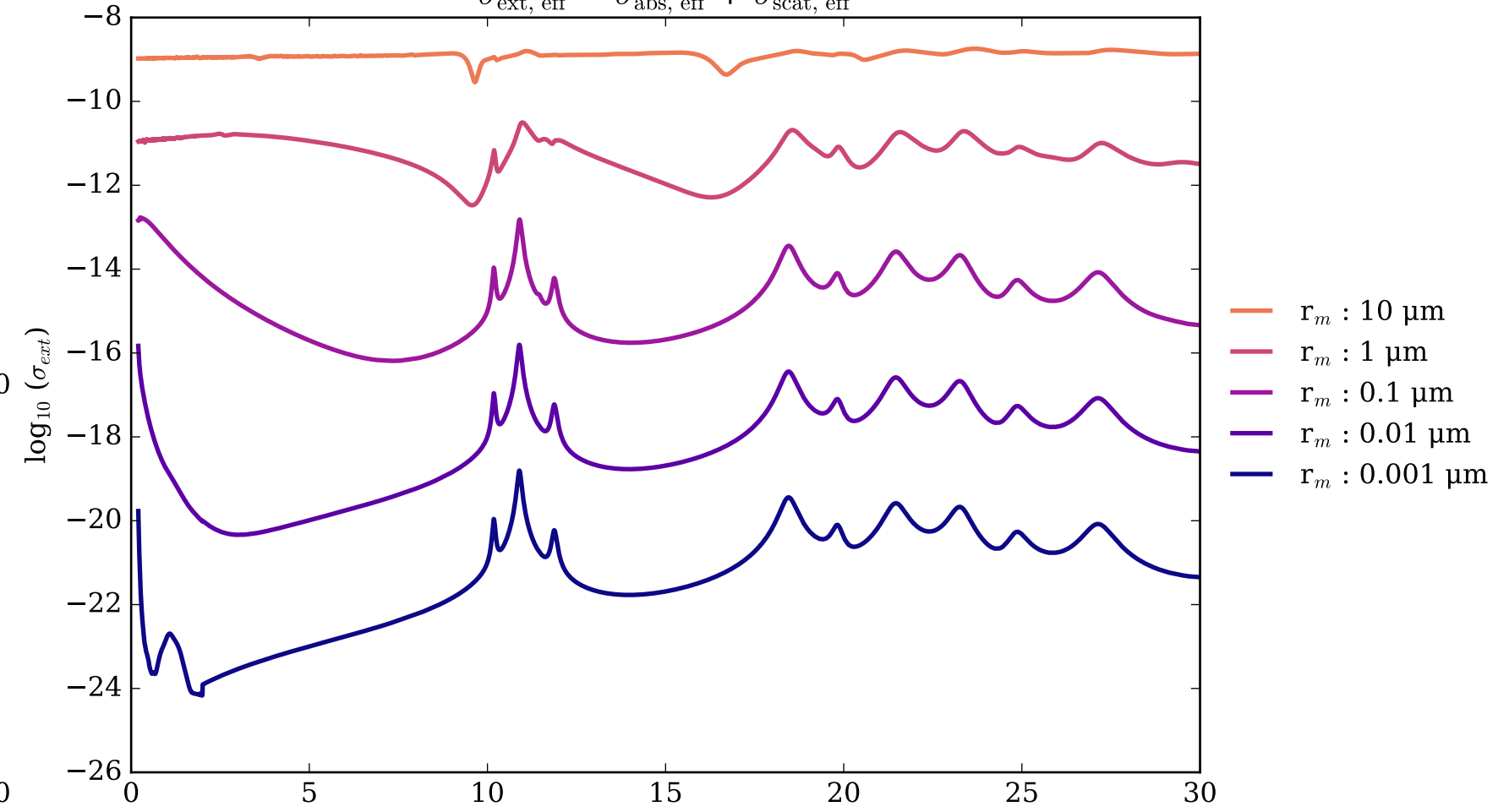
KCl Asymmetry Parameter  $g$   
0 (Rayleigh Limit) to 1 (Total Forward Scattering)



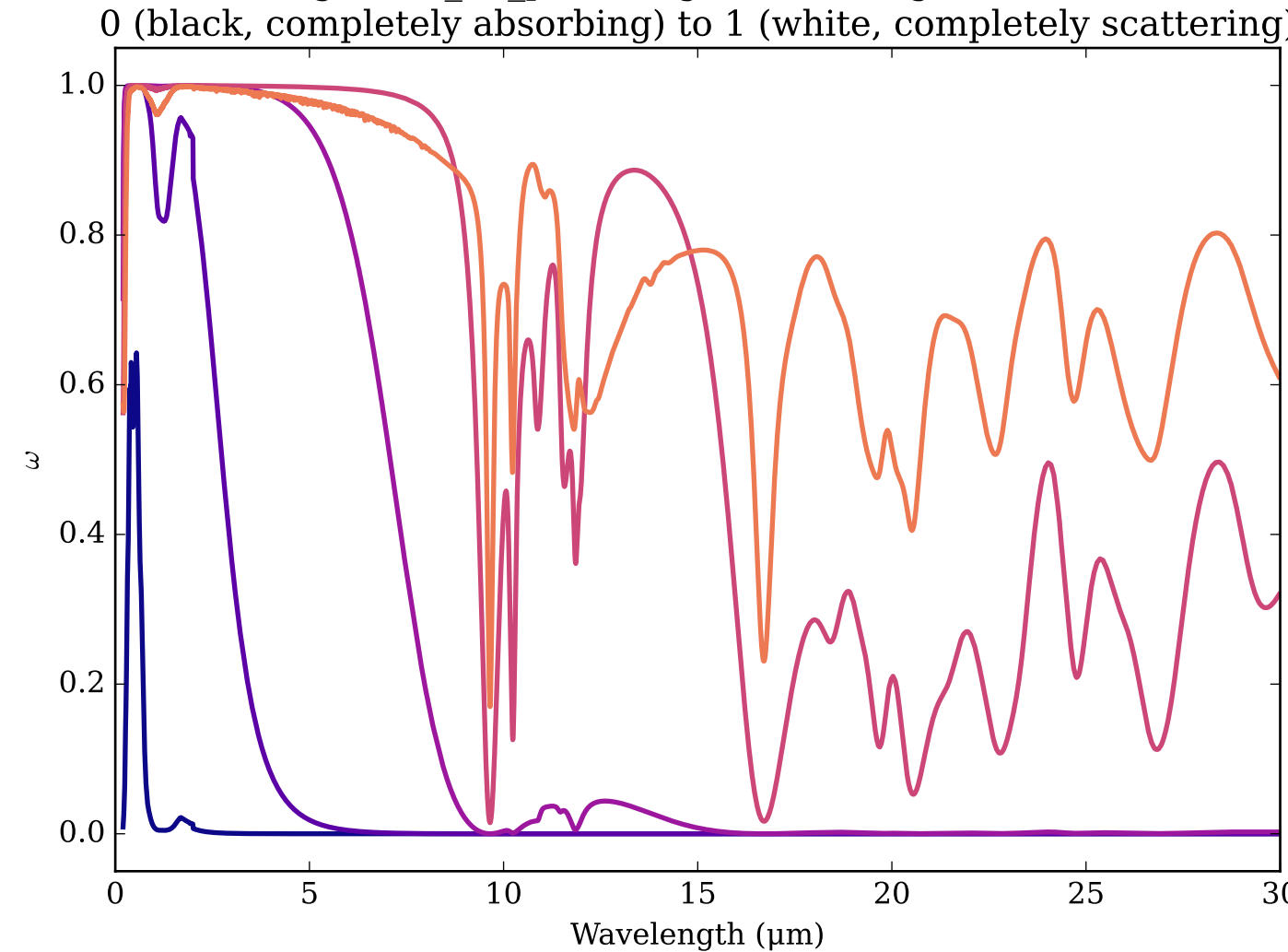
Refractive Indices for Mg<sub>2</sub>SiO<sub>4</sub>  
(0.2, 30.0)  $\mu\text{m}$



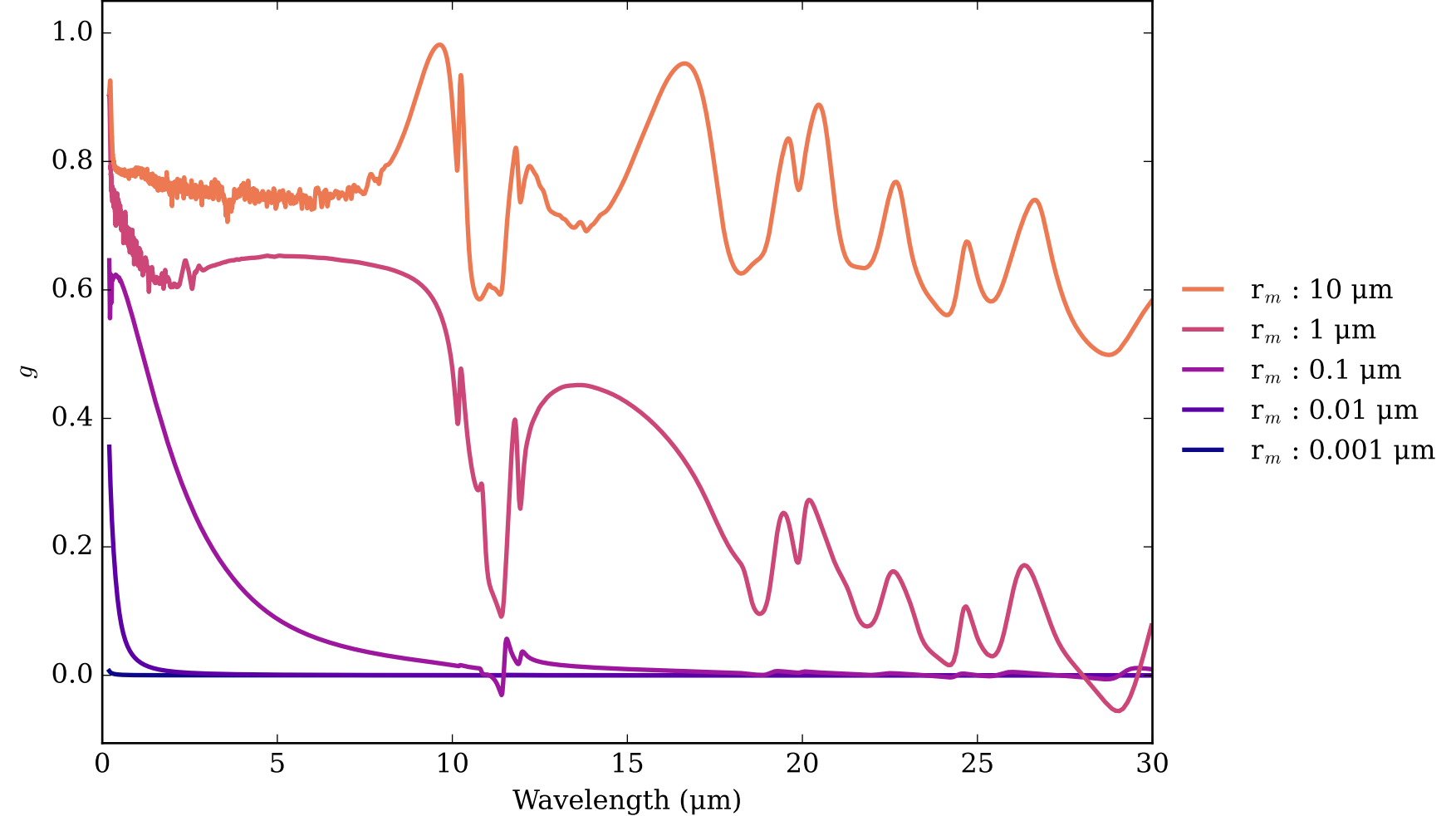
Mg<sub>2</sub>SiO<sub>4</sub>\_Fe\_poor Effective Extinction Cross Section  
 $\sigma_{\text{ext, eff}} = \sigma_{\text{abs, eff}} + \sigma_{\text{scat, eff}}$



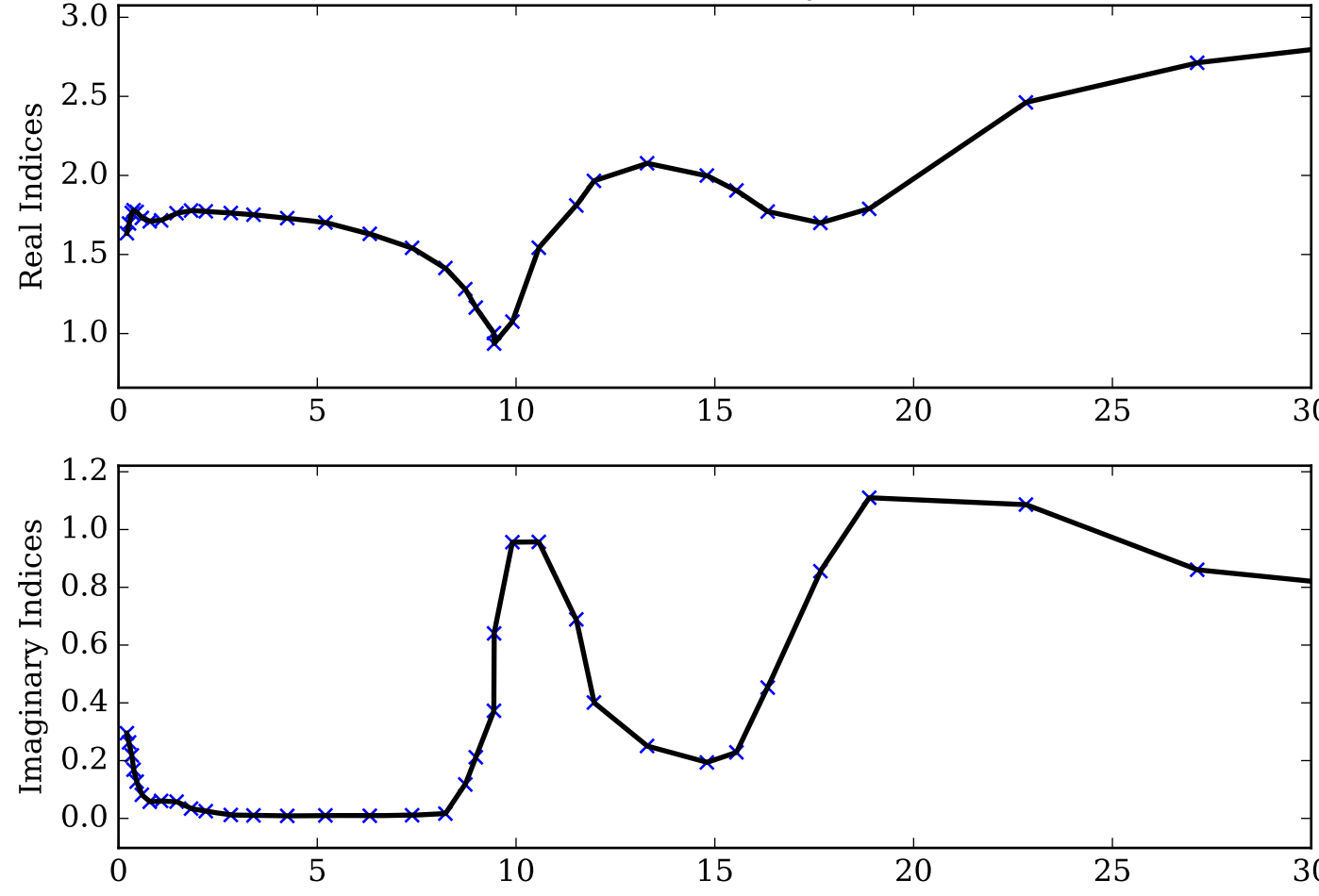
Mg<sub>2</sub>SiO<sub>4</sub>\_Fe\_poor Single Scattering Albedos  $\omega$



Mg<sub>2</sub>SiO<sub>4</sub>\_Fe\_poor Asymmetry Parameter  $g$   
0 (Rayleigh Limit) to 1 (Total Forward Scattering)

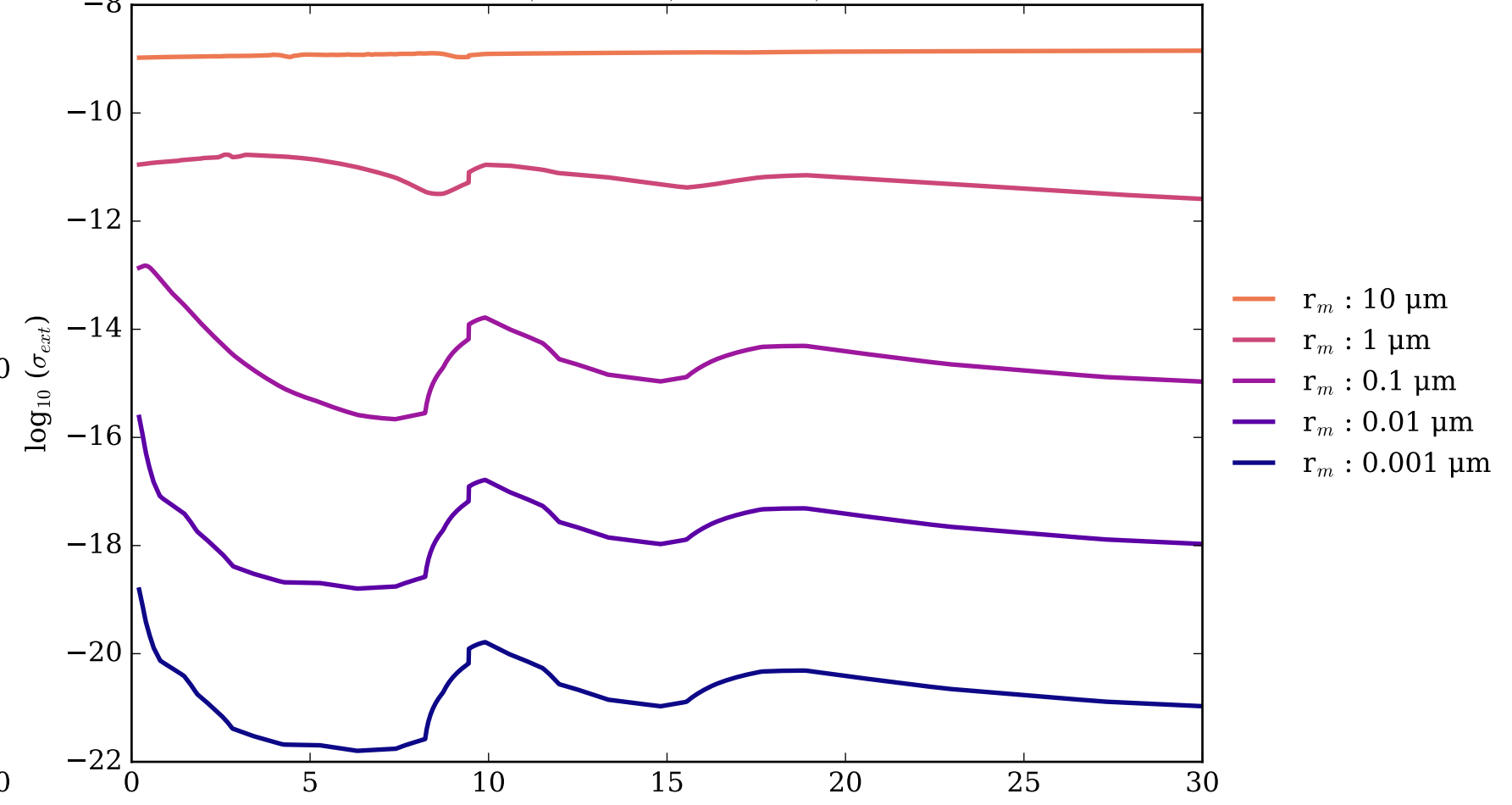


Refractive Indices for Mg<sub>2</sub>SiO<sub>4</sub>  
(0.21, 30.0)  $\mu\text{m}$

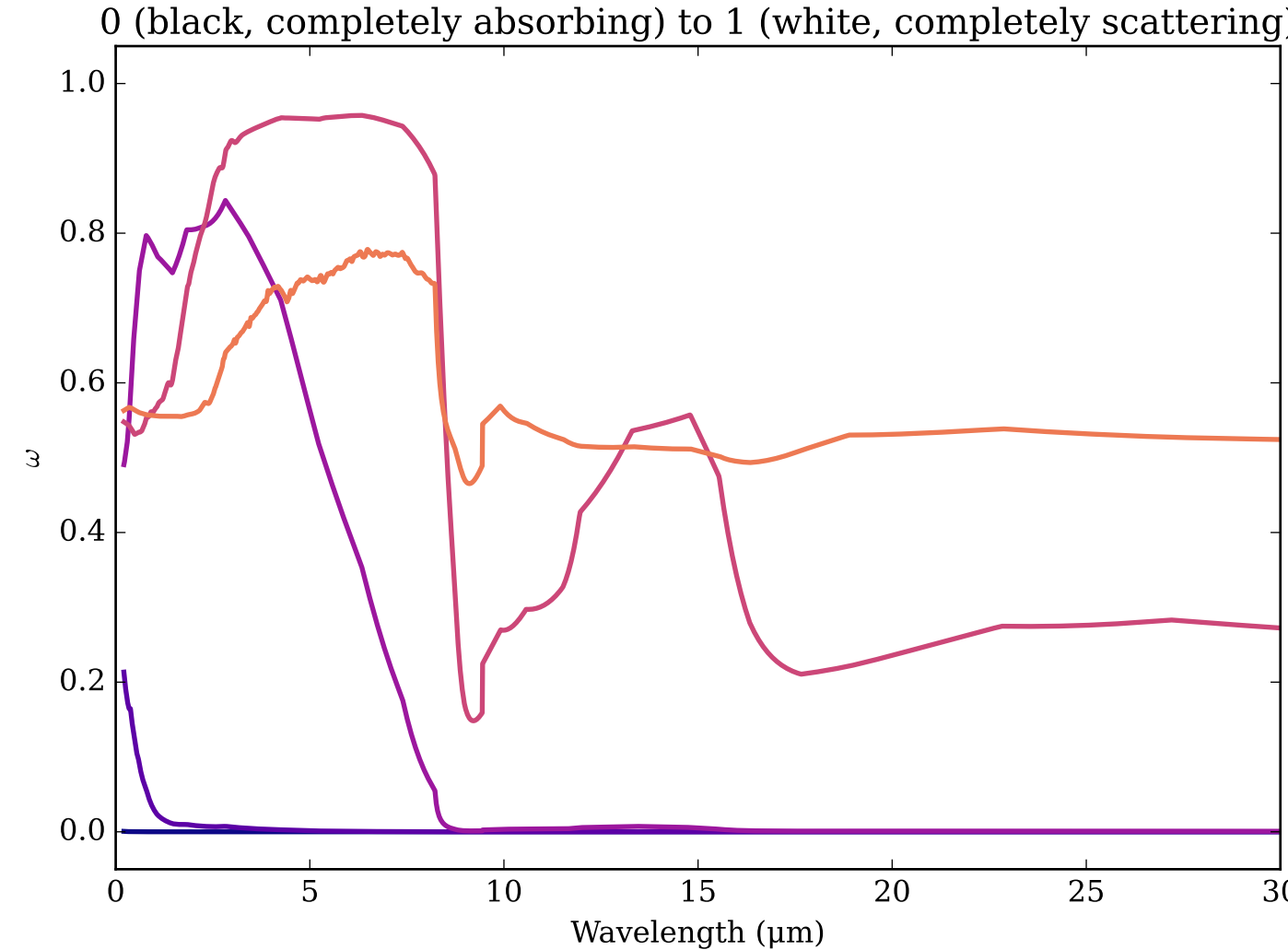


Mg<sub>2</sub>SiO<sub>4</sub>\_Fe\_rich Effective Extinction Cross Section

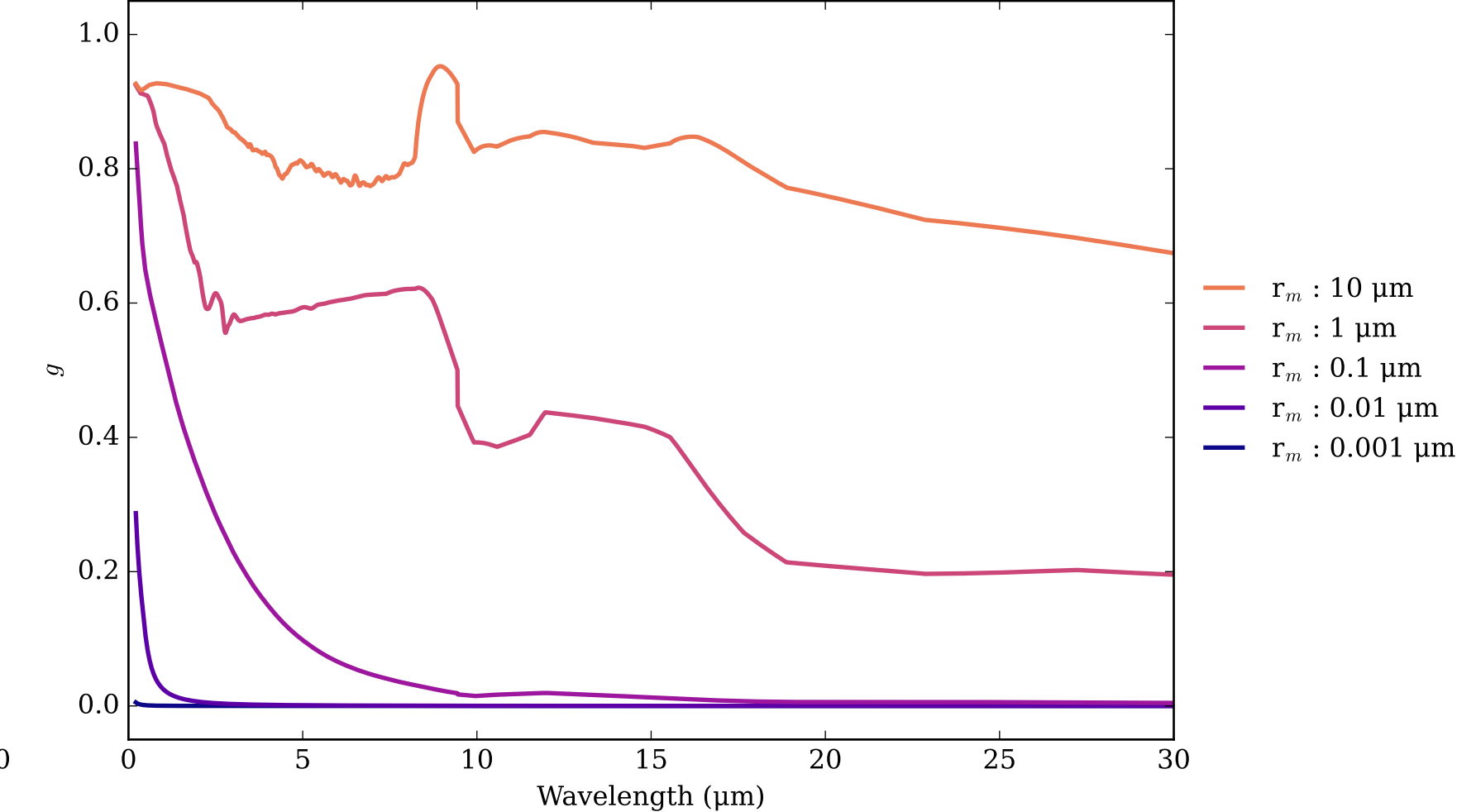
$$\sigma_{\text{ext, eff}} = \sigma_{\text{abs, eff}} + \sigma_{\text{scat, eff}}$$



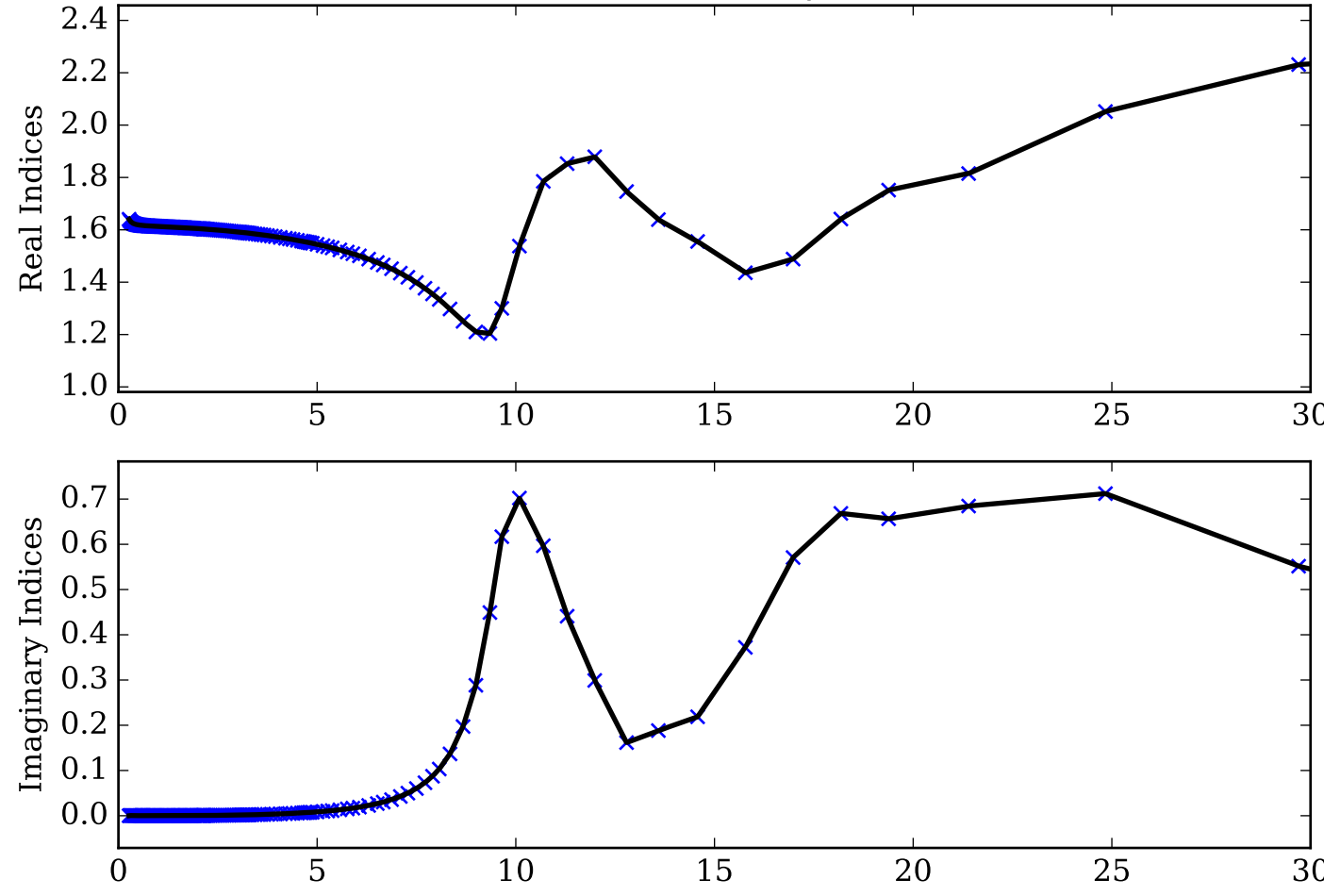
Mg<sub>2</sub>SiO<sub>4</sub>\_Fe\_rich Single Scattering Albedos  $\omega$



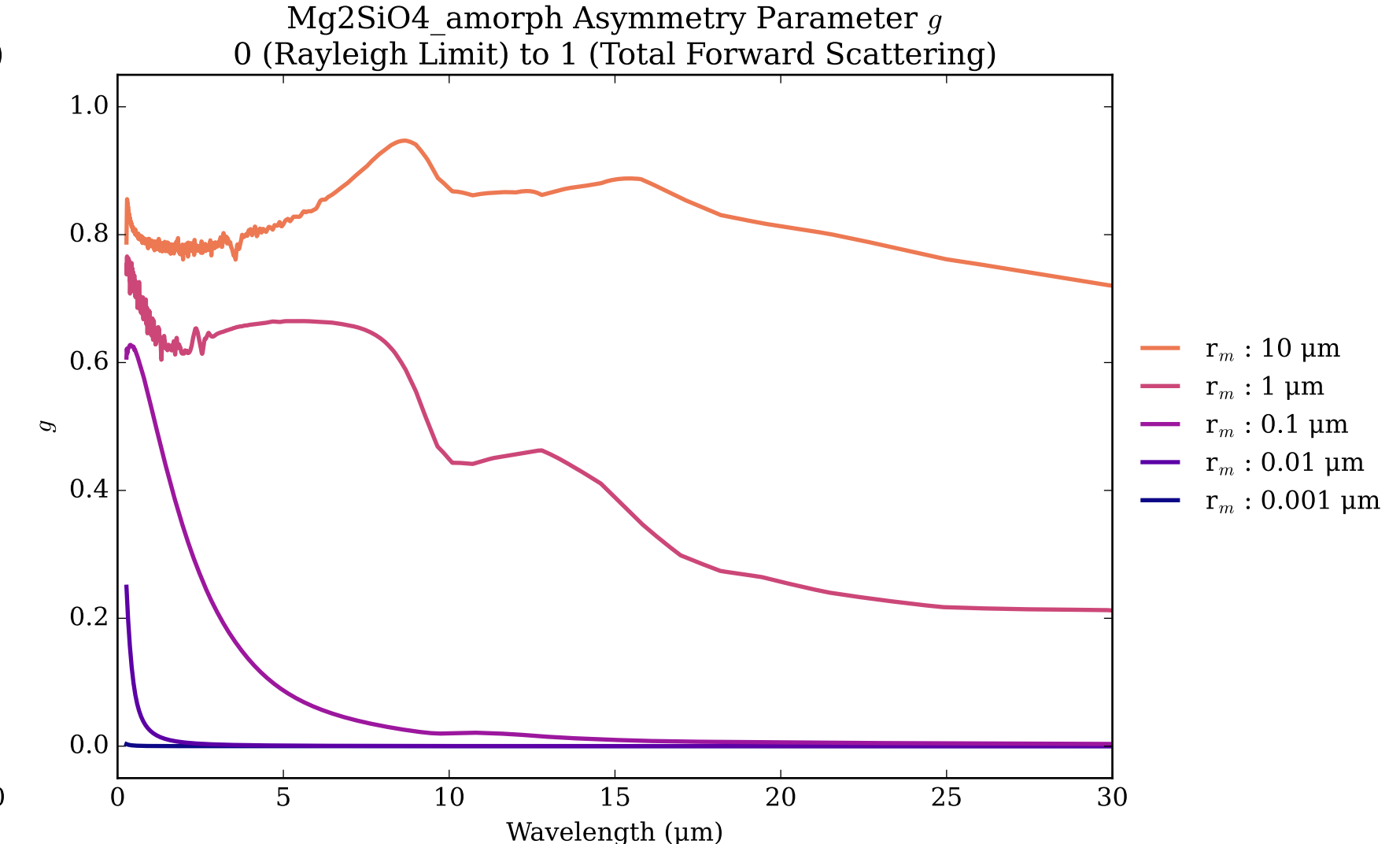
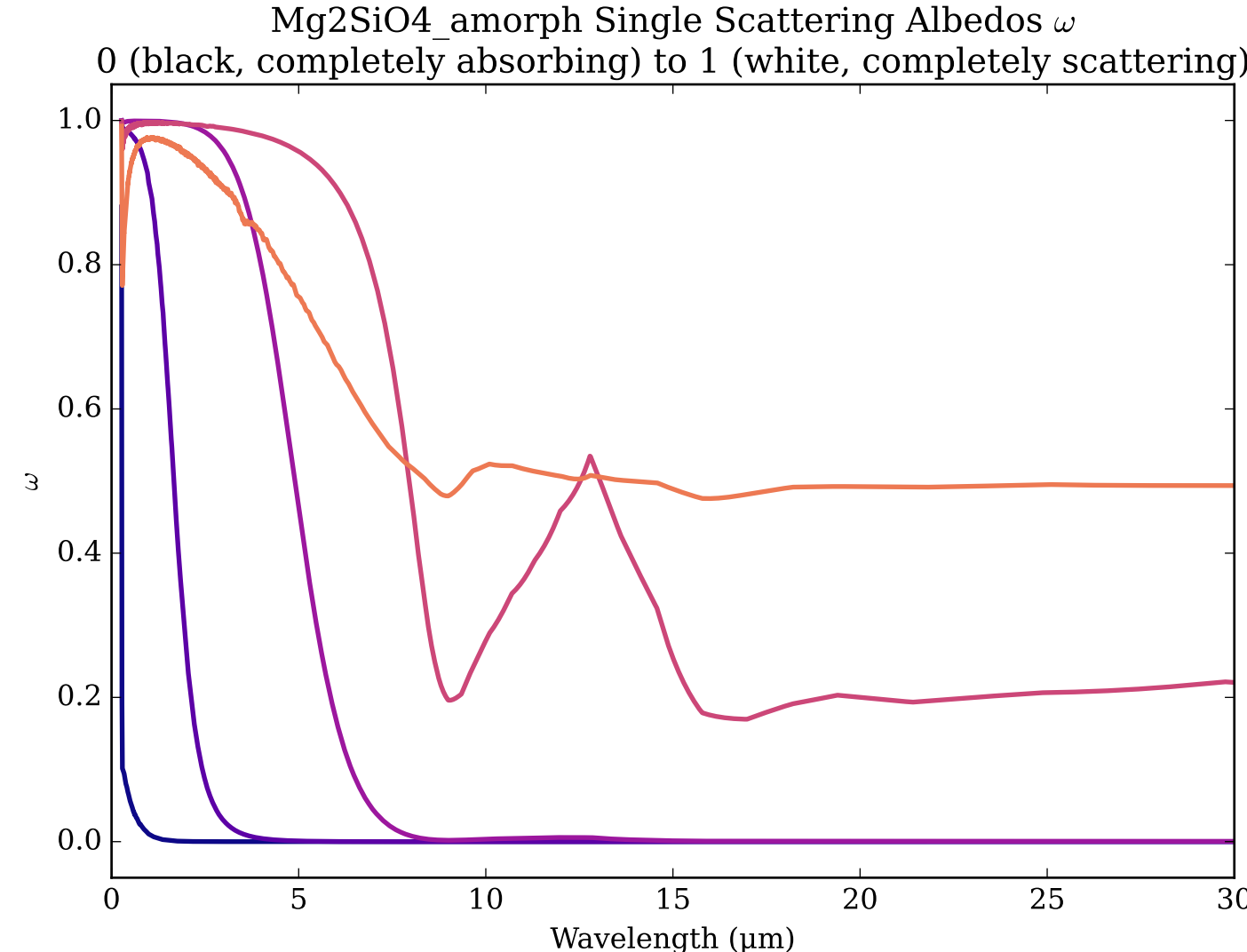
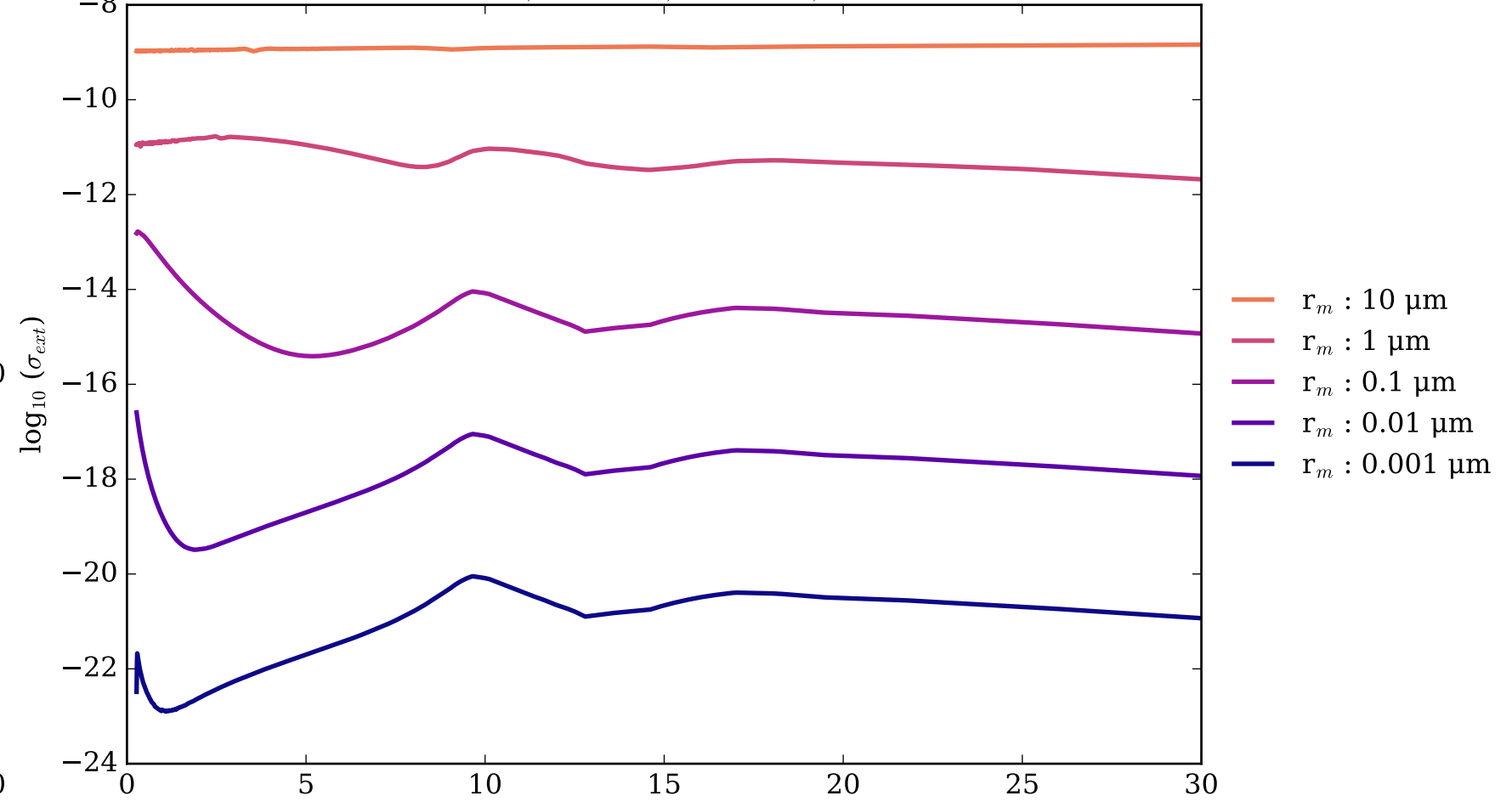
Mg<sub>2</sub>SiO<sub>4</sub>\_Fe\_rich Asymmetry Parameter  $g$   
0 (Rayleigh Limit) to 1 (Total Forward Scattering)



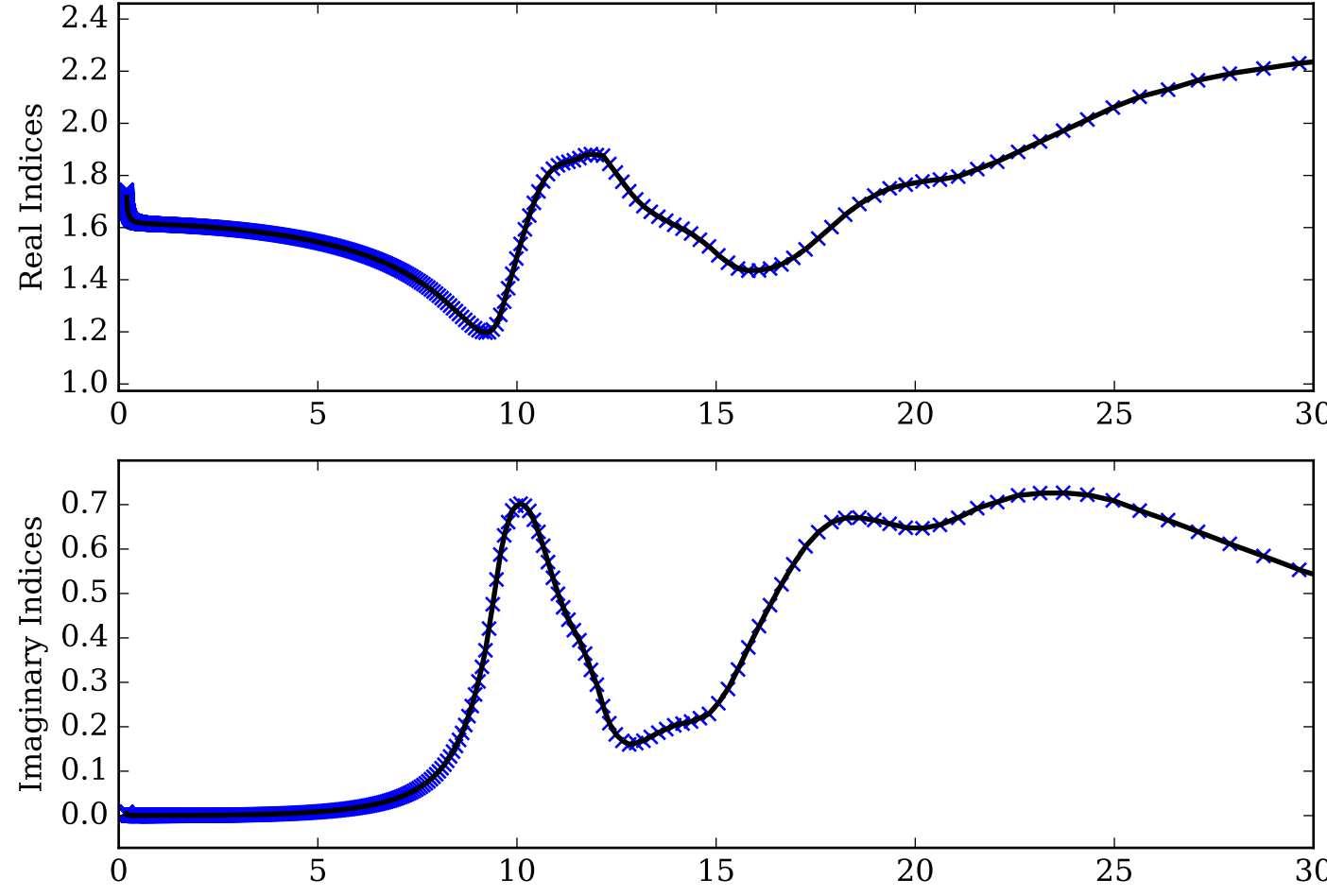
Refractive Indices for Mg<sub>2</sub>SiO<sub>4</sub>  
(0.27, 30.0)  $\mu\text{m}$



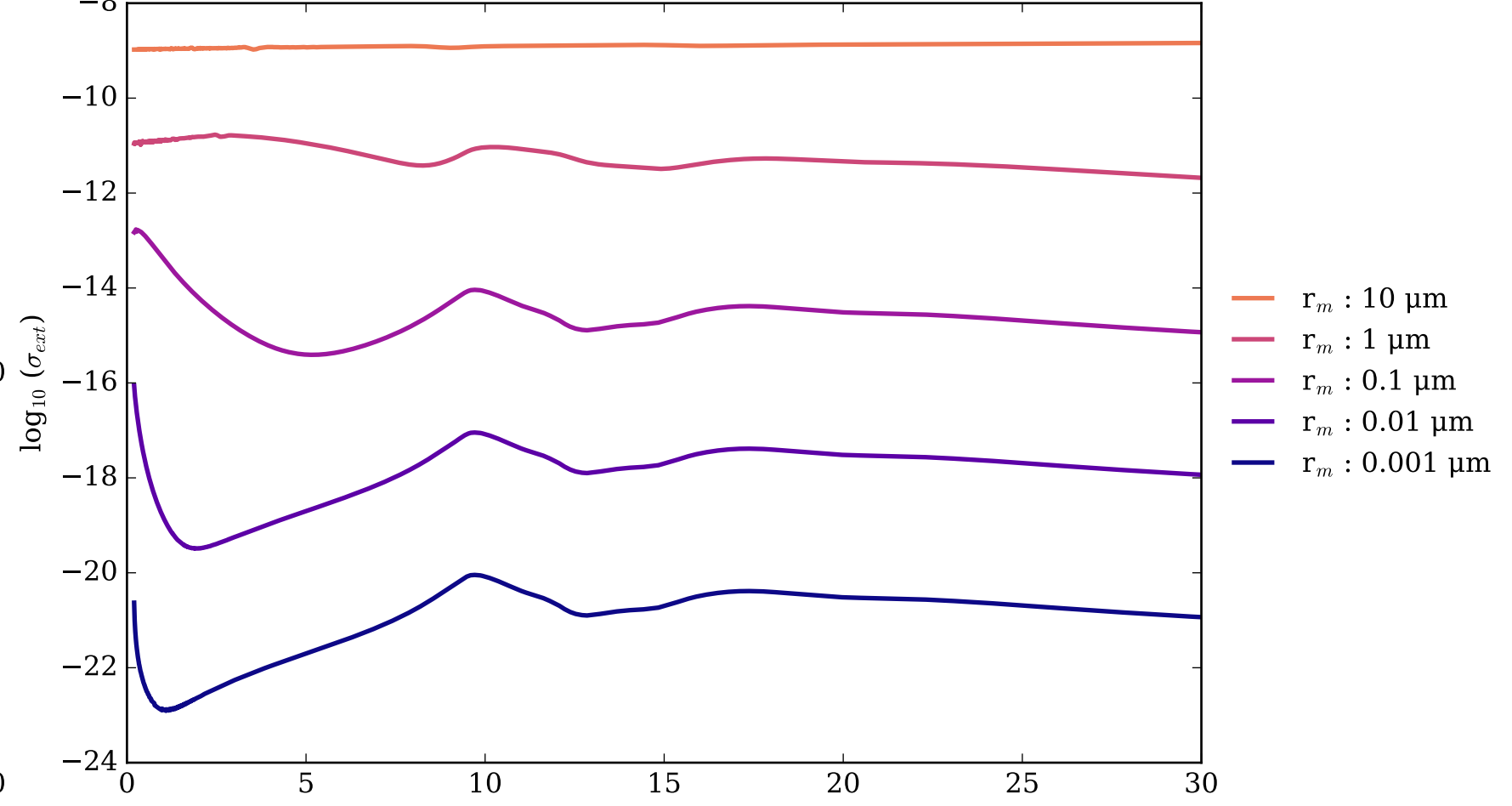
Mg<sub>2</sub>SiO<sub>4</sub>\_amorph Effective Extinction Cross Section  
 $\sigma_{\text{ext, eff}} = \sigma_{\text{abs, eff}} + \sigma_{\text{scat, eff}}$



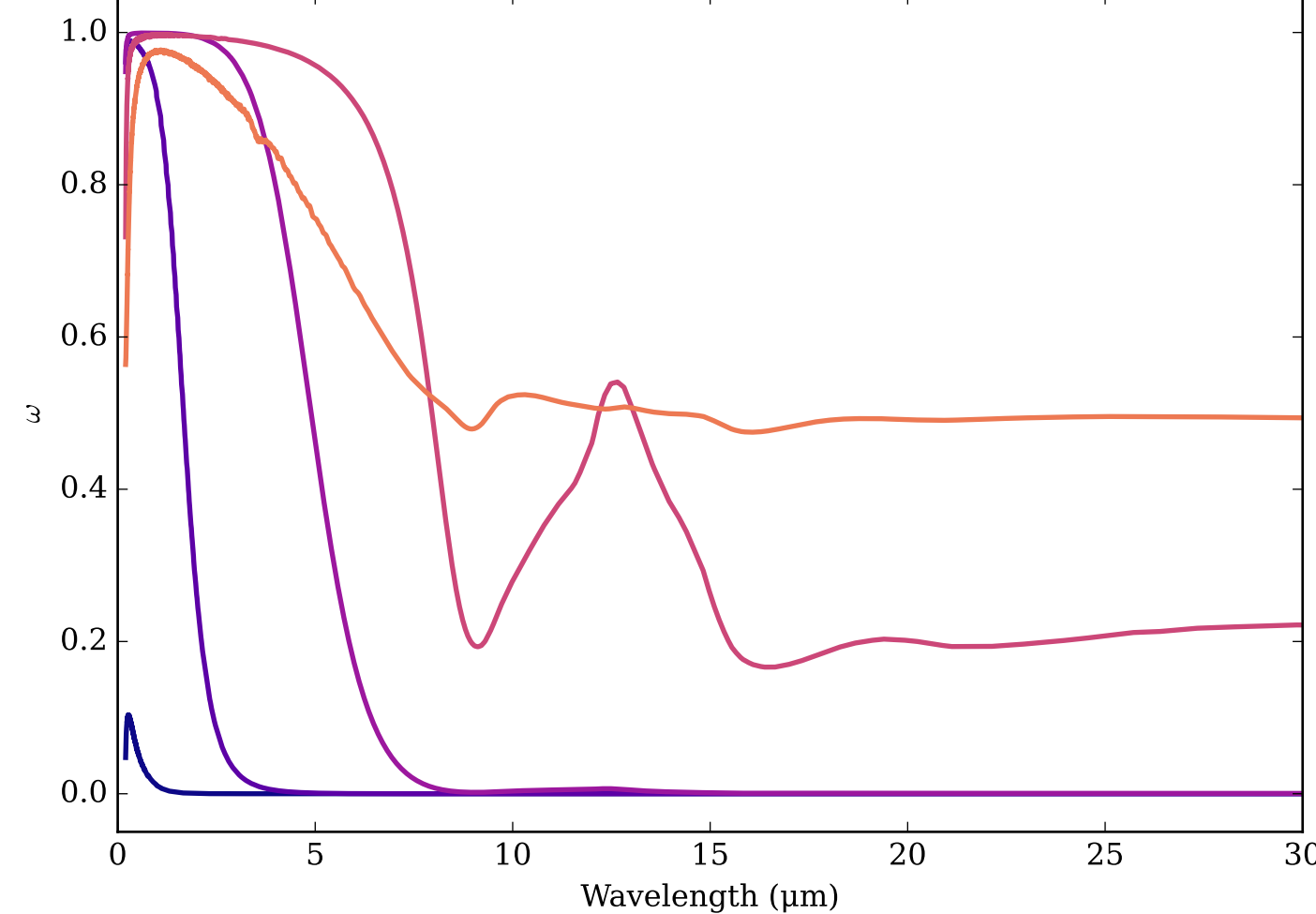
Refractive Indices for Mg<sub>2</sub>SiO<sub>4</sub>  
(0.2, 30.0)  $\mu\text{m}$



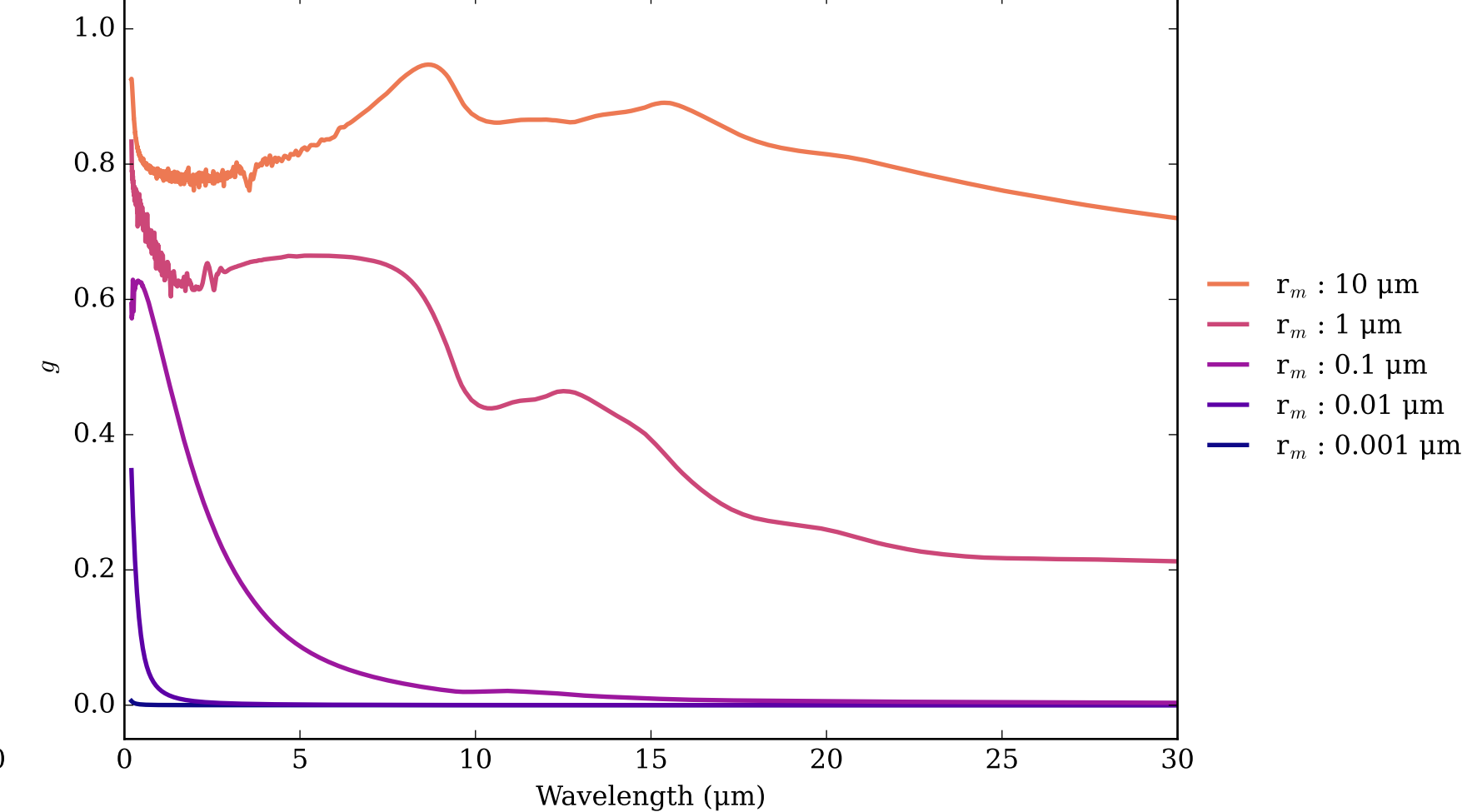
Mg<sub>2</sub>SiO<sub>4</sub>\_amorph\_sol\_gel Effective Extinction Cross Section



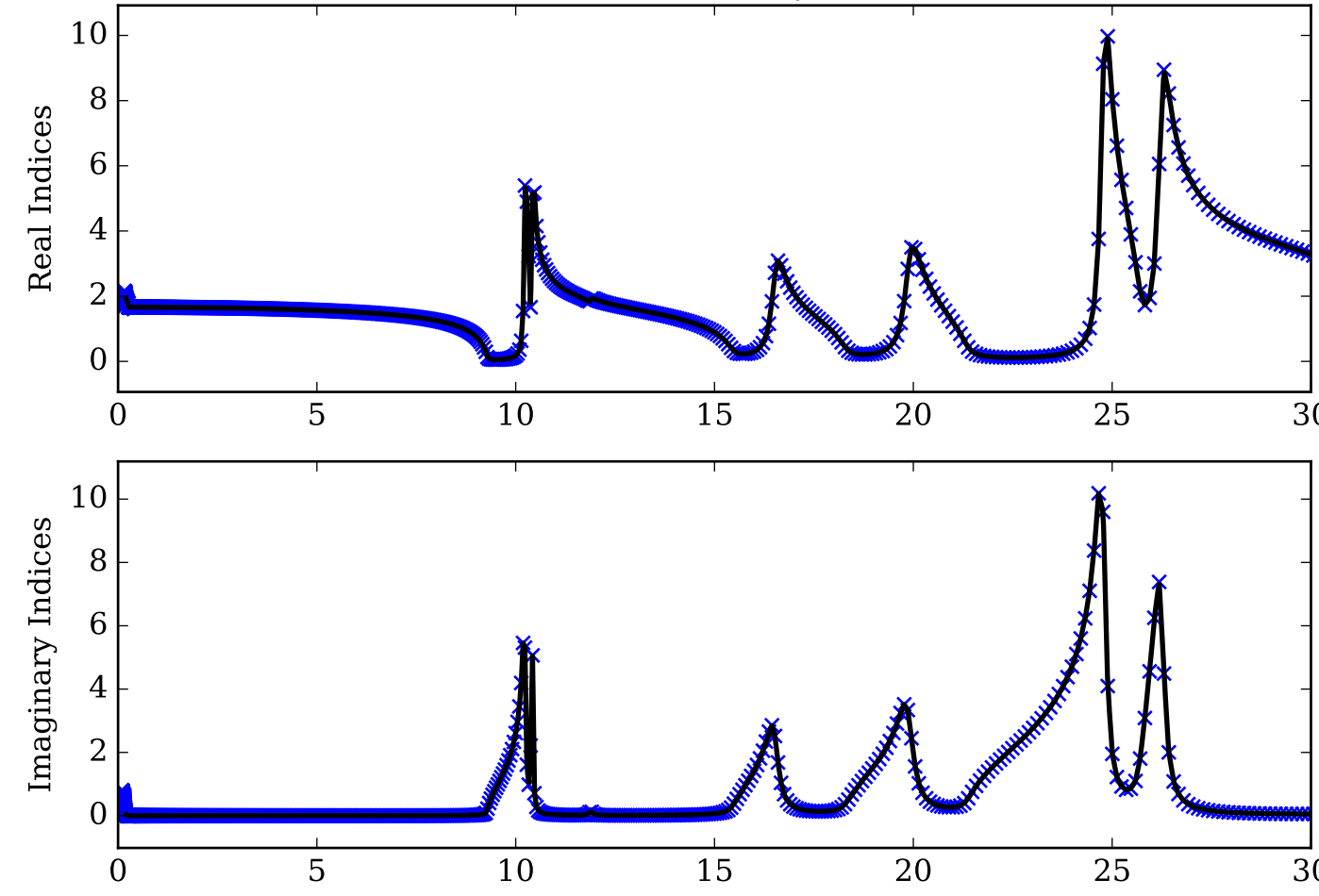
Mg<sub>2</sub>SiO<sub>4</sub>\_amorph\_sol\_gel Single Scattering Albedos  $\omega$   
0 (black, completely absorbing) to 1 (white, completely scattering)



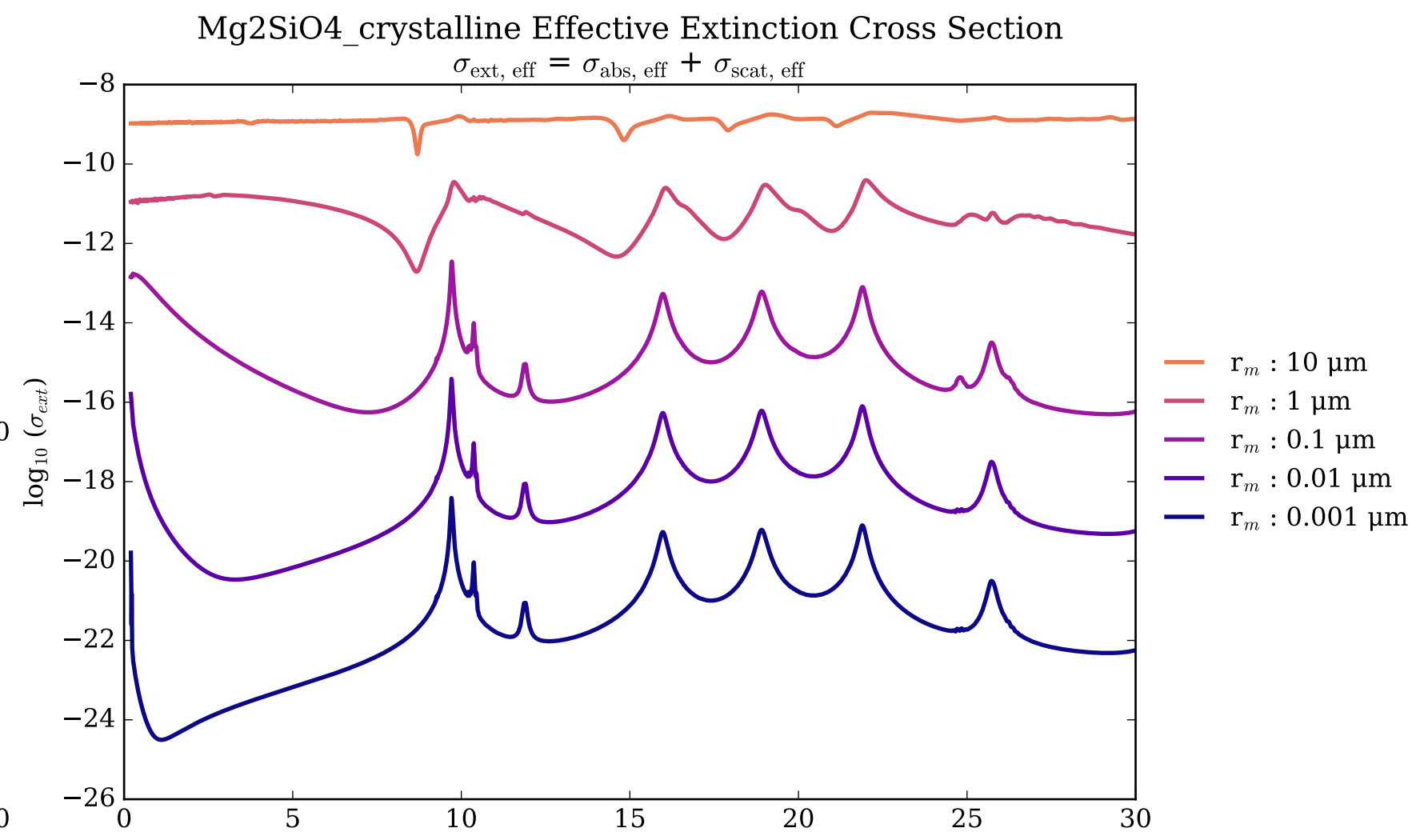
Mg<sub>2</sub>SiO<sub>4</sub>\_amorph\_sol\_gel Asymmetry Parameter  $g$   
0 (Rayleigh Limit) to 1 (Total Forward Scattering)



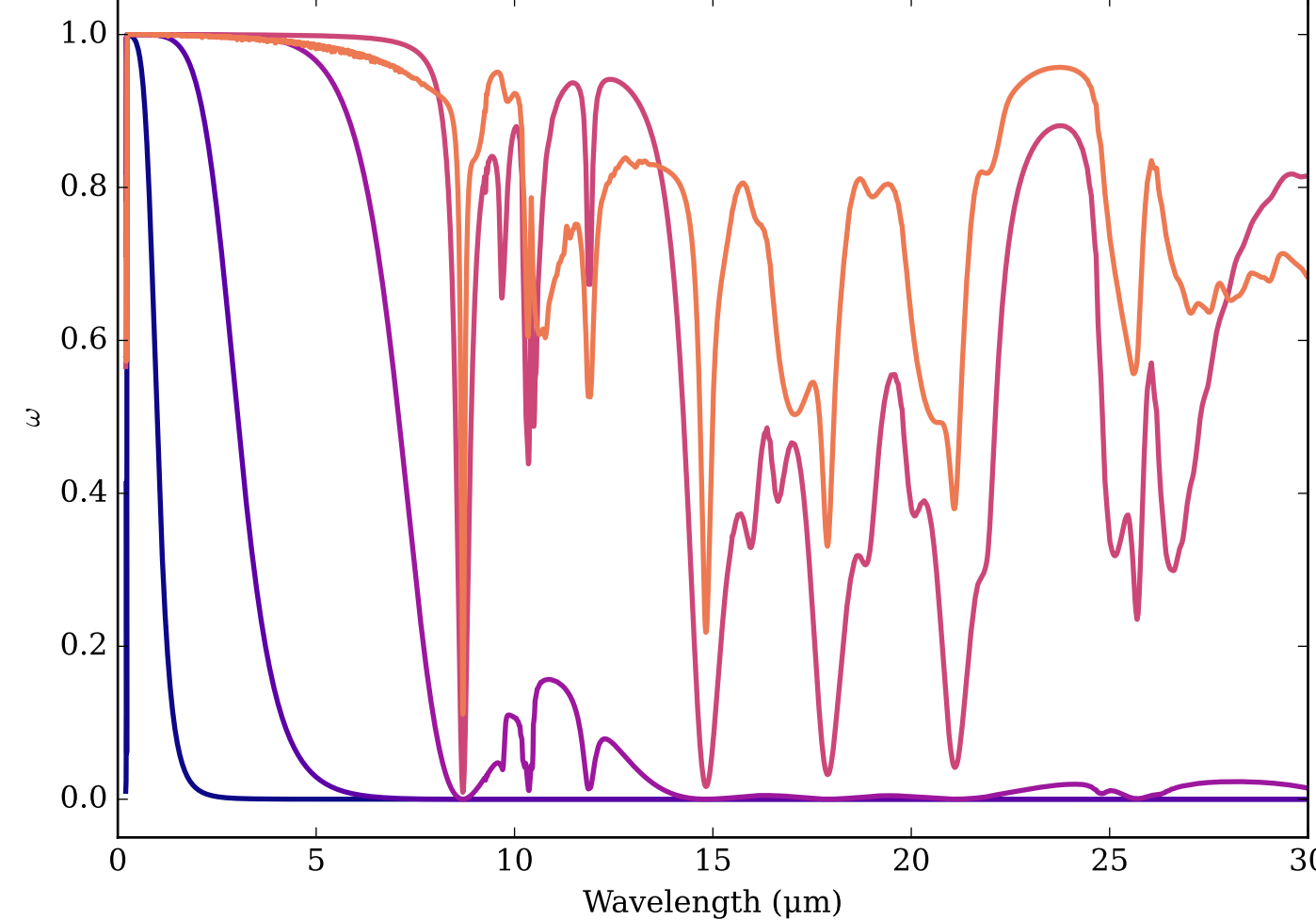
Refractive Indices for Mg<sub>2</sub>SiO<sub>4</sub>  
(0.2, 30.0)  $\mu\text{m}$



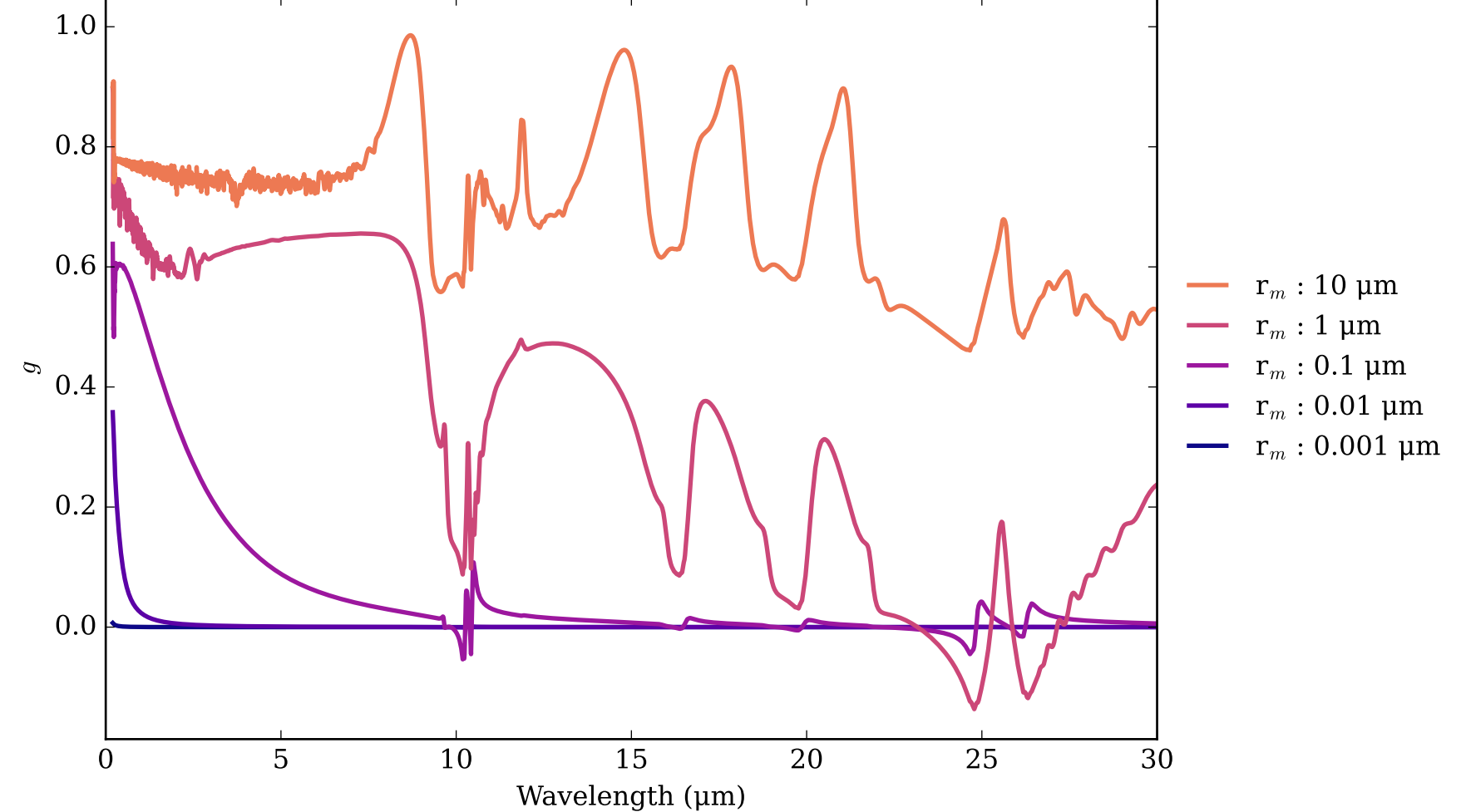
Mg<sub>2</sub>SiO<sub>4</sub>\_crystalline Effective Extinction Cross Section



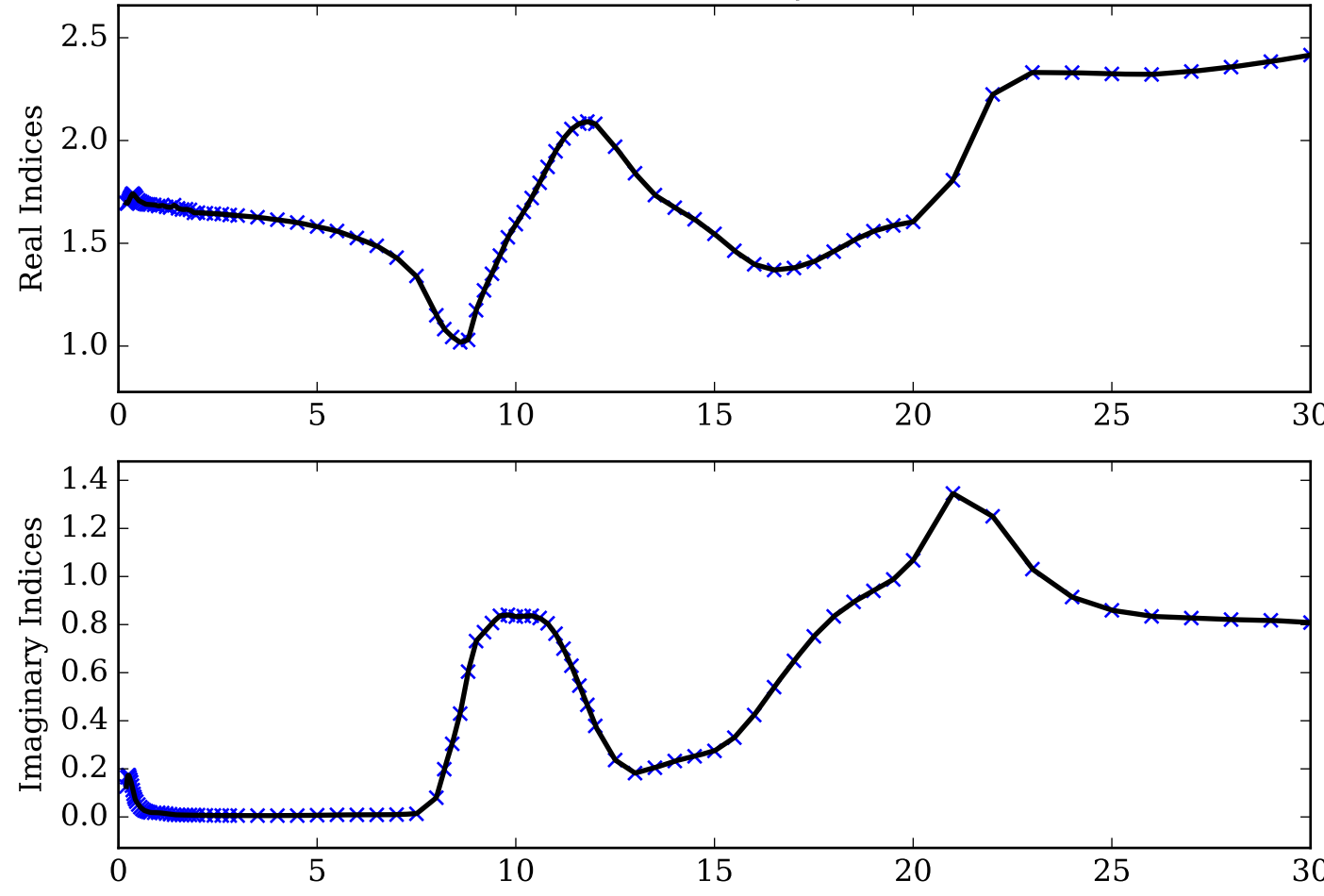
Mg<sub>2</sub>SiO<sub>4</sub>\_crystalline Single Scattering Albedos  $\omega$   
0 (black, completely absorbing) to 1 (white, completely scattering)



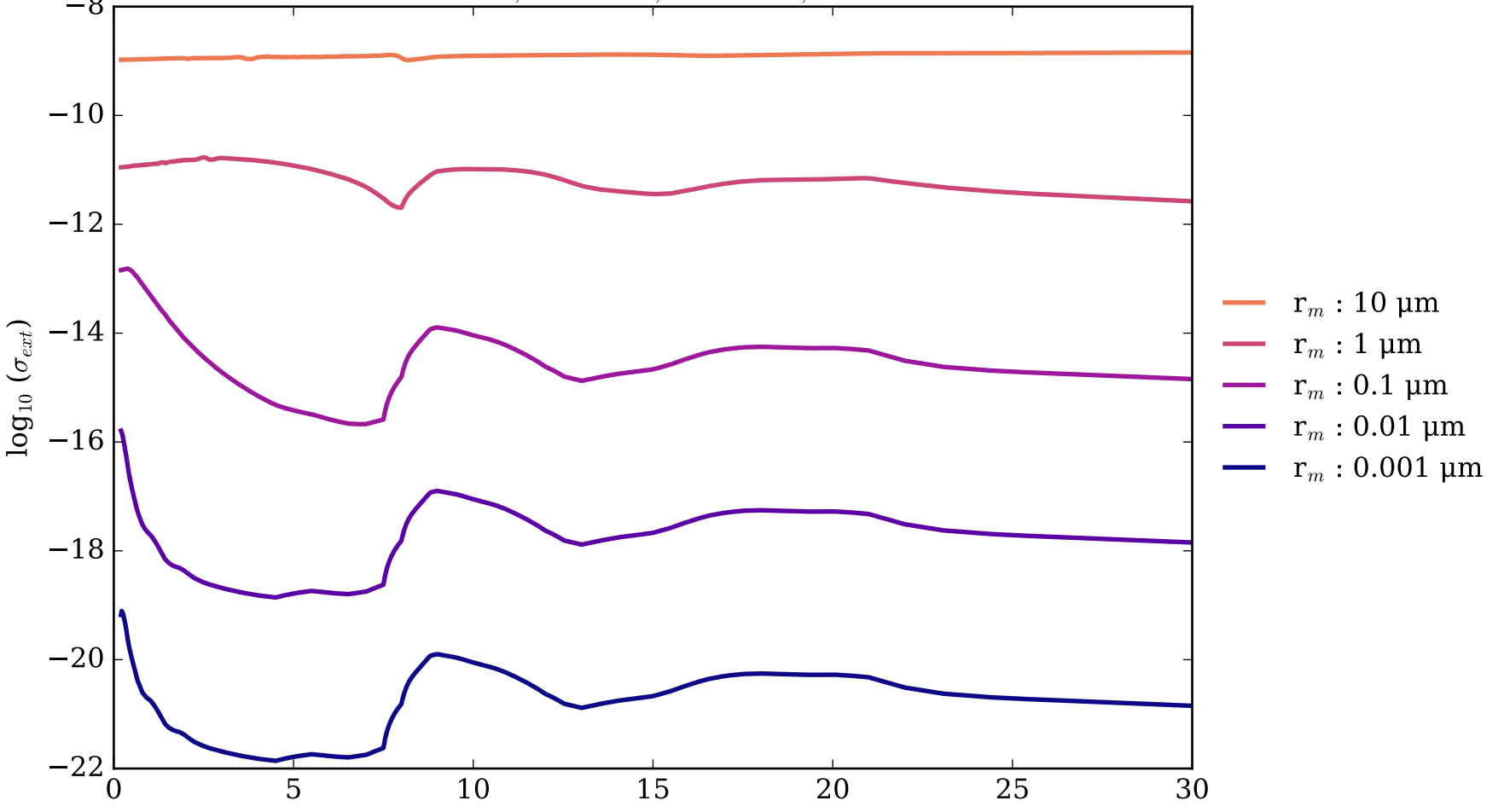
Mg<sub>2</sub>SiO<sub>4</sub>\_crystalline Asymmetry Parameter  $g$   
0 (Rayleigh Limit) to 1 (Total Forward Scattering)



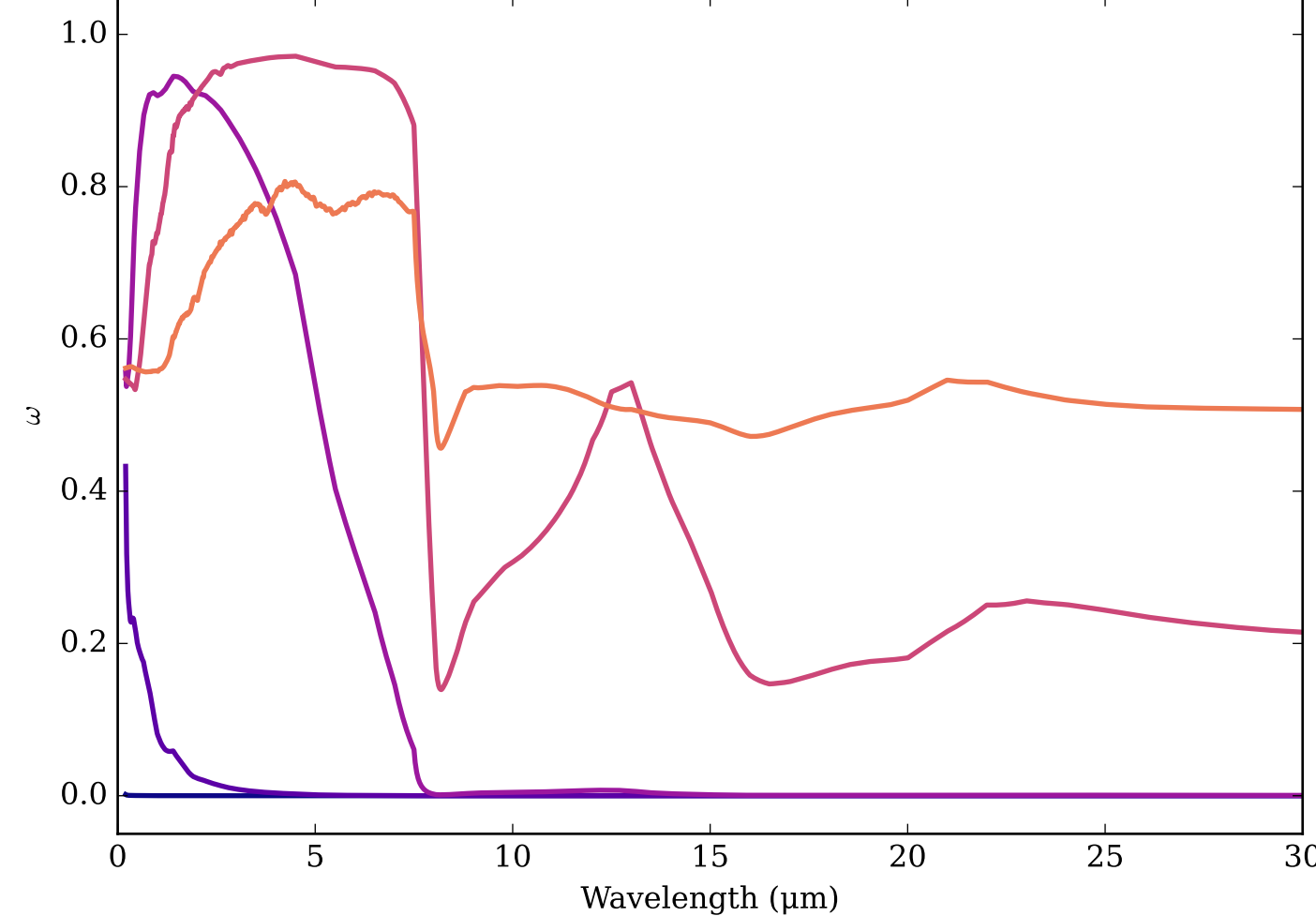
Refractive Indices for Mg<sub>4</sub>Fe<sub>6</sub>SiO<sub>3</sub>  
(0.2, 30.0)  $\mu\text{m}$



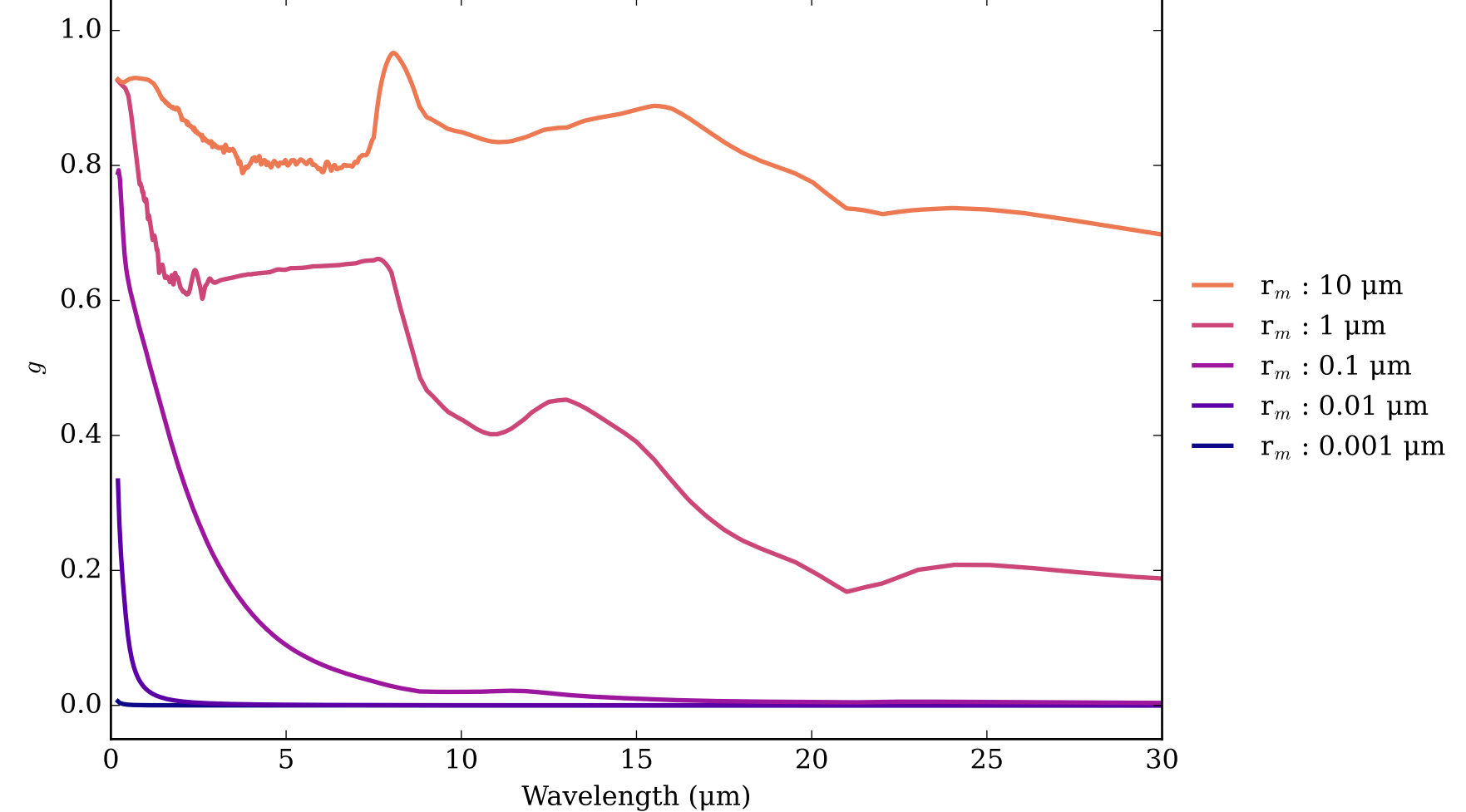
Mg<sub>4</sub>Fe<sub>6</sub>SiO<sub>3</sub>\_amorph\_glass Effective Extinction Cross Section



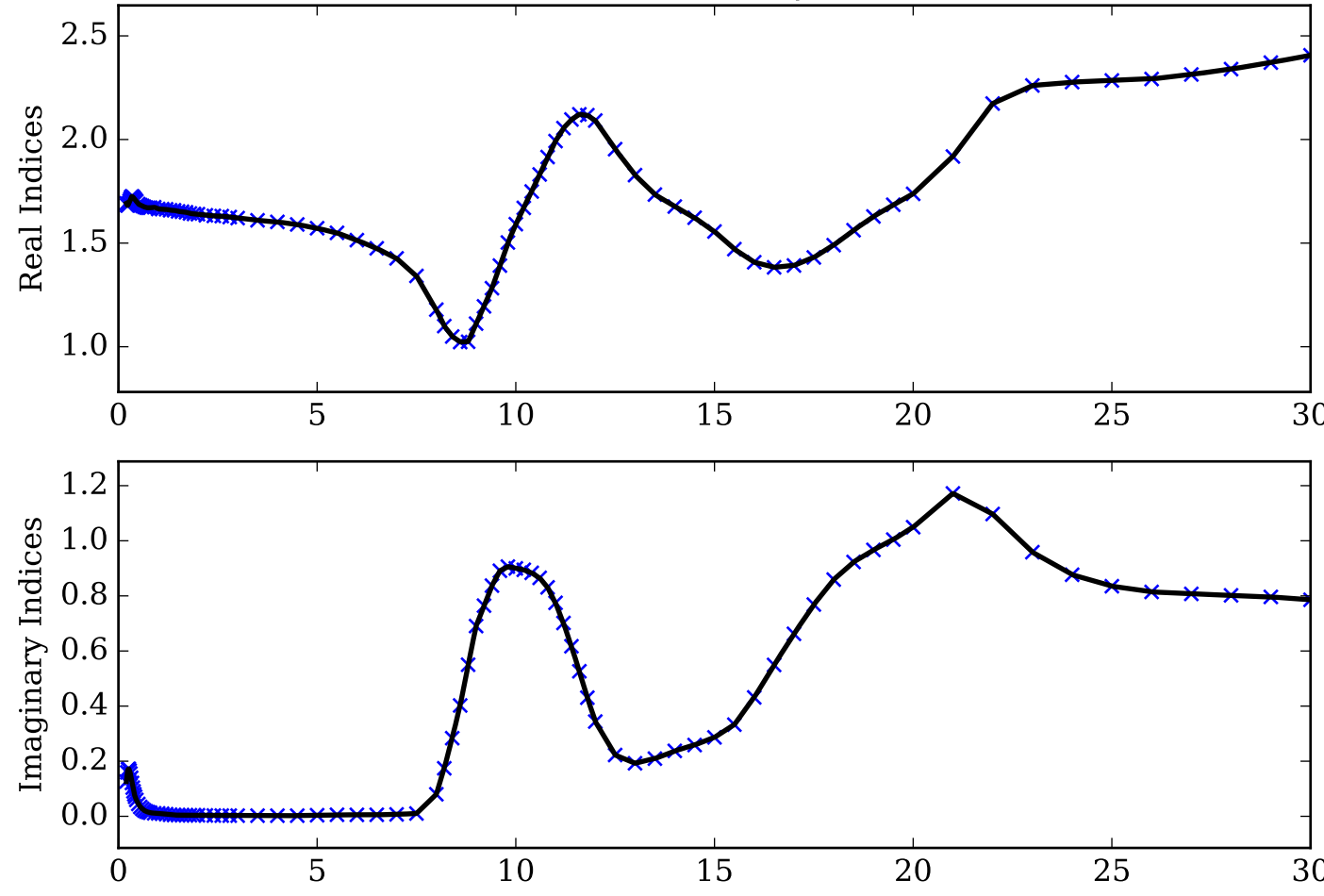
Mg<sub>4</sub>Fe<sub>6</sub>SiO<sub>3</sub>\_amorph\_glass Single Scattering Albedos  $\omega$   
0 (black, completely absorbing) to 1 (white, completely scattering)



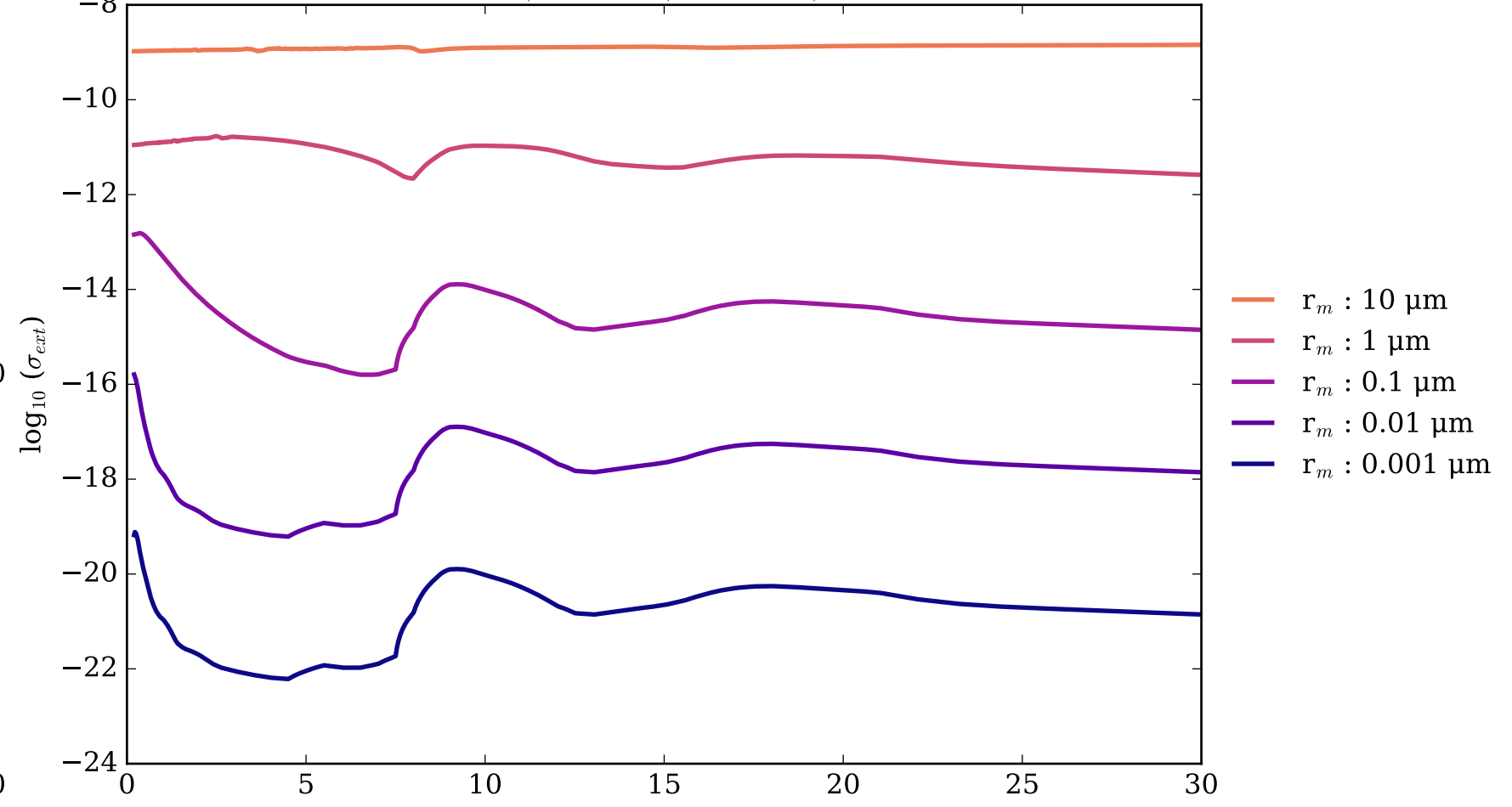
Mg<sub>4</sub>Fe<sub>6</sub>SiO<sub>3</sub>\_amorph\_glass Asymmetry Parameter  $g$   
0 (Rayleigh Limit) to 1 (Total Forward Scattering)



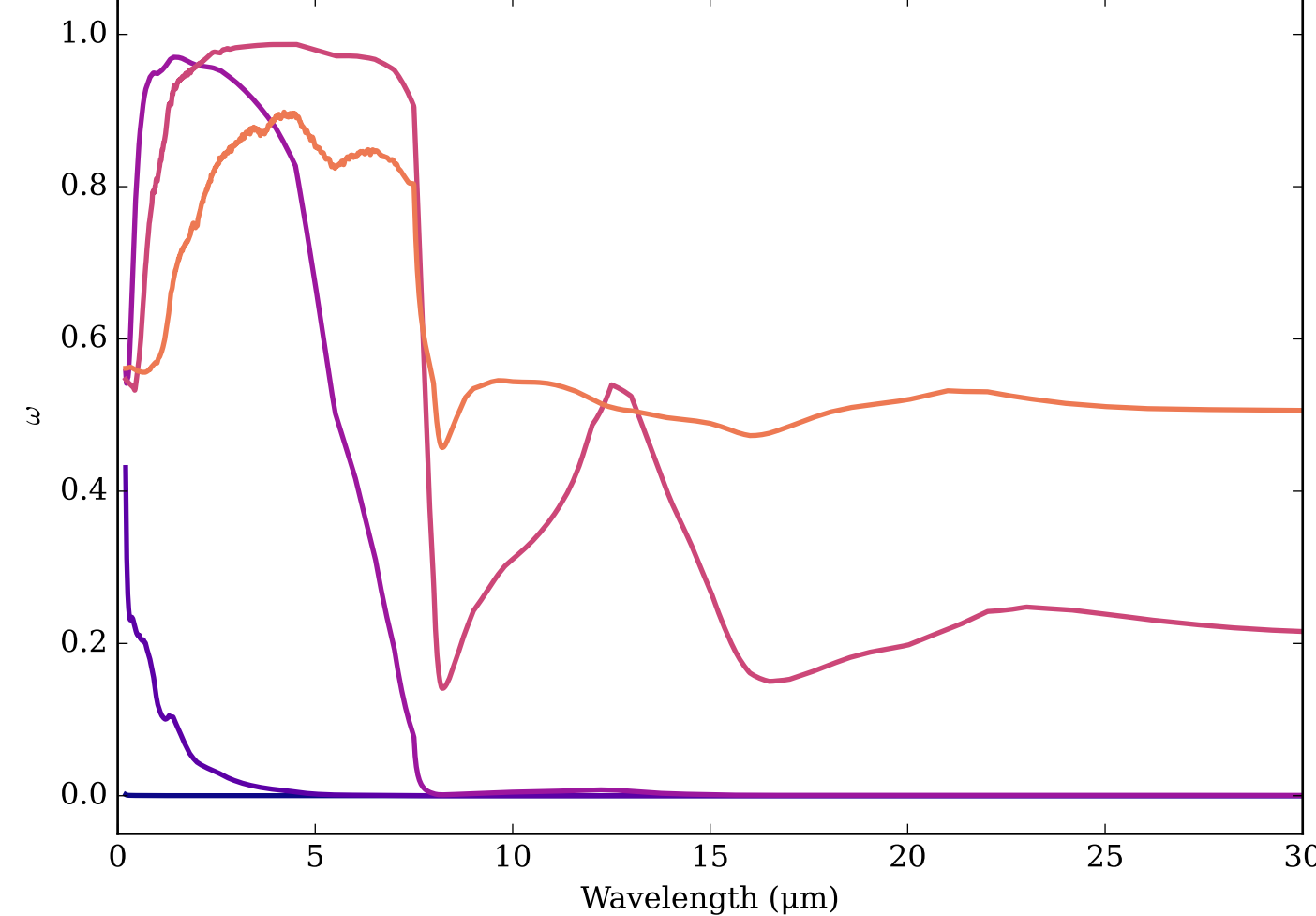
Refractive Indices for Mg<sub>5</sub>Fe<sub>5</sub>SiO<sub>3</sub>  
(0.2, 30.0)  $\mu\text{m}$



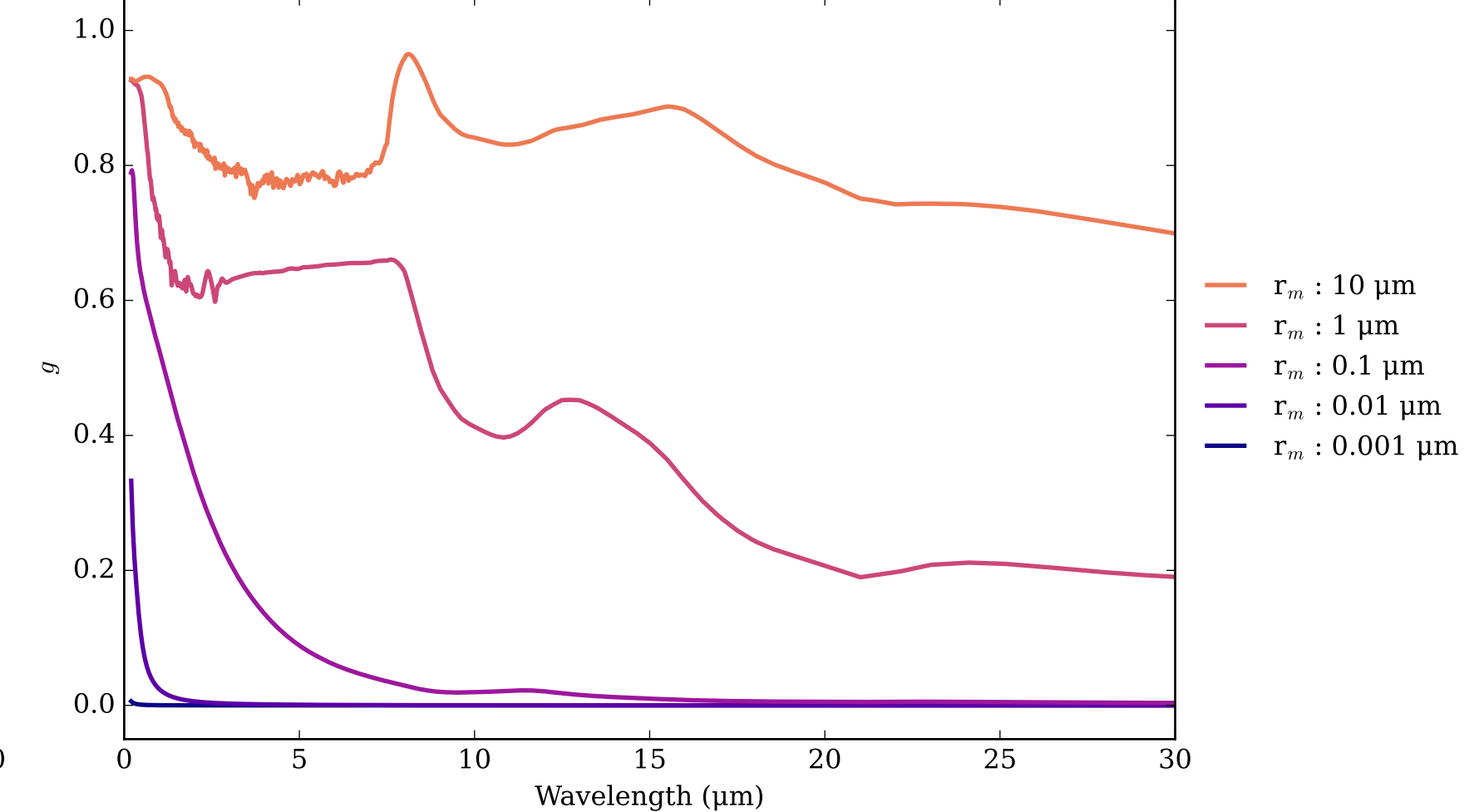
Mg<sub>5</sub>Fe<sub>5</sub>SiO<sub>3</sub>\_amorph\_glass Effective Extinction Cross Section



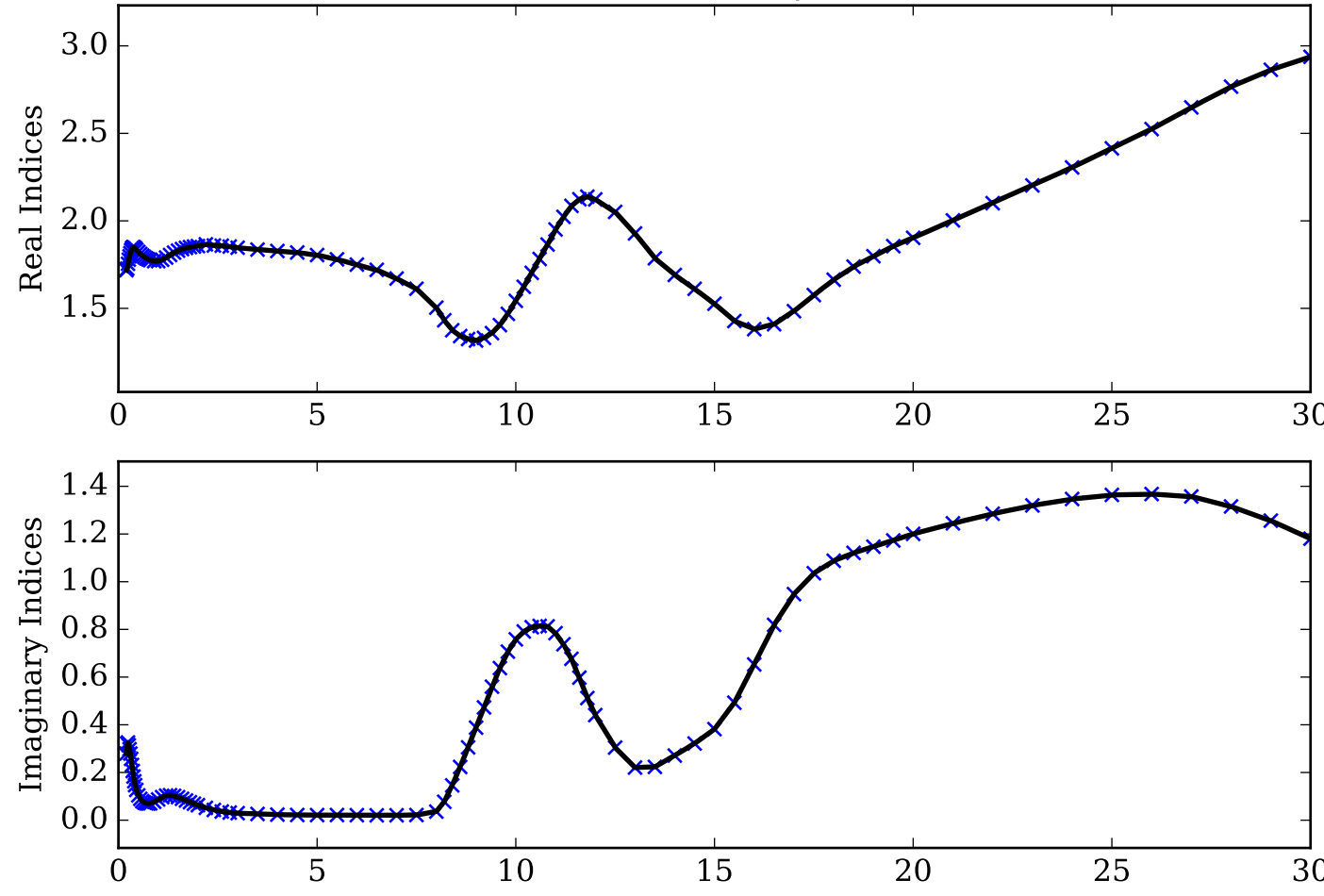
Mg<sub>5</sub>Fe<sub>5</sub>SiO<sub>3</sub>\_amorph\_glass Single Scattering Albedos  $\omega$   
0 (black, completely absorbing) to 1 (white, completely scattering)



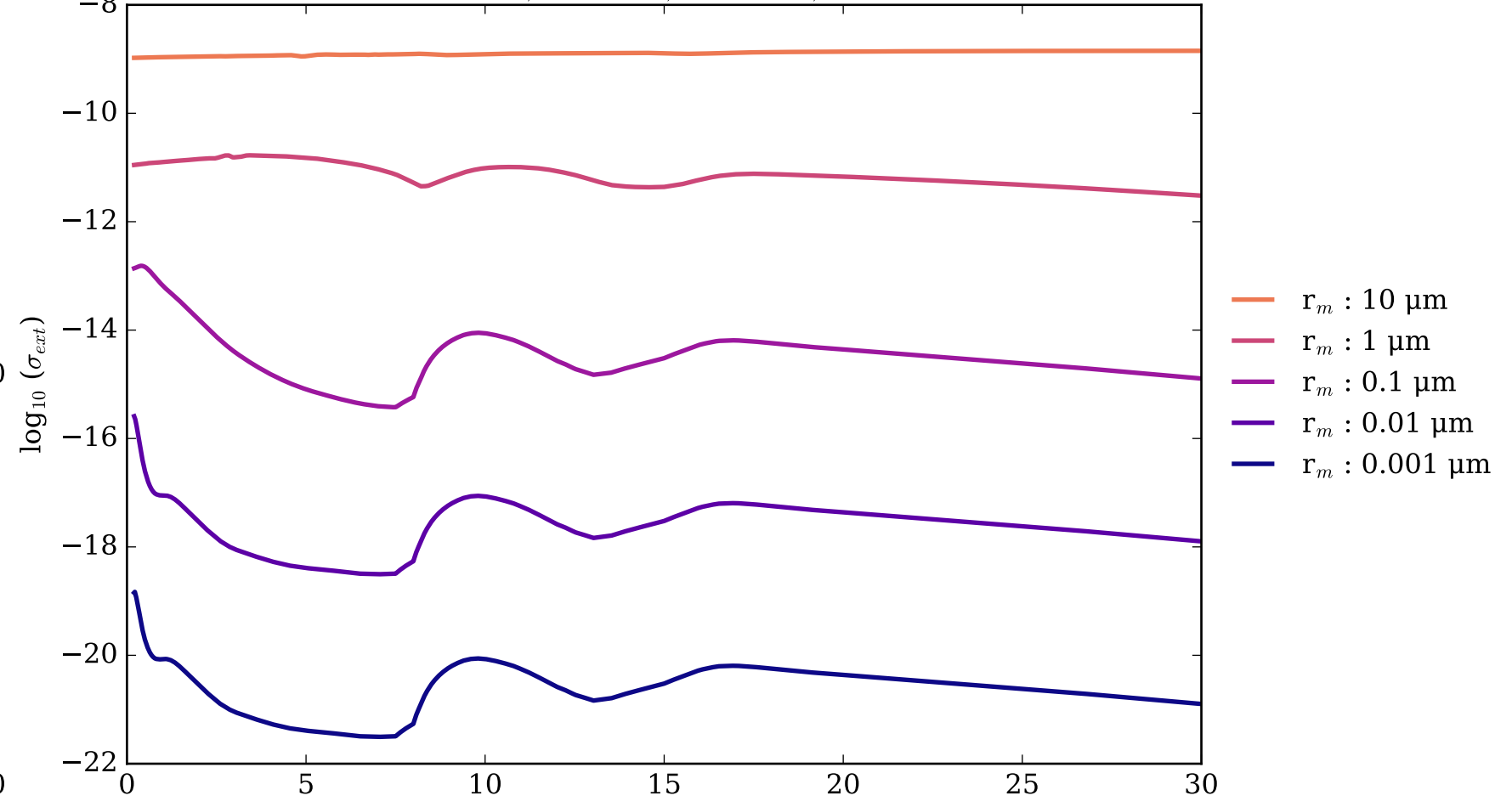
Mg<sub>5</sub>Fe<sub>5</sub>SiO<sub>3</sub>\_amorph\_glass Asymmetry Parameter  $g$   
0 (Rayleigh Limit) to 1 (Total Forward Scattering)



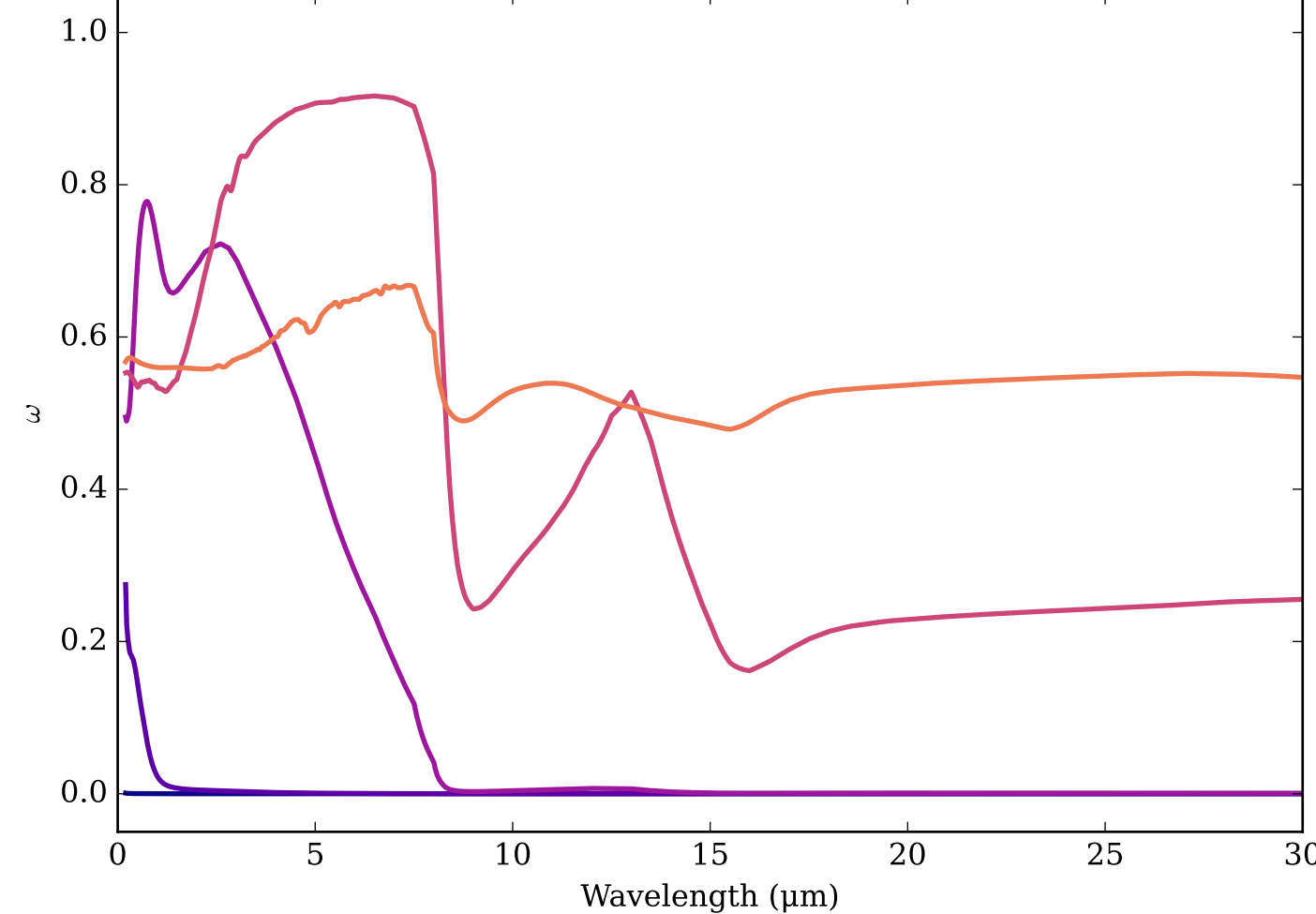
Refractive Indices for Mg8Fe12SiO<sub>4</sub>  
 (0.2, 30.0) μm



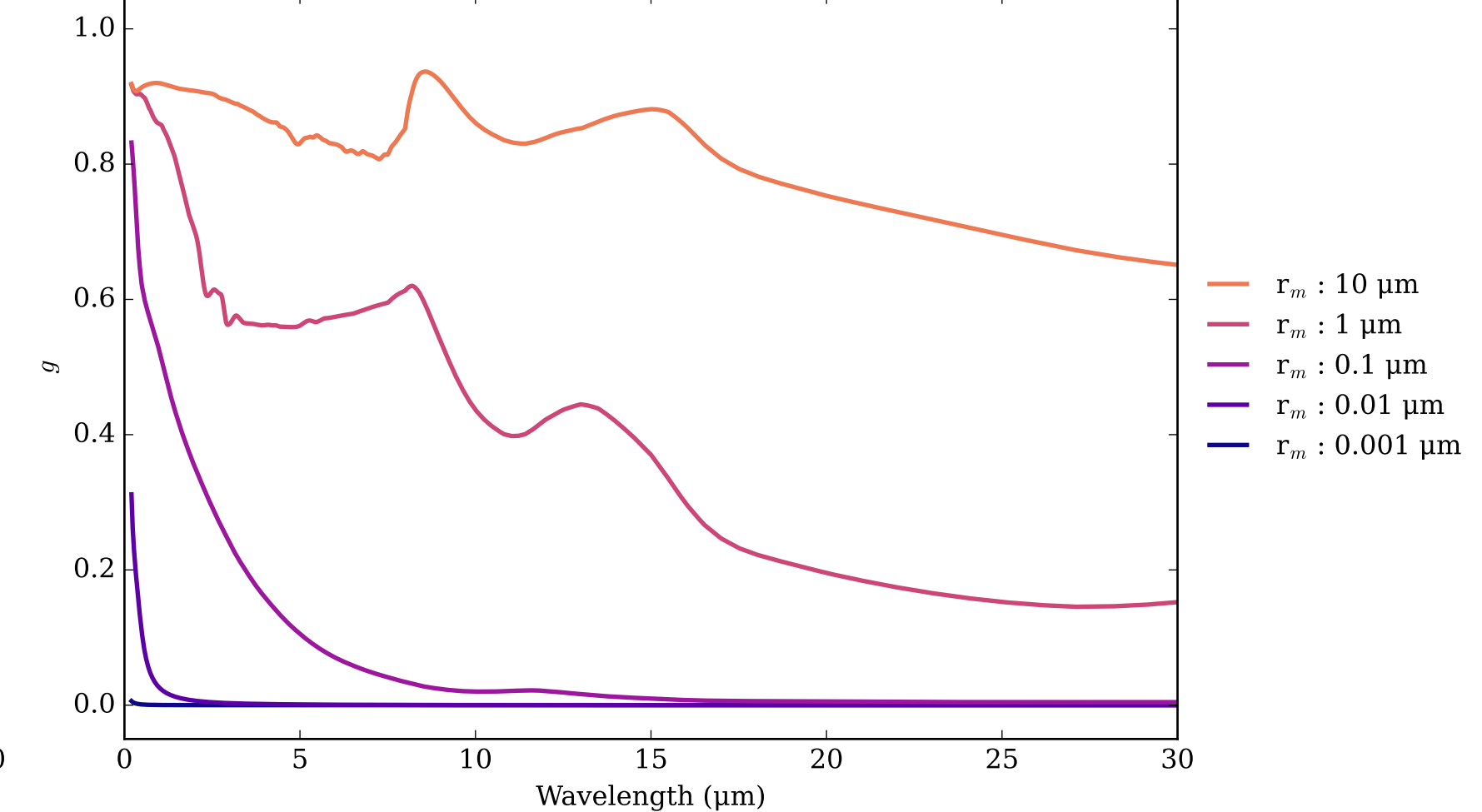
Mg8Fe12SiO<sub>4</sub>\_amorph\_glass Effective Extinction Cross Section  
 $\sigma_{ext, eff} = \sigma_{abs, eff} + \sigma_{scat, eff}$



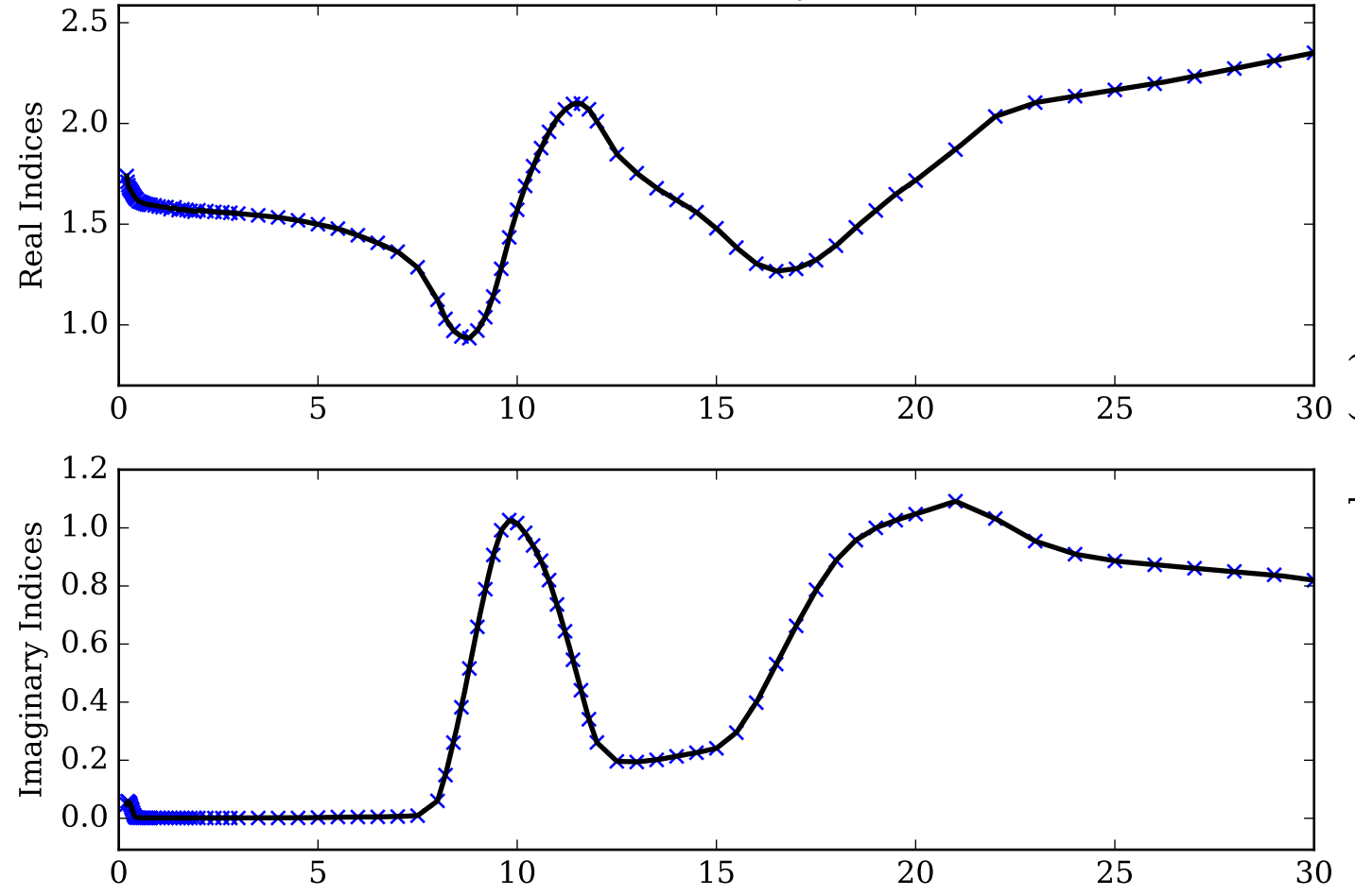
Mg8Fe12SiO<sub>4</sub>\_amorph\_glass Single Scattering Albedos  $\omega$   
 0 (black, completely absorbing) to 1 (white, completely scattering)



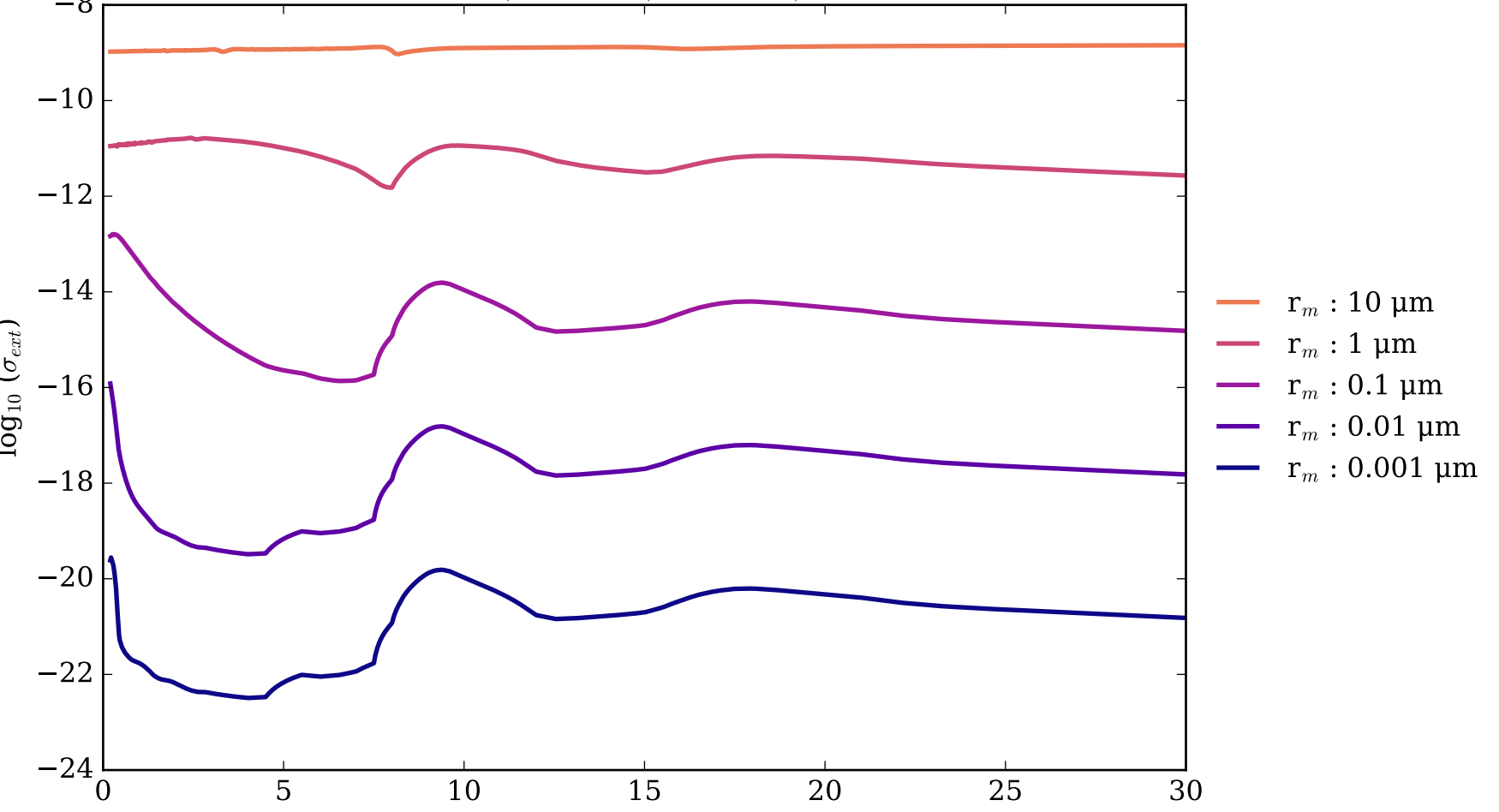
Mg8Fe12SiO<sub>4</sub>\_amorph\_glass Asymmetry Parameter  $g$   
 0 (Rayleigh Limit) to 1 (Total Forward Scattering)



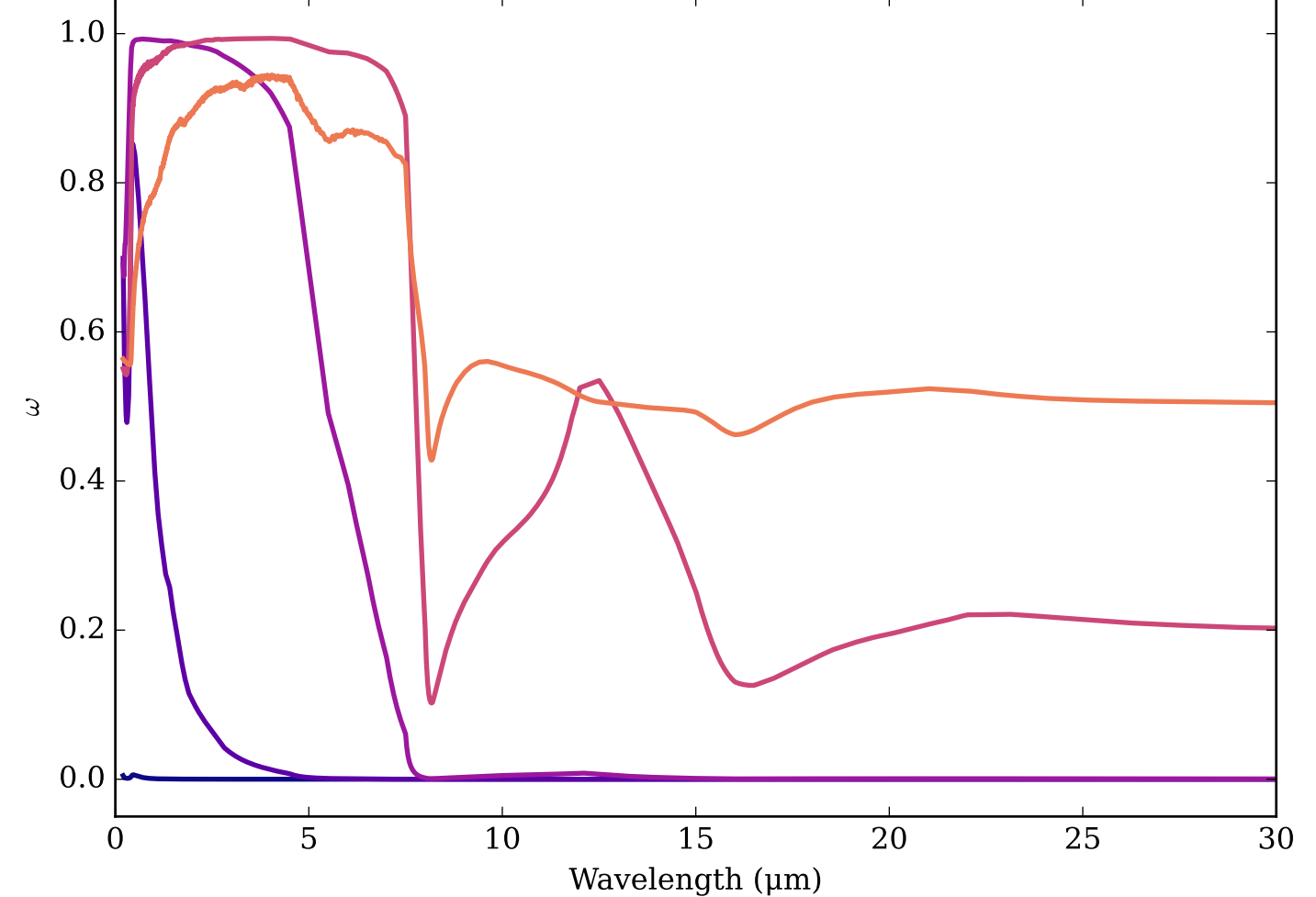
Refractive Indices for Mg8Fe2SiO<sub>3</sub>  
(0.2, 30.0) μm



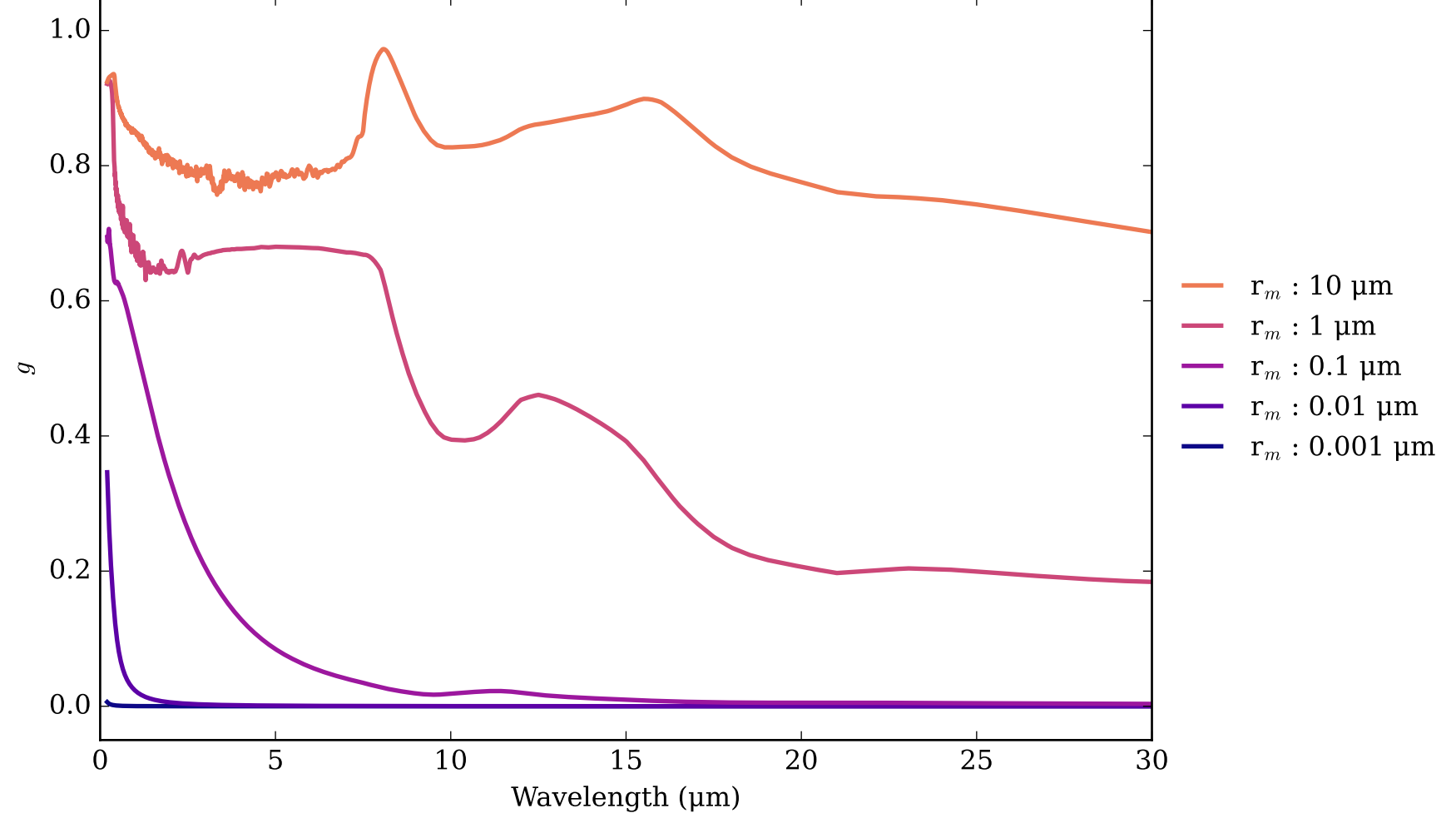
Mg8Fe2SiO<sub>3</sub>\_amorph\_glass Effective Extinction Cross Section



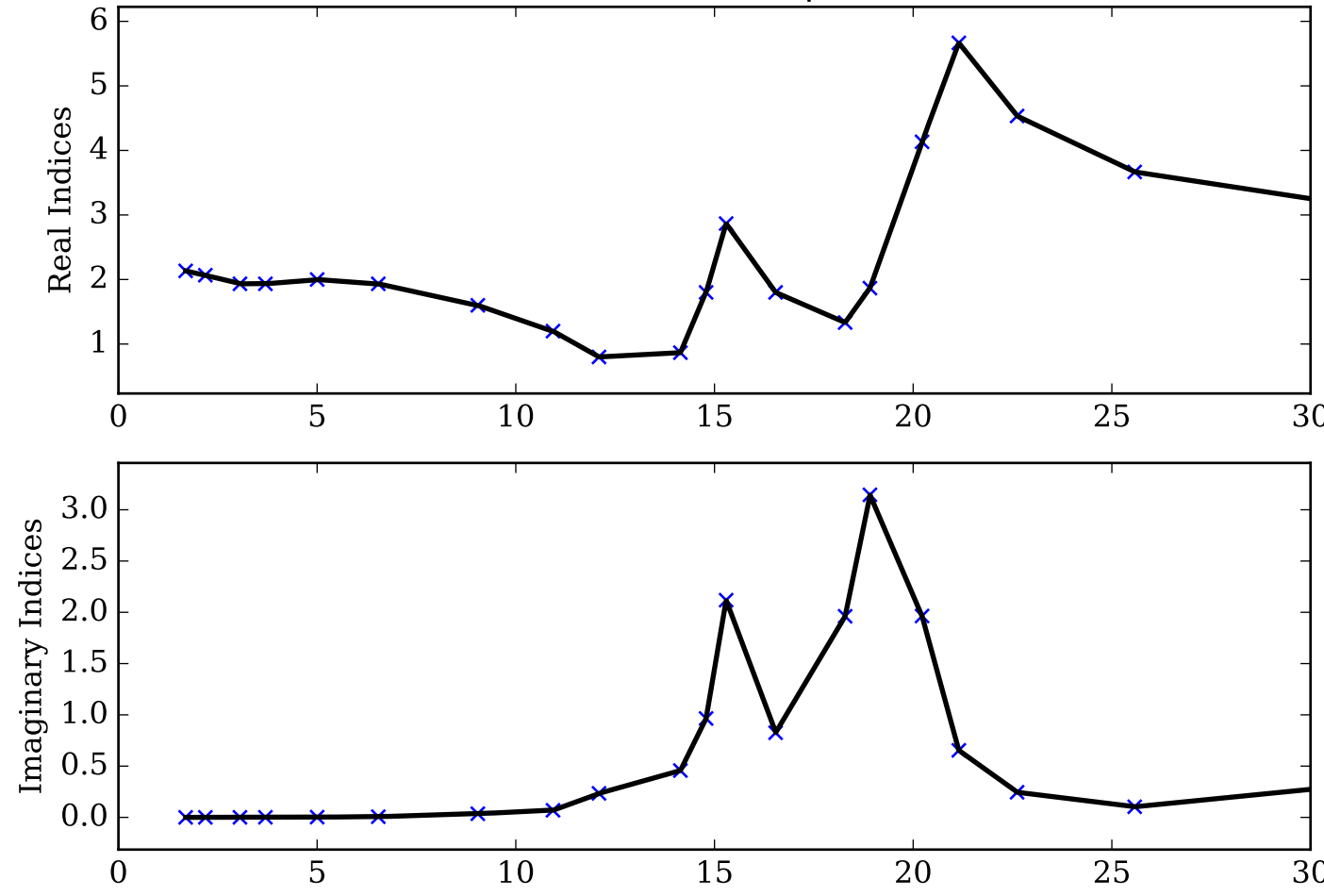
Mg8Fe2SiO<sub>3</sub>\_amorph\_glass Single Scattering Albedos  $\omega$   
0 (black, completely absorbing) to 1 (white, completely scattering)



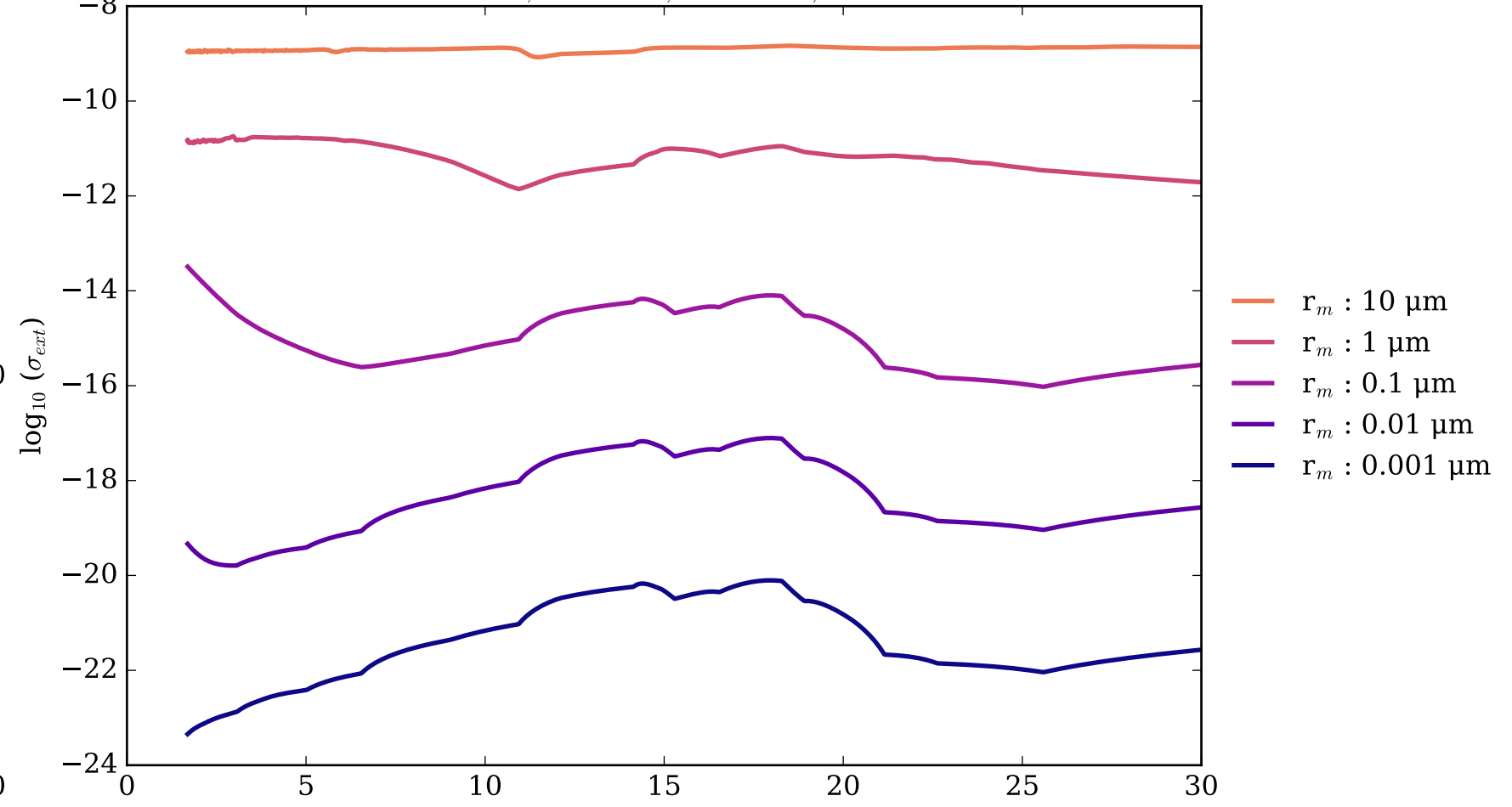
Mg8Fe2SiO<sub>3</sub>\_amorph\_glass Asymmetry Parameter  $g$   
0 (Rayleigh Limit) to 1 (Total Forward Scattering)



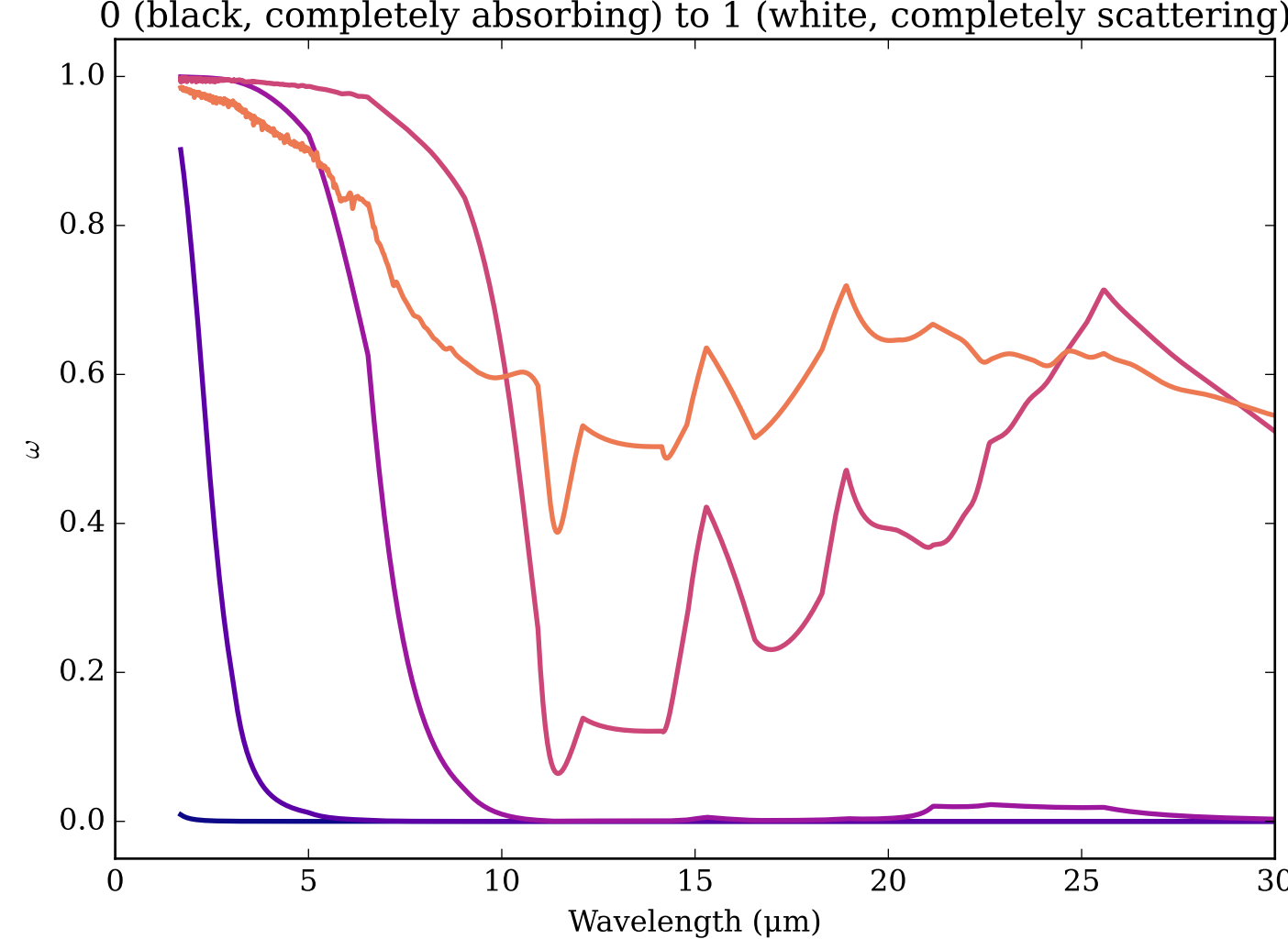
Refractive Indices for MgAl<sub>2</sub>O<sub>4</sub>  
(1.69, 30.0)  $\mu\text{m}$



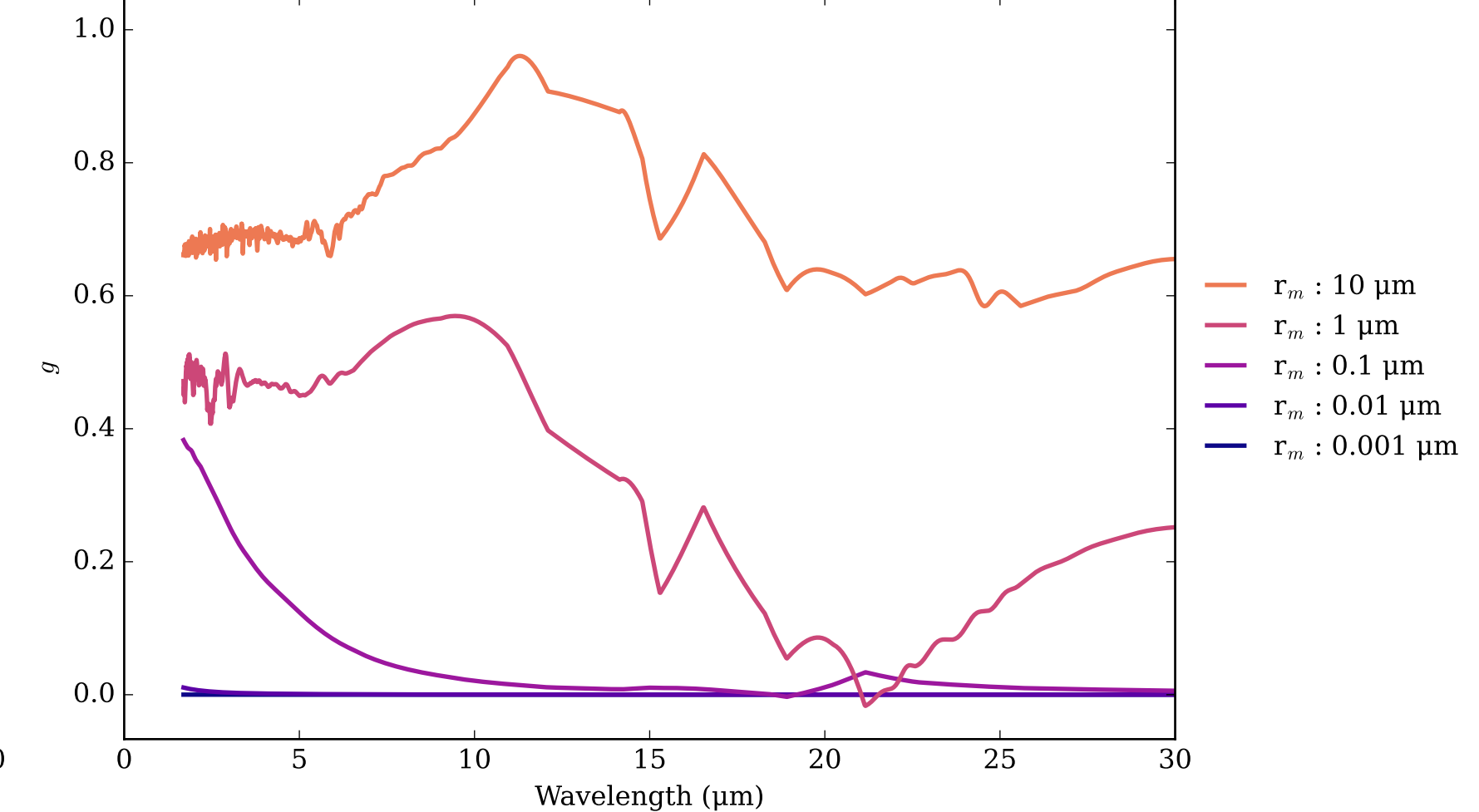
MgAl<sub>2</sub>O<sub>4</sub> Effective Extinction Cross Section  
 $\sigma_{\text{ext, eff}} = \sigma_{\text{abs, eff}} + \sigma_{\text{scat, eff}}$



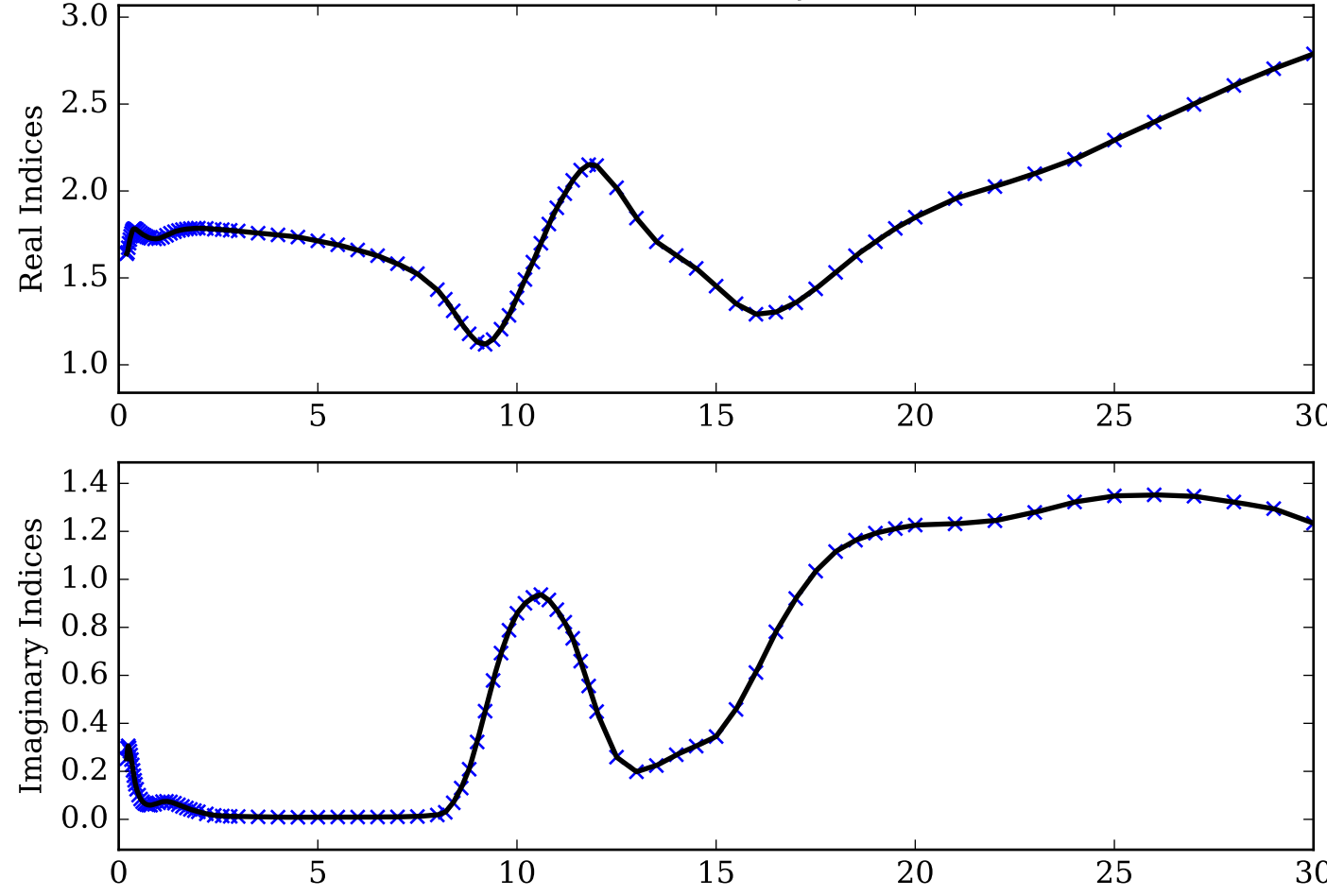
MgAl<sub>2</sub>O<sub>4</sub> Single Scattering Albedos  $\omega$



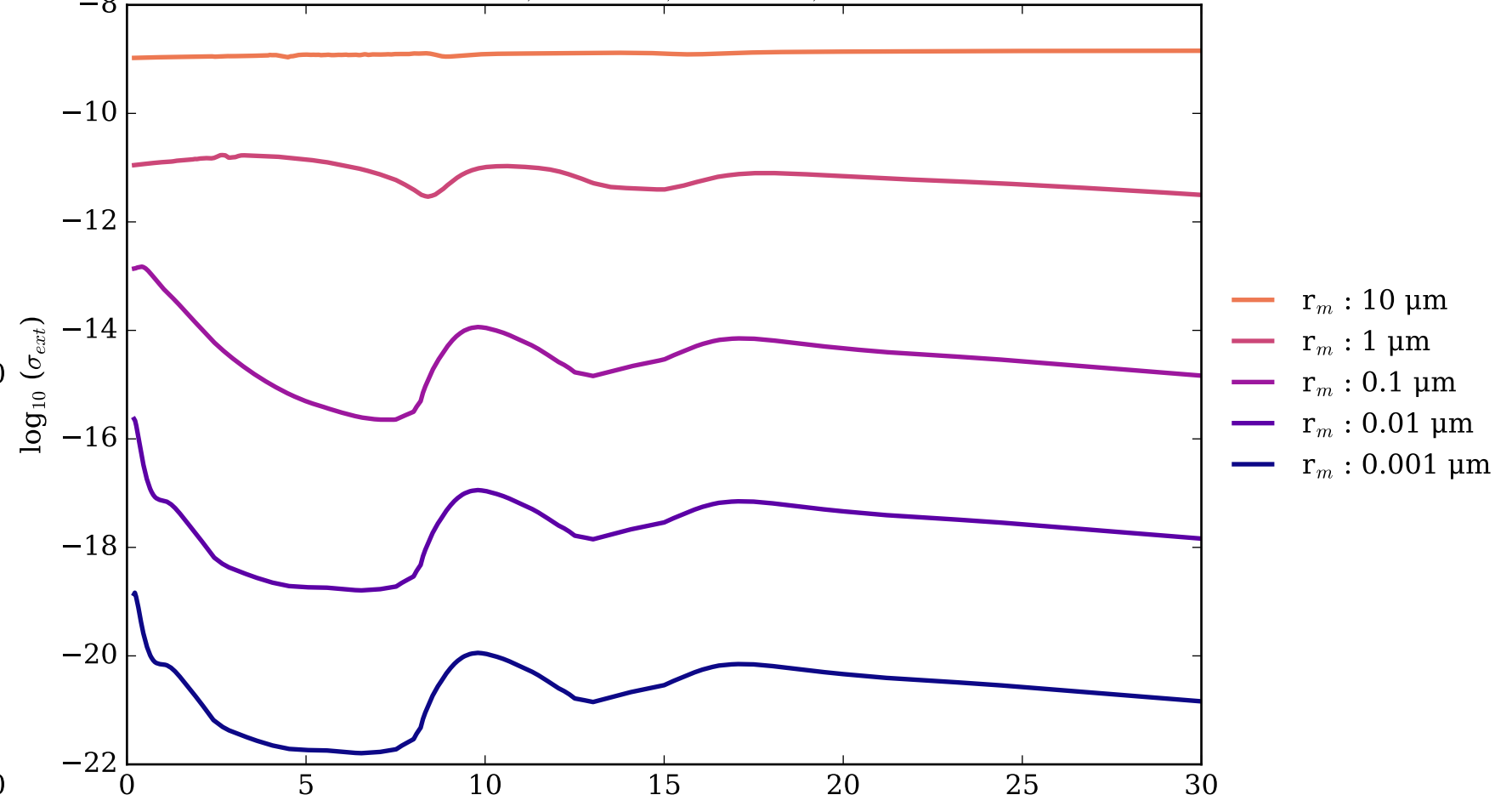
MgAl<sub>2</sub>O<sub>4</sub> Asymmetry Parameter  $g$   
0 (Rayleigh Limit) to 1 (Total Forward Scattering)



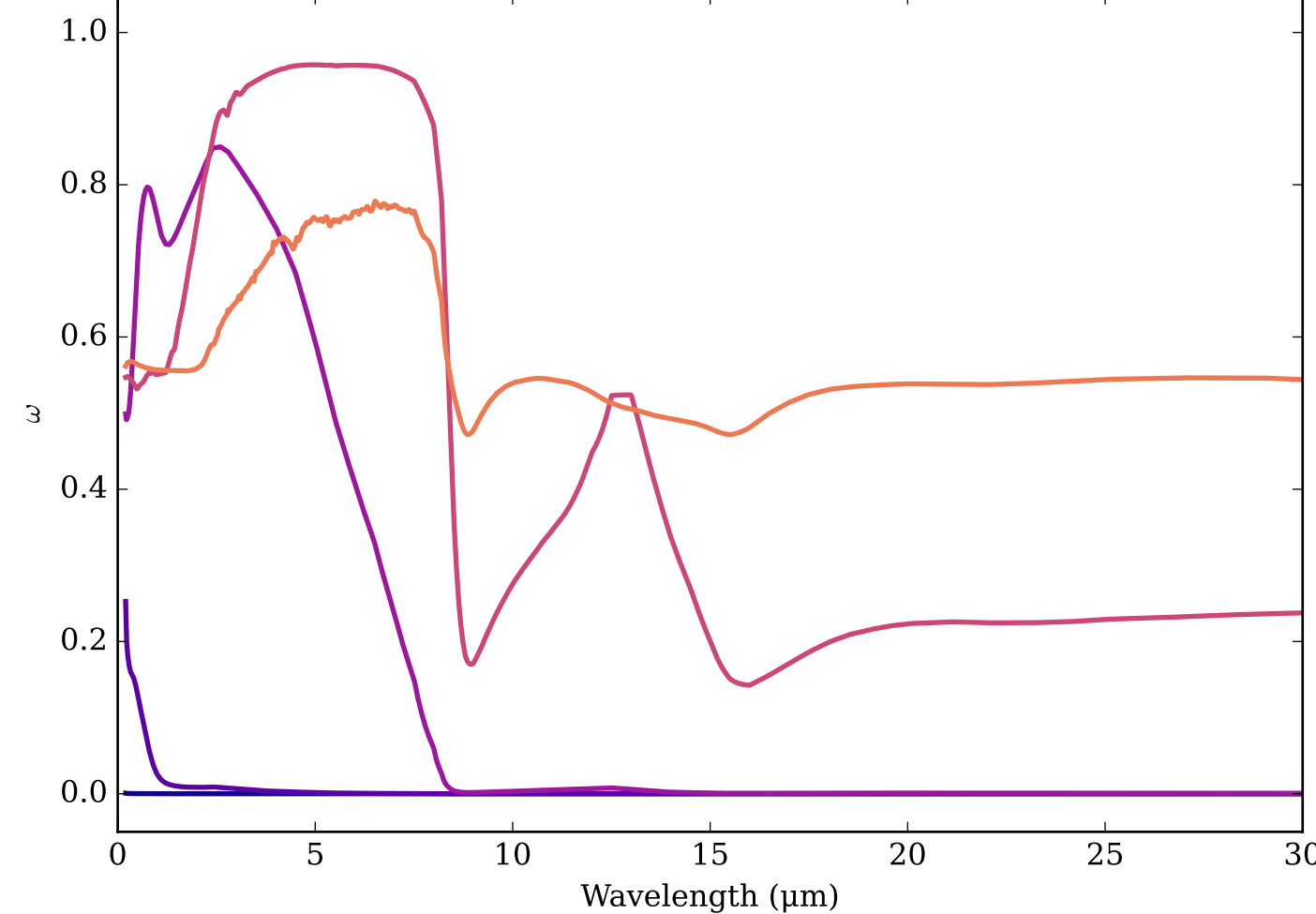
Refractive Indices for MgFeSiO<sub>4</sub>  
(0.2, 30.0)  $\mu\text{m}$



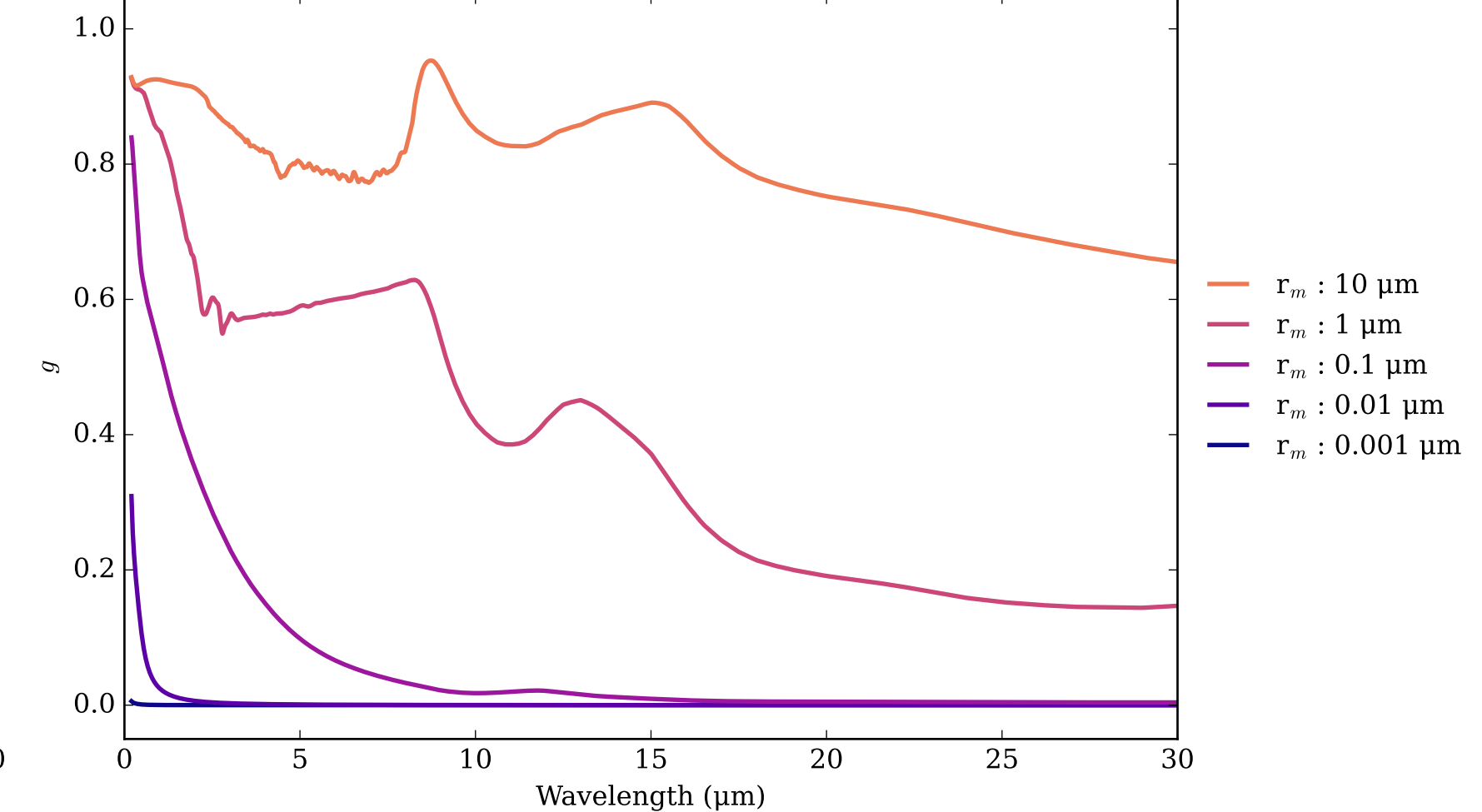
MgFeSiO<sub>4</sub>\_amorph\_glass Effective Extinction Cross Section  
 $\sigma_{\text{ext, eff}} = \sigma_{\text{abs, eff}} + \sigma_{\text{scat, eff}}$



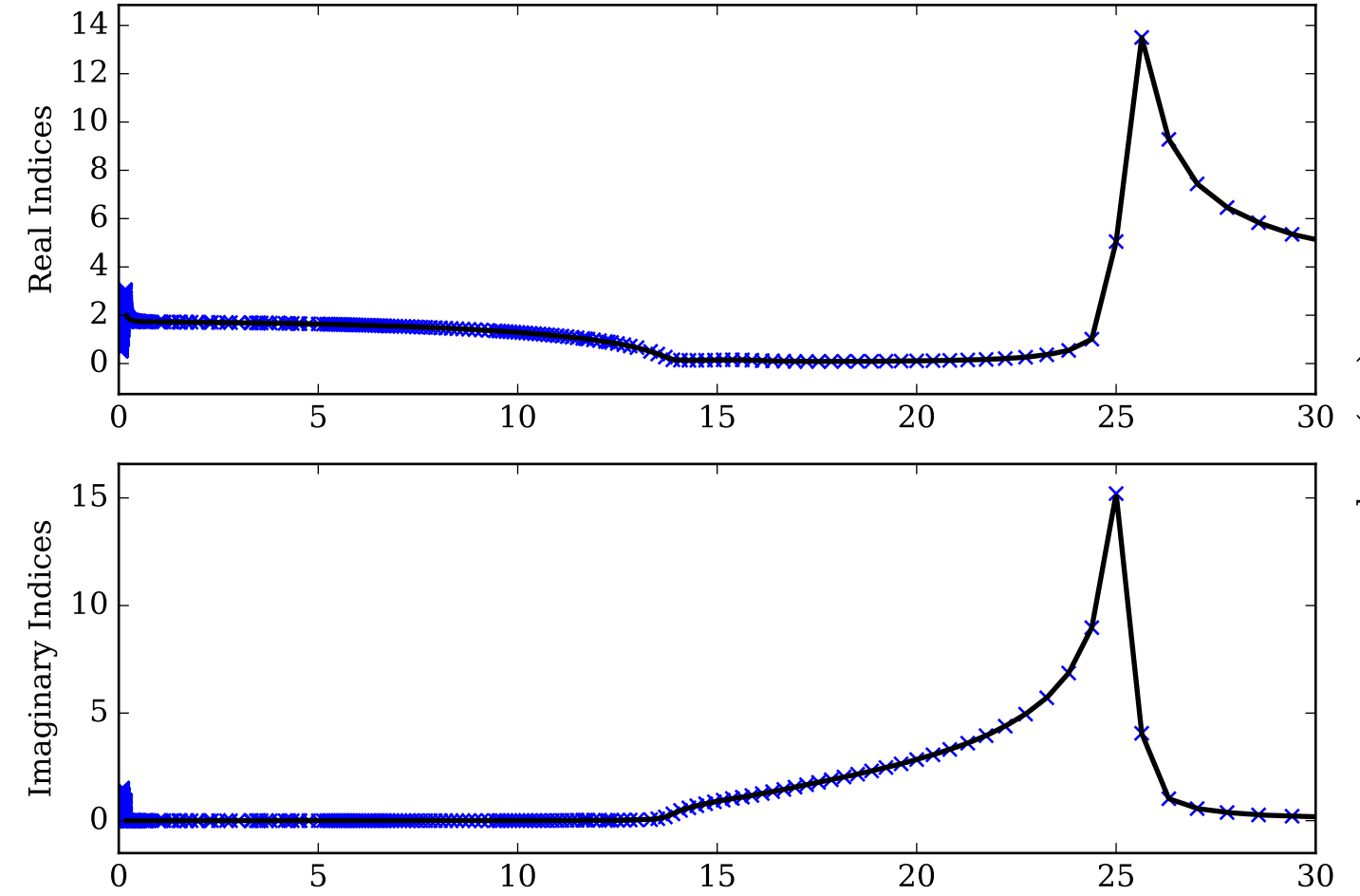
MgFeSiO<sub>4</sub>\_amorph\_glass Single Scattering Albedos  $\omega$   
0 (black, completely absorbing) to 1 (white, completely scattering)



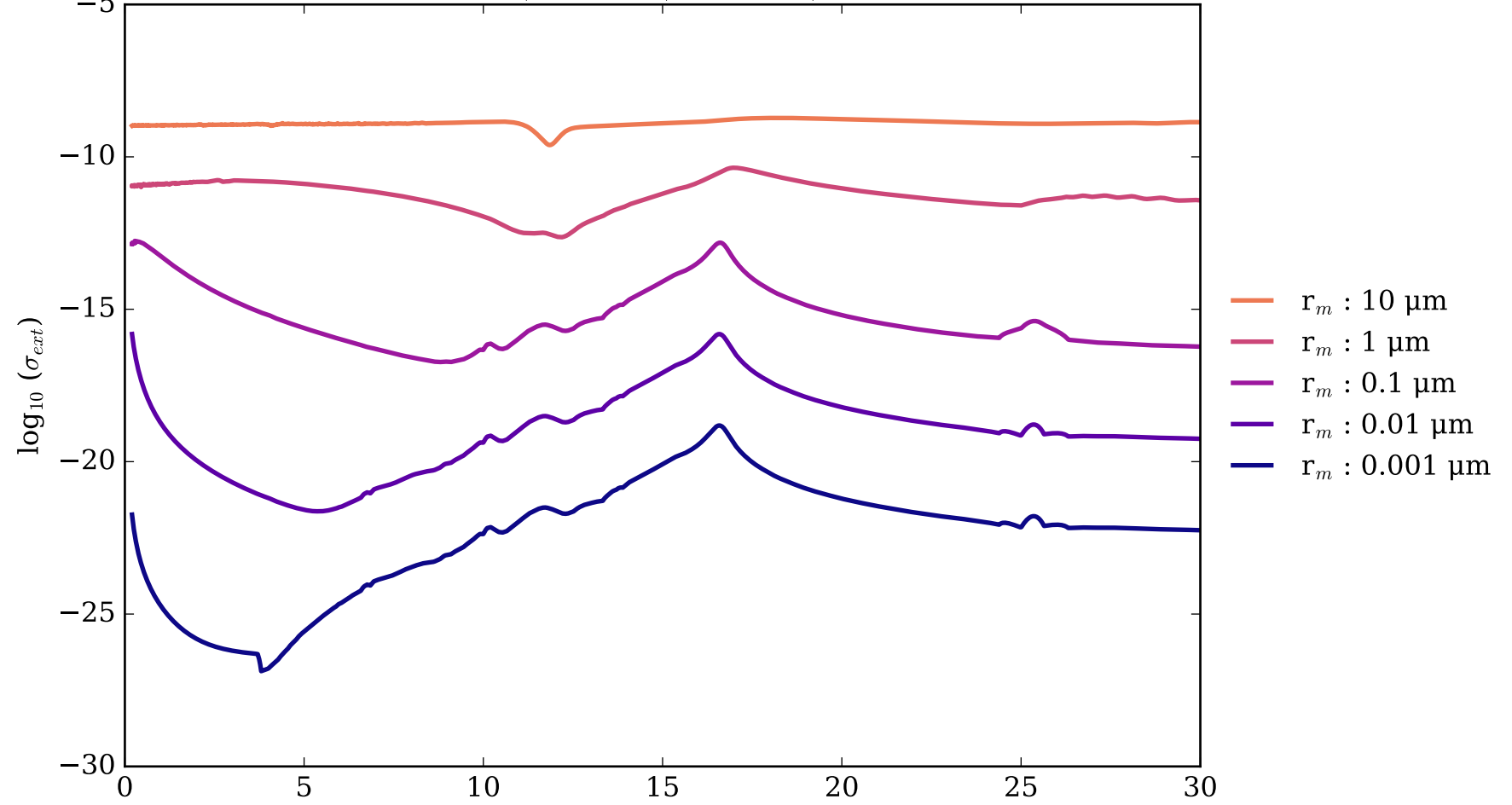
MgFeSiO<sub>4</sub>\_amorph\_glass Asymmetry Parameter  $g$   
0 (Rayleigh Limit) to 1 (Total Forward Scattering)



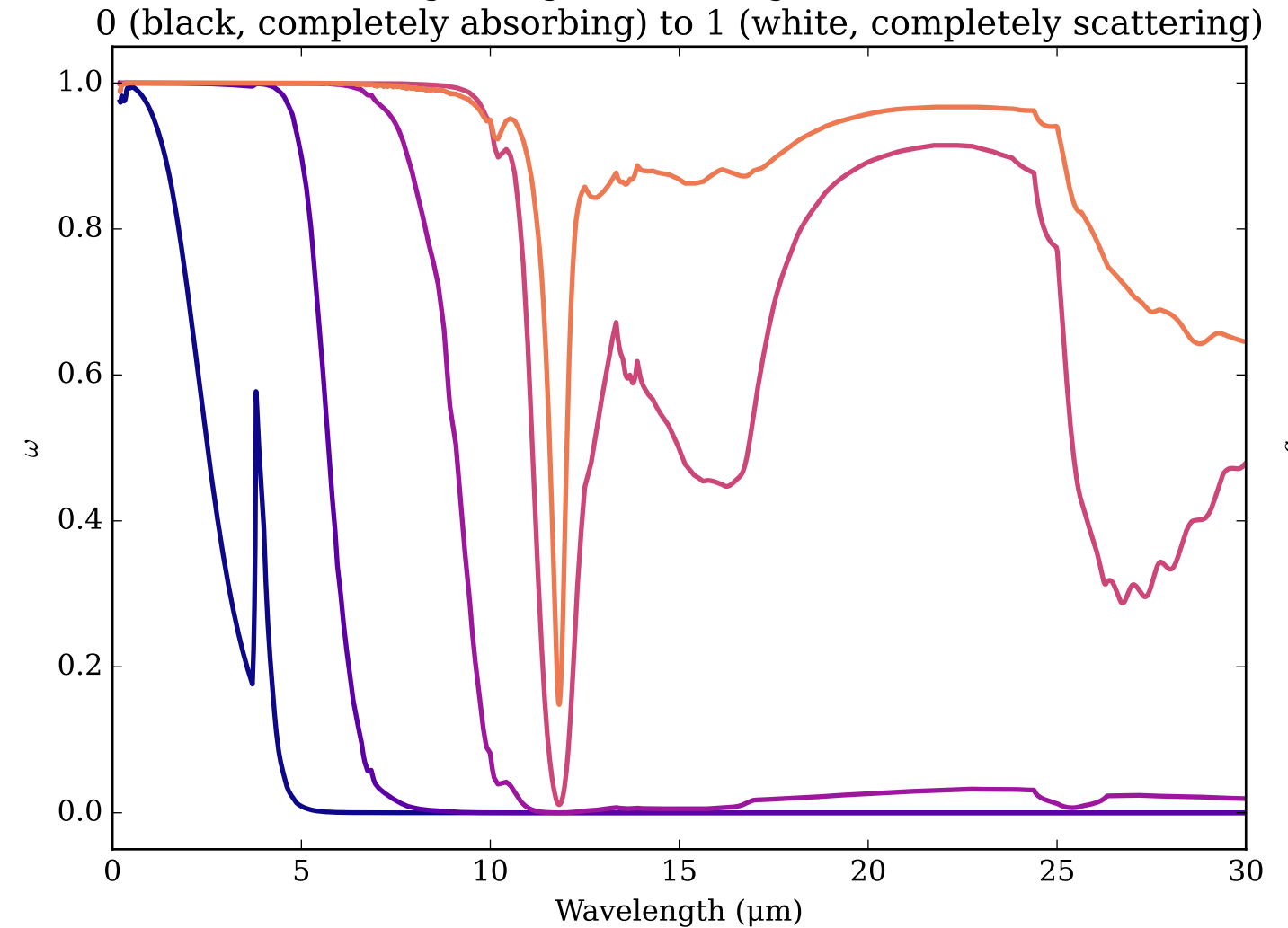
Refractive Indices for MgO  
(0.2, 30.0)  $\mu\text{m}$



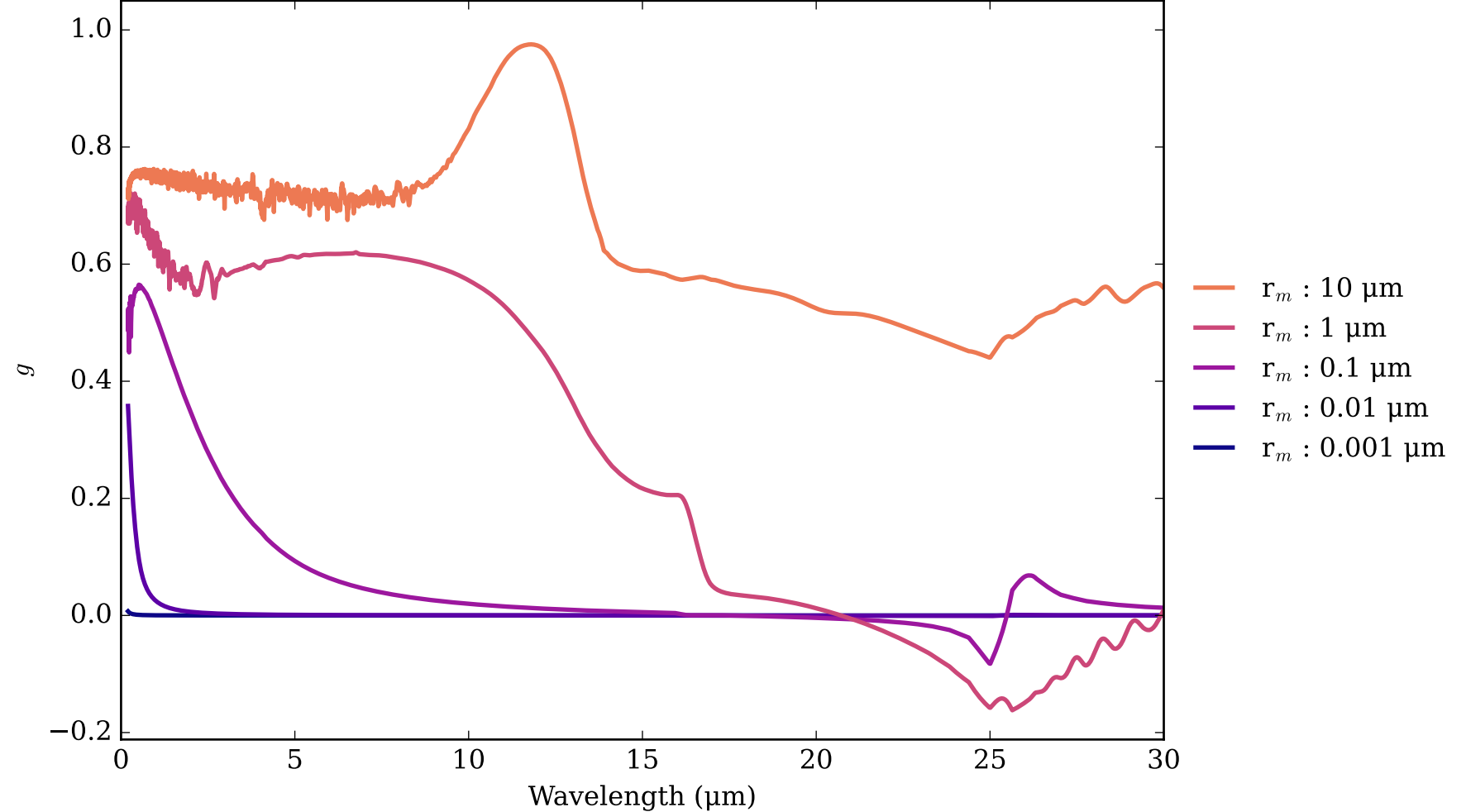
MgO Effective Extinction Cross Section  
 $\sigma_{\text{ext, eff}} = \sigma_{\text{abs, eff}} + \sigma_{\text{scat, eff}}$



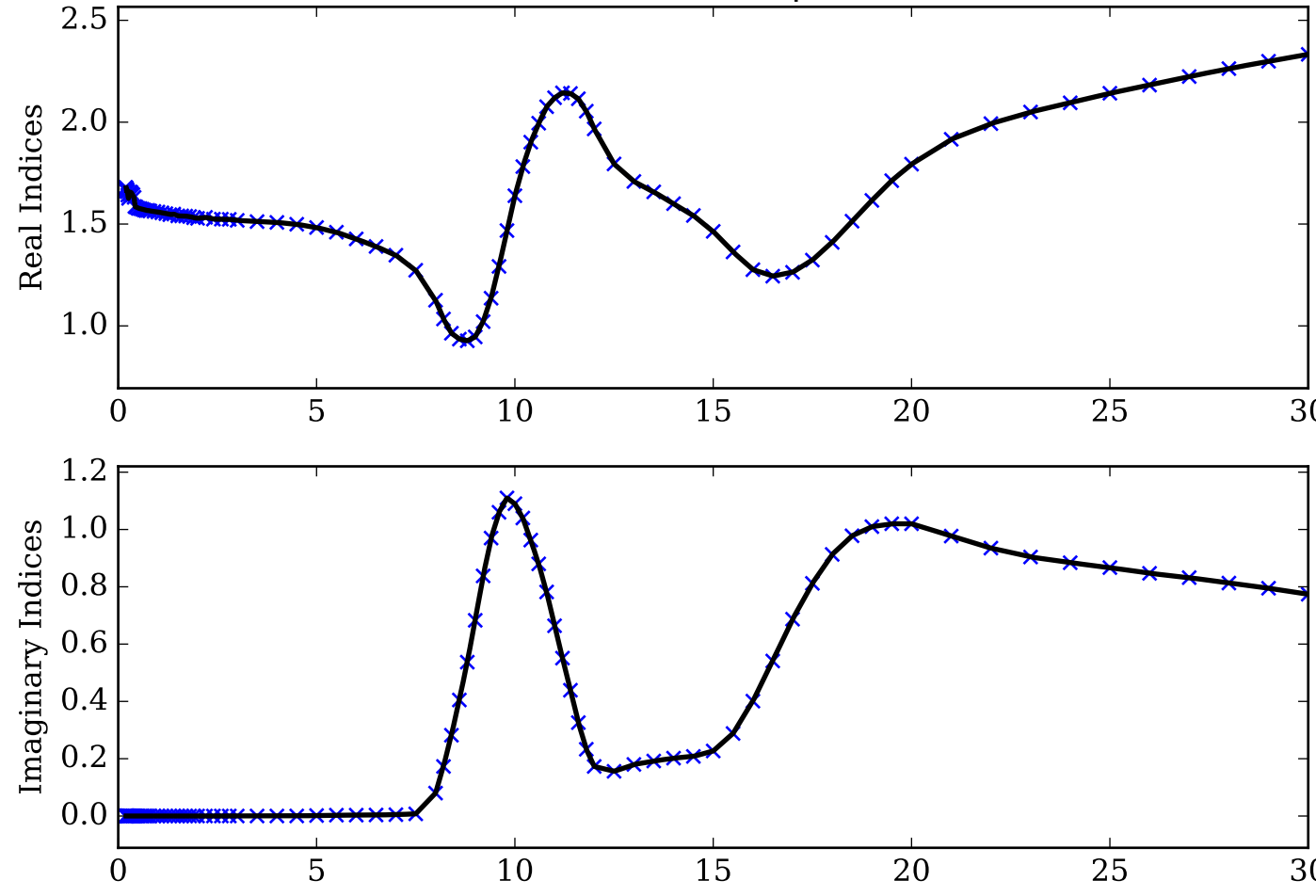
MgO Single Scattering Albedos  $\omega$



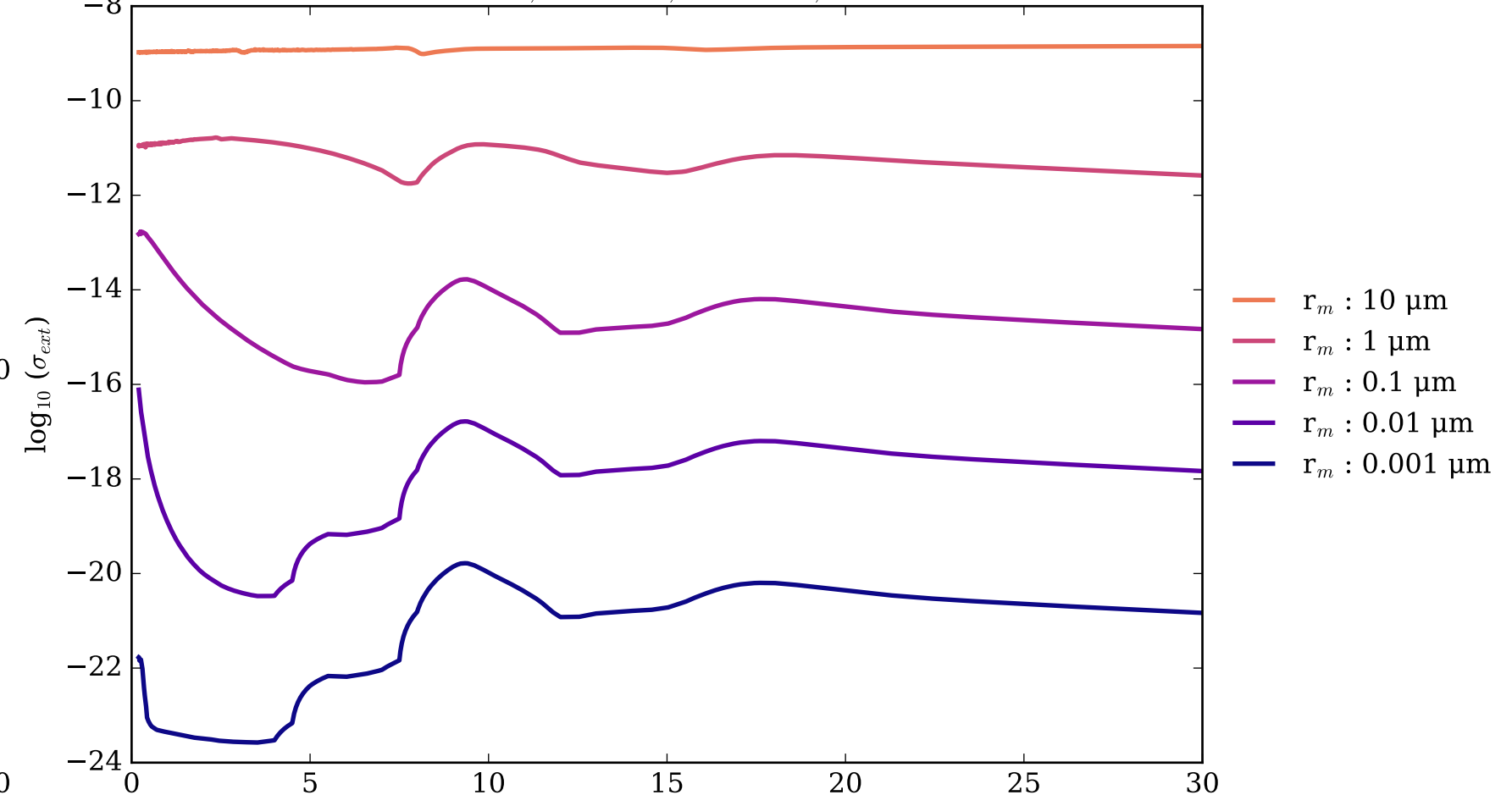
MgO Asymmetry Parameter  $g$   
0 (Rayleigh Limit) to 1 (Total Forward Scattering)



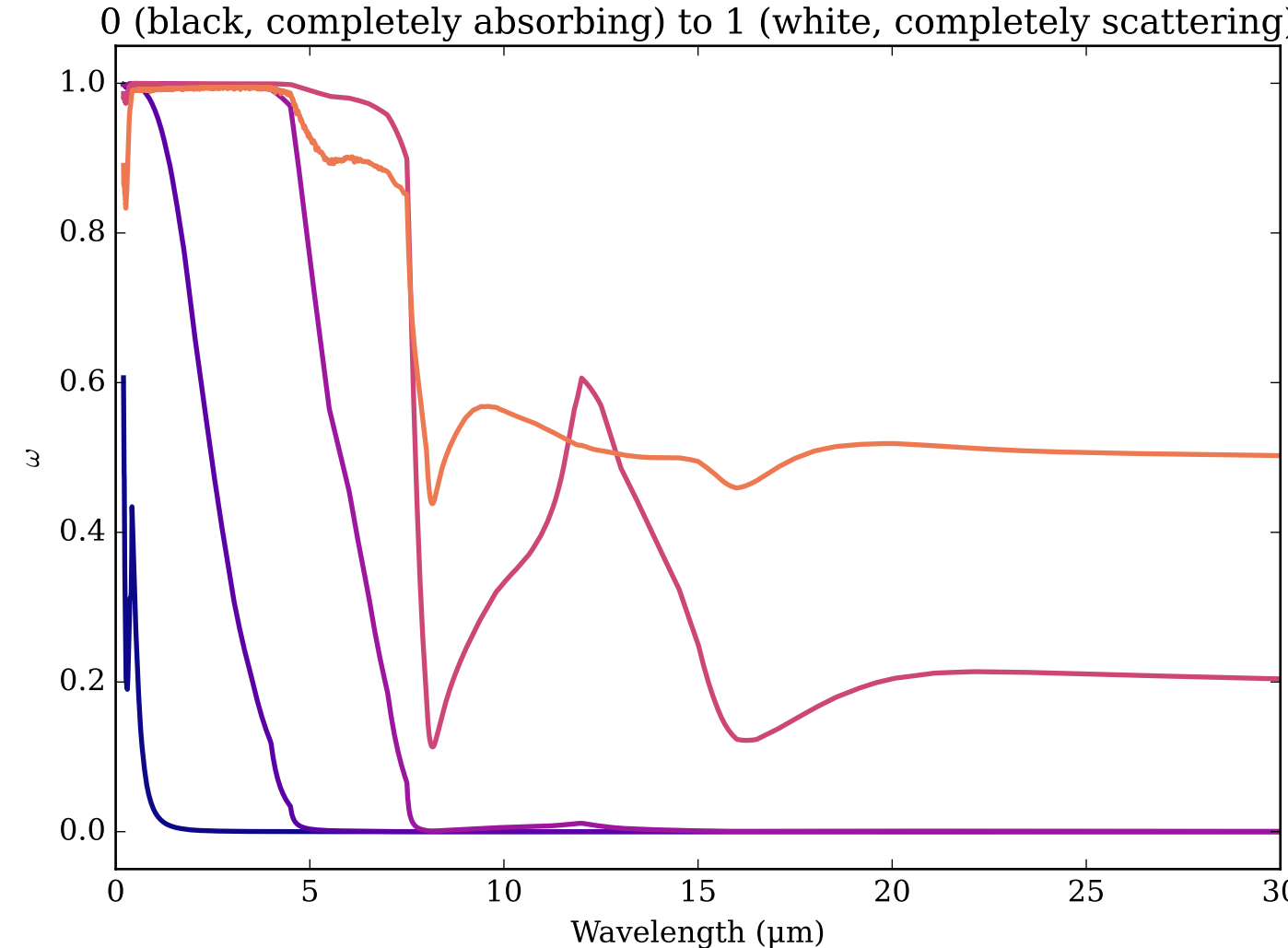
Refractive Indices for MgSiO<sub>3</sub>  
(0.2, 30.0) μm



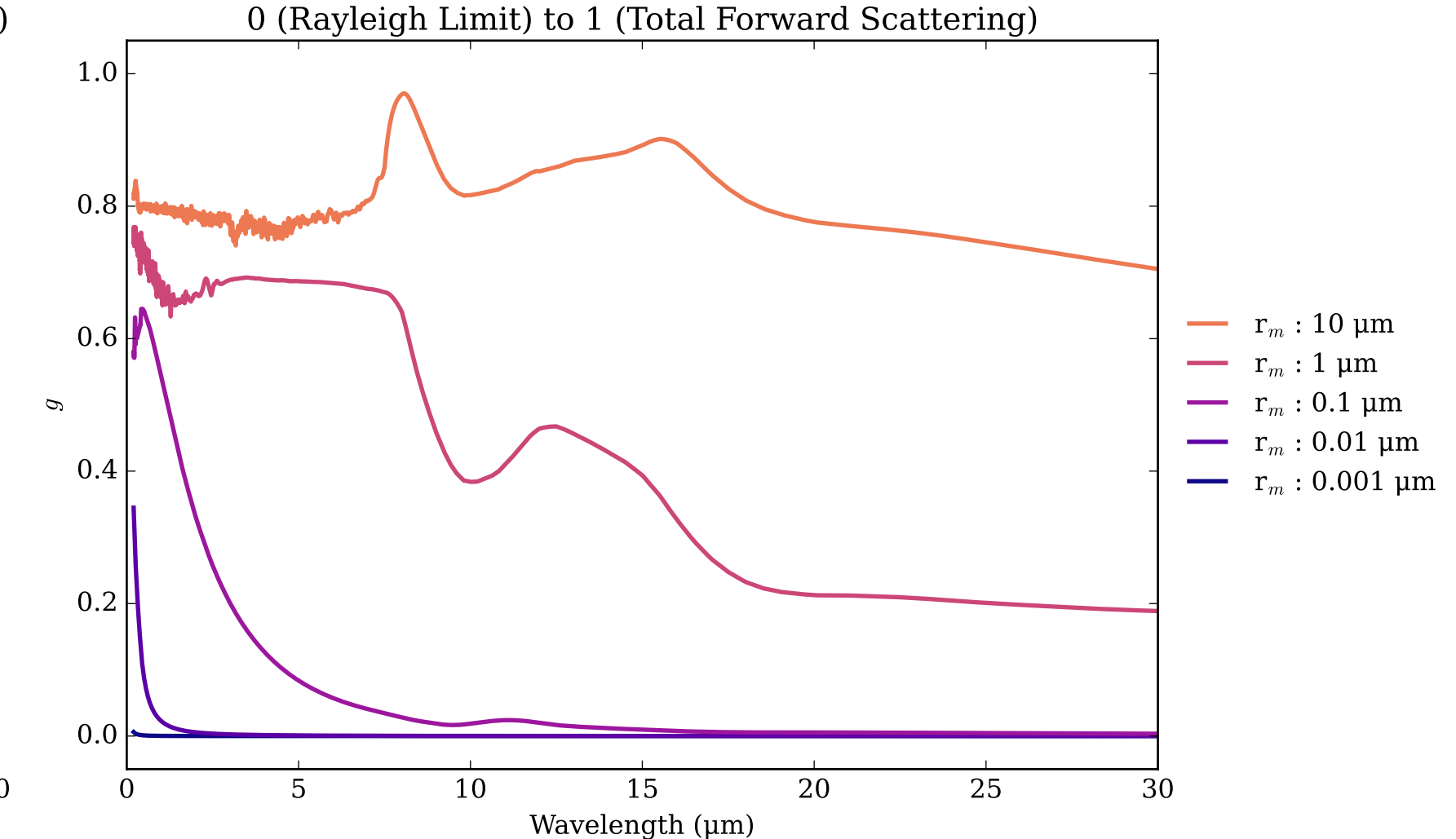
MgSiO<sub>3</sub> Effective Extinction Cross Section



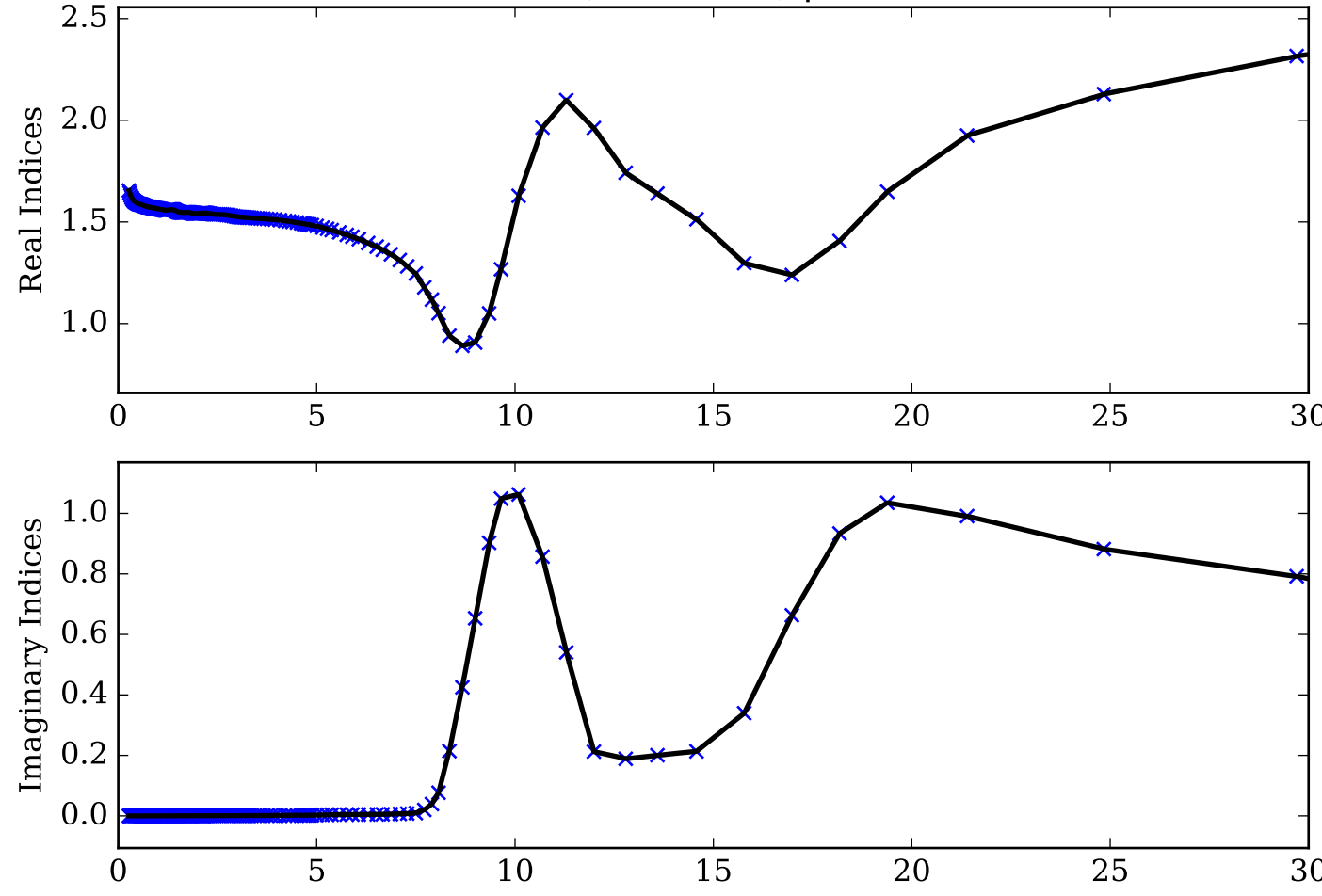
MgSiO<sub>3</sub> Single Scattering Albedos  $\omega$



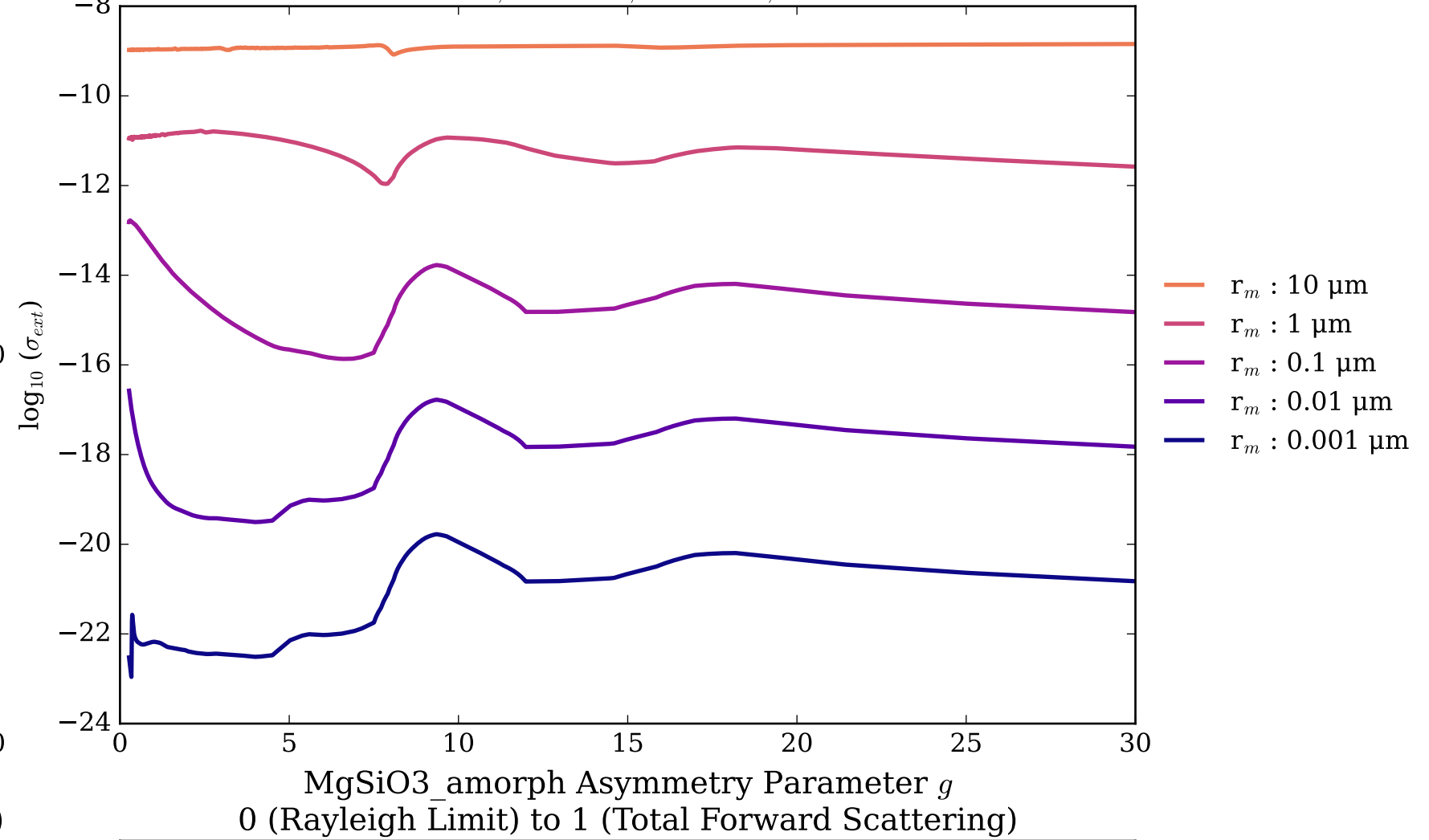
MgSiO<sub>3</sub> Asymmetry Parameter  $g$



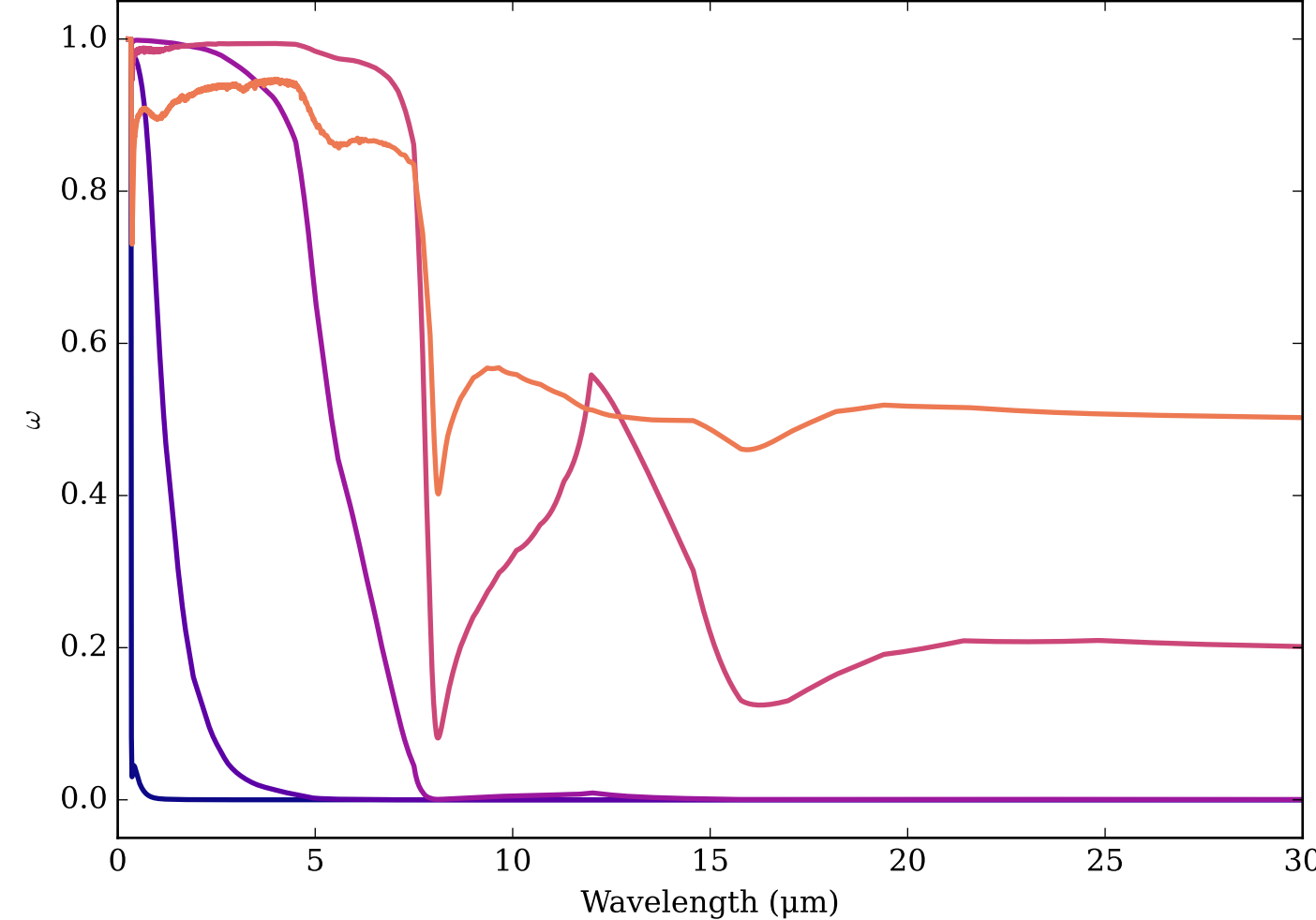
Refractive Indices for MgSiO<sub>3</sub>  
(0.27, 30.0)  $\mu\text{m}$



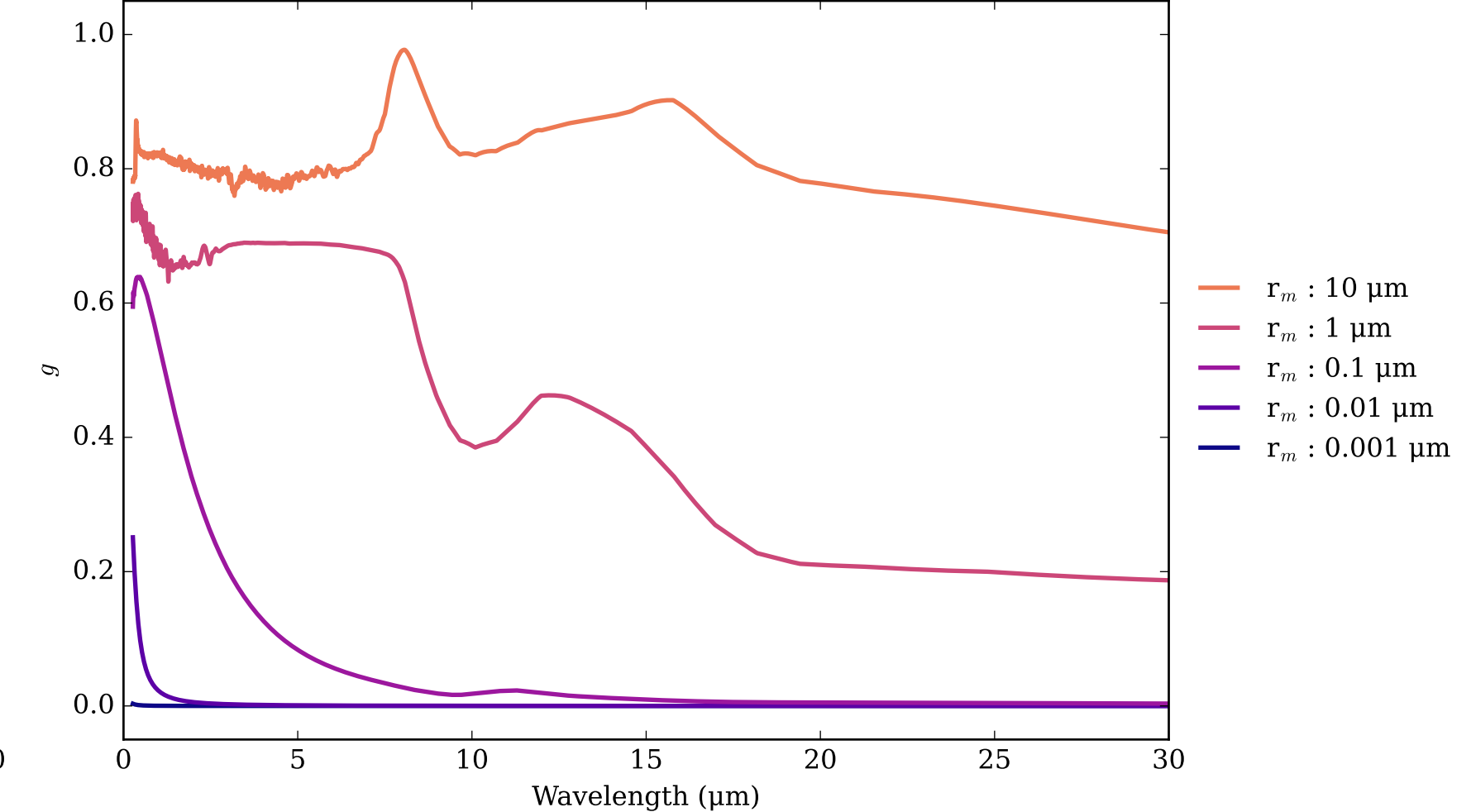
MgSiO<sub>3</sub>\_amorph Effective Extinction Cross Section



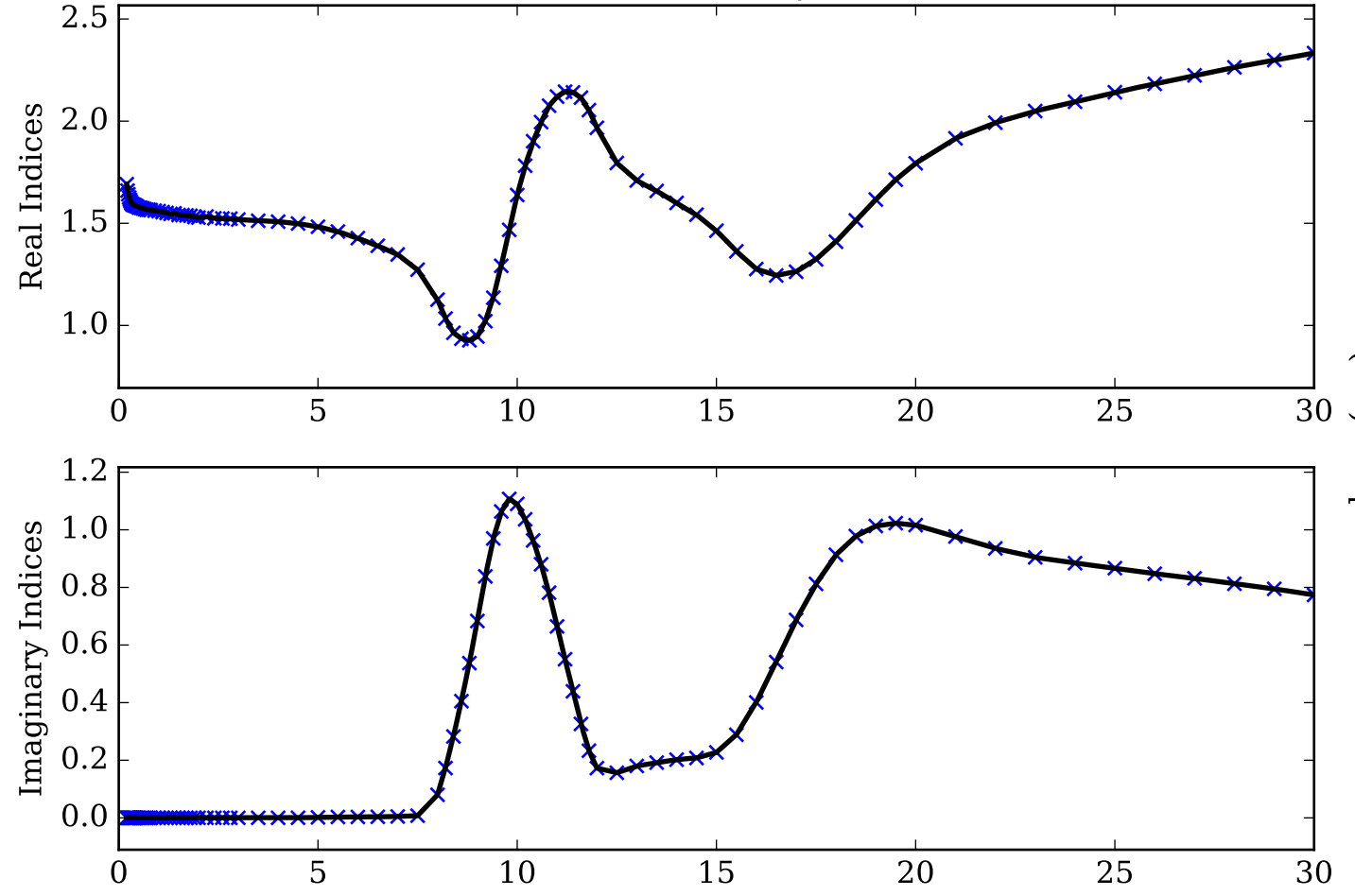
MgSiO<sub>3</sub>\_amorph Single Scattering Albedos  $\omega$   
0 (black, completely absorbing) to 1 (white, completely scattering)



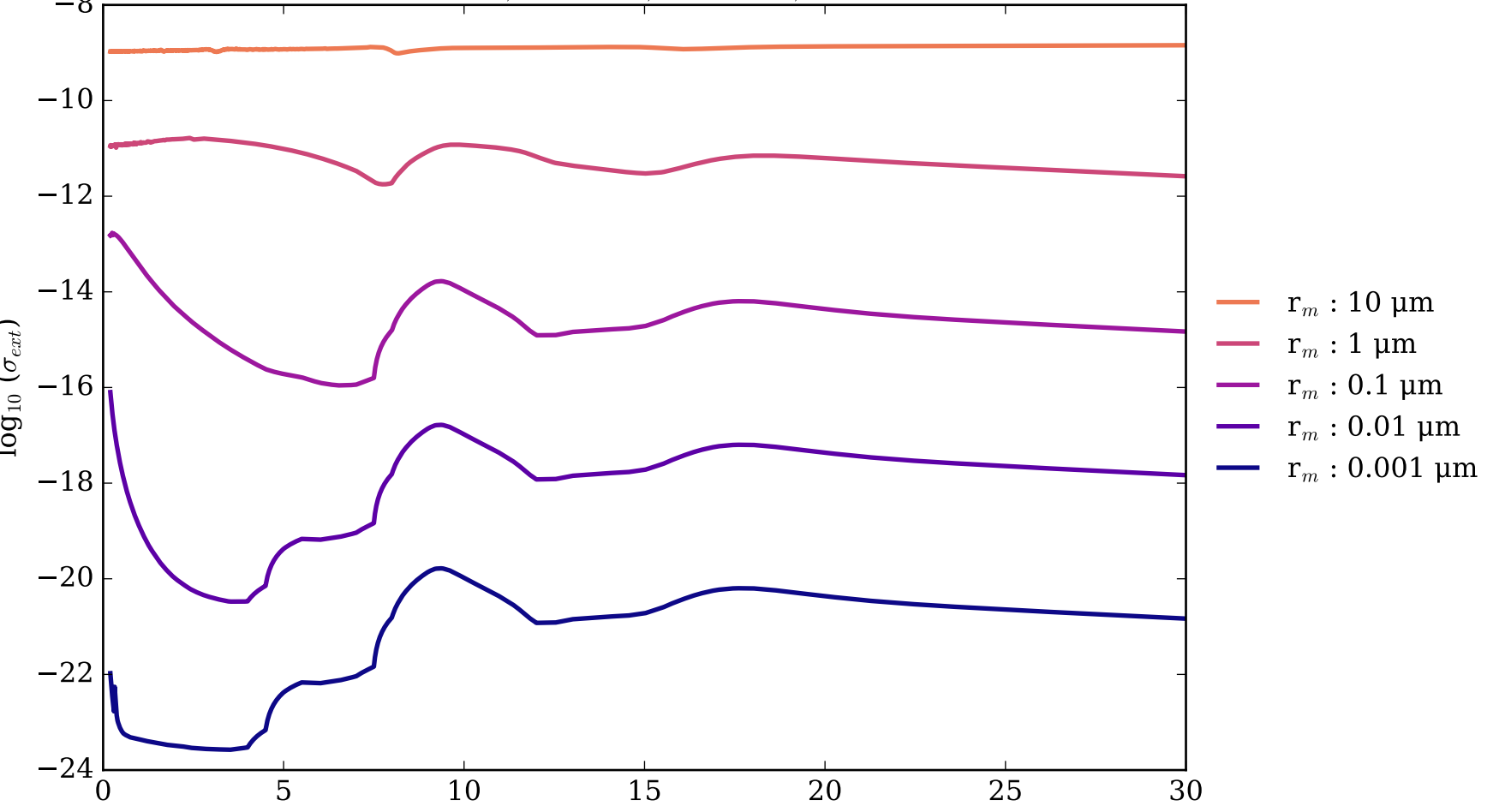
MgSiO<sub>3</sub>\_amorph Asymmetry Parameter  $g$   
0 (Rayleigh Limit) to 1 (Total Forward Scattering)



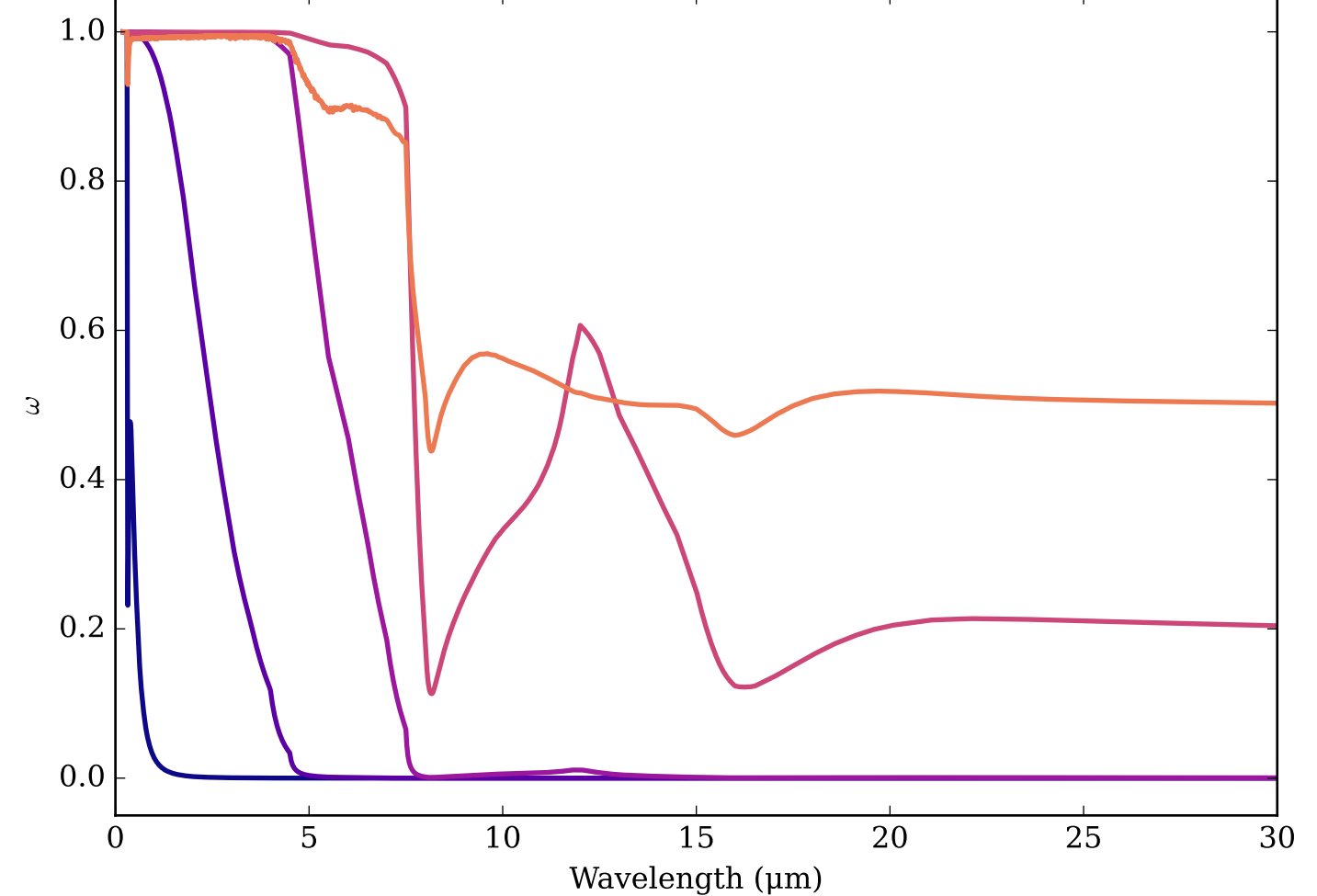
Refractive Indices for MgSiO<sub>3</sub>  
(0.2, 30.0)  $\mu\text{m}$



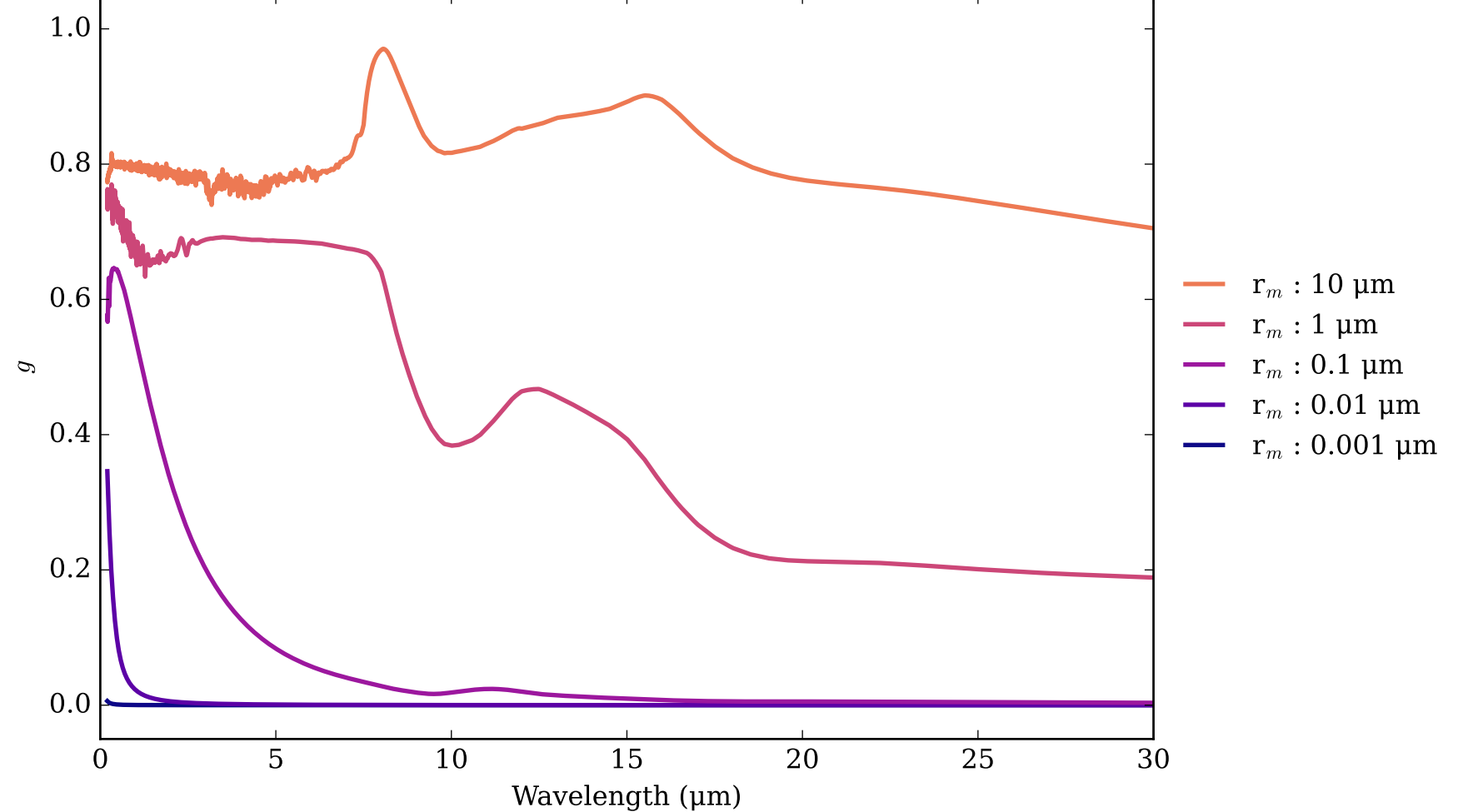
MgSiO<sub>3</sub>\_amorph\_glass Effective Extinction Cross Section  
 $\sigma_{\text{ext, eff}} = \sigma_{\text{abs, eff}} + \sigma_{\text{scat, eff}}$



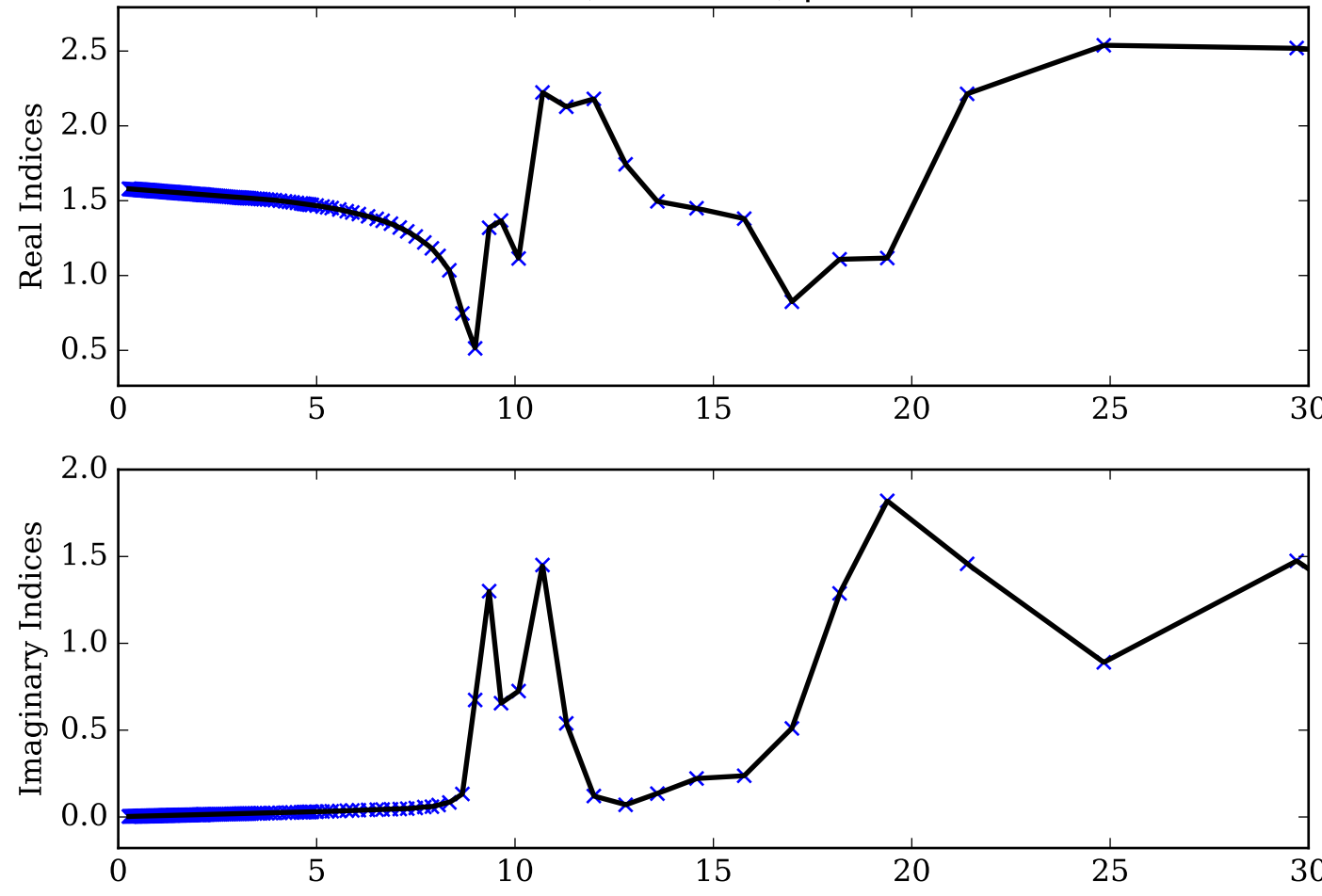
MgSiO<sub>3</sub>\_amorph\_glass Single Scattering Albedos  $\omega$   
0 (black, completely absorbing) to 1 (white, completely scattering)



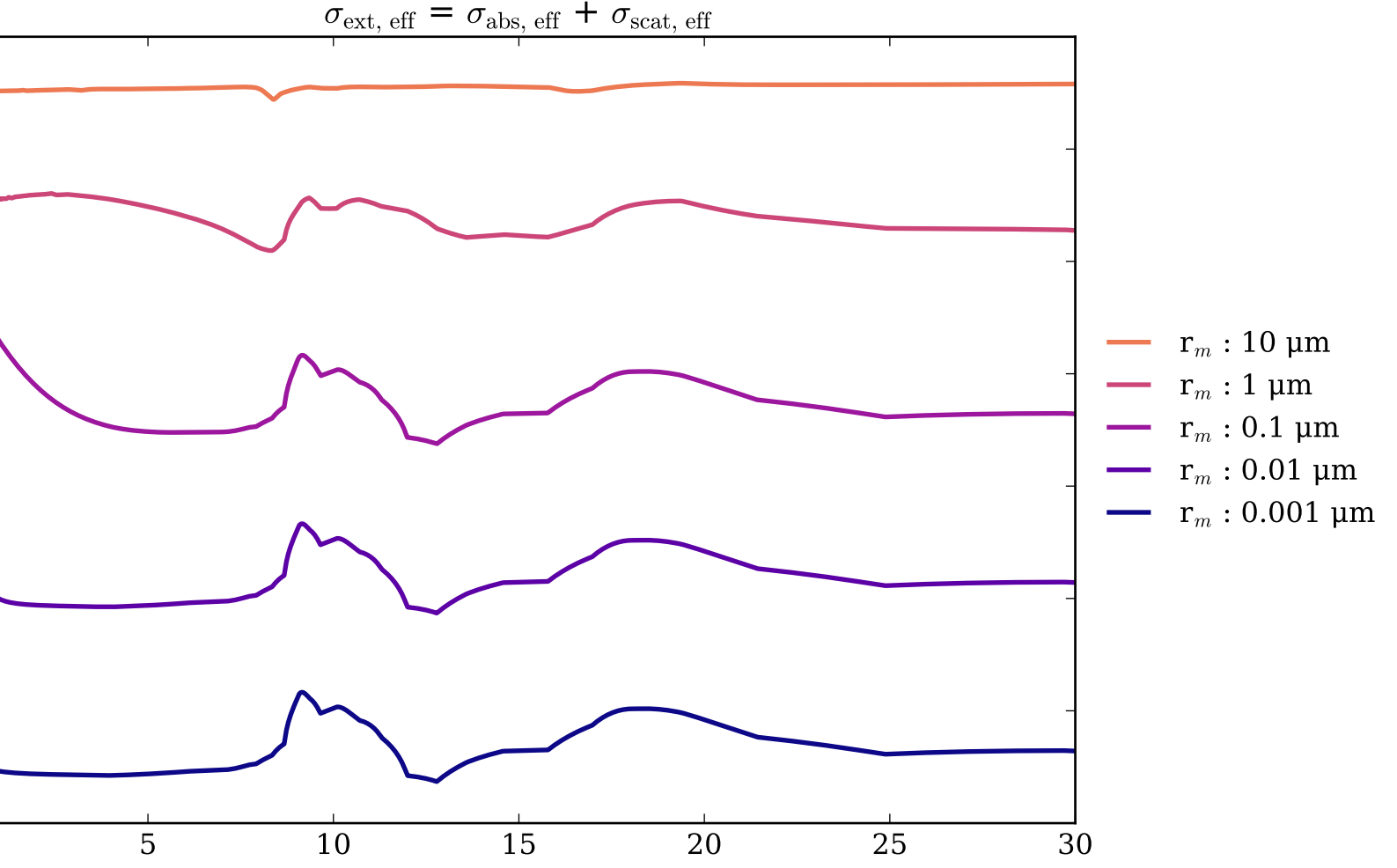
MgSiO<sub>3</sub>\_amorph\_glass Asymmetry Parameter  $g$   
0 (Rayleigh Limit) to 1 (Total Forward Scattering)



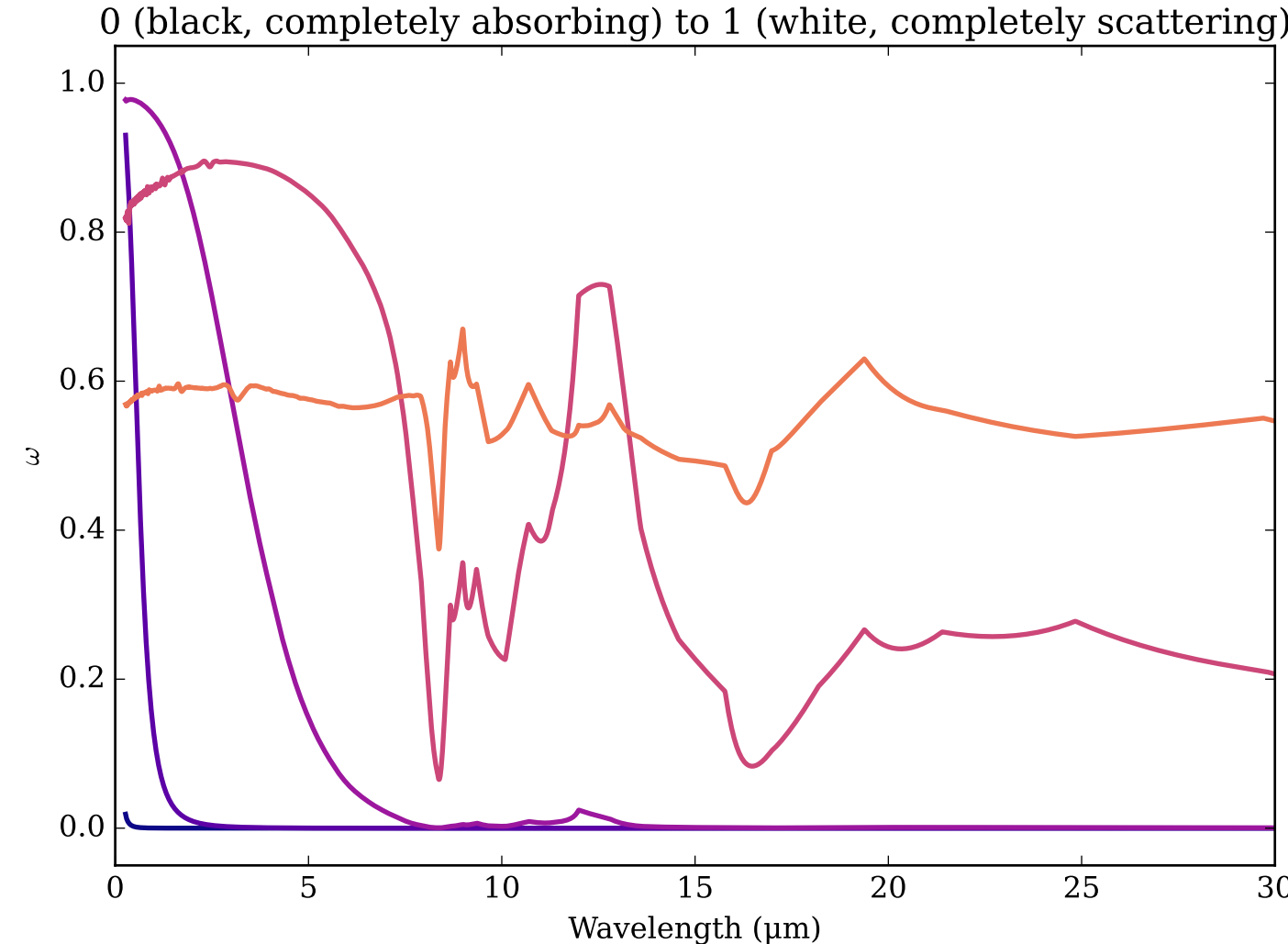
Refractive Indices for MgSiO<sub>3</sub>  
(0.27, 30.0)  $\mu\text{m}$



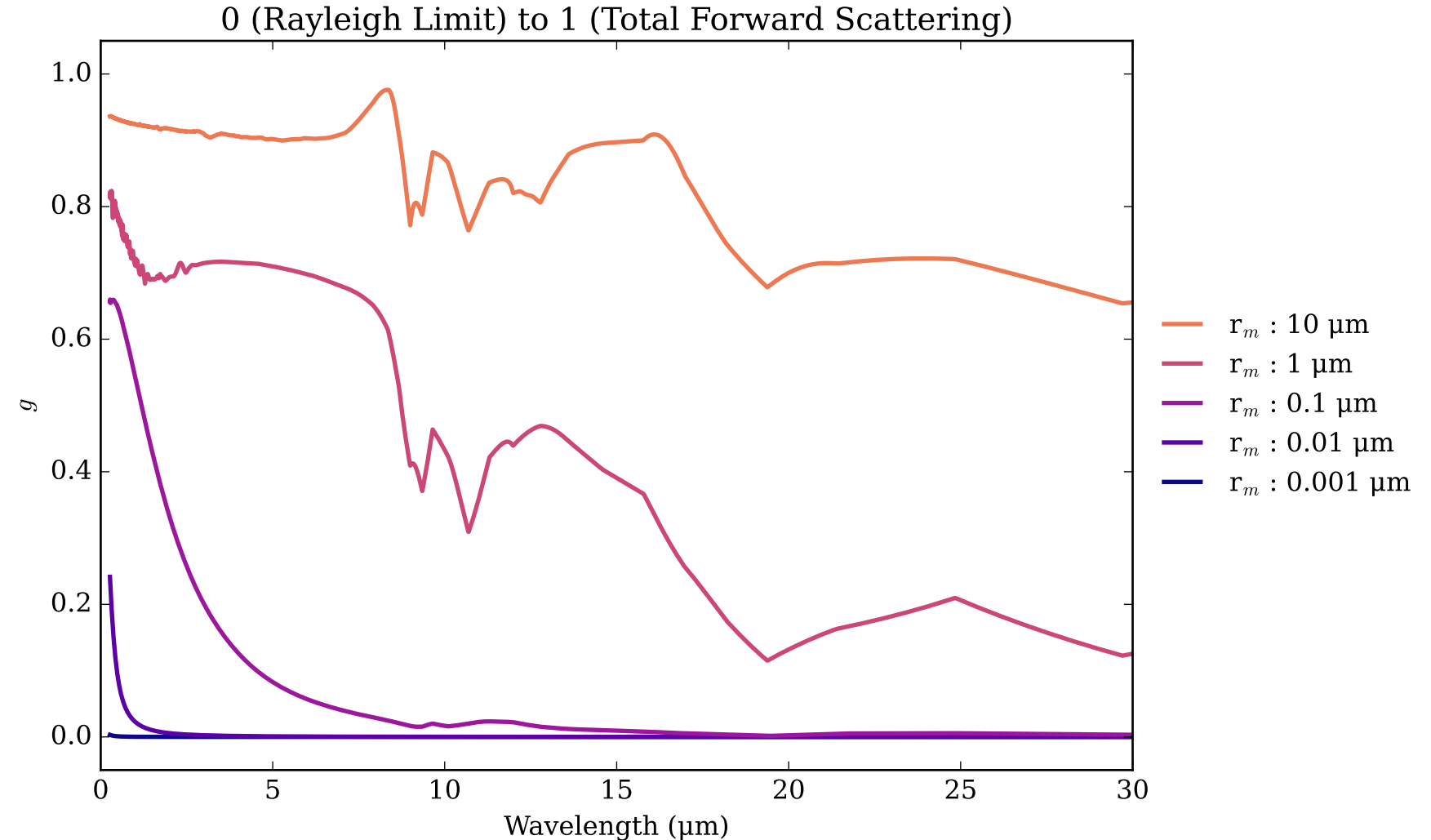
MgSiO<sub>3</sub>\_crystalline Effective Extinction Cross Section



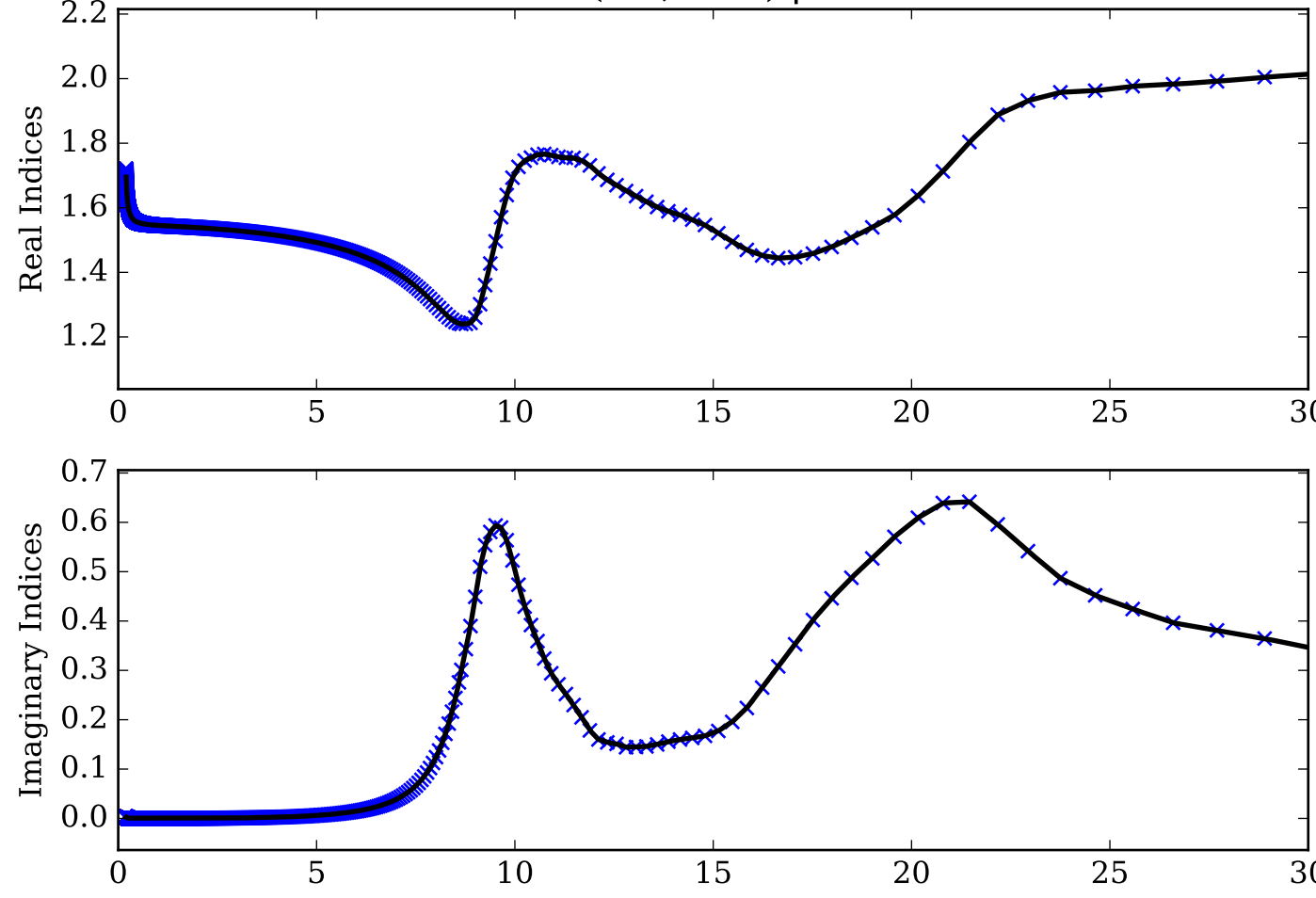
MgSiO<sub>3</sub>\_crystalline Single Scattering Albedos  $\omega$



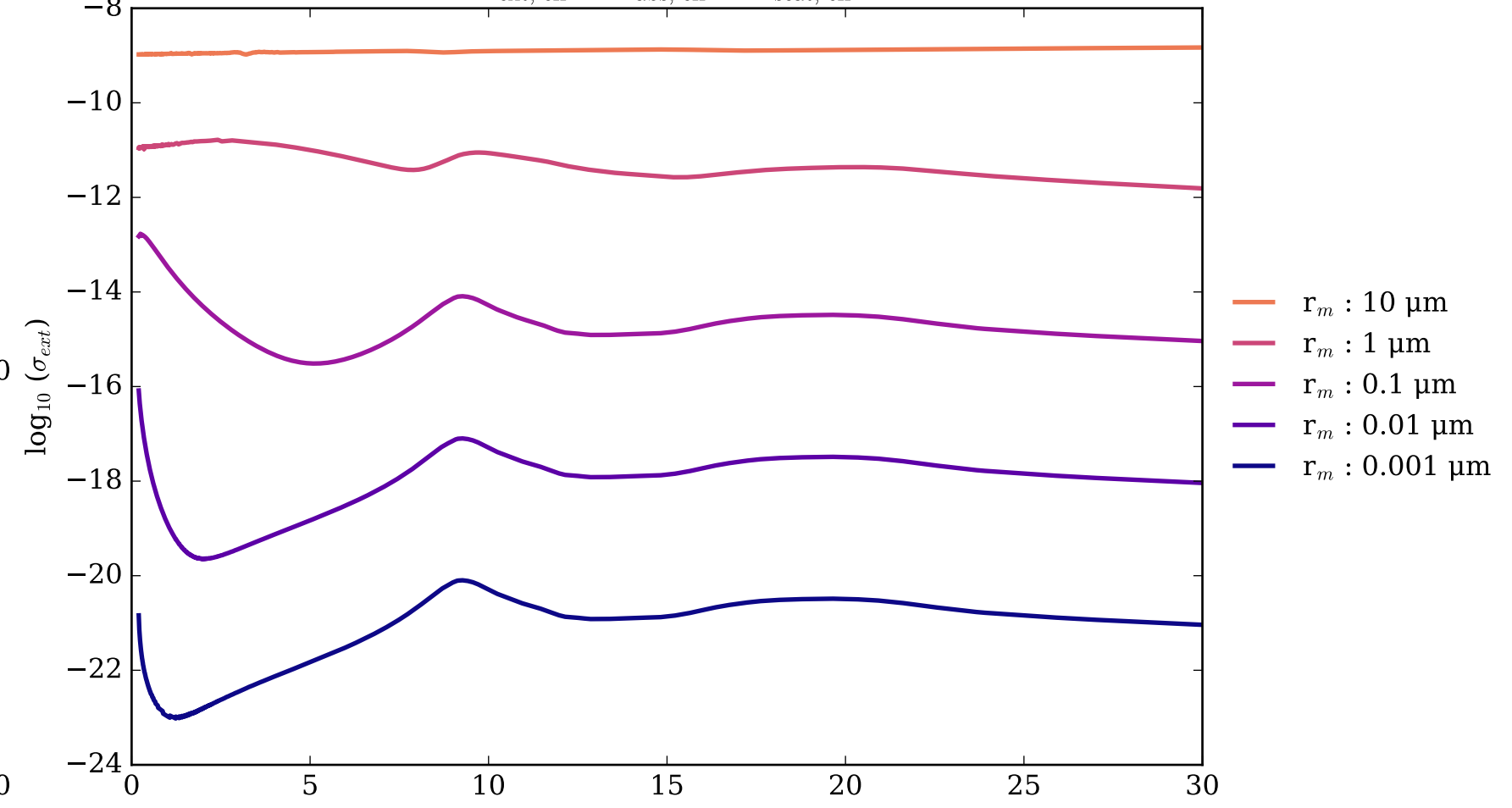
MgSiO<sub>3</sub>\_crystalline Asymmetry Parameter  $g$



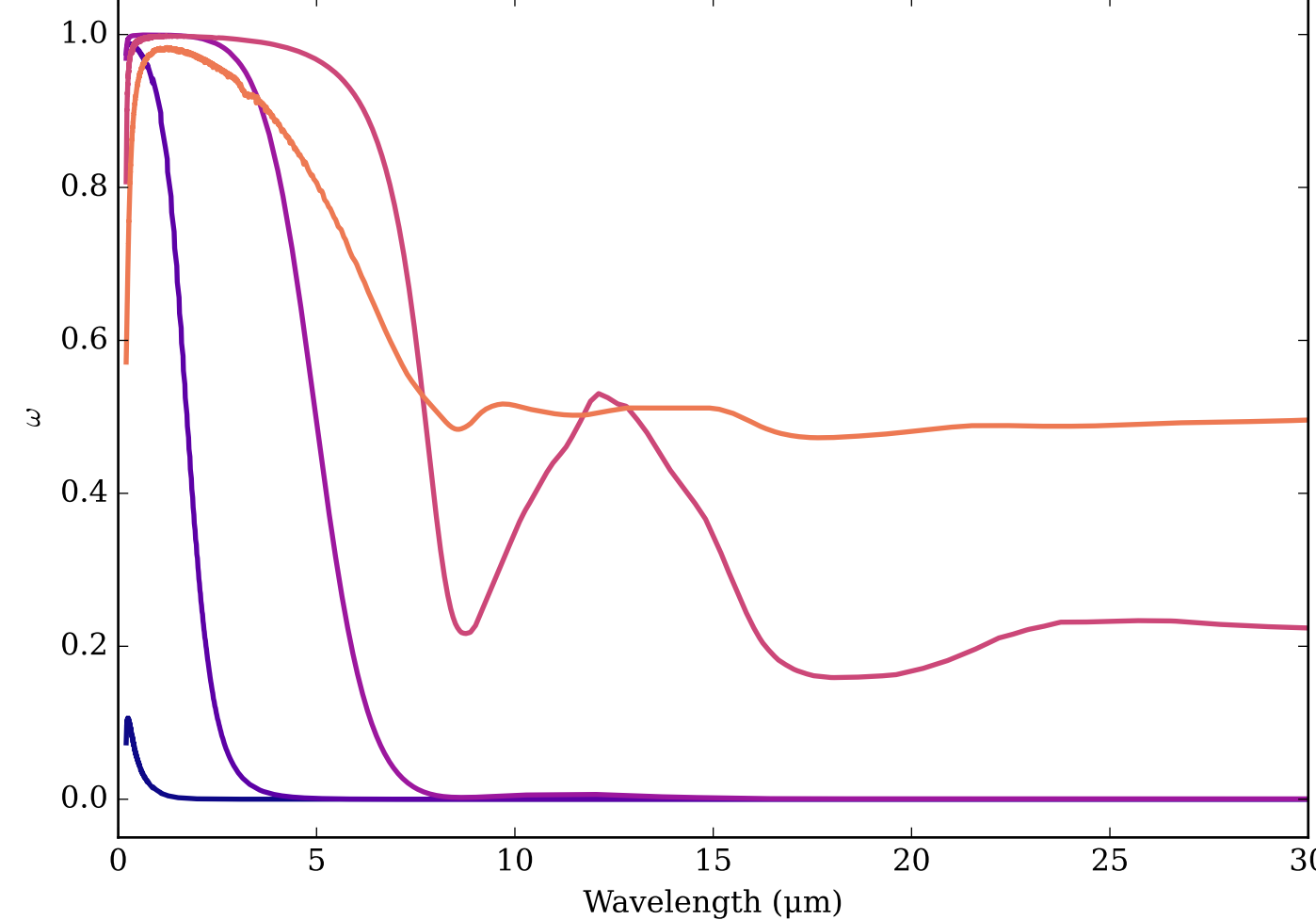
Refractive Indices for MgSiO<sub>3</sub>  
(0.2, 30.0)  $\mu\text{m}$



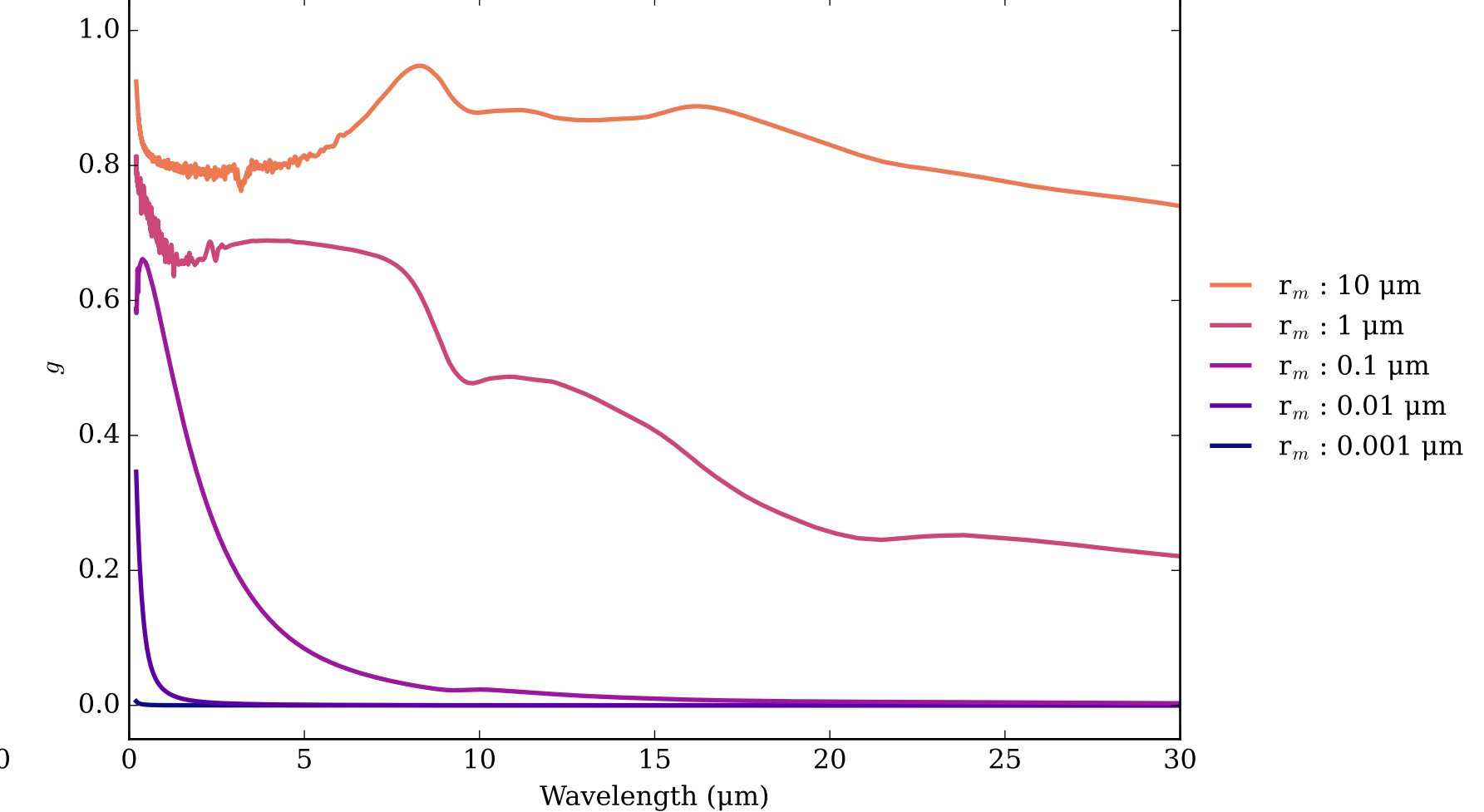
MgSiO<sub>3</sub>\_sol\_gel Effective Extinction Cross Section  
 $\sigma_{\text{ext, eff}} = \sigma_{\text{abs, eff}} + \sigma_{\text{scat, eff}}$



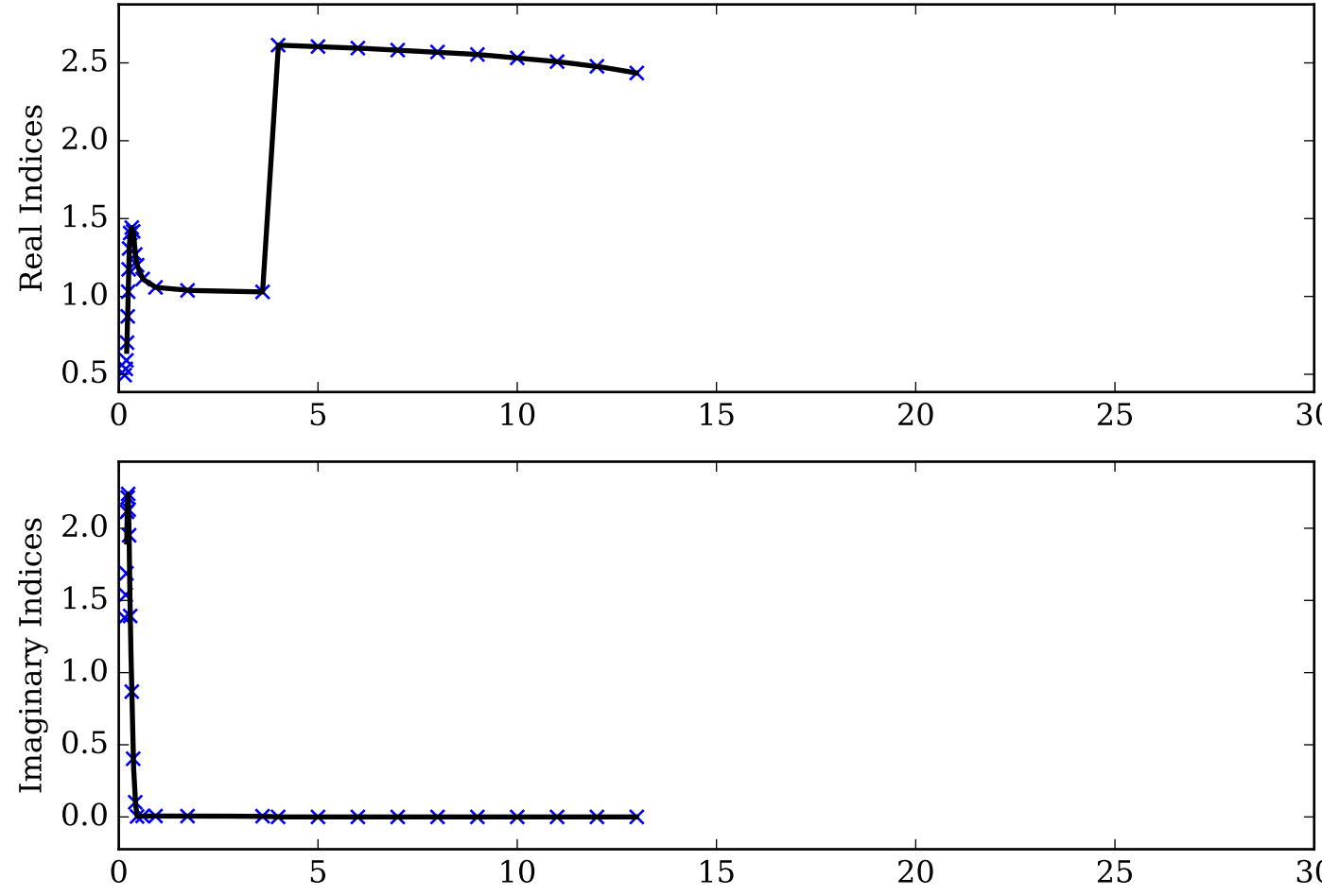
MgSiO<sub>3</sub>\_sol\_gel Single Scattering Albedos  $\omega$   
0 (black, completely absorbing) to 1 (white, completely scattering)



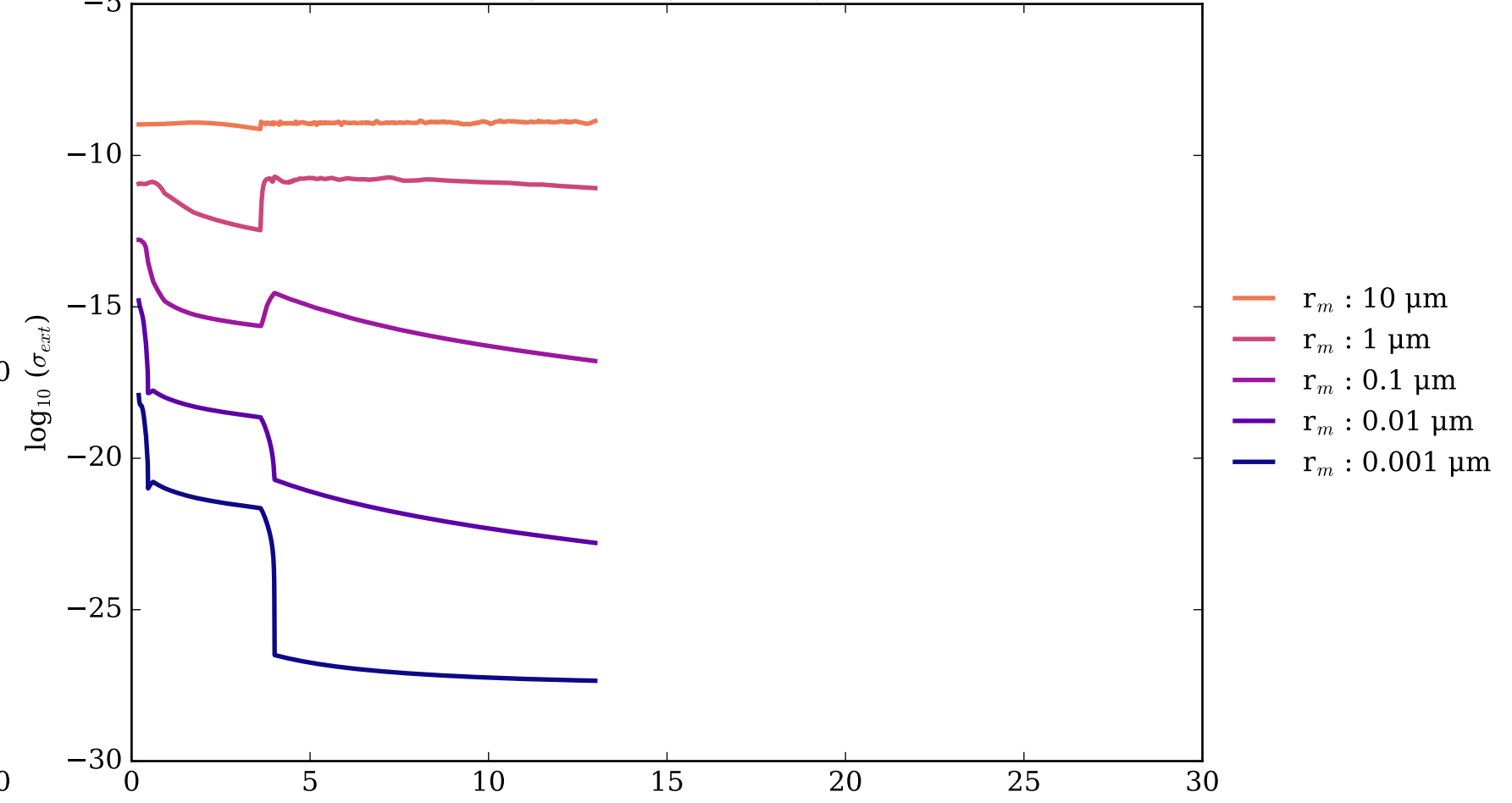
MgSiO<sub>3</sub>\_sol\_gel Asymmetry Parameter  $g$   
0 (Rayleigh Limit) to 1 (Total Forward Scattering)



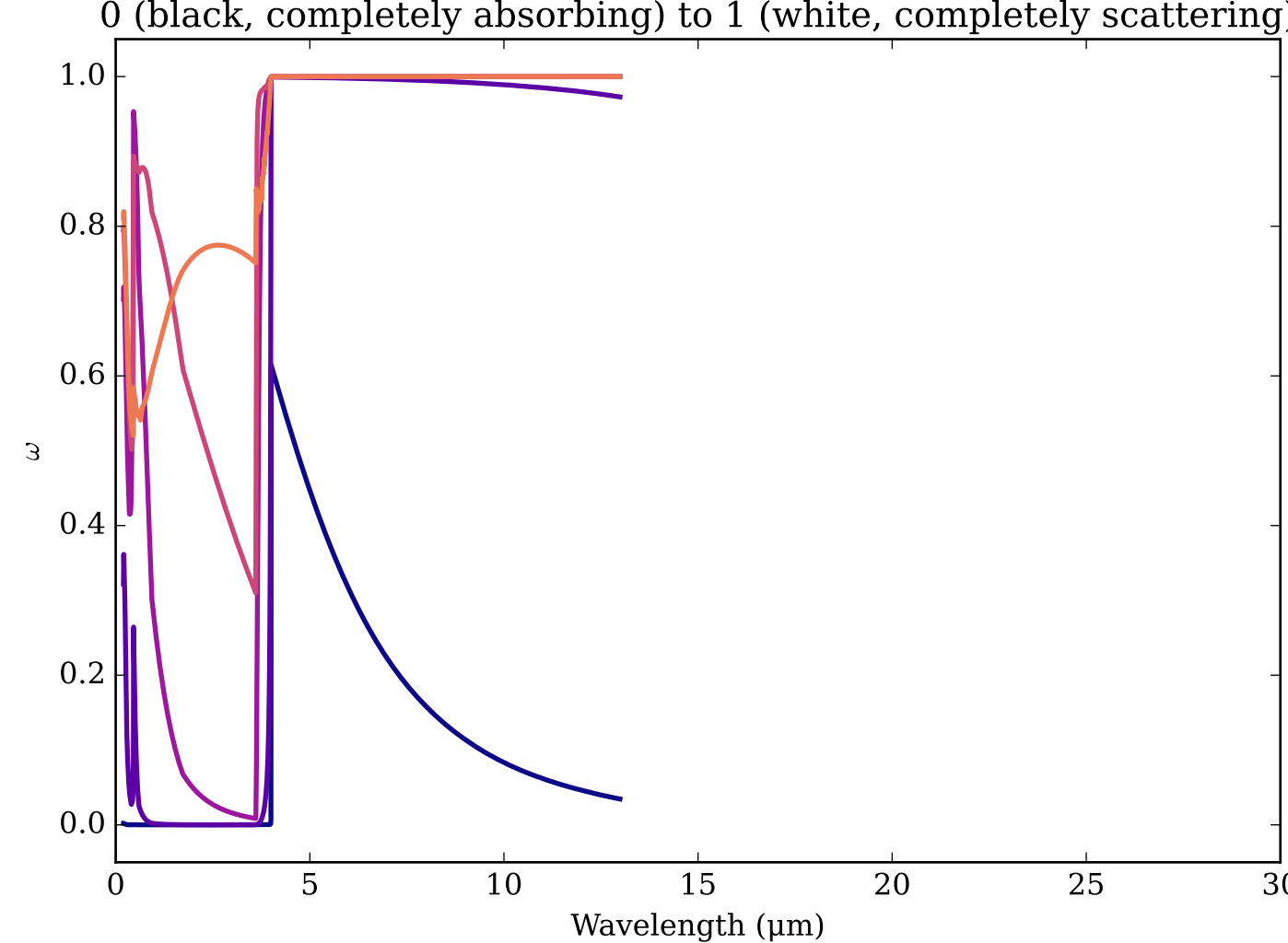
Refractive Indices for MnS  
(0.2, 12.99)  $\mu\text{m}$



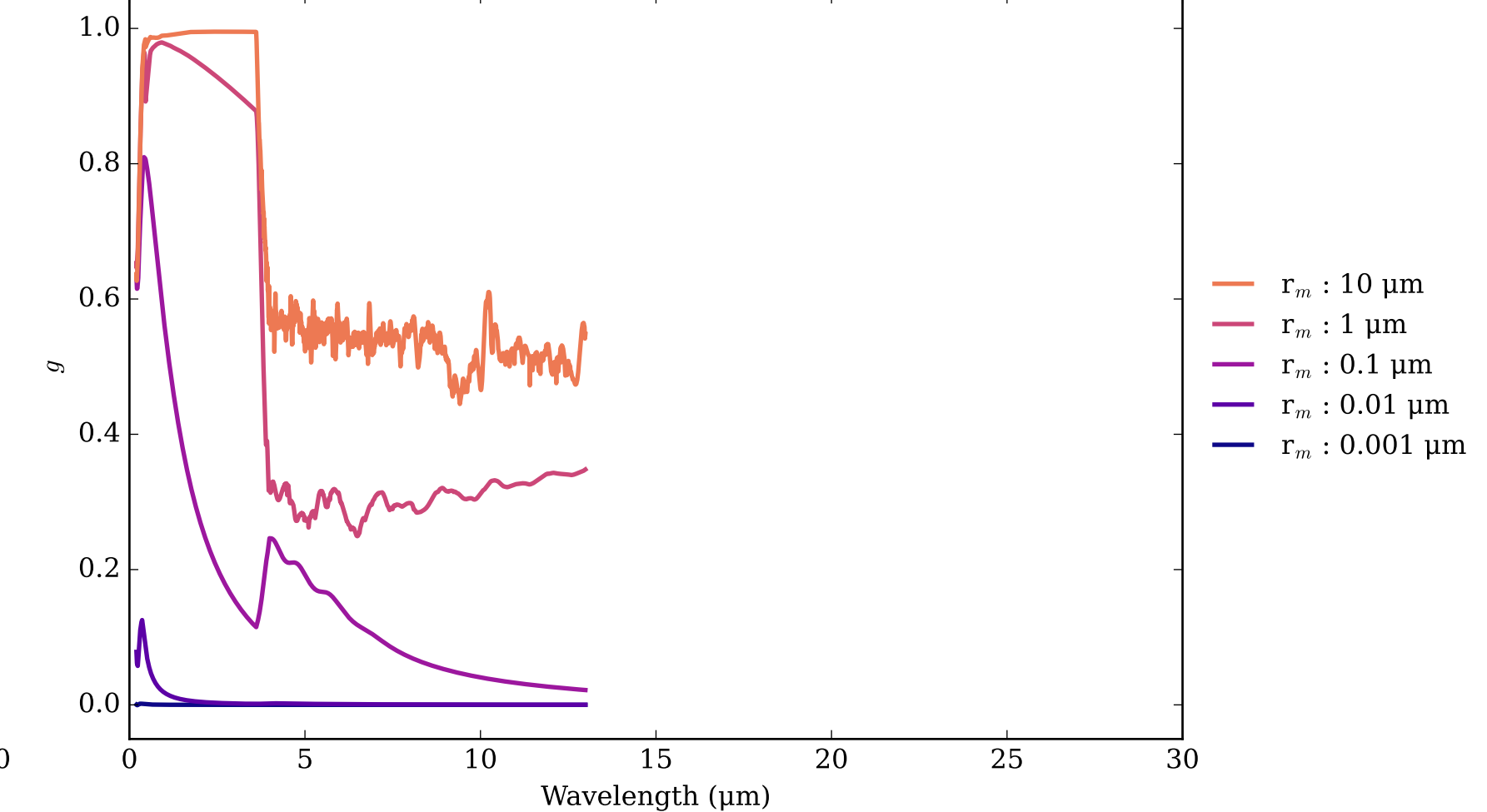
MnS Effective Extinction Cross Section  
 $\sigma_{\text{ext, eff}} = \sigma_{\text{abs, eff}} + \sigma_{\text{scat, eff}}$



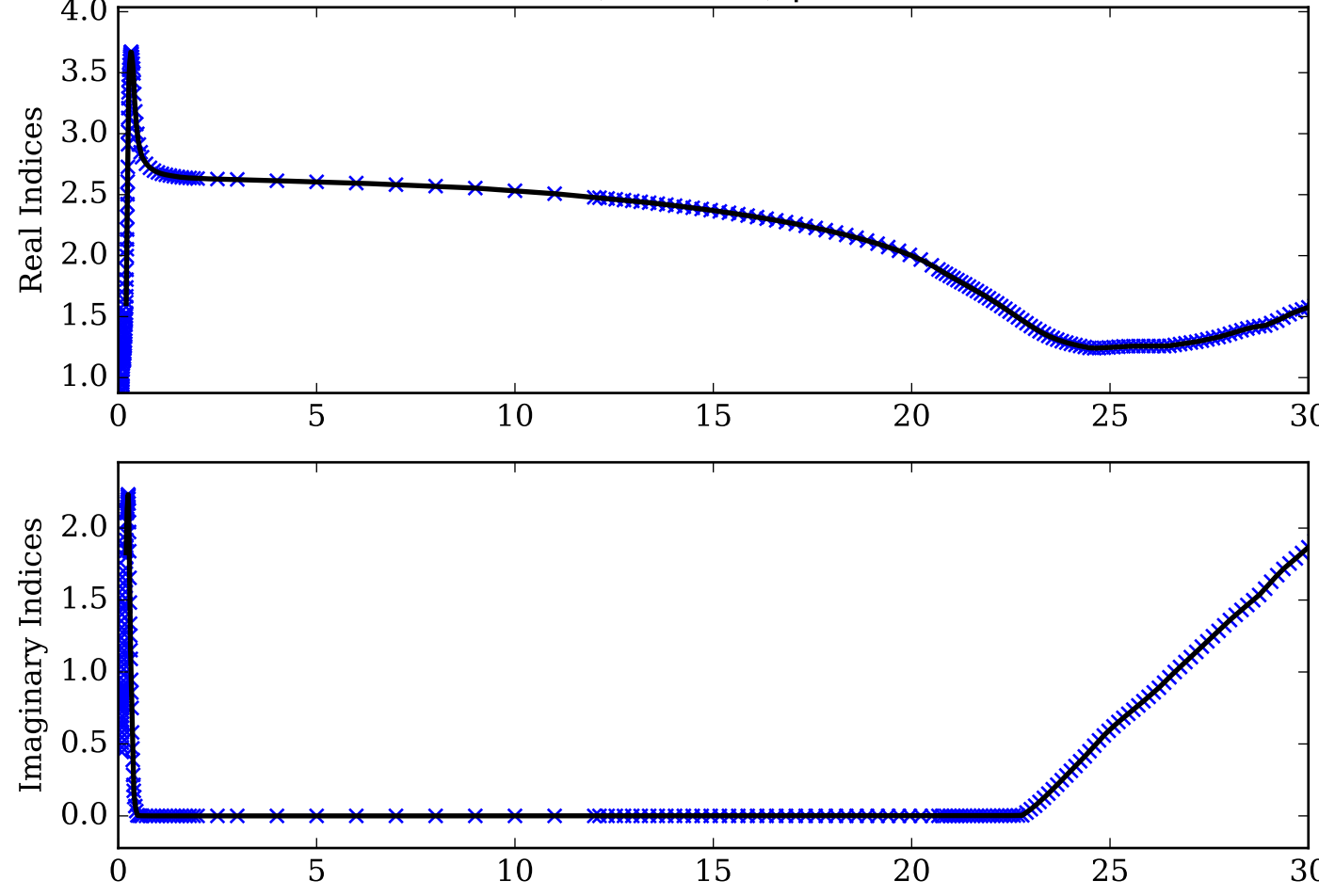
MnS Single Scattering Albedos  $\omega$



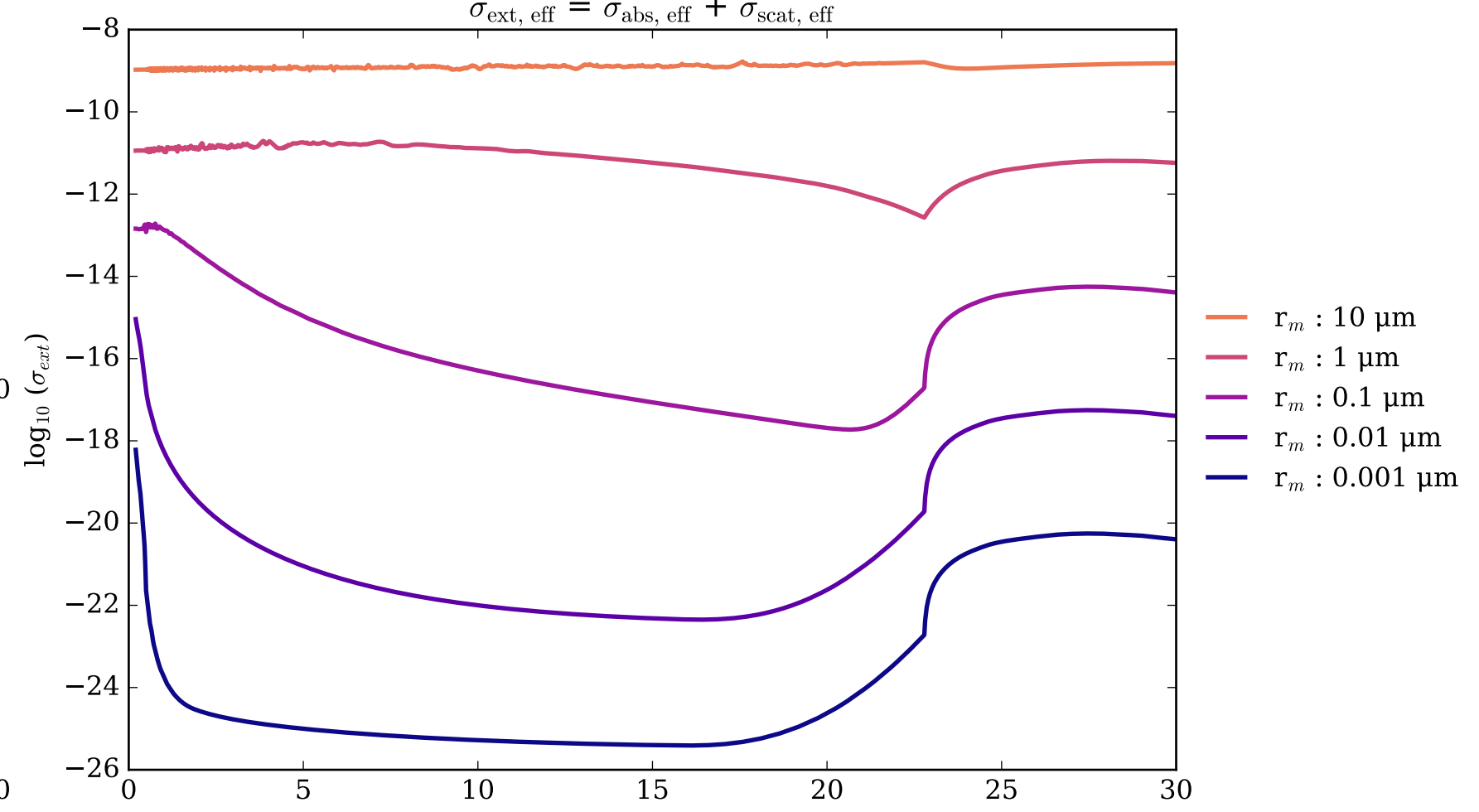
MnS Asymmetry Parameter  $g$   
0 (Rayleigh Limit) to 1 (Total Forward Scattering)



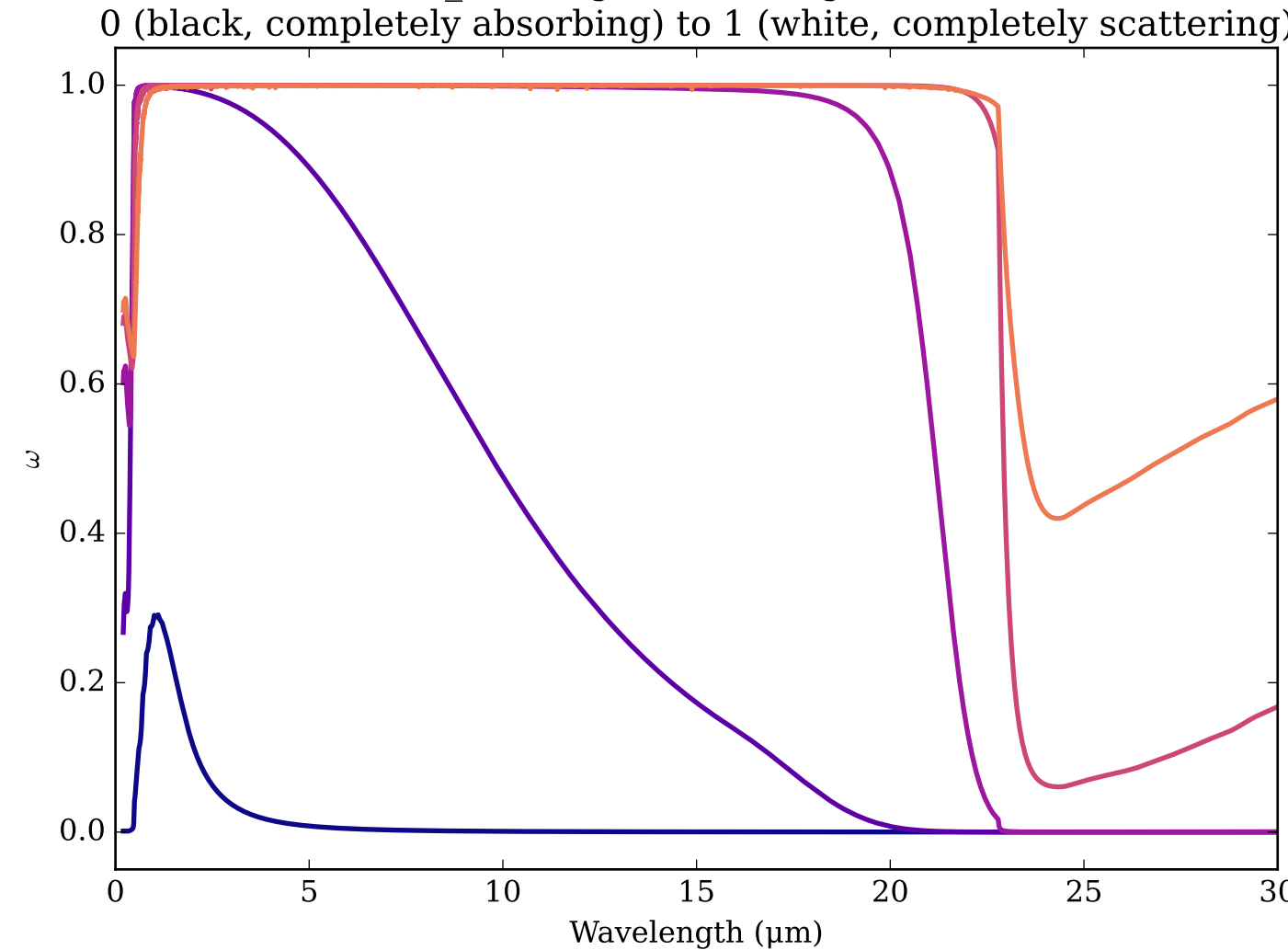
Refractive Indices for MnS  
(0.2, 30.0)  $\mu\text{m}$



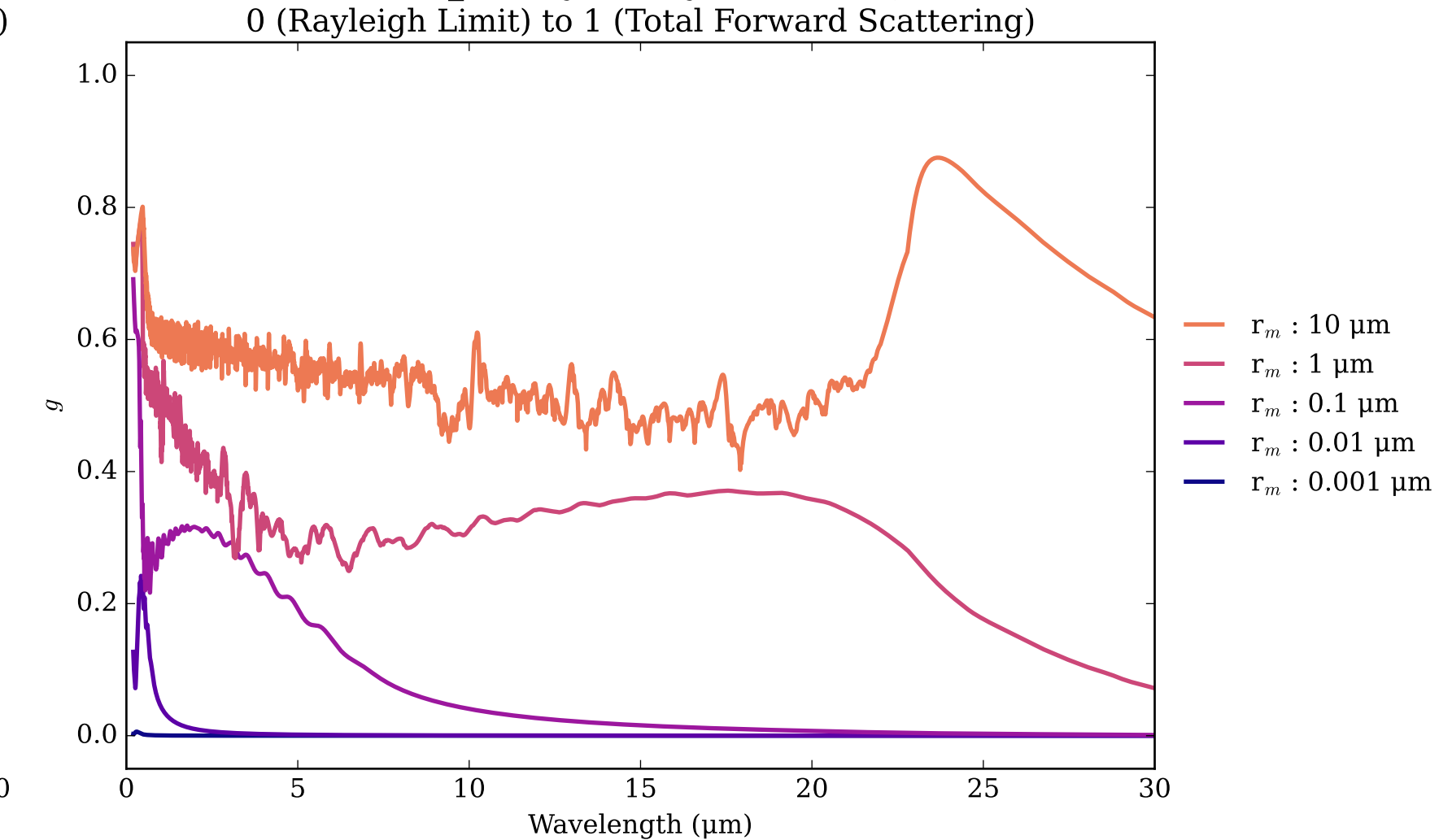
MnS\_KH Effective Extinction Cross Section



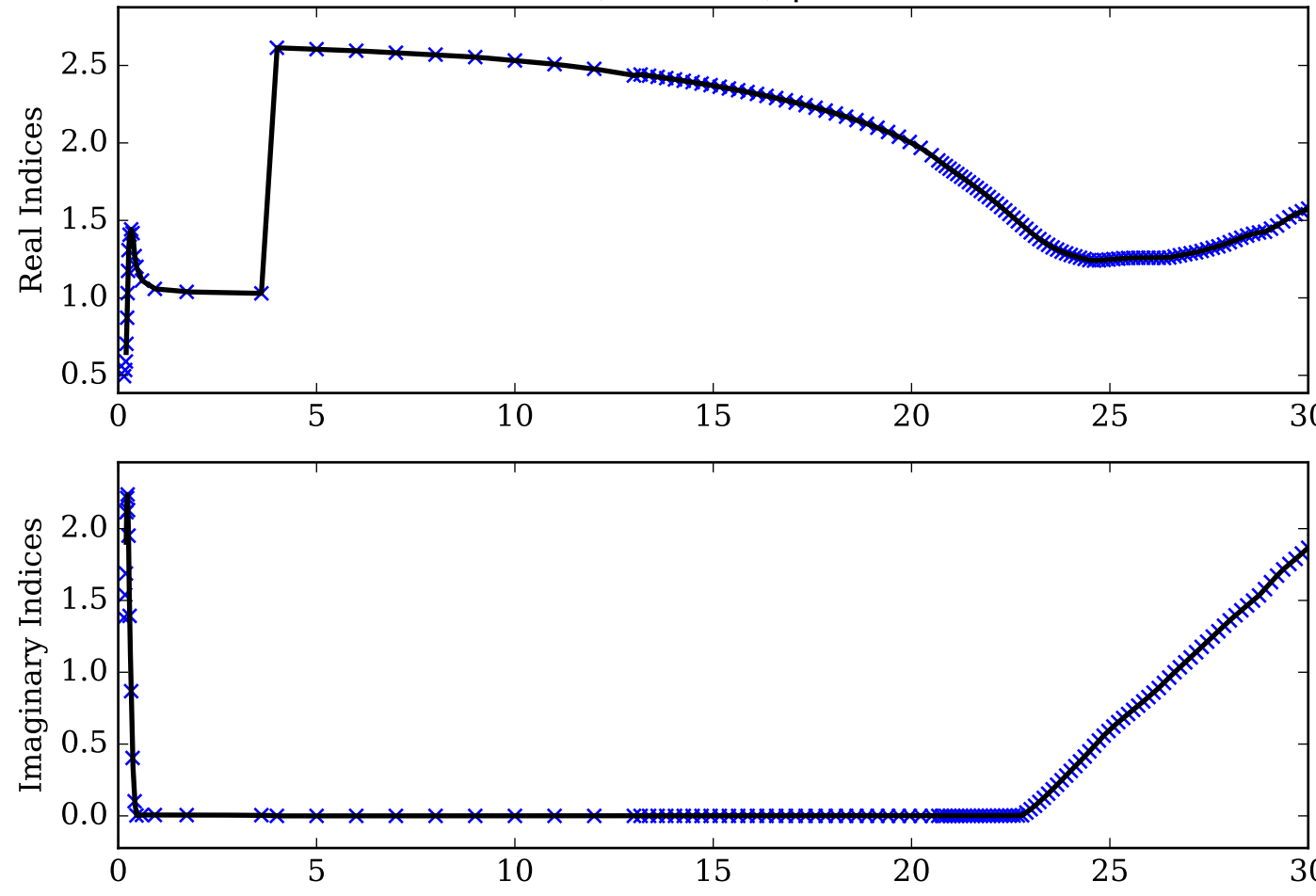
MnS\_KH Single Scattering Albedos  $\omega$



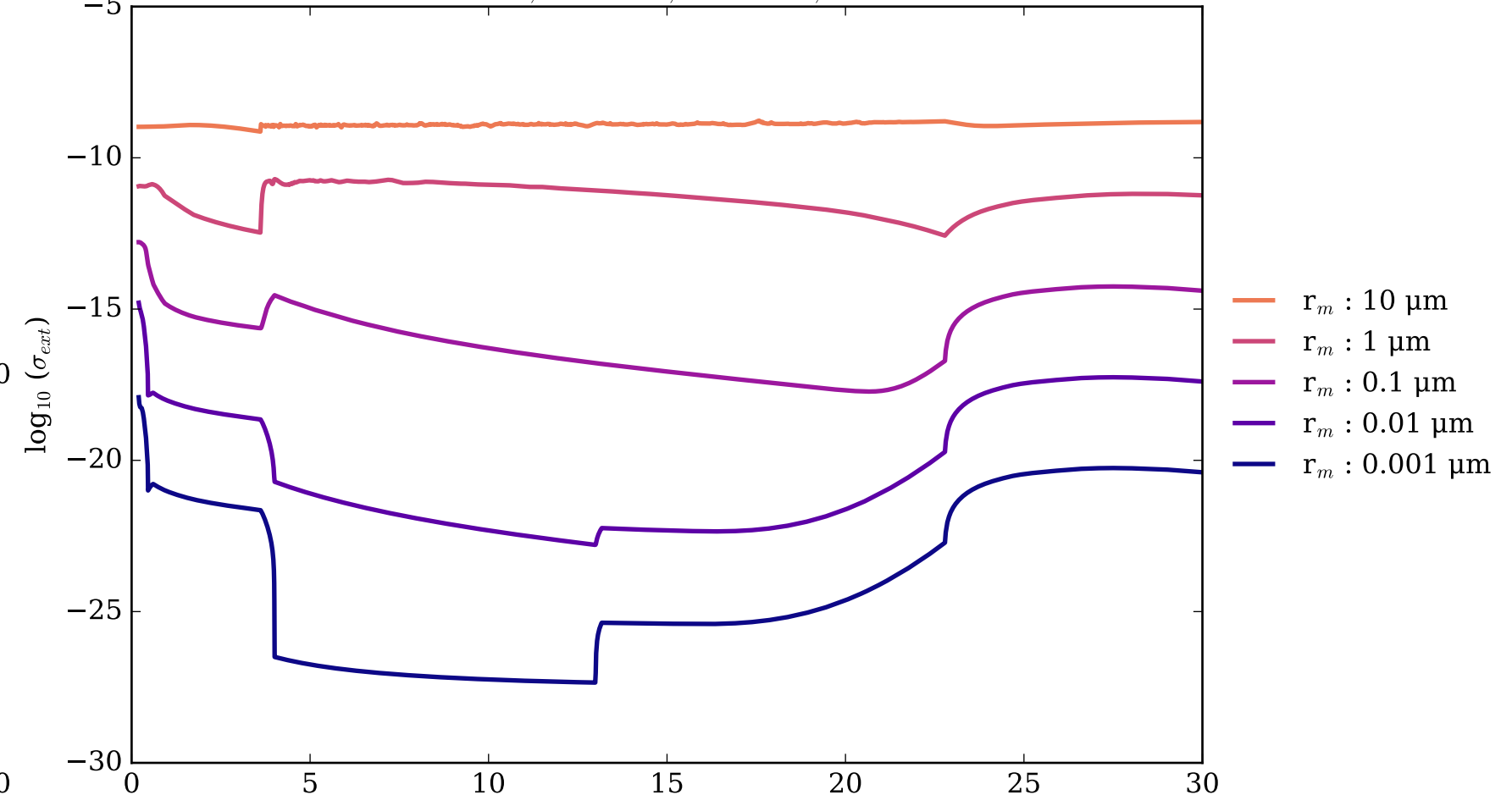
MnS\_KH Asymmetry Parameter  $g$



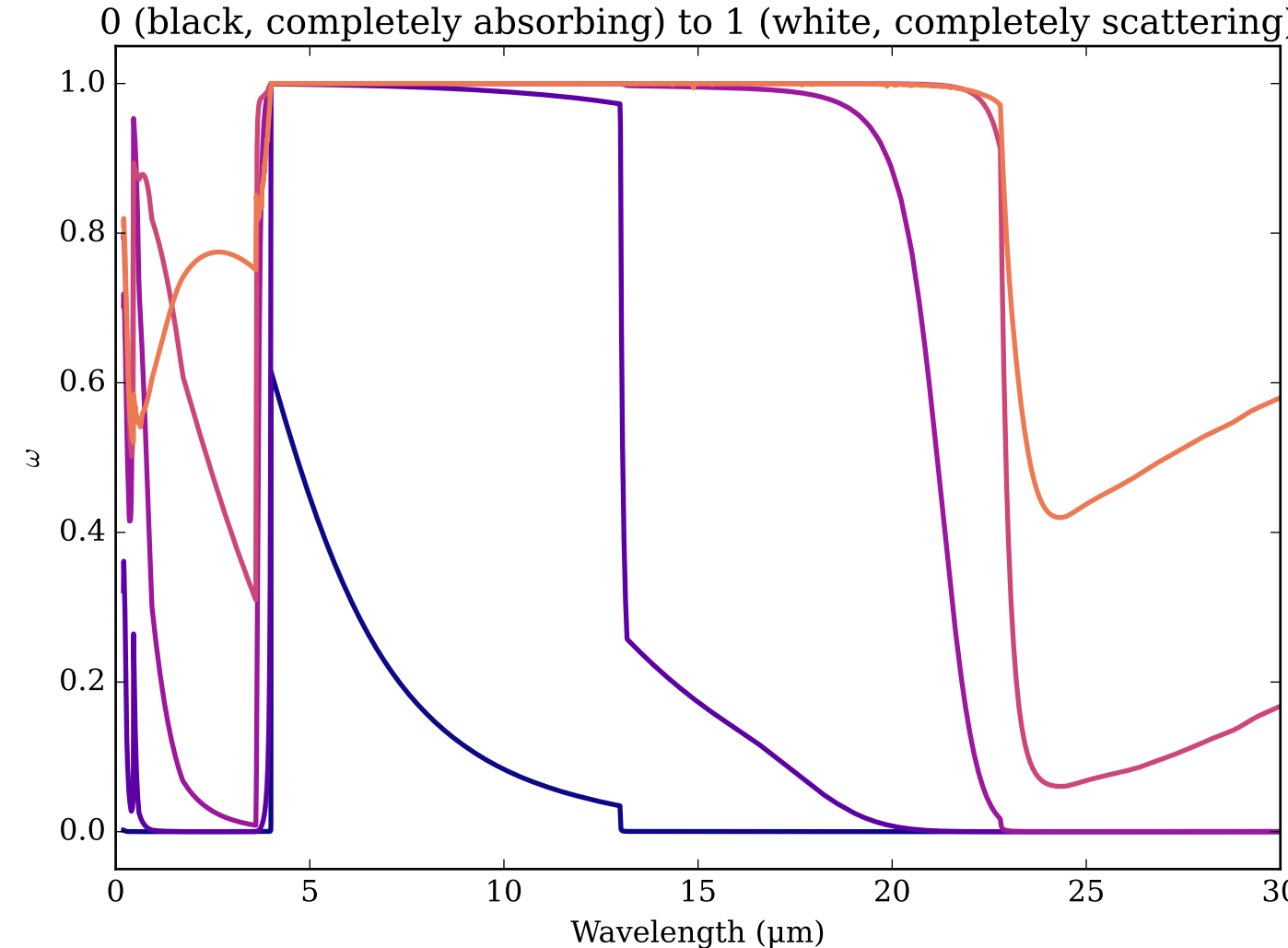
Refractive Indices for MnS  
(0.2, 30.0)  $\mu\text{m}$



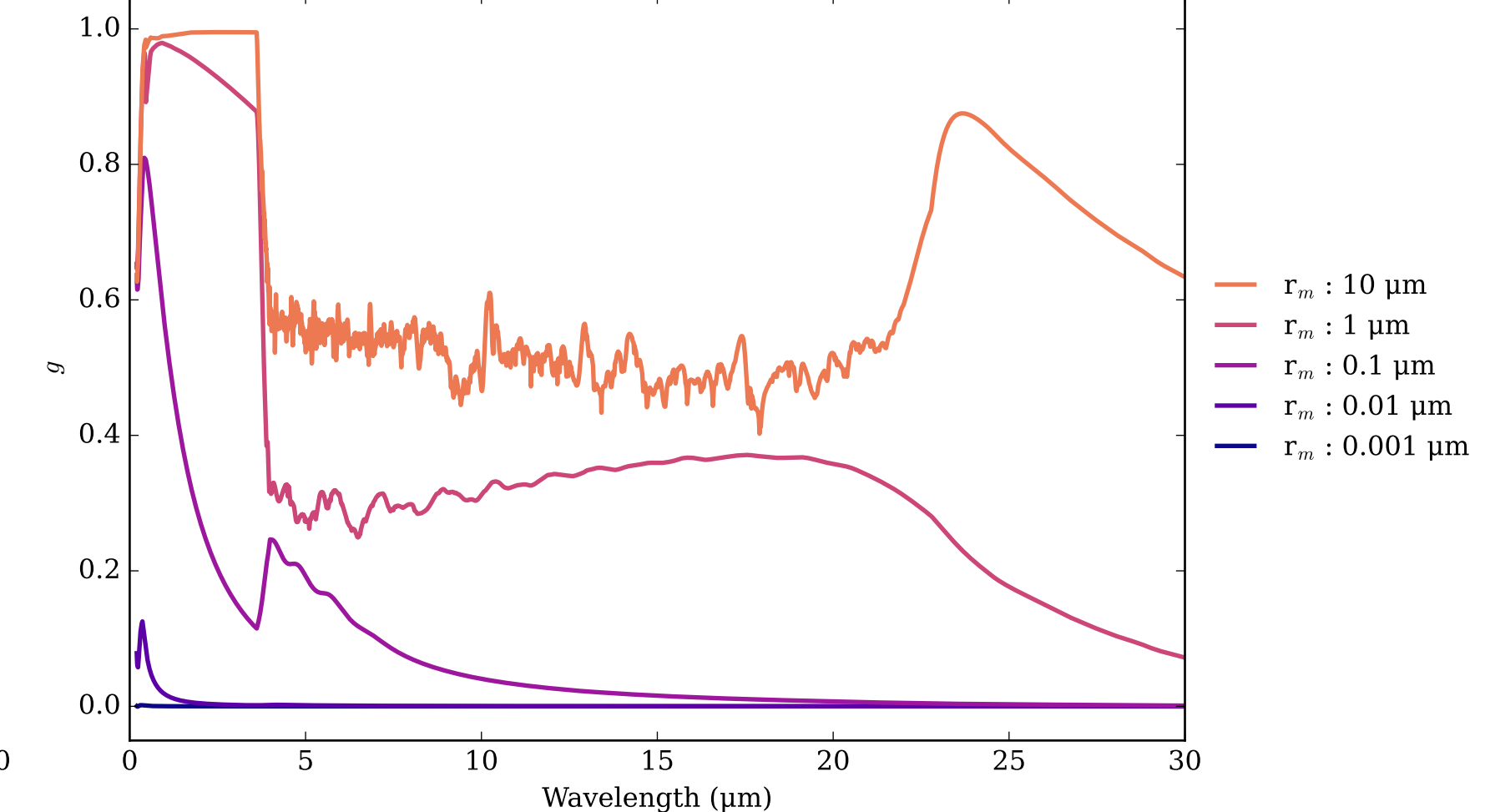
MnS\_Mor Effective Extinction Cross Section  
 $\sigma_{\text{ext, eff}} = \sigma_{\text{abs, eff}} + \sigma_{\text{scat, eff}}$



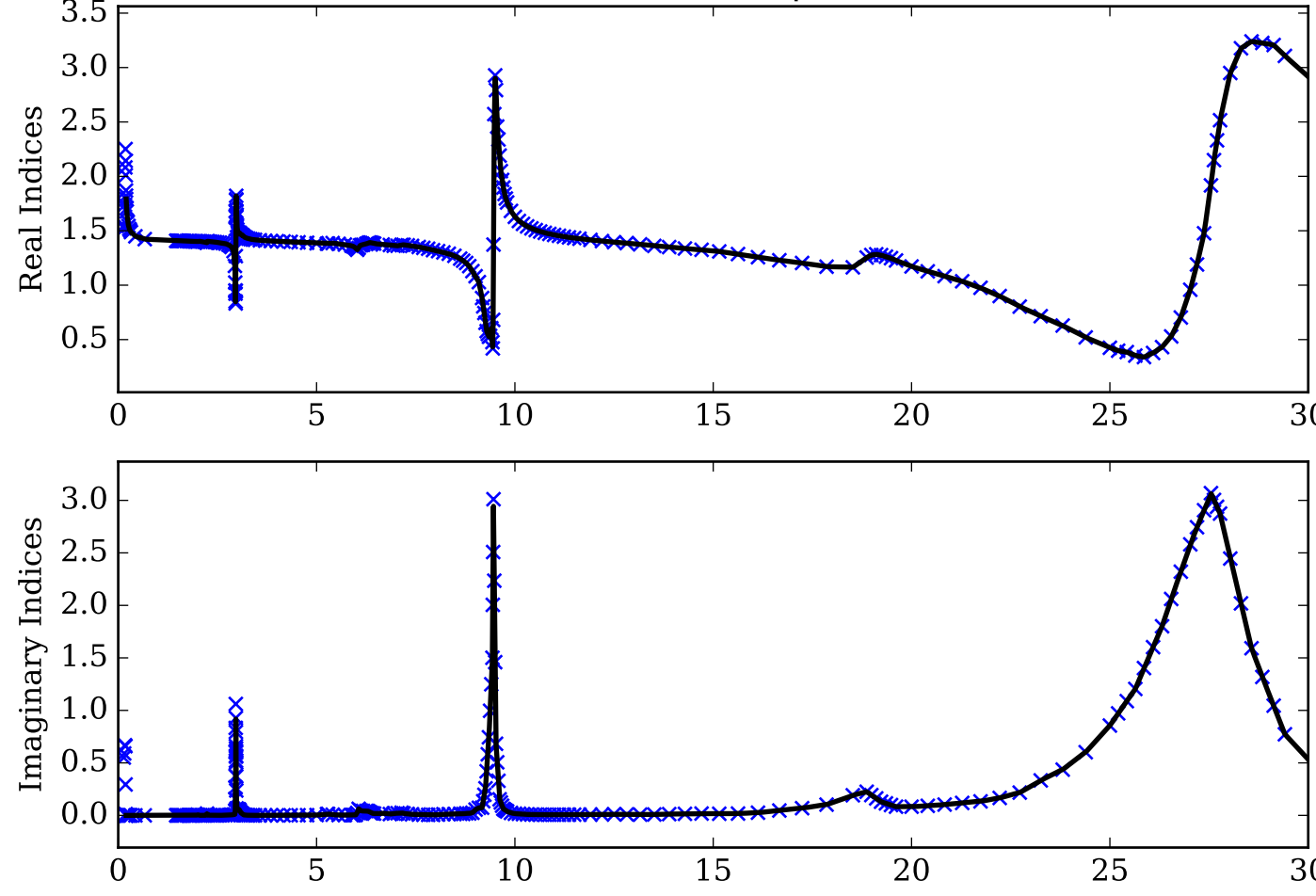
MnS\_Mor Single Scattering Albedos  $\omega$



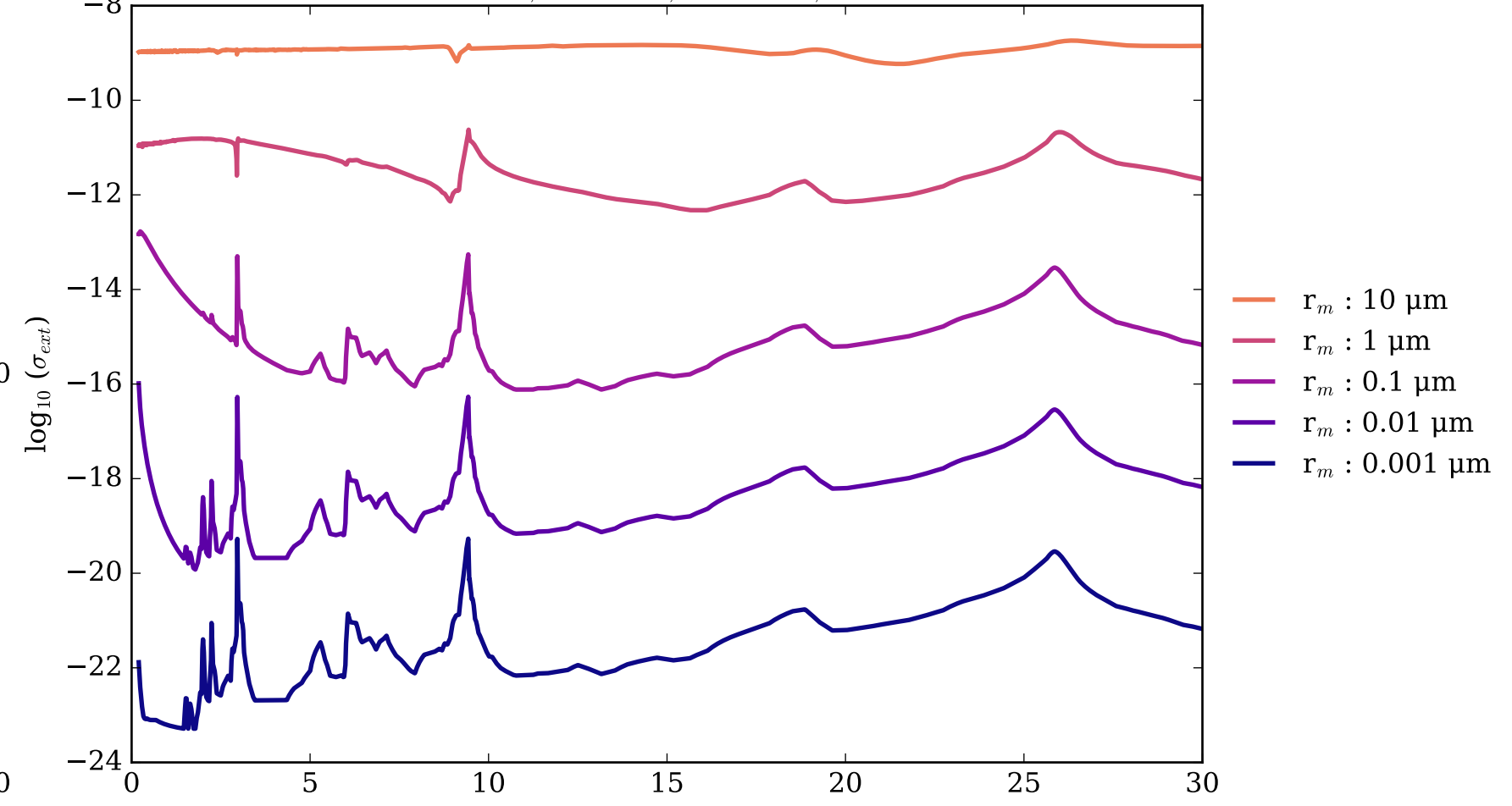
MnS\_Mor Asymmetry Parameter  $g$   
0 (Rayleigh Limit) to 1 (Total Forward Scattering)



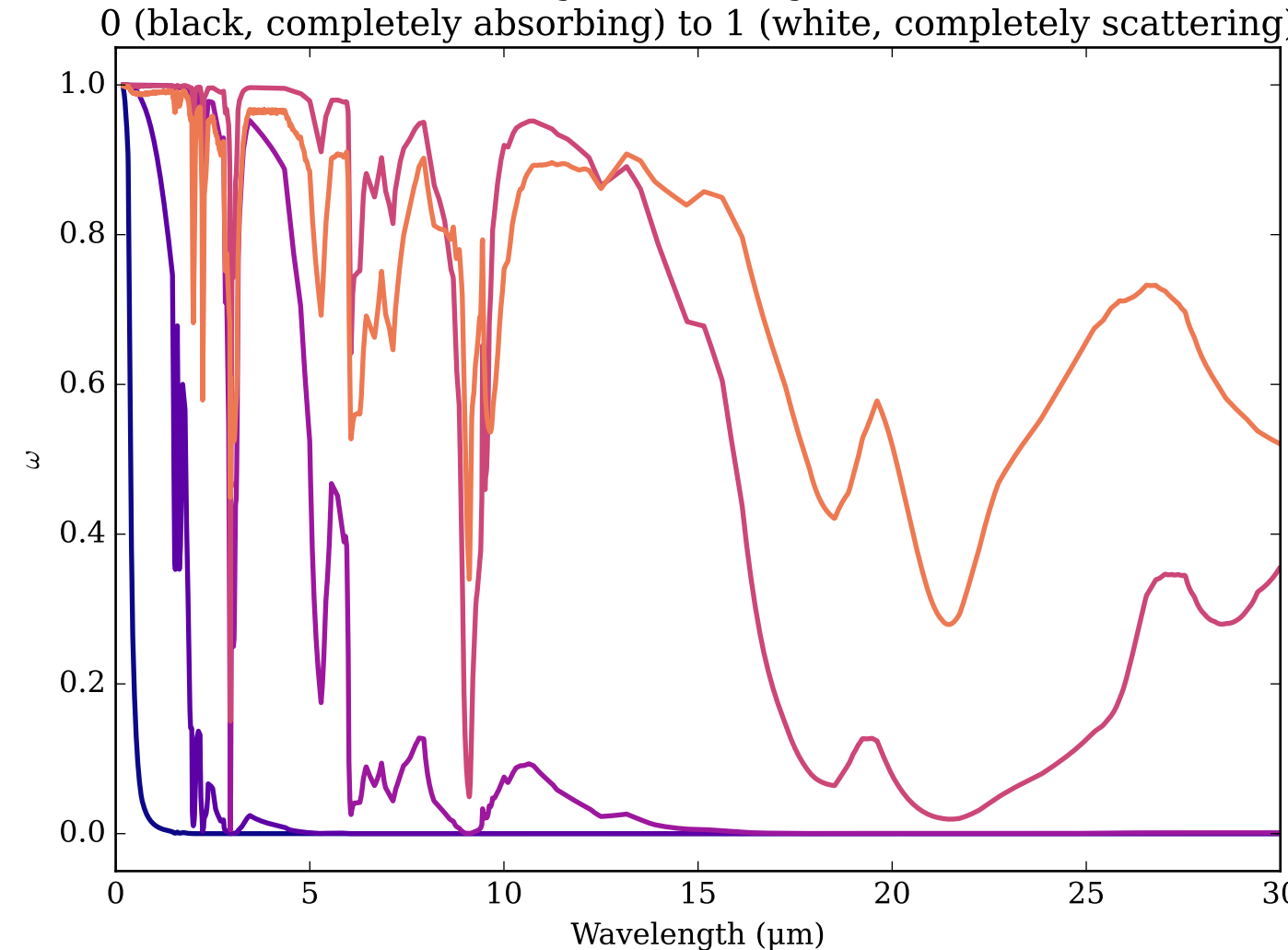
Refractive Indices for NH<sub>3</sub>  
(0.2, 30.0)  $\mu\text{m}$



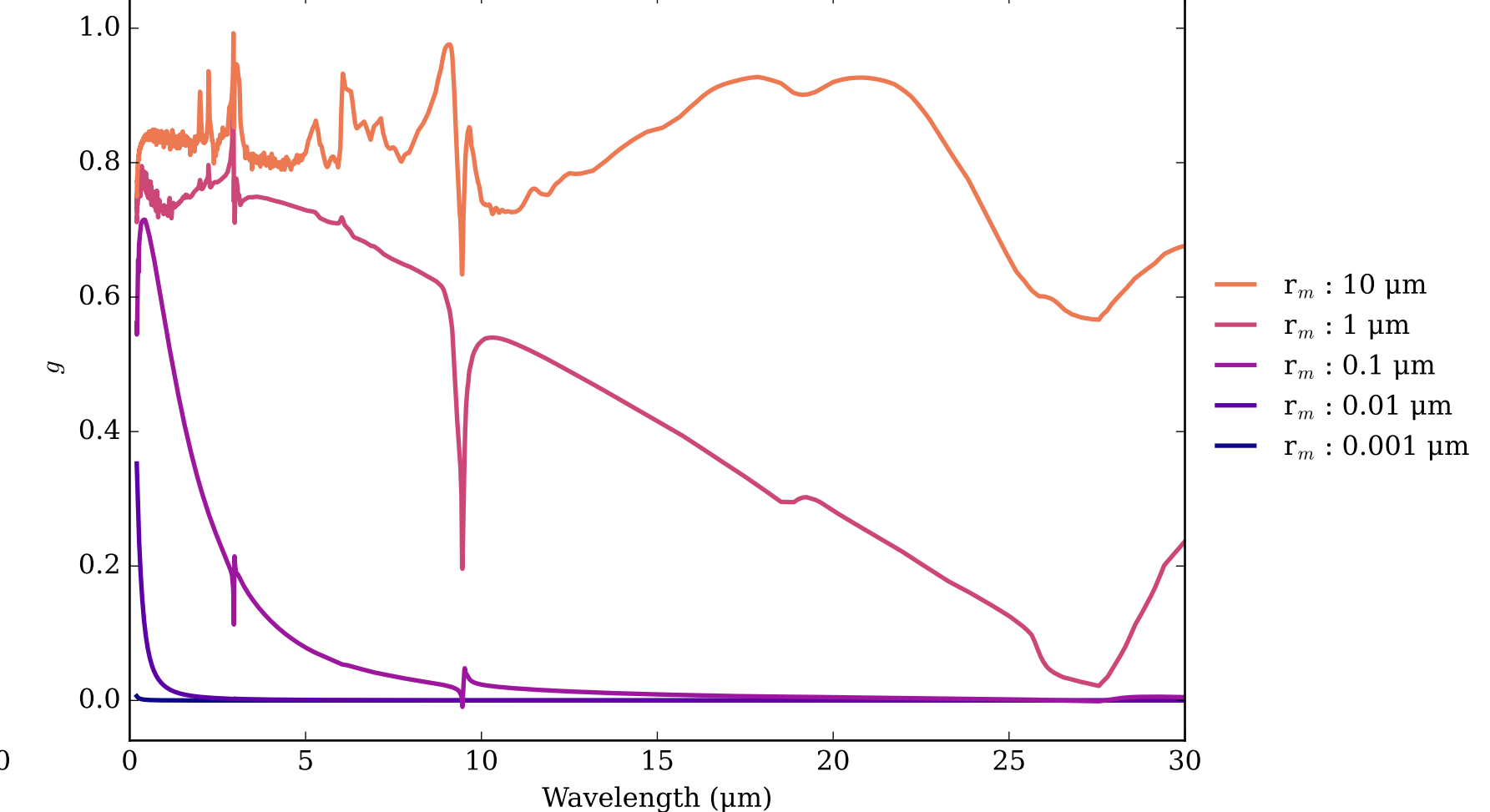
NH<sub>3</sub> Effective Extinction Cross Section  
 $\sigma_{\text{ext, eff}} = \sigma_{\text{abs, eff}} + \sigma_{\text{scat, eff}}$



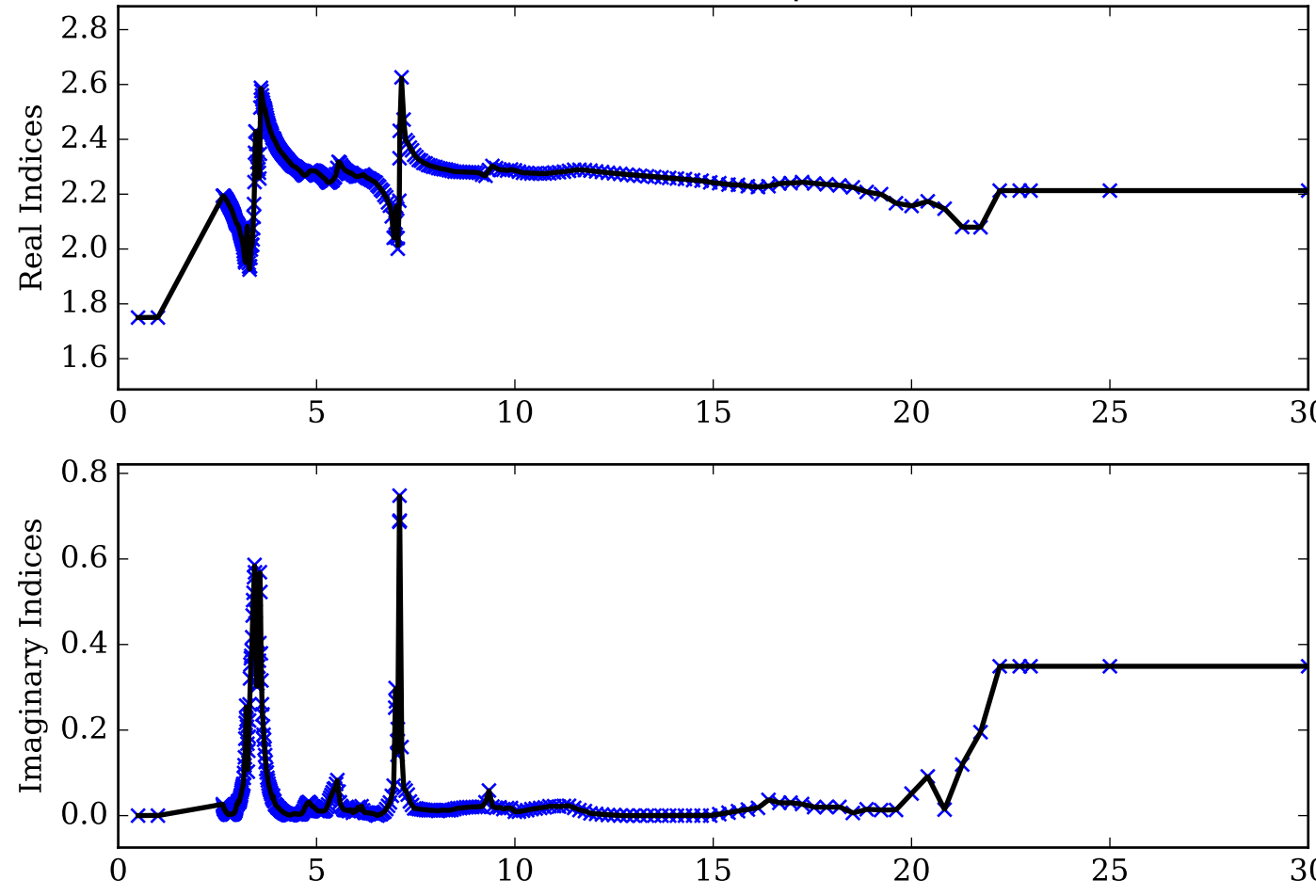
NH<sub>3</sub> Single Scattering Albedos  $\omega$



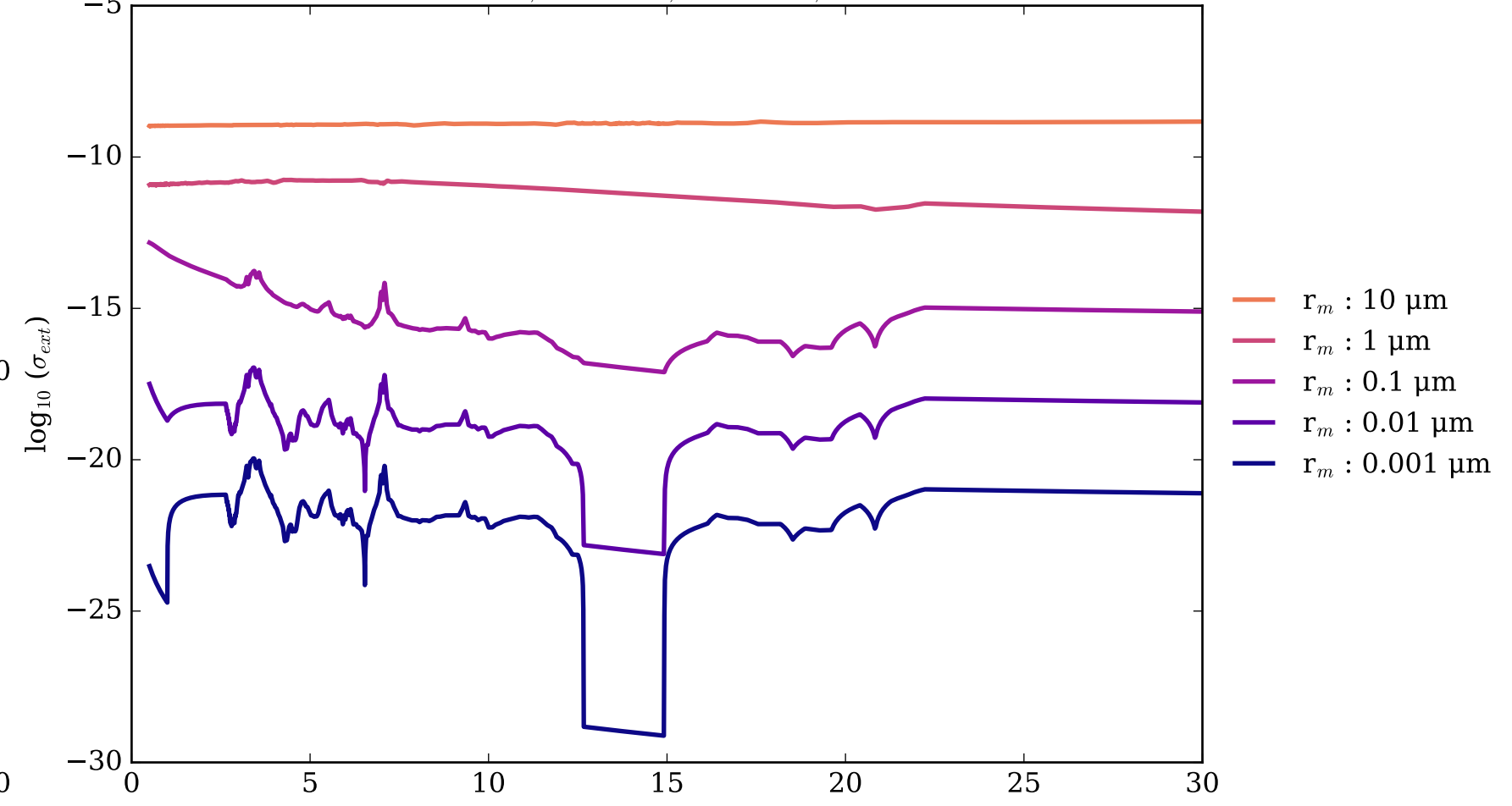
NH<sub>3</sub> Asymmetry Parameter  $g$   
0 (Rayleigh Limit) to 1 (Total Forward Scattering)



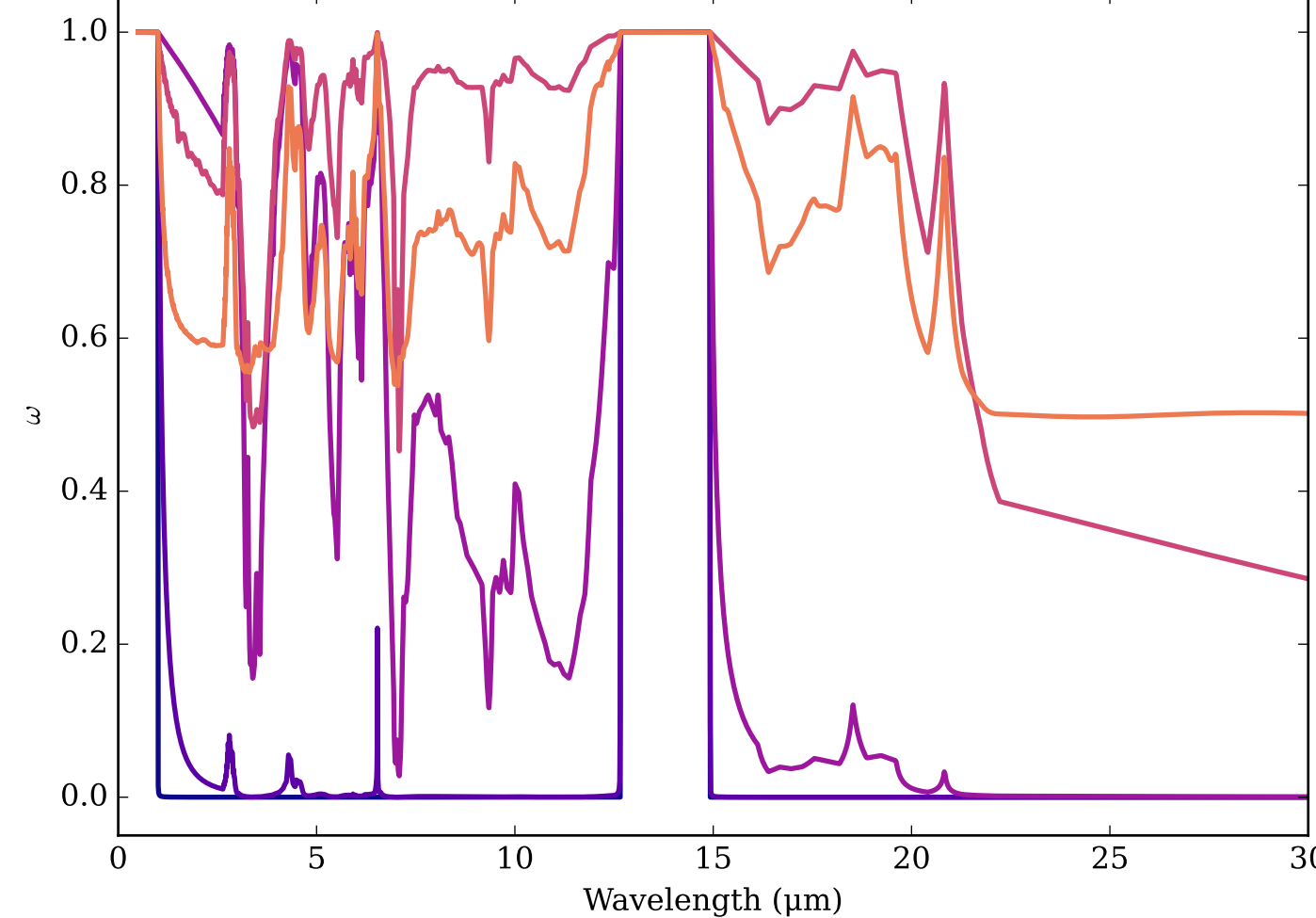
Refractive Indices for NH<sub>4</sub>SH  
(0.5, 30.0)  $\mu\text{m}$



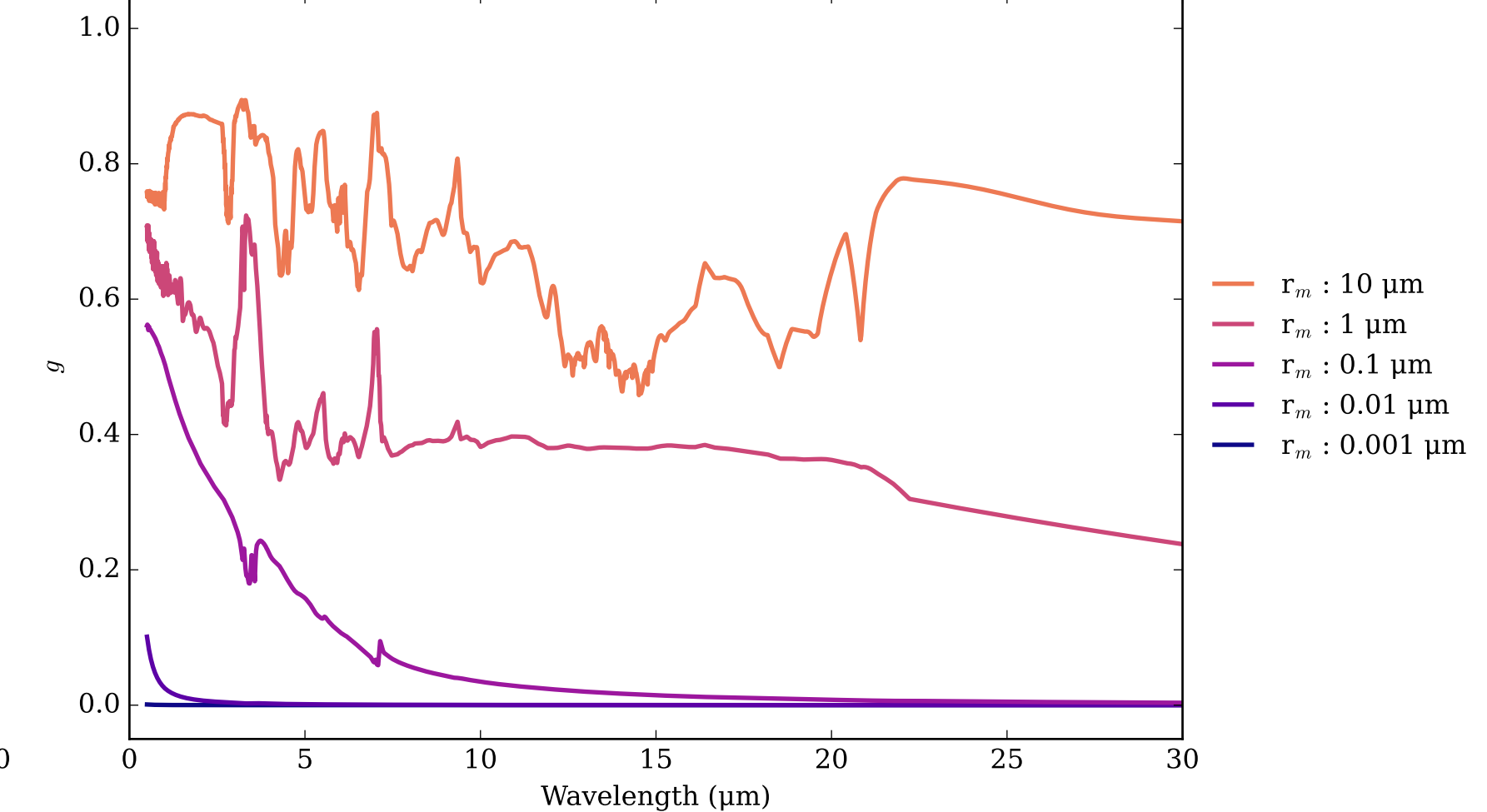
NH<sub>4</sub>SH Effective Extinction Cross Section  
 $\sigma_{\text{ext, eff}} = \sigma_{\text{abs, eff}} + \sigma_{\text{scat, eff}}$



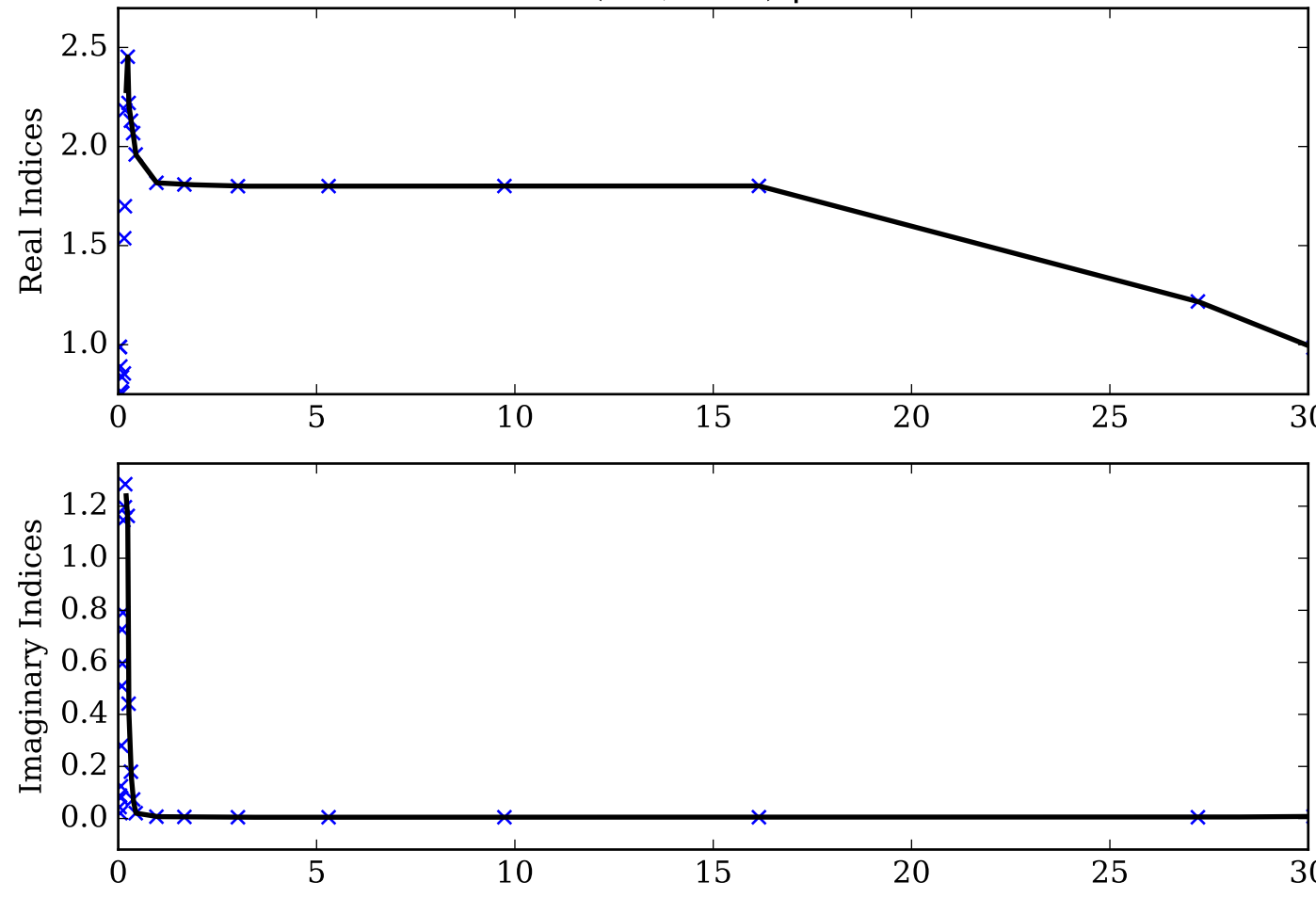
NH<sub>4</sub>SH Single Scattering Albedos  $\omega$   
0 (black, completely absorbing) to 1 (white, completely scattering)



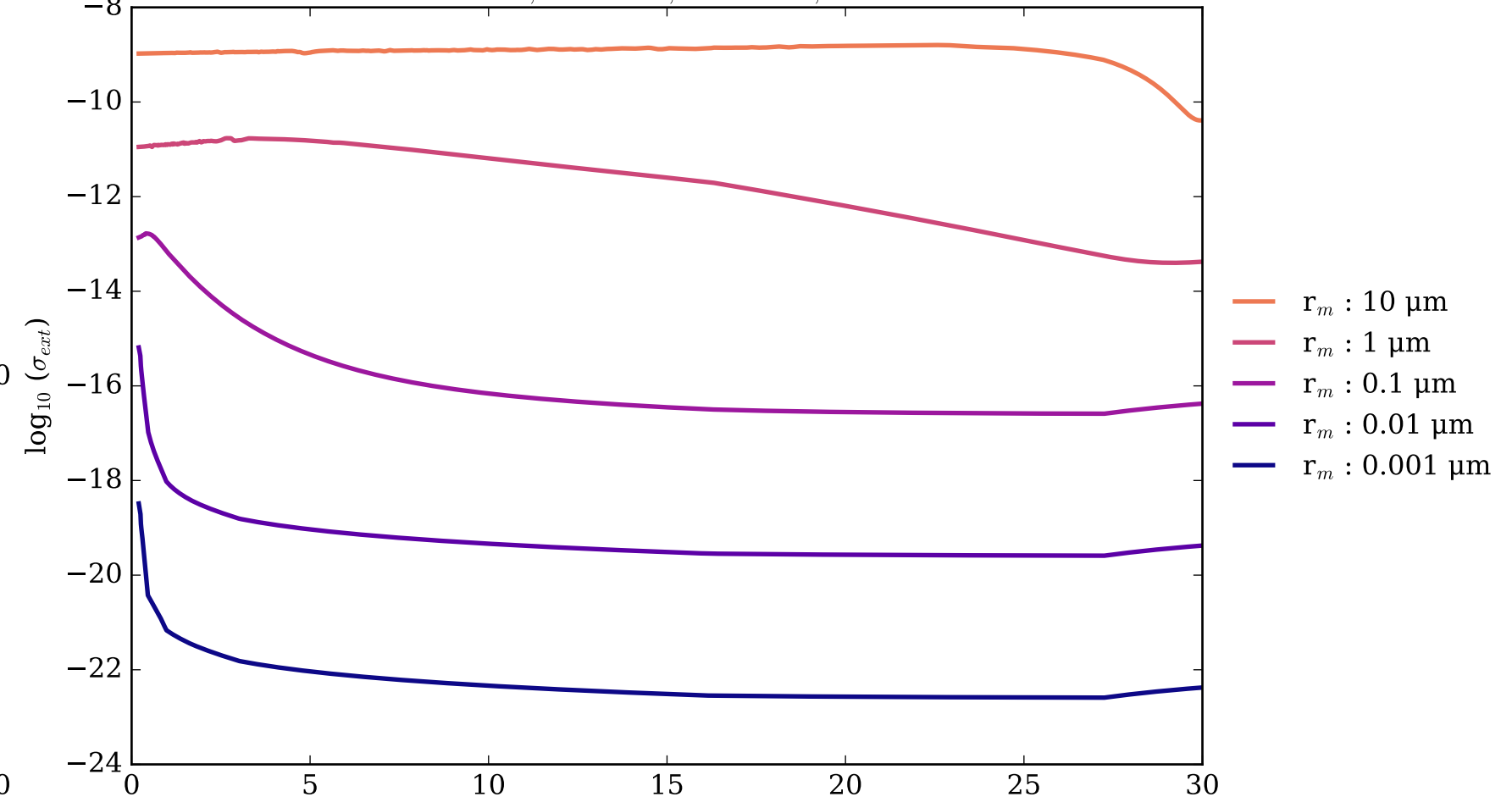
NH<sub>4</sub>SH Asymmetry Parameter  $g$   
0 (Rayleigh Limit) to 1 (Total Forward Scattering)



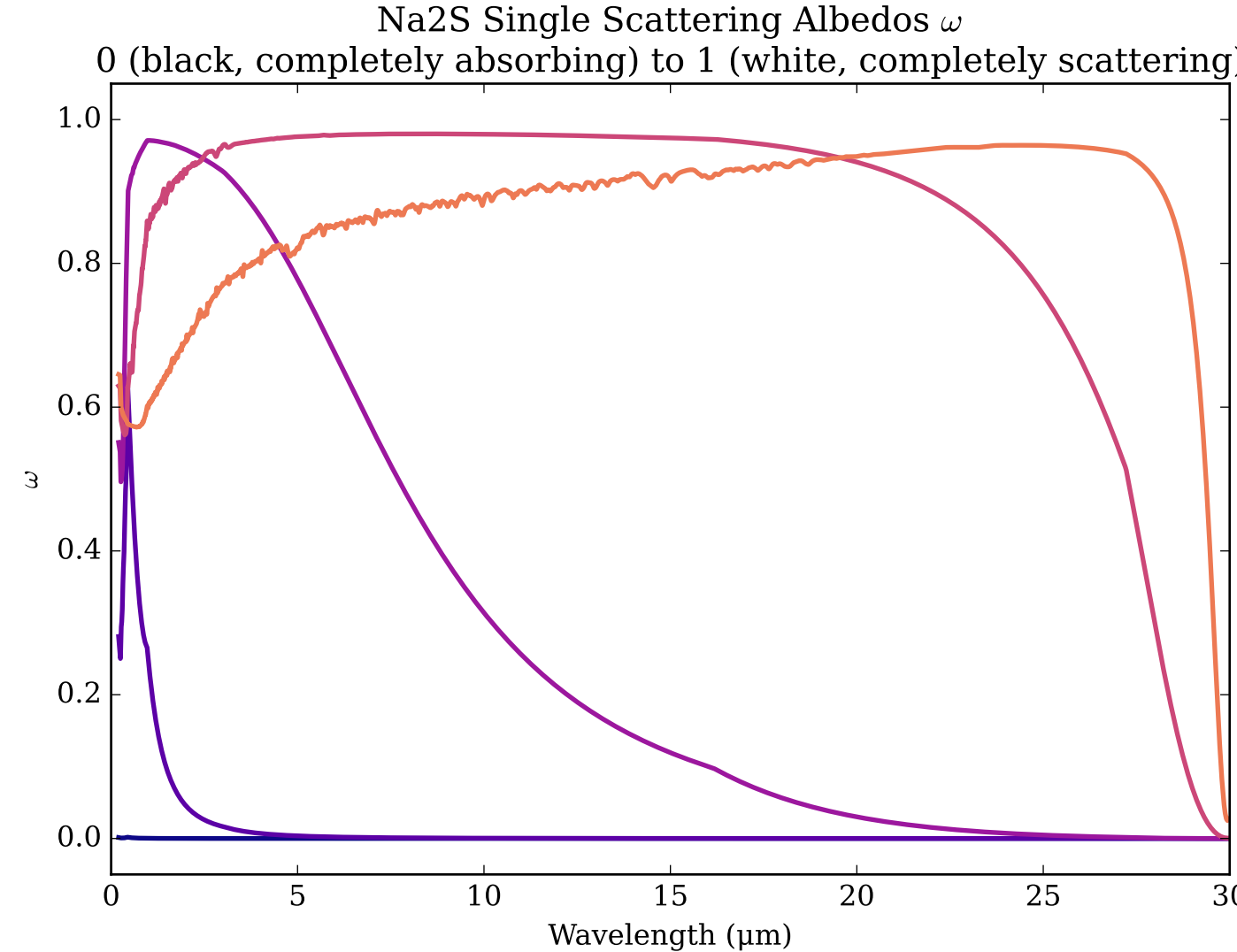
Refractive Indices for Na<sub>2</sub>S  
(0.2, 30.0)  $\mu\text{m}$



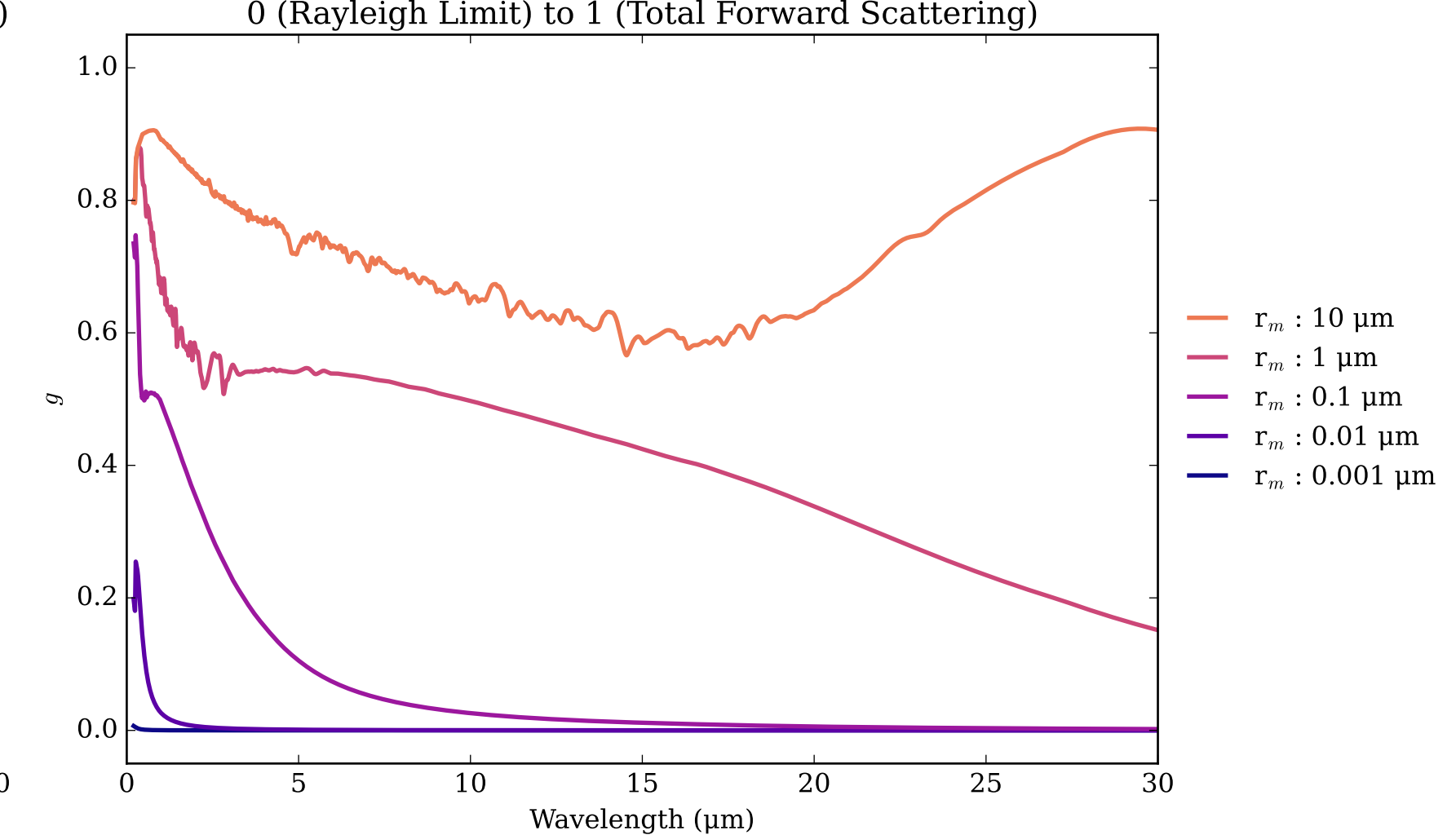
Na<sub>2</sub>S Effective Extinction Cross Section



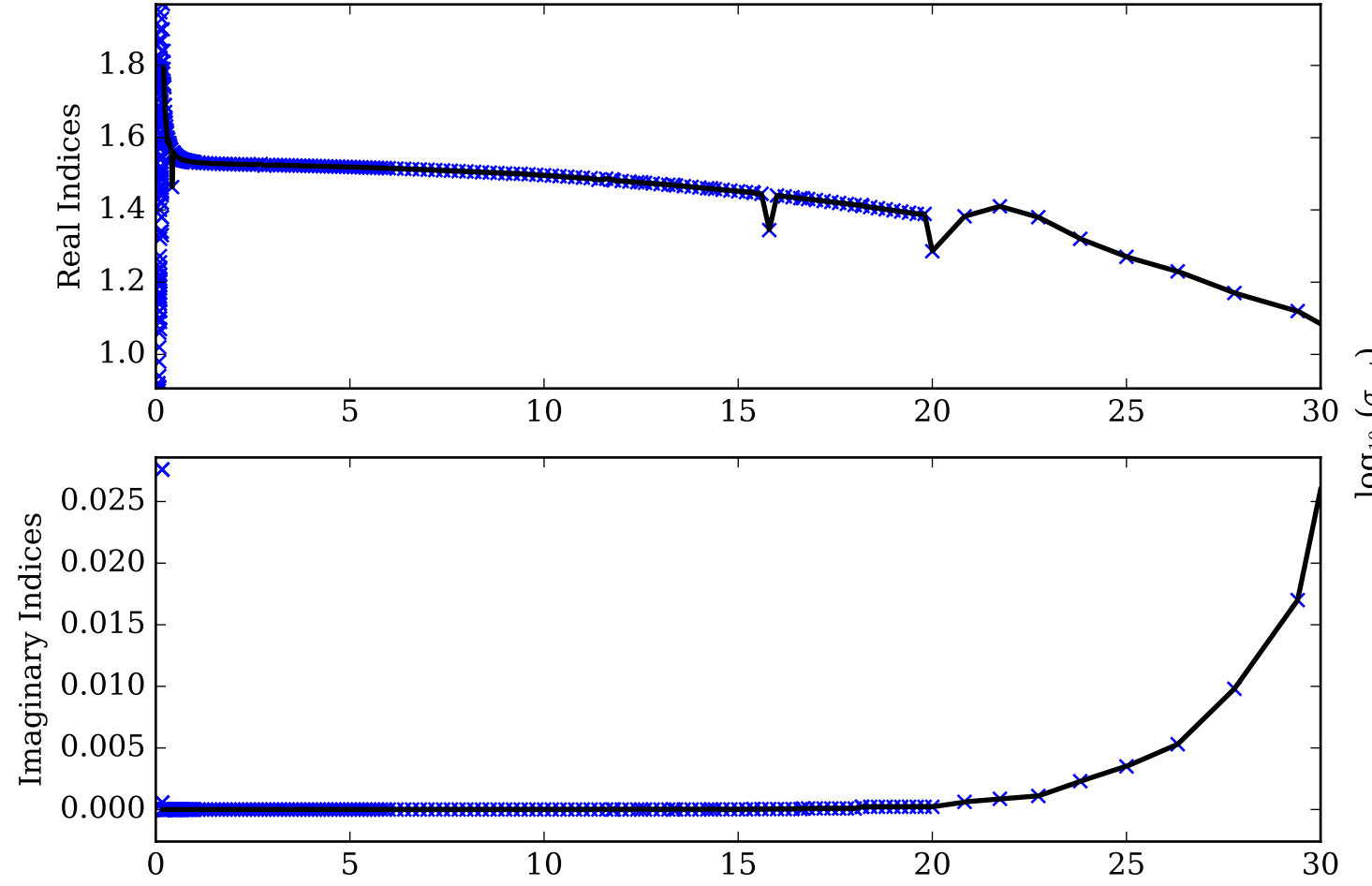
Na<sub>2</sub>S Single Scattering Albedos  $\omega$



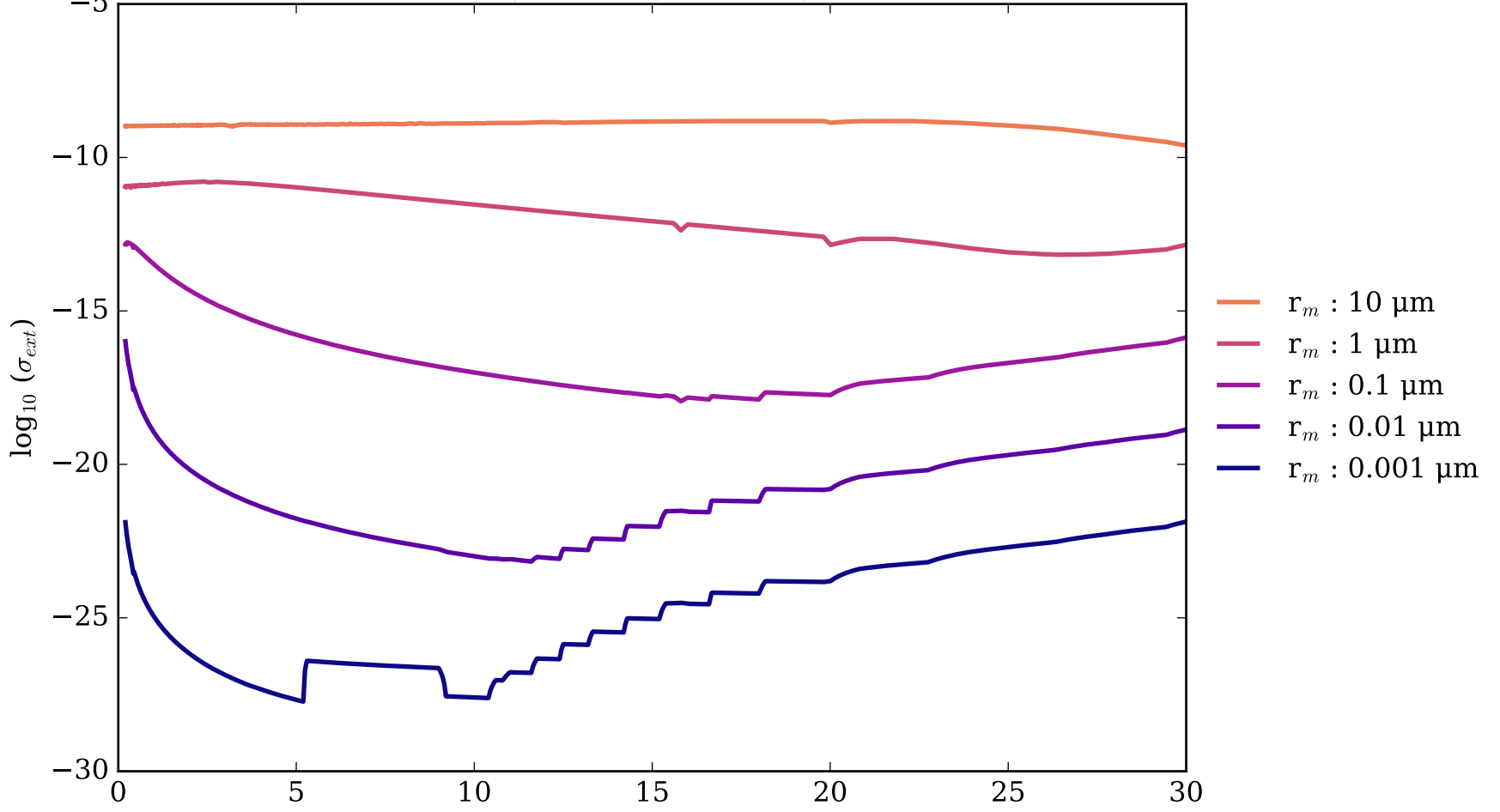
Na<sub>2</sub>S Asymmetry Parameter  $g$



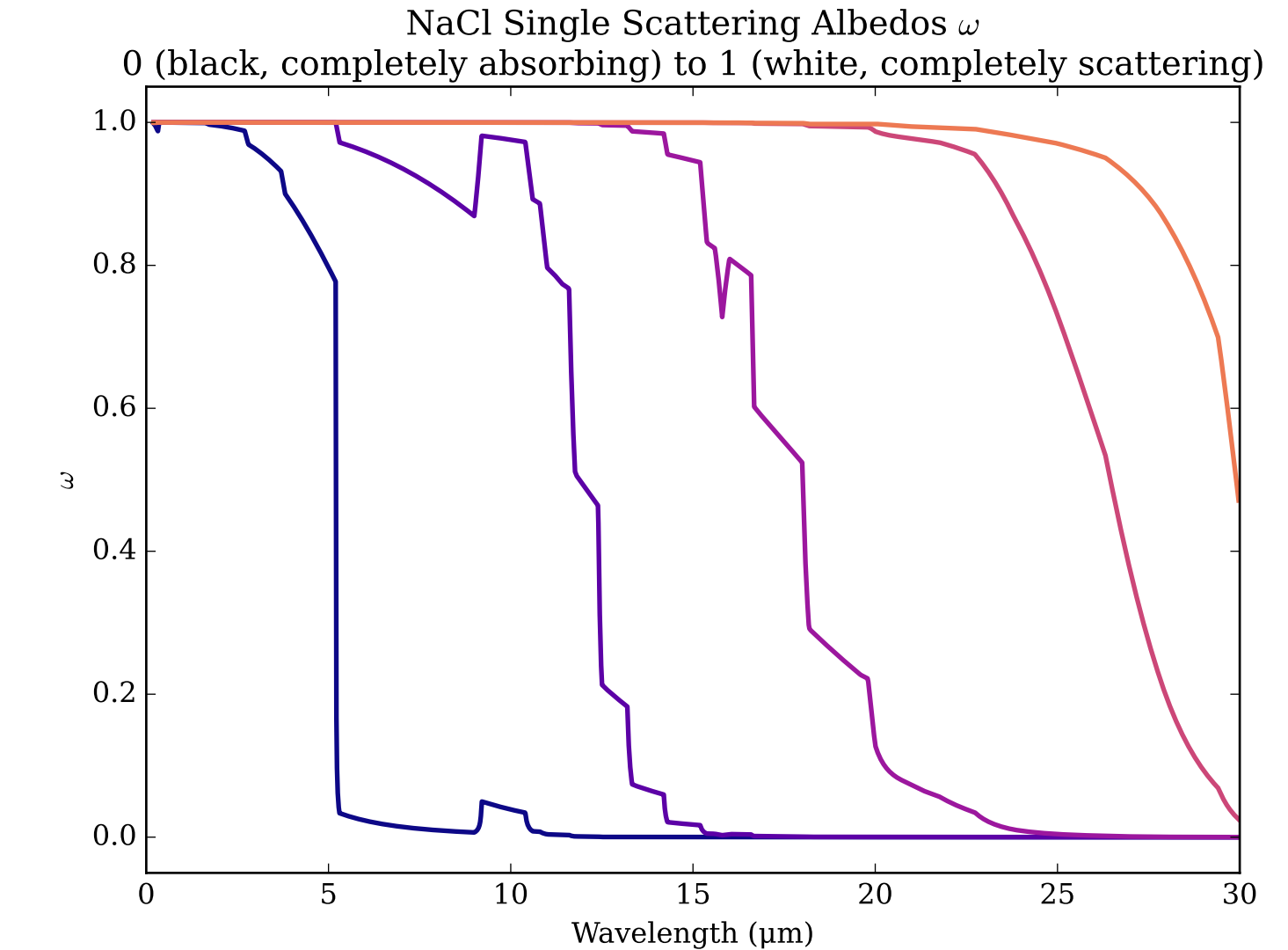
Refractive Indices for NaCl  
(0.2, 30.0)  $\mu\text{m}$



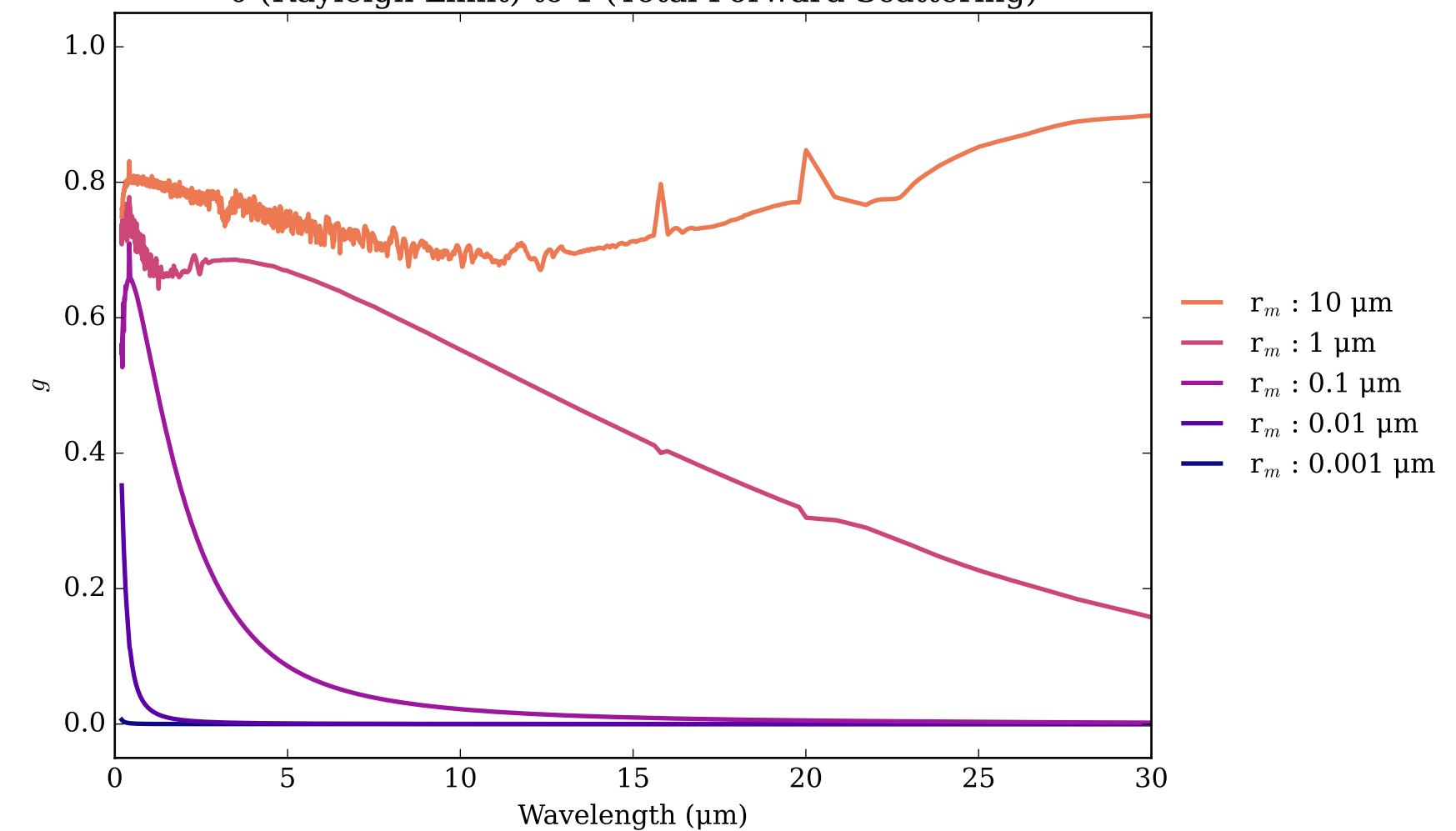
NaCl Effective Extinction Cross Section  
 $\sigma_{\text{ext, eff}} = \sigma_{\text{abs, eff}} + \sigma_{\text{scat, eff}}$



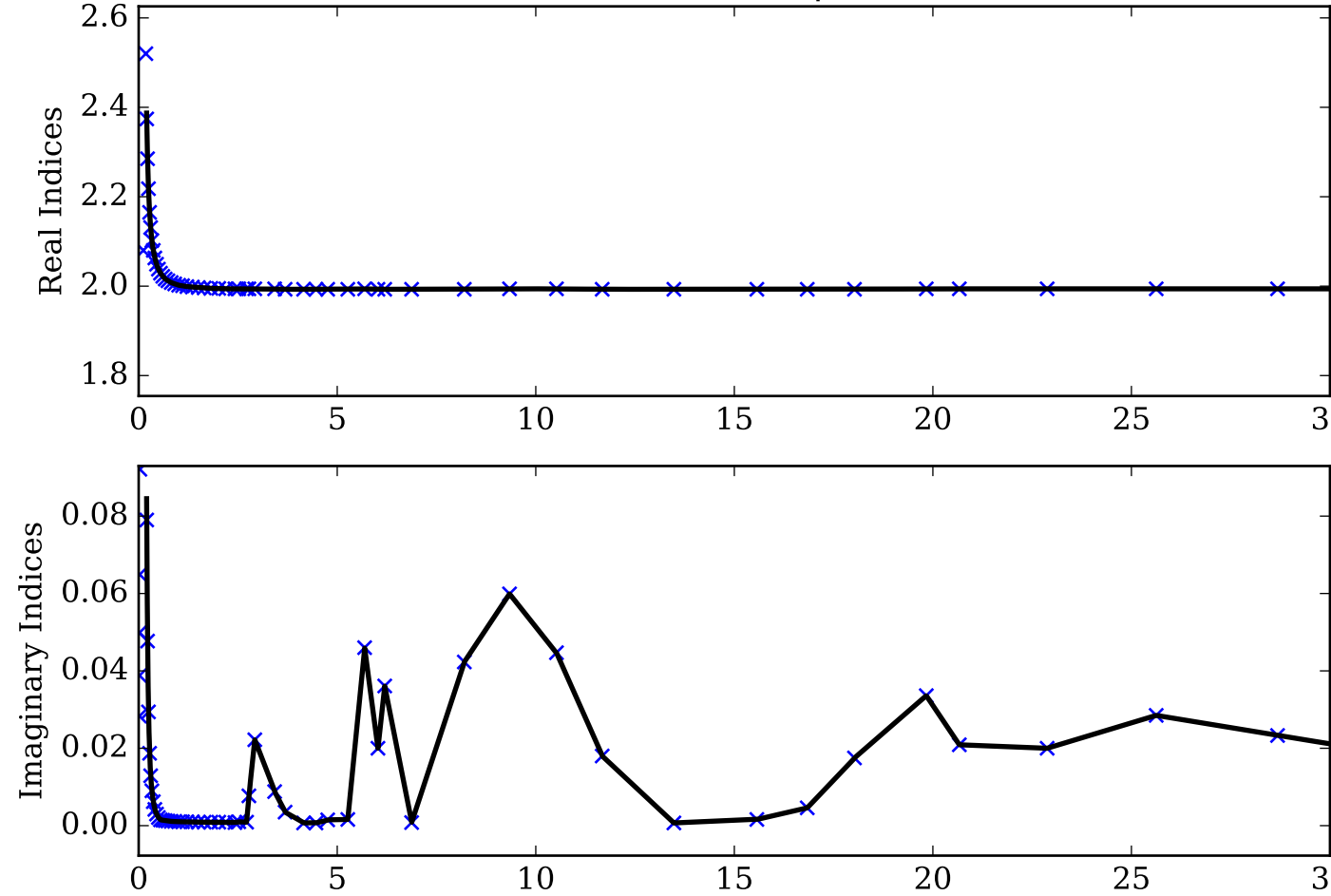
NaCl Single Scattering Albedos  $\omega$



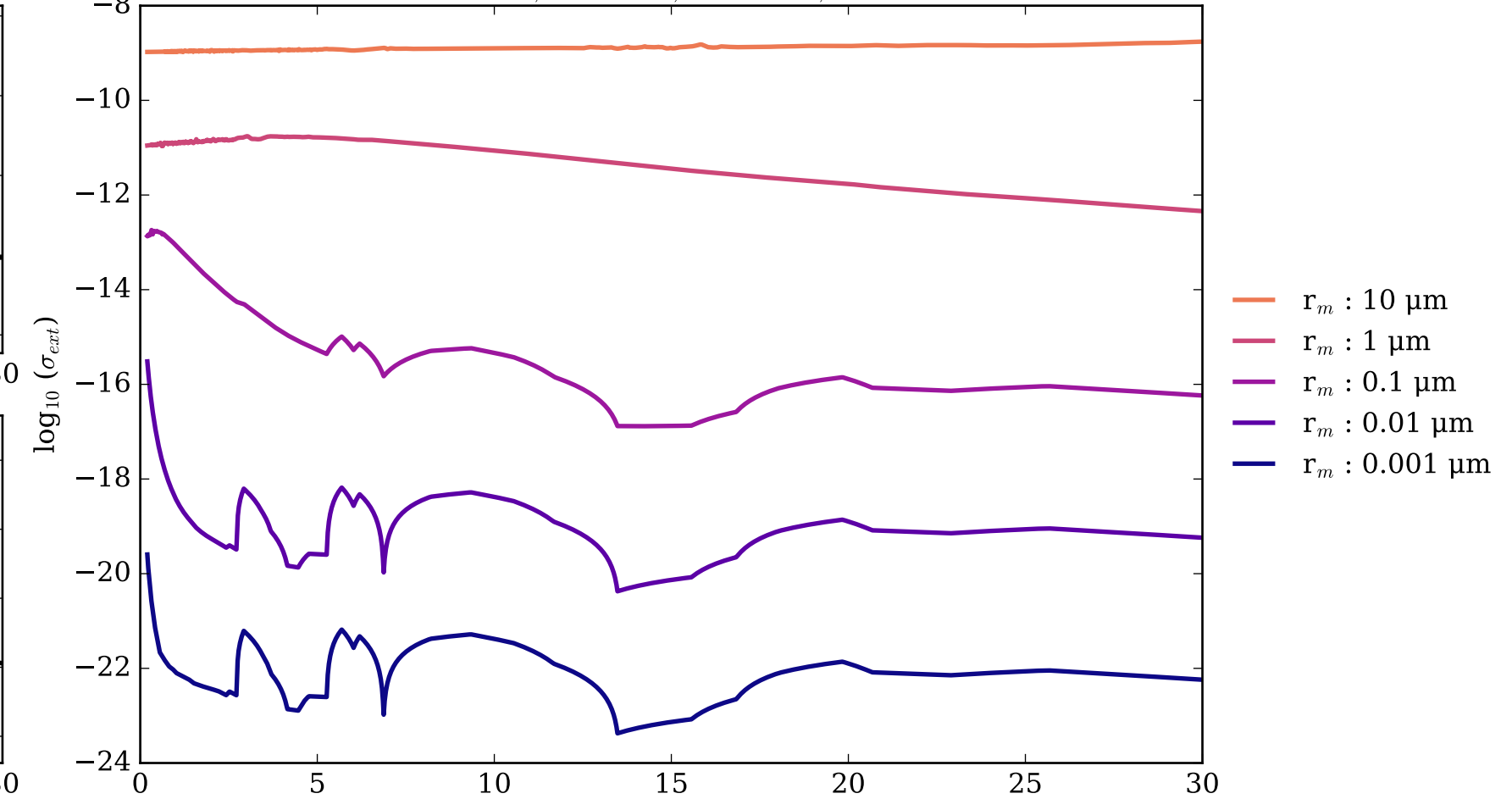
NaCl Asymmetry Parameter  $g$   
0 (Rayleigh Limit) to 1 (Total Forward Scattering)



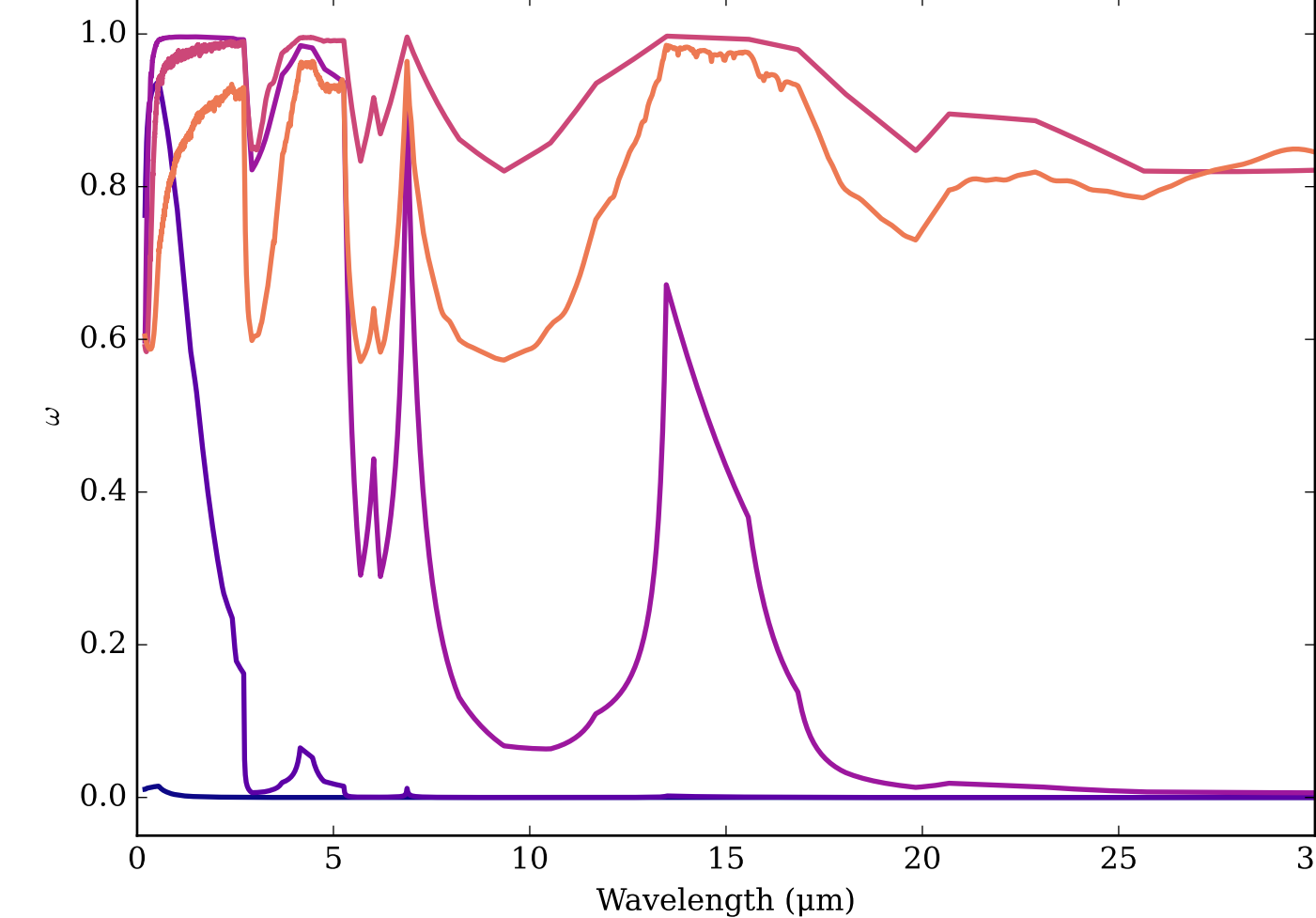
Refractive Indices for NanoDiamonds  
(0.2, 30.0)  $\mu\text{m}$



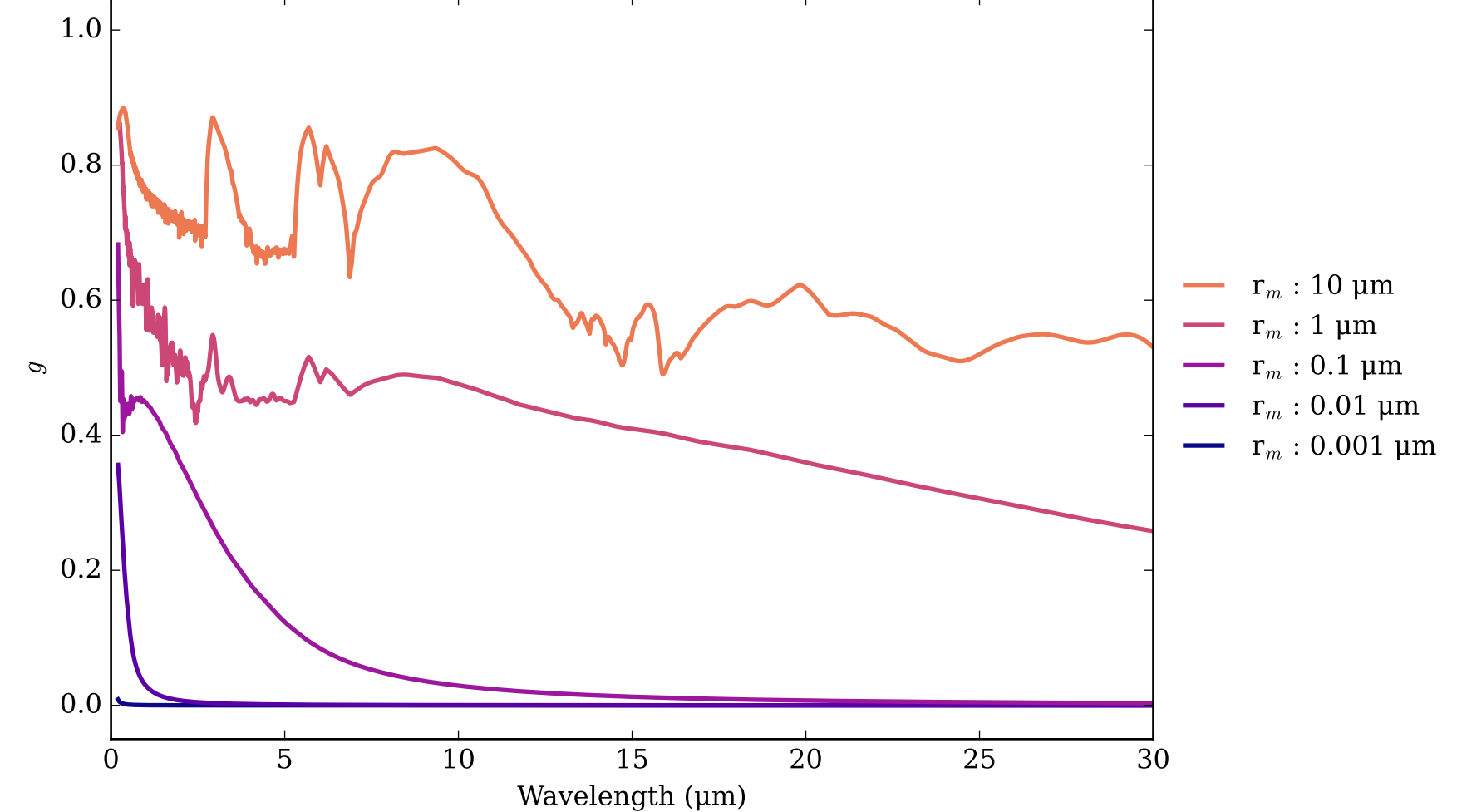
NanoDiamonds Effective Extinction Cross Section



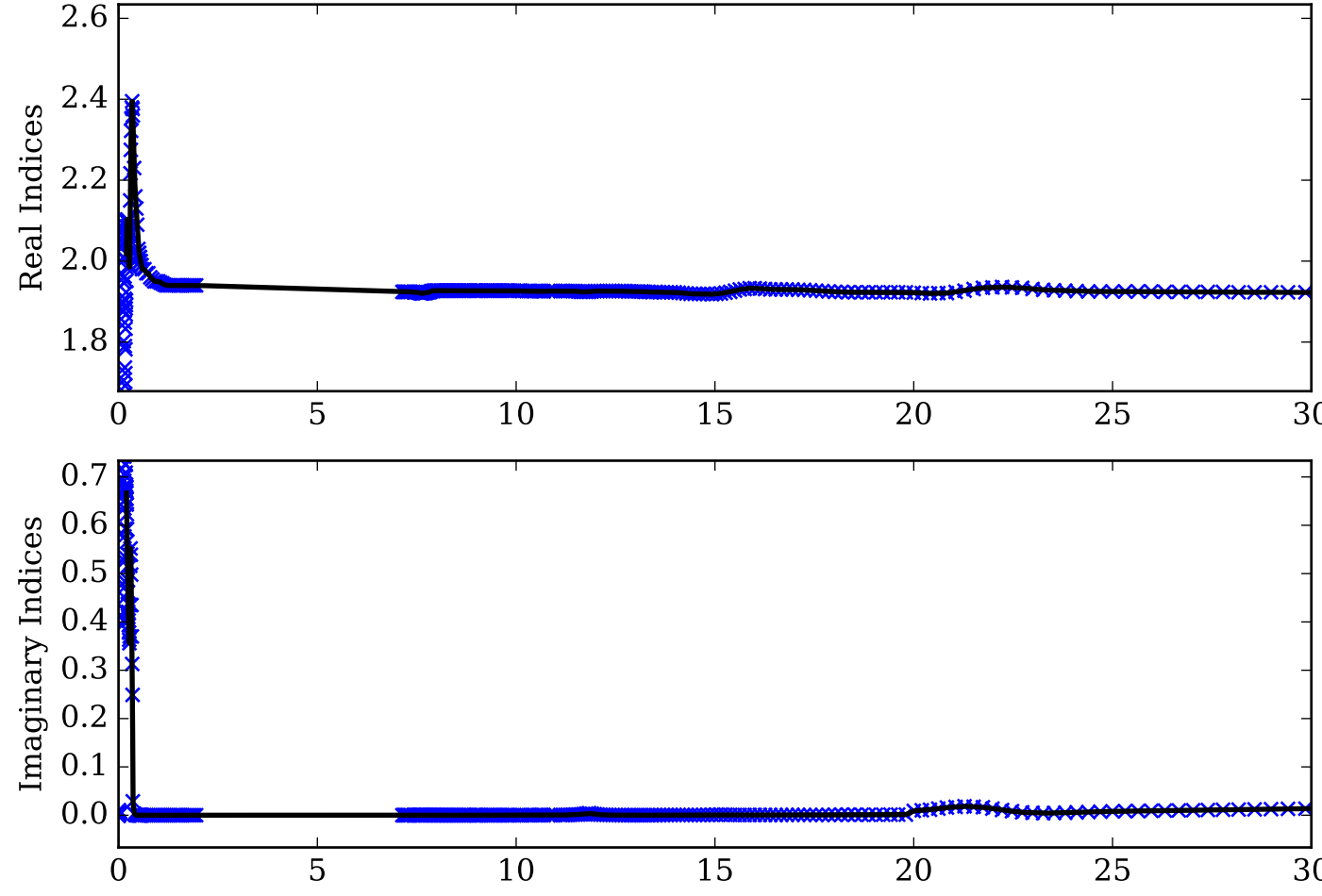
NanoDiamonds Single Scattering Albedos  $\omega$   
0 (black, completely absorbing) to 1 (white, completely scattering)



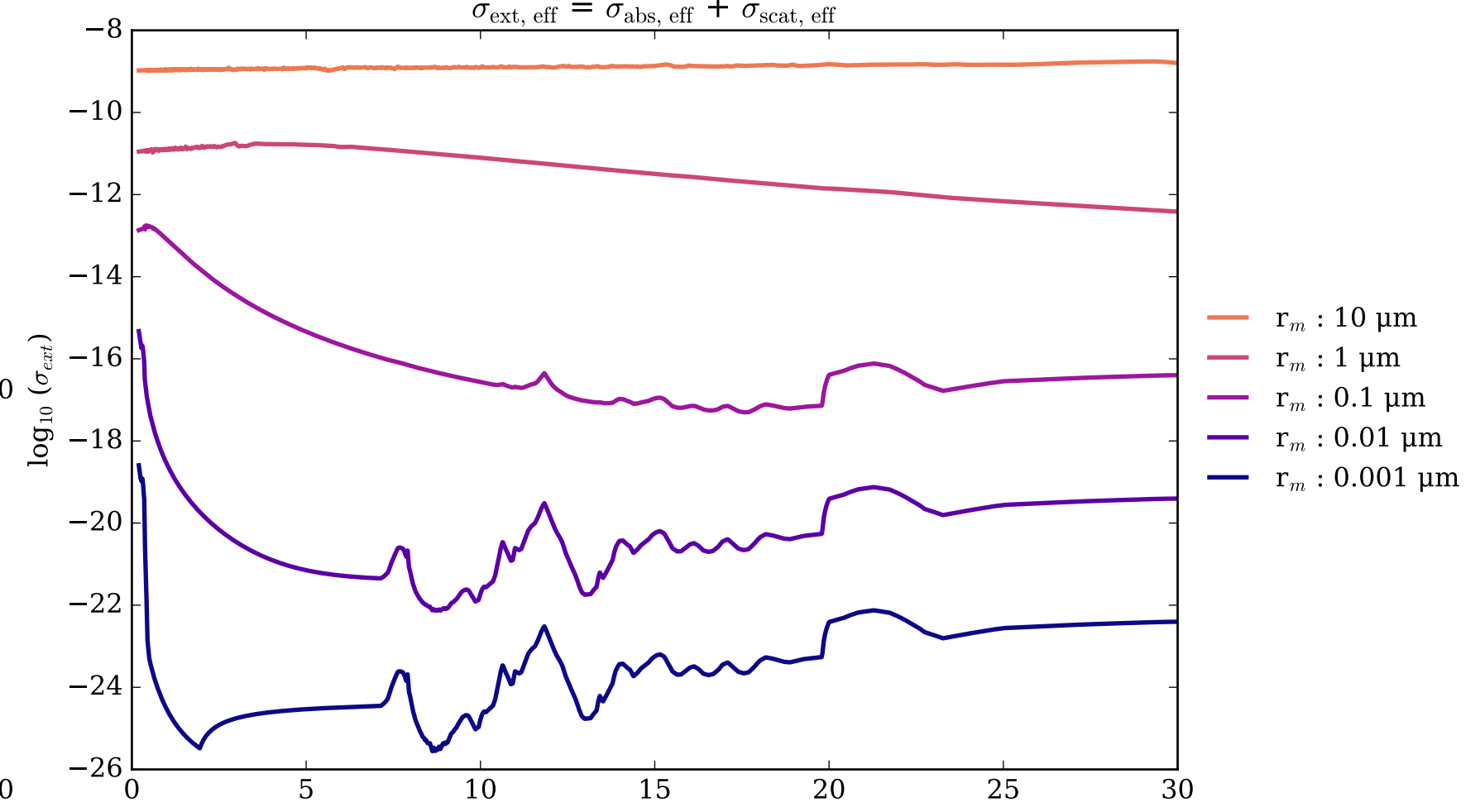
NanoDiamonds Asymmetry Parameter  $g$   
0 (Rayleigh Limit) to 1 (Total Forward Scattering)



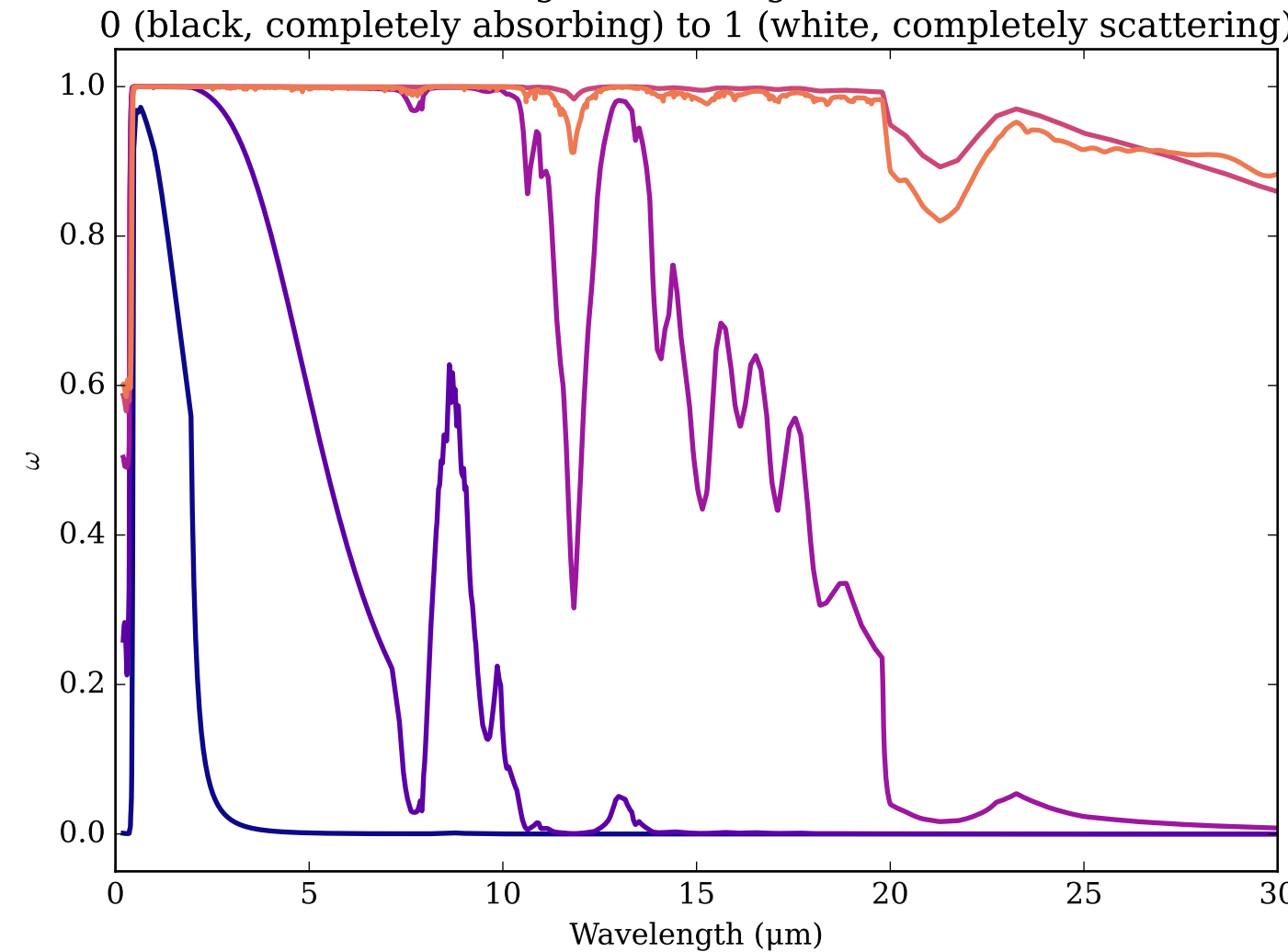
Refractive Indices for S8  
 $(0.2, 30.0) \mu\text{m}$



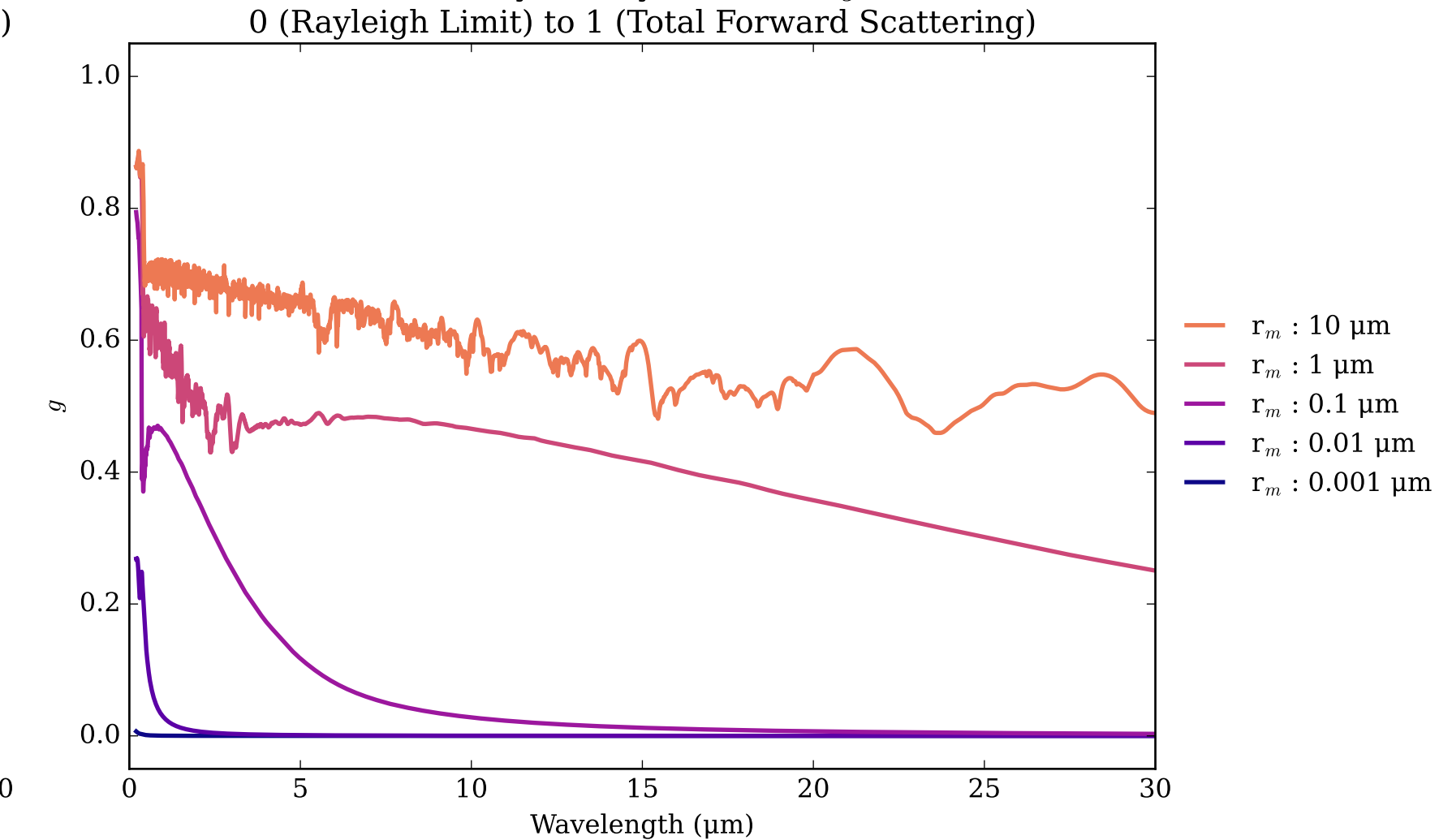
S8 Effective Extinction Cross Section



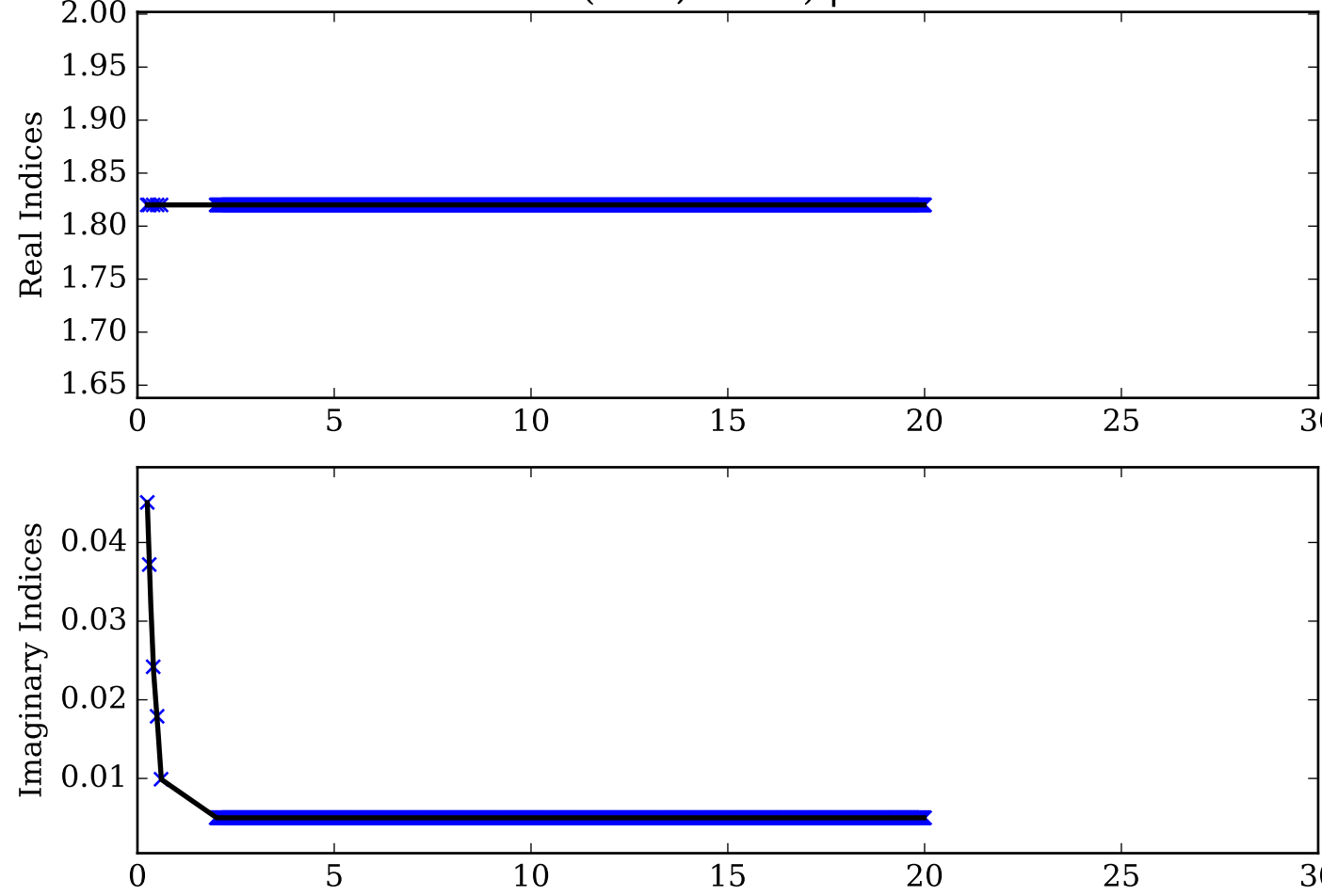
S8 Single Scattering Albedos  $\omega$



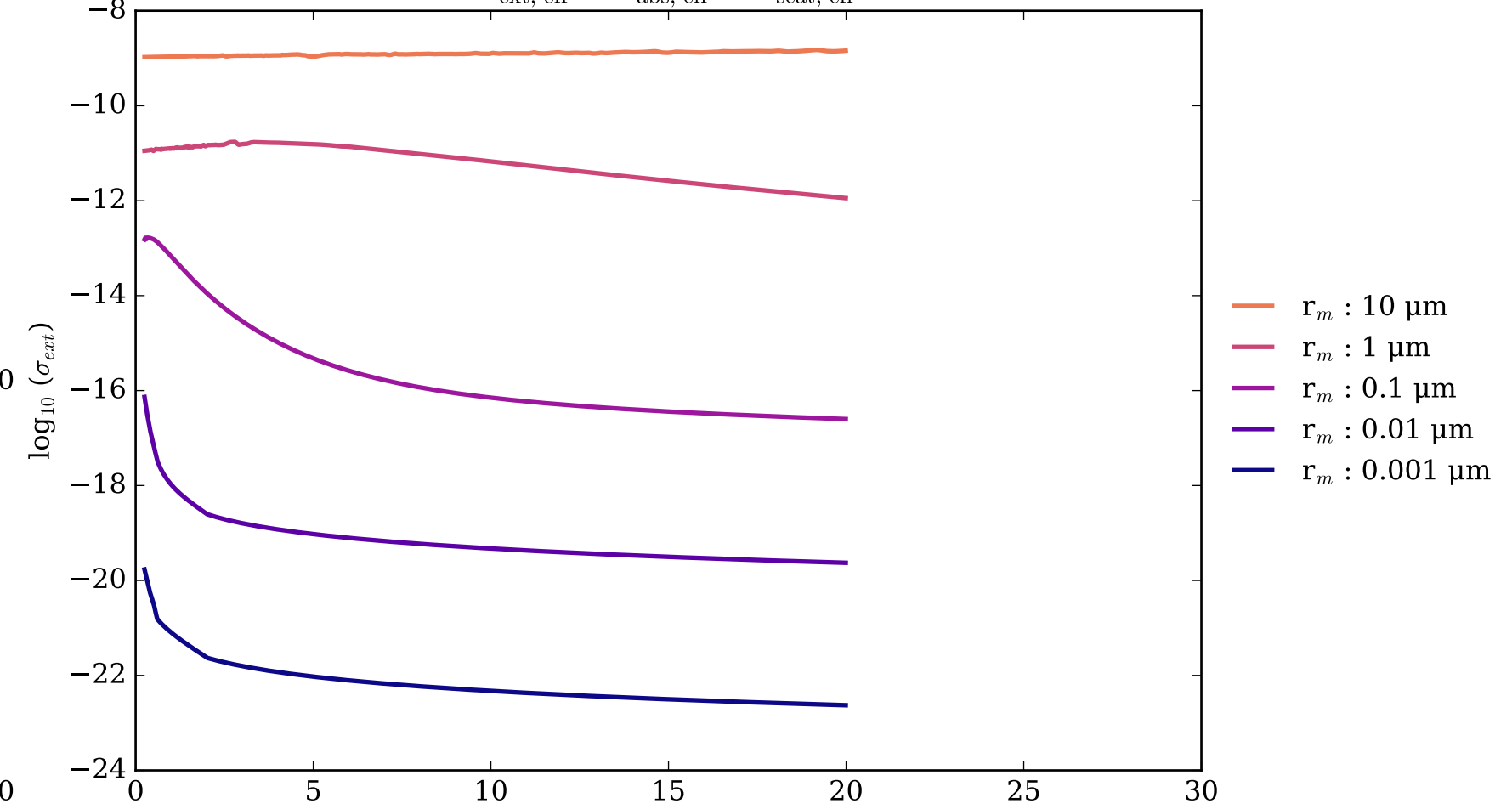
S8 Asymmetry Parameter  $g$



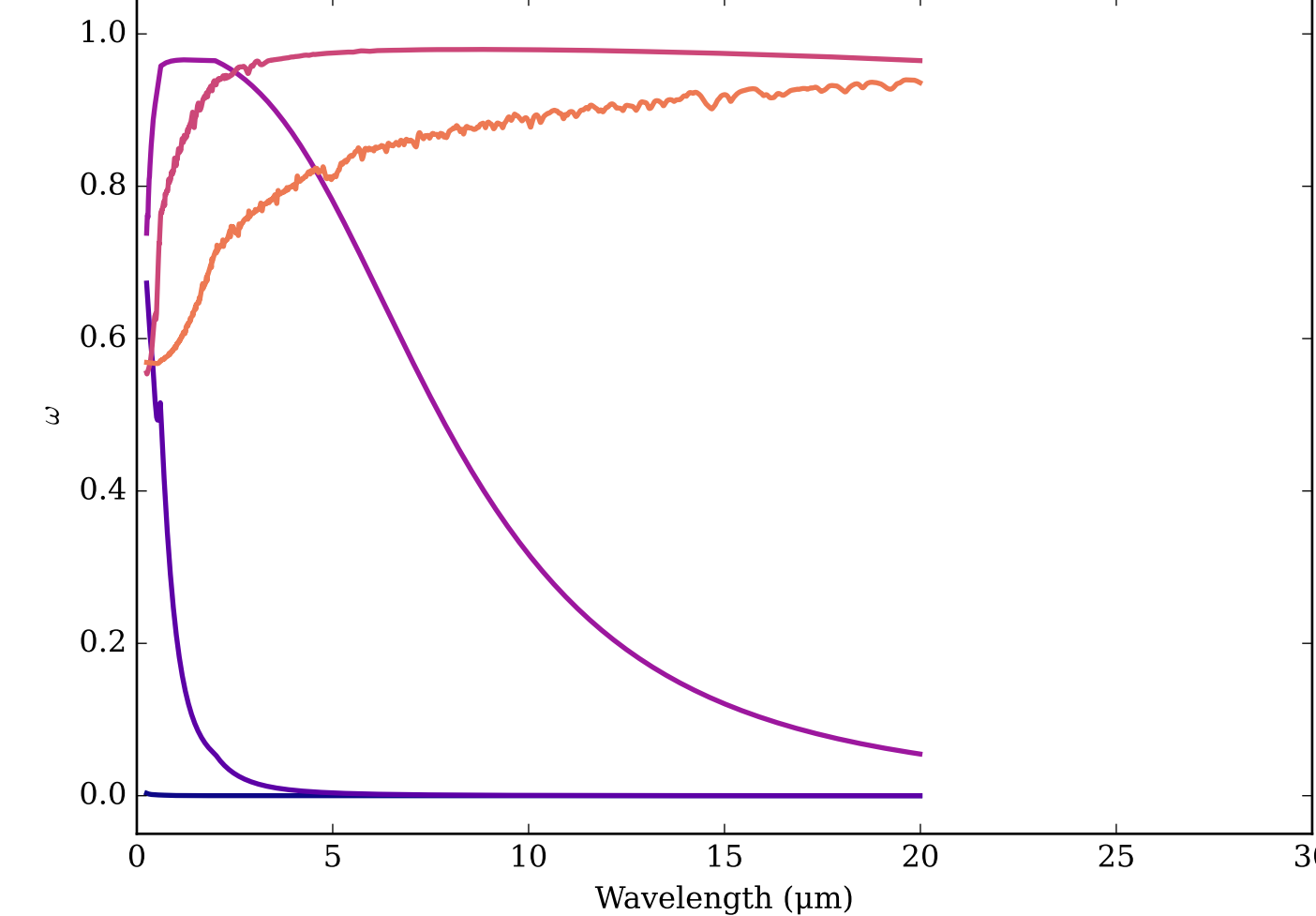
Refractive Indices for Saturn-Phosphorus-Haze  
(0.25, 19.99)  $\mu\text{m}$



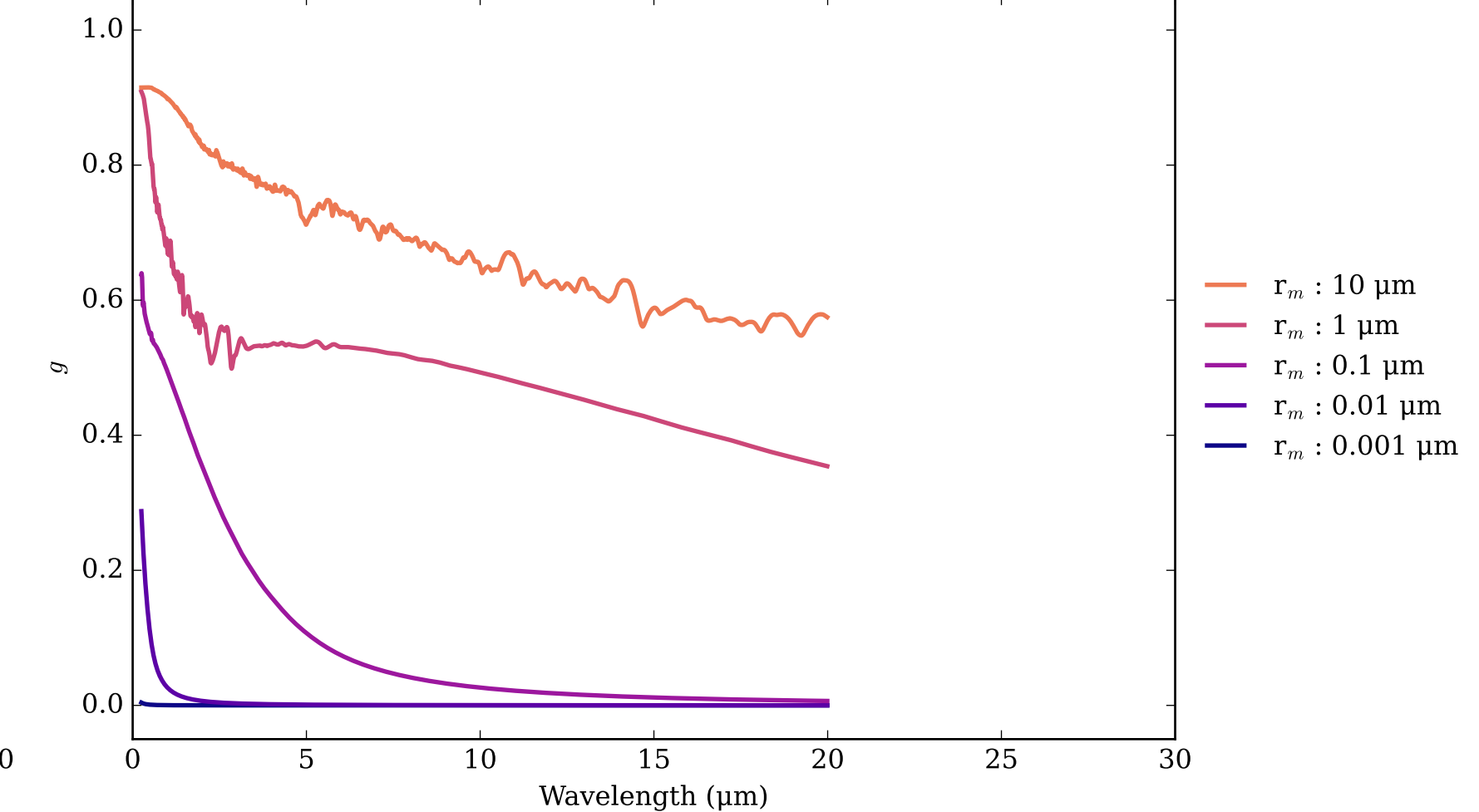
Saturn-Phosphorus-Haze Effective Extinction Cross Section



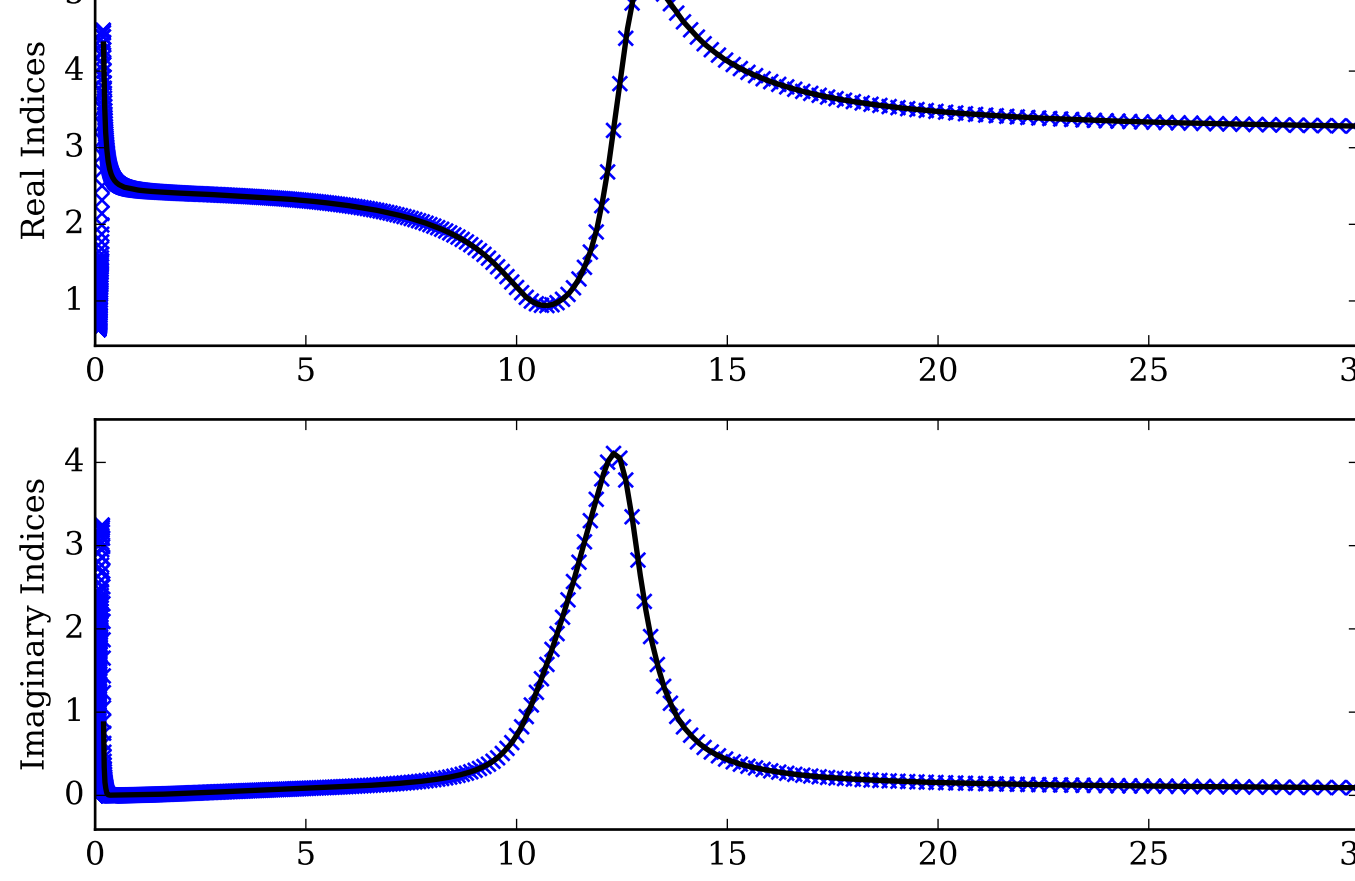
Saturn-Phosphorus-Haze Single Scattering Albedos  $\omega$   
0 (black, completely absorbing) to 1 (white, completely scattering)



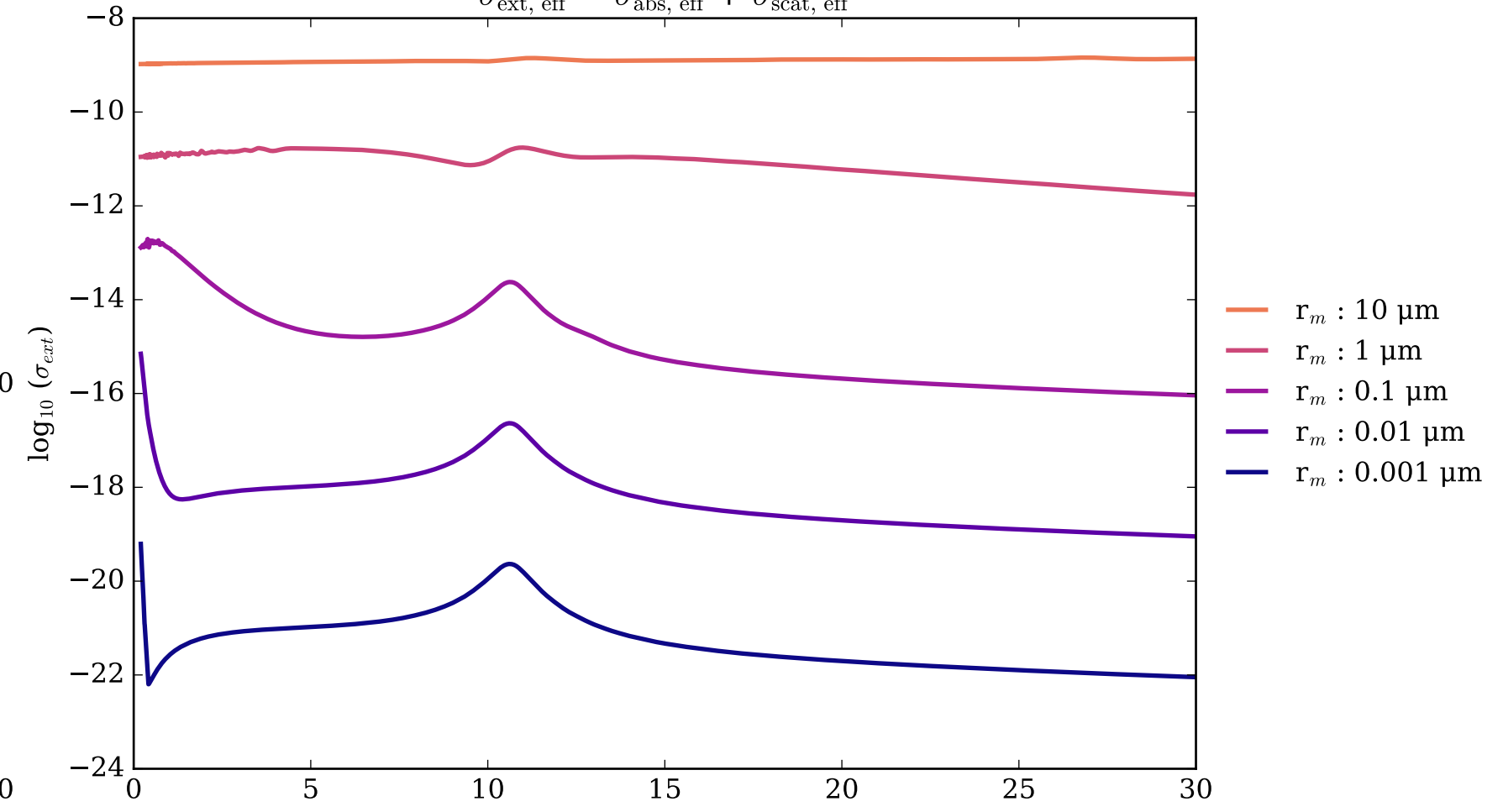
Saturn-Phosphorus-Haze Asymmetry Parameter  $g$   
0 (Rayleigh Limit) to 1 (Total Forward Scattering)



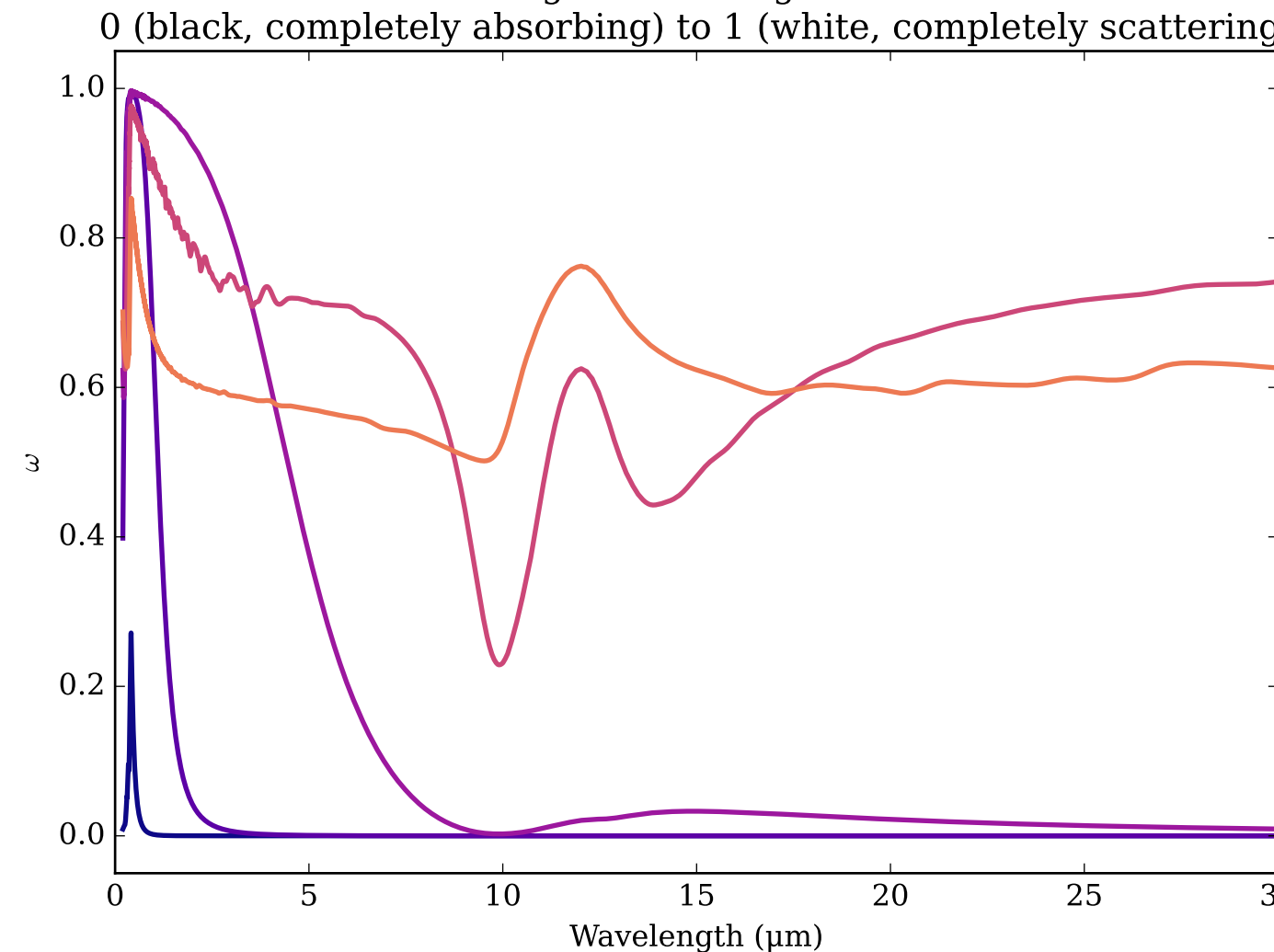
Refractive Indices for SiC  
(0.2, 30.0)  $\mu\text{m}$



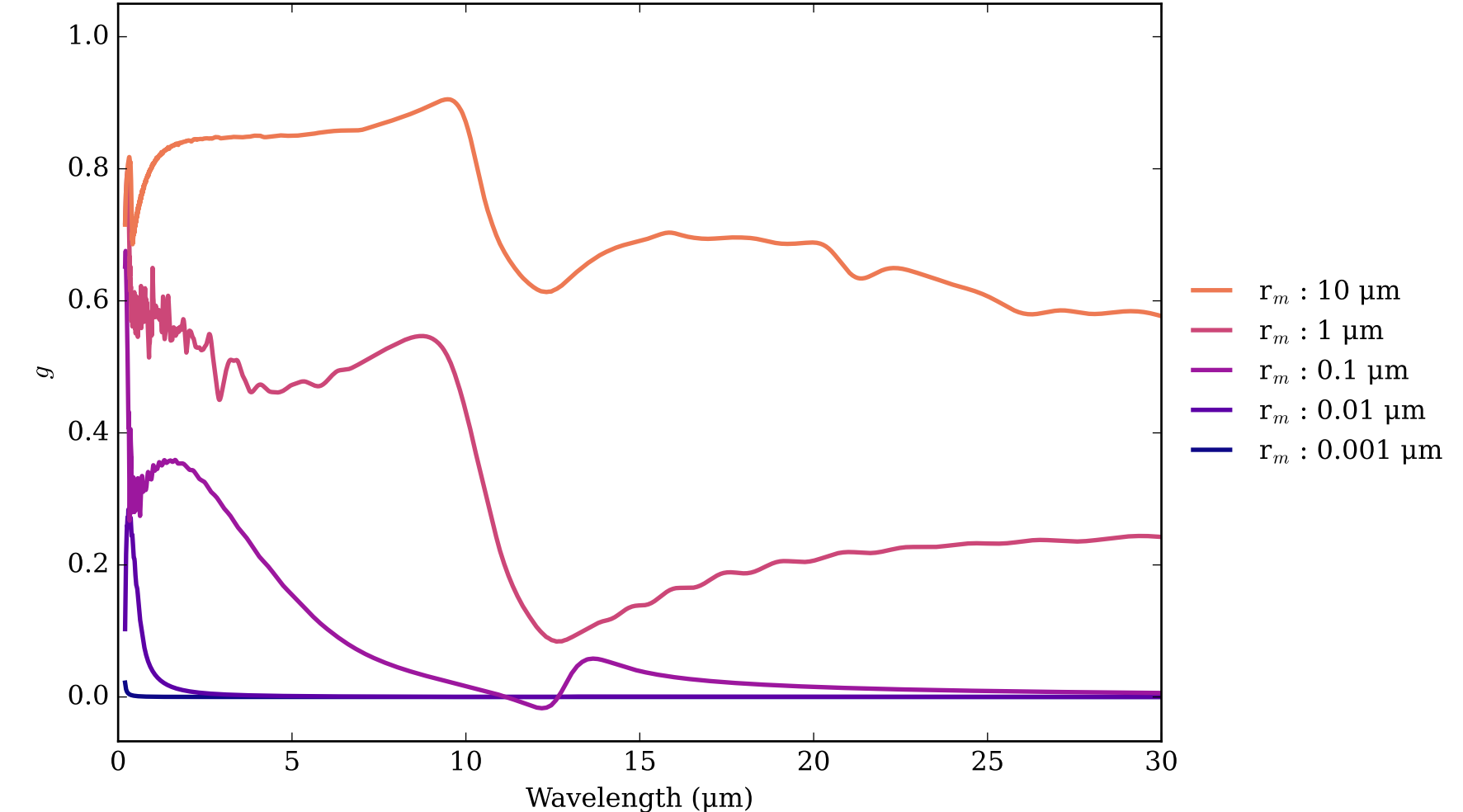
SiC Effective Extinction Cross Section  
 $\sigma_{\text{ext, eff}} = \sigma_{\text{abs, eff}} + \sigma_{\text{scat, eff}}$



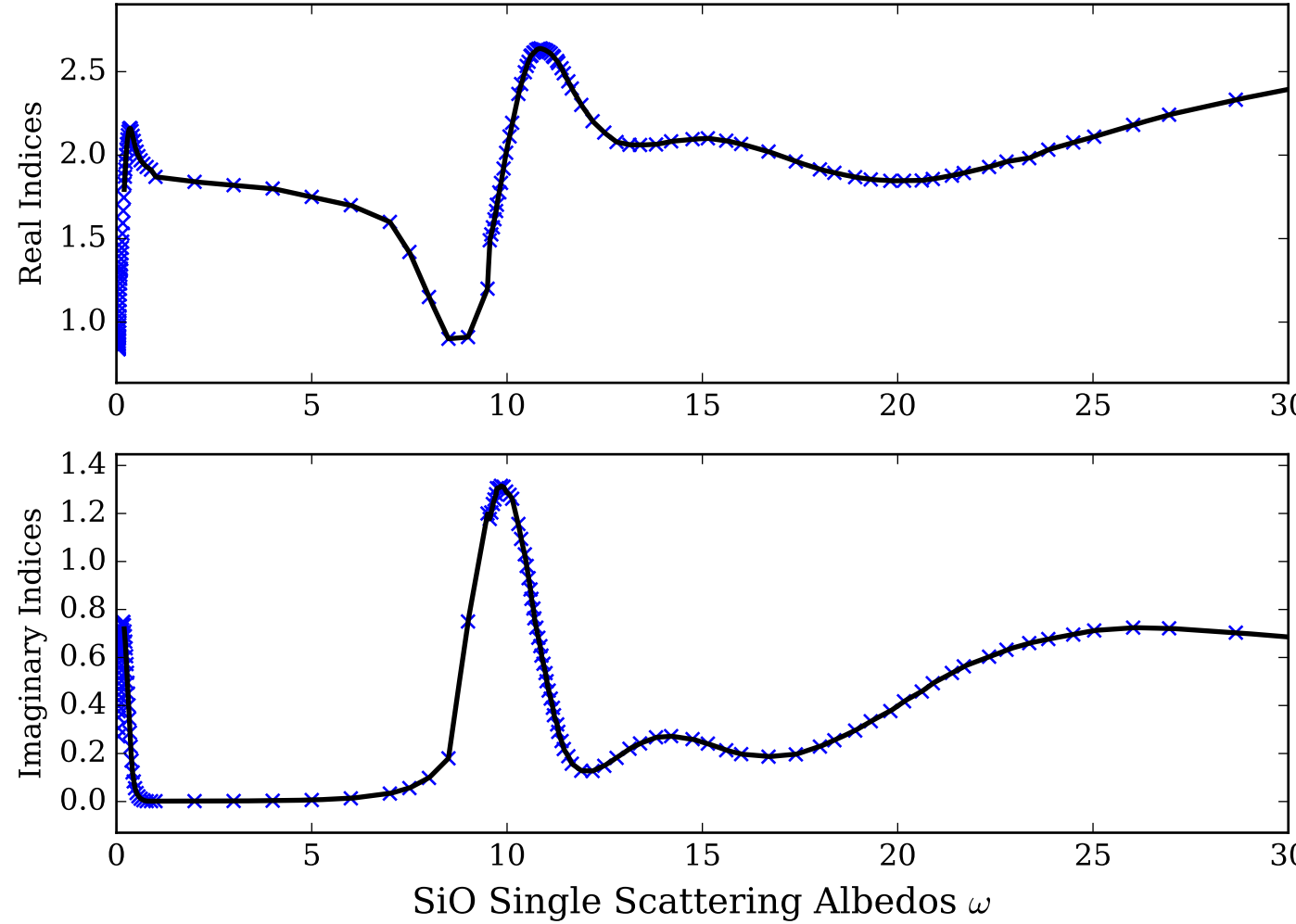
SiC Single Scattering Albedos  $\omega$



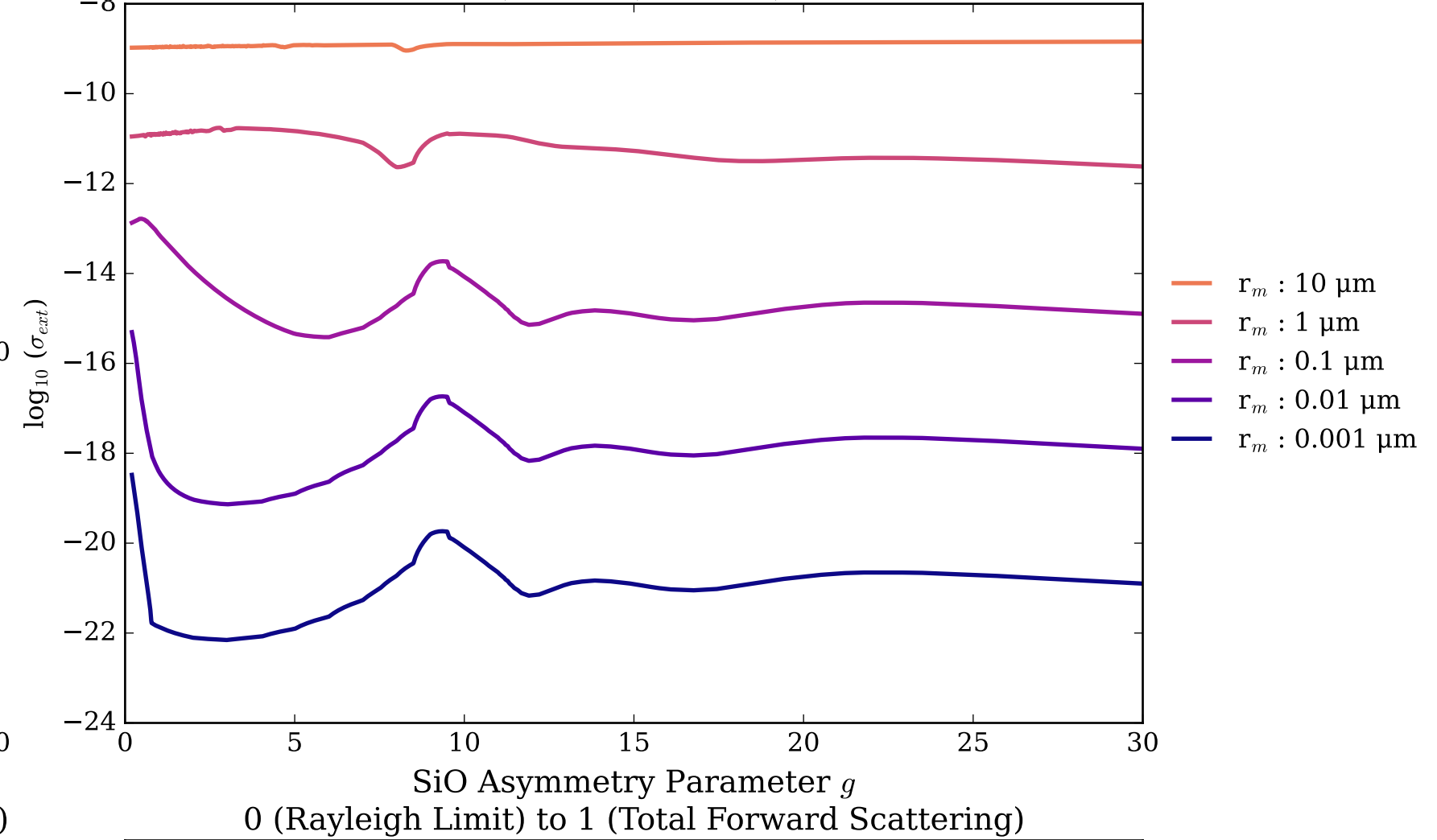
SiC Asymmetry Parameter  $g$   
0 (Rayleigh Limit) to 1 (Total Forward Scattering)



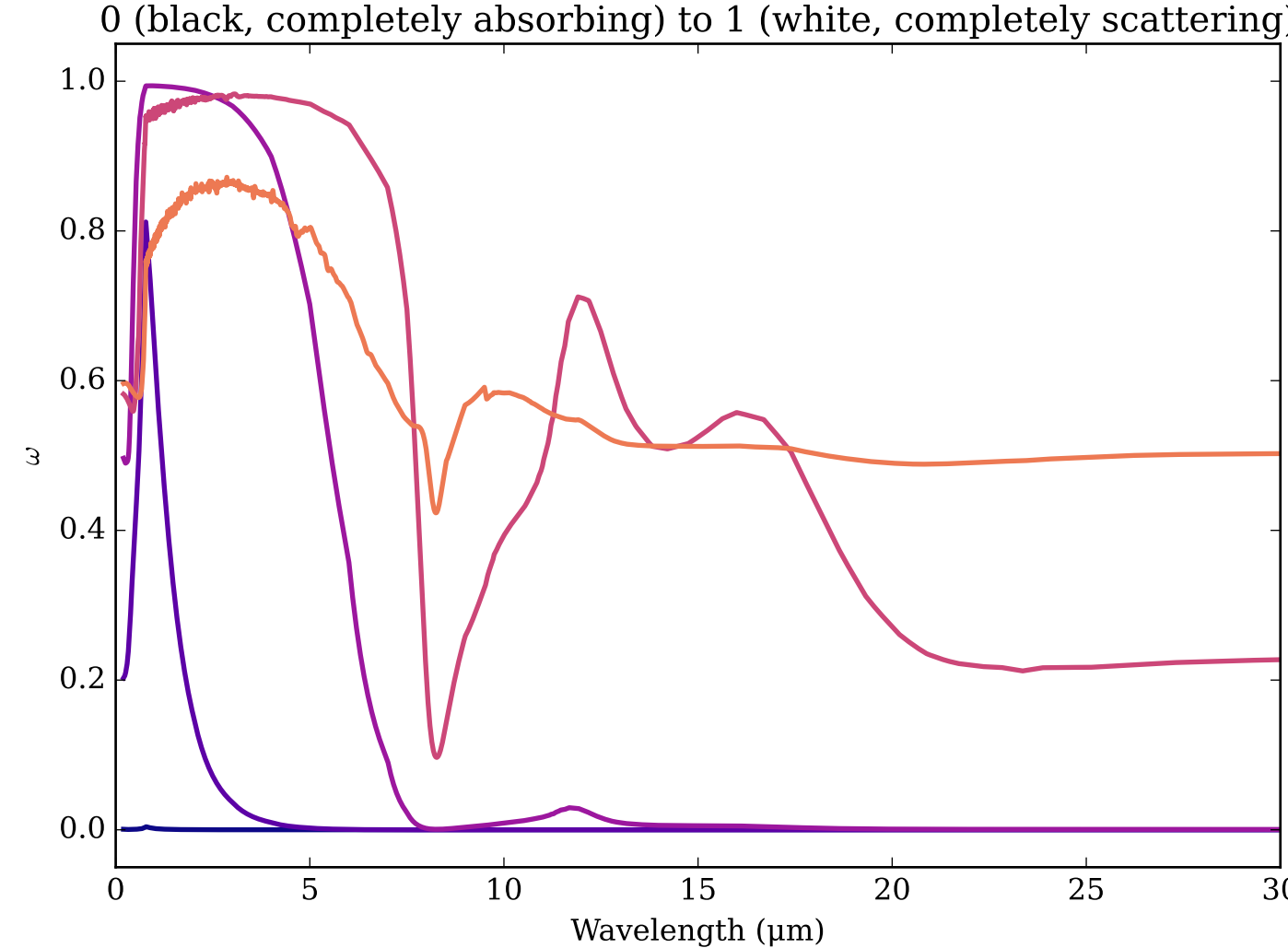
Refractive Indices for SiO  
(0.2, 30.0)  $\mu\text{m}$



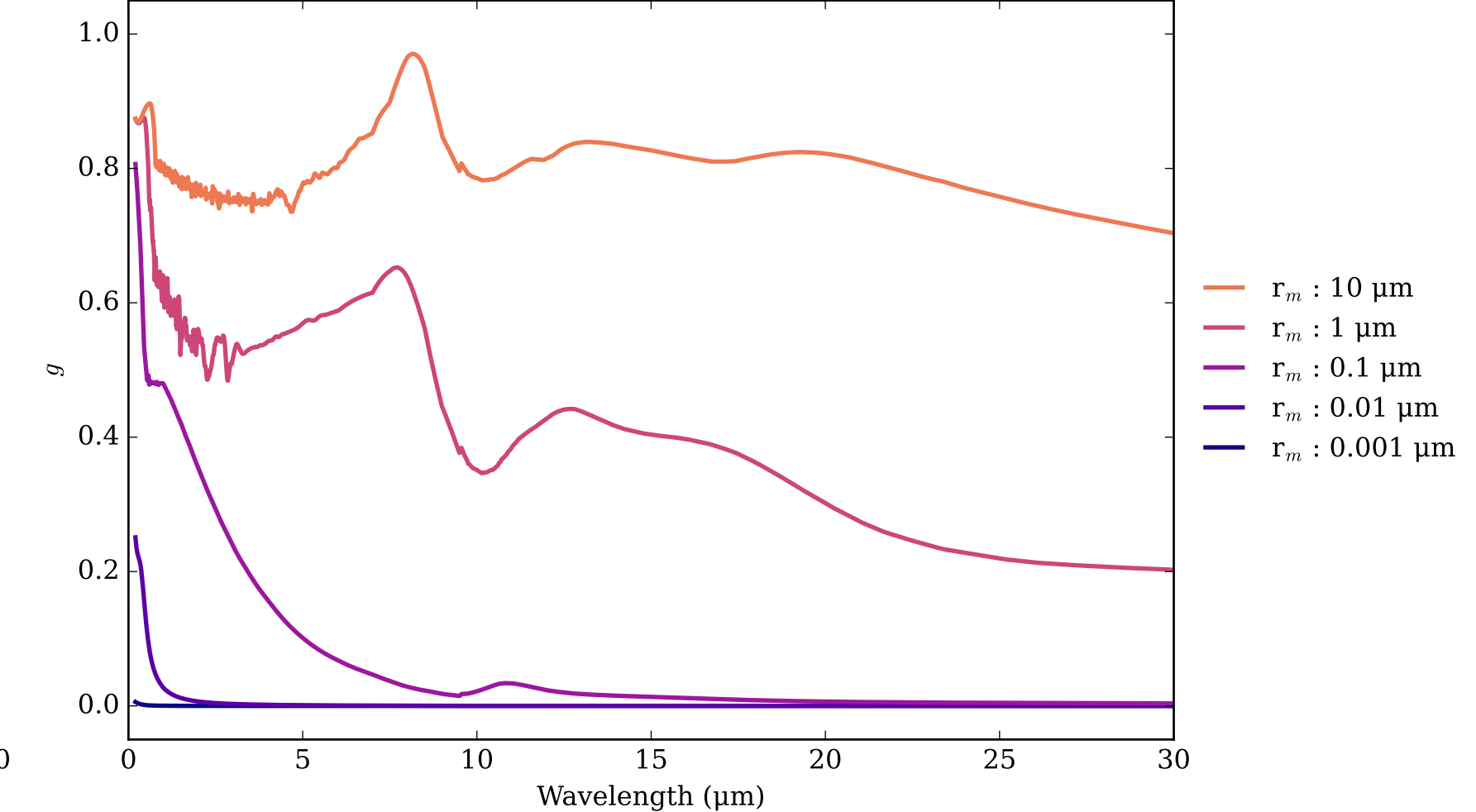
SiO Effective Extinction Cross Section  
 $\sigma_{\text{ext, eff}} = \sigma_{\text{abs, eff}} + \sigma_{\text{scat, eff}}$



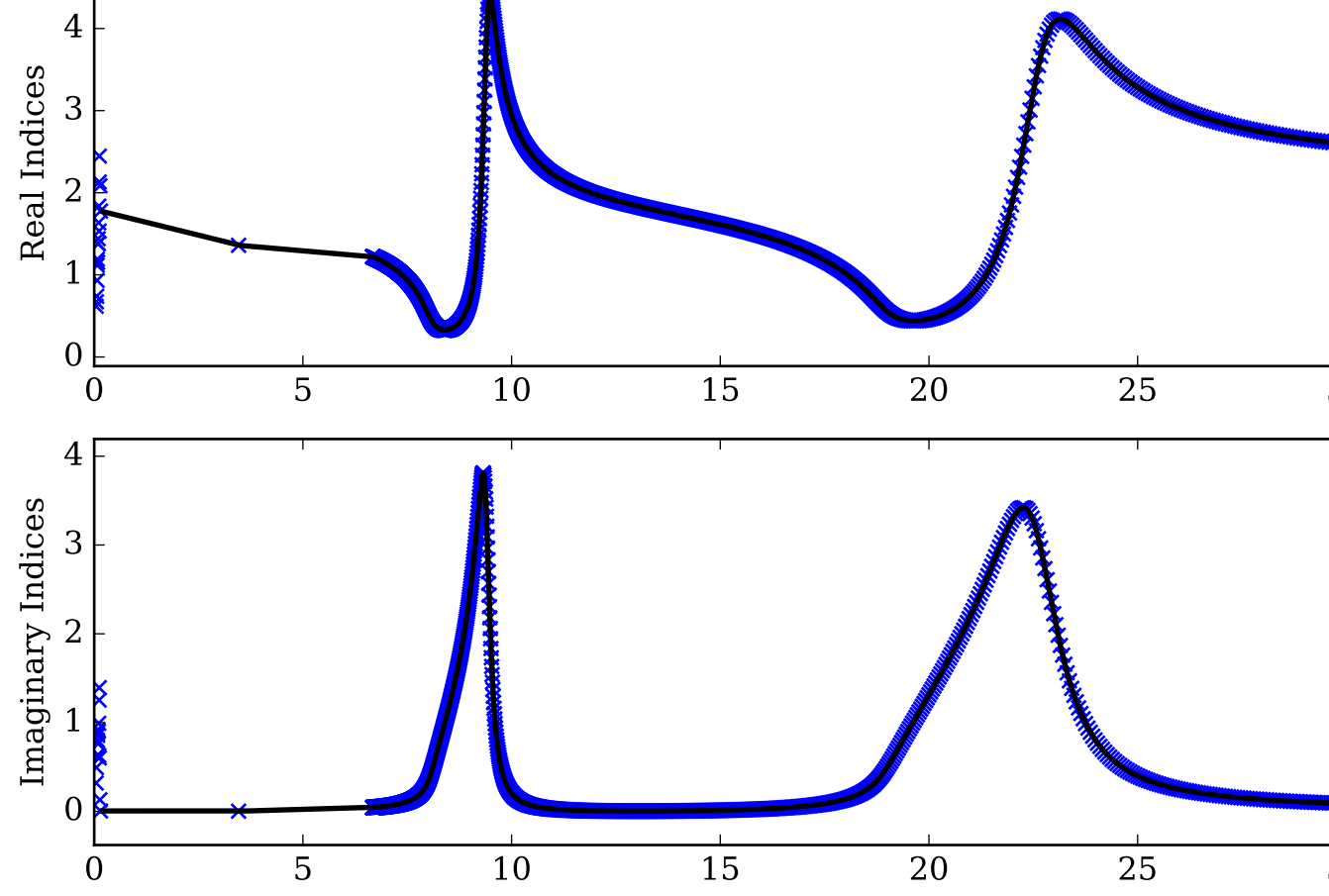
SiO Single Scattering Albedos  $\omega$



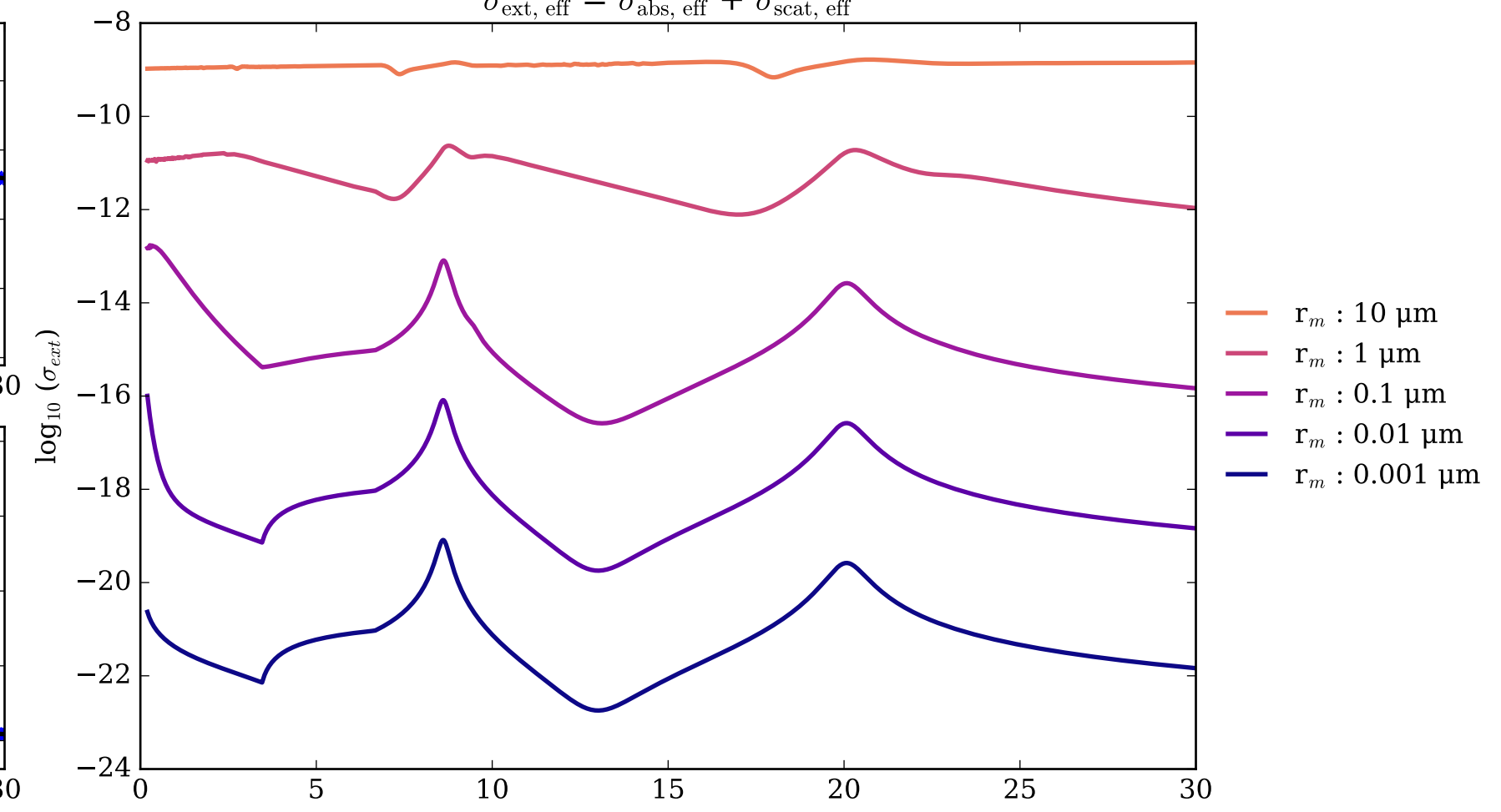
SiO Asymmetry Parameter  $g$   
0 (Rayleigh Limit) to 1 (Total Forward Scattering)



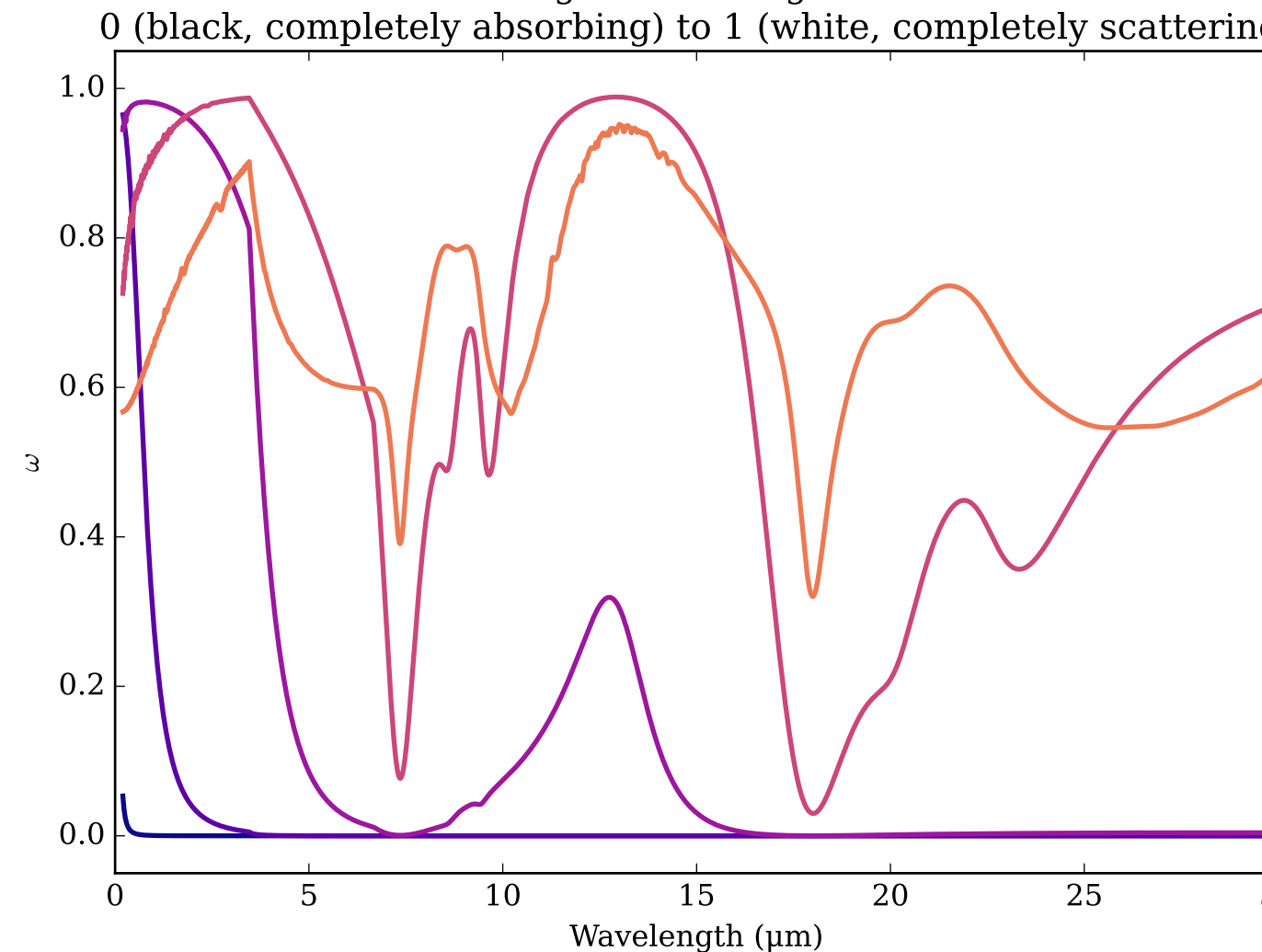
Refractive Indices for SiO<sub>2</sub>  
(0.2, 30.0) μm



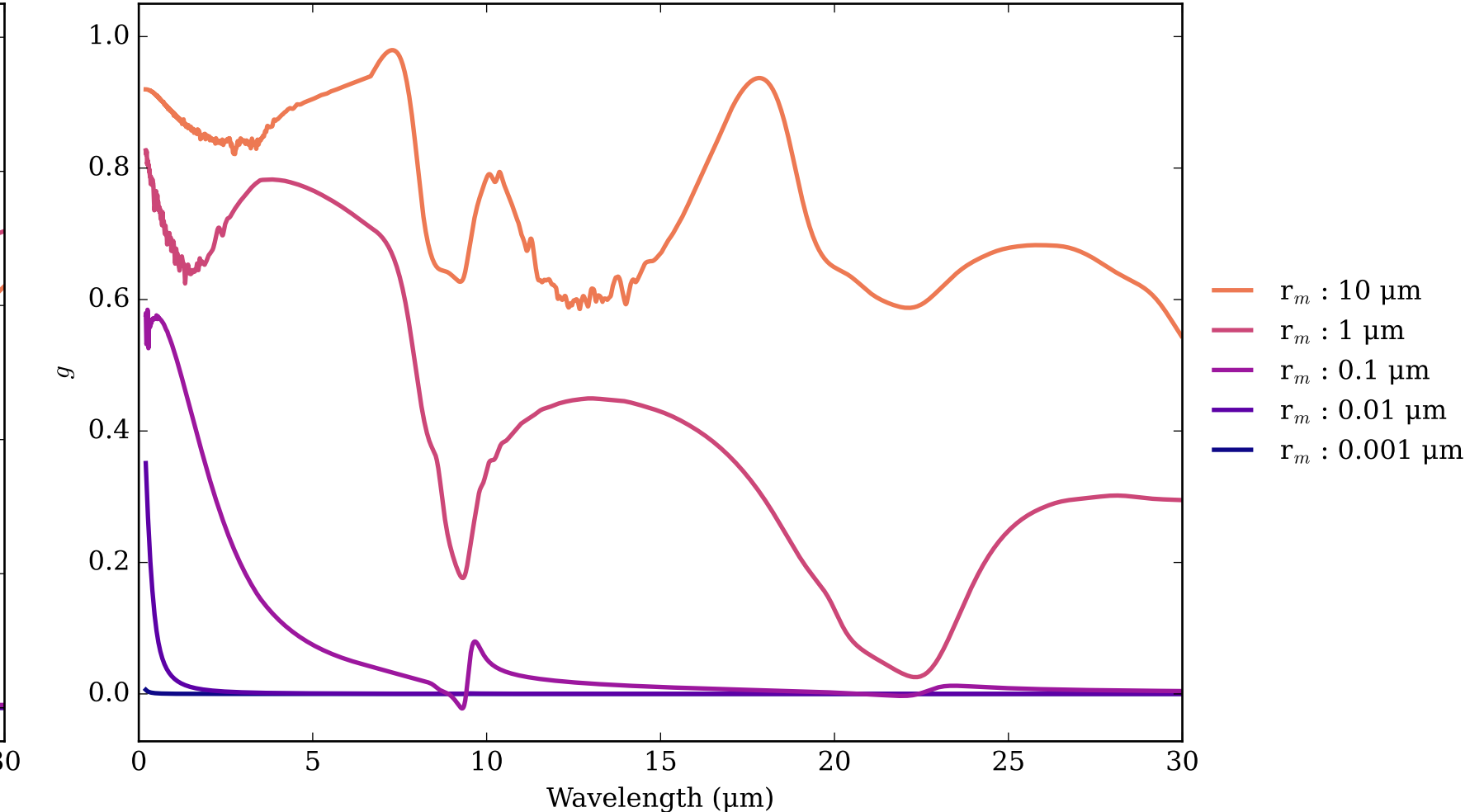
SiO<sub>2</sub> Effective Extinction Cross Section  
 $\sigma_{\text{ext, eff}} = \sigma_{\text{abs, eff}} + \sigma_{\text{scat, eff}}$



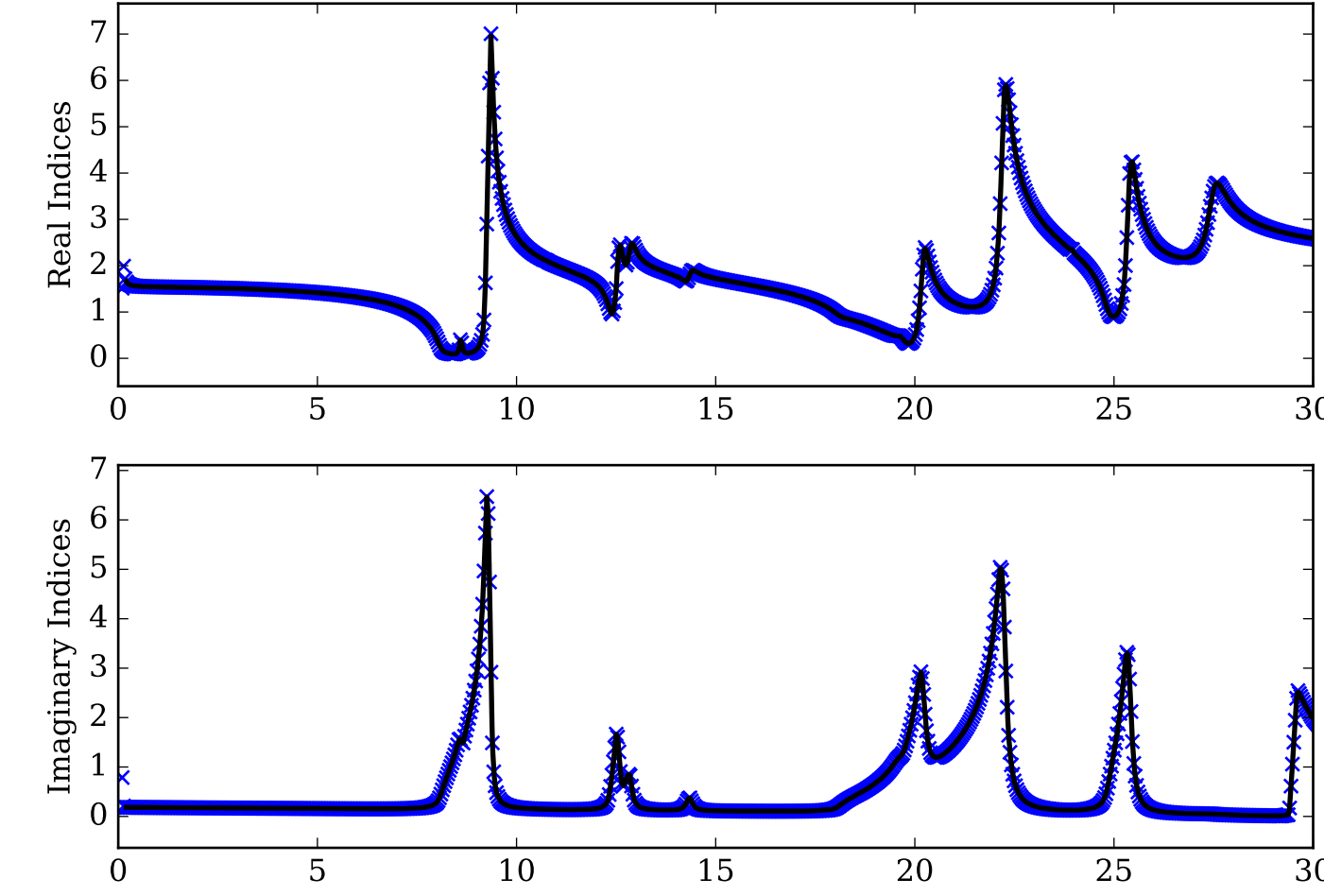
SiO<sub>2</sub> Single Scattering Albedos  $\omega$



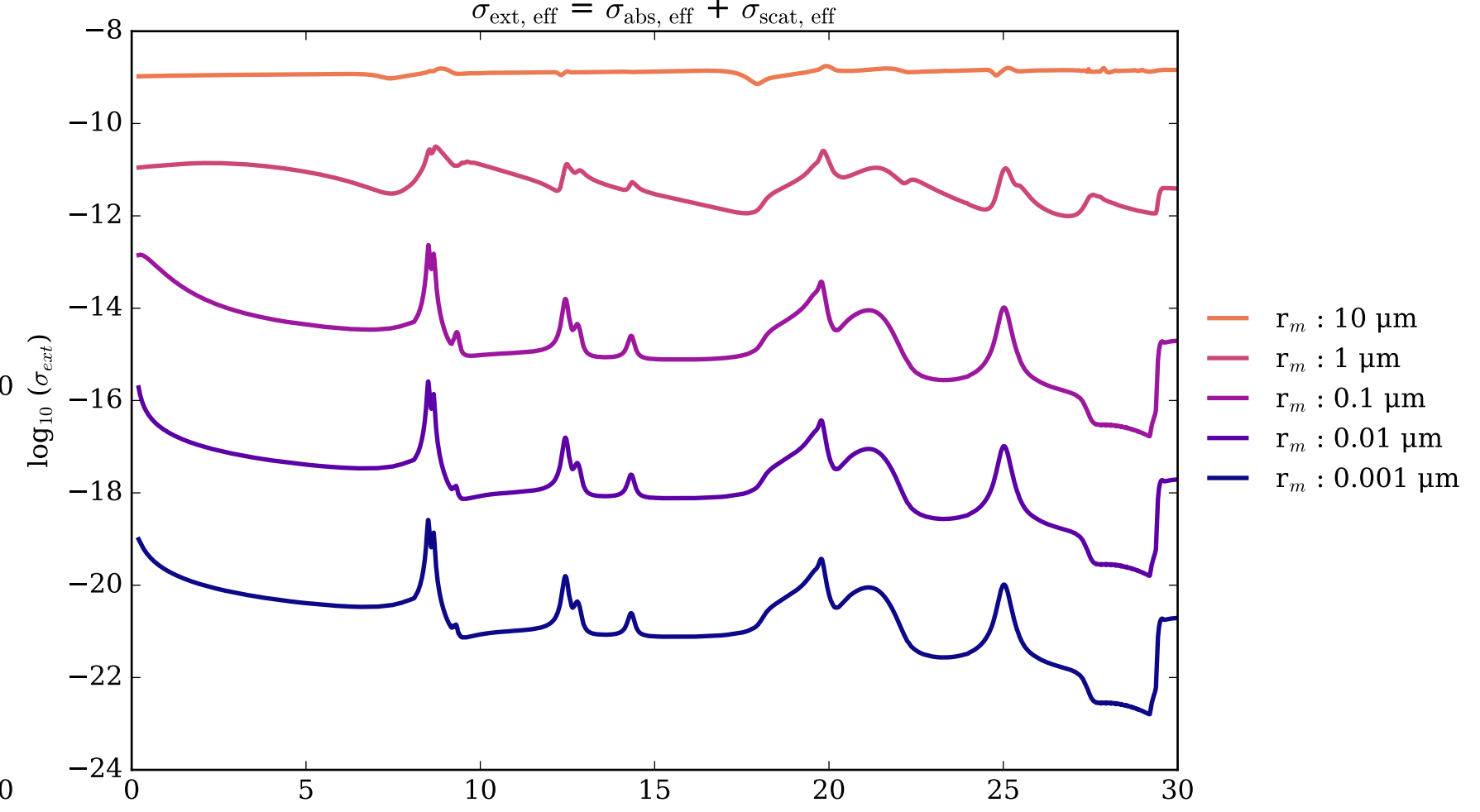
SiO<sub>2</sub> Asymmetry Parameter  $g$   
0 (Rayleigh Limit) to 1 (Total Forward Scattering)



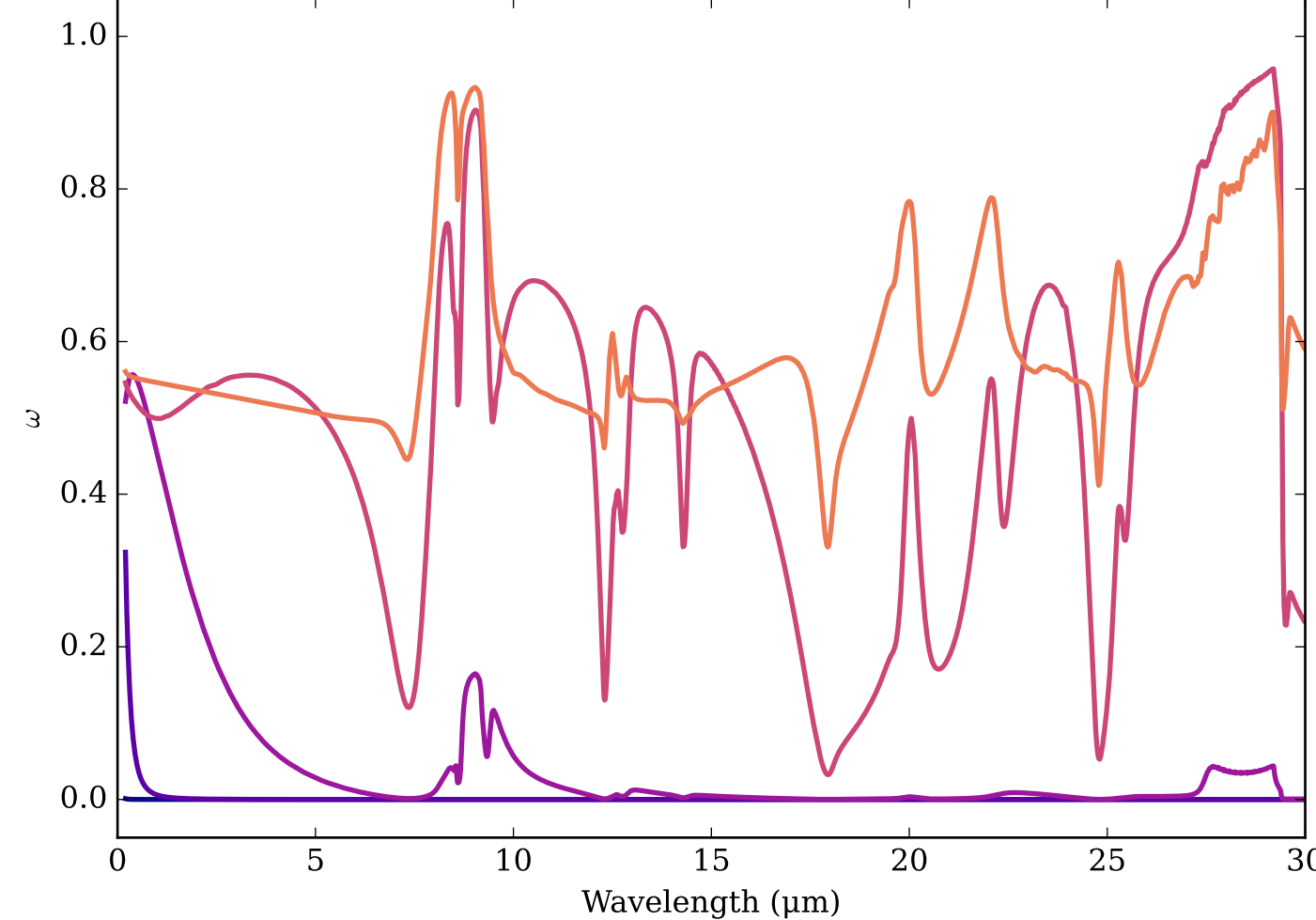
Refractive Indices for SiO<sub>2</sub>  
(0.2, 30.0)  $\mu\text{m}$



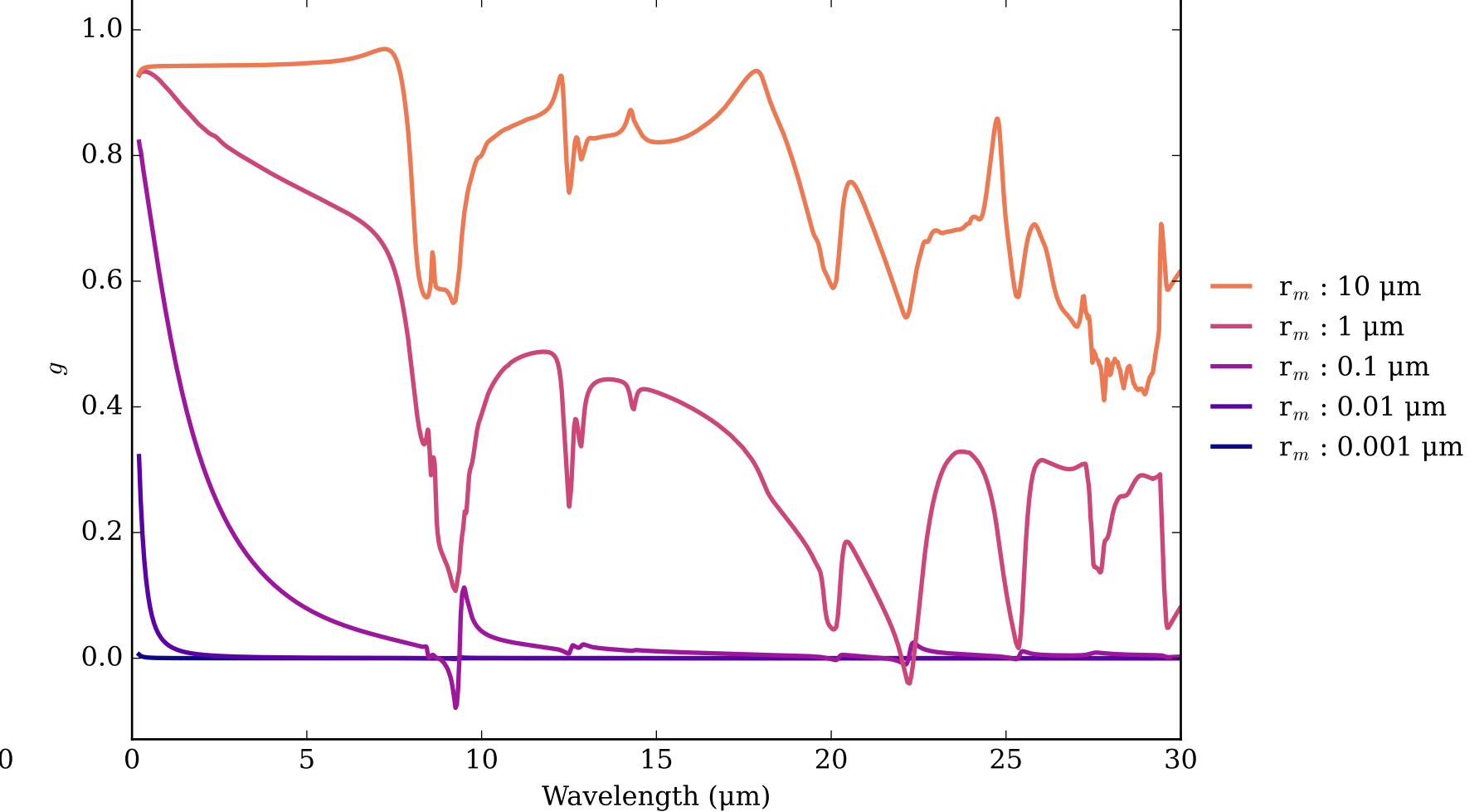
SiO<sub>2</sub>\_alpha\_palik Effective Extinction Cross Section



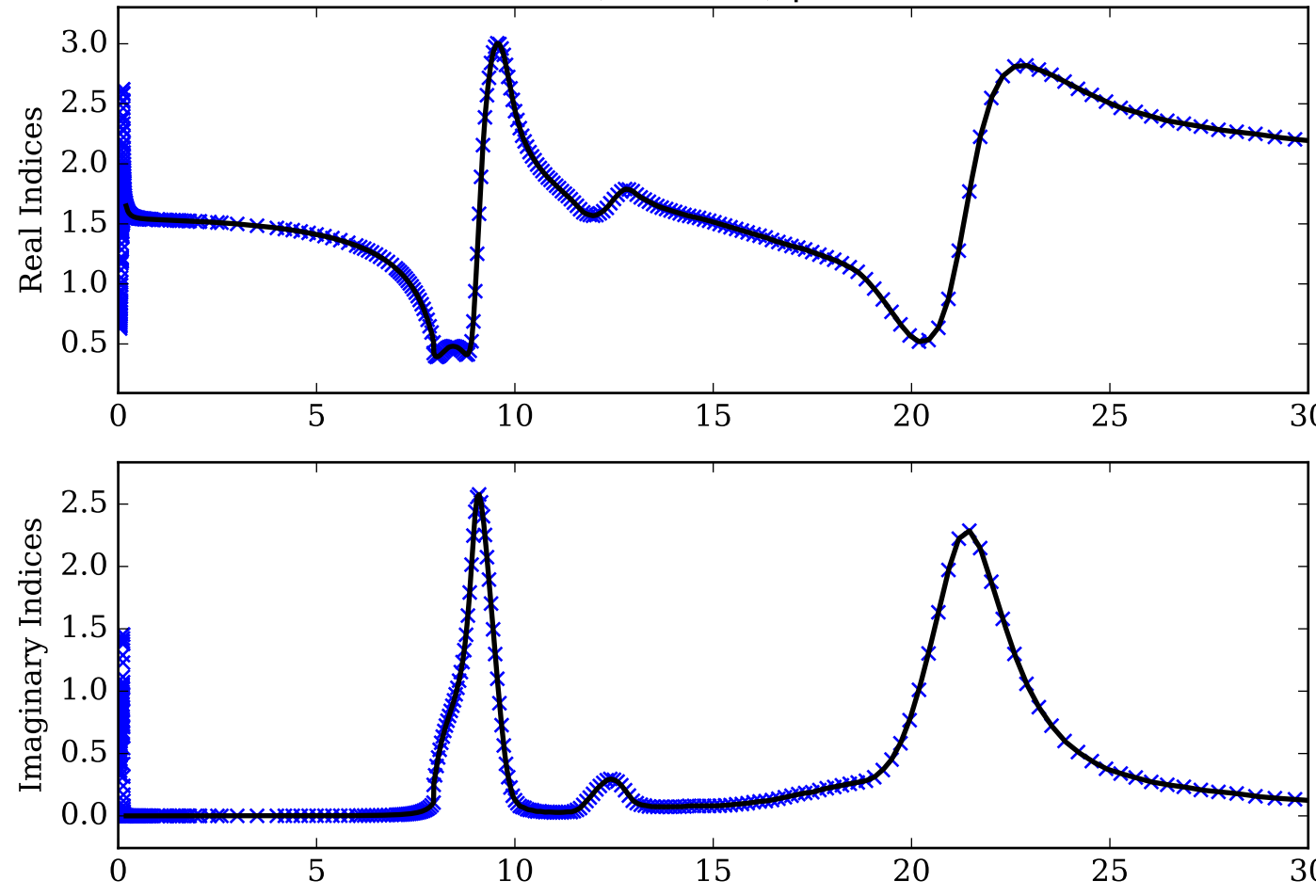
SiO<sub>2</sub>\_alpha\_palik Single Scattering Albedos  $\omega$   
0 (black, completely absorbing) to 1 (white, completely scattering)



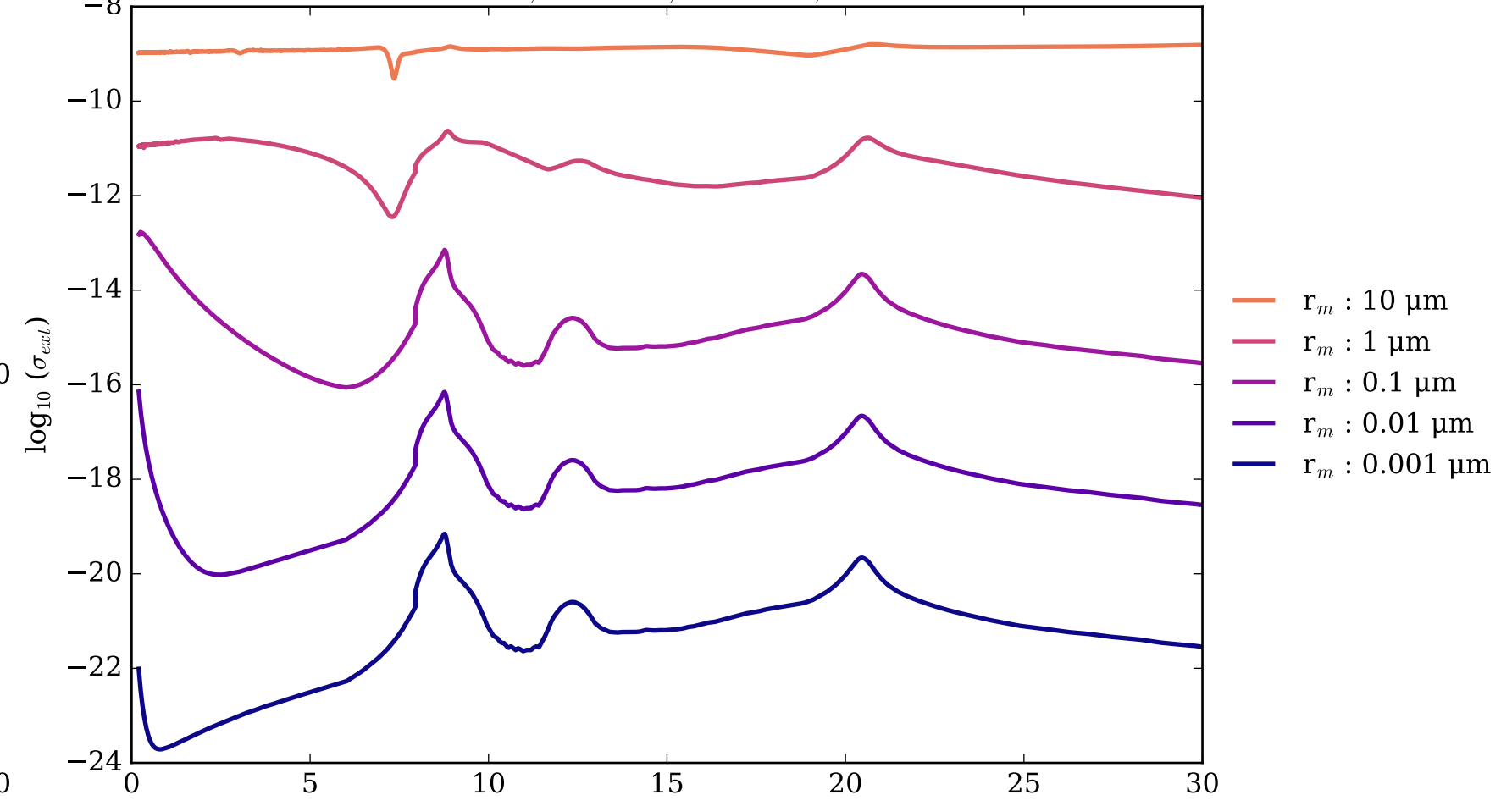
SiO<sub>2</sub>\_alpha\_palik Asymmetry Parameter  $g$   
0 (Rayleigh Limit) to 1 (Total Forward Scattering)



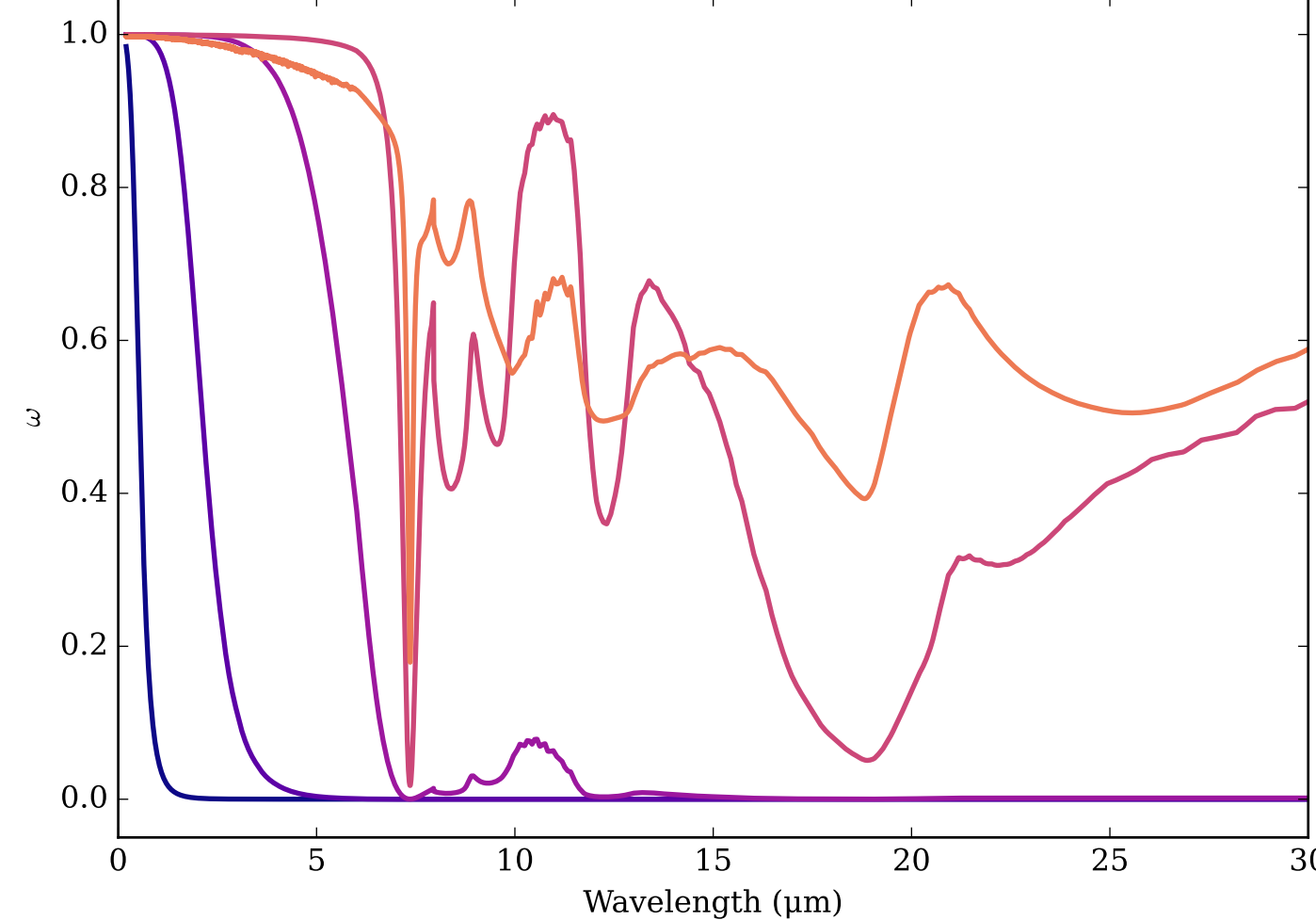
Refractive Indices for SiO<sub>2</sub>  
(0.2, 30.0)  $\mu\text{m}$



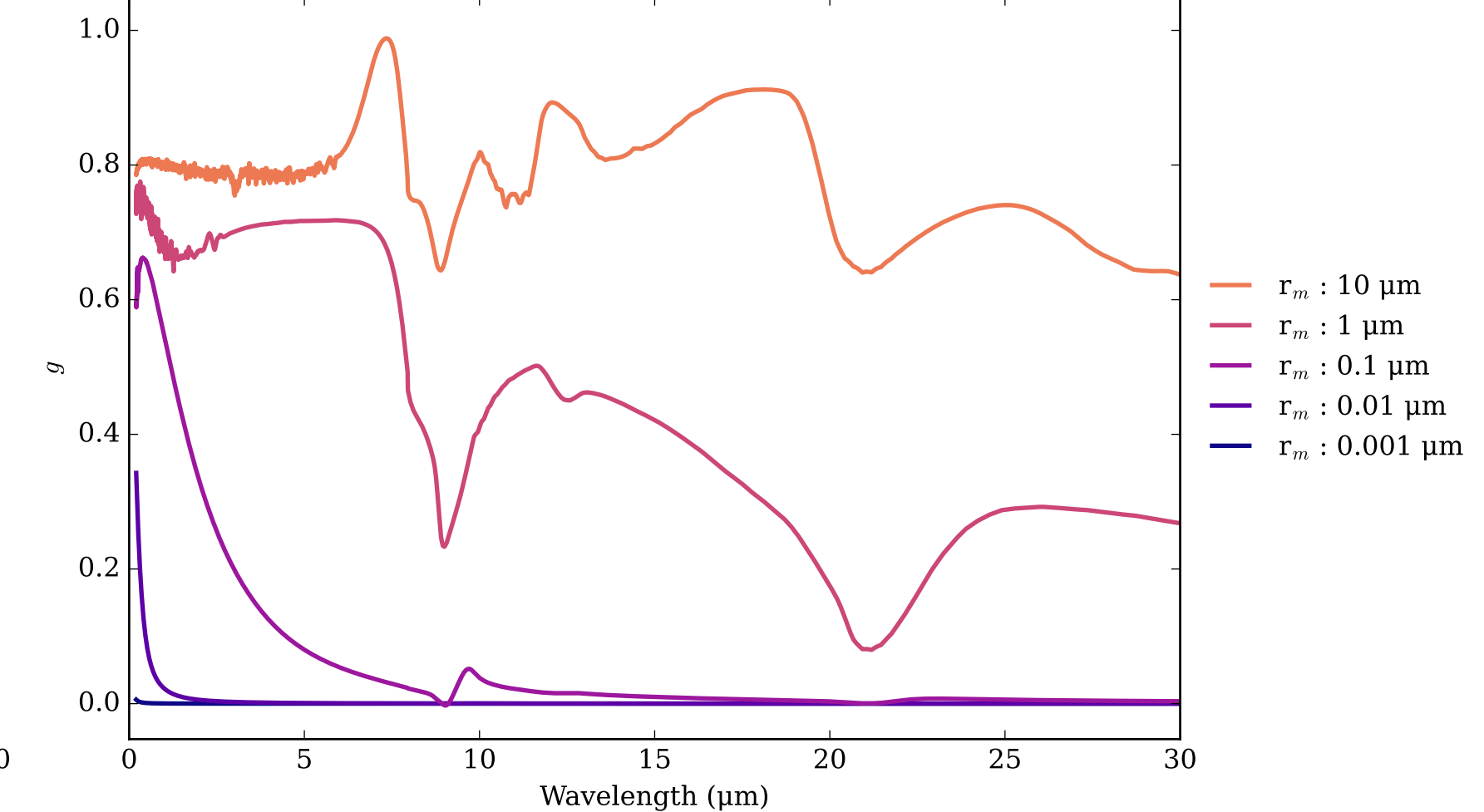
SiO<sub>2</sub>\_amorph Effective Extinction Cross Section  
 $\sigma_{\text{ext, eff}} = \sigma_{\text{abs, eff}} + \sigma_{\text{scat, eff}}$



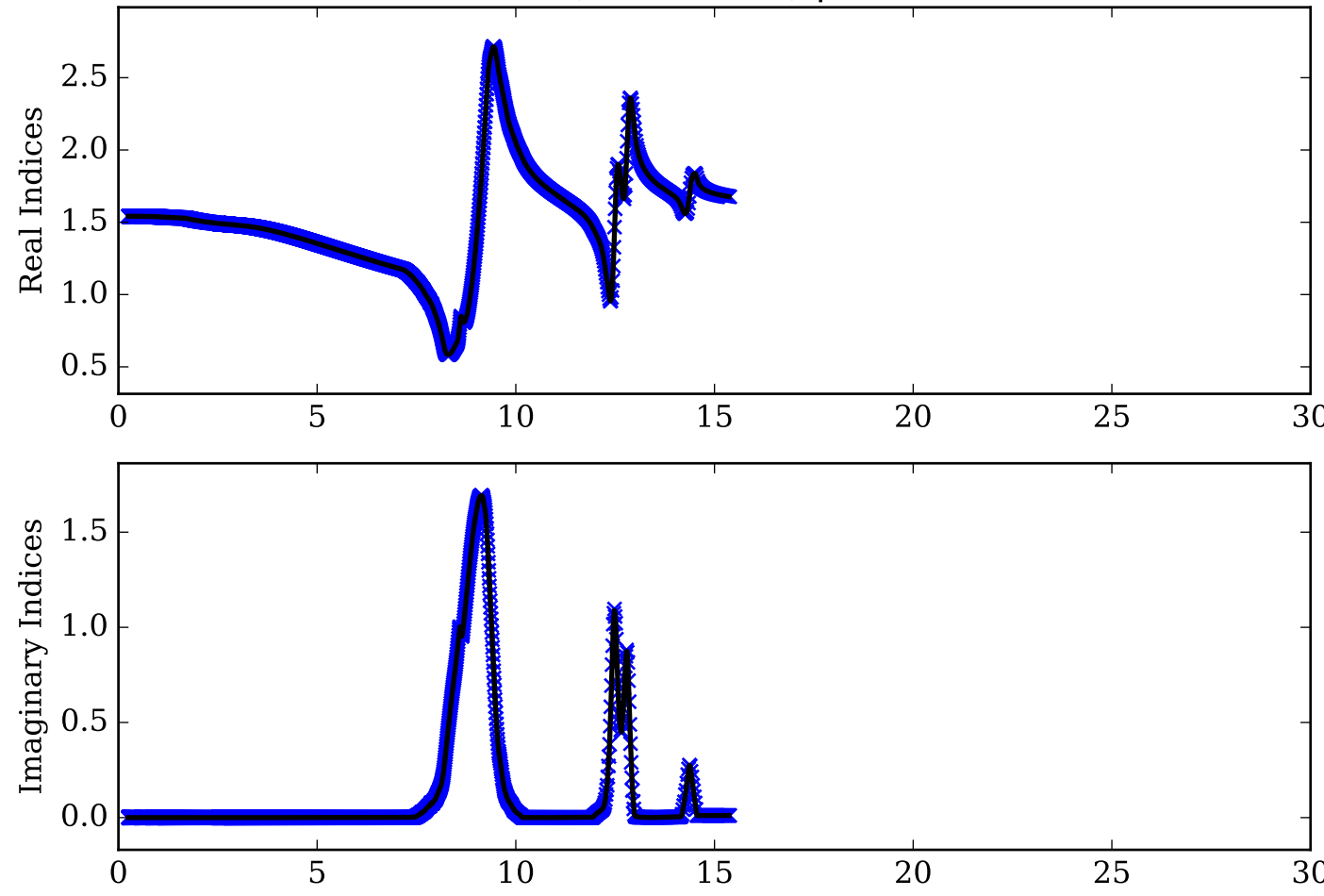
SiO<sub>2</sub>\_amorph Single Scattering Albedos  $\omega$   
0 (black, completely absorbing) to 1 (white, completely scattering)



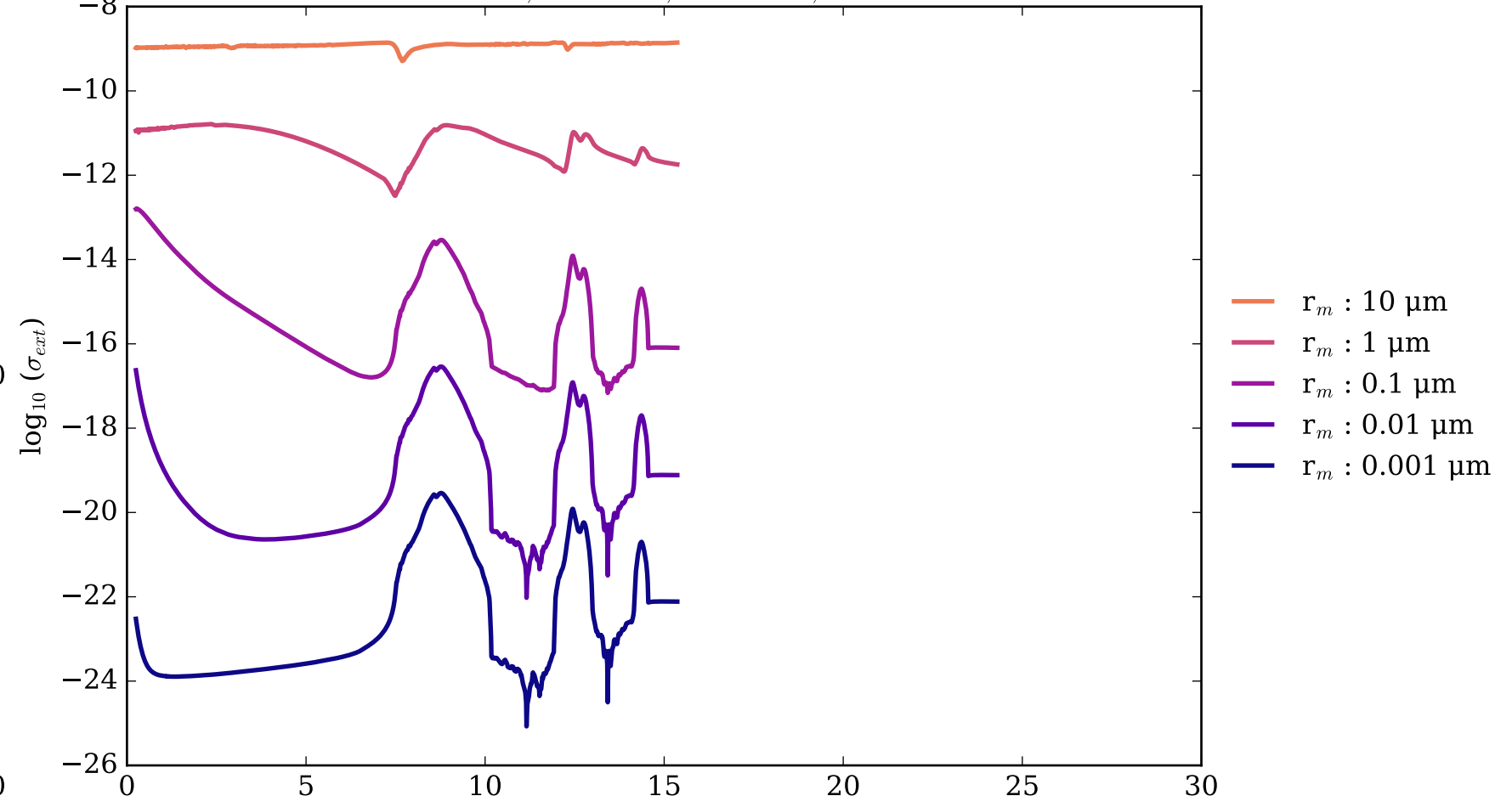
SiO<sub>2</sub>\_amorph Asymmetry Parameter  $g$   
0 (Rayleigh Limit) to 1 (Total Forward Scattering)



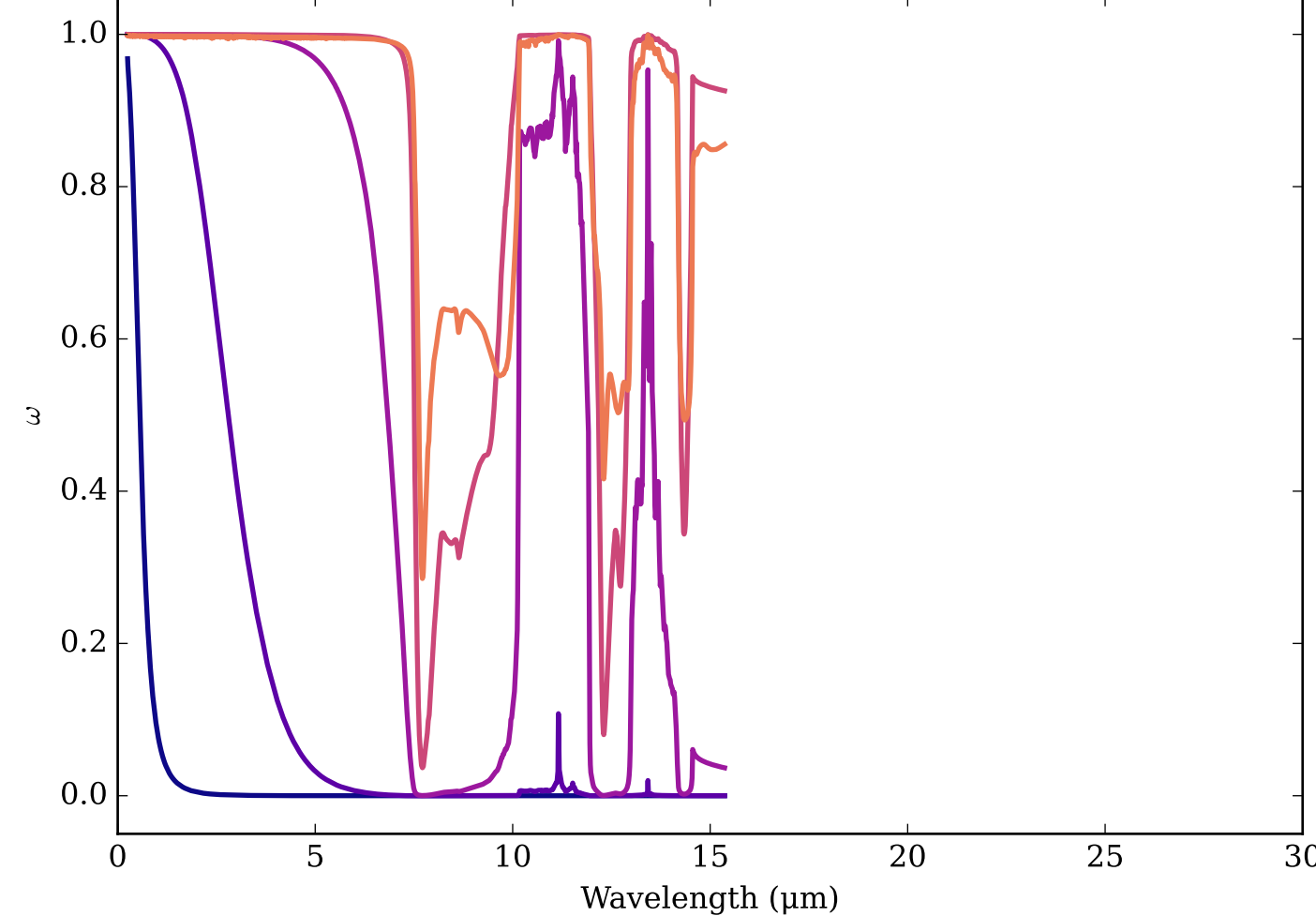
Refractive Indices for SiO<sub>2</sub>  
(0.25, 15.37) μm



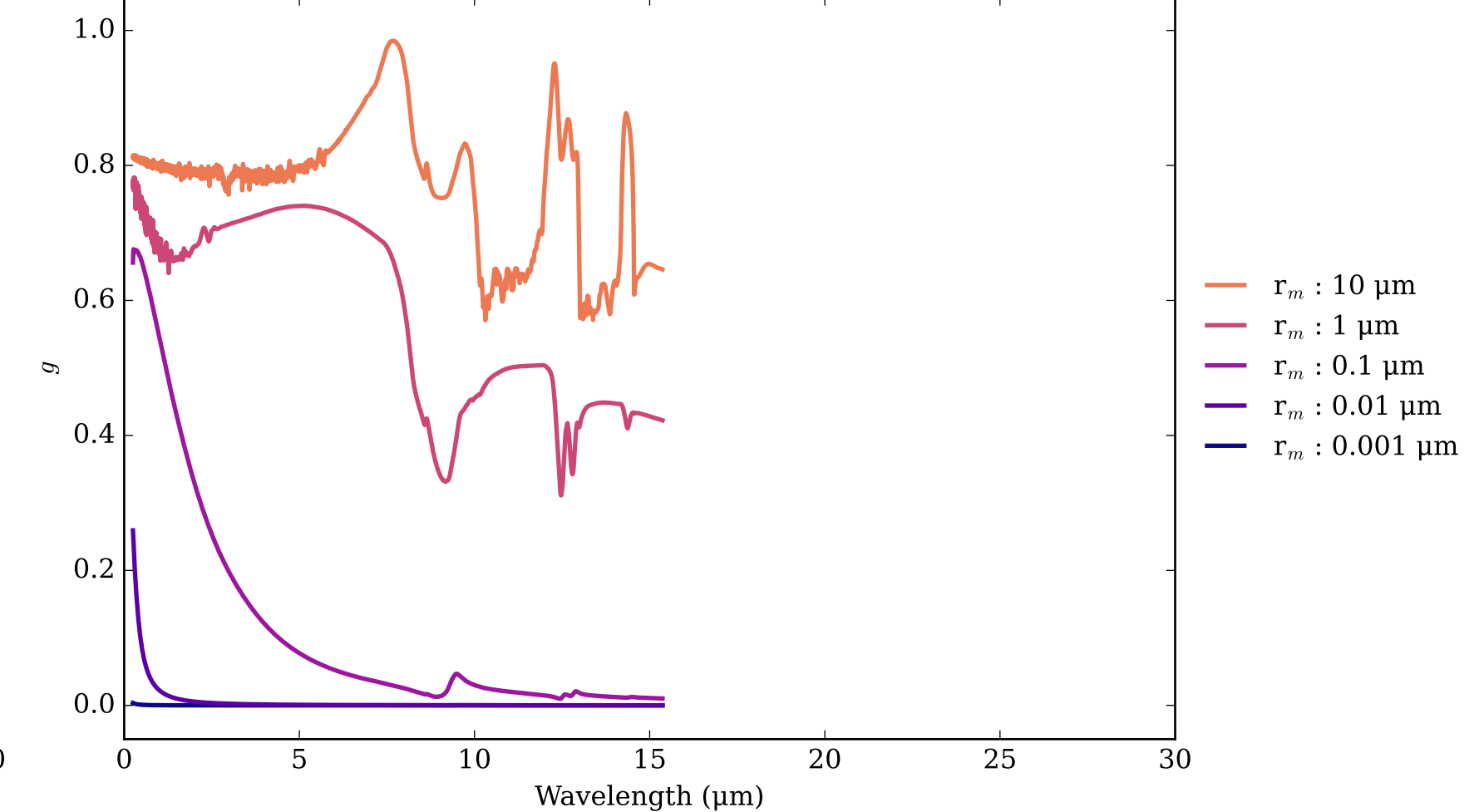
SiO<sub>2</sub>\_crystalline\_2023 Effective Extinction Cross Section  
 $\sigma_{ext, eff} = \sigma_{abs, eff} + \sigma_{scat, eff}$



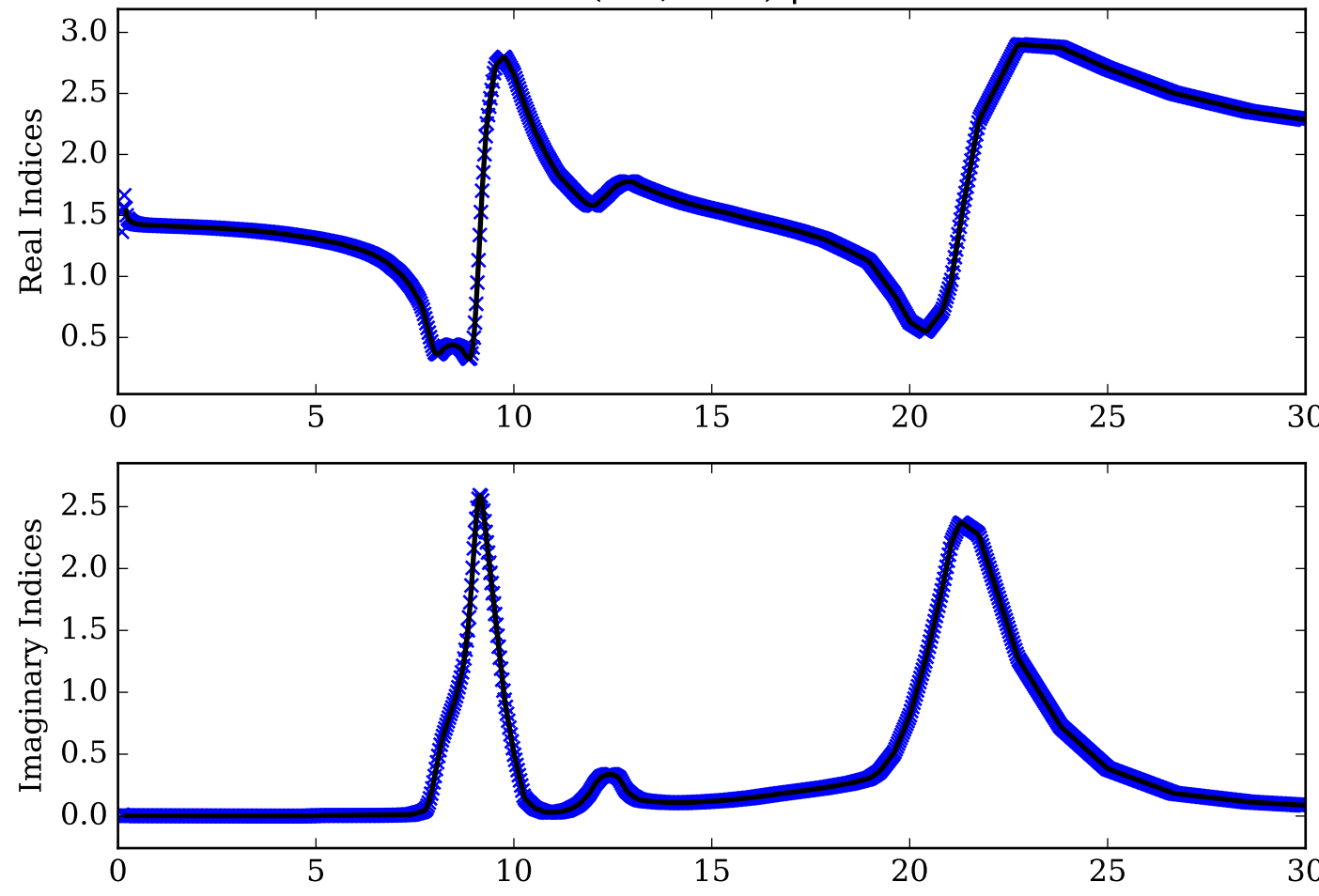
SiO<sub>2</sub>\_crystalline\_2023 Single Scattering Albedos ω  
0 (black, completely absorbing) to 1 (white, completely scattering)



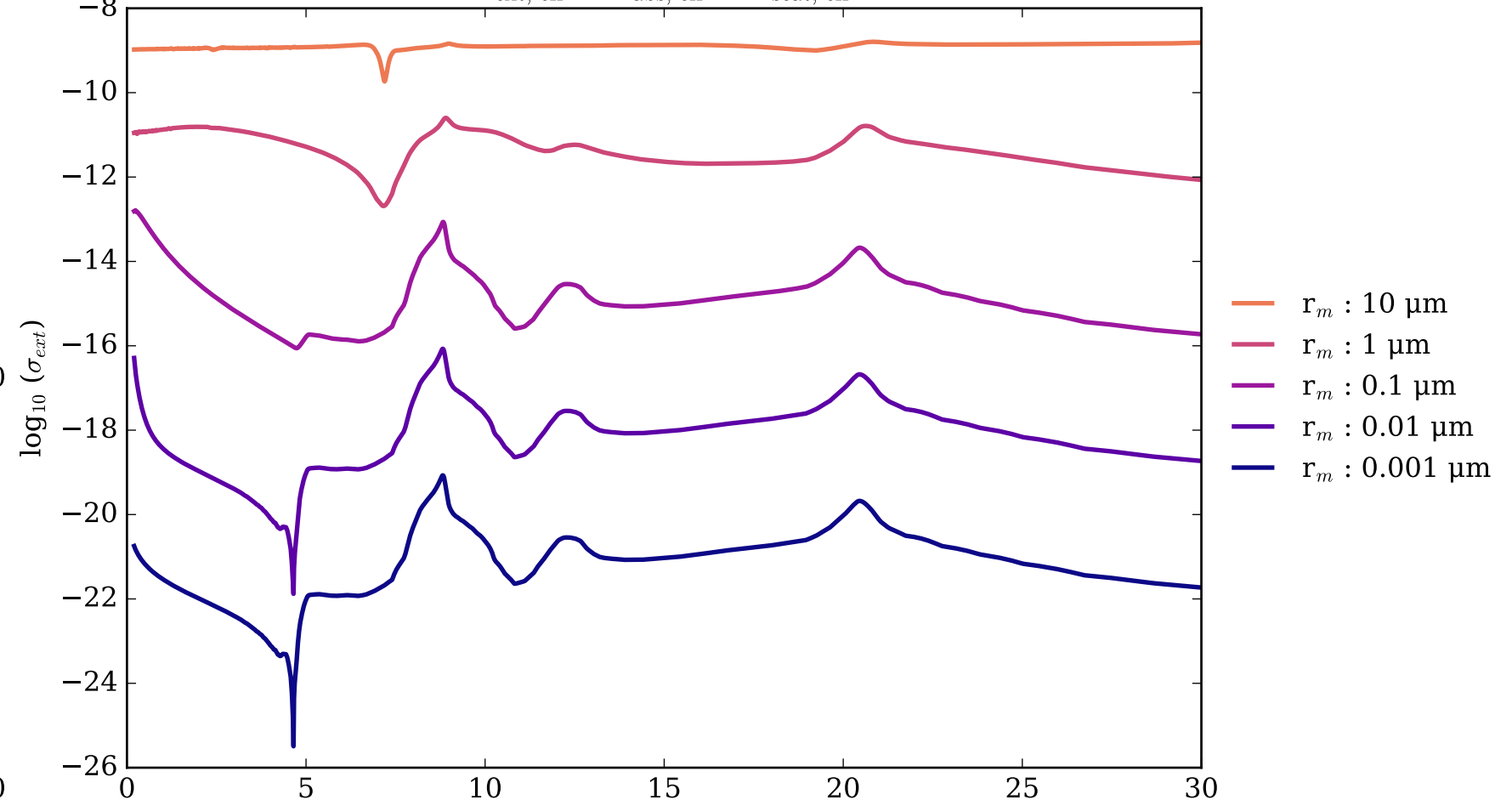
SiO<sub>2</sub>\_crystalline\_2023 Asymmetry Parameter g  
0 (Rayleigh Limit) to 1 (Total Forward Scattering)



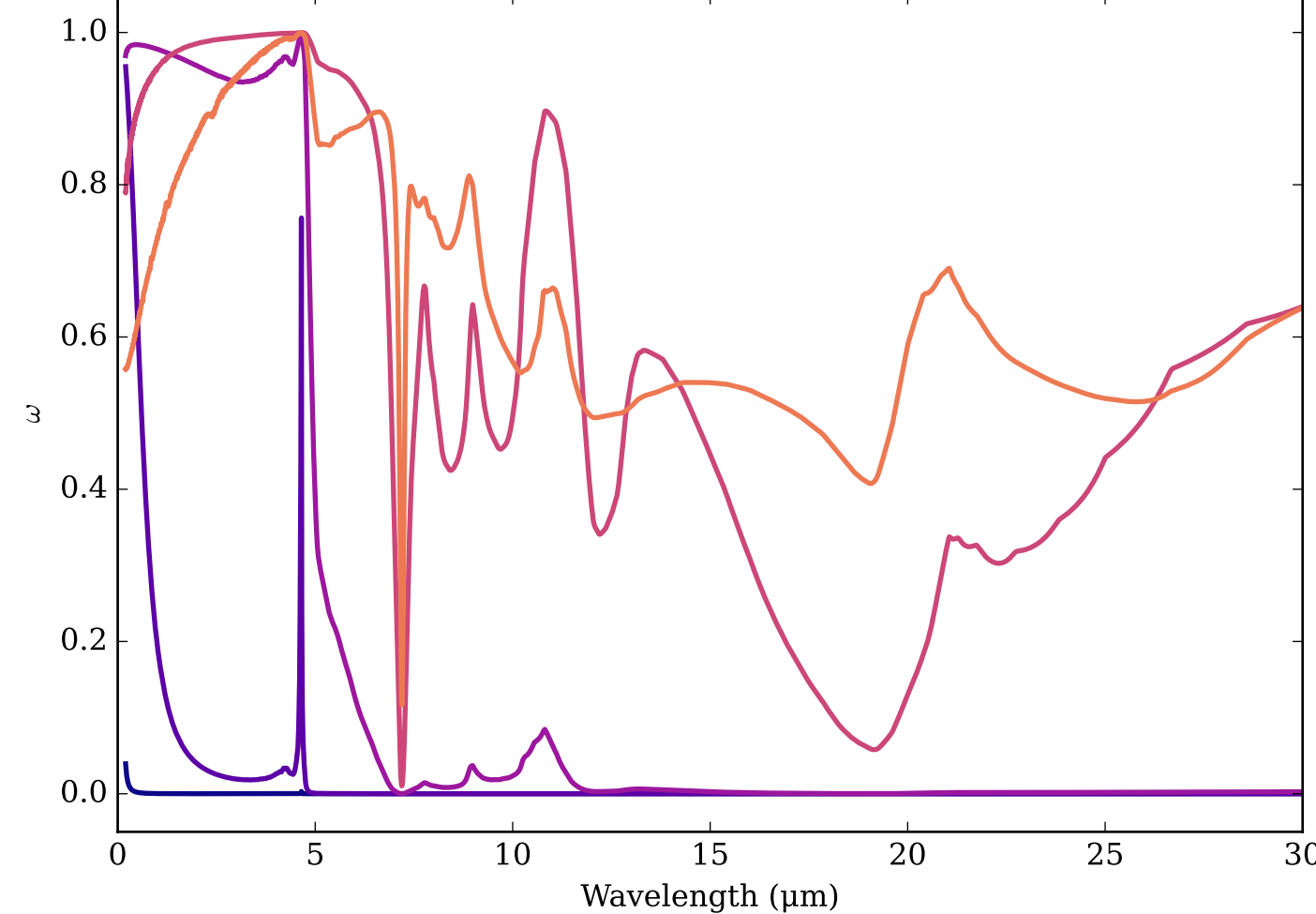
Refractive Indices for SiO<sub>2</sub>  
(0.2, 30.0) μm



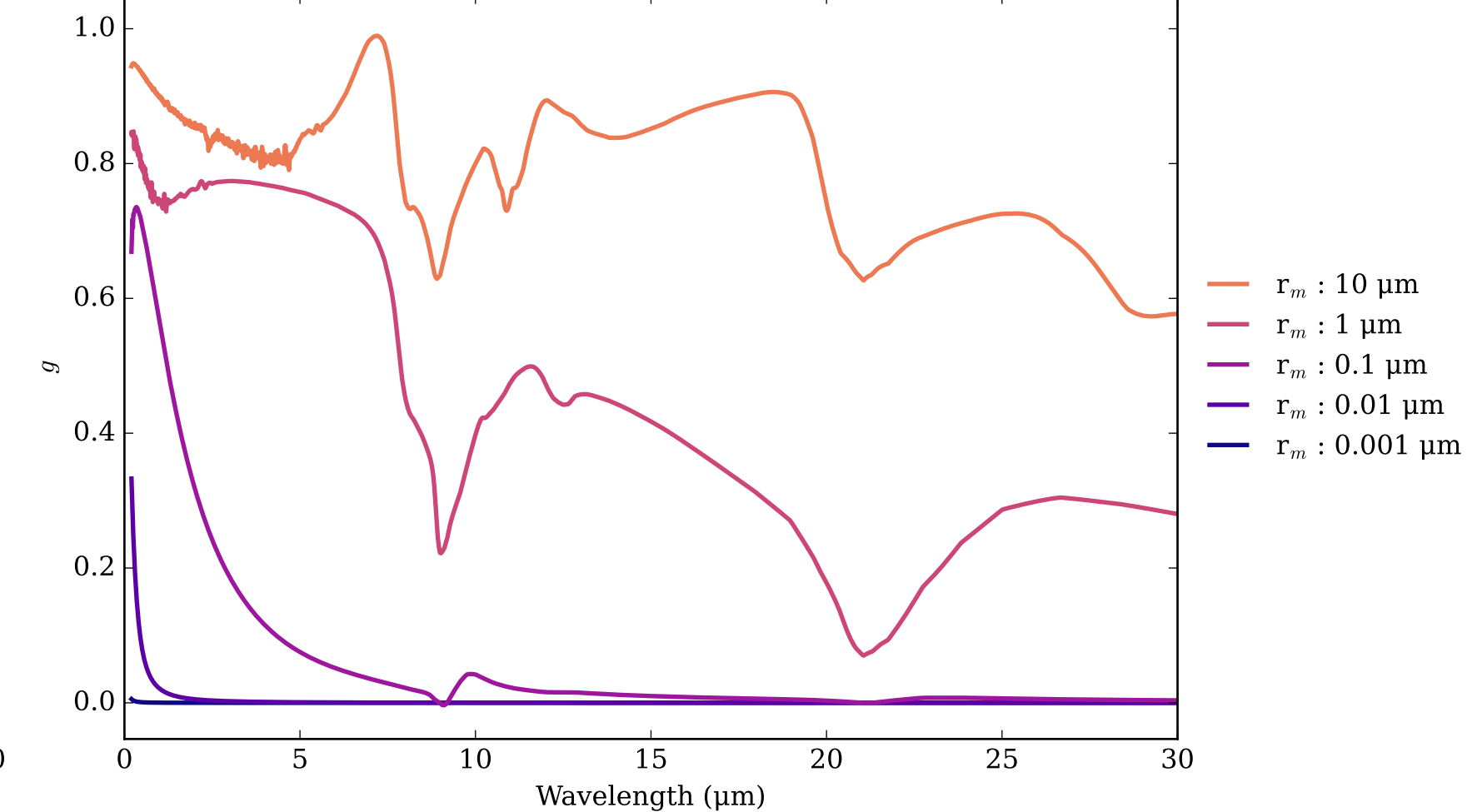
SiO<sub>2</sub>\_glass\_palik Effective Extinction Cross Section  
 $\sigma_{ext, eff} = \sigma_{abs, eff} + \sigma_{scat, eff}$



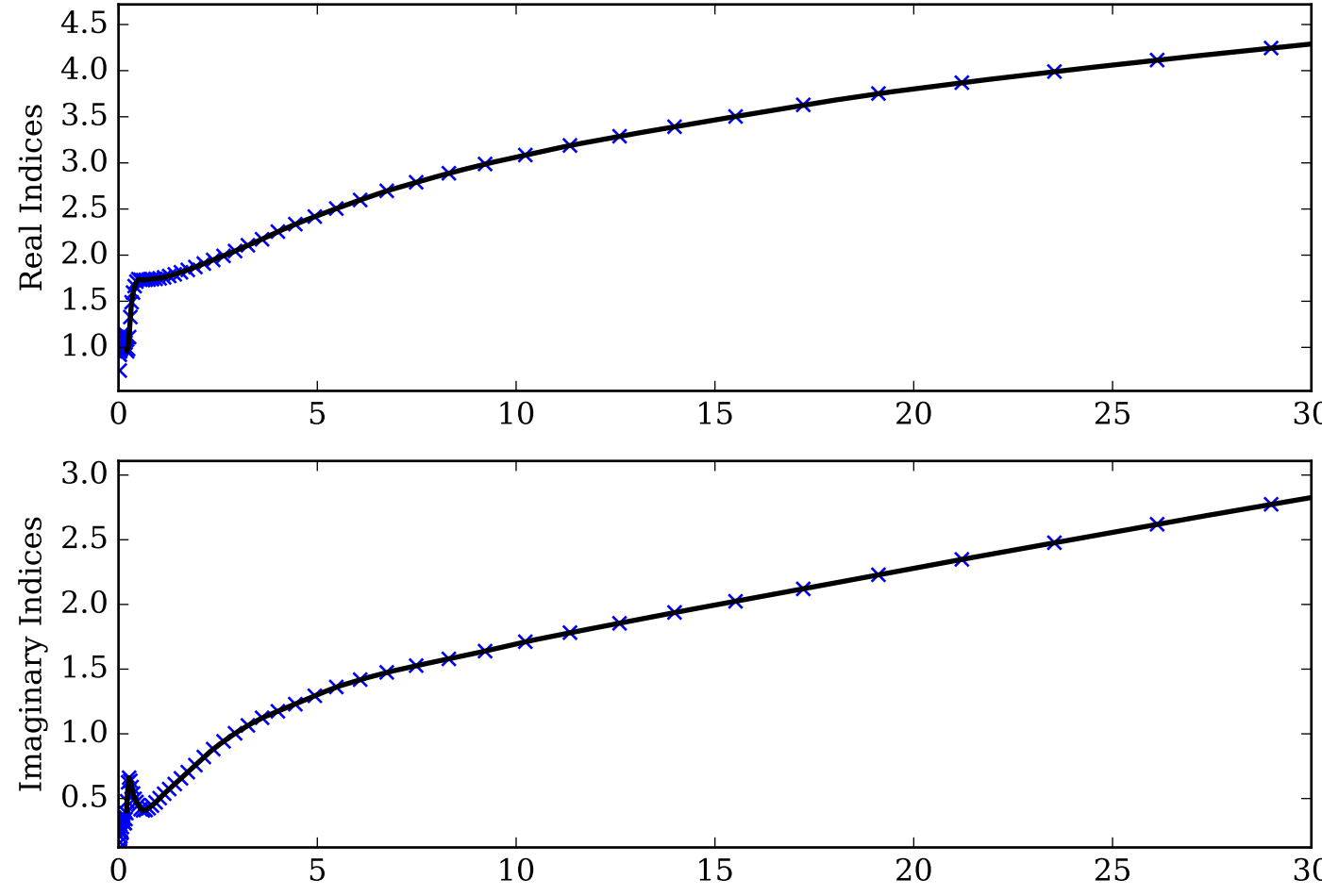
SiO<sub>2</sub>\_glass\_palik Single Scattering Albedos ω  
0 (black, completely absorbing) to 1 (white, completely scattering)



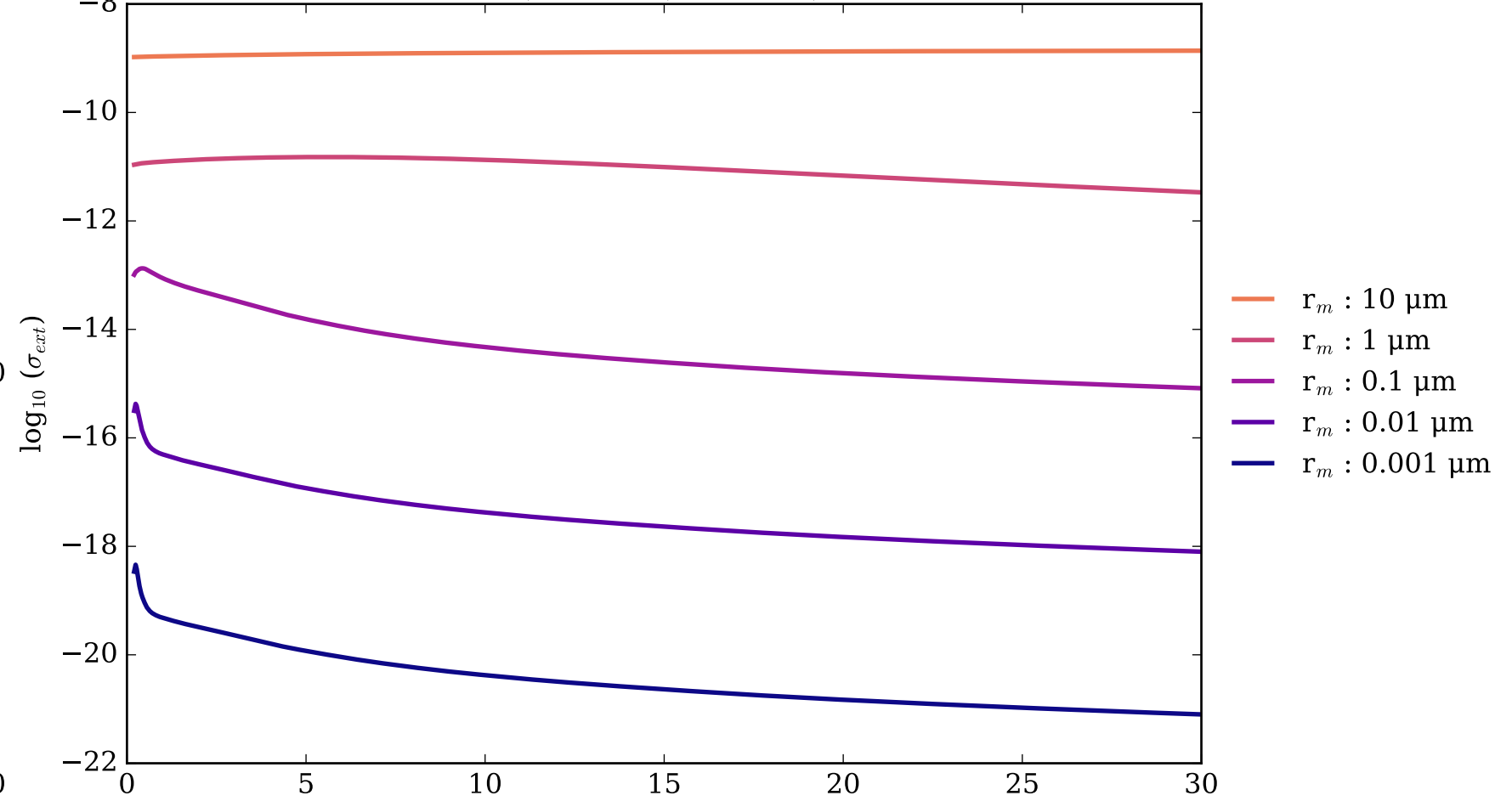
SiO<sub>2</sub>\_glass\_palik Asymmetry Parameter g  
0 (Rayleigh Limit) to 1 (Total Forward Scattering)



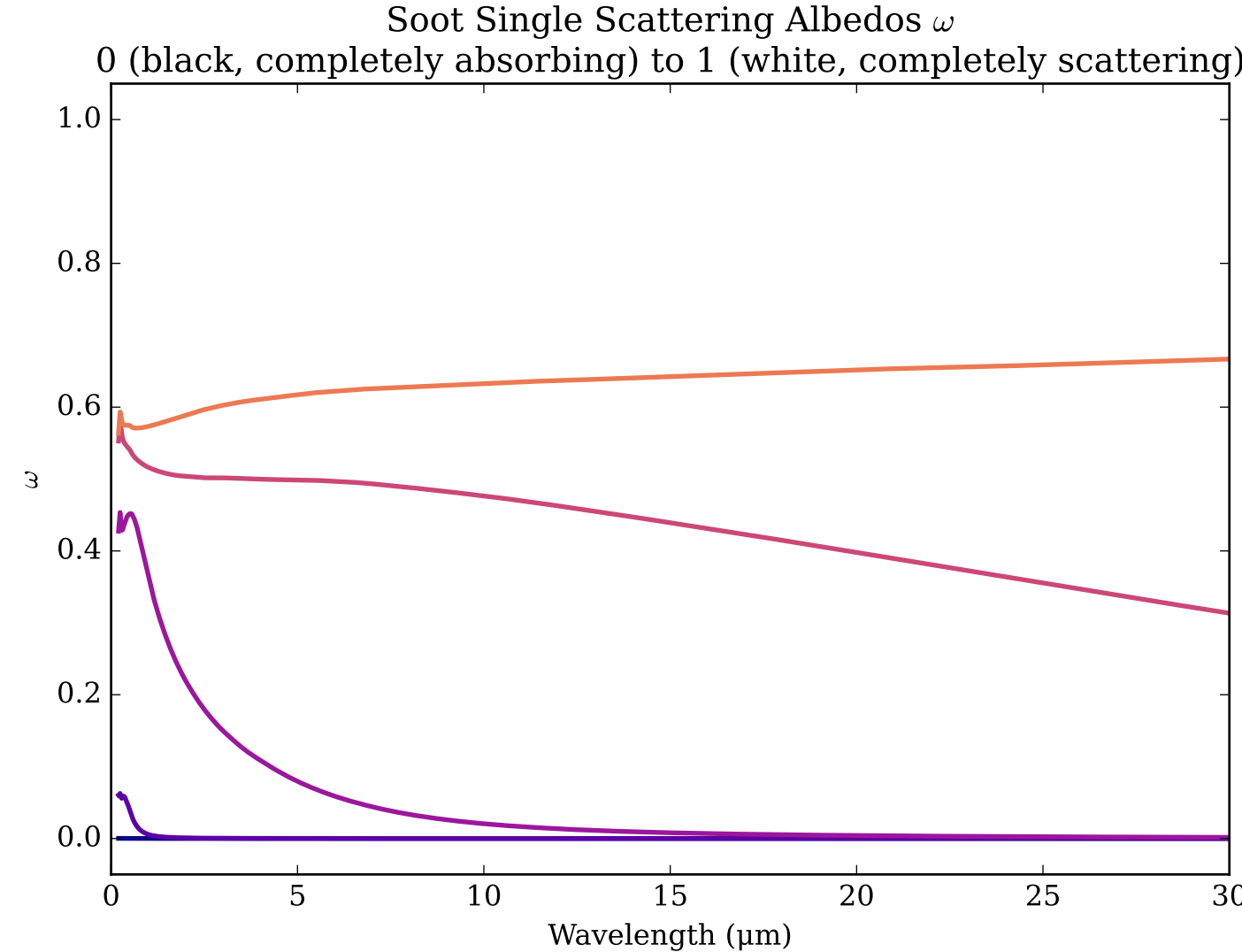
Refractive Indices for Soot  
(0.2, 30.0)  $\mu\text{m}$



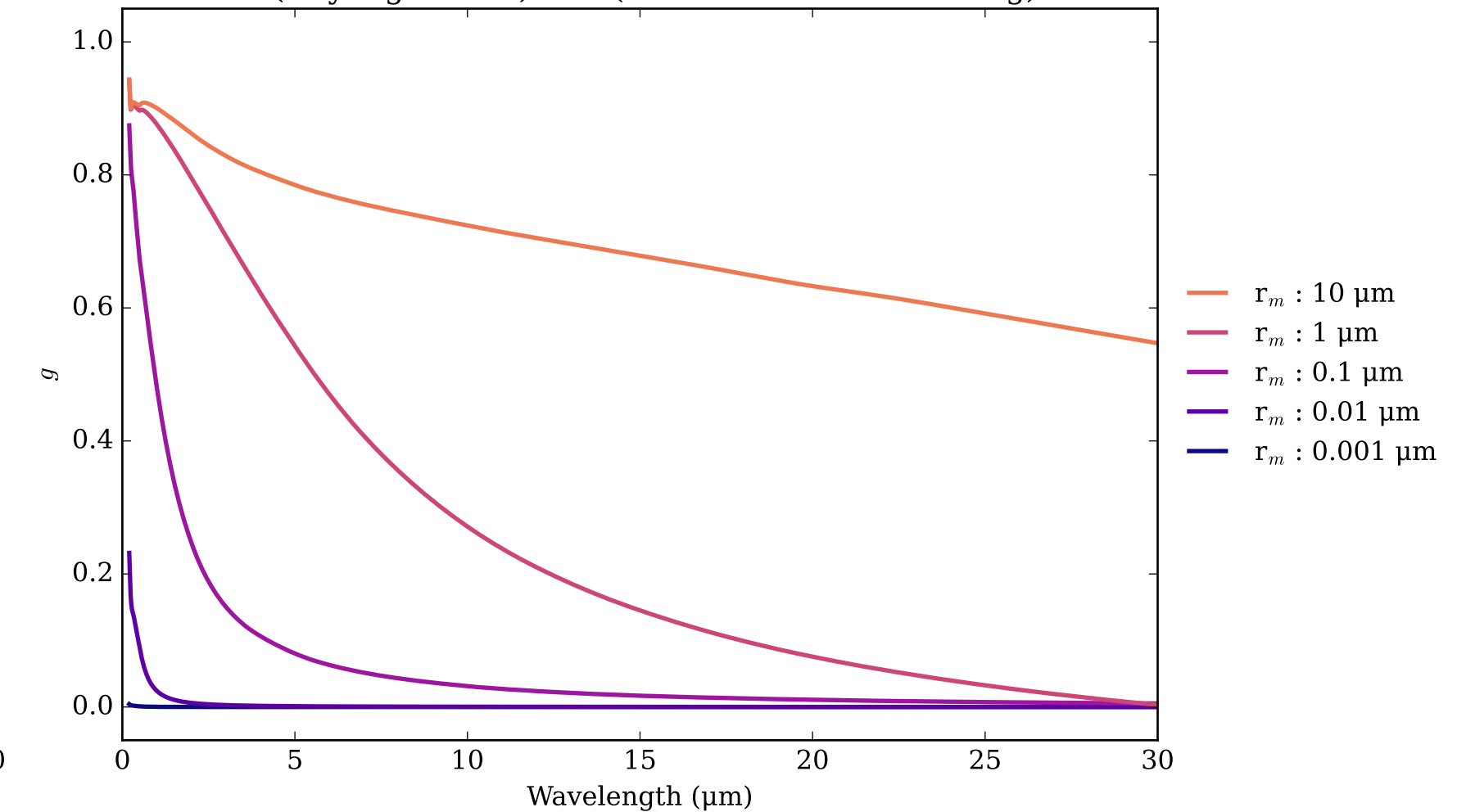
Soot Effective Extinction Cross Section



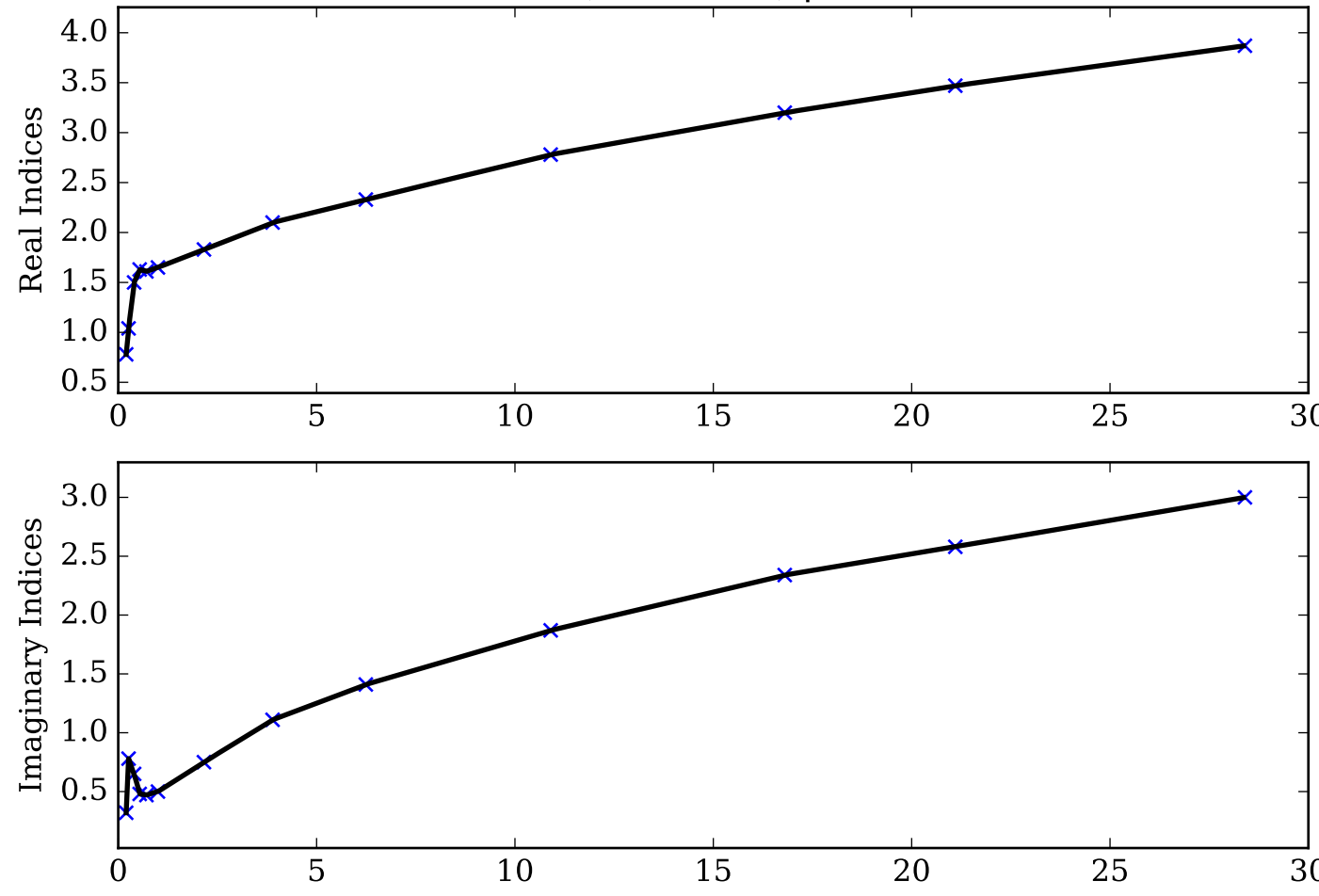
Soot Single Scattering Albedos  $\omega$



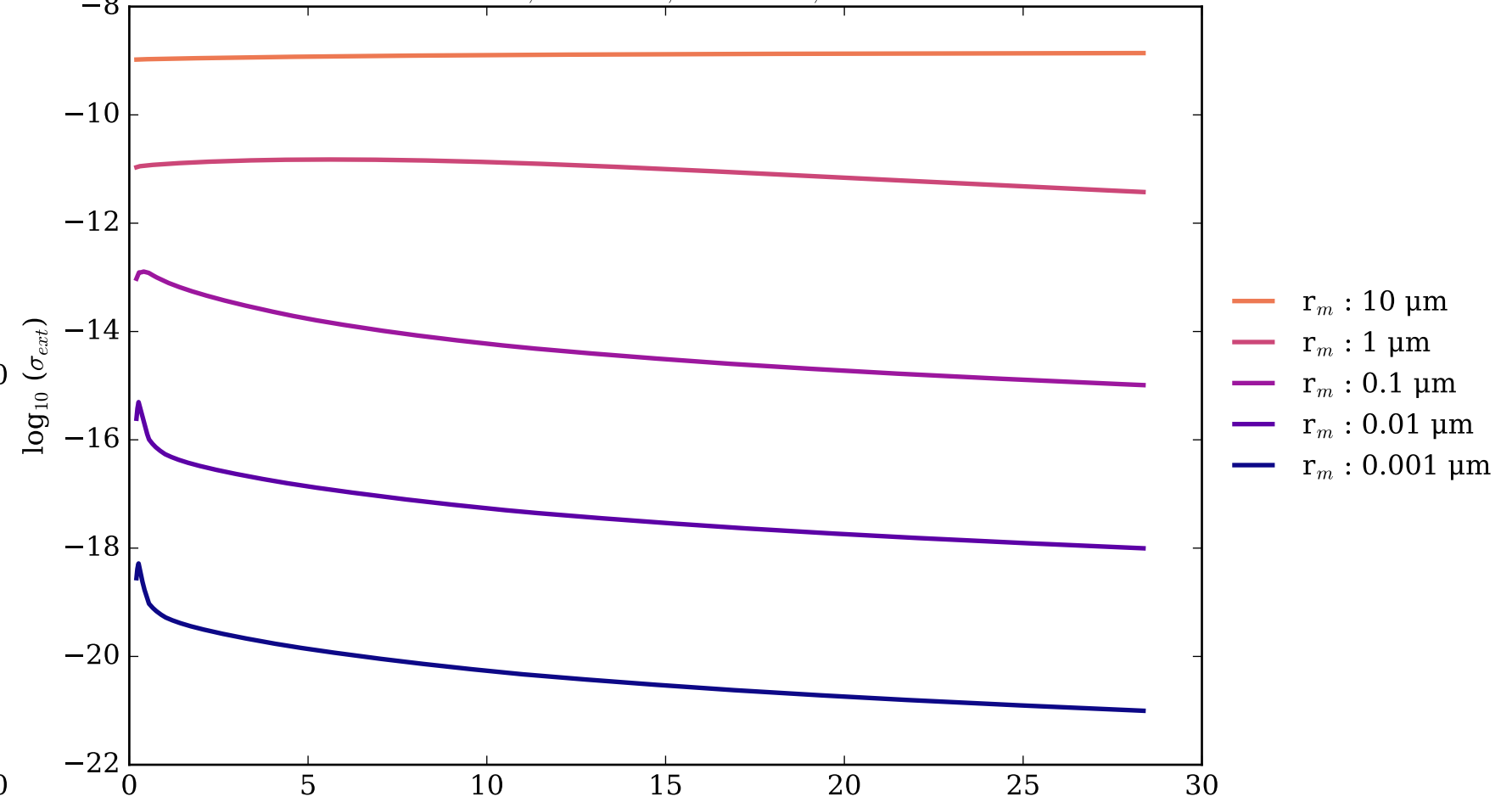
Soot Asymmetry Parameter  $g$



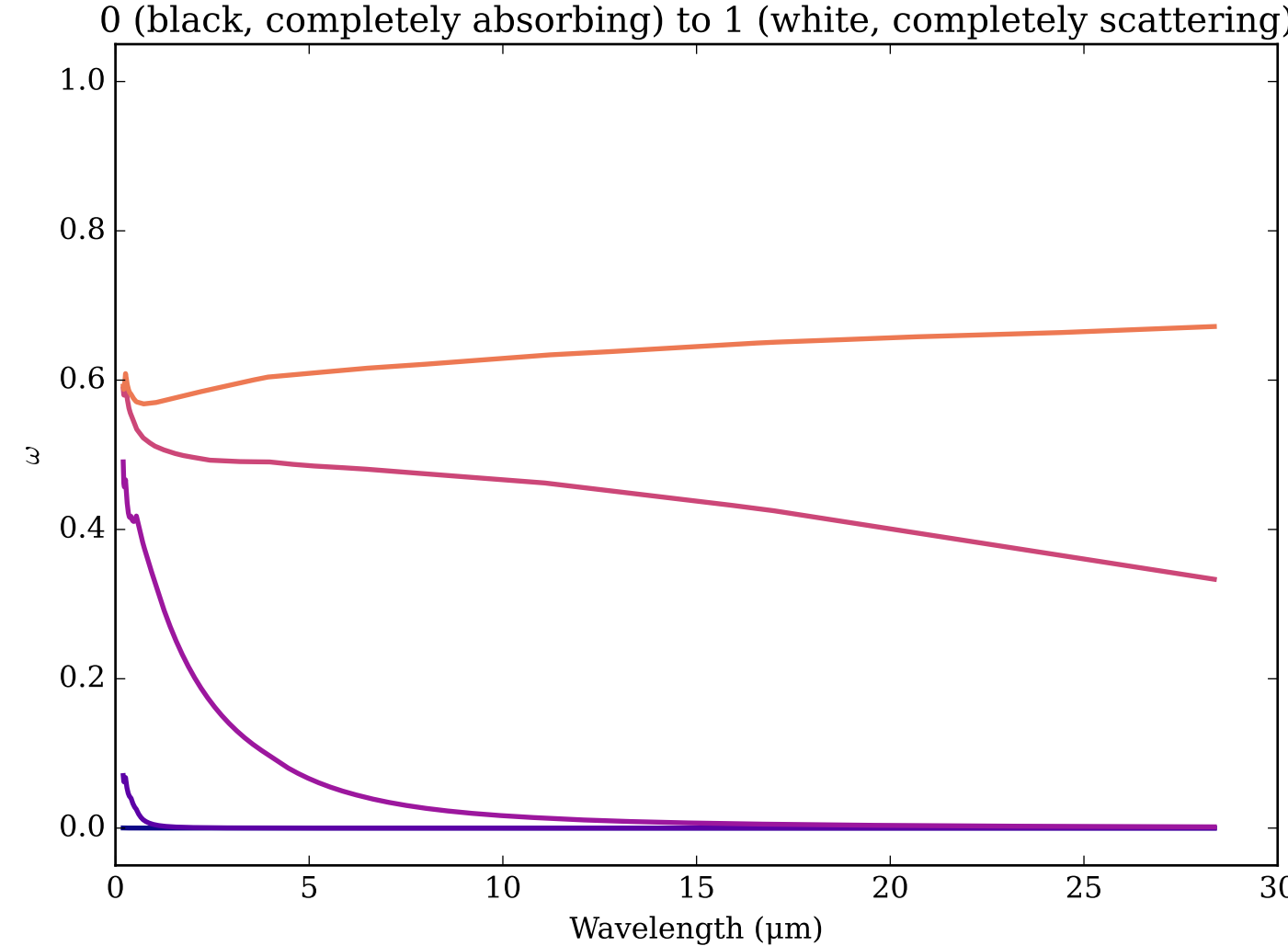
Refractive Indices for Soot  
(0.2, 28.37)  $\mu\text{m}$



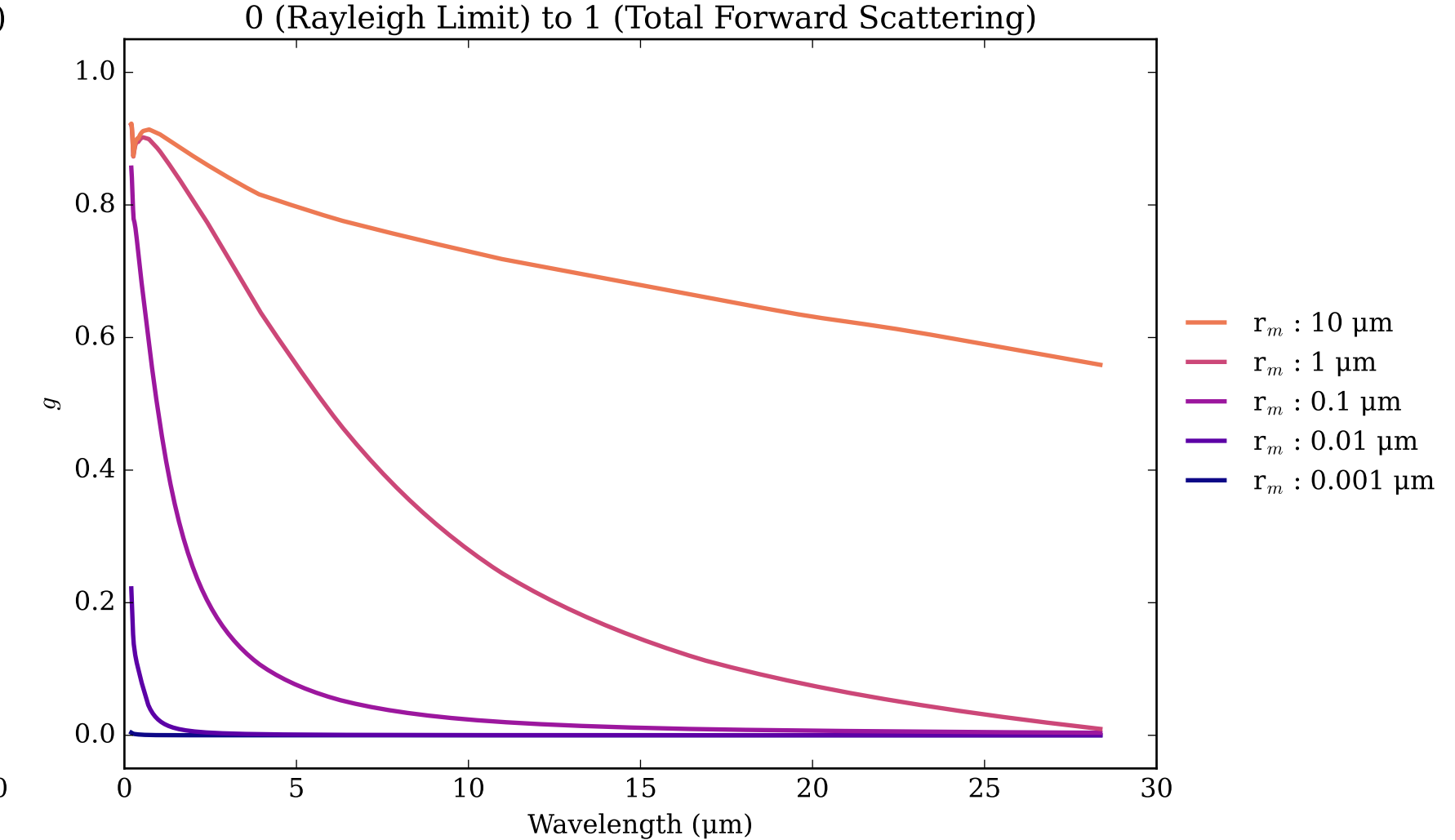
Soot\_6mm Effective Extinction Cross Section



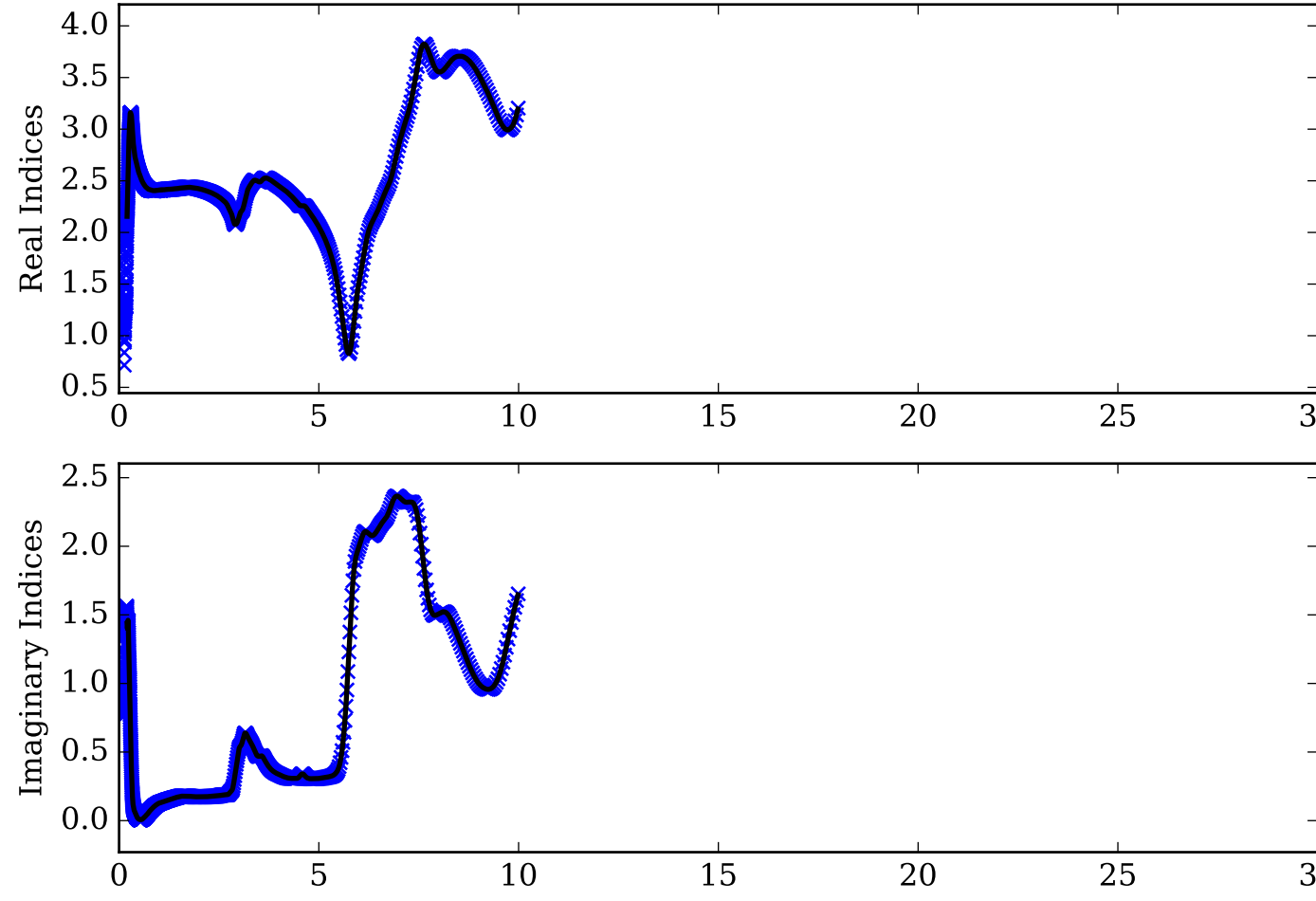
Soot\_6mm Single Scattering Albedos  $\omega$



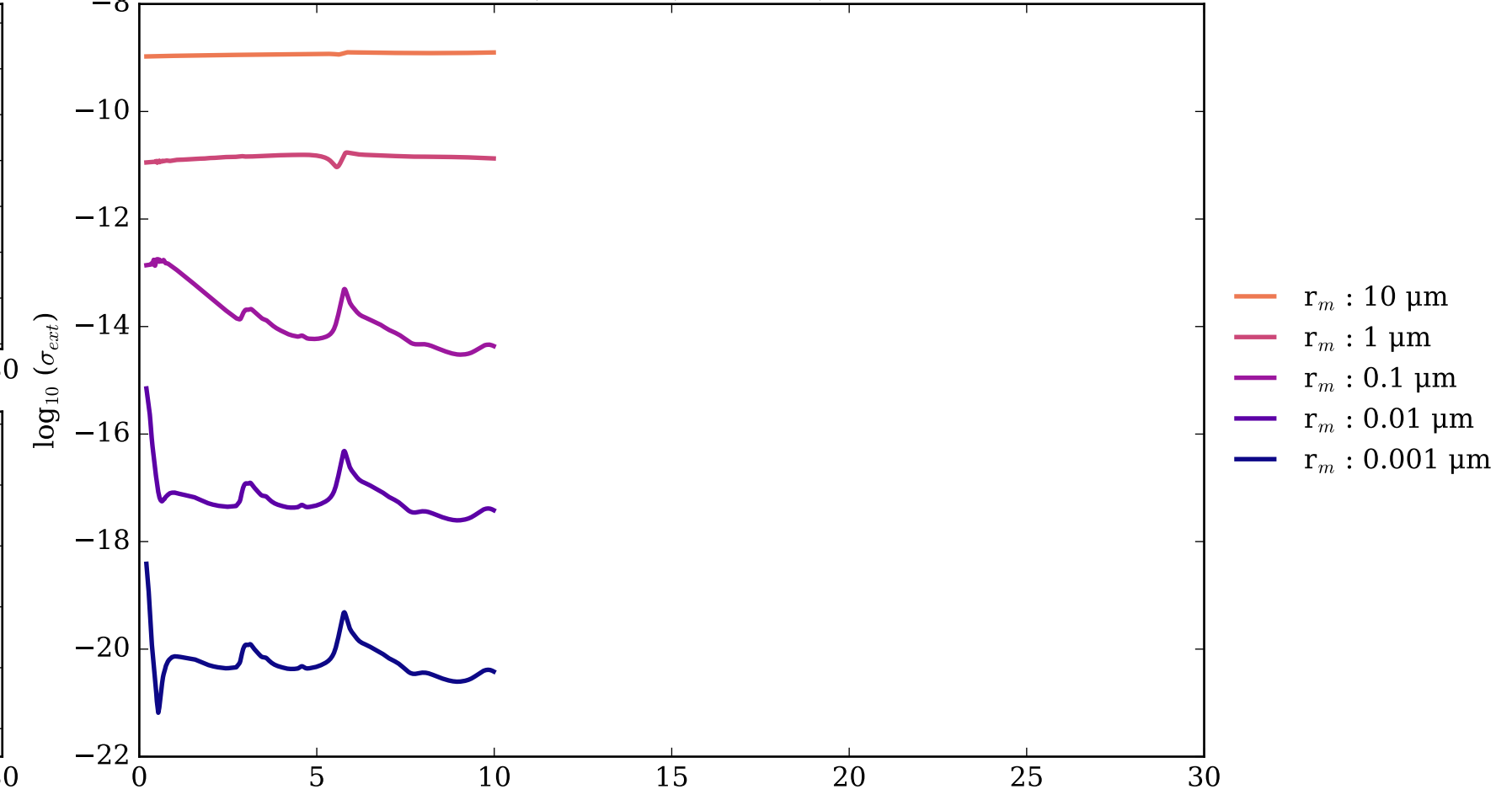
Soot\_6mm Asymmetry Parameter  $g$



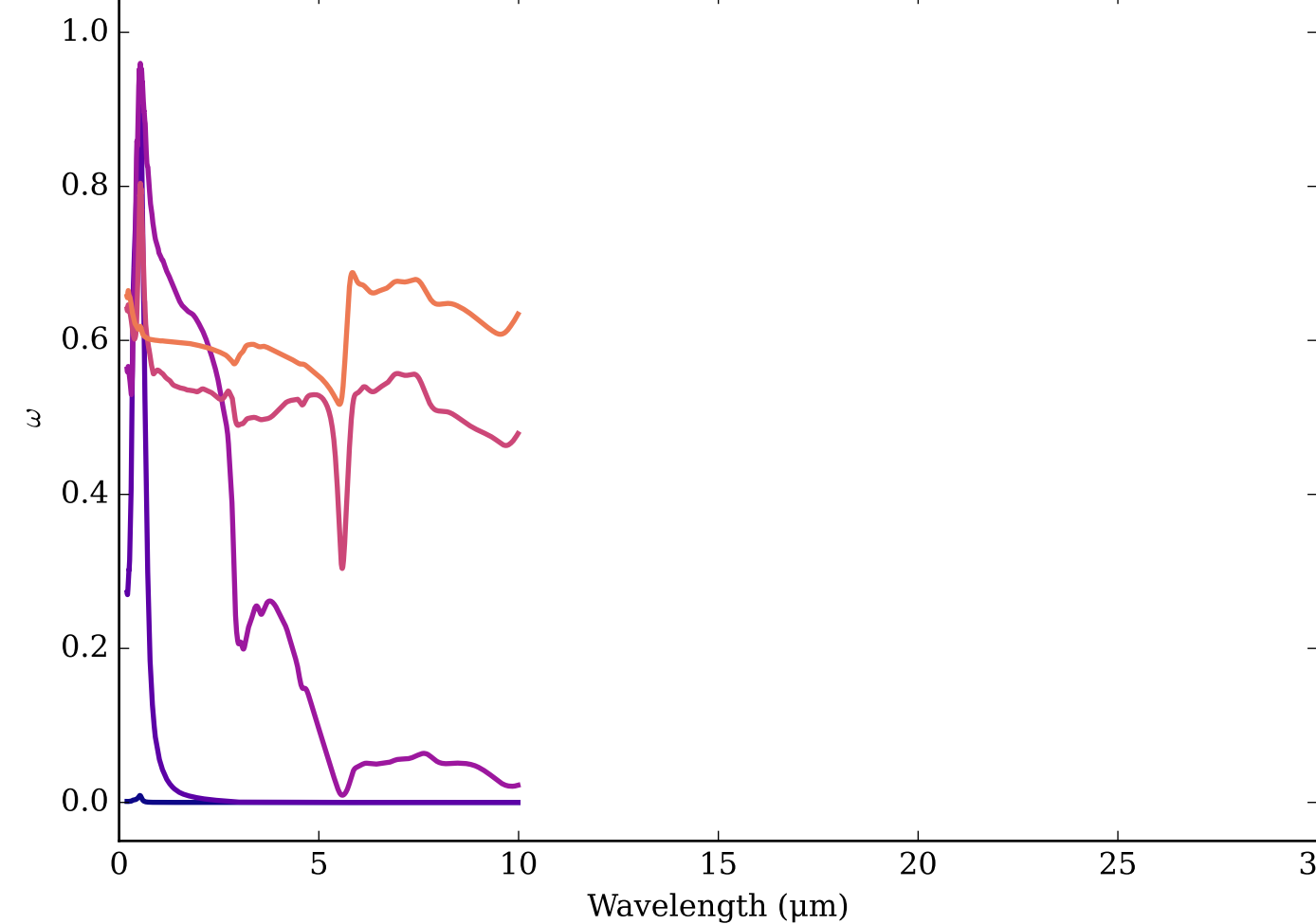
Refractive Indices for Tholin-CO-0625  
(0.2, 9.98)  $\mu\text{m}$



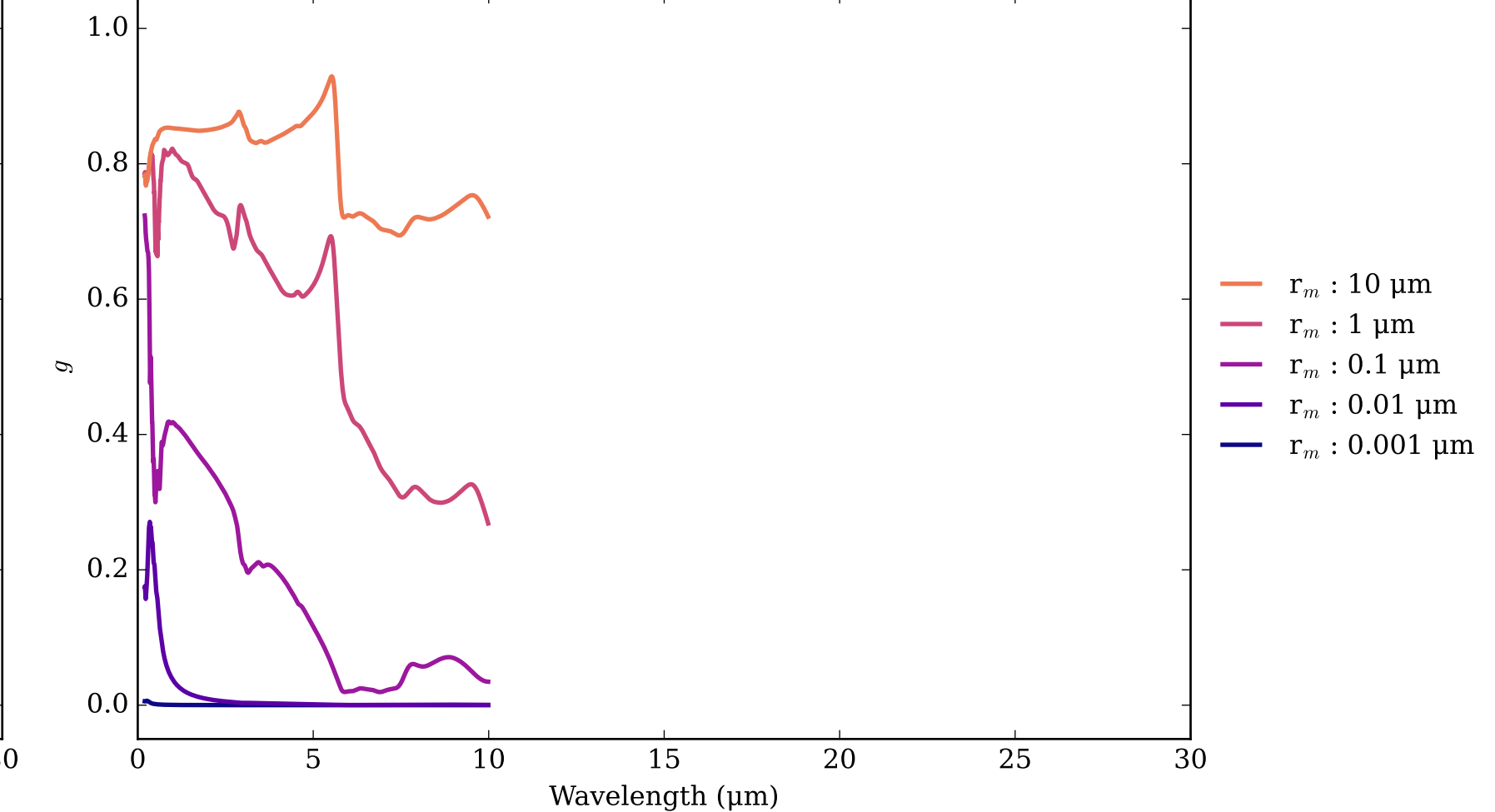
Tholin-CO-0625 Effective Extinction Cross Section



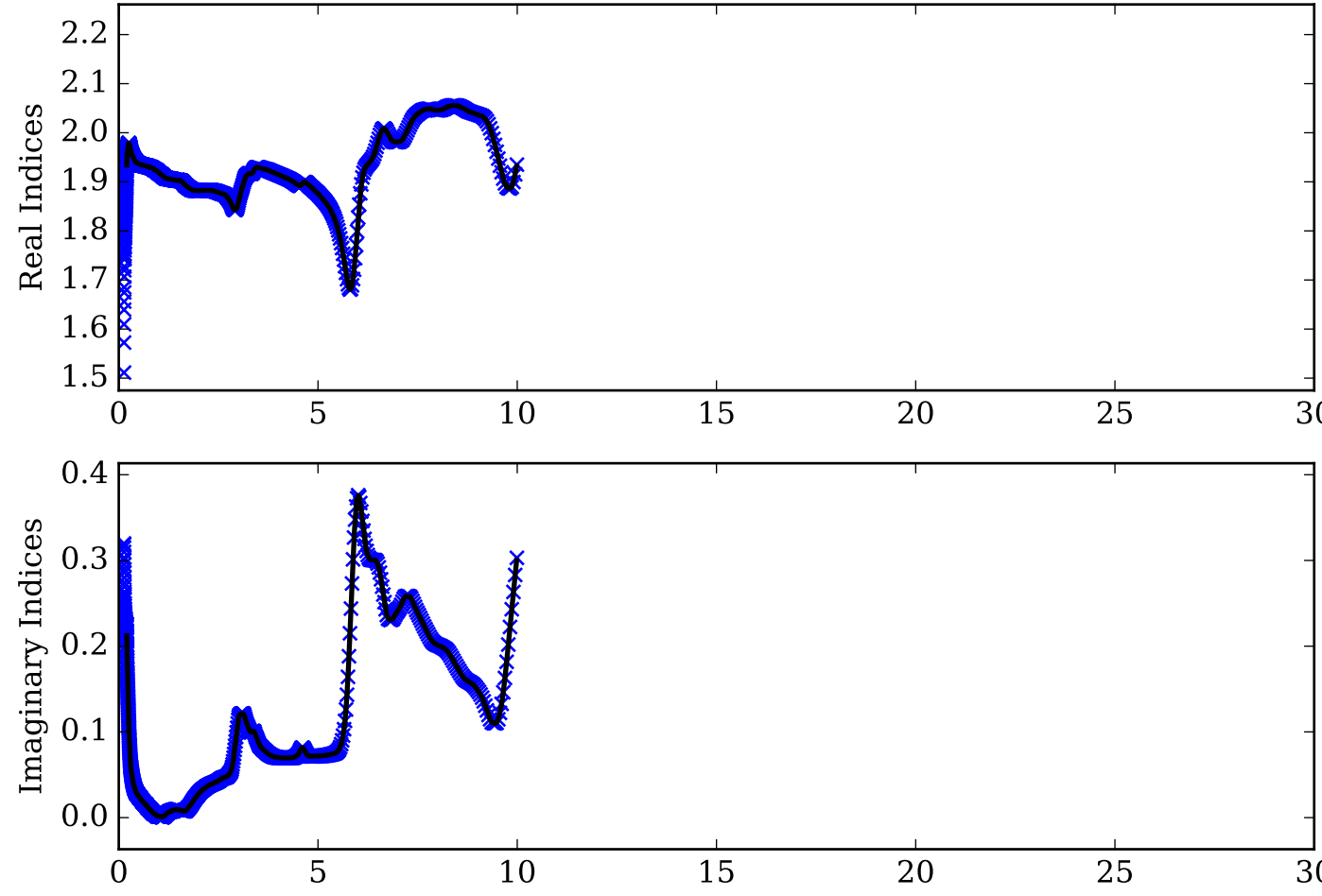
Tholin-CO-0625 Single Scattering Albedos  $\omega$   
0 (black, completely absorbing) to 1 (white, completely scattering)



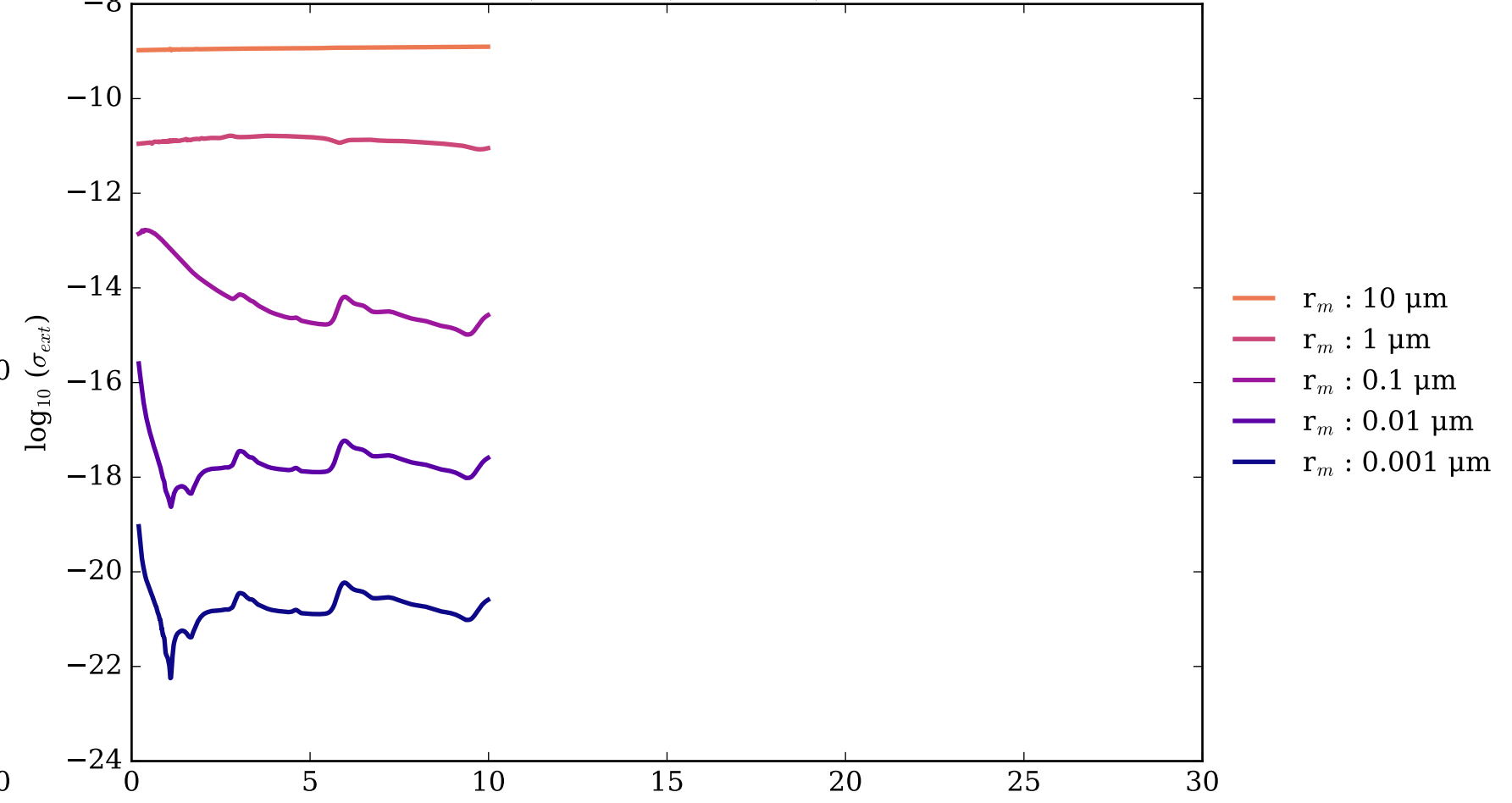
Tholin-CO-0625 Asymmetry Parameter  $g$   
0 (Rayleigh Limit) to 1 (Total Forward Scattering)



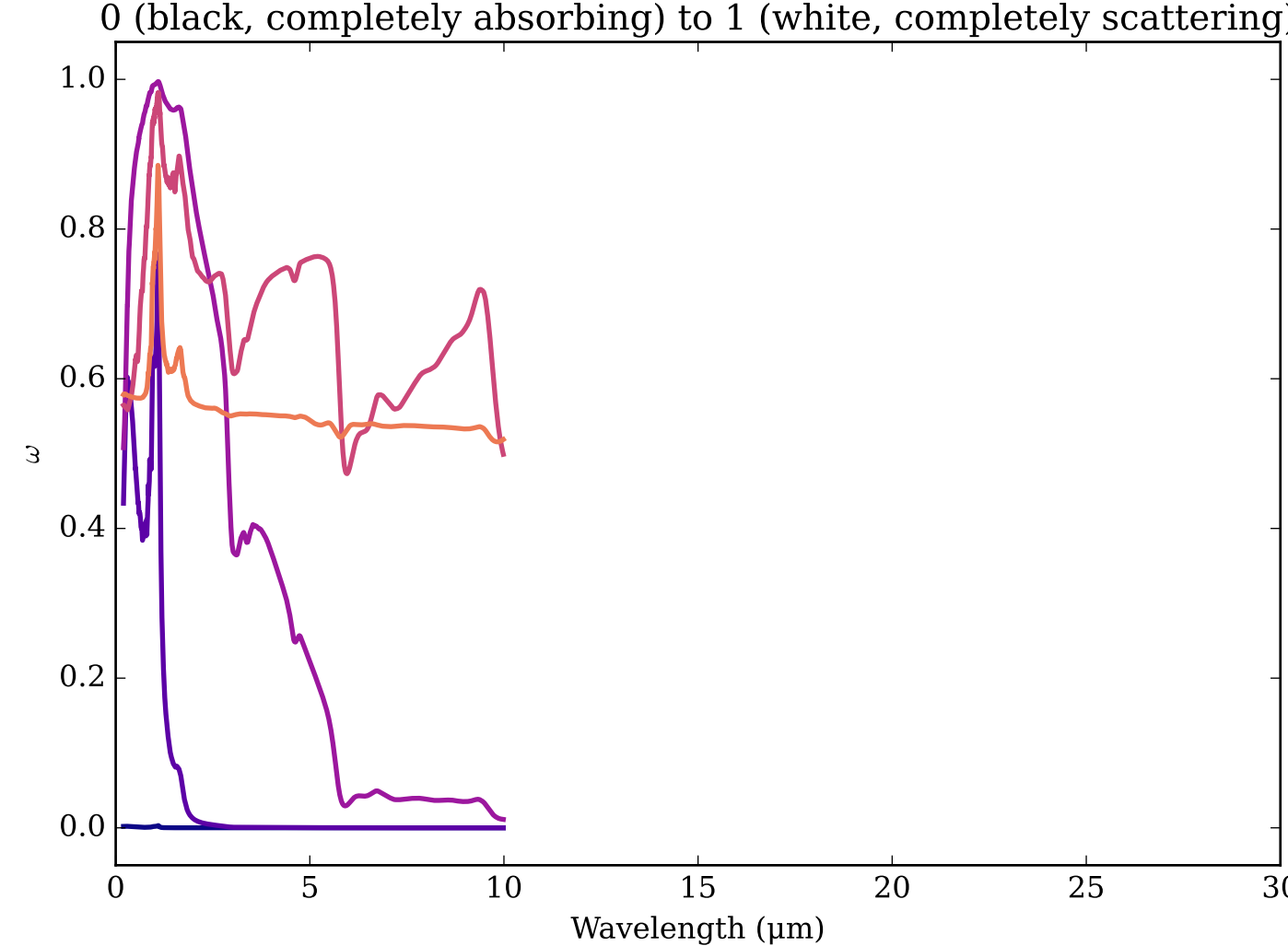
Refractive Indices for Tholin-CO-1  
(0.2, 9.98)  $\mu\text{m}$



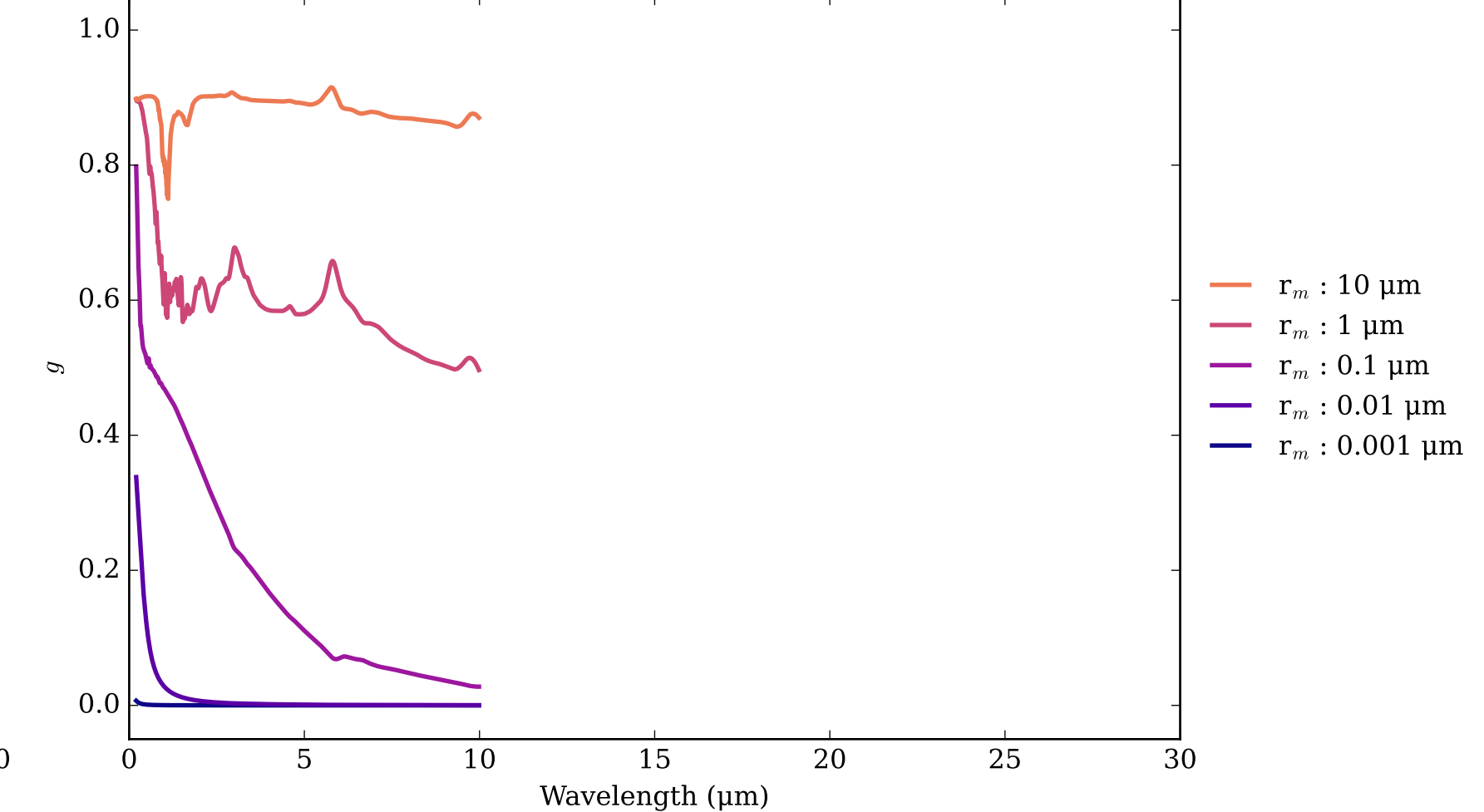
Tholin-CO-1 Effective Extinction Cross Section  
 $\sigma_{\text{ext, eff}} = \sigma_{\text{abs, eff}} + \sigma_{\text{scat, eff}}$



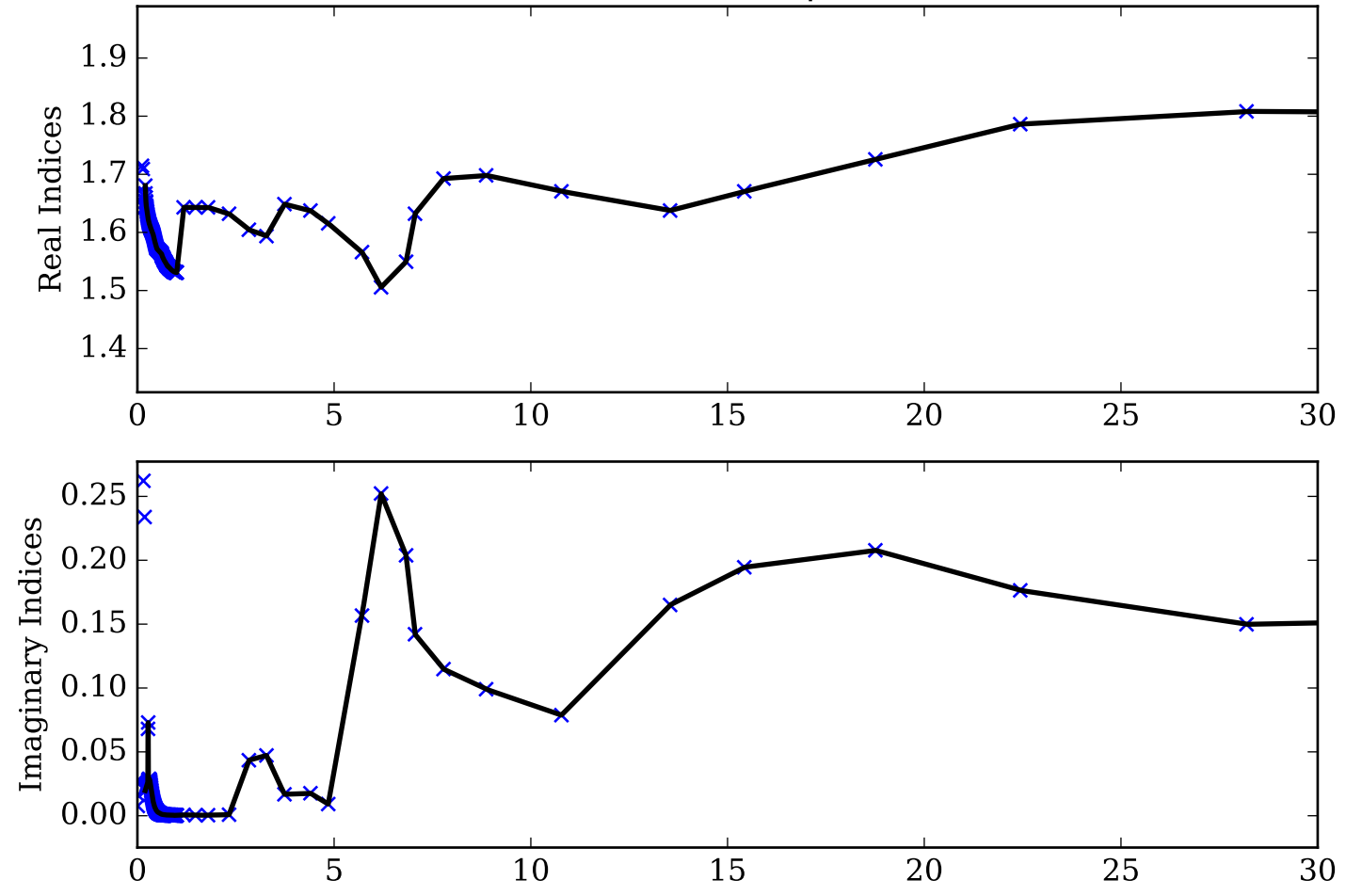
Tholin-CO-1 Single Scattering Albedos  $\omega$



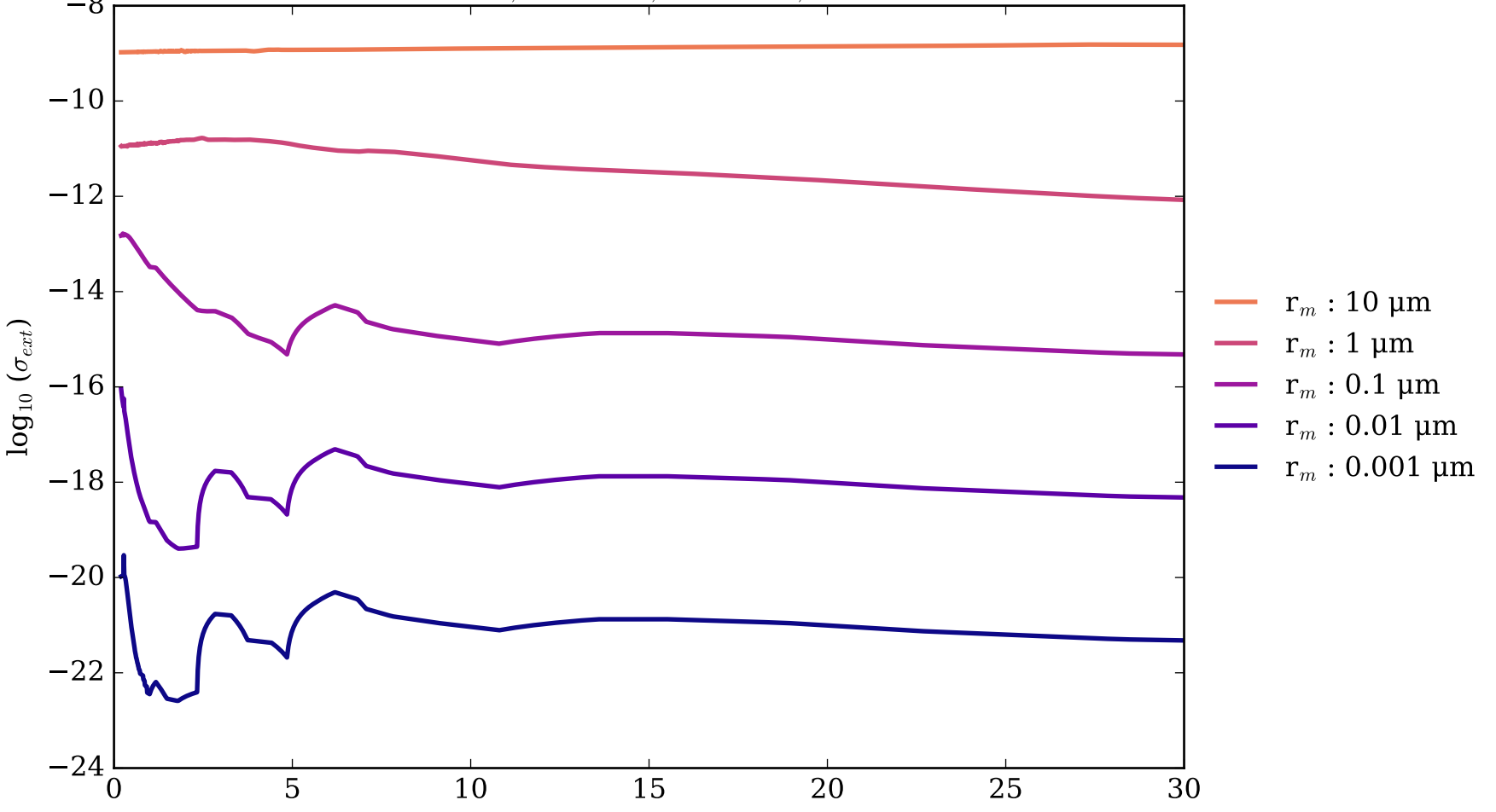
Tholin-CO-1 Asymmetry Parameter  $g$   
0 (Rayleigh Limit) to 1 (Total Forward Scattering)



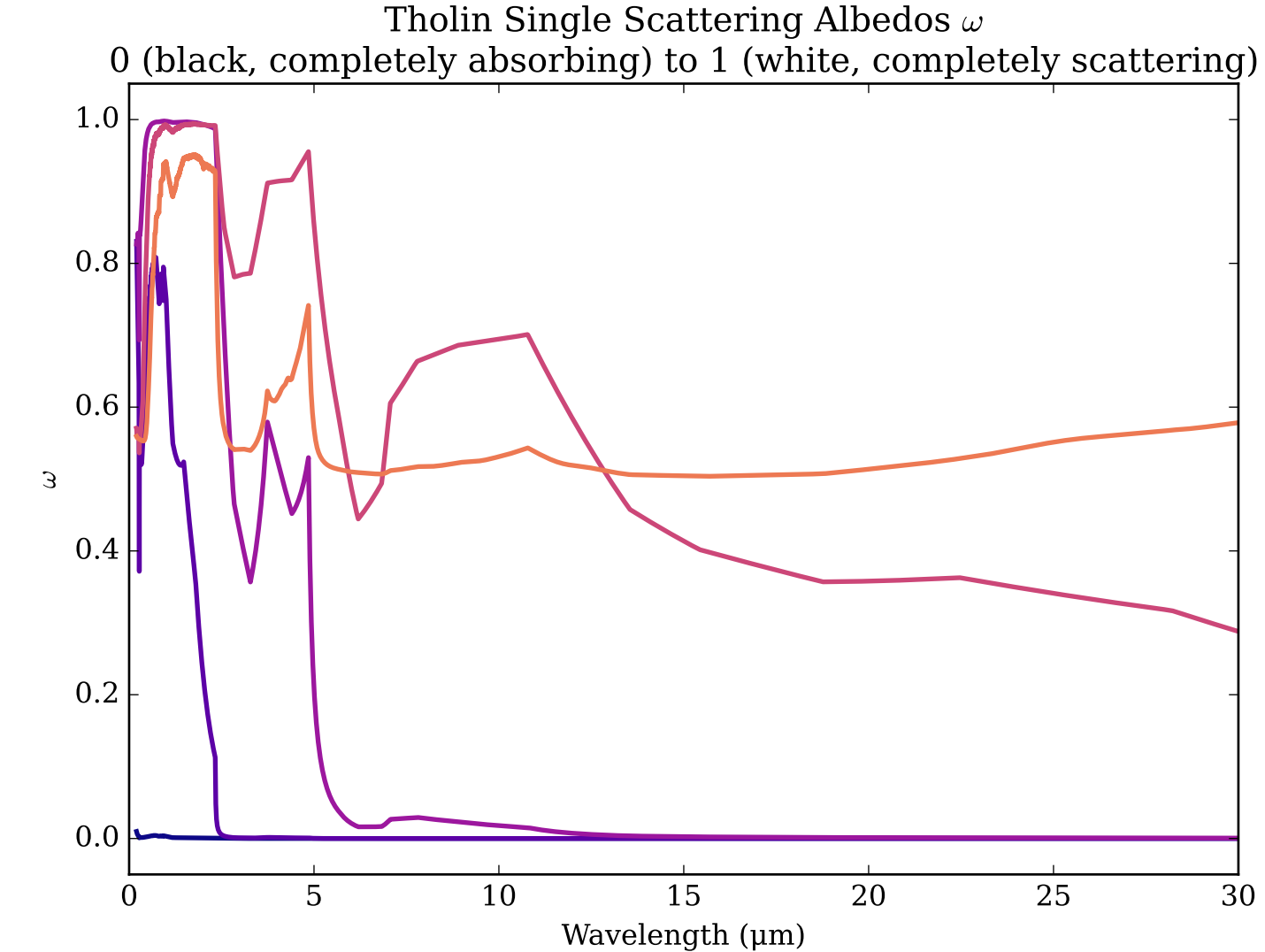
Refractive Indices for Tholin  
(0.2, 30.0)  $\mu\text{m}$



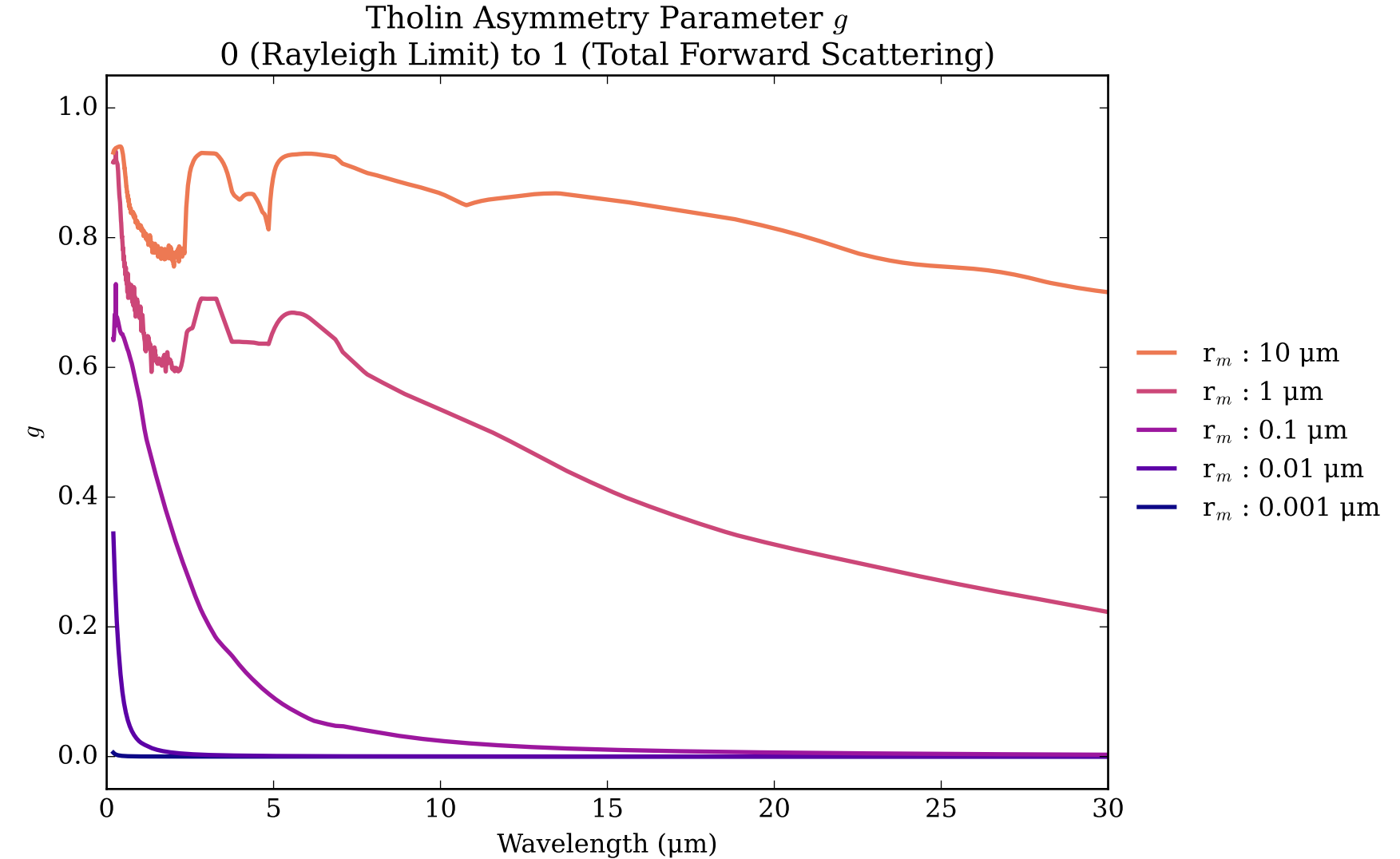
Tholin Effective Extinction Cross Section  
 $\sigma_{\text{ext, eff}} = \sigma_{\text{abs, eff}} + \sigma_{\text{scat, eff}}$



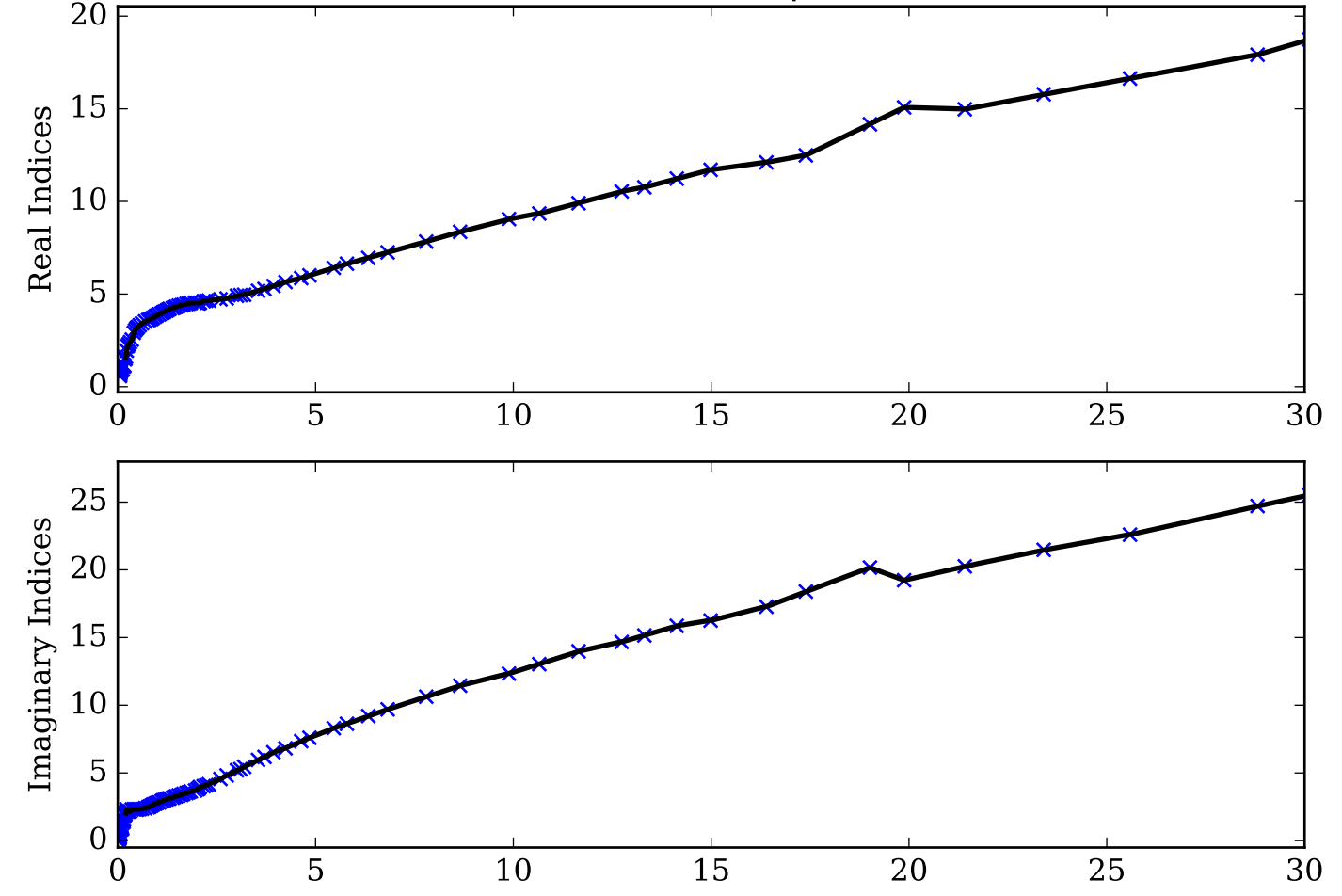
Tholin Single Scattering Albedos  $\omega$



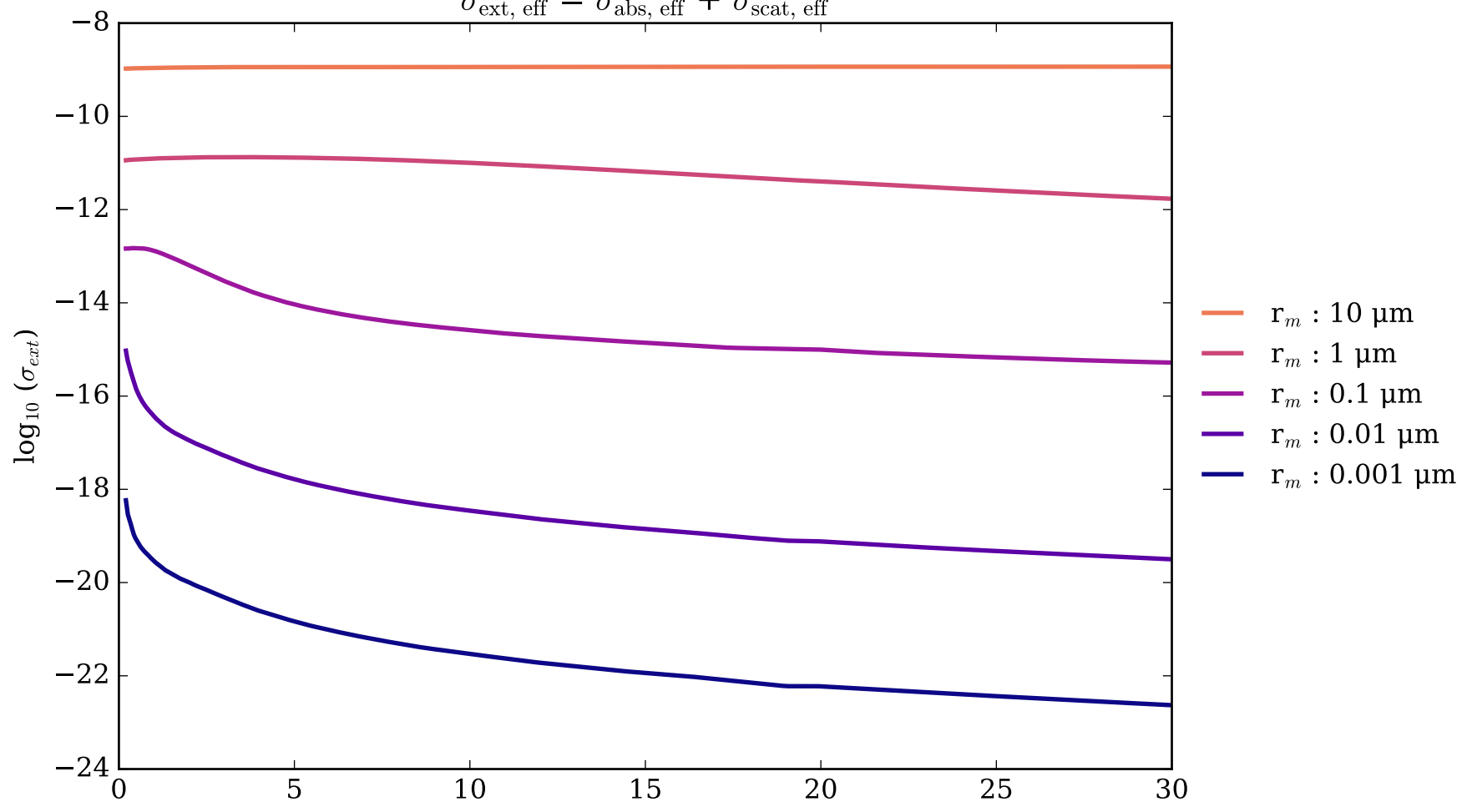
Tholin Asymmetry Parameter  $g$



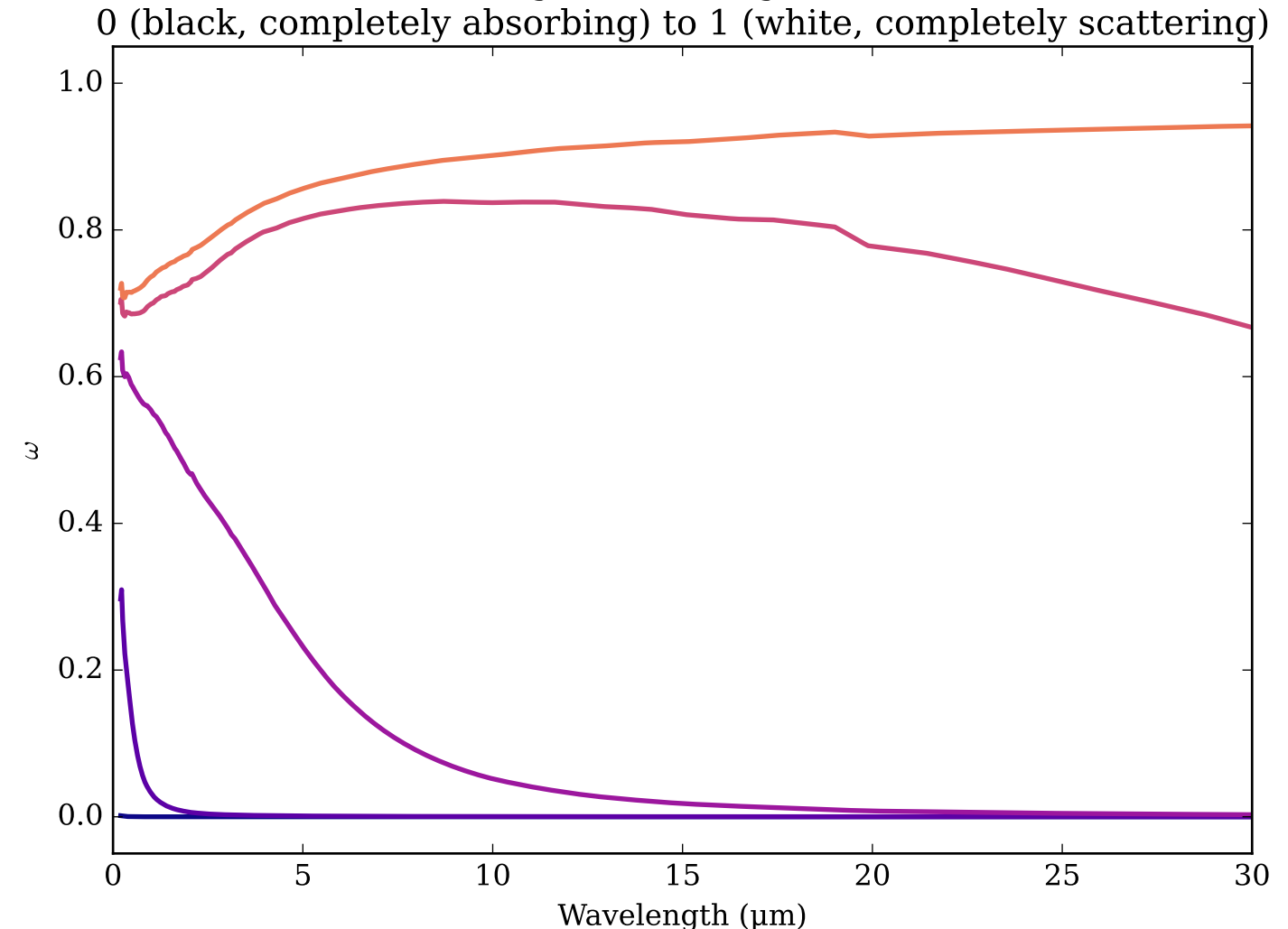
Refractive Indices for TiC  
(0.2, 30.0)  $\mu\text{m}$



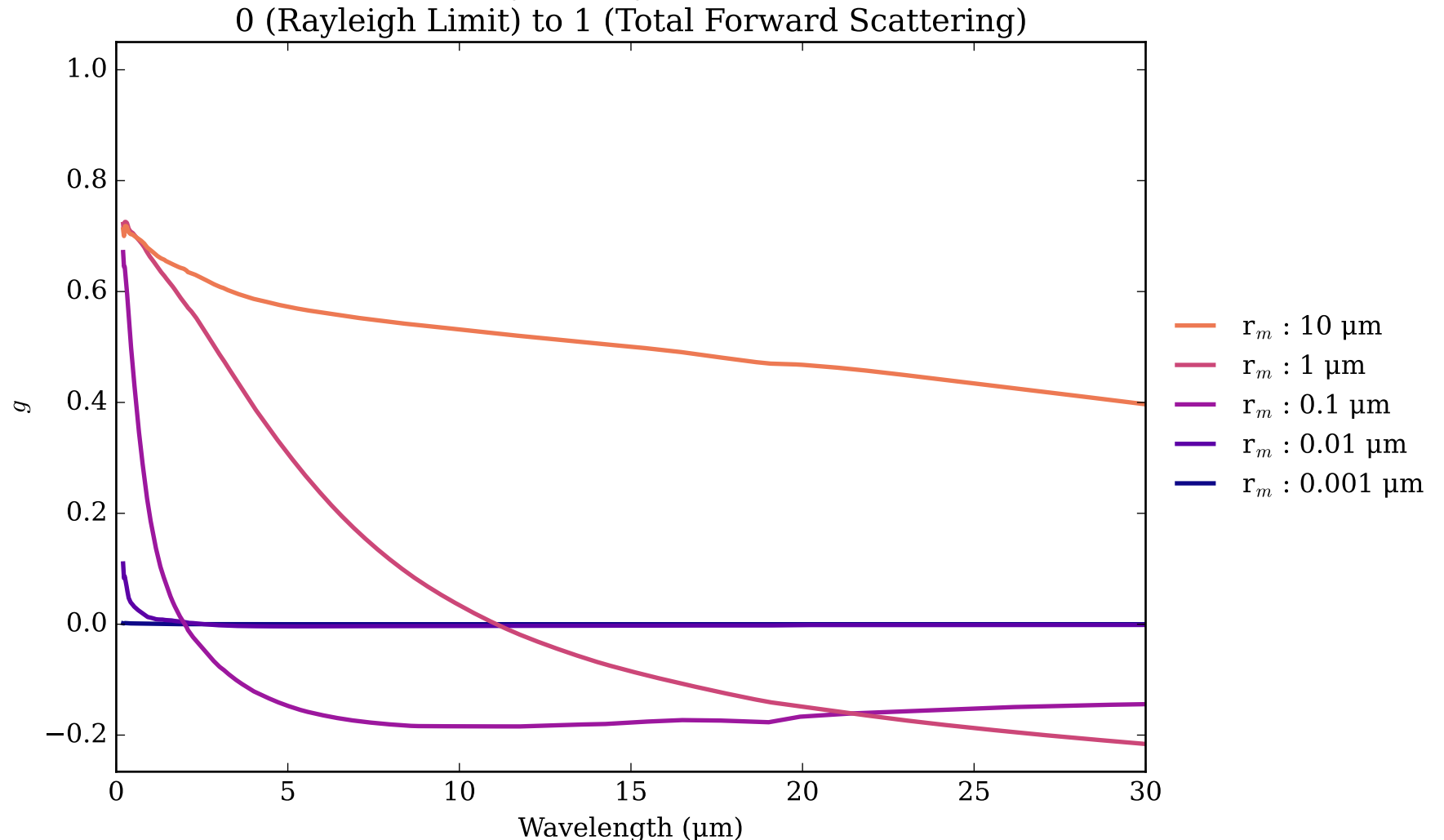
TiC Effective Extinction Cross Section



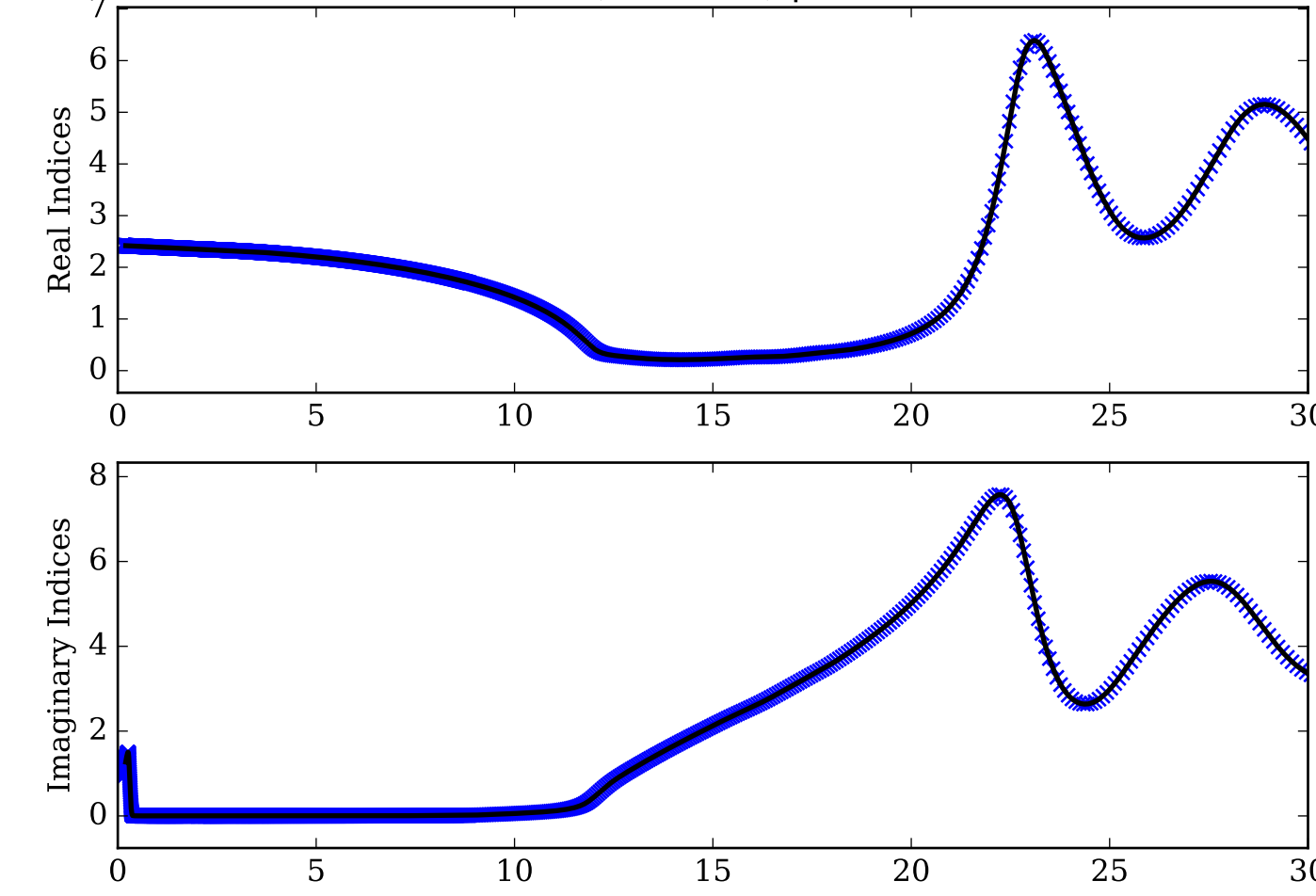
TiC Single Scattering Albedos  $\omega$



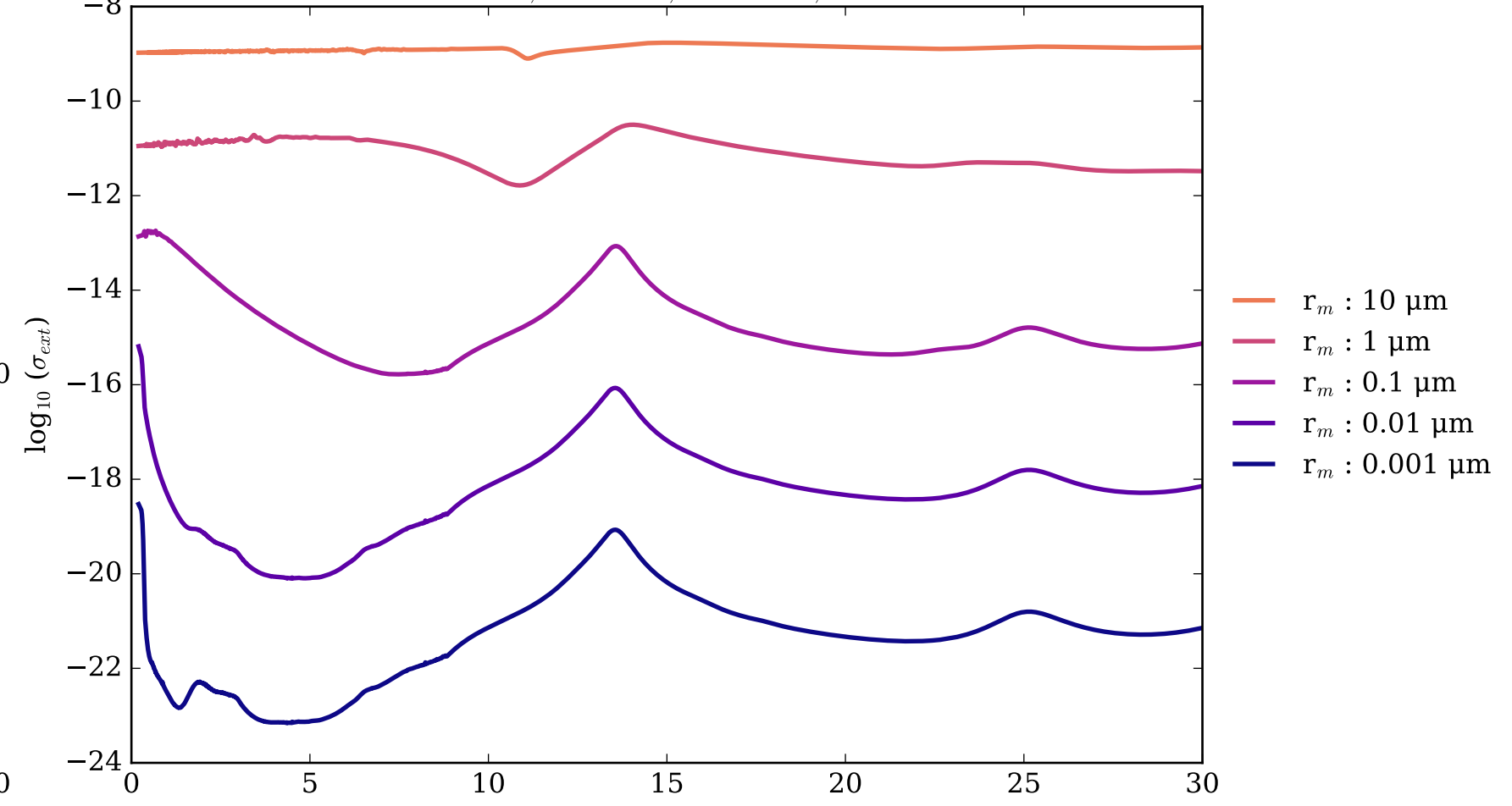
TiC Asymmetry Parameter  $g$



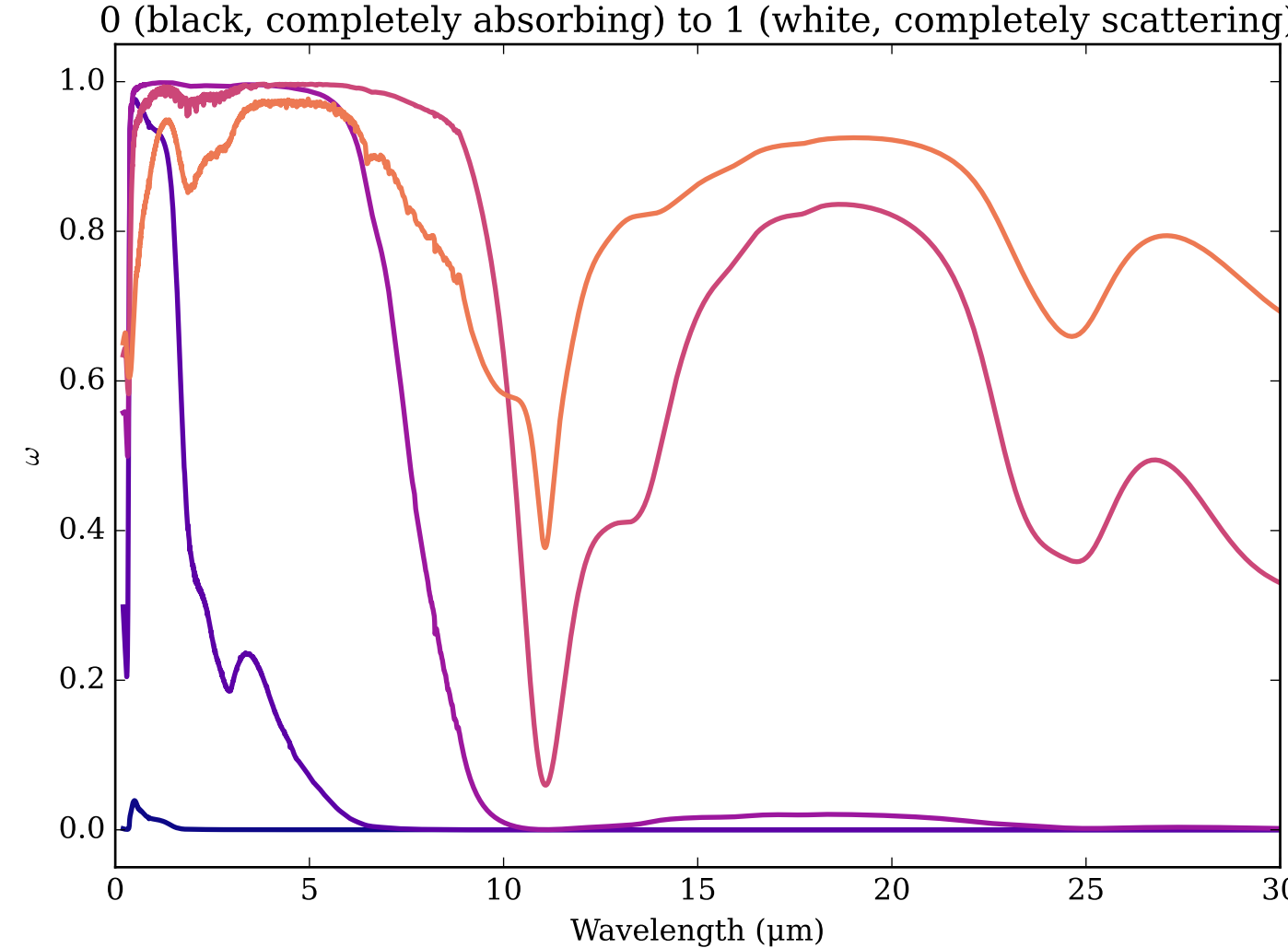
Refractive Indices for TiO<sub>2</sub>  
(0.2, 30.0) μm



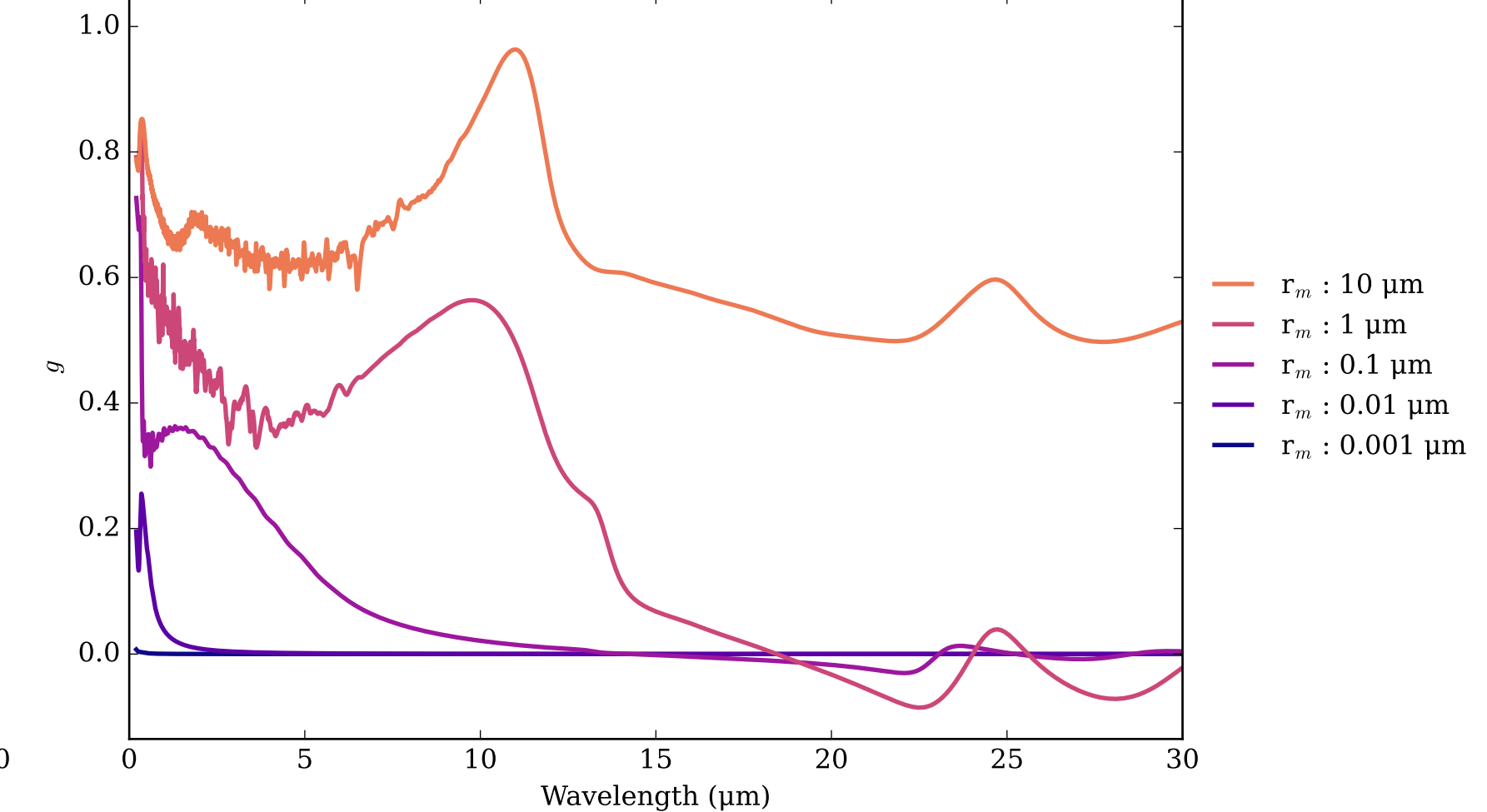
TiO<sub>2</sub>\_anatase Effective Extinction Cross Section  
 $\sigma_{\text{ext, eff}} = \sigma_{\text{abs, eff}} + \sigma_{\text{scat, eff}}$



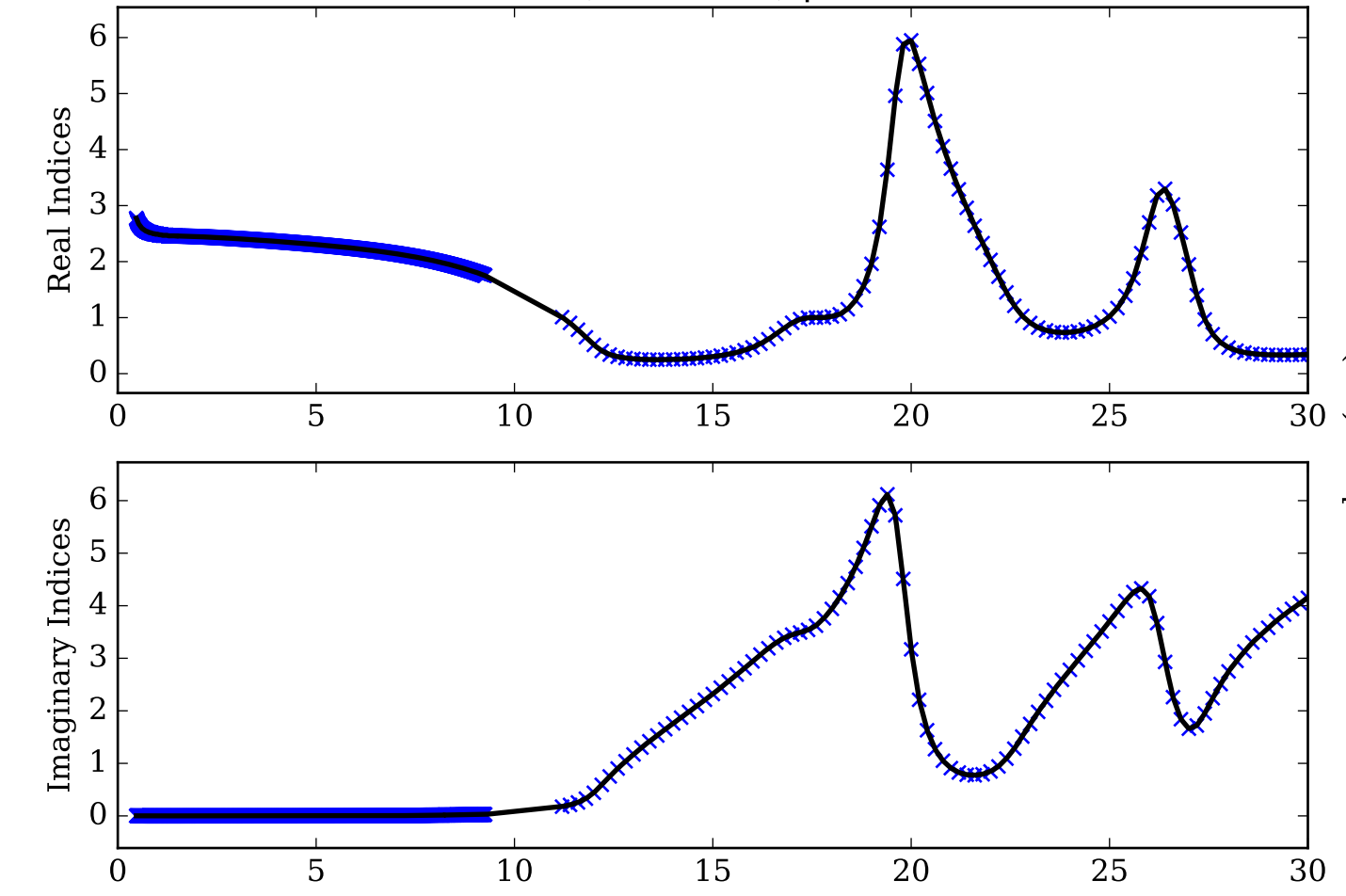
TiO<sub>2</sub>\_anatase Single Scattering Albedos  $\omega$



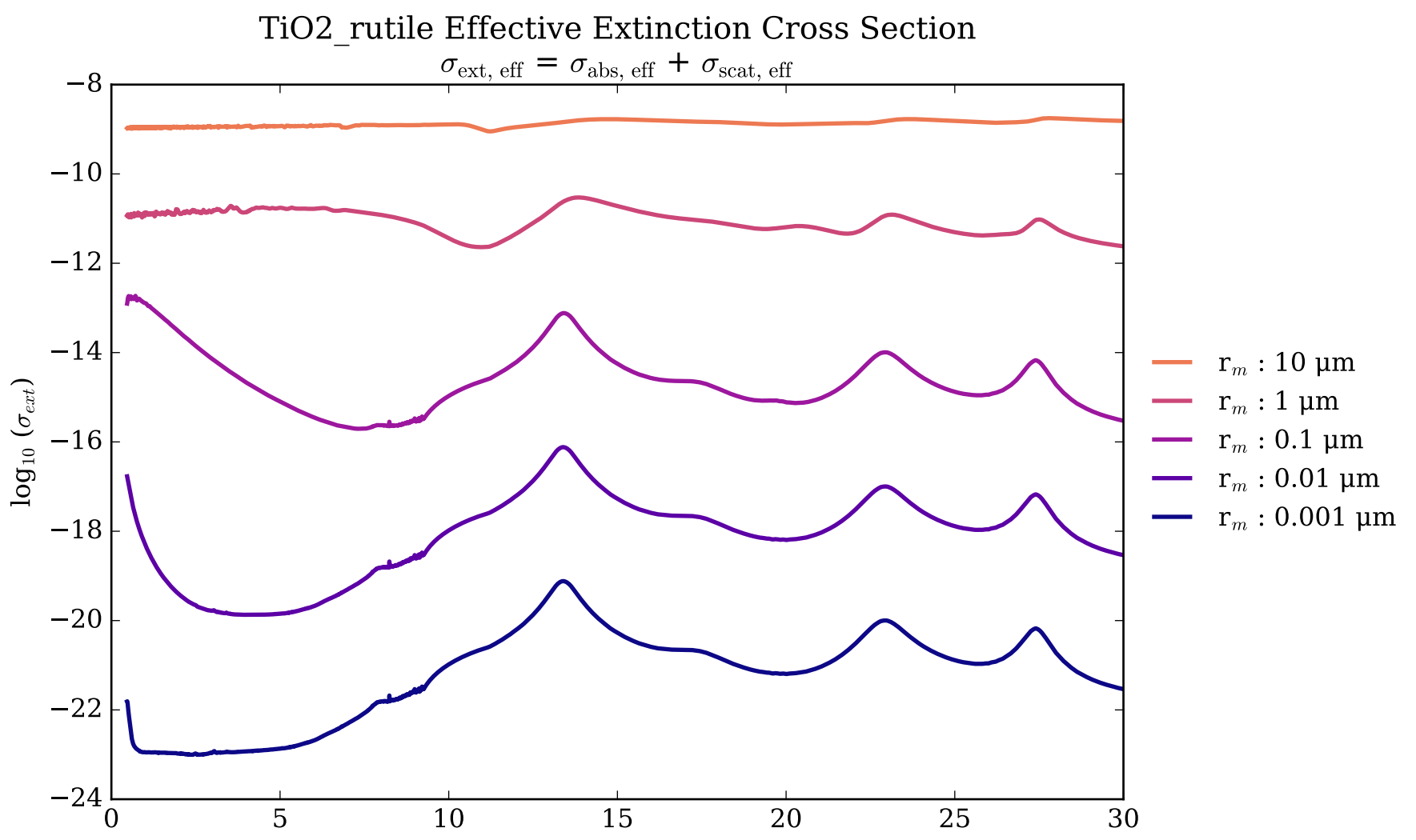
TiO<sub>2</sub>\_anatase Asymmetry Parameter  $g$   
0 (Rayleigh Limit) to 1 (Total Forward Scattering)



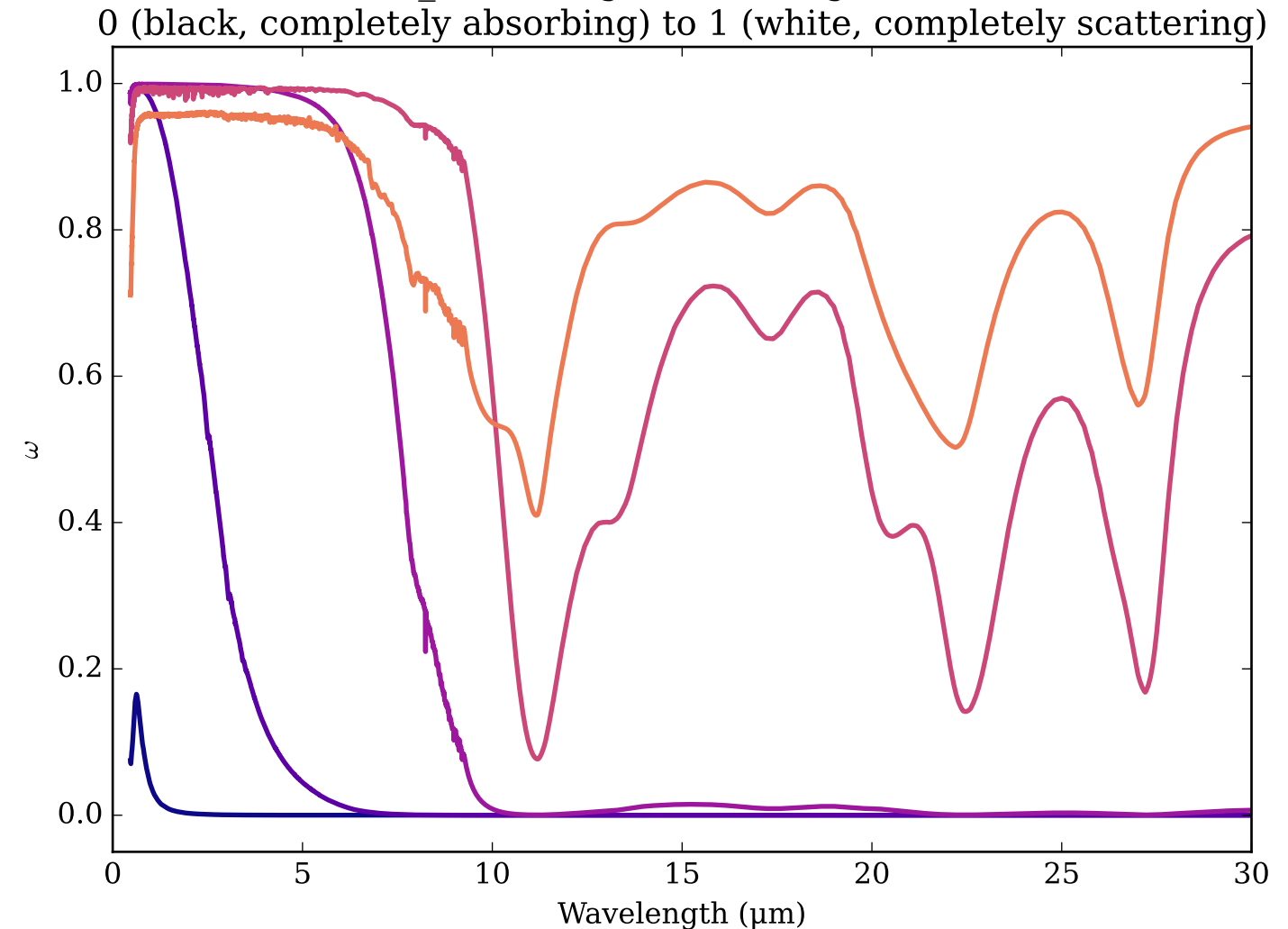
Refractive Indices for TiO<sub>2</sub>  
(0.47, 30.0)  $\mu\text{m}$



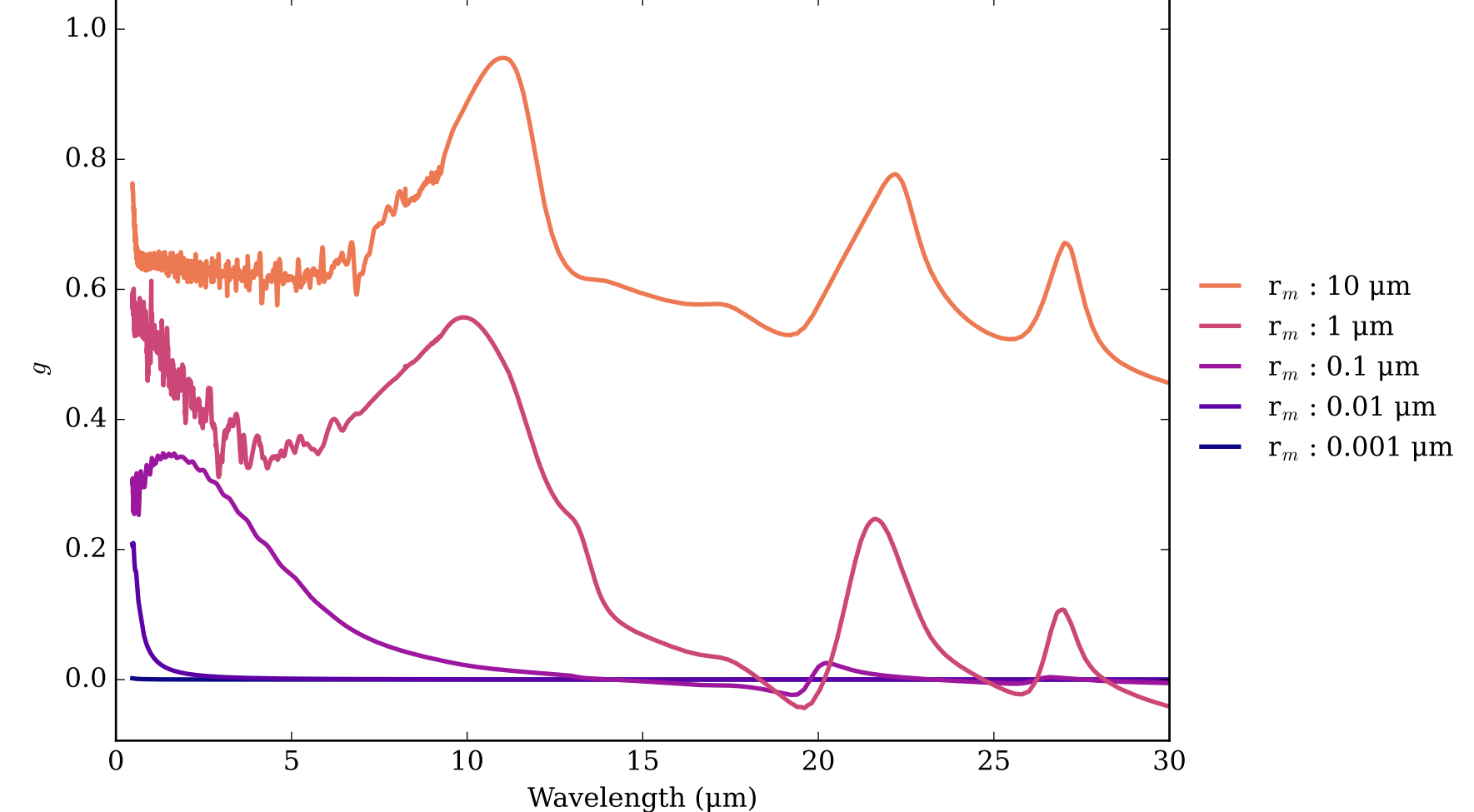
TiO<sub>2</sub>\_rutile Effective Extinction Cross Section



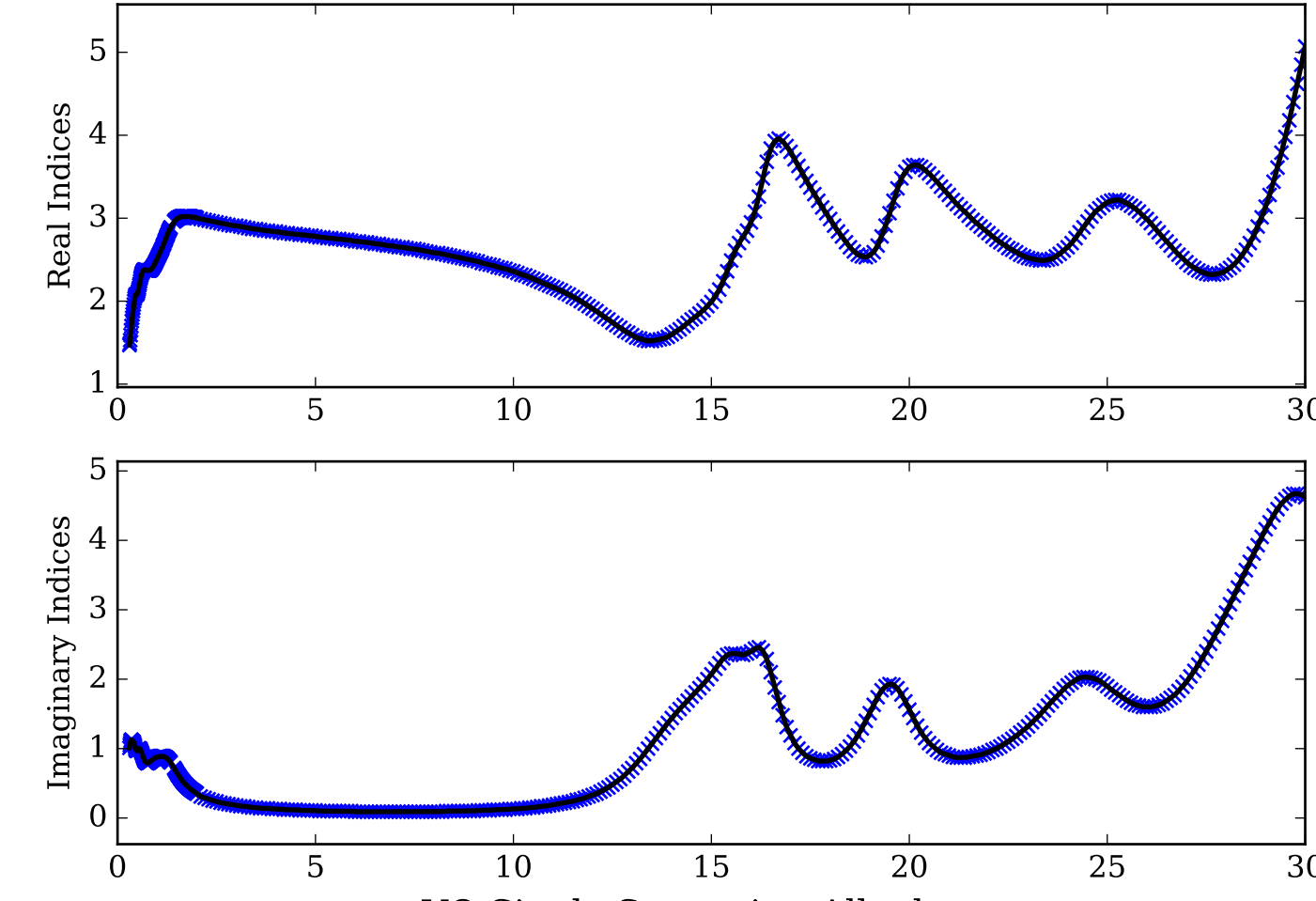
TiO<sub>2</sub>\_rutile Single Scattering Albedos  $\omega$



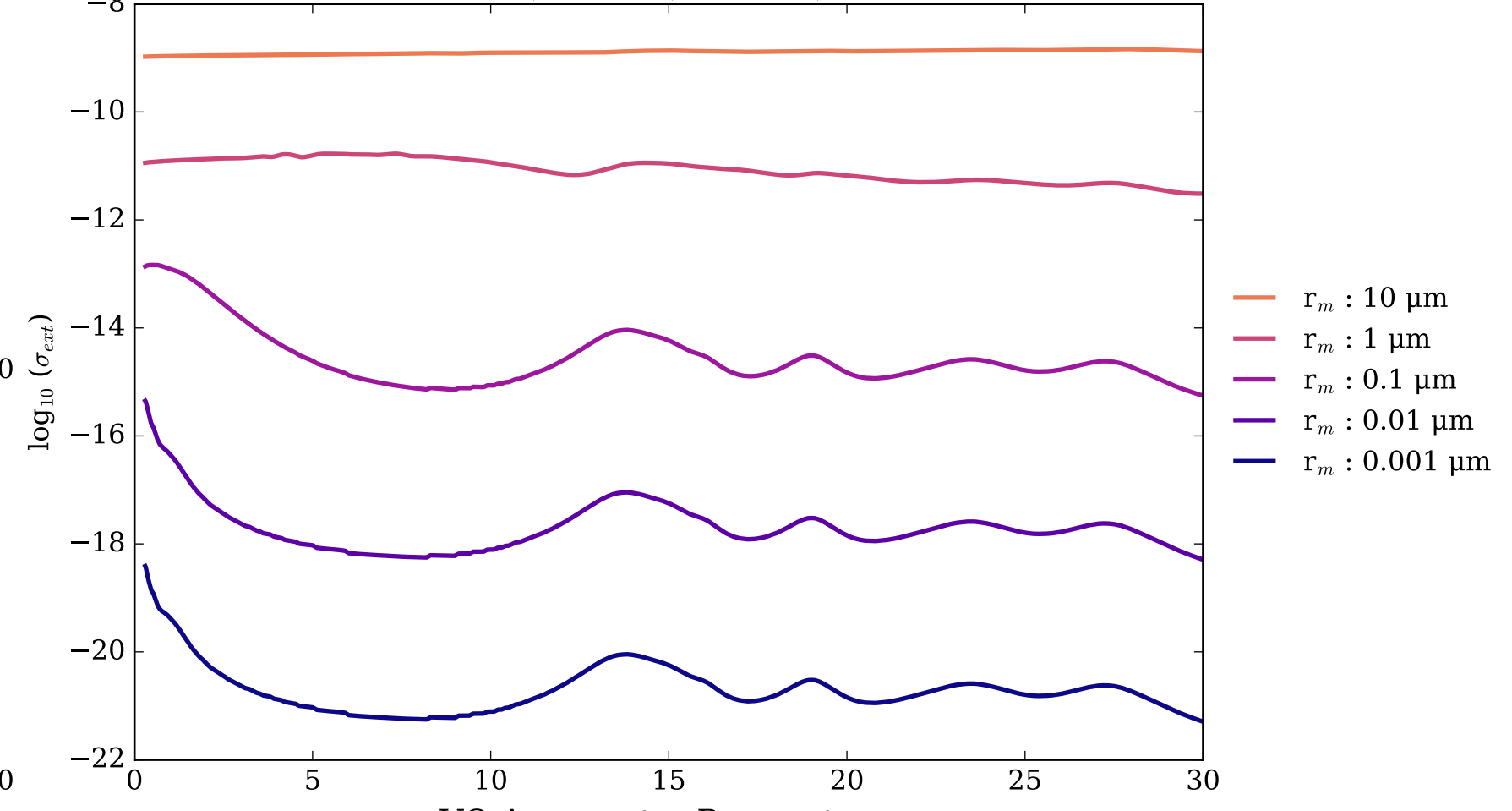
TiO<sub>2</sub>\_rutile Asymmetry Parameter  $g$   
0 (Rayleigh Limit) to 1 (Total Forward Scattering)



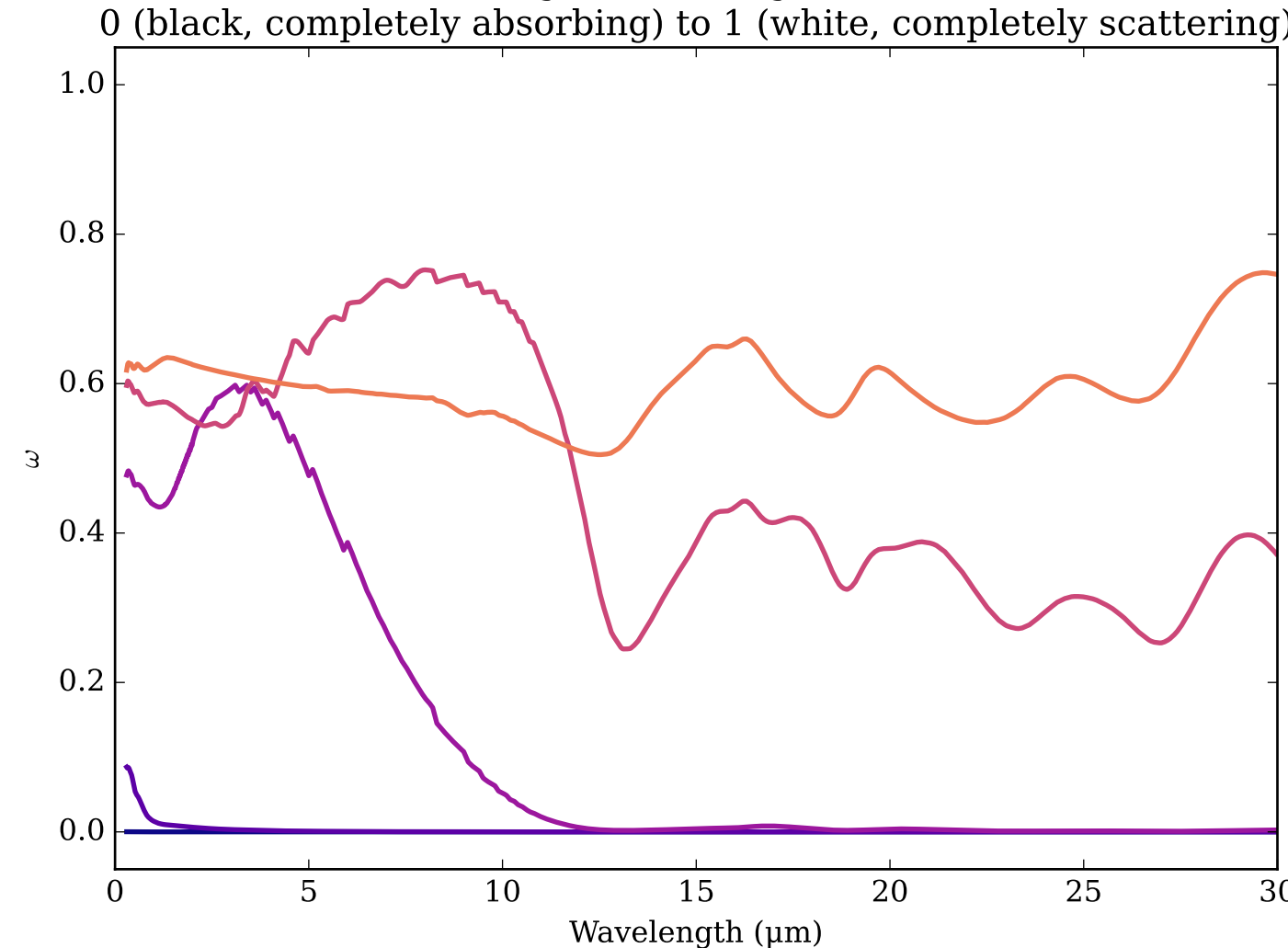
Refractive Indices for VO  
(0.3, 30.0)  $\mu\text{m}$



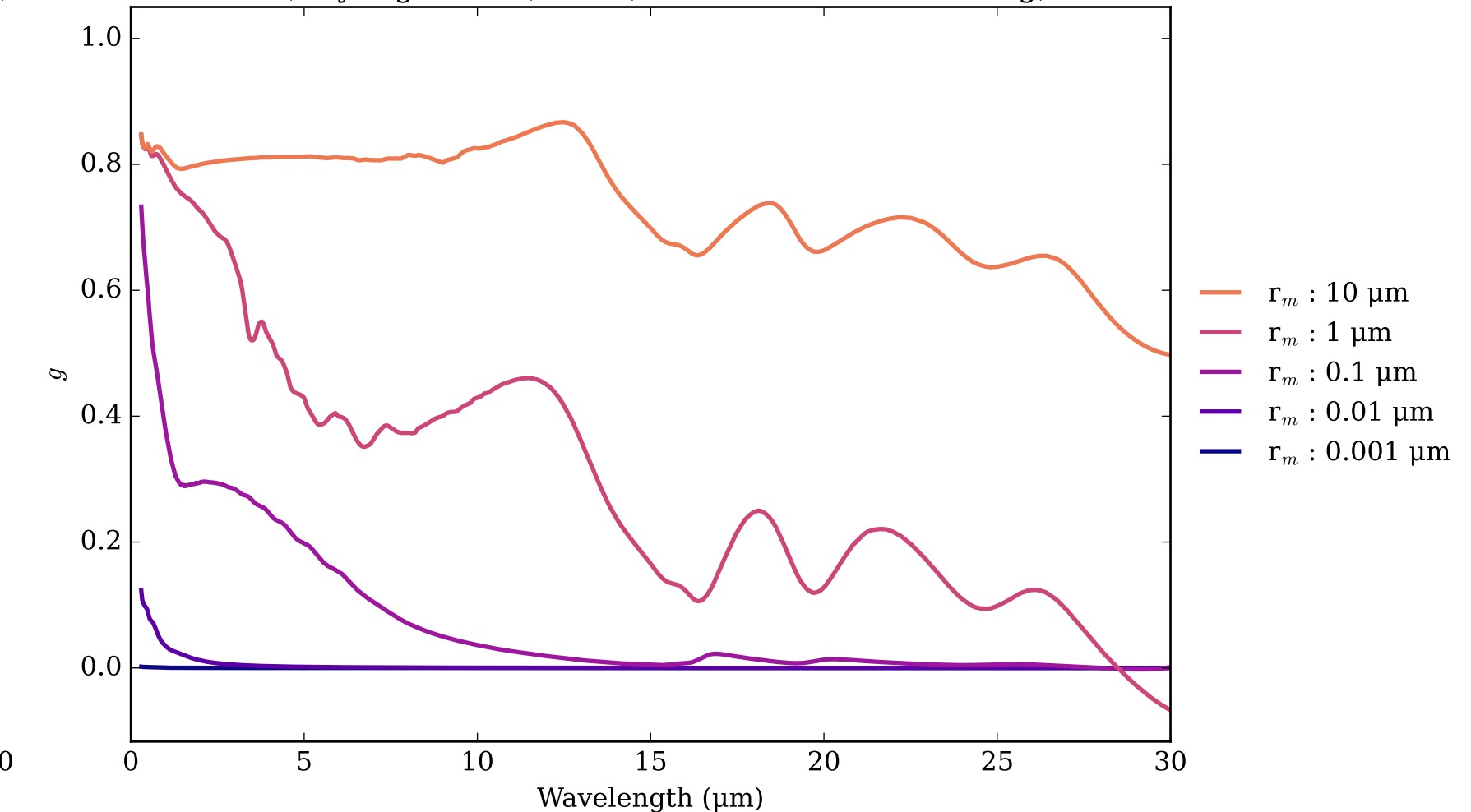
VO Effective Extinction Cross Section  
 $\sigma_{\text{ext, eff}} = \sigma_{\text{abs, eff}} + \sigma_{\text{scat, eff}}$



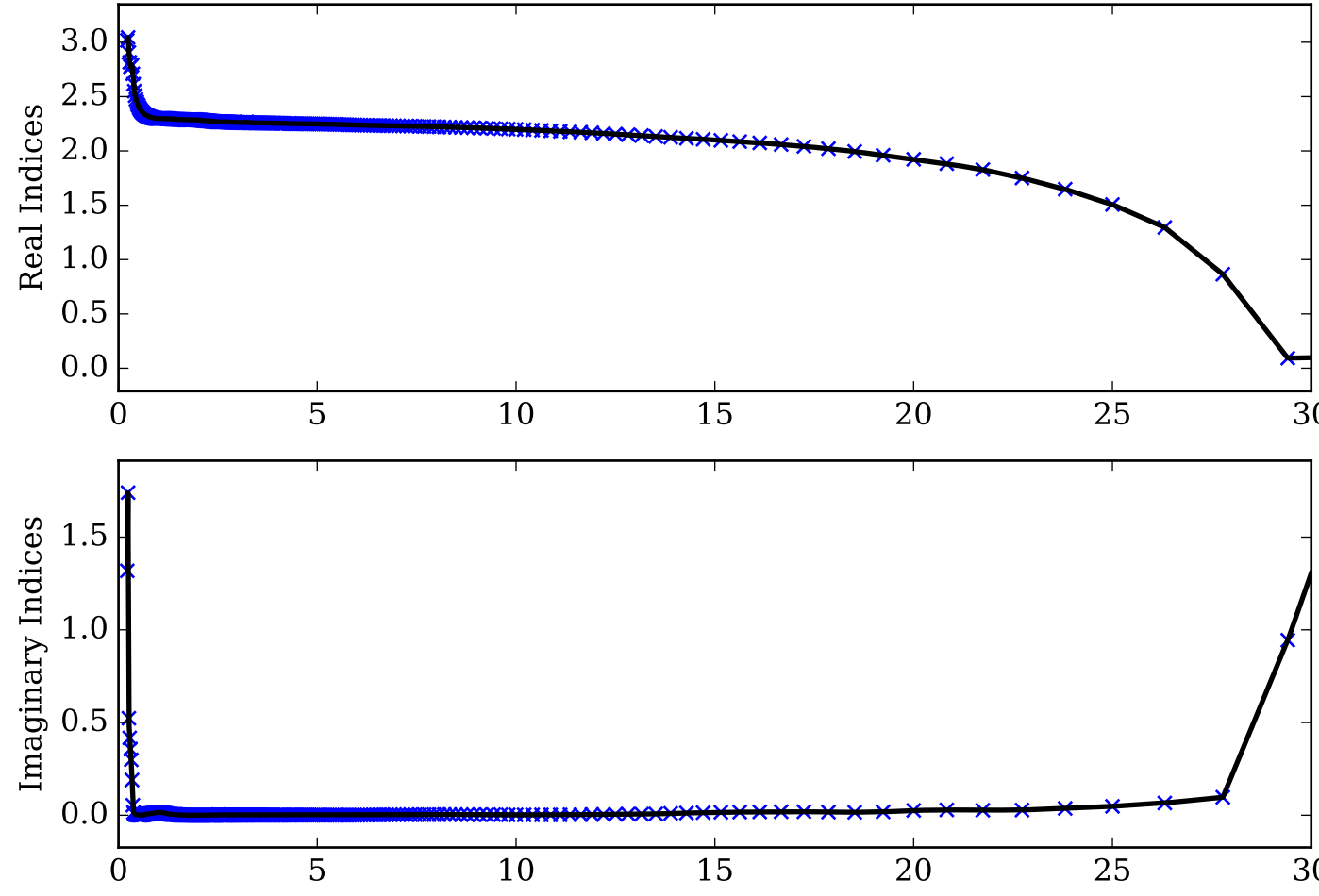
VO Single Scattering Albedos  $\omega$



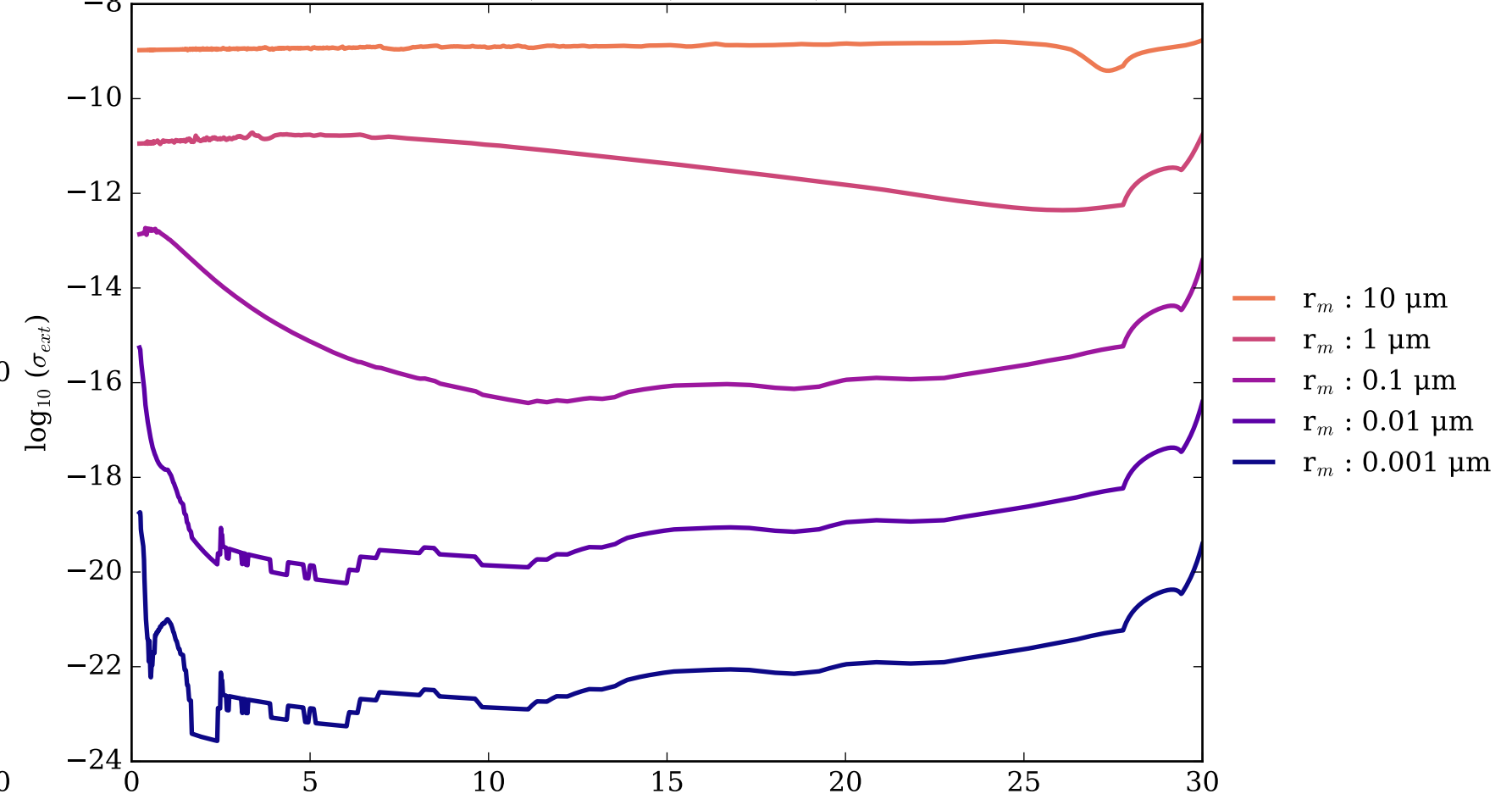
VO Asymmetry Parameter  $g$   
0 (Rayleigh Limit) to 1 (Total Forward Scattering)



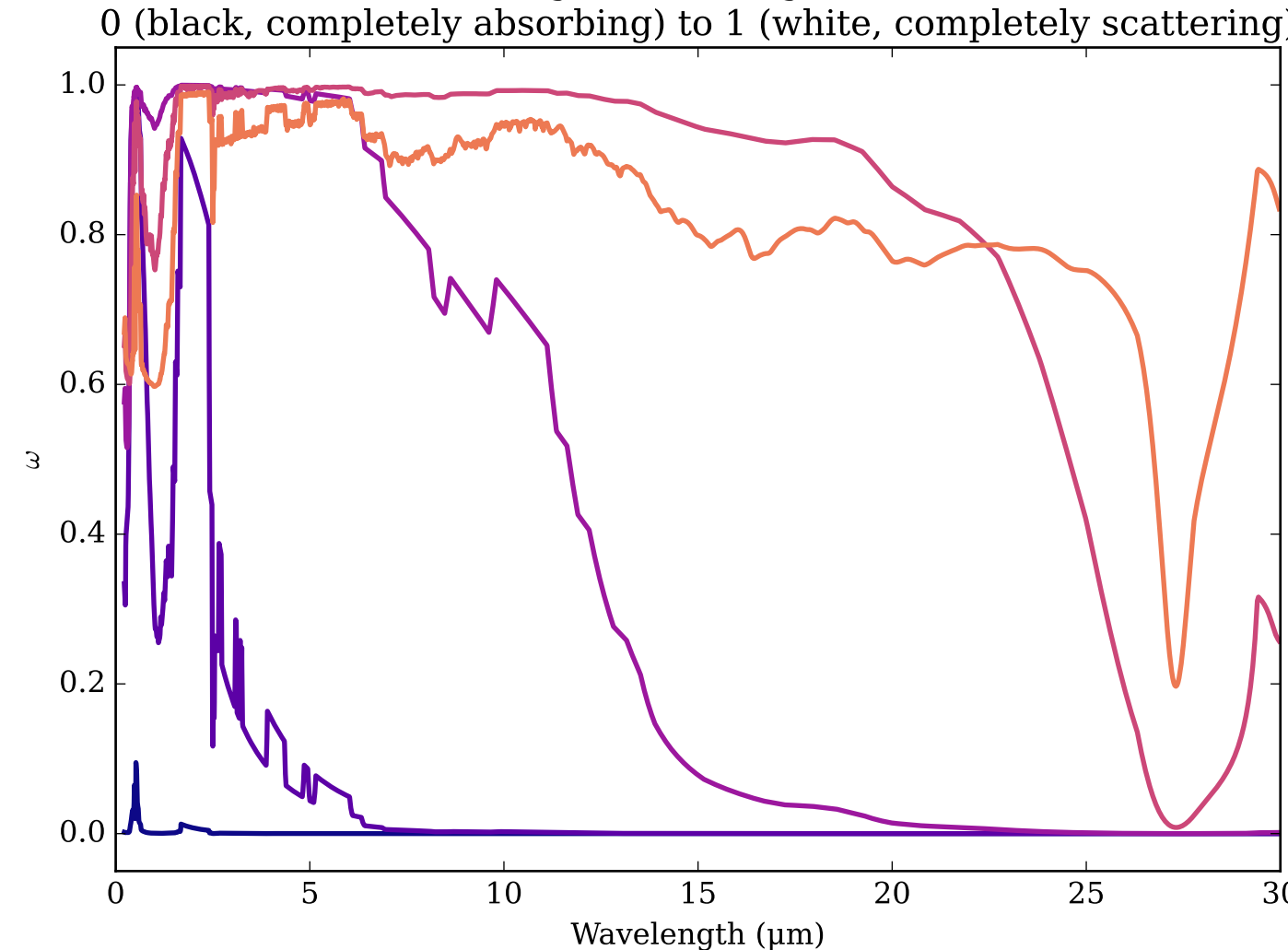
Refractive Indices for ZnS  
(0.22, 30.0)  $\mu\text{m}$



ZnS Effective Extinction Cross Section  
 $\sigma_{\text{ext, eff}} = \sigma_{\text{abs, eff}} + \sigma_{\text{scat, eff}}$



ZnS Single Scattering Albedos  $\omega$



ZnS Asymmetry Parameter  $g$   
0 (Rayleigh Limit) to 1 (Total Forward Scattering)

